
Strain-promoted Stapled Peptides for Inhibiting Protein-protein Interactions

Krishna Sharma

September 2018



UNIVERSITY OF
CAMBRIDGE

Department of Chemistry
Cambridge CB2 1EW



Trinity College
Cambridge CB2 1TQ

This dissertation is submitted for the degree of Doctor of Philosophy

Declaration

This dissertation is the result of my own work and includes nothing which is the outcome of work done in collaboration except where specifically indicated in the text. It does not exceed the word limit specified by the Physics and Chemistry Degree Committee.

Krishna Sharma

September 2018

For my late maternal grandparents Prof. V. N. Dixit and Dr Manorama Dixit.

Acknowledgements

I would like to take this opportunity to thank my supervisor Prof. David Spring for his constant motivation, encouragement and support. I would also like to thank my previous boss Prof. Martin Smith for being a great mentor during my masters at Oxford, which paved a way for me to come to Cambridge. Thanks to Dr Yu Heng Lau for being an amazing mentor and co-supervisor during the first year of my PhD. I am grateful to Trinity College, Cambridge Trust, Cambridge Nehru Trust and Cambridge Philosophical Society for funding my PhD. Many thanks to Dr Warren Galloway, Dr Matthew Grayson, Stephen Walsh, Josie Gaynord, and Jonny Bargh for taking out their precious time to proof-read this thesis.

I thank Dr Andrew Bond and Dr Xuelu Wang for their help with X-ray crystallography. I also thank the NMR staff members Duncan Howe, Peter Grice and Andrew Mason for their help with NMR spectroscopy. I am also thankful to Dr Wenshu Xu, Elaine Fowler, Dr Yuteng Wu and Alexander Strizhak for their help with biological testing of molecules. Thanks to all the current members of the Spring group for their support, invaluable advice and creating a cheerful and friendly atmosphere in the lab. Thanks also to the past group members Mareike Wiedmann, Claudia Fusco, James Hodgkinson, Jamie Stokes, David Twigg, Moni Gupta, Laura Santos, Eddy Sotelo, Claus Jensen and Andrea Renzetti.

A big thank you goes to my family for having supported me at all times. My maternal grandparents: Prof. V. N. Dixit and Dr Manorama Dixit have always been a great source of support and motivation and have played an integral role in shaping my life. My parents: Prof. R. K. Sharma and Dr Ranjana Sharma, who happen to be chemist have been a tremendous source of inspiration and enthusiasm and it would not have been possible to pursue my studies without their support. I thank my brother Pranav Sharma for all the support and also my maternal uncle Dr Lalit Dixit and aunt Dr Purnima Dixit. Furthermore, I am grateful to my wonderful undergraduate chemistry teachers from St Stephen's College for their continued guidance and support; in particular to Dr Shabnam Johry, Dr Rene Saksena, Dr Vibha Sharma, and Dr Rashmi Sachdeva. Thanks to all my Trinity and Indian friends at Cambridge for having made me feel at home while being miles away from home.

Finally, thanks to the Almighty!

Abbreviations

Ac	Acetyl
Aib	2-Aminoisobutyric acid
Ar	Aryl
BAK	Bcl-2 homologous antagonist killer
BCL-X _L	β-cell lymphoma-extra large
BID	BH3 interacting-domain death agonist
B3LYP	Becke 3-parameter Lee-Yang-Parr
Boc	<i>tert</i> -butyloxycarbonyl
BOP	(Benzotriazol-1-yloxy)tris(dimethylamino)phosphonium hexafluorophosphate
BPO	Benzoyl peroxide
CD	Circular dichroism
COSY	Correlation spectroscopy
CPCM	Conductor-like polarisable continuum model
CuAAC	Cu(I)-catalysed azide-alkyne cycloaddition
DEPT	Distortionless enhancement by polarisation transfer
DIBAL-H	Diisobutylaluminium hydride
DIBAC	Dibenzoazacyclooctyne
DIBO	Dibenzocyclooctyne
DIFO	Difluorinated cyclooctyne
DIMAC	Dimethoxyazacyclooctyne
DIPEA	<i>N,N</i> -diisopropylethylamine
DMF	<i>N,N</i> -dimethylformamide
DMP	Dess-Martin periodinane
DMSO	Dimethyl sulfoxide
DNA	Deoxyribonucleic acid
DOS	Diversity-oriented synthesis
eq	Equivalents
FBS	Fragment-based screening
Fmoc	9-fluorenylmethyloxycarbonyl
FP	Fluorescence Polarisation
h	Hour
HER2	Human epidermal growth factor receptor 2
HIV	Human immunodeficiency virus
HMBC	Heteronuclear multiple bond correlation spectroscopy

HPLC	High-performance liquid chromatography
HTS	High-throughput screening
HRMS	High-resolution mass spectrum
HSQC	Heteronuclear single-quantum correlation spectroscopy
IR	Infrared
LCMS	Liquid chromatography-mass spectrometry
LDA	Lithium diisopropylamide
LiHMDS	Lithium Hexamethyldisilazide
Lys	Lysine
MCL	Myeloid cell leukemia
m.p.	Melting point
<i>m</i> -CPBA	<i>meta</i> -Chloroperoxybenzoic acid
MDM2	Mouse double minute 2
MOFO	Monofluorinated cyclooctyne
M06	Minnesota 06
NBS	<i>N</i> -bromosuccinimide
NMR	Nuclear magnetic resonance
Orn(N ₃)	azidoornithine
PBS	Phosphate-buffered saline
Ph	Phenyl
R _f	Retention factor
PPI	Protein-protein interaction
PS	Polystyrene
RCM	Ring-closing metathesis
rt	Room temperature
SPAAC	Strain-promoted azide-alkyne cycloaddition
TCEP	tris(2-carboxyethyl)phosphine
TFE	2,2,2-trifluoroethanol
THF	Tetrahydrofuran
THPTA	tris(3-hydroxypropyltriazolylmethyl)amine
TLC	Thin-layer chromatography
TMS	trimethylsilyl
Tris	tris(hydroxymethyl)aminomethane
UV	Ultra-violet
X	Azido amino acid

Standard one and three letter codes are used for amino acids.

Abstract

Protein-protein interactions (PPIs) are responsible for the regulation of a variety of important functions within living organisms. Compounds which can selectively modulate aberrant PPIs are novel therapeutic candidates for treating human diseases. Whilst PPIs have traditionally been considered as “undruggable”, research in this area has led to the emergence of several effective methodologies for targeting PPIs. One such methodology is peptide stapling, which involves constraining a short peptide into its native alpha-helical form by forming a covalent link between two of its amino acid side-chains. The Sondheimer dialkyne reagent has previously been used in strain-promoted double-click cycloadditions with diazidopeptides to generate stapled peptides that are capable of inhibiting PPIs. However, the Sondheimer dialkyne suffers from poor water-solubility; it decomposes rapidly in aqueous solutions which limits its application in biological systems. This dissertation describes the design and synthesis of new substituted variants of the Sondheimer dialkyne with increased solubility and stability, that are suitable for application in strain-promoted double-click peptide stapling. In total, ten different derivatives were generated; of these, a *meta*-trimethylammonium substituted variant was found to have particularly high water-solubility and aqueous stability, as well as high azide-reactivity. The substituted Sondheimer dialkynes were applied to the strain-promoted double-click stapling of p53-based diazido peptides in an effort to generate stapled peptide-based inhibitors of the oncogenic p53-MDM2 PPI, a validated target for anticancer therapeutics. Three stapled peptides were found to have inhibitory activity, thus demonstrating the utility of the novel dialkynes in the preparation of PPI inhibitors. The functionalised stapled peptide formed from a *meta*-fluoro substituted Sondheimer dialkyne was found to be the most potent inhibitor. All *ortho*-substituted Sondheimer dialkynes were found to be unreactive, whereas those with a *meta*-trimethylammonium substituent were highly reactive when compared to other *meta*-substituted dialkynes. These patterns in azide reactivity could be explained through X-ray crystallographic studies and density functional theory calculations.

Table of Contents

Declaration	i
Acknowledgements	iii
List of abbreviations	iv
Abstract	vi
Table of Contents	vii
1. Introduction	1
1.1 Protein-protein interactions as therapeutic targets	1
1.2 Strategies for targeting PPIs	1
1.2.1 Small molecule PPI inhibitors	1
1.2.2 Biologics	4
1.2.3 Peptidomimetics	4
1.3 Stapled peptides as alpha helix mimetics	5
1.4 Peptide stapling techniques	6
1.4.1 One-component peptide-stapling	6
1.4.1.1 Hydrocarbon stapling	6
1.4.1.2 Lactamisation	7
1.4.1.3 Cycloadditions	8
1.4.1.4 Disulphide linking	9
1.4.2 Two-component peptide-stapling	9
1.4.2.1 Photoswitchable linkers	10
1.4.2.2 Alkylation/arylation on cysteine residues	11
1.5 Previous work in the Spring group	12

1.5.1 Cu(I)-catalysed double-click peptide stapling	12
1.5.2 Strain-promoted double-click peptide stapling	13
1.6 Project aim and thesis overview	14
2. Synthesis of substituted Sondheimer dialkynes	16
2.1 Synthesis of tetramethoxy substituted Sondheimer dialkyne	17
2.2 Synthesis of <i>meta</i> -methoxy substituted Sondheimer dialkyne	19
2.3 Synthesis of <i>meta</i> -fluoro substituted Sondheimer dialkyne	20
2.4 Synthesis of <i>ortho</i> -fluoro substituted Sondheimer dialkyne	21
2.5 Synthesis of <i>meta</i> -nitro substituted Sondheimer dialkyne	22
2.6 Synthesis of <i>ortho</i> -nitro substituted Sondheimer dialkyne	23
2.7 Synthesis of <i>ortho</i> -dimethylamine substituted Sondheimer dialkyne	24
2.8 Synthesis of <i>meta</i> -dimethylamine substituted Sondheimer dialkyne	27
2.9 Synthesis of quaternary-ammonium substituted Sondheimer dialkynes	28
2.9.1. Water solubility of quaternary ammonium substituted dialkynes	29
2.9.2. Stability of quaternary ammonium substituted dialkynes	30
2.10 Synthesis of heteroaromatic based Sondheimer dialkynes	31
2.10.1. Synthesis of pyridine-based Sondheimer dialkyne	31
2.10.2. Synthesis of furan-based Sondheimer dialkyne	34
3. Strain-promoted double-click peptide stapling	36
3.1 p53-MDM2 interaction	36
3.2 Peptide stapling with substituted Sondheimer dialkynes	38
3.3 Biological evaluation of functionalised stapled peptides	42

4.	SPAAC reactivity of substituted Sondheimer dialkynes: Experimental investigations	47
4.1	Kinetic analysis	47
4.2	X-ray crystallographic analysis	67
5.	Computational Studies: Prediction of SPAAC reactivity	70
5.1	Prediction of alkyne bond angles and strain energies of substituted Sondheimer dialkynes	70
5.2	Transition state barriers	74
5.3	Distortion/Interaction analysis	88
6.	Conclusions and future work	91
7.	Experimental	94
7.1	General Information	94
7.1.1	Solvents and Reagents	94
7.1.2	Chromatography	94
7.1.3	NMR Spectroscopy	94
7.1.4	IR Spectroscopy	94
7.1.5	High Resolution Mass Spectrometry	94
7.1.6	Liquid Chromatography-Mass Spectrometry	95
7.1.7	UV Spectroscopy	95
7.1.8	High-performance Liquid Chromatography	95
7.1.9	Melting points	95
7.1.10	Naming and numbering of compounds	95
7.2	Experimental Procedures and Data	96
7.2.1	Peptide synthesis procedure	193

7.2.2 General strain-promoted double-click peptide stapling procedure	193
7.2.3 Peptide LCMS and HPLC data	194
7.2.4 X-ray crystallography	203
7.2.5 Competitive fluorescence polarisation assay	216
7.2.6 Cellular p53 reporter assay	218
7.2.7 Kinetic analysis method	219
7.2.8 log P determination of <i>meta</i> -amine substituted diynes	220
8. Computational data	223
8.1 Cartesian coordinates and energies of all stationary points	224
References	300
Appendix: DFT studies with benzyl azide	312

1. Introduction

1.1 Protein-protein interactions as therapeutic targets

Proteins form an integral part of the cellular machinery and are responsible for carrying out a diverse range of important functions within living organisms, such as cell growth, DNA replication, enzymatic catalysis and signal transduction. Each of these functions is regulated by a complex network of proteins consisting of interactions between various proteins.^{1,2} Loss of an essential protein-protein interaction (PPI) or formation/stabilisation of a protein complex at an inappropriate time or location can lead to the onset of human diseases.³ Therefore, selective modulation of such aberrant PPIs can lead to the development of novel therapeutic agents for treating human diseases.

Despite the importance of PPIs, research in this area is still under development due to two main challenges:

- 1) PPI interfaces are large ($\sim 1000\text{-}2000\text{ \AA}^2$) suggesting the need of large molecules to compete effectively with the natural protein partner in contrast to ‘drug-like’ small molecules which have been employed in enzyme inhibition.⁴⁻⁵
- 2) PPI interfaces often lack deep, well-defined pockets for small molecules to bind, in contrast to enzymes and G-protein-coupled receptors which possess well-defined binding cavities.⁶ Moreover, the lack of natural small molecule binders as a starting point for PPI inhibition poses difficulties for structure-based drug design.

Therefore, twenty years ago PPIs were considered to be “intractable” or “undruggable”.⁷ Despite these challenges, there has been considerable amount of research in this area for the past two decades and a number of different approaches have been reported for inhibiting PPIs.⁸

1.2 Strategies for targeting PPIs

1.2.1 Small molecule PPI inhibitors

Most of the drugs available at present are small organic molecules.⁹ Traditionally, competitive inhibition of protein function has been achieved by using molecules that can mimic enzyme substrates (Figure 1a).^{6, 10} Crystallographic studies have demonstrated that PPI interfaces are generally large and flat.¹¹ This suggests that effective inhibition of PPIs using small molecules would require the small molecule to bind over a much larger surface area ($800\text{-}1100\text{ \AA}^2$) on

the protein surface as compared to the potential binding-area of small-molecules (100-600 Å²), and complement the poorly defined projections on the protein surface (Figure 1b).^{6, 12}

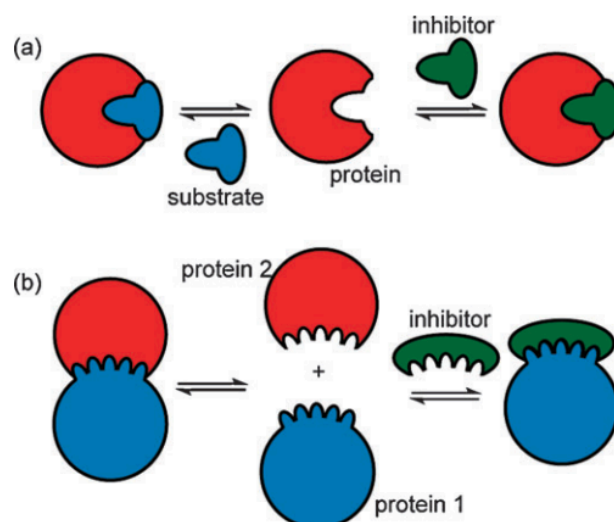


Figure 1: (a) Recognition and inhibition of enzymes; (b) recognition and inhibition of PPIs (from Wilson *et al.*⁶).

However, Wells *et al.* have shown that not all residues at the PPI interface are important, but rather only a small fraction of the interface residues known as “hot spots” contribute to the majority of the total free energy of binding between proteins.¹³⁻¹⁴ Since then several examples of PPI inhibitors that target “hot spots” have been reported.¹⁵

An established drug-discovery process which allows screening of a large number of drug-like compounds for a specific biological target is high-throughput screening (HTS). Hoffmann-La Roche employed HTS to discover a series of small molecule inhibitors (Nutlins) of the p53/MDM2 interaction.¹⁶ They found that (-)-Nutlin-3 (Figure 2) was the most potent derivative which has progressed to clinical trials. HTS has also led to the discovery of another PPI inhibitor Maraviroc (Selzentry), which is a commercial drug and functions as a CCR5 receptor antagonist for the treatment of HIV infection (Figure 2).¹⁷

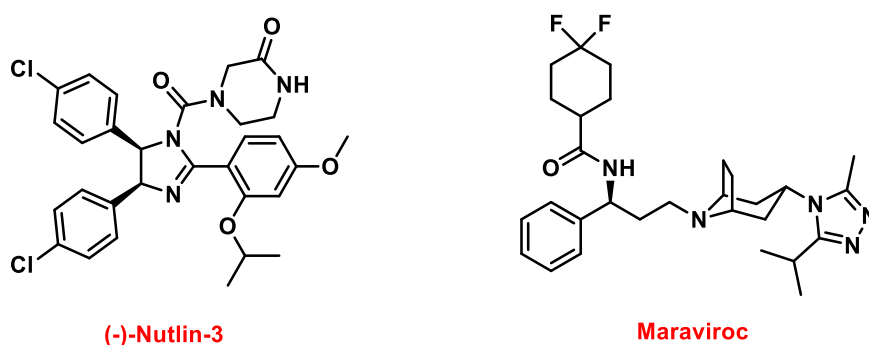


Figure 2: Small molecule PPI inhibitors.

However, many HTS libraries consists of structurally similar compounds biased towards traditional drug targets and thereby do not show hits for PPIs. To address this issue, new combinatorial approaches were developed. These are fragment-based screening (FBS) and diversity-oriented synthesis (DOS)¹⁸. FBS involves screening of small chemical fragments and identifying those that can bind weakly to the biological target, and then building upon them or combining them to produce a lead compound possessing higher affinity for the target. On the other hand, DOS involves the efficient simultaneous synthesis of a whole library of chemical compounds that are structurally different from each other, thus occupying a larger region of chemical space (Figure 3).¹⁹⁻²⁰

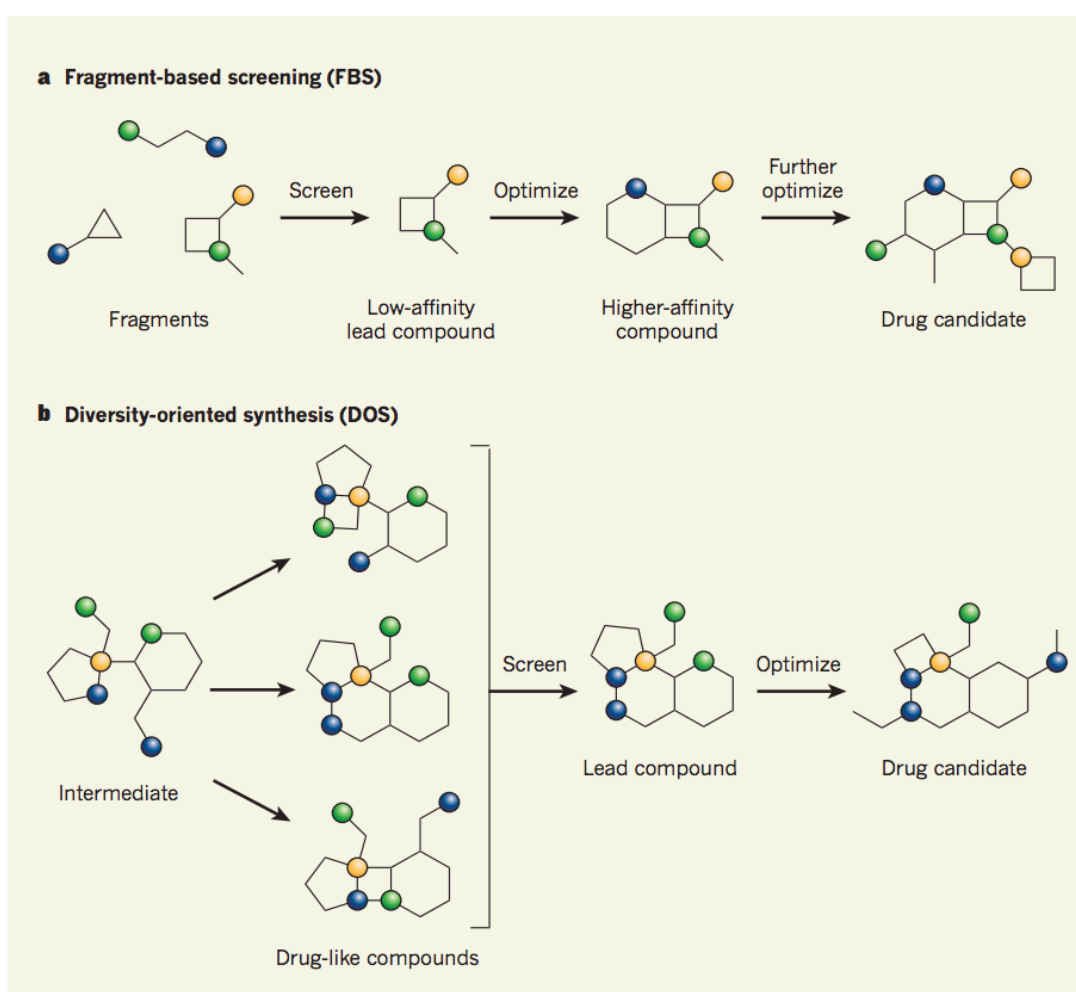


Figure 3: a) Fragment-based approach; b) Diversity-oriented approach¹⁸ (from Hajduk *et al.*¹⁸).

1.2.2 Biologics

Another established class of inhibitors for targeting PPIs is biologics which are typically protein-based drugs, such as monoclonal antibodies, that are derived from biological sources. They all have a high-molecular weight which allows them to bind targets with greater specificity and affinity by allowing contacts with the protein surface over a larger area.²¹

However, the large size of biologics renders them unsuitable for binding intracellular targets due to poor membrane permeability. Despite this drawback, a number of therapeutic antibodies which target PPIs are now commercially available. For instance, Herceptin, a humanised monoclonal antibody has been developed which helps treat breast cancer (Figure 4).²²⁻²³

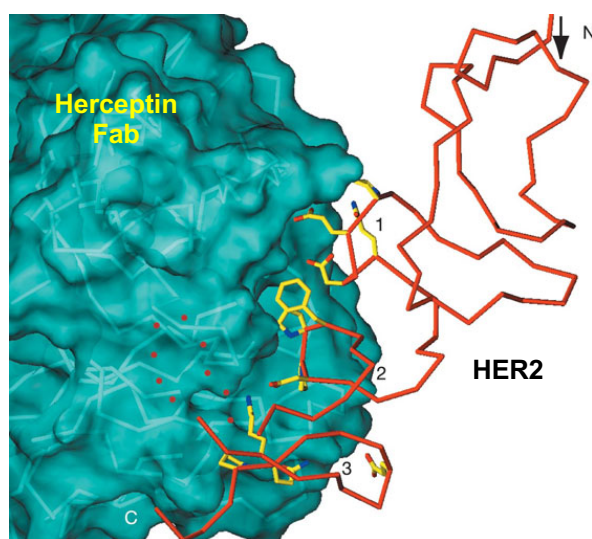


Figure 4: Crystal structure showing the binding of Herceptin Fab with the extracellular region of HER2 (human epidermal growth factor receptor 2) (from Cho *et al.*²³).

1.2.3 Peptidomimetics

Peptidomimetics are small molecules designed to mimic the three-dimensional structure of peptides. They have the ability to interact with biological targets in the same way as the natural peptide or protein from which their structure was derived.²⁴⁻²⁶ A range of peptidomimetics have been developed, including cyclic peptides, beta-peptides and non-peptide based mimetics.^{2, 6} For example, Hamilton *et al.* have inhibited the BCL-X_L/BAK interaction using a non-peptide based alpha-helix mimetic having a terphenyl backbone (Figure 5).²⁷⁻²⁹ Moreover, Schepartz and coworkers have employed the use of helical beta-peptides for inhibiting p53/MDM2 interaction (Figure 5).³⁰⁻³¹

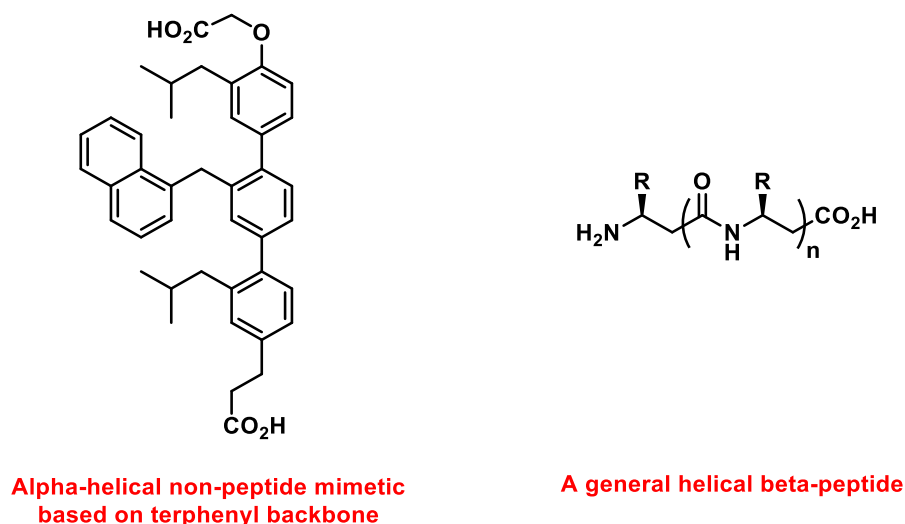


Figure 5: Non-peptide based and helical beta-peptide mimetics²⁷.

1.3 Stapled peptides as alpha helix mimetics

Alpha-helices are the most common secondary structure in proteins.³² An alpha-helix is a right-handed coiled conformation consisting of 3.6 amino acid residues per turn with a distance of 1.5 Å between consecutive turns along the helical axis. It consists of a H-bond between the N-H group of an amino acid and the C=O group of the amino acid four residues earlier ($i+4 \rightarrow i$), thereby stabilising the alpha-helix.³³⁻³⁵

Synthetic mimics of alpha-helices hold great potential as they play an important role in many PPIs.³⁶⁻³⁷ Despite the stabilising factors, in isolation short peptides usually do not retain their native alpha-helical conformation and binding properties due to the lack of structural enforcement provided by the rest of the protein. Also, peptides are unstable in living organisms due to proteolytic degradation, and generally cannot penetrate the cell membrane. Due to these reasons, currently research is being carried out to develop new synthetic methods for constraining peptides into their native conformation, thereby improving their stability, cell permeability and biological activity towards protein targets.

Peptide stapling is a strategy to constrain short linear peptides into alpha-helical conformation by covalently linking two amino acid side-chains through synthetic transformations.³⁸ For the stapling process, two amino acids which lie on the same face of the linear peptide chain are chosen. Typically these are amino acid residues with $i, i+4$; $i, i+7$; or $i, i+11$ spacing on the peptide chain as these lie approximately on the same face of an alpha-helix (Figure 6).

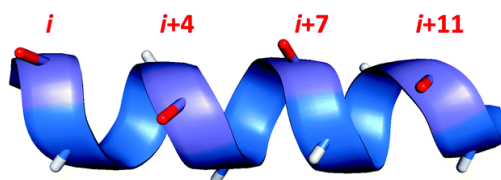


Figure 6: Amino acid residues on the same face of an alpha helix are depicted in red (from Spring *et al.*³⁸).

These two residues are then substituted with two unnatural amino acids having side-chains which can be joined together covalently or ‘stapled’. Depending upon the length of the two side-chains and position of the non-native amino acids, this process can constrain the peptide into an alpha-helical conformation. Since its introduction a number of peptide stapling techniques have been developed utilising different types of chemistry.

1.4 Peptide stapling techniques

These can be broadly classified as one- and two-component stapling.

1.4.1 One-component peptide-stapling

One-component stapling involves direct bond formation between the side-chains of the two unnatural amino acids (Figure 7).³⁸ Thus a variation in either length of covalent staple or its position would require the synthesis of a new linear peptide.

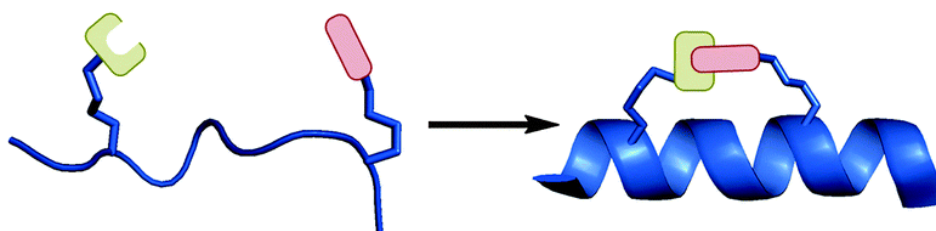


Figure 7: One-component stapling (from Spring *et al.*³⁸).

The following section describes some of the different one-component approaches reported in the literature.

1.4.1.1 Hydrocarbon stapling

Hydrocarbon stapling is one of the most well-studied and successful techniques for peptide stapling to date. Grubbs and Blackwell reported the first attempts to use ring-closing metathesis (RCM) for cross-linking two *O*-allylserine side chains on a peptide.³⁹ Following this work, Verdine *et al.* synthesised the first all-hydrocarbon stapled alpha-helical peptide.⁴⁰

This was achieved by cross-linking two unnatural α,α -disubstituted amino acids bearing olefinic side chains by using RCM (Figure 8).⁴¹

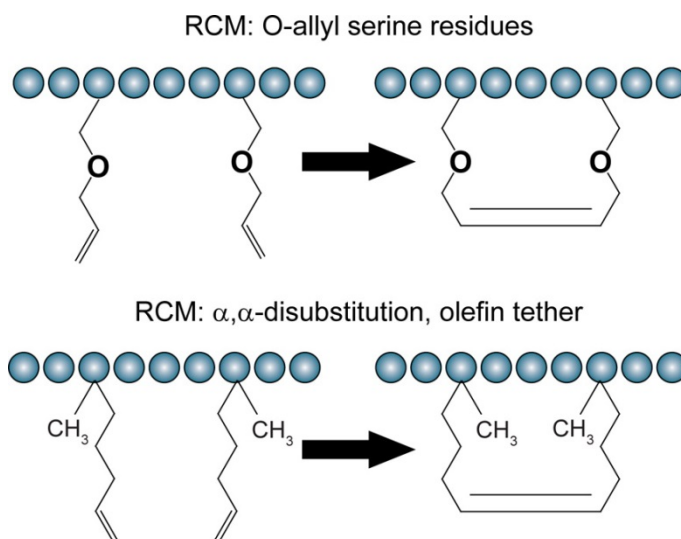
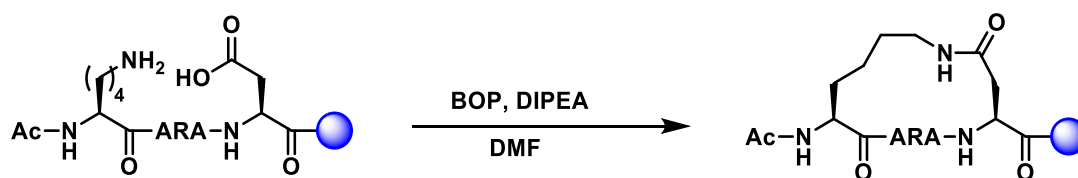


Figure 8: Hydrocarbon stapling (from Walensky *et al.*⁴¹).

Verdine, Walensky and coworkers have successfully applied this technique to target a range of PPIs. For example, they have developed BID BH₃ stapled peptides which showed increased helicity and *in vivo* stability, and were able to bind proteins of the BCL-2 family with greater affinity than the wild type peptide.⁴¹ Overexpression of the anti-apoptotic members of the BCL-2 family protein (involved in regulation of apoptotic cell death) such as MCL-1 causes cancer that is often intractable and chemoresistant.⁴²

1.4.1.2 Lactamisation

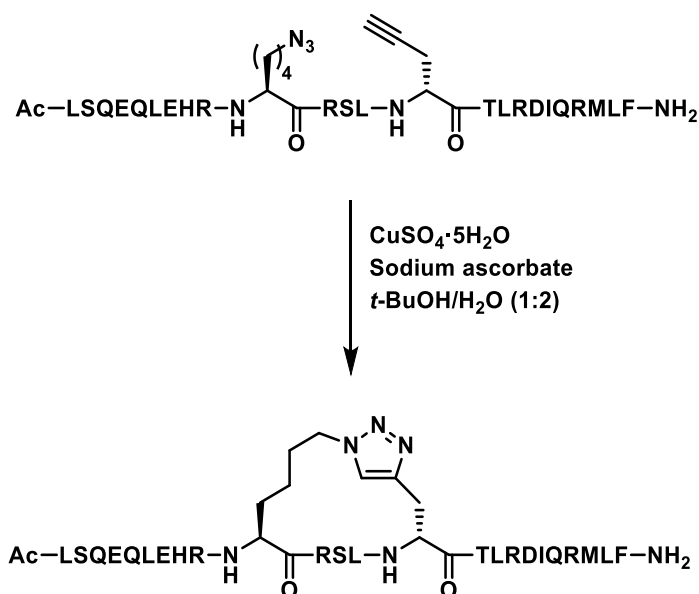
Another technique developed for stapling peptides is utilising a lactam formation reaction for cross-linking amino-acid side chains. At first Felix *et al.* investigated the possibility of using this process in shortened analogues of growth hormone releasing factor by coupling the side chains of Lys and Asp residues.⁴³ They were successful in preserving helicity and bioactivity of growth hormone after lactamisation process. Since then a number of examples have been reported for developing lactam-stapled peptides.⁴⁴ Recently Fairlie *et al.* have utilised this approach to create the shortest lactam-stapled peptides which are alpha-helical in water (Scheme 1) and have also applied this technique to a number of biologically important targets.⁴⁵⁻⁴⁷



Scheme 1: Peptide stapling using lactamisation by Fairlie *et al.*⁴⁵

1.4.1.3 Cycloadditions

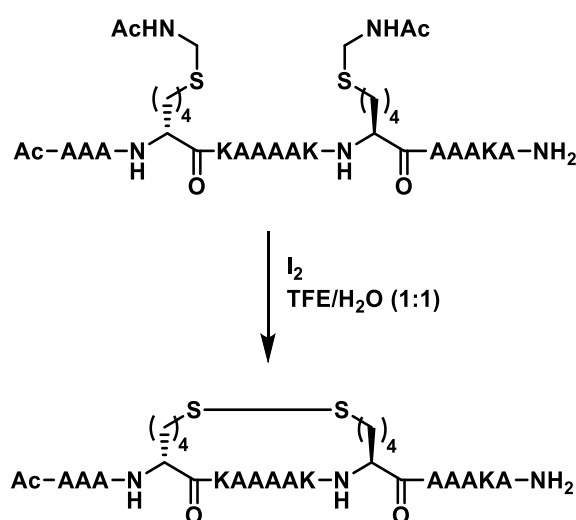
D'Ursi *et al.* utilised the Cu(I)-catalysed azide-alkyne cycloaddition (CuAAC) 'click' reaction discovered by Sharpless⁴⁸ and Meldal⁴⁹ in 2002, to develop a new peptide stapling technique. The idea was to have two unnatural amino acid side-chains bearing terminal alkyne and azide groups on the peptide which can be cross-linked, forming a triazole ring and giving an alpha-helical stapled peptide.⁵⁰ Wang *et al.* have applied this technique for inhibiting oncogenic BCL9/ β -catenin PPI.⁵¹ They carried out optimisation on their Cu(I) click peptide stapling process by screening different linker lengths, position of triazole ring on the staple loop, and spacing between the unnatural amino acids on the peptide. The stapled peptide obtained from the optimised stapling process showed an increased *in vitro* binding affinity along with increased proteolytic stability in cell media (Scheme 2).



Scheme 2: Optimised CuAAC stapling of BCL9 peptides by Wang *et al.*⁵¹

1.4.1.4 Disulphide linking

Schultz *et al.* have developed an *i,i*+7 peptide stapling technique utilising a disulphide formation between two amino acid side chains bearing thiol-group.⁵² Stapled peptides were found to have greatly increased alpha-helicity (Scheme 3). The major disadvantage of this stapling technique is that disulphide linkages are unstable in the reducing environment of the cells, restricting its application for intracellular targets. The research groups of Mieke and Spatola have successfully applied this technique to target nuclear-receptor co-activator interactions.⁵³⁻⁵⁴



Scheme 3: Schultz *et al.* *i,i*+7 disulphide stapling.⁵²

1.4.2 Two-component peptide-stapling

In contrast to the one-component stapling, a two-component stapling makes use of a separate bifunctional linker to staple the two non-native side chains together. This method has the advantage of generating stapled peptides with varying staple lengths starting from a common linear peptide by just varying the bifunctional linker and thereby imparting new properties to the stapled peptide (Figure 9).³⁸

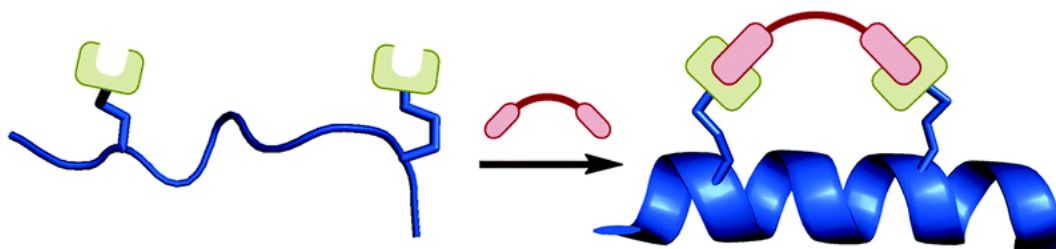


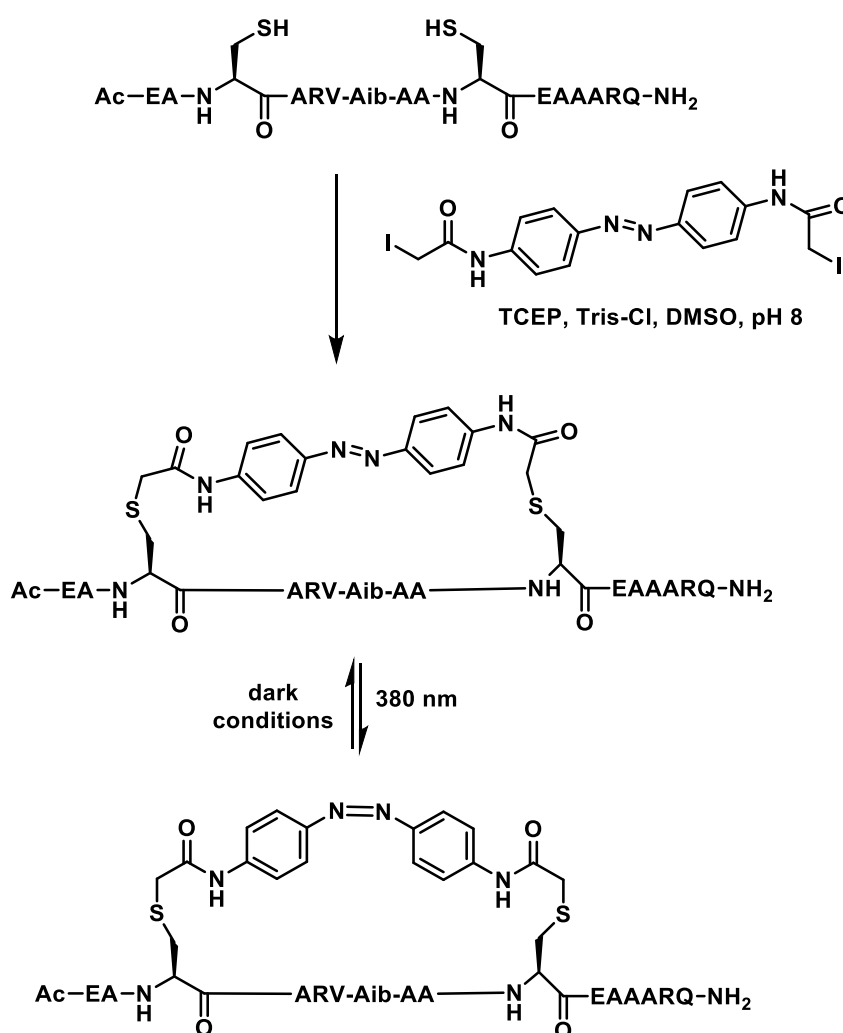
Figure 9: Two-component stapling (from Spring *et al.*³⁸).

A disadvantage of this technique is that more by-products are possible here due to the additional complexity involved in the process.

Two-component stapling methods can be categorised into the following sections on the basis of their functional features.

1.4.2.1 Photoswitchable linkers

Kumita *et al.* made use of an azobenzene-based linker having 2-iodoacetamide groups for attachment to cysteine residues on the peptide to develop the first photoswitchable stapled peptide.⁵⁵ They observed that the model non-helical *trans*-form of the azobenzene stapled peptide could be converted to the helical *cis*-azobenzene stapled peptide under irradiation at 380 nm for 5 minutes. This process could be reversed simply by leaving the peptide under dark conditions for several hours (Scheme 4).

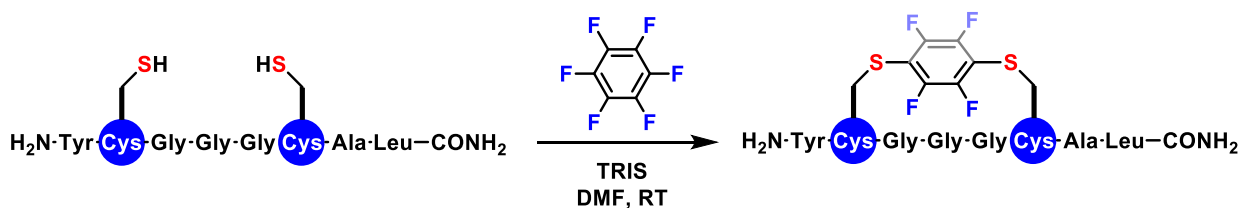


Scheme 4: Photoswitchable linkers for peptide stapling.⁵⁵

This ability of controlling peptide helicity using UV/visible light is useful for studying the effect of conformational changes of peptides in biological systems. Allemann *et al.* have applied this technique to target oncogenic protein BCL-X_L and they found that switching the helicity of the stapled peptide changes its *in vitro* binding properties with the protein BCL-X_L.⁵⁶

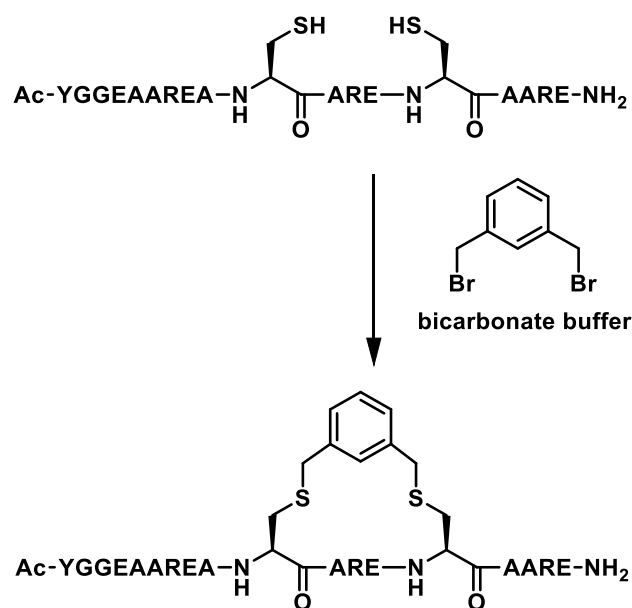
1.4.2.2 Alkylation/arylation on cysteine residues

Penetelute *et al.* have developed a two-component stapling technique by utilising an S_NAr reaction to couple an aryl linker with *i,i*+4 Cys residues on the peptide chain.⁵⁷ Hexafluorobenzene was used as the linker and was linked with the Cys residues on peptide chain in the presence of Tris base and DMF (Scheme 5). This technique was applied to a peptide binder of HIV-1 capsid assembly polyprotein, which resulted in an improvement in helicity, proteolytic stability, *in vitro* binding properties and cellular uptake of the peptide binder.



Scheme 5: Perfluoroaryl-Cysteine S_NAr peptide stapling by Penetelute *et al.*⁵⁷

Jo *et al* reported another similar stapling method.⁵⁸ They used bis-electrophilic linkers in the presence of weak basic conditions to couple with *i,i*+4 Cys residues on the peptide chain through an alkylation step (Scheme 6). This technique has been applied to inhibit the calpastatin/calpain PPI.



Scheme 6: Coupling Cys residues using bis-electrophilic linker by Jo *et al.*⁵⁸

1.5 Previous work in the Spring group

1.5.1 Cu(I)-catalysed double-click peptide stapling

In 2003, Carolyn Bertozzi introduced the term bioorthogonal chemistry to describe reactions that can occur inside of living systems without interfering with native biochemical processes.⁵⁹⁻⁶⁰ One of the most widely used biorthogonal reactions is the Cu(I)-catalysed azide-alkyne cycloaddition also known as a ‘click’ reaction, developed independently by Sharpless⁴⁸ and Meldal⁴⁹ in 2002 (Figure 10). Click reaction refers to the class of reactions where the two reagents would ‘click’ together selectively to deliver the desired product in high yields with minimal by-products.

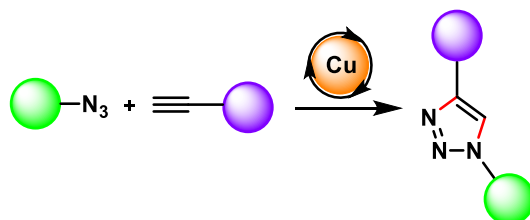
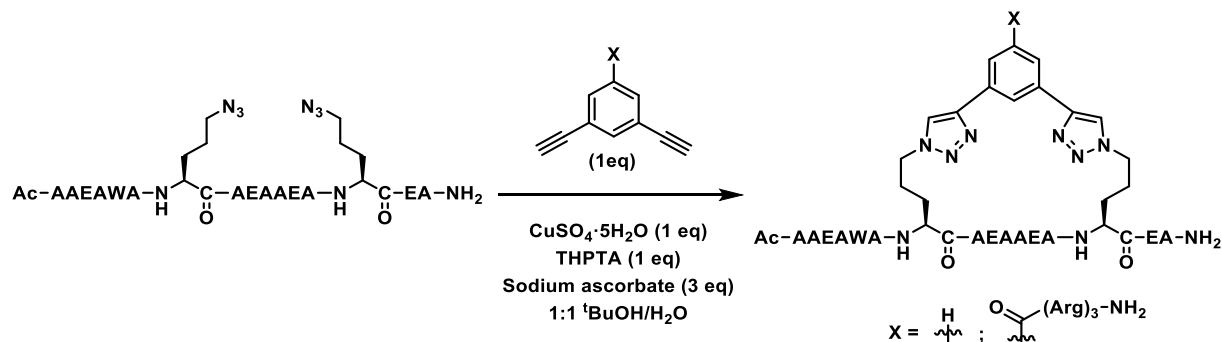


Figure 10: General schematic of the Cu(I)-catalysed click reaction by Sharpless and Meldal.

Utilising this Cu(I)-catalysed click chemistry, a two-component double-click peptide stapling strategy was developed within the Spring group (Scheme 7).⁶¹ Dialkynyl linkers bearing different functional motifs were coupled with unnatural amino acid side-chains bearing azide groups on the peptides, forming triazole rings and hence constraining the peptides into an

alpha-helical conformation. An increased level of helicity was observed for the stapled peptides. This method has the advantage of being highly chemoselective and functional group tolerant, thus minimising the possibility of side reactions due to other functional groups on the linker or the peptide.



Scheme 7: Two examples of Cu(I) catalysed double-click peptide stapling that use the same peptide sequence but different linkers.⁶¹

This technique has been successfully applied to target the oncogenic p53/MDM2 PPI (Scheme 7). The stapled peptides were found to have high binding affinity towards MDM2 and increased cell permeability. It was also observed that the introduction of cationic arginine groups on the dialkynyl linker, was crucial for cellular uptake and p53 activation.

1.5.2 Strain-promoted double-click peptide stapling

Despite the widespread utility of Cu(I)-catalysed click chemistry, its use inside living systems is limited due to the cytotoxicity of Cu(I) catalyst involved. A copper-free click reaction was developed by Bertozzi in 2004 which utilises a high-energy strained cyclooctyne molecule to increase the rate of reaction without the need for a catalyst.⁶² As the ring strain of the cyclic molecule drives the click reaction forward, the reaction is also referred to as the strain-promoted azide-alkyne cycloaddition (SPAAC) (Figure 11a).⁶²

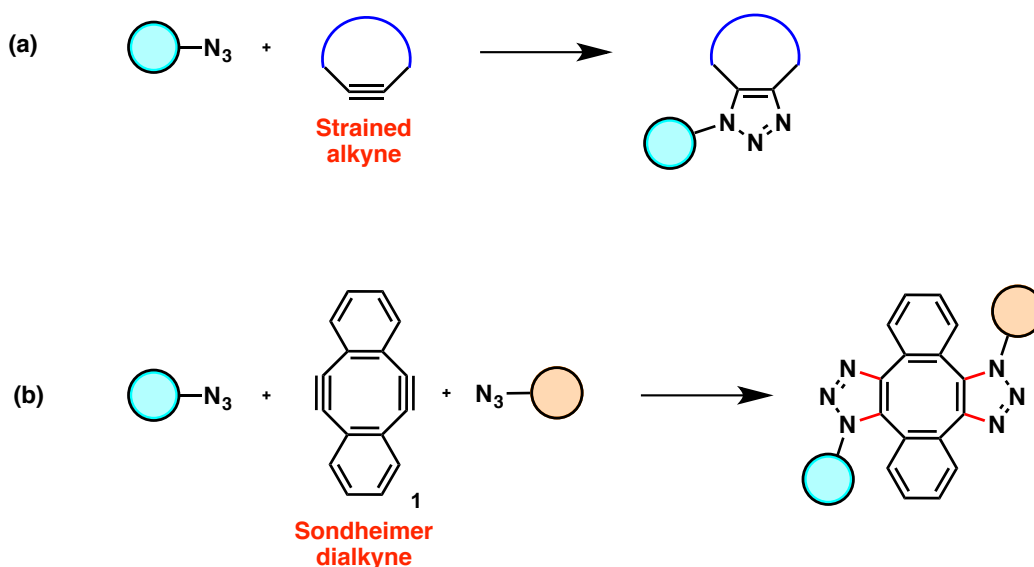
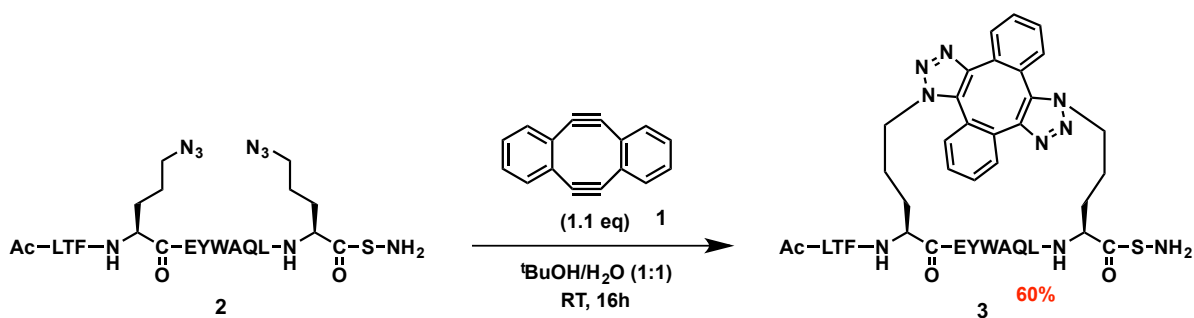


Figure 11: a) General schematic: Strain-promoted azide-alkyne cycloaddition (SPAAC).⁶²
b) Double SPAAC or strain-promoted double-click reaction.

Utilising this strain-promoted click chemistry, a strain-promoted double-click stapling methodology was developed within the Spring group (Figure 11b). A double strained Sondheimer dialkyne⁶³⁻⁶⁴ reagent **1** was employed to undergo metal-free double-click stapling of a p53-based peptide **2** (Scheme 8).⁶⁵ The stapled peptide **3** was found to be a potent helical inhibitor of the p53-MDM2 interaction.



Scheme 8: Strain-promoted double-click peptide stapling.

1.6 Project aim and thesis overview

At the point of initiation of this Ph.D. research project, three main limitations of the Spring group's metal-free double-click stapling methodology were identified:

- The poor water solubility of Sondheimer dialkyne **1**, which leads to its precipitation during stapling.

- ii) The instability of Sondheimer dialkyne **1** in aqueous solutions. Compound **1** decompose rapidly in aqueous solutions ($\tau_{1/2} \sim 10$ min at pH = 7.4), which limits its applications in biological systems.⁶⁶ Moreover, even when it is kept in the neat form at room temperature it decomposes completely within 2 days.⁶⁶
- iii) The lack of functional groups on Sondheimer dialkyne **1** to which other motifs could be attached, which limits the potential to fully exploit the two-component stapling methodology. It was envisaged that the use of substituted Sondheimer dialkynes for stapling would allow for the facile introduction of added functionalities into staple peptides, which could impart novel physical properties and modify biological activity.

Chapter 2 describes the development of substituted variants of Sondheimer dialkyne **1** in an attempt to achieve water-soluble, stable and azide-reactive strained dialkyne reagents for biocompatible strain-promoted click chemistry. In general, highly azide-reactive strained alkyne reagents are desirable, as they allow probing of fast biological processes and enable reactions in biological systems at lower reagent concentrations.

Chapter 3 describes the use of these substituted Sondheimer dialkynes synthesised in metal-free double-click stapling to generate functionalised p53-based stapled peptides for inhibiting the p53-MDM2 PPI (Figure 12). Structural evidence obtained through X-ray crystallography for the binding mode of a functionalised stapled peptide with MDM2 is also presented.

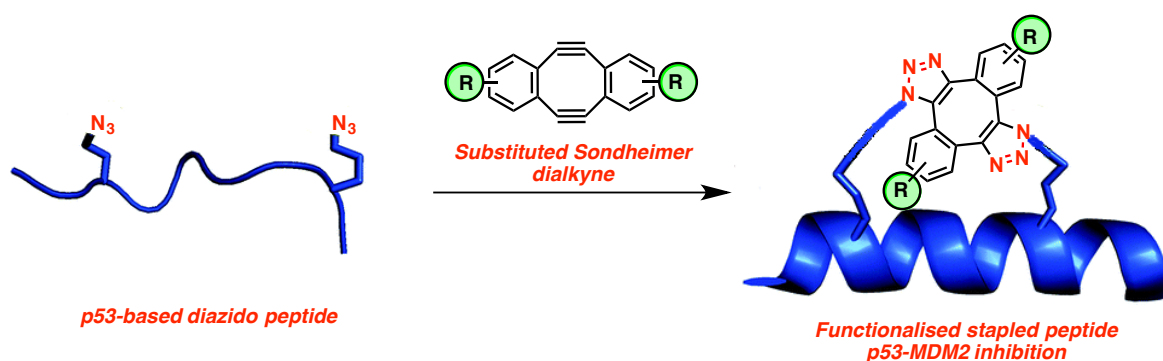


Figure 12: Application of substituted Sondheimer dialkynes in the generation of functionalised stapled peptides for p53-MDM2 inhibition.

In Chapter 4, a detailed kinetic analysis of all substituted Sondheimer dialkynes synthesised is presented. Chapter 5 describes a computational study designed to elucidate the experimentally observed contrast in the reactivity of differentially substituted Sondheimer dialkynes.

2. Synthesis of substituted Sondheimer dialkynes

It was envisaged that the presence of substituents on the aromatic rings of Sondheimer diyne could result in the modification of its water-solubility, water-stability and SPAAC reactivity. Moreover, we conceived that the position and nature (electron donating/withdrawing) of these substituents would also influence the SPAAC reactivity. Previous studies have demonstrated that the water-solubility⁶⁷, stability⁶⁸⁻⁷¹ and SPAAC reactivity^{67-69, 71-74} of cyclooctyne based reagents can all be changed through the introduction of substituents. For instance, the introduction of fluorine atoms at the propargylic position of cyclooctyne (difluorinated cyclooctyne DIFO) was found to increase the SPAAC reactivity relative to the unsubstituted parent compound (Figure 13).^{69, 72} Furthermore, introduction of sp²-like centres into the cyclooctyne ring (dibenzoazacyclooctyne DIBAC, dimethoxyazacyclooctyne DIMAC, biarylazacyclooctyne BARAC) has also been shown to increase the SPAAC reactivity relative to the unsubstituted parent cyclooctyne (Figure 13).^{67, 71, 73} Boons *et al.* demonstrated that an increase in the stability and reactivity of cyclooctyne can be achieved by the introduction of fused aryl rings on cyclooctyne (dibenzocyclooctyne DIBO).^{68, 74} The methoxy-functionalised compound DIMAC demonstrated superior water-solubility compared to cyclooctyne.⁶⁷

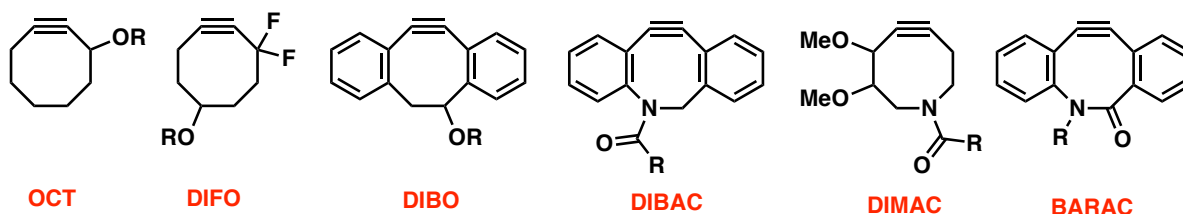


Figure 13: Modified strained cyclooctyne reagents utilized for SPAAC.⁷⁵

Hence, we planned to prepare a series of substituted variants (**4-17**) of Sondheimer diyne **1** and examine their water-solubility and SPAAC reactivity (Figure 14). Octanol-water partition coefficient values (clogP) for substituted diynes **4-17** were predicted using ACD/Labs software (I-Lab 2.0) and are indicated below in Figure 14.

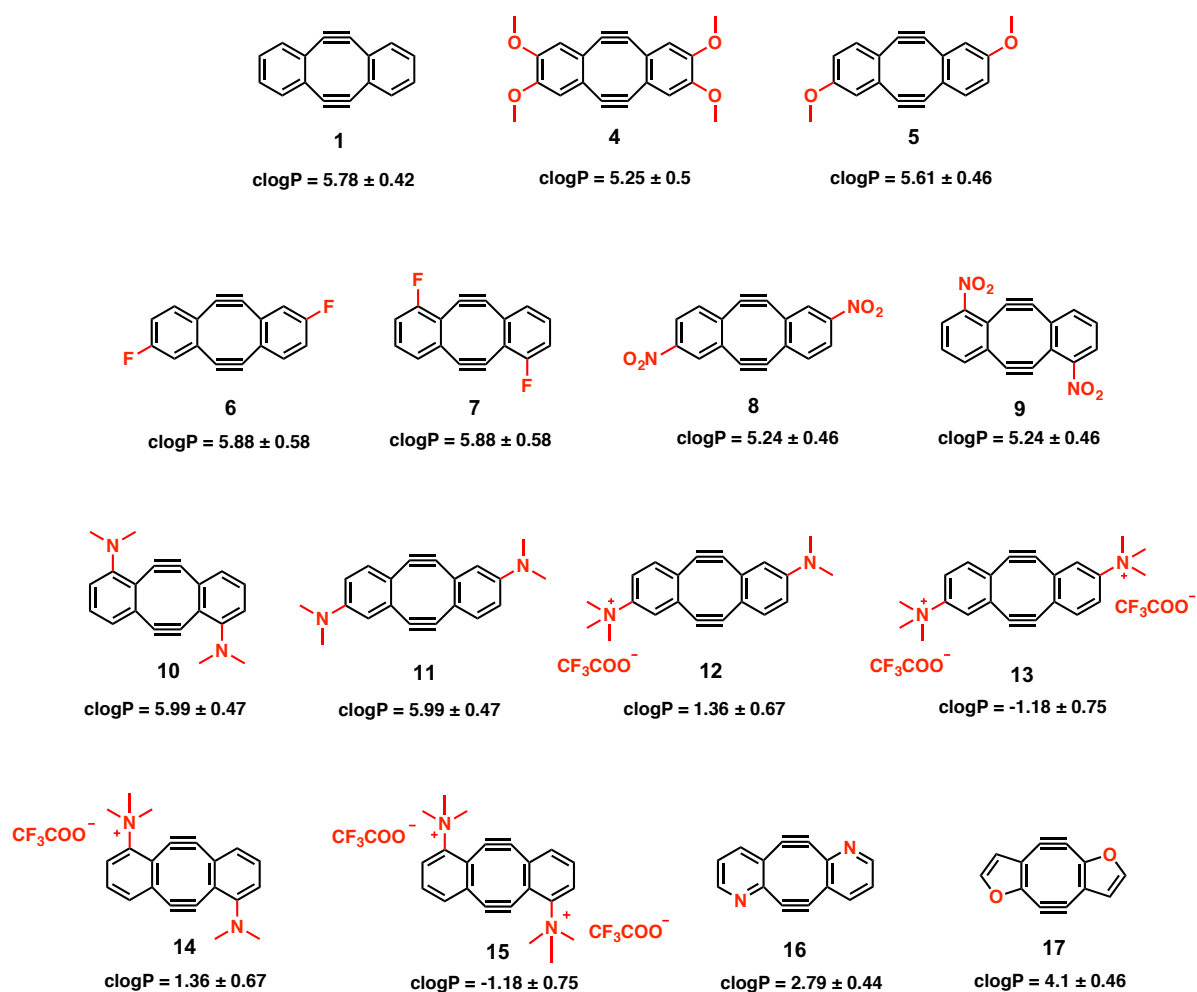
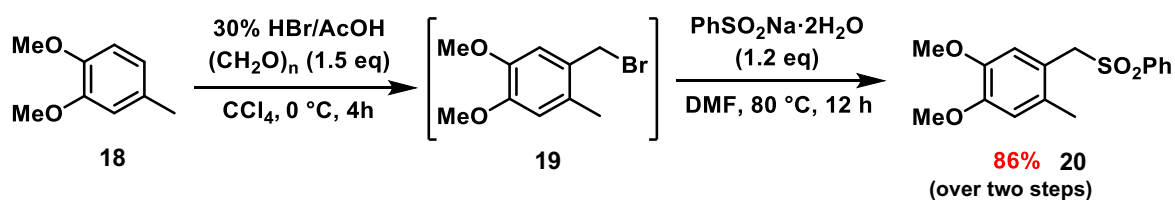


Figure 14: Substituted variants of Sondheimer dialkyne that we planned to prepare.

Orita *et al.* had previously reported the generation of **1** and **4** by the route outlined in Scheme 11.^{64, 76} It was envisaged that this route could be adapted to enable access to the target Sondheimer diynes **5-17**.

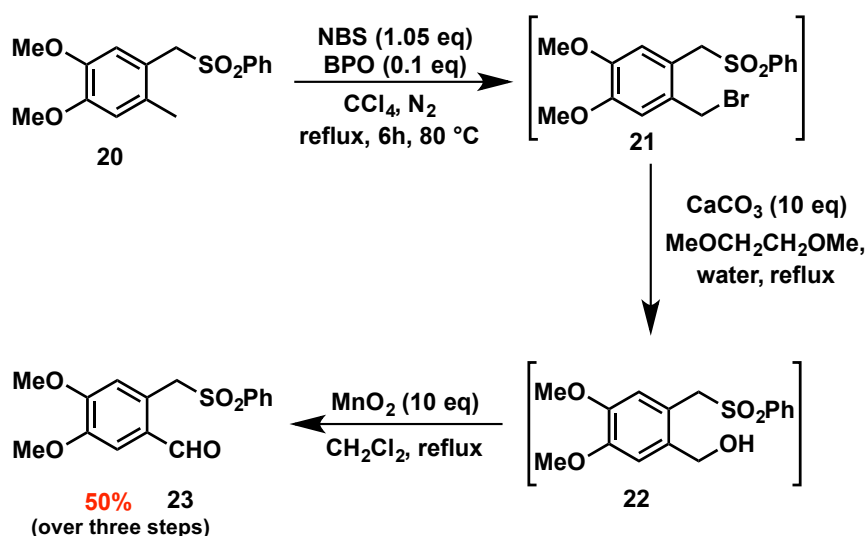
2.1 Synthesis of tetramethoxy substituted Sondheimer dialkyne **4**

The synthesis of 2,3,8,9-tetramethoxy substituted Sondheimer dialkyne **4** was carried out, by following the synthetic route reported by Orita *et al.*⁷⁶ Commercially available 3,4-dimethoxytoluene **18** was treated with paraformaldehyde to give bromomethylated compound **19** and subsequent nucleophilic substitution with benzenesulfinic acid sodium salt afforded dimethoxy-substituted sulfone **20** in a good yield over the two steps (Scheme 9).



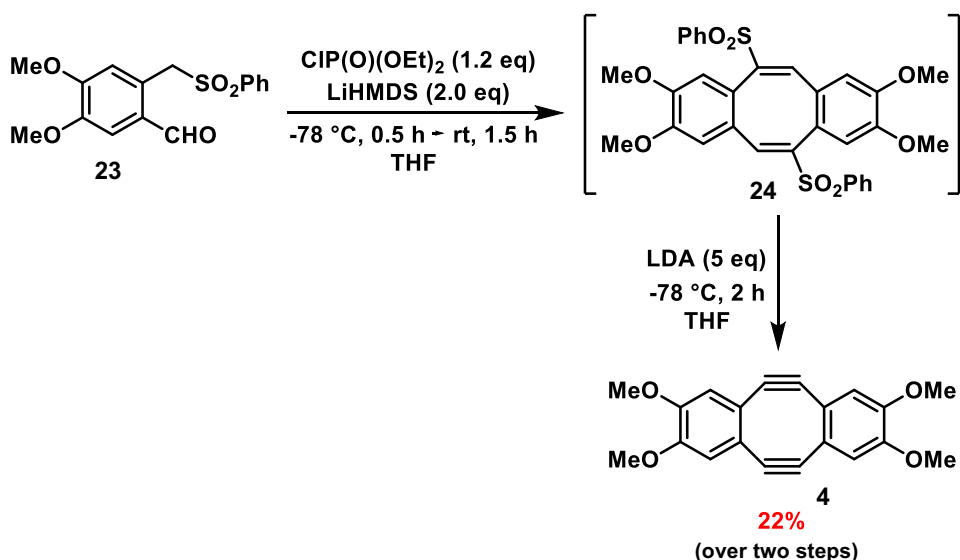
Scheme 9: Synthesis of dimethoxy-substituted sulfone.

Sulfone **20** was then subjected to Wohl-Ziegler bromination followed by nucleophilic hydroxylation to give hydroxybenzyl sulfone **22**. This hydroxyl-substituted sulfone **22** was then converted to the corresponding aldehyde **23** by oxidation with MnO_2 (Scheme 10).



Scheme 10: Synthesis of dimethoxysubstituted aldehyde.

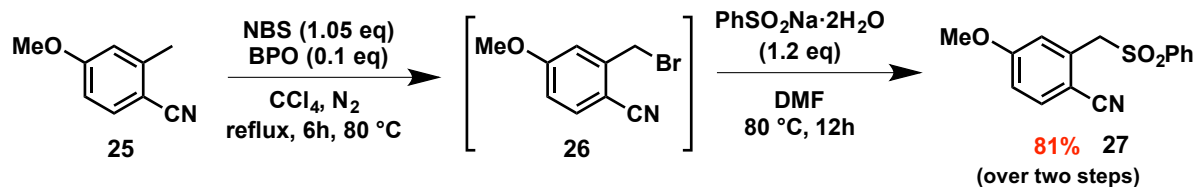
Finally, the conversion of sulfone **23** to the target Sondheimer diyne derivative **4** using Orita's one-pot double elimination protocol was attempted.⁶⁴ Thus sulfone **23** was subjected to Wittig-Horner conditions in the presence of LiHMDS and diethyl chlorophosphate to form the cyclized intermediate **24**. This was then treated *in situ* with LDA to affect consecutive elimination of the two phenylsulfonyl groups and thus generate the target compound **4** (Scheme 11).



Scheme 11: Synthesis of tetramethoxy substituted Sondheimer diyne.

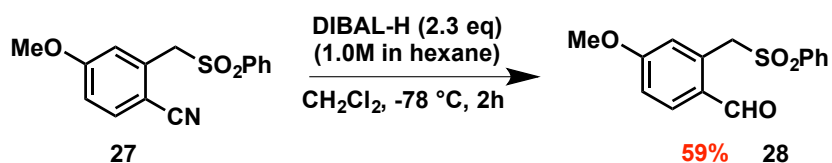
2.2 Synthesis of *meta*-methoxy substituted Sondheimer dialkyne ⁵⁷⁷

The commercially available *meta*-methoxy substituted nitrile arene substrate **25** was subjected to Wohl-Ziegler bromination to give **26**. Subsequent substitution with benzenesulfinic acid sodium salt afforded *meta*-methoxy substituted sulfone nitrile **27** (Scheme 12).



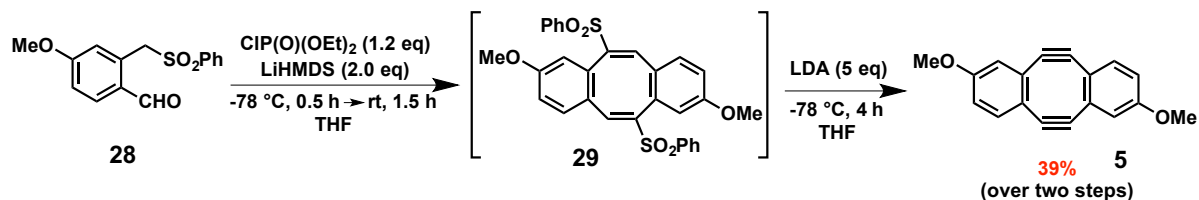
Scheme 12: Synthesis of *meta*-methoxy substituted sulfone nitrile.

Reduction of sulfone nitrile **27** with DIBAL-H gave the corresponding aldehyde **28** (Scheme 13).



Scheme 13: DIBAL-H reduction of *meta*-methoxy substituted sulfone nitrile.

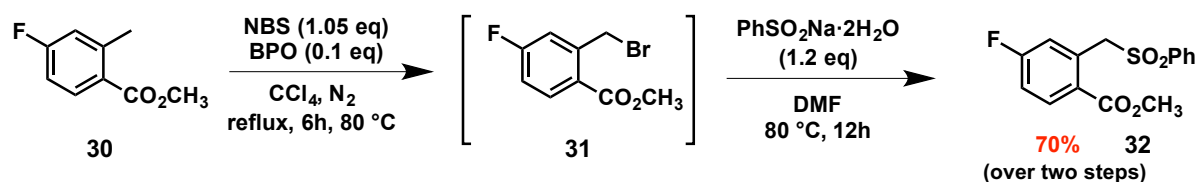
Compound **28** was then subjected to Orita's one-pot double elimination protocol to generate the desired *meta*-methoxy substituted Sondheimer diyne **5** (Scheme 14).



Scheme 14: Synthesis of *meta*-methoxy substituted Sondheimer diyne.

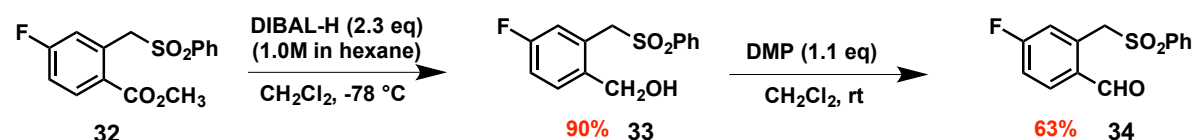
2.3 Synthesis of *meta*-fluoro substituted Sondheimer dialkyne **6**

Wohl-Ziegler bromination of commercially available *meta*-fluoro substituted ester **30** generated **31** and subsequent treatment with benzenesulfinic acid afforded sulfone ester **32** (Scheme 15).



Scheme 15: Synthesis of *meta*-fluoro substituted sulfone ester.

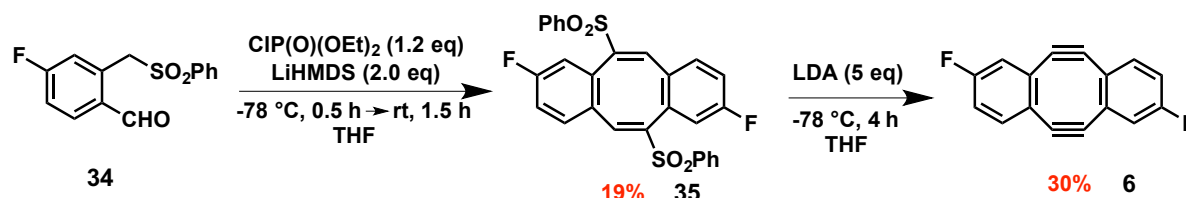
Treatment of the sulfone ester **32** with DIBAL-H led to complete over-reduction of the ester to alcohol **33** (Scheme 16). The desired aldehyde **34** could be readily accessed from **33** by Dess-Martin oxidation (Scheme 16).⁷⁸



Scheme 16: Synthesis of *meta*-fluoro substituted aldehyde.

Having the desired *meta*-fluoro substituted sulfone aldehyde **34** in hand, we attempted its transformation to the cyclic diacetylene **6**. A stepwise synthesis procedure was employed as the use of one-pot double elimination protocol resulted in poor yields of the desired diyne **6**. The substituted sulfone aldehyde **34** was subjected to Wittig-Horner conditions in the presence

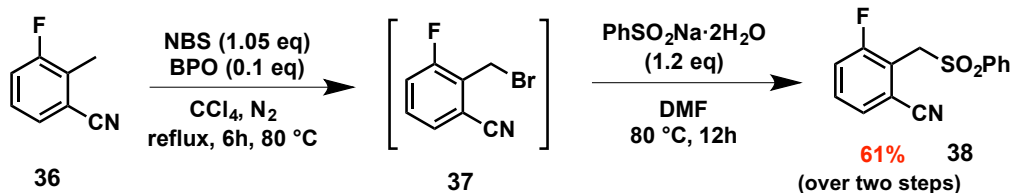
of LiHMDS and diethyl chlorophosphate to form the cyclized intermediate **35** in 19% yield (Scheme 17). The cyclized intermediate **35** was then further treated with LDA to undergo consecutive elimination of the two phenylsulfonyl groups affording the desired *meta*-fluoro substituted Sondheimer diyne **6** in 30% yield (Scheme 17).



Scheme 17: Synthesis of *meta*-fluoro substituted Sondheimer diyne.

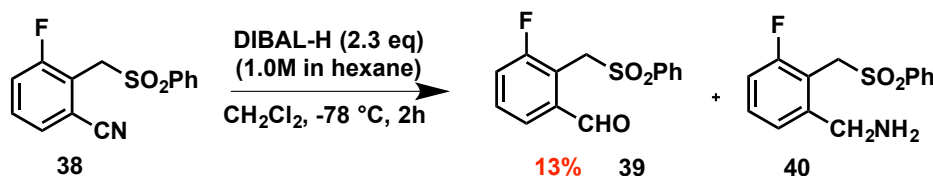
2.4 Synthesis of *ortho*-fluoro substituted Sondheimer dialkyne 7

Compound **38** was generated from commercially available *ortho*-fluoro substituted nitrile arene **36** by Wohl-Ziegler bromination followed by substitution with benzenesulfinic acid sodium salt (Scheme 18).



Scheme 18: Synthesis of *ortho*-fluoro substituted sulfone nitrile.

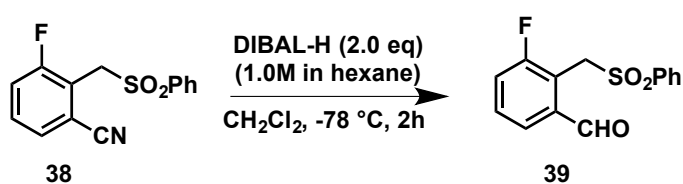
Treatment of **38** with 2.3 equivalents of DIBAL-H for 2h afforded a mixture of the desired aldehyde **39** and amine **40** (by LCMS analysis) due to over-reduction of nitrile (Scheme 19).



Scheme 19: DIBAL-H reduction of *ortho*-fluoro substituted sulfone nitrile.

In an attempt to improve the yield of the aldehyde **39** a reduced reaction time of 20 min was investigated. This did not show any change in the reaction conversion and again resulted in a

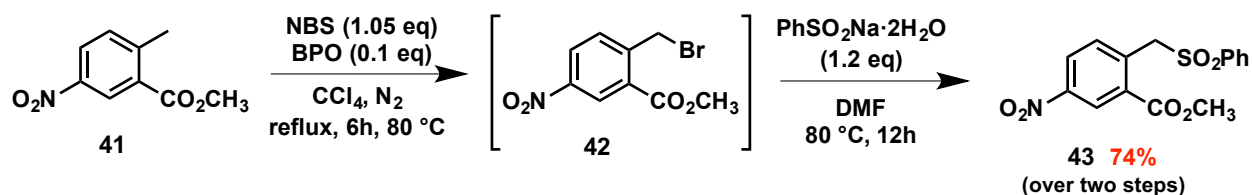
mixture of aldehyde **39** and amine **40**. Furthermore, two-fold dilution of the reaction mixture also did not have any effect on the reaction conversion.



This mixture was subjected to Wittig-Horner conditions in the presence of LiHMDS and diethyl chlorophosphate to form the cyclized intermediate **40** (Scheme **21**). The cyclized intermediate **40** was then further treated with LDA to afford the desired *ortho*-fluoro substituted Sondheimer diyne **7** (Scheme **21**).

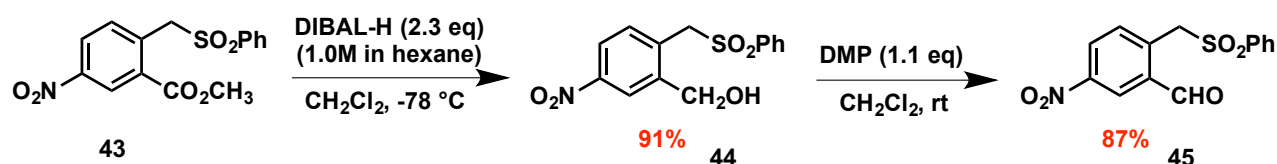
Scheme 21: Synthesis of *ortho*-fluoro substituted Sondheimer diyne.

Nitro-substituted Sondheimer dialkyne **8** was targeted as it was thought that the nitro group could later be reduced to an amine for improved water-solubility and for the purpose of functionalisation of the stapled peptide.

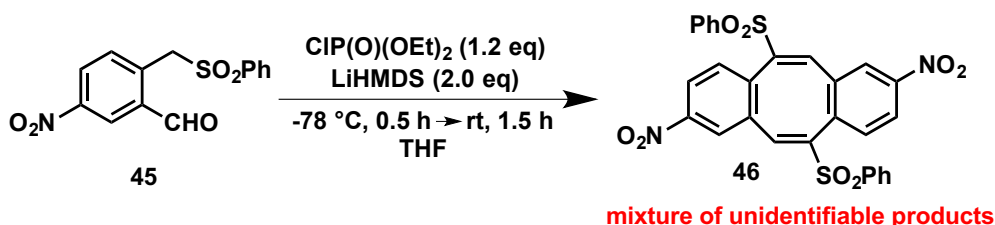


Scheme 22: Synthesis of *meta*-nitro substituted sulfone ester.

Reduction of the ester **43** with 2.3 eq. DIBAL-H afforded the corresponding alcohol **44** in 91% yield. Subsequent Dess-Martin oxidation delivered the desired aldehyde **45** in a good yield (Scheme 23).⁷⁸ Unfortunately, the attempted conversion of **45** to **46** through the use of Wittig-Horner conditions resulted in a complex intractable mixture of unidentifiable products, as determined by LCMS and ¹H NMR analysis of the crude reaction material obtained after work-up (Scheme 24).



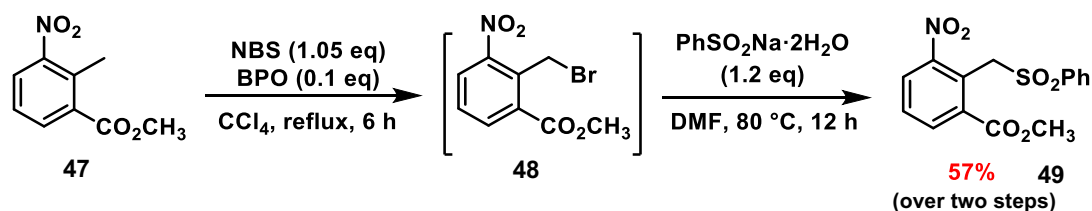
Scheme 23: Synthesis of *meta*-nitro substituted aldehyde.



Scheme 24: Subjecting *meta*-nitro substituted aldehyde to Wittig-Horner conditions.

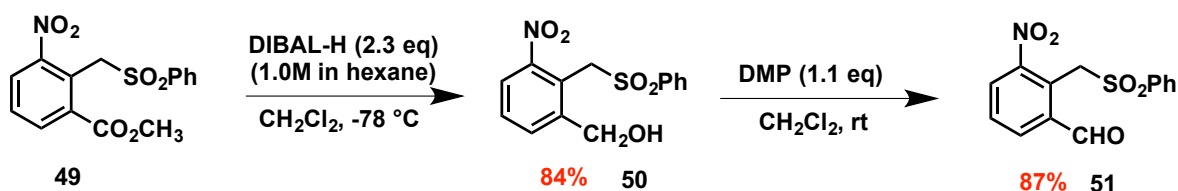
2.6 Synthesis of *ortho*-nitro substituted Sondheimer dialkyne **9**

ortho-Nitro substituted sulfone ester **49** was accessed from **47** by the standard two-step sequence of Wohl-Ziegler bromination followed by nucleophilic substitution with benzenesulfinic acid sodium salt (Scheme 25).

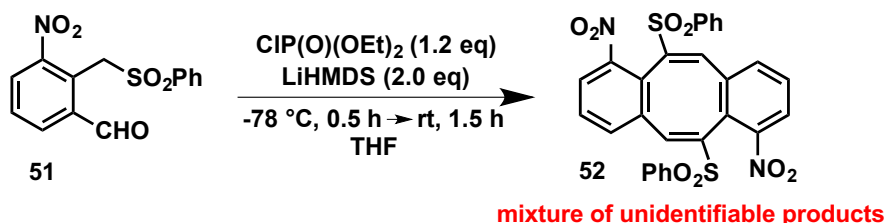


Scheme 25: Synthesis of *ortho*-nitro substituted sulfone ester.

Complete reduction of **49** to alcohol **50** was followed by Dess-Martin oxidation to afford aldehyde **51** (Scheme 26).⁷⁸ Unfortunately, the attempted conversion of **51** to **52** through the use of Wittig-Horner conditions resulted in a complex intractable mixture of unidentifiable products by LCMS and ¹H NMR analysis (Scheme 27), as was also observed in the attempted conversion of *meta*-nitro substituted aldehyde **45** to the corresponding cyclooctene **46** (Scheme 24).



Scheme 26: Synthesis of *ortho*-nitro substituted aldehyde.

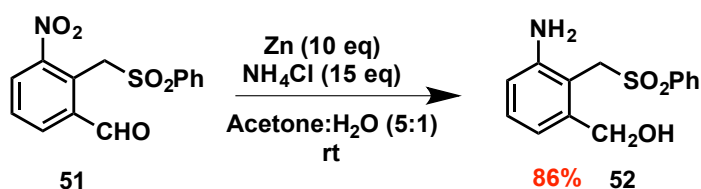


Scheme 27: Subjecting *ortho*-nitro substituted aldehyde to Wittig-Horner conditions.

We believe that the presence of a strong electron-withdrawing nitro substituent renders the substrates **45** and **51** highly reactive and unstable to Wittig-Horner conditions.

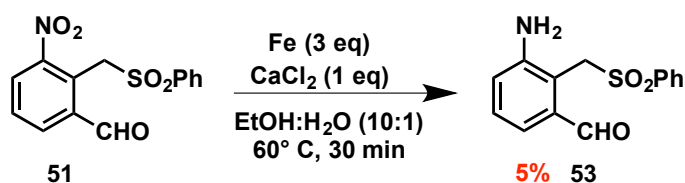
2.7 Synthesis of *ortho*-dimethylamine substituted Sondheimer dialkyne **10**

The synthesis of *ortho*-dimethylamine substituted dialkyne **10** from *ortho*-nitro substituted aldehyde **51** was next investigated. Subjection of **51** to Zn/NH₄Cl reduction conditions.⁷⁹ resulted in the reduction of both nitro and aldehyde groups to afford **52** rather than the desired amine aldehyde derivative **53** (Scheme 28).



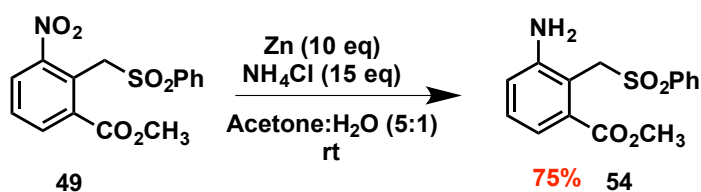
Scheme 28: Zn/NH₄Cl nitro-reduction of *ortho*-nitro substituted aldehyde.

Selective reduction of the nitro group in **51** to form **53** could be achieved⁸⁰ by treatment with iron powder and calcium chloride in ethanol (Scheme 29). However, the isolated yield of **53** was very low, with a large amount of unreacted starting material **51** recovered.



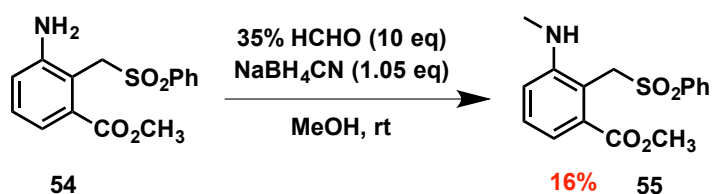
Scheme 29: Fe/CaCl₂ nitro-reduction of *ortho*-nitro substituted aldehyde.

Therefore, an alternative synthesis route was investigated, which started from the *ortho*-nitro substituted ester **49**. Selective reduction of the nitro group of **49** was achieved by application of Zn/NH₄Cl conditions⁷⁹ to afford amine **54** in a good yield (Scheme 30).



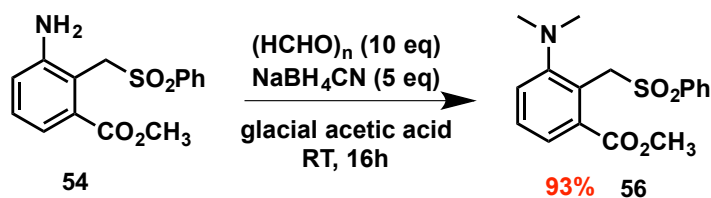
Scheme 30: Zn/NH₄Cl nitro-reduction of *ortho*-nitro substituted ester.

Reductive methylation of **54** was attempted by treatment with aqueous formaldehyde solution and sodium cyanoborohydride in methanol (Scheme 31). However, this resulted in the formation of monomethylated amine **55** and unreacted **54**.⁸¹



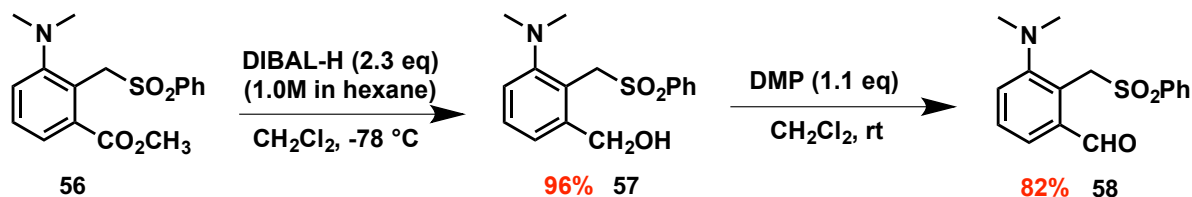
Scheme 31: Reductive methylation of *ortho*-amine substituted ester in methanol.

Reductive methylation of **54** under an alternative set of conditions (paraformaldehyde and sodium cyanoborohydride in glacial acetic acid) pleasingly resulted in the formation of the desired dimethylated amine **56** in an excellent yield (Scheme 32).⁸²



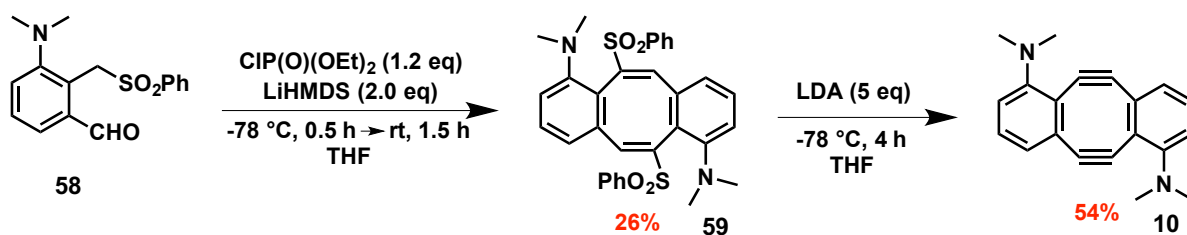
Scheme 32: Reductive methylation of *ortho*-amine substituted ester in glacial acetic acid.

Reduction of the ester in **56** with DIBAL-H afforded the corresponding alcohol **57** and subsequent Dess-Martin oxidation provided the desired aldehyde **58** (Scheme 33).⁷⁸



Scheme 33: Synthesis of *ortho*-dimethylamine substituted aldehyde.

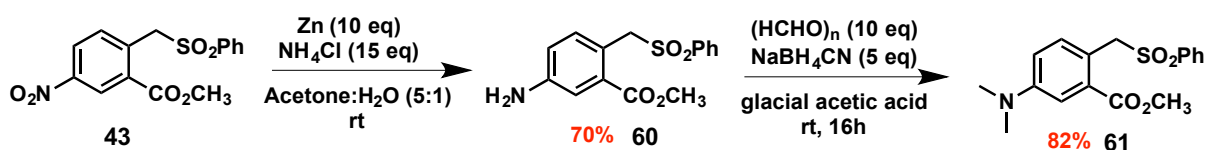
Compound **58** was then successfully converted into the desired *ortho*-dimethylamine substituted Sondheimer diyne **10** using Orita's double elimination protocol, proceeding *via* isolated intermediate **59** (Scheme 34).



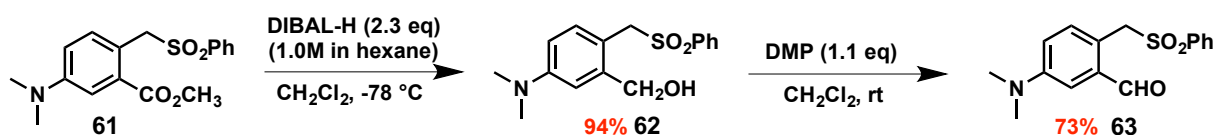
Scheme 34: Synthesis of *ortho*-dimethylamine substituted Sondheimer diyne.

2.8 Synthesis of *meta*-dimethylamine substituted Sondheimer dialkyne 11

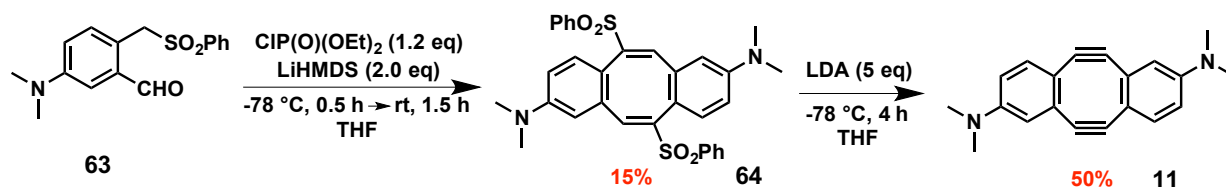
Reduction of nitro-group in *meta*-nitro substituted sulfone ester **43** with Zn/NH₄Cl⁷⁹ afforded amine **60** (Scheme 35). Reductive methylation of amine **60** with paraformaldehyde and sodium cyanoborohydride in glacial acetic acid delivered dimethylated amine **61** (Scheme 35).⁸² Subsequent ester reduction with DIBAL-H afforded alcohol **62** and Dess-Martin oxidation delivered the desired aldehyde **63** (Scheme 36). Compound **63** was then successfully converted into the desired *ortho*-dimethylamine substituted Sondheimer diyne **11** using Orita's double elimination protocol, proceeding *via* isolated intermediate **64** (Scheme 37).



Scheme 35: Reductive methylation of *meta*-amine substituted ester.



Scheme 36: Synthesis of *meta*-dimethylamine substituted aldehyde.

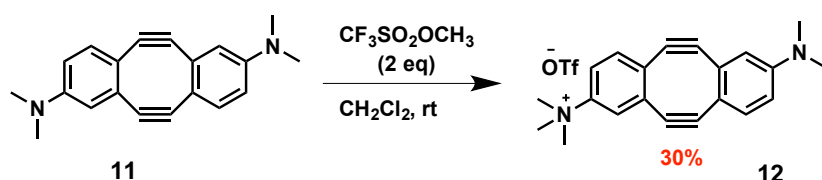


Scheme 37: Synthesis of *meta*-dimethylamine substituted Sondheimer diyne.

2.9 Synthesis of quaternary-ammonium substituted Sondheimer dialkynes 12-15

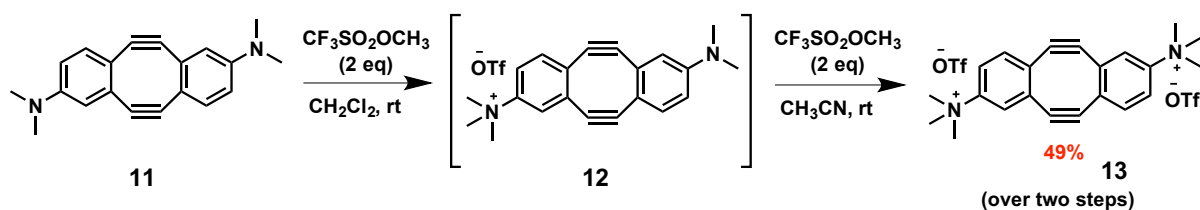
In an attempt to access water-soluble strained dialkyne reagents, we attempted further functionalisation of *meta*- and *ortho*-dimethylamine substituted dialkynes **11** and **10** to synthesise charged quaternary ammonium substituted dialkynes **12-15**.

Due to the unstable nature of the strained dialkynes present in **10** and **11**, mild methylation conditions were desired. Thus, compound **11** was treated with an excess of methyl trifluoromethanesulfonate in dichloromethane at room temperature (Scheme 38).⁸³ This resulted in the formation of mono-methylated quaternary ammonium substituted dialkyne **12** along with trace amounts of di-methylated dialkyne **13**. This reaction showed only partial conversion and unreacted starting dialkyne **11** was recovered. Preparative HPLC purification gave mono-methylated quaternary ammonium substituted dialkyne **12** in 30% yield.



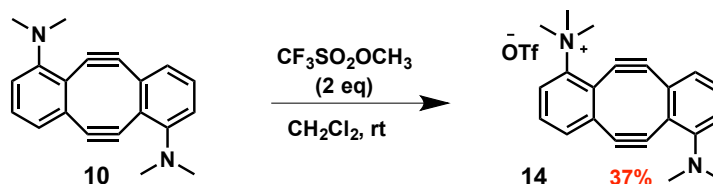
Scheme 38: Synthesis of mono-methylated quaternary ammonium *meta*-substituted diyne.

Further methylation of mono-methylated dialkyne **12** under the same reaction conditions was unsuccessful due to the insolubility of **12** in dichloromethane. This was addressed by a change of solvent; the mono-methylated dialkyne **12** was treated with an excess of methyl trifluoromethanesulfonate in acetonitrile which pleasingly delivered the desired di-methylated quaternary ammonium substituted dialkyne **13** in 49% isolated yield along with unreacted starting material **12** (Scheme 39).

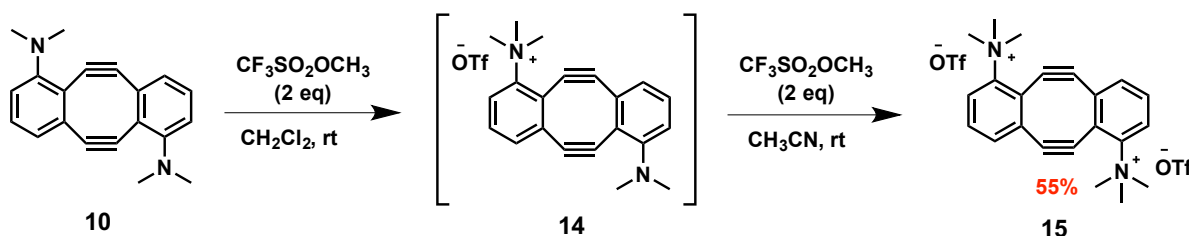


Scheme 39: Synthesis of di-methylated quaternary ammonium *meta*-substituted diyne.

Similarly, methylation of *ortho*-dimethylamine substituted dialkyne **10** to obtain mono-methylated **14** and di-methylated **15** quaternary ammonium substituted dialkynes was achieved (Scheme 40, 41).⁷⁷



Scheme 40: Synthesis of mono-methylated quaternary ammonium *ortho*-substituted diyne.



Scheme 41: Synthesis of di-methylated quaternary ammonium *ortho*-substituted diyne.

2.9.1. Water solubility of quaternary ammonium substituted dialkynes

Gratifyingly, all of the quaternary ammonium substituted dialkynes **12-15** were found to be readily soluble in water as observed by visual inspection.

The water-solubility of quaternary ammonium *meta*-substituted dialkyne **13** was determined experimentally by measuring its octanol-water partition coefficient using shake-flask method.⁸⁴ Similarly, the water solubility of uncharged dimethylamine substituted dialkyne **11** was determined for comparison. These experiments demonstrated quaternary ammonium substituted dialkyne **13** (log P = -1.50) to be more soluble than the uncharged dialkyne **11** (log P = 1.11).

This observed increase in solubility on methylation was consistent with the solubility trend predicted earlier through calculations (Figure 14), which had indicated di-methylated diyne **13** (clogP = -1.18 ± 0.75) to be more water-soluble than mono-methylated diyne **12** (clogP = 1.36 ± 0.67) and its uncharged counterpart **11** (clogP = 5.99 ± 0.47).

2.9.2. Stability of quaternary ammonium substituted dialkynes

The aqueous stability of the two highly water-soluble quaternary ammonium substituted diynes **12** and **13** was next examined. Solutions of dialkynes **12** and **13** (1mM concentration for each) were prepared in 20% MeOH/PBS (pH 7.4). The decomposition of **12** and **13** was monitored by UV spectroscopy by following the decrease in absorbance of **12** and **13** with time at 385 and 372 nm respectively (Figure 15).

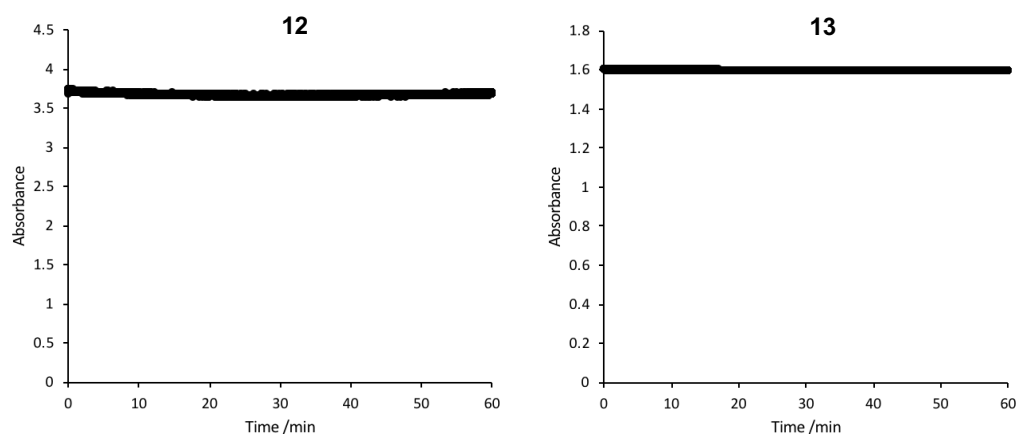


Figure 15. Absorbance of dialkynes **12** (left) and **13** (right) with time in aqueous buffer.

Pleasingly, no decomposition of **12** and **13** was observed after a period of seven days (Figure 16), whereas Sondheimer diyne **1** is known to have a decomposition half lifetime of 10 ± 2 minutes under the same conditions.⁶⁶

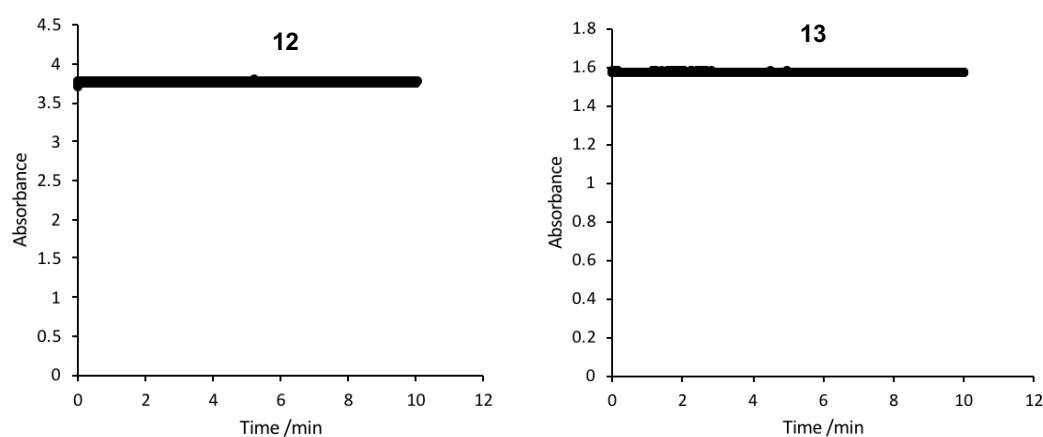


Figure 16. Absorbance of dialkynes **12** (left) and **13** (right) with time in aqueous buffer measured after leaving the sample (1 mM solution in 20% MeOH/PBS) for 7 days at room temperature.

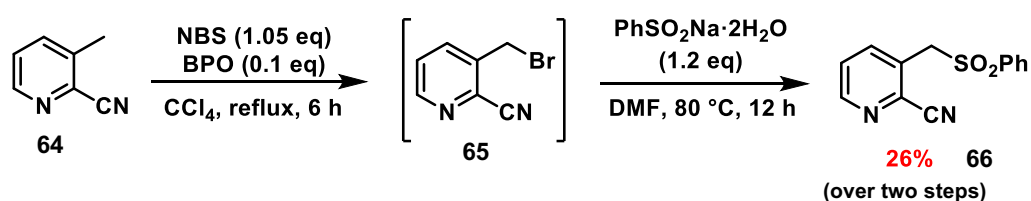
Moreover, a neat sample of **13** at room temperature did not show any decomposition after two weeks, whereas Sondheimer diyne **1** is known to completely decompose within two days.⁶⁶

2.10 Synthesis of heteroaromatic based Sondheimer dialkynes

Next, the synthesis of heteroaromatic pyridine-based **16** and furan-based **17** strained dialkynes was attempted (Figure 14).

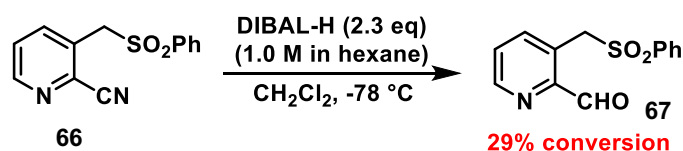
2.10.1. Synthesis of pyridine-based Sondheimer dialkyne **16**

Commercially available 3-methylpicolinonitrile **64** was subjected to Wohl-Ziegler bromination to give 3-(bromomethyl)picolinonitrile **65** which was then further treated with benzenesulfinic acid sodium salt in DMF to afford 3-((phenylsulfonyl)methyl)picolinonitrile **66** (Scheme 42).



Scheme 42: Synthesis of phenylsulfonyl-substituted cyanopyridine.

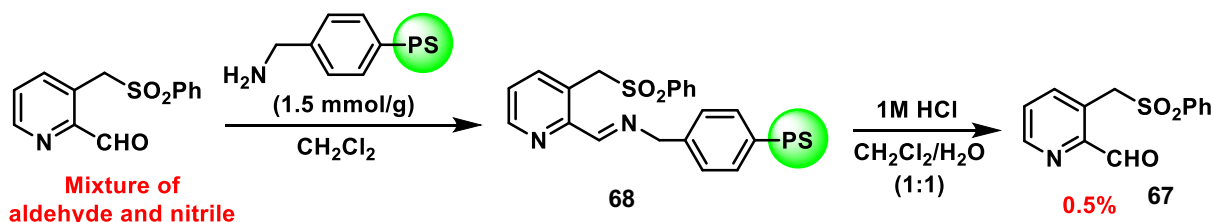
Reduction of the phenylsulfonyl-substituted cyanopyridine **66** was attempted using DIBAL-H under the standard conditions (Scheme 43). The reaction gave the corresponding aldehyde **67**, as a mixture together with the cyano starting material **66** in a ratio of 1:2.5 (**67**:**66**) as determined by ¹H NMR analysis of the crude material obtained after reaction work-up. These two compounds **66** and **67** were found to have very similar R_f values on SiO₂ and it was therefore not possible to separate them *via* flash column chromatography on SiO₂. Any attempts towards optimising the reaction conditions by increasing the temperature or the equivalents of DIBAL-H led to complete over-reduction of cyano group to the corresponding amine. Substitution of solvent to THF also did not show any change in reaction conversion.



Scheme 43: DIBAL-H reduction of substituted cyanopyridine.

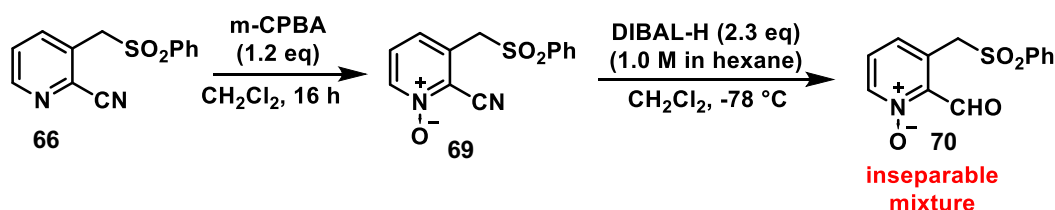
An attempt was made to isolate **67** through the use of a solid-supported scavenger.⁸⁵⁻⁸⁶ The reaction mixture resulting from the application of the reaction conditions shown in Scheme 43 to **66** was treated with benzylamine supported on polystyrene beads. Compound **67** underwent imine formation with the polystyrene-supported benzylamine and the beads were then filtered

to separate them from the mixture. The polystyrene beads were then subjected to imine hydrolysis in the presence of 1M HCl in dichloromethane/water mixture to deliver an analytically pure samples of the desired aldehyde **67**, albeit in trace yield (Scheme 44).



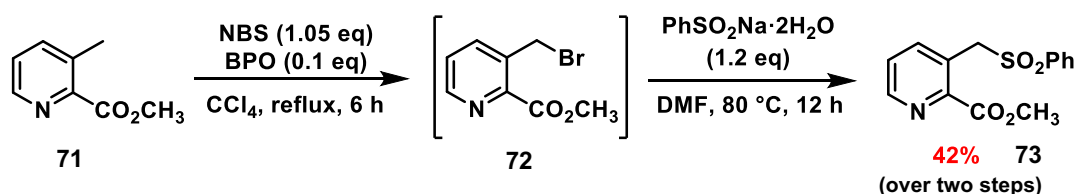
Scheme 44: Separation by solid-supported scavenging.

Since the desired aldehyde **67** could be isolated in only very poor yields using the solid-supported scavenging method, alternative routes towards this compound were investigated. It was hoped that **69**, the pyridine *N*-oxide of **67**, would display modified reactivity with DIBAL-H and thus allow more facile access to the corresponding aldehyde derivative. Compound **69** was readily prepared from phenylsulfonyl-substituted pyridine cyanide **66** by treatment with *m*-CPBA in dichloromethane (Scheme 45). Unfortunately, an inseparable mixture of starting material and aldehyde was obtained when **70** was treated under the same DIBAL-H reduction conditions. Hence, we decided to start with an alternative substrate to attain the desired aldehyde **67**.



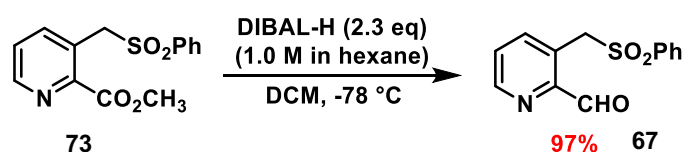
Scheme 45: Synthesis of phenylsulfonyl-substituted pyridine *N*-oxide.

It was envisaged that the use of pyridine ester instead of pyridine cyanide might allow an alternative reaction profile for DIBAL-H reduction and afford the desired aldehyde with good conversion. Hence, commercially available methyl 3-methylpyridine-2-carboxylate **71** was subjected to Wohl-Ziegler bromination to give methyl 3-(bromomethyl)picolinate **72** which was then treated with benzenesulfinic acid sodium salt to afford phenylsulfonyl-substituted picolinate **73** (Scheme 46).



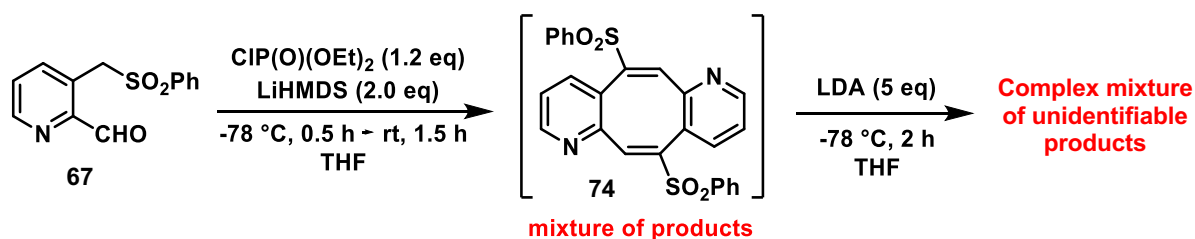
Scheme 46: Synthesis of phenylsulfonyl-substituted pyridine ester.

Reduction of the phenylsulfonyl-substituted pyridine ester compound **73** was attempted using DIBAL-H in dichloromethane (Scheme 47). Gratifyingly, the reaction went to completion without any over-reduction of the ester, affording the desired phenylsulfonyl-substituted pyridine aldehyde **67** in 97% yield.



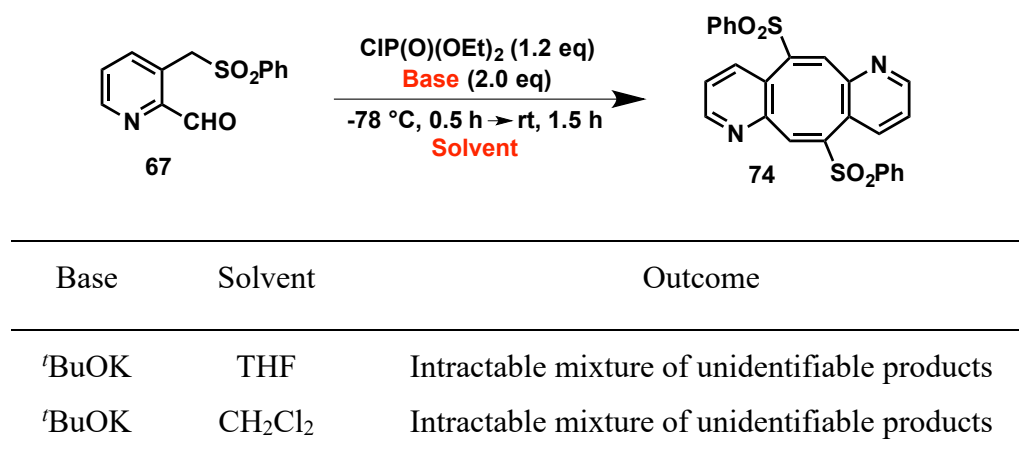
Scheme 47: DIBAL-H reduction of phenylsulfonyl-substituted pyridine ester.

The transformation of **67** to the cyclic diacetylene **16** using Orita's double elimination protocol was next investigated.⁶⁴ Compound was subjected to the Wittig-Horner conditions employed earlier. The one-pot reaction gave a complex intractable mixture of unidentifiable products and the desired product **74** could not be detected (Scheme 48). The reaction was then attempted again and the individual steps monitored by LCMS. It was observed that upon addition of LiHMDS at -78° C the reaction turns into a mixture of products and the desired intermediate **74** could be identified as one of them, as determined by LCMS analysis of reaction mixture. Addition of LDA to this mixture at -78° C turned it completely into a complex intractable mixture of unidentifiable products as observed by ¹H NMR analysis of the crude reaction material obtained after work-up.



Scheme 48: Attempted synthesis of pyridine-based Sondheimer diyne.

Variation of the reaction parameters (base and solvent conditions) did not show any improvement (Scheme 49).

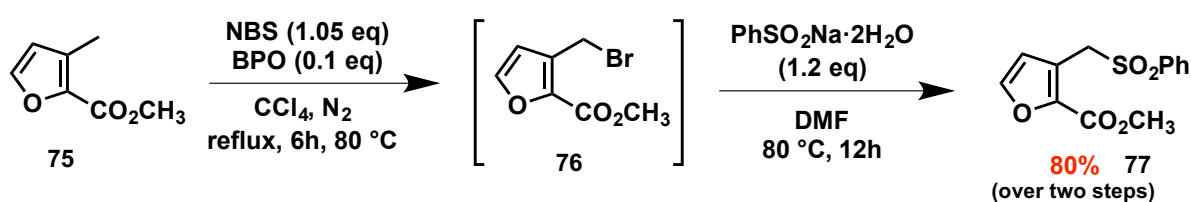


Scheme 49: Attempted synthesis of pyridine-based Sondheimer diyne: Variation of reaction parameters.

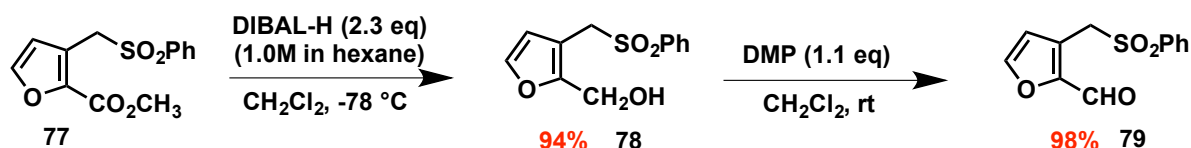
We believe that the fusion of a heteroaromatic pyridine ring renders the aldehyde substrate **67** highly reactive and unstable under the Wittig-Horner conditions for the formation of cyclic intermediate **74**.

2.10.2. Synthesis of furan-based Sondheimer dialkyne **17**

Methyl 3-methylfuran-2-carboxylate **75** was subjected to Wohl-Ziegler bromination to give **76** which was then further treated with benzenesulfinic acid sodium salt to afford furan-based sulfone ester **77** in 80% yield (Scheme 50). Treatment with 2.3 equivalents of DIBAL-H led to alcohol **78**, which was then oxidized to furan-based sulfone aldehyde **79** using Dess-Martin conditions (Scheme 51).

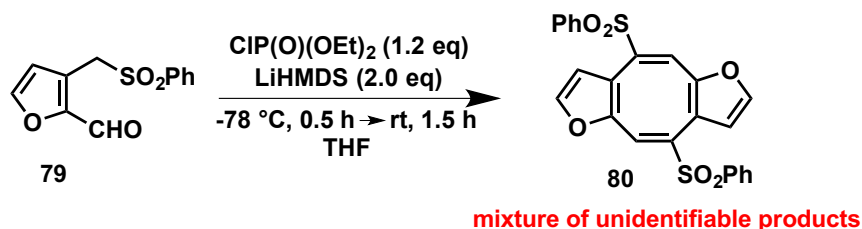


Scheme 50: Synthesis of furan-based sulfone ester.



Scheme 51: Synthesis of furan-based aldehyde.

The transformation of aldehyde **79** to cyclic diacetylene **17** was investigated but treatment under previously used conditions unfortunately resulted in a complex intractable mixture of unidentifiable products (Scheme 52).



Scheme 52: Attempted synthesis of furan-based Sondheimer diyne.

We believe that the fusion of a five-membered furan ring imposes additional strain on the substrate and renders it unstable to the Wittig-Horner conditions for the formation of the cyclic intermediate.

In summary, ten different substituted variants of Sondheimer dialkyne (**4-7**, **10-15**) were successfully synthesised (Figure 17). Out of these, dialkynes with trimethylammonium substituent **12-15** were found to be highly water-soluble and aqueous stable.

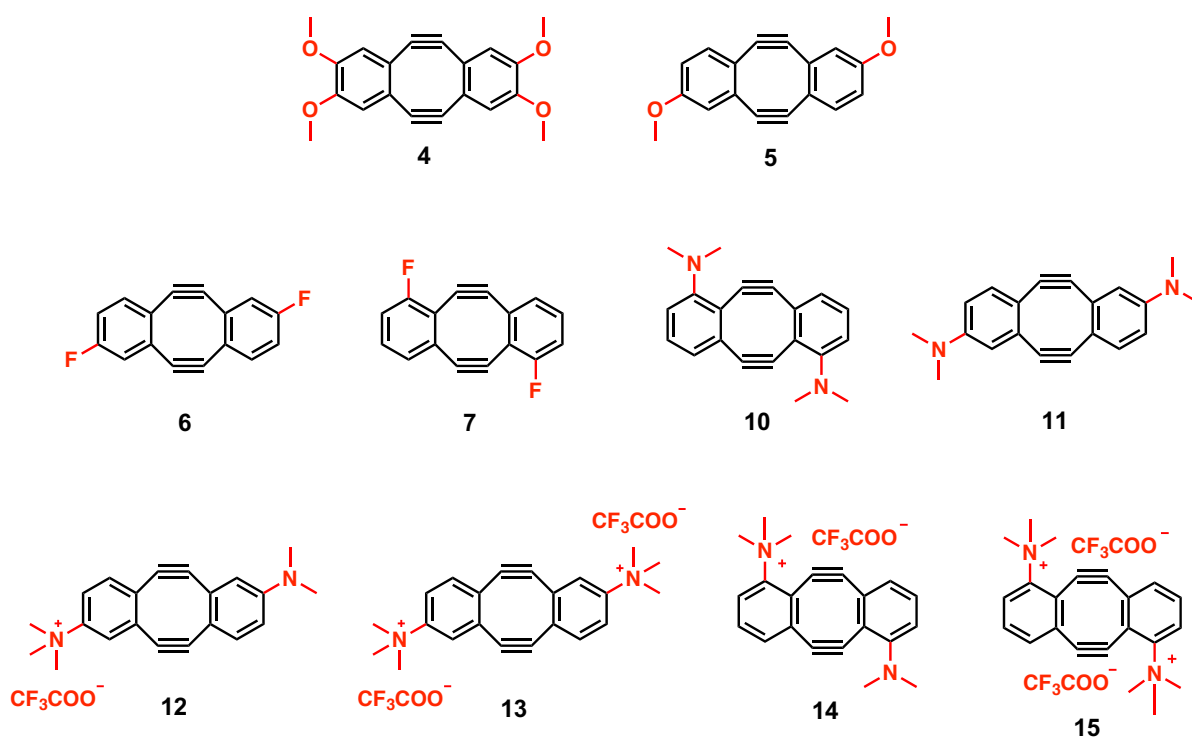


Figure 17: Substituted variants of Sondheimer dialkyne successfully synthesised.

3. Strain-promoted double-click peptide stapling

Having the substituted Sondheimer diynes **4-7** and **10-15** in hand we investigated their application in stapling phage display peptide⁸⁷⁻⁸⁸ PDI-E **2** (Ac-LTFXEYWAQLXS-NH₂, **X** = Orn(N₃)) for targeting the oncogenic p53-MDM2 interaction. Phage display is a high throughput screening method used for studying the interaction of peptides with proteins or other biomolecules. Peptides with high affinity for a particular protein target can be identified by *in vitro* selection from large libraries of peptides. The PDI-E peptide **2** was synthesized by Alexander Strizhak in the Spring group. Peptide **2** was chosen for stapling as previous work within our group has shown that the stapled PDI-E peptide with Sondheimer diyne **1** is a potent inhibitor of the p53-MDM2 interaction.⁸⁹

3.1 p53-MDM2 interaction

The p53 protein is a tumour suppressing transcription factor which plays a very important role in controlling cell cycle and division.⁹⁰ p53 is activated in response to stress signals such as DNA damage, heat shock, hyperoxia, and hypoxia. This leads to an increase in the concentration of p53 in the cells followed by binding with p53-response elements in its tetrameric form, thus activating genes for apoptosis (programmed cell death), growth arrest or altered DNA repair (Figure 18).⁹¹⁻⁹² It is estimated that about 50-55% of all human cancers are due to mutations in the p53-related pathways.⁹³

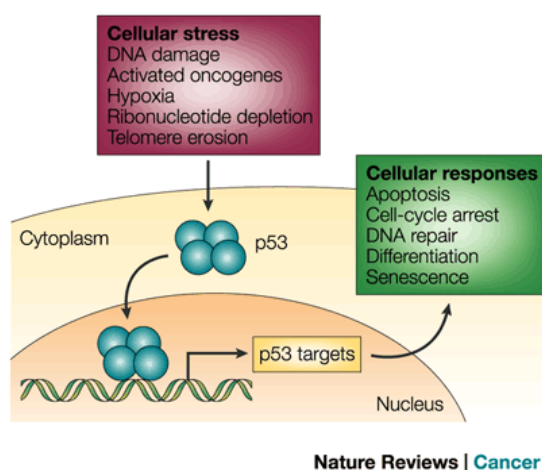


Figure 18: Activation of p53 in response to stress (from Chene⁹⁴).

MDM2 is an E3 ubiquitin ligase protein⁹⁵⁻⁹⁶ and plays an important role in regulating the activity of p53 in cells by either blocking its transcriptional activity, exporting p53 to the cytoplasm, or by promoting degradation of p53 *via* ubiquitin-mediated proteolysis.^{95, 97-98}

Thus, in a normal cell, p53 is only present in low levels due to its continuous degradation by MDM2 (half-life 5-20 minutes).⁹⁹⁻¹⁰⁰ Stress signals such as from DNA damage promotes p53 phosphorylation, thereby inhibits its degradation by preventing its binding with MDM2.¹⁰¹⁻¹⁰² In fact, MDM2 is itself activated by p53 transcriptional activity and hence p53 and MDM2 are said to form an auto-regulatory feedback loop (Figure 19).^{94, 103}

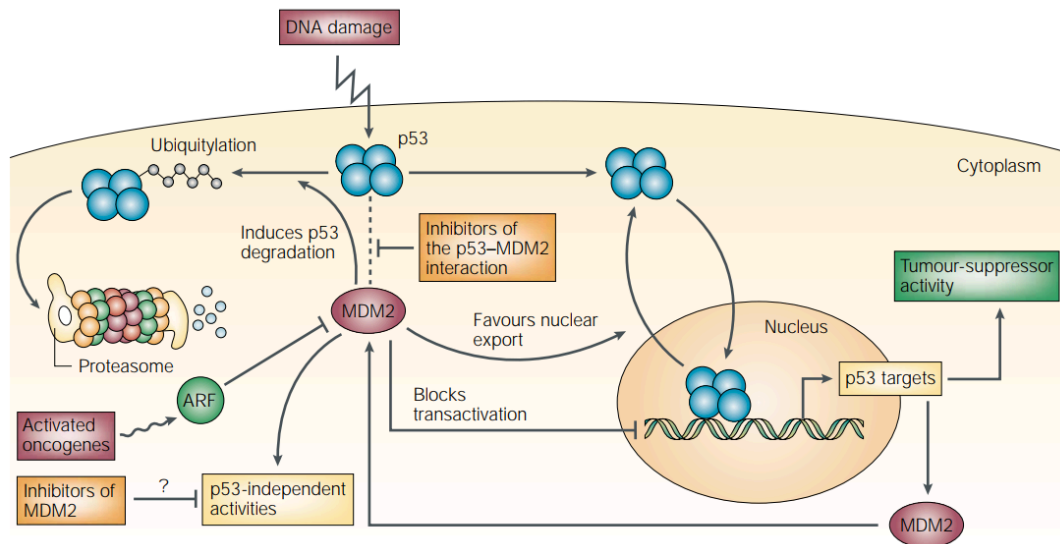


Figure 19: p53 regulation by MDM2 (from Chene⁹⁴).

Overexpression of MDM2 can inhibit the transcriptional activity of p53 leading to the halt of apoptosis, growth arrest and DNA repair mechanism, resulting in a cancerous growth of cells.¹⁰⁴⁻¹⁰⁶ This can be controlled by inhibiting the p53/MDM2 PPI which will make p53 free and transcriptionally active in response to stress signals.

In 1996, Pavletich *et al.* obtained a crystal structure of the p53-MDM2 complex which revealed the molecular interactions between the two proteins (Figure 20).¹⁰⁷ They observed that only MDM2 has a well-defined binding site. Moreover, only the p53 interface consists of a single contiguous stretch of amino acids. This suggests that inhibitors of p53/MDM2 PPI should mimic p53.¹⁰⁰ It was also observed that three amino acid residues- Phe19, Trp23 and Leu26 contribute for most of the interaction and binding energy between p53 and MDM2. Hence potential inhibitors for this PPI should aim to have mimics of at least these three amino acid residues.

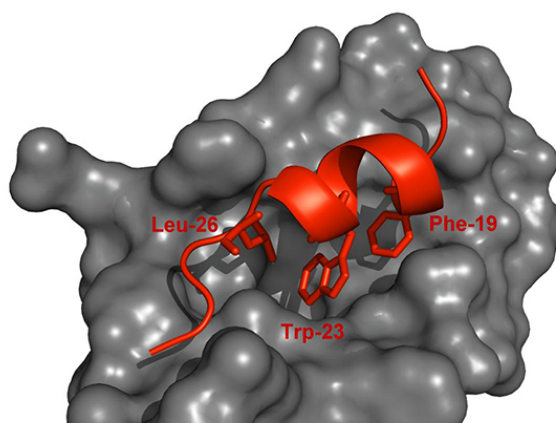
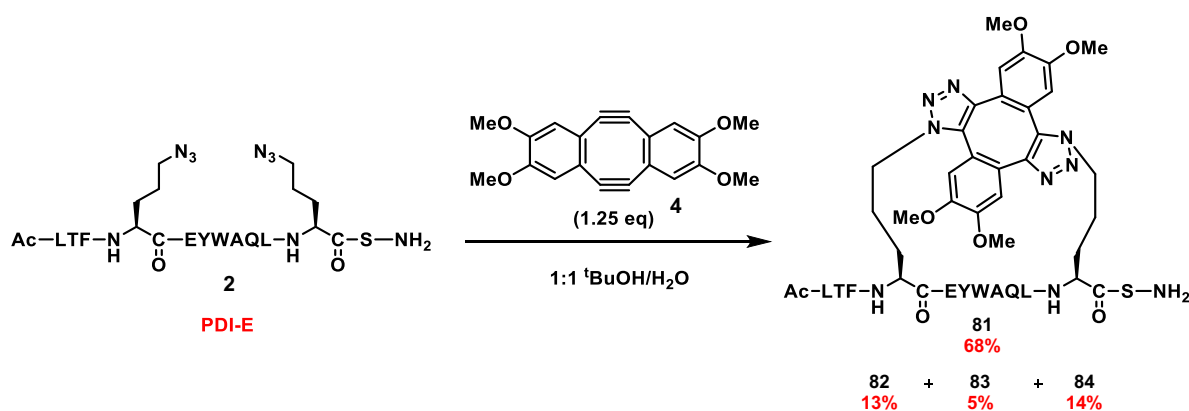


Figure 20: Crystal structure of p53-MDM2 complex (from Hupp *et al.*¹⁰⁸).

The p53-MDM2 interaction has been well studied with a great wealth of literature present on it. Due to this, development of p53/MDM2 PPI inhibitors as an anti-cancer therapy is an attractive research field.

3.2 Peptide stapling of **2** with substituted Sondheimer dialkynes

The stapling investigations began with C₂-symmetric tetramethoxy substituted Sondheimer dialkyne **4**. Linear diazido peptide **2** was treated with **4** in 1:1 ^tBuOH/H₂O (Scheme **53**). Reaction was stirred at room temperature and monitored by liquid chromatography mass spectrometry (LCMS). Peptide stapling of PDI-E **2** with **4** proceeded successfully to give functionalised stapled peptide **81** as the major product in 68% yield (by HPLC) within 24 hours (Scheme **53**). Preparative HPLC purification provided **81** in 39% isolated yield. HPLC analysis of the reaction mixture indicated that along with the major product **81**, there were three other by-products **82**, **83** and **84**, all with the same mass (Figure **21**).



Scheme 53: Strain-promoted double-click peptide stapling with **4**.

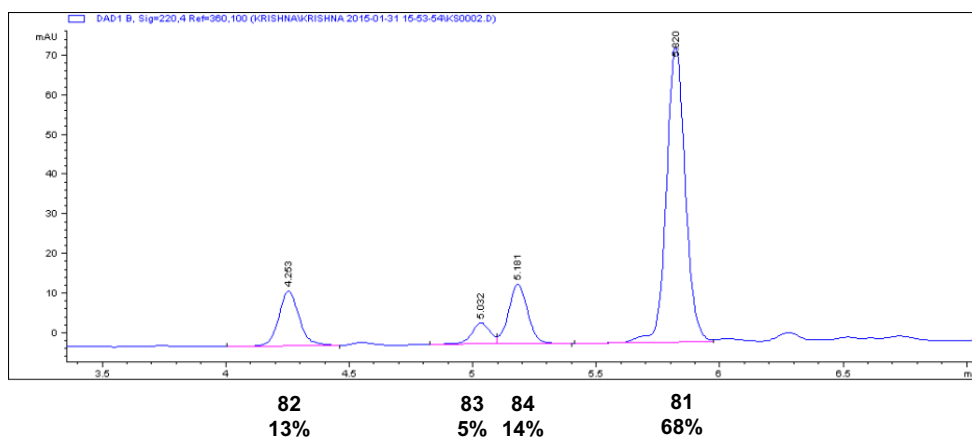


Figure 21: HPLC trace of the peptide stapling reaction of **2** with **4** at 220 nm.

There were four isomers possible for the stapled peptide:- the *trans*-form and the *cis*-form with two different conformers each (Figure 22). The X-ray crystal structure of MDM2-bound stapled peptide with unsubstituted dialkyne **1**, obtained in the group previously has demonstrated the formation of the *trans*-isomer. Therefore, by analogy it is likely that the *trans*-isomer of the stapled peptide **81** is formed.

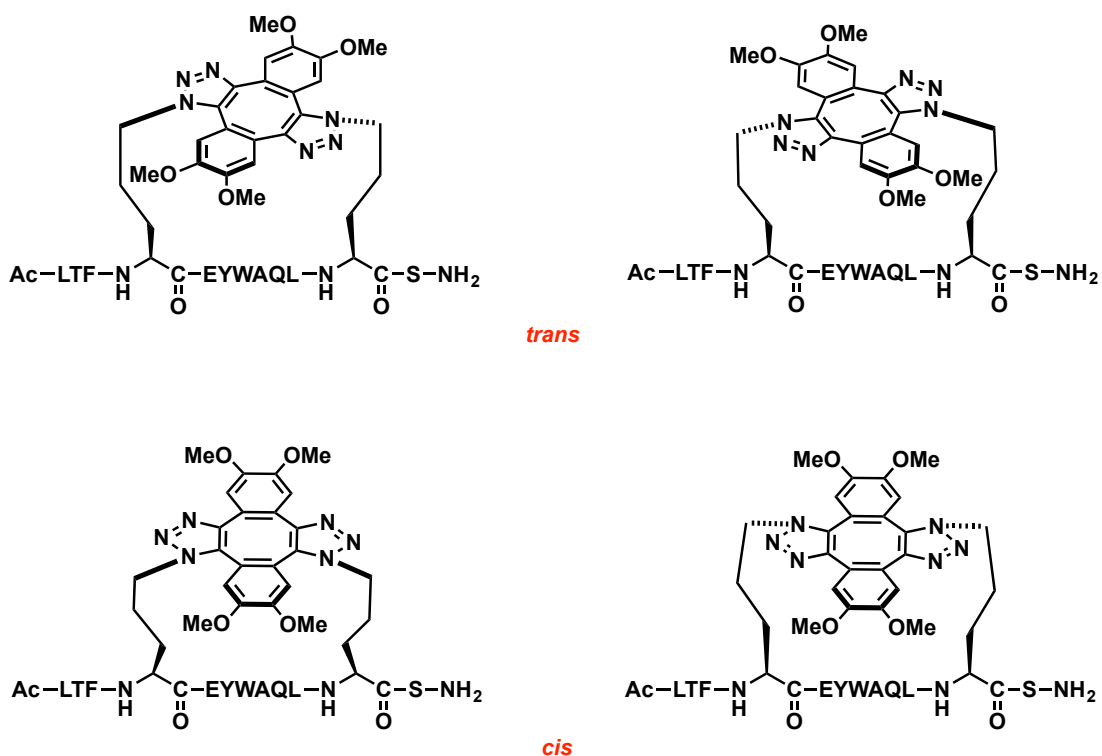


Figure 22: Possible isomers of the product from stapling reaction with dialkyne **4**.

IR spectra of by-products **82**, **83** and **84** suggested that these are not linear coupling products **85**, **86** due to the absence of an azide-group absorption peak (Figure 23). High-resolution mass spectrum of the **82**, **83** and **84** ruled out the possibility of higher order oligomer formation due to the observance of isotopic spacing expected for monomeric stapled products. It was concluded that the by-products are possibly different conformational forms of the *cis*- and *trans*-stapled peptides.

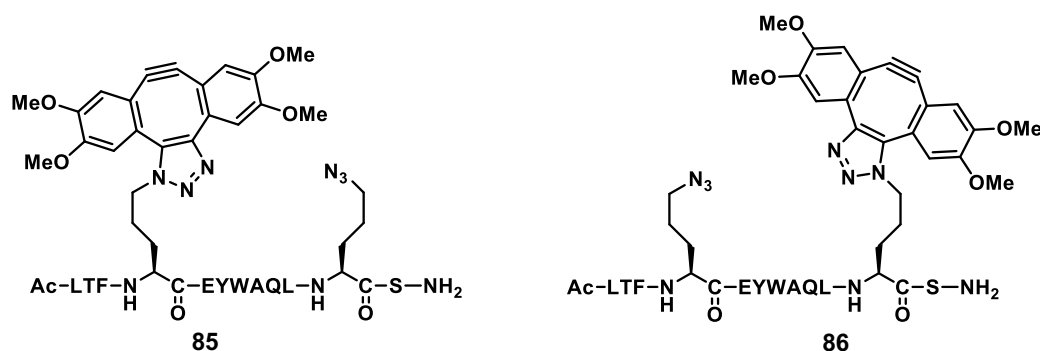


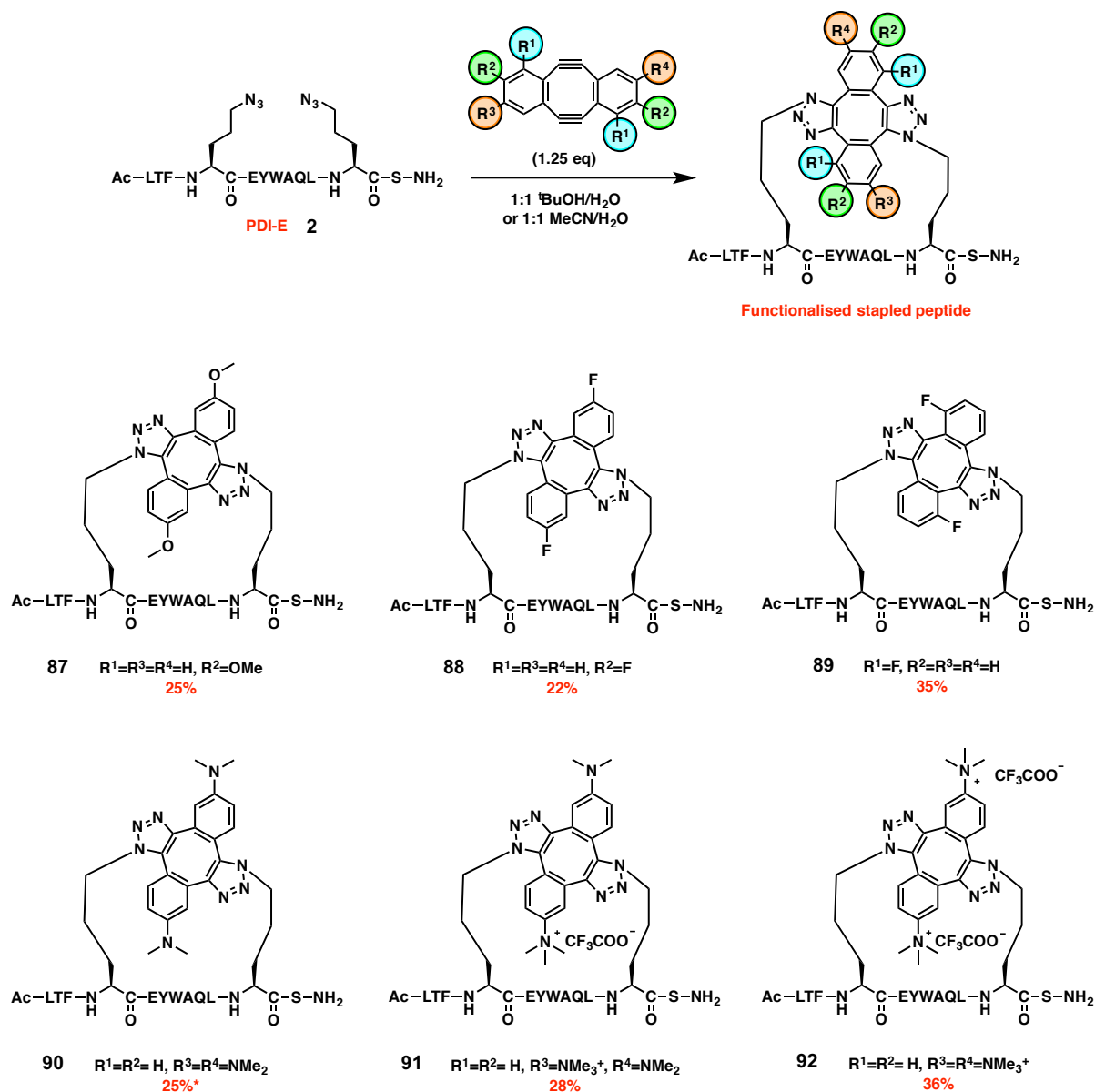
Figure 23: Possible linear coupling products from peptide stapling with dialkyne **4**.

To improve the yield of the major product **81**, peptide stapling was attempted at 0° C under the same reaction conditions. Unfortunately, reducing temperature did not have any effect on the selectivity of the process and the by-products **82**, **83** and **84** were formed again in the same relative proportions. Since the focus of the project was screening of substituted diynes to demonstrate their application in stapling a diazido peptide for inhibition of protein-protein interactions, no more effort was put into further optimisation of the reaction conditions to improve the yield.

Having established a peptide stapling protocol with tetramethoxy substituted **4**, we moved on to investigate our stapling reaction with substituted dialkynes **5-7**, **10-15**. Stapling reactions with highly-water soluble quaternary ammonium substituted dialkynes **12-15** were carried out in 1:1 MeCN/H₂O. Stapling reaction with dialkynes **5-7**, **11-13** proceeded successfully to give desired functionalised stapled peptides **87-92** in 22-36% yield* (Scheme 54). Stapling with disubstituted Sondheimer dialkynes **5-7**, **11-13** can result in two different *anti*-isomers of stapled peptide. In the scheme is shown the one with least steric hindrance involved as a representative structure for the major isomer of functionalised stapled product. Stapling

* Yields depicted are the isolated yields of the major fraction of the stapled peptides obtained after HPLC purification. It is possible that some of these fractions were an inseparable mixture of conformational isomers.

reactions with dialkynes **5**, **6**, and **11** went to completion within 24 hours. Stapling with *ortho*-fluoro dialkyne **7** was found to be very slow (~72 h, by LCMS), whereas, stapling with quaternary ammonium substituted dialkynes **12**, **13** was found to be much faster (~8 h, by LCMS). Dialkynes **10**, **14**, **15**, all bearing an amine substituent *ortho* to the alkyne were found to be unreactive under the given reaction conditions.



Scheme 54: Strain-promoted double-click stapling with substituted dialkynes **5-7**, **11-13**.

***90** was obtained as an inseparable mixture of two conformational isomers.

3.3 Biological evaluation of functionalised stapled peptides

Functionalised stapled peptides **81**, **87-92**^{*} were tested in a competitive fluorescence polarisation (FP)^{61, 109} assay for MDM2 binding affinity (Table 1). This assay was carried out by Dr Laura Itzhaki's group at Department of Pharmacology, University of Cambridge and conducted by Dr Wenshu Xu.

In particular, *meta*-methoxy **87** (8.5 ± 1.9 nM), *meta*-fluoro **88** (17.3 ± 7.7 nM), and quaternary ammonium **91**, **92** functionalised stapled peptides were found to be potent binders of MDM2 (Table 1). On the other hand, tetramethoxy **81** (130.1 ± 28.3), *ortho*-fluoro **89** (501.4 ± 107.5), and *meta*-dimethylamine **90** (35.3 ± 0.1) functionalised stapled peptides were found to be weak binders of MDM2. Out of all, the stapled peptide with single charge (quaternary ammonium substituted) functionalisation **91** was found to exhibit highest binding affinity (7.0 ± 3.9 nM). Installation of a second charge on the linker slightly reduced the binding affinity of the stapled peptide (**92**, 17.0 ± 6.2 nM). The binding data for unstapled diazido peptide **2** (PDI-E) and its corresponding stapled form **3** with Sondheimer dialkyne were available from previous work.⁸⁹

Peptide	K_d / nM
87	8.5 ± 1.9
81	130.1 ± 28.3
88	17.3 ± 7.7
89	501.4 ± 107.5
90	35.3 ± 0.1
91	7.0 ± 3.9
92	17.0 ± 6.2
3	7.5 ± 0.7
2	6.5 ± 0.6

Table 1: *In vitro* MDM2 binding affinity of functionalised stapled peptides.

^{*} Major isomer of functionalised stapled peptides separated by HPLC purification were tested for biological activity.

We were also interested in investigating whether the charged trimethylammonium group in functionalised peptide **91** is involved in any interaction with MDM2. Previously reported studies on stapled peptide **3** have indicated the involvement of the staple moiety of the peptide in forming interactions with the protein.^{89, 110-113} For this purpose, we determined the crystal structure of functionalised peptide **91** in complex with MDM2 (17-108, E69A/K70A;¹¹⁴ Figure **24**). These studies were carried out by Dr Xuelu Wang at the Department of Biochemistry, University of Cambridge.

The MDM2-bound functionalised stapled peptide **91** was found to be in an α -helical conformation, and with the binding triad (F3, W7, L10) being in the correct orientation for engaging the binding hotspot on MDM2 (Figure **24**: Top view).⁸⁹ The bis(triazolyl) staple of the bound peptide **91** was found to exist as *anti* regioisomer with the charged trimethylammonium group pointing away from MDM2 surface (Figure **24**: Side view).

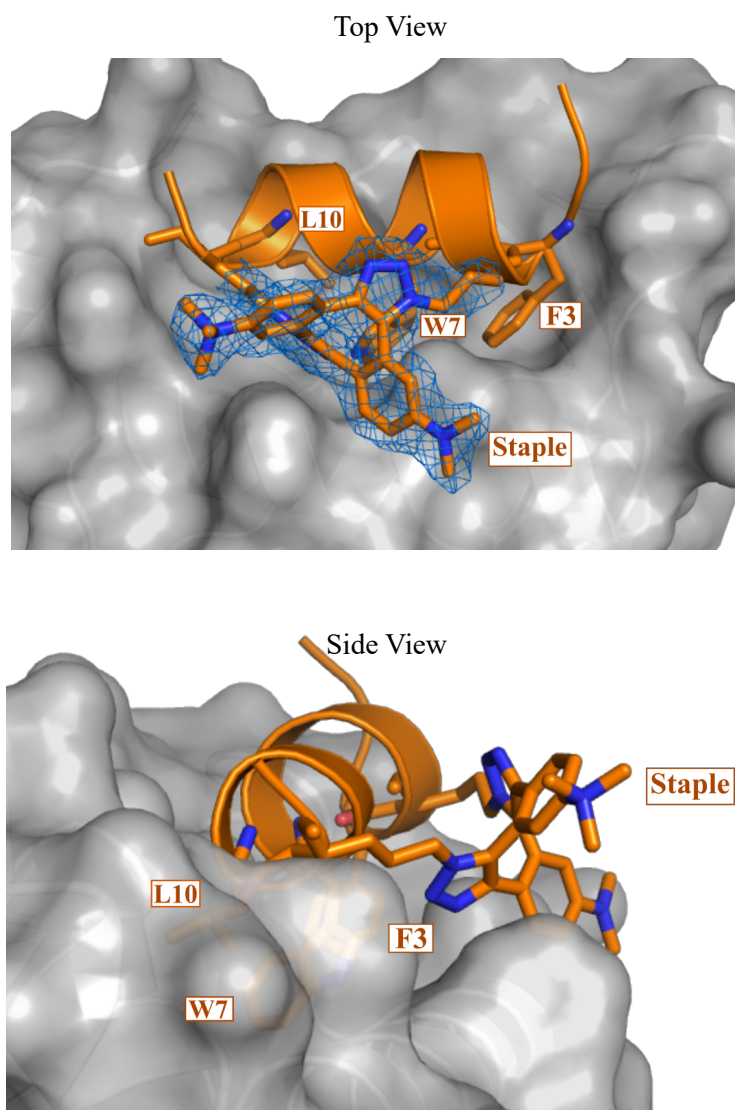


Figure 24: Crystal structure of **91** bound to MDM2 at 2.0 Å resolution (PDB ID: 6H22). Top and side views depicting the bound stapled peptide **91** in α -helical conformation and the staple

as *anti* regioisomer (only the staple and side chains of the three binding residues are shown for clarity). The 2Fo-Fc electron density map is contoured at 1 σ .

In comparison with the structure of MDM2-**3** peptide complex (PDB ID: 5AFG), both peptides **3** and **91** form hydrophobic interactions with MDM2 through residue F3, W7, and L10 (Figure 25a). However, the staple moiety of peptide **91** was found to be shifted away from the MDM2 protein surface (Figure 25b). The charged trimethylammonium group moves even further compared to the dimethylamine group, indicating that the hydrophobic interface on MDM2 seem to expel the staple compound due to its charged group.

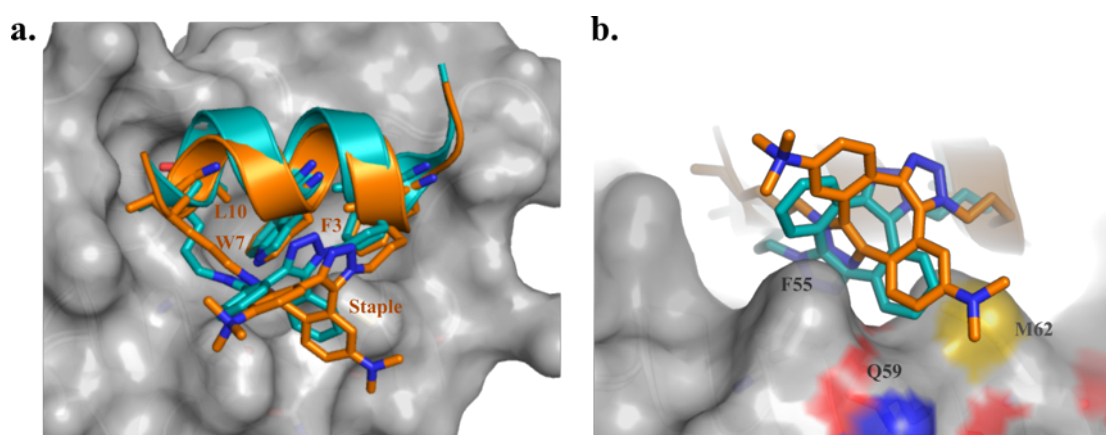


Figure 25: Comparison of structures of MDM2-**91** peptide complex (PDB ID: 6H22) and MDM2-**3** peptide complex (PDB ID: 5AFG). The structure of MDM2 is shown as surface and coloured in grey. The peptides are shown as cartoon and the staple shown as sticks. **3** peptide is coloured in cyan and **91** peptide is in orange. a. **91** peptide associates with MDM2 through hydrophobic interactions mediated by residue F3, W7, and L10, which is conserved in **3** peptide-MDM2 interactions. b. The staple of peptide **91** shifts away from the MDM2 surface formed by F55, Q59, and M62 compared to the staple of peptide **3**.

Next, we tested the ability of functionalised stapled peptides **81**, **87-92** to inhibit the p53-MDM2 interaction in an established p53 reporter cell-based assay.¹⁰⁹ These studies were conducted by Elaine Fowler at the Department of Pharmacology, University of Cambridge. p53 reporter cells taken in a 96-well format were treated with linear diazido peptide **2** and substituted diynes **4-7**, **11-13** in Dulbecco's Modified Eagle's medium (DMEM). This technique of stapling a linear diazido peptide **2** with multiple substituted diynes in parallel, directly in the cellular medium, provides a faster way of screening a large dialkyne library without performing a separate stapling reaction and purification for each diyne variant.⁸⁹ The

negative control for the assay was treatment with 1% DMSO. p53 activation values are reported as fold activation over 1% DMSO, indicating an indirect comparative measure of the cellular p53 levels.

We found *meta*-fluoro functionalised peptide **88** (fold activation: 3.9 ± 0.7) to be the most potent inhibitor, and twice as active than peptide **2** stapled with Sondheimer dialkyne **1** (fold activation: 1.9 ± 0.1 , Figure 26). No p53 activation was observed with dialkynes **4**, **5**, **7** and **13**. Only slight p53 activation values were observed with dialkynes **11** and **12**.

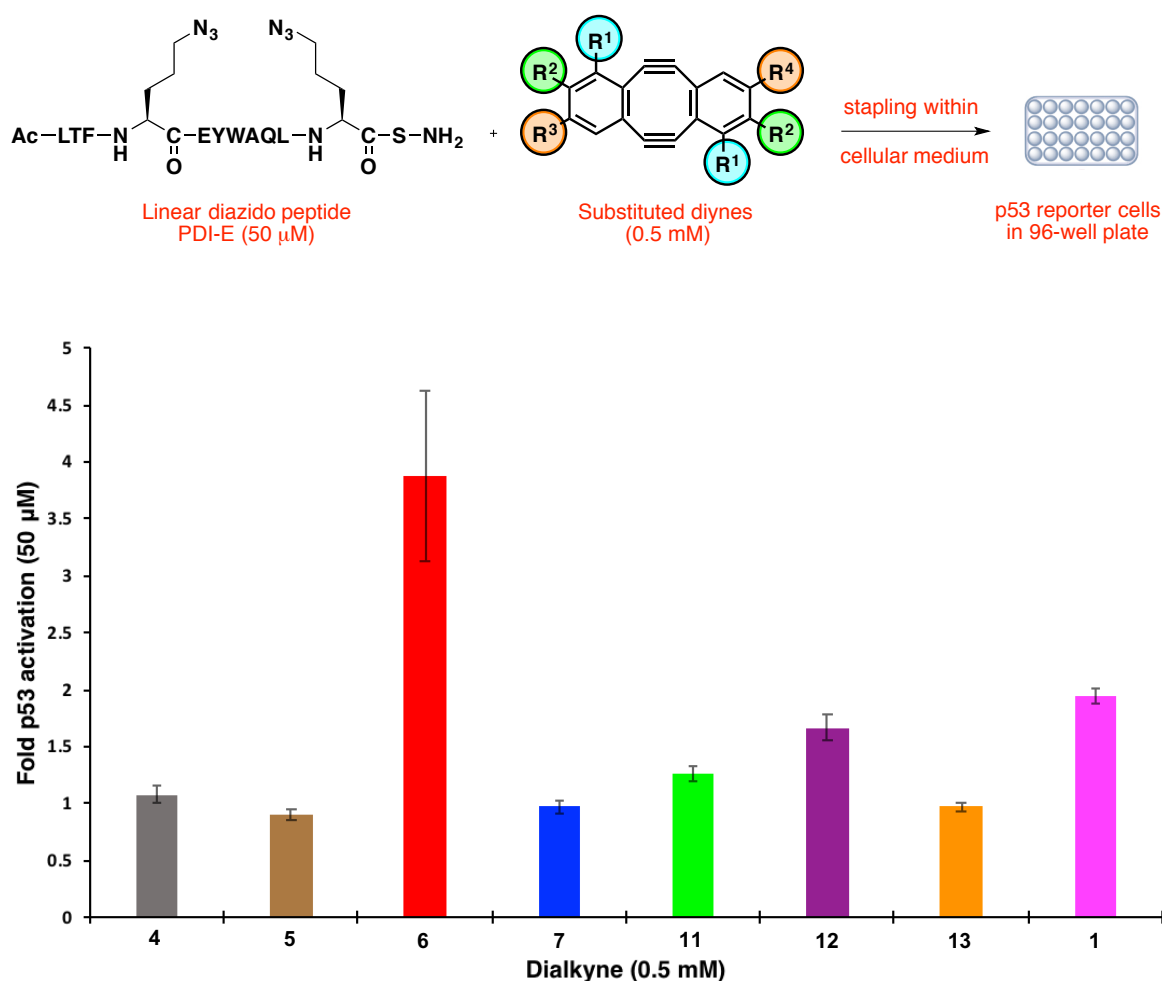


Figure 26: p53 activation in a cellular reporter assay for stapling of peptide **2** (50 μM) with substituted diynes **4-7**, **11-13** (0.5 mM) in parallel, directly within the cellular medium (performed as technical triplicate). Data reported as fold activation over 1% DMSO.

Purified stapled peptides **81**, **87-92** were also tested separately for p53 activation to confirm the potency (Figure 27). This assay also showed **88** to be the most potent. Moreover, **87** and **89** were also found to exhibit slight inhibitory activity in this assay.

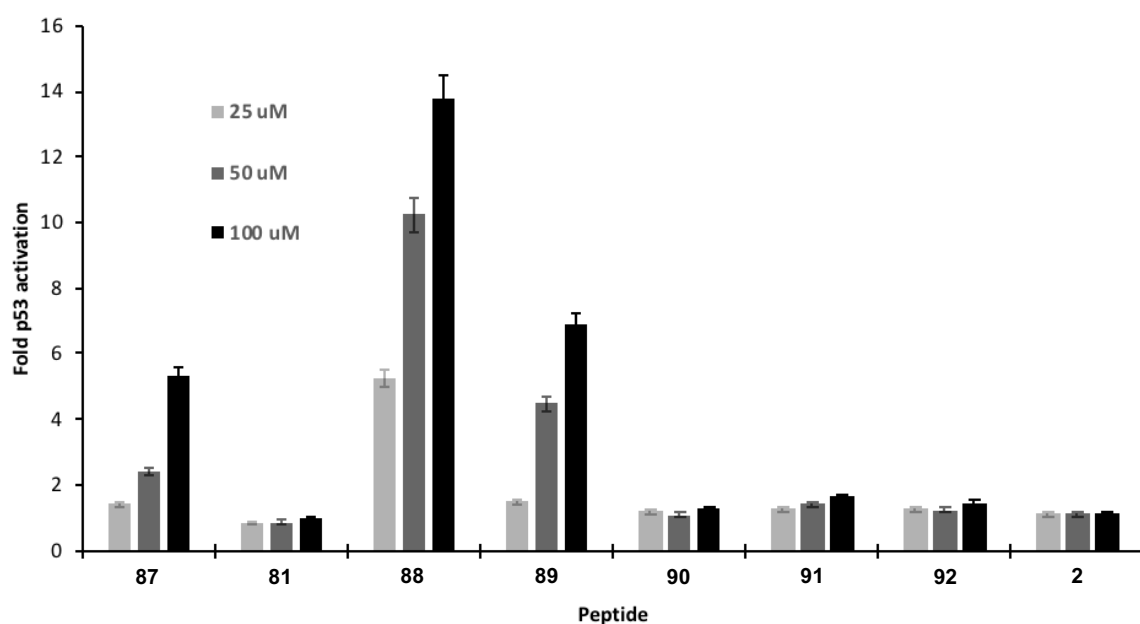


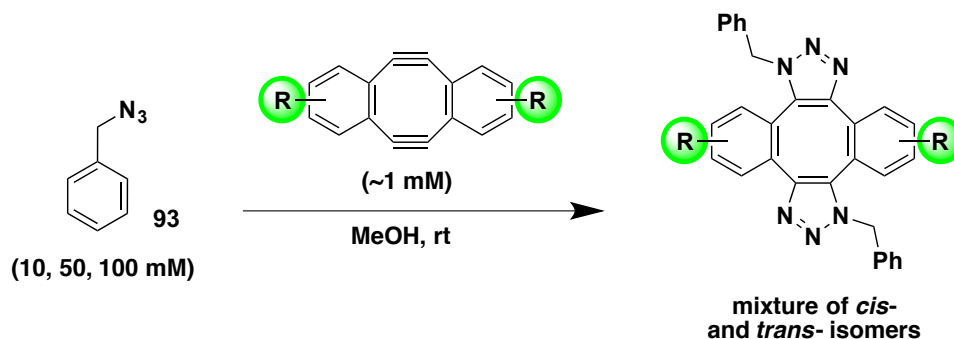
Figure 27: p53 activation in the cellular reporter assay with pre-stapled purified peptides **81**, **87-92**. Data is reported as fold activation over 1% DMSO.

These results suggest that slight variation in the aromatic substitution pattern of the dialkyne can have a drastic effect on the biological activity of the stapled peptide, modifying its binding affinity and cellular activity.

4. SPAAC reactivity of substituted Sondheimer dialkynes: Experimental investigations

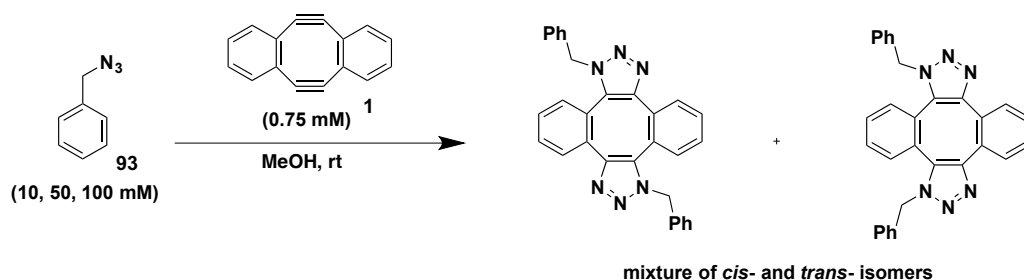
4.1 Kinetic analysis

During the strain-promoted peptide stapling with substituted Sondheimer dialkynes an unusually decreased rate of reaction was observed with *ortho*-substituted dialkynes (**7**, **10**, **14**, **15**), whereas, an increased rate was observed with *meta*-substituted charged dialkynes (**12**, **13**). These observations prompted kinetic investigations into the effect of different substituents on the SPAAC reactivity of Sondheimer dialkyne. Reaction kinetics was studied by monitoring the consumption of dialkynes **1**, **4**, **6**, **7**, **10-13** in a SPAAC with benzyl azide **93** in methanol using UV spectroscopy and their second-order rate constants were determined (see Experimental 7.2.7 for further details). The rate measurement was performed by monitoring the absorbance of dialkynes in the presence of an excess amount of benzyl azide (Scheme 55).^{76, 115} It has been demonstrated previously with Sondheimer diyne **1** that the first cycloaddition leading to the formation of monoyne intermediate is the rate-determining step of the reaction.¹¹⁵



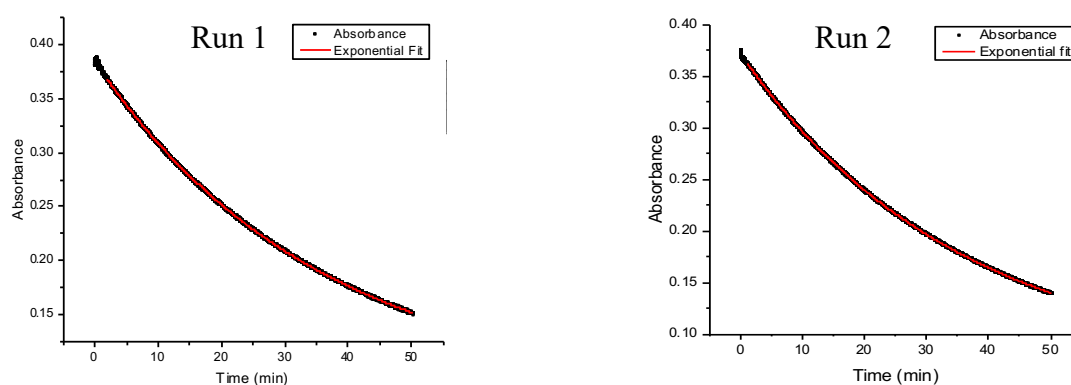
Scheme 55: Kinetic analysis of substituted Sondheimer dialkynes.

4.1.1 Kinetic analysis of diyne **1**¹¹⁵

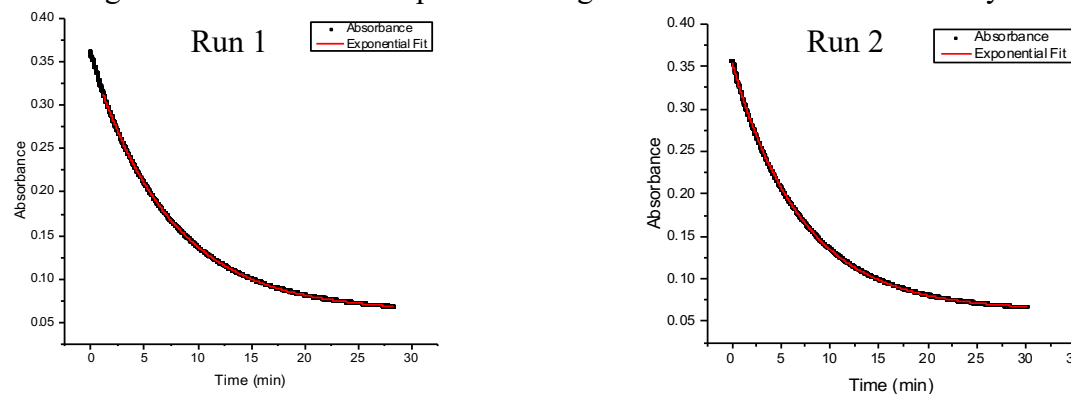


Scheme 56: SPAAC of diyne **1** with benzyl azide.

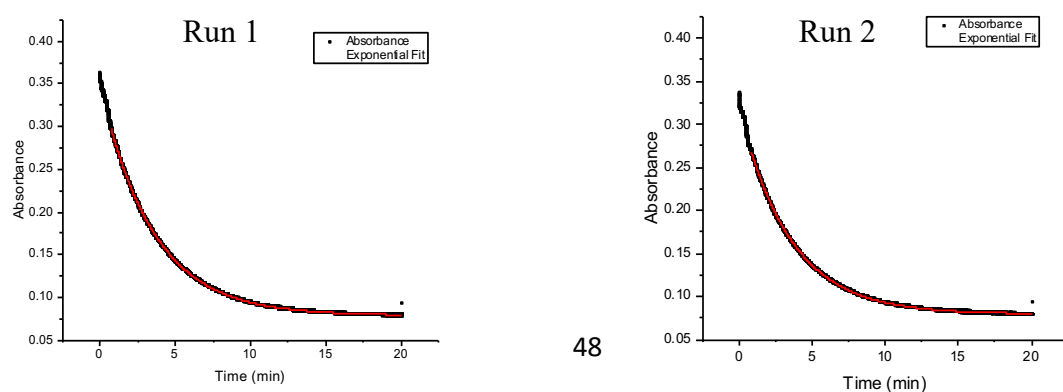
Time-dependent absorbance of diyne **1** (initial concentration of 1.5 mM) at 370 nm of wavelength was monitored in duplicate during the reaction with 10 mM benzyl azide.



Time-dependent absorbance of diyne **1** (initial concentration of 1.5 mM) at 370 nm of wavelength was monitored in duplicate during the reaction with 50 mM benzyl azide.



Time-dependent absorbance of diyne **1** (initial concentration of 1.5 mM) at 370 nm of wavelength was monitored in duplicate during the reaction with 100 mM benzyl azide.

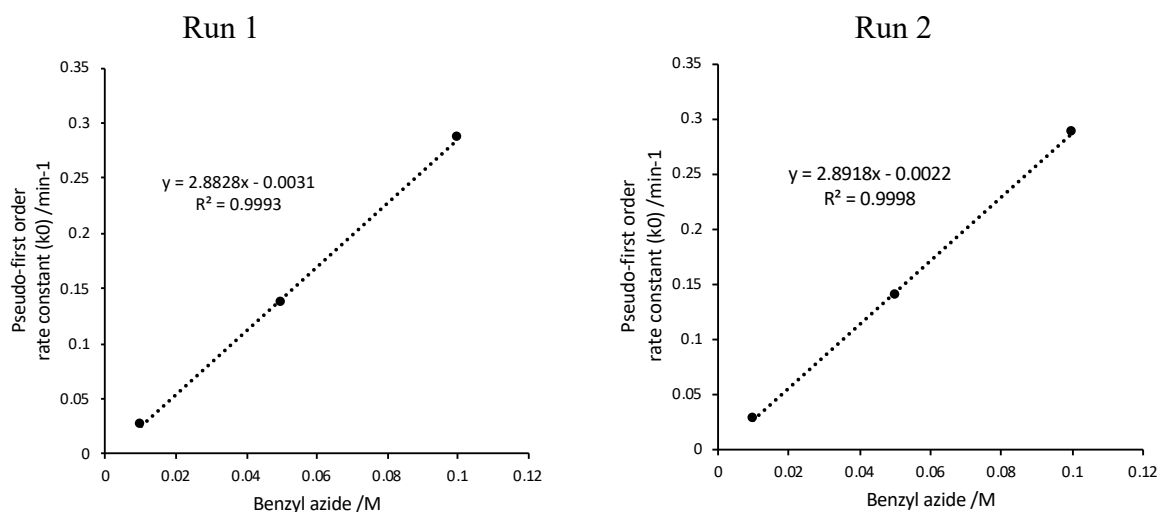


Pseudo-first order rate constants (k_0) were determined for diyne **1** by fitting of the absorbance versus time data to the following exponential equation ($y = A \cdot \exp(-k_0 \cdot x) + y_0$) using Origin.

Benzyl azide	Run	Pseudo-first order rate constant k_0 (min ⁻¹)	Standard error	R ²
10 mM	1	0.028	4.28E-6	0.99998
	2	0.028	4.23E-6	0.99998
50 mM	1	0.137	1.18E-5	0.99998
	2	0.140	2.66E-5	0.9999
100 mM	1	0.287	3.81E-5	0.99998
	2	0.288	6.03E-5	0.9999

Table 2: Pseudo-first order rate constants for SPAAC with diyne **1**.

Pseudo-first order rate constants (k_0) obtained were plotted against the concentration of benzyl azide for the determination of second order rate constant (k).

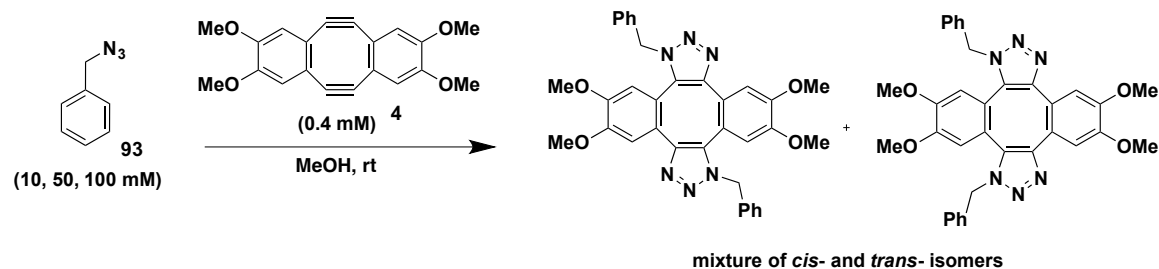


Run	Second order rate constant (M ⁻¹ min ⁻¹)	Second order rate constant (M ⁻¹ s ⁻¹)	Mean second order rate constant k (M ⁻¹ s ⁻¹)	Standard error
1	2.883	0.04805	0.048125	7.5E-5
2	2.892	0.0482		

Table 3: Second order rate constants for SPAAC with diyne **1**.

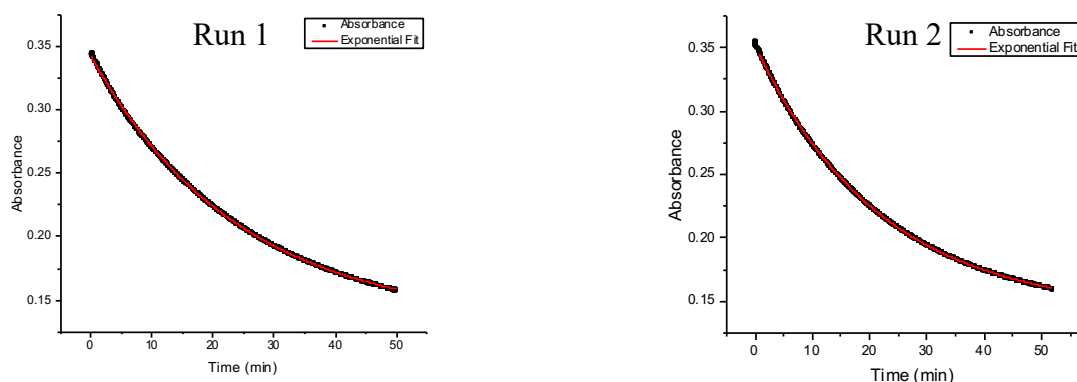
Mean second order rate constant, $k = 0.048 \pm 7.5E-5$ M⁻¹ s⁻¹

4.1.2 Kinetic analysis of diyne **4**⁷⁶

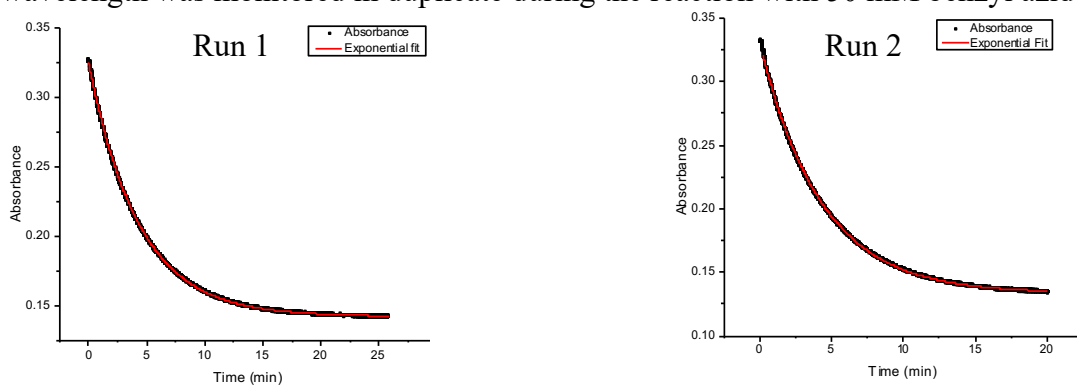


Scheme 57: SPAAC of diyne **4** with benzyl azide.

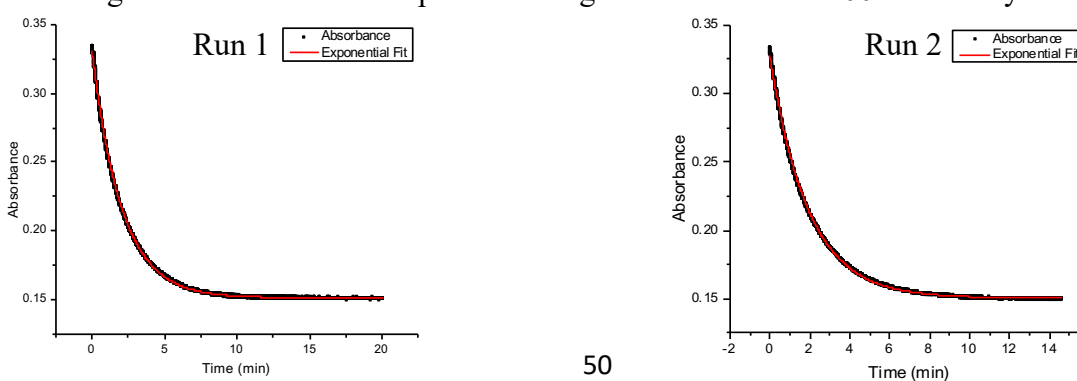
Time-dependent absorbance of diyne **4** (initial concentration of 0.8 mM) at 363 nm of wavelength was monitored in duplicate during the reaction with 10 mM benzyl azide.



Time-dependent absorbance of diyne **4** (initial concentration of 0.8 mM) at 363 nm of wavelength was monitored in duplicate during the reaction with 50 mM benzyl azide.



Time-dependent absorbance of diyne **4** (initial concentration of 0.8 mM) at 363 nm of wavelength was monitored in duplicate during the reaction with 100 mM benzyl azide.

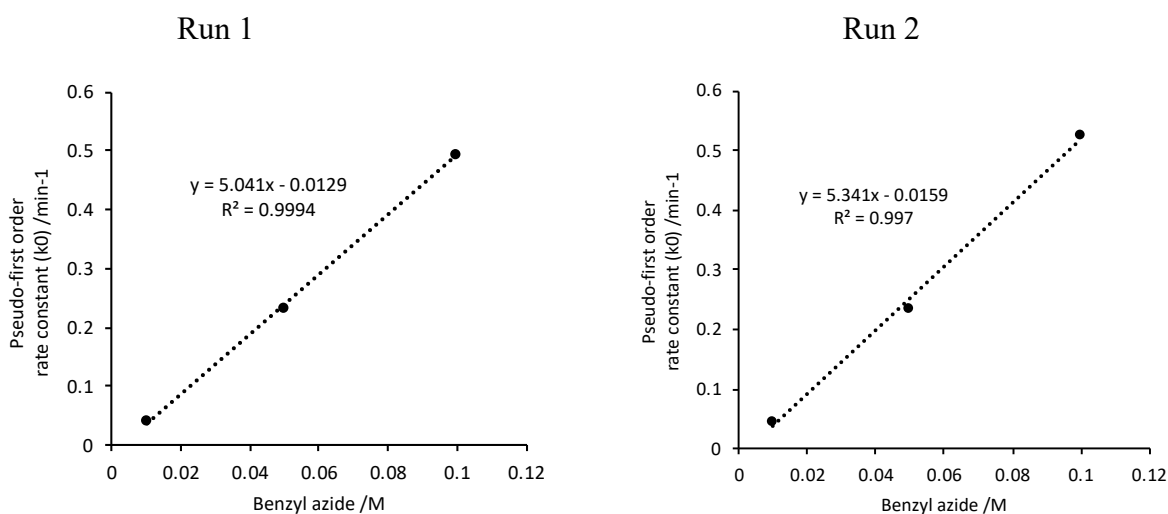


Pseudo-first order rate constants (k_0) were determined for diyne **4** by fitting of the absorbance versus time data to the following exponential equation ($y = A \cdot \exp(-k_0 \cdot x) + y_0$) using Origin.

Benzyl azide	Run	Pseudo-first order rate constant k_0 (min ⁻¹)	Standard error	R ²
10 mM	1	0.041	1.26E-5	0.99983
	2	0.046	8.75E-6	0.99992
50 mM	1	0.233	1.18E-5	0.99992
	2	0.236	6.27E-5	0.99986
100 mM	1	0.494	1.88E-4	0.99959
	2	0.525	2.57E-4	0.99954

Table 4: Pseudo-first order rate constants for SPAAC with diyne **4**.

Pseudo-first order rate constants (k_0) obtained were plotted against the concentration of benzyl azide for the determination of second order rate constant (k).

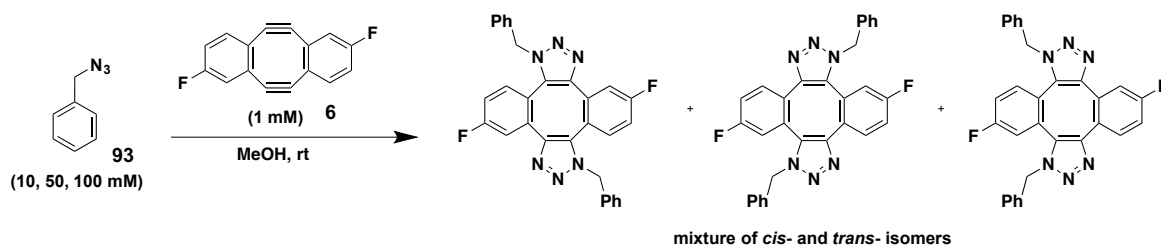


Run	Second order rate constant (M ⁻¹ min ⁻¹)	Second order rate constant (M ⁻¹ s ⁻¹)	Mean second order rate constant k (M ⁻¹ s ⁻¹)	Standard error
1	5.041	0.084	0.0865	2.5E-3
2	5.341	0.089		

Table 5: Second order rate constants for SPAAC with diyne **4**.

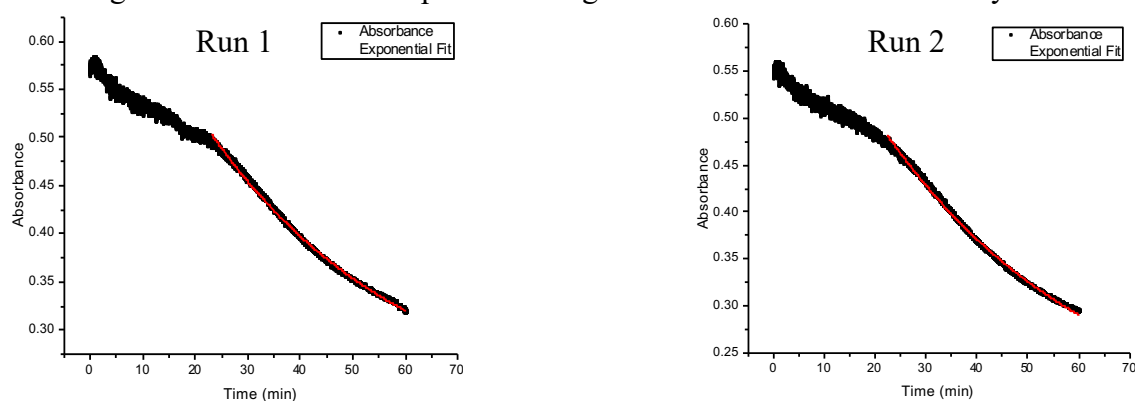
Mean second order rate constant, $k = 0.086 \pm 2.5E-3$ M⁻¹ s⁻¹

4.1.3 Kinetic analysis of diyne 6

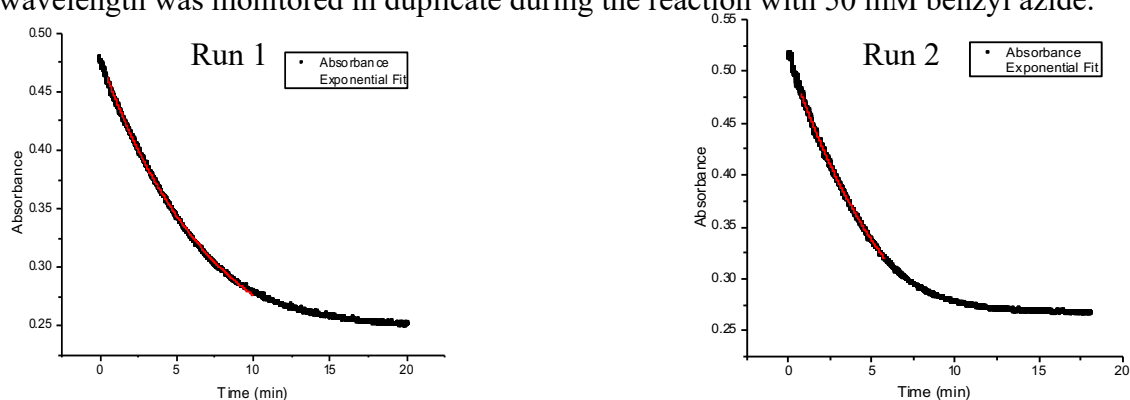


Scheme 58: SPAAC of diyne **6** with benzyl azide.

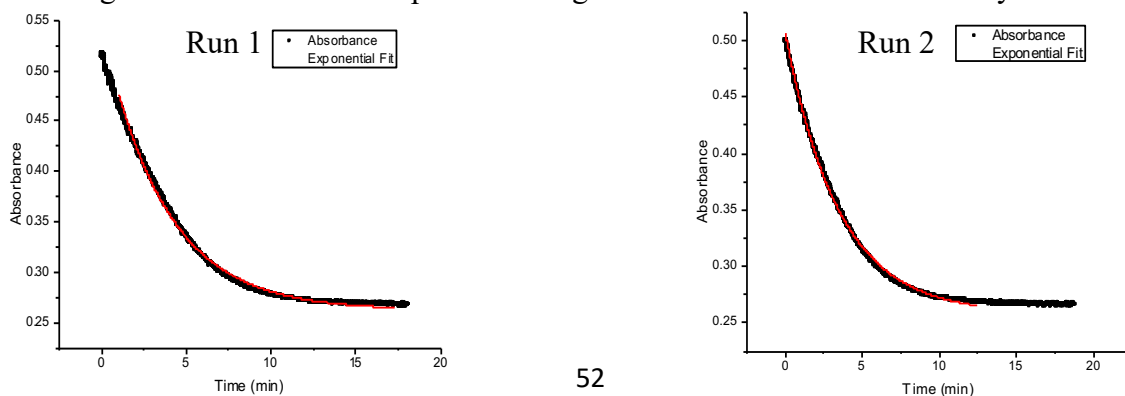
Time-dependent absorbance of diyne **6** (initial concentration of 2.0 mM) at 370 nm of wavelength was monitored in duplicate during the reaction with 10 mM benzyl azide.



Time-dependent absorbance of diyne **6** (initial concentration of 2.0 mM) at 370 nm of wavelength was monitored in duplicate during the reaction with 50 mM benzyl azide.



Time-dependent absorbance of diyne **6** (initial concentration of 2.0 mM) at 370 nm of wavelength was monitored in duplicate during the reaction with 100 mM benzyl azide.

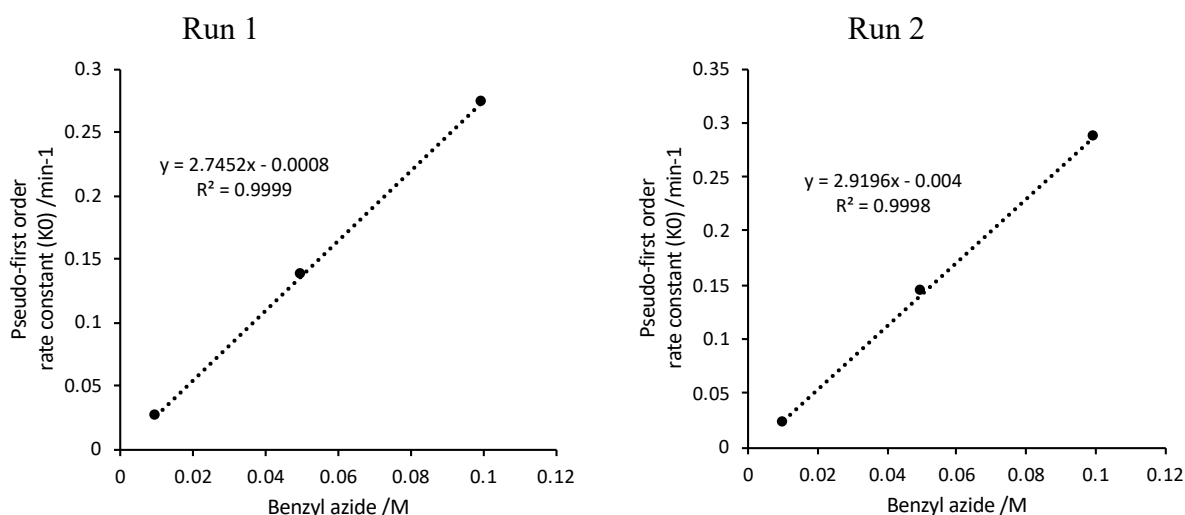


Pseudo-first order rate constants (k_0) were determined for diyne **6** by fitting of the absorbance versus time data to the following exponential equation ($y = A \cdot \exp(-k_0 \cdot x) + y_0$) using Origin.

Benzyl azide	Run	Pseudo-first order rate constant k_0 (min ⁻¹)	Standard error	R ²
10 mM	1	0.026	6.66E-5	0.99785
	2	0.024	7.16E-5	0.99734
50 mM	1	0.138	3.06E-4	0.99925
	2	0.144	1.01E-3	0.99878
100 mM	1	0.273	4.18E-4	0.99635
	2	0.287	3.72E-4	0.99838

Table 6: Pseudo-first order rate constants for SPAAC with diyne **6**.

Pseudo-first order rate constants (k_0) obtained were plotted against the concentration of benzyl azide for the determination of second order rate constant (k).

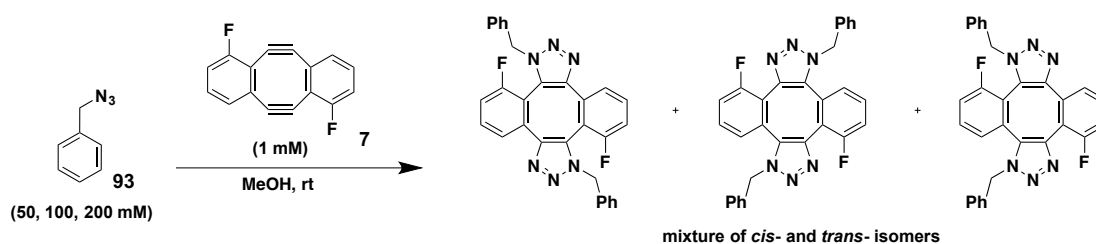


Run	Second order rate constant (M ⁻¹ min ⁻¹)	Second order rate constant (M ⁻¹ s ⁻¹)	Mean second order rate constant k (M ⁻¹ s ⁻¹)	Standard error
1	2.745	0.04575	0.04721	1.5E-3
2	2.920	0.04867		

Table 7: Second order rate constants for SPAAC with diyne **6**.

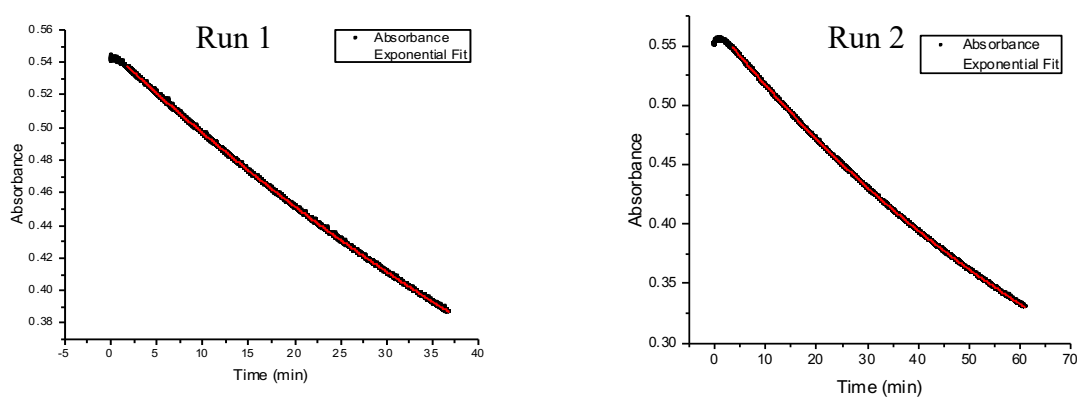
Mean second order rate constant, $k = 0.047 \pm 1.5E-3$ M⁻¹ s⁻¹

4.1.4 Kinetic analysis of diyne 7

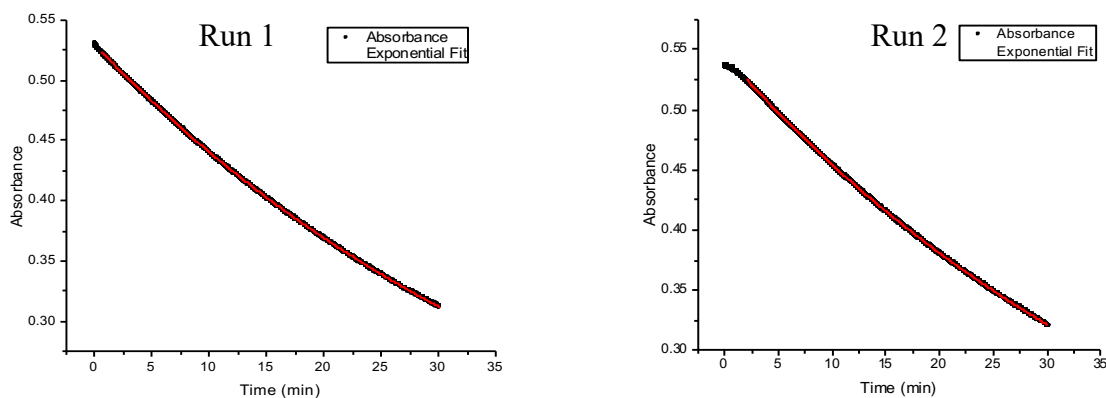


Scheme 59: SPAAC of diyne **7** with benzyl azide.

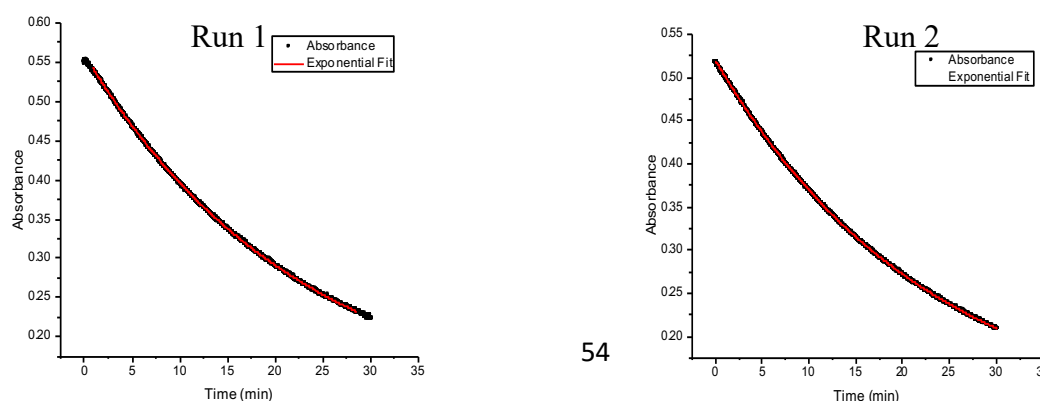
Time-dependent absorbance of diyne **7** (initial concentration of 2.0 mM) at 394 nm of wavelength was monitored in duplicate during the reaction with 50 mM benzyl azide.



Time-dependent absorbance of diyne **7** (initial concentration of 2.0 mM) at 394 nm of wavelength was monitored in duplicate during the reaction with 100 mM benzyl azide.



Time-dependent absorbance of diyne **7** (initial concentration of 2.0 mM) at 394 nm of wavelength was monitored in duplicate during the reaction with 200 mM benzyl azide.

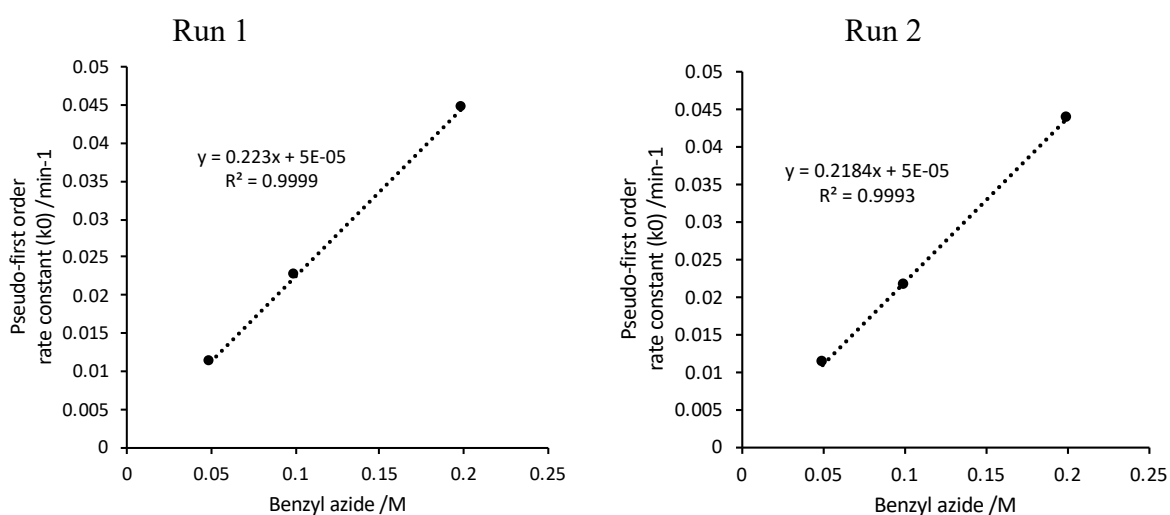


Pseudo-first order rate constants (k_0) were determined for diyne **7** by fitting of the absorbance versus time data to the following exponential equation ($y = A \cdot \exp(-k_0 \cdot x) + y_0$) using Origin.

Benzyl azide	Run	Pseudo-first order rate constant k_0 (min ⁻¹)	Standard error	R ²
50 mM	1	0.011	1.23E-6	0.99994
	2	0.011	3.53E-6	0.99998
100 mM	1	0.022	8.51E-6	0.99998
	2	0.021	9.23E-6	0.99998
200 mM	1	0.045	1.73E-5	0.99994
	2	0.044	1.02E-5	0.99997

Table 8: Pseudo-first order rate constants for SPAAC with diyne **7**.

Pseudo-first order rate constants (k_0) obtained were plotted against the concentration of benzyl azide for the determination of second order rate constant (k).

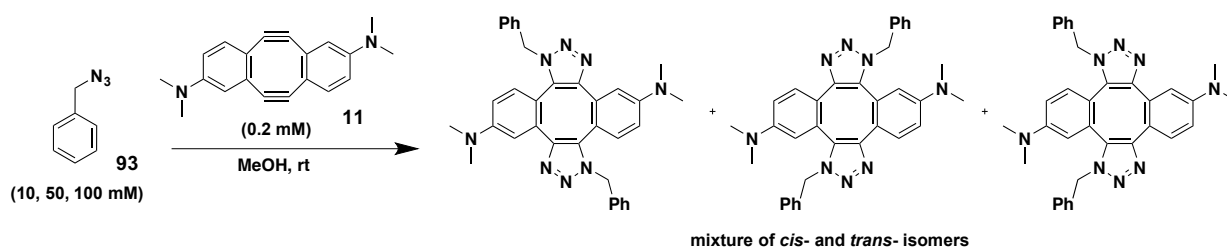


Run	Second order rate constant (M ⁻¹ min ⁻¹)	Second order rate constant (M ⁻¹ s ⁻¹)	Mean second order rate constant k (M ⁻¹ s ⁻¹)	Standard error
1	0.223	0.003717	0.00367	4.2E-5
2	0.218	0.003633		

Table 9: Second order rate constants for SPAAC with diyne **7**.

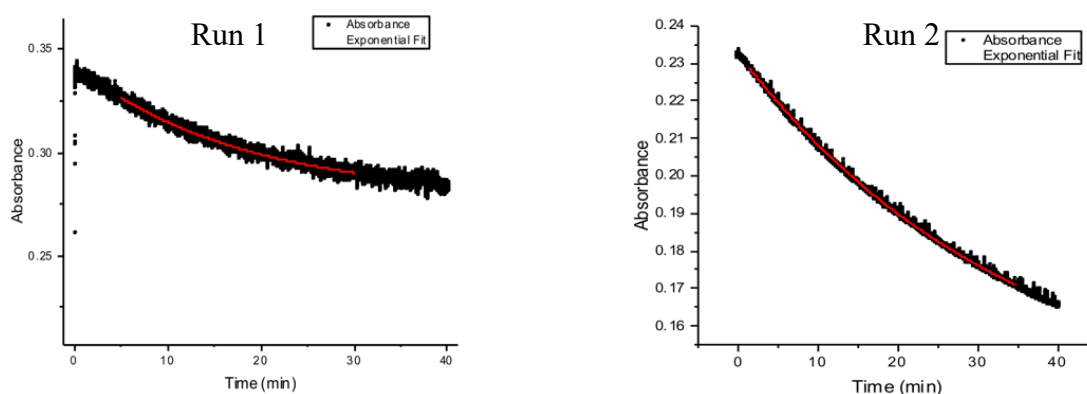
Mean second order rate constant, $k = 0.003 \pm 4.2E-5$ M⁻¹ s⁻¹

4.1.5 Kinetic analysis of diyne **11**

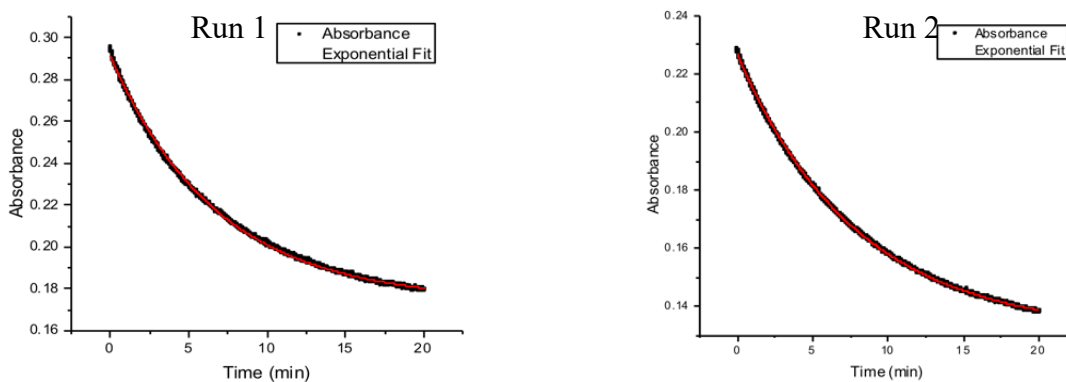


Scheme 60: SPAAC of diyne **11** with benzyl azide.

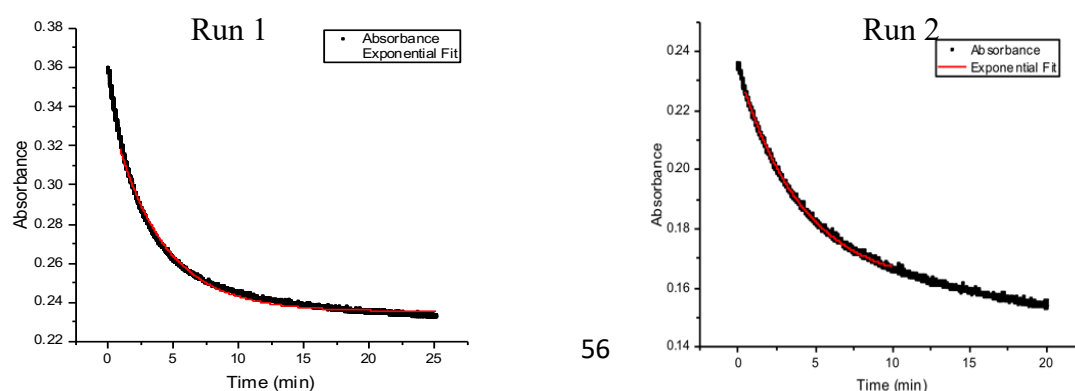
Time-dependent absorbance of diyne **11** (initial concentration of 0.4 mM) at 372 nm of wavelength was monitored in duplicate during the reaction with 10 mM benzyl azide.



Time-dependent absorbance of diyne **11** (initial concentration of 0.4 mM) at 372 nm of wavelength was monitored in duplicate during the reaction with 50 mM benzyl azide.



Time-dependent absorbance of diyne **11** (initial concentration of 0.4 mM) at 372 nm of wavelength was monitored in duplicate during the reaction with 100 mM benzyl azide.

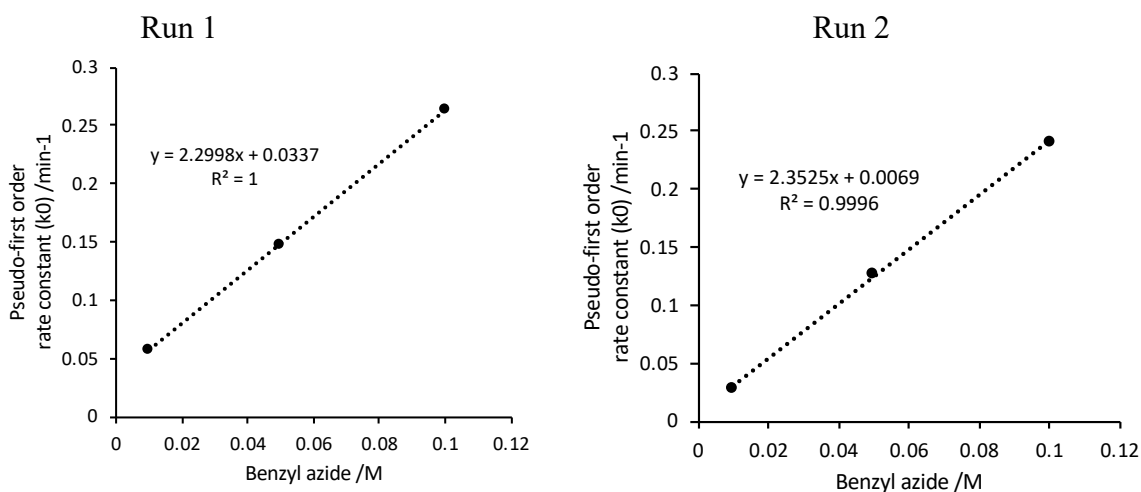


Pseudo-first order rate constants (k_0) were determined for diyne **11** by fitting of the absorbance versus time data to the following exponential equation ($y = A \cdot \exp(-k_0 \cdot x) + y_0$) using Origin.

Benzyl azide	Run	Pseudo-first order rate constant k_0 (min ⁻¹)	Standard error	R ²
10 mM	1	0.057	4.59E-4	0.97066
	2	0.029	4.40E-5	0.99931
50 mM	1	0.148	8.51E-6	0.99998
	2	0.127	6.09E-5	0.99977
100 mM	1	0.264	3.77E-4	0.99939
	2	0.241	3.84E-4	0.99899

Table 10: Pseudo-first order rate constants for SPAAC with diyne **11**.

Pseudo-first order rate constants (k_0) obtained were plotted against the concentration of benzyl azide for the determination of second order rate constant (k).

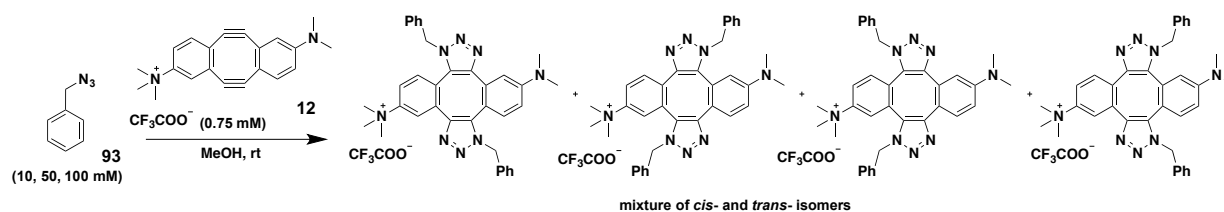


Run	Second order rate constant (M ⁻¹ min ⁻¹)	Second order rate constant (M ⁻¹ s ⁻¹)	Mean second order rate constant k (M ⁻¹ s ⁻¹)	Standard error
1	2.300	0.038333	0.038683	3.50E-4
2	2.342	0.039033		

Table 11: Second order rate constants for SPAAC with diyne **11**.

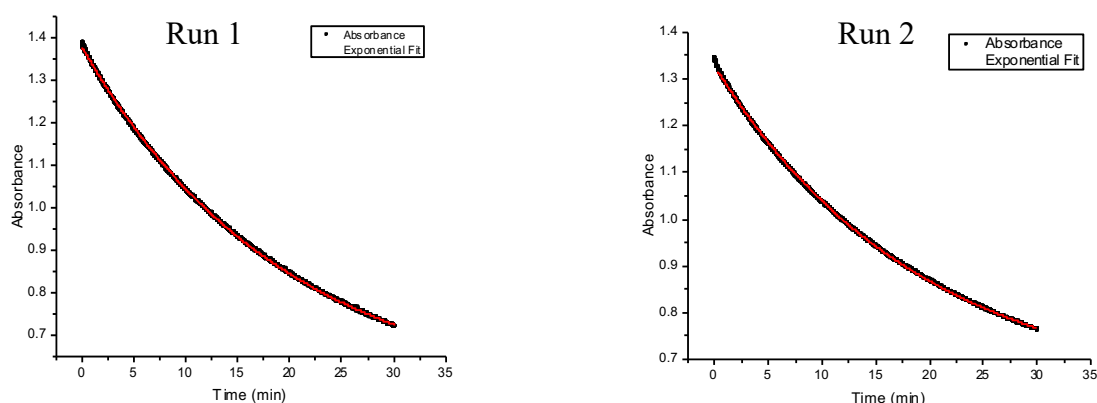
Mean second order rate constant, $k = 0.039 \pm 3.5\text{E-}4 \text{ M}^{-1} \text{ s}^{-1}$

4.1.6 Kinetic analysis of diyne **12**

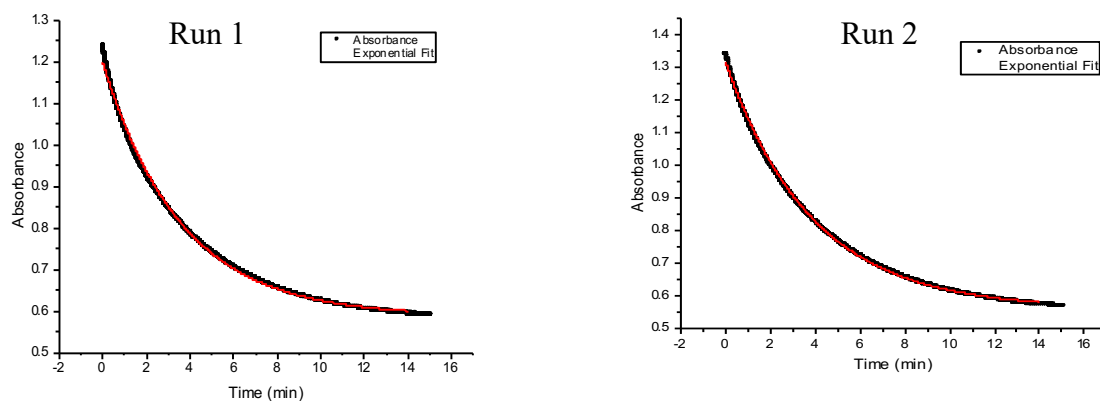


Scheme 61: SPAAC of diyne **12** with benzyl azide.

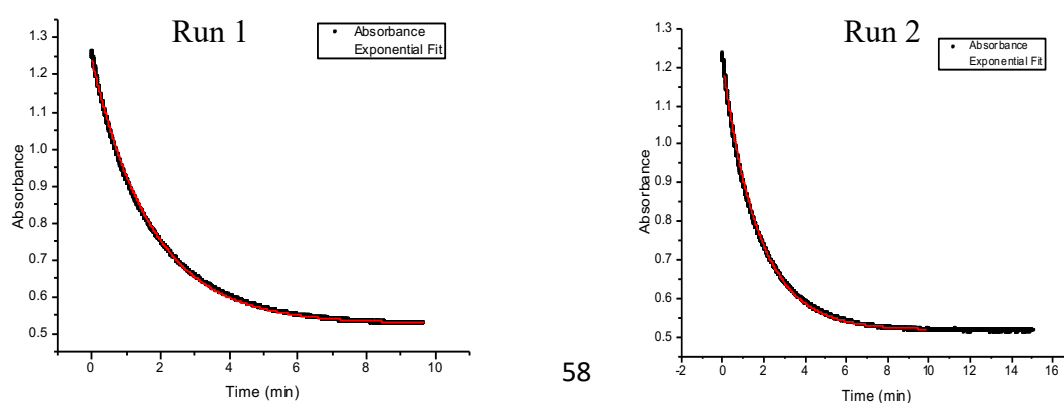
Time-dependent absorbance of diyne **12** (initial concentration of 1.5 mM) at 385 nm of wavelength was monitored in duplicate during the reaction with 10 mM benzyl azide.



Time-dependent absorbance of diyne **12** (initial concentration of 1.5 mM) at 385 nm of wavelength was monitored in duplicate during the reaction with 50 mM benzyl azide.



Time-dependent absorbance of diyne **12** (initial concentration of 1.5 mM) at 385 nm of wavelength was monitored in duplicate during the reaction with 100 mM benzyl azide.

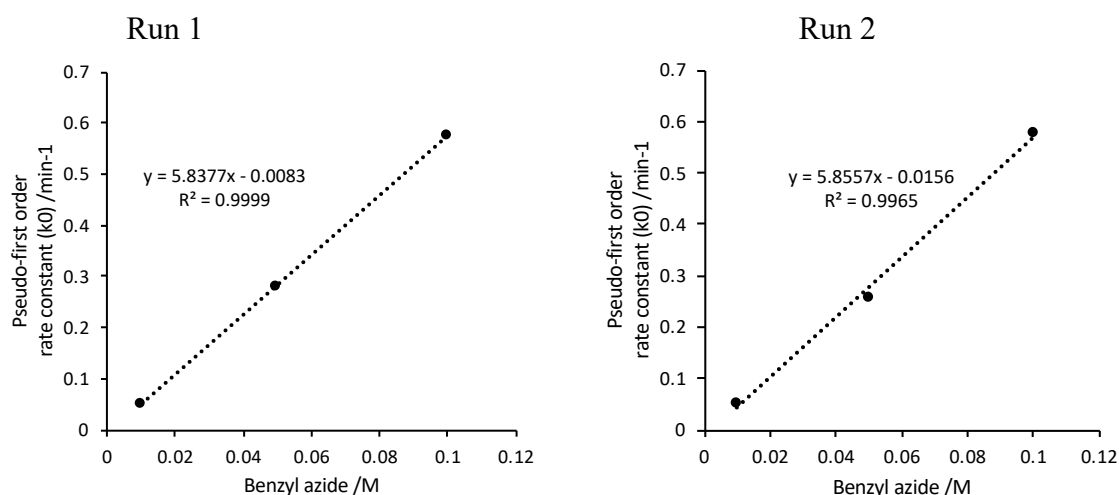


Pseudo-first order rate constants (k_0) were determined for diyne **12** by fitting of the absorbance versus time data to the following exponential equation ($y = A \cdot \exp(-k_0 \cdot x) + y_0$) using Origin.

Benzyl azide	Run	Pseudo-first order rate constant k_0 (min ⁻¹)	Standard error	R ²
10 mM	1	0.052	2.14E-5	0.99989
	2	0.053	2.26E-5	0.99988
50 mM	1	0.280	3.25E-4	0.99899
	2	0.259	1.94E-4	0.99938
100 mM	1	0.577	4.15E-4	0.99943
	2	0.578	3.58E-4	0.99956

Table 12: Pseudo-first order rate constants for SPAAC with diyne **12**.

Pseudo-first order rate constants (k_0) obtained were plotted against the concentration of benzyl azide for the determination of second order rate constant (k).

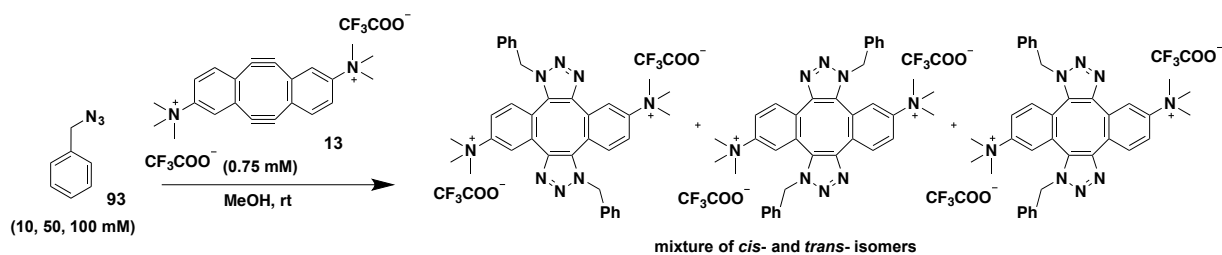


Run	Second order rate constant (M ⁻¹ min ⁻¹)	Second order rate constant (M ⁻¹ s ⁻¹)	Mean second order rate constant k (M ⁻¹ s ⁻¹)	Standard error
1	5.838	0.0973	0.09745	1.50E-4
2	5.856	0.0976		

Table 13: Second order rate constants for SPAAC with diyne **12**.

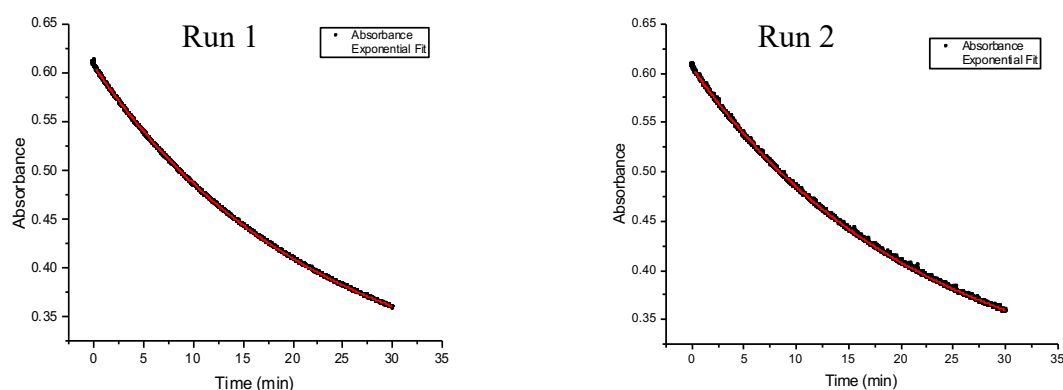
Mean second order rate constant, $k = 0.097 \pm 1.5\text{E-}4 \text{ M}^{-1} \text{ s}^{-1}$

4.1.7 Kinetic analysis of diyne **13**

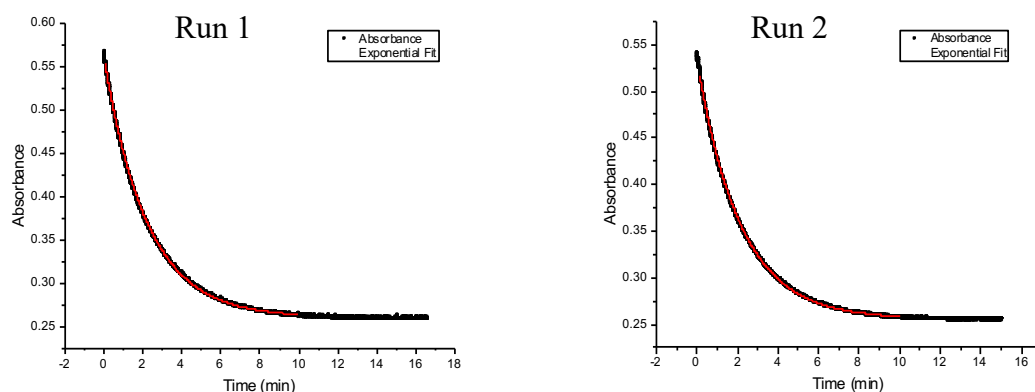


Scheme 62: SPAAC of diyne **13** with benzyl azide.

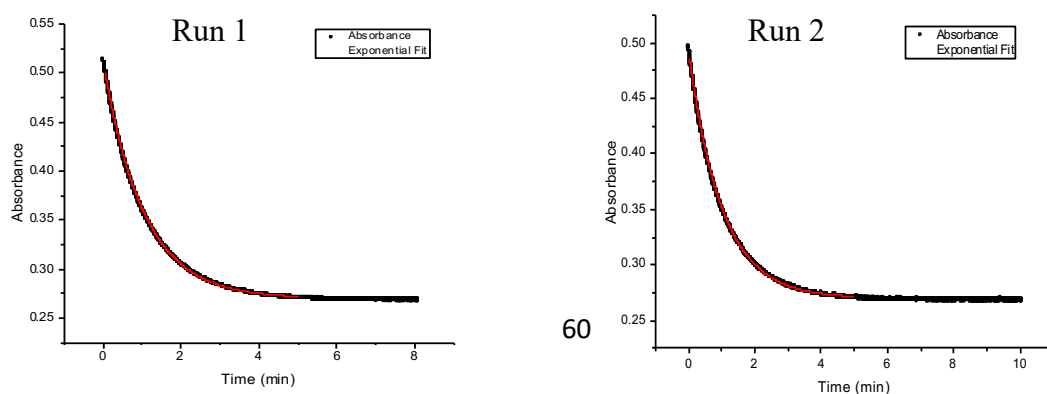
Time-dependent absorbance of diyne **13** (initial concentration of 1.5 mM) at 372 nm of wavelength was monitored in duplicate during the reaction with 10 mM benzyl azide.



Time-dependent absorbance of diyne **13** (initial concentration of 1.5 mM) at 372 nm of wavelength was monitored in duplicate during the reaction with 50 mM benzyl azide.



Time-dependent absorbance of diyne **13** (initial concentration of 1.5 mM) at 372 nm of wavelength was monitored in duplicate during the reaction with 100 mM benzyl azide.

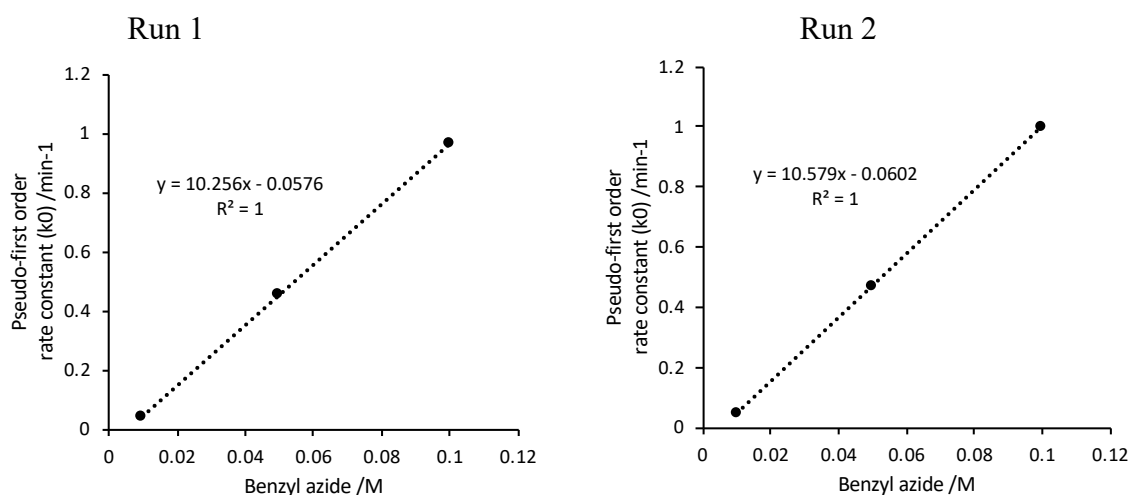


Pseudo-first order rate constants (k_0) were determined for diyne **13** by fitting of the absorbance versus time data to the following exponential equation ($y = A \cdot \exp(-k_0 \cdot x) + y_0$) using Origin.

Benzyl azide	Run	Pseudo-first order rate constant k_0 (min ⁻¹)	Standard error	R ²
10 mM	1	0.045	1.40E-5	0.99995
	2	0.046	2.56E-5	0.99984
50 mM	1	0.455	2.12E-4	0.99979
	2	0.468	2.24E-4	0.99977
100 mM	1	0.968	6.00E-4	0.9998
	2	0.998	7.33E-4	0.99972

Table 14: Pseudo-first order rate constants for SPAAC with diyne **13**.

Pseudo-first order rate constants (k_0) obtained were plotted against the concentration of benzyl azide for the determination of second order rate constant (k).

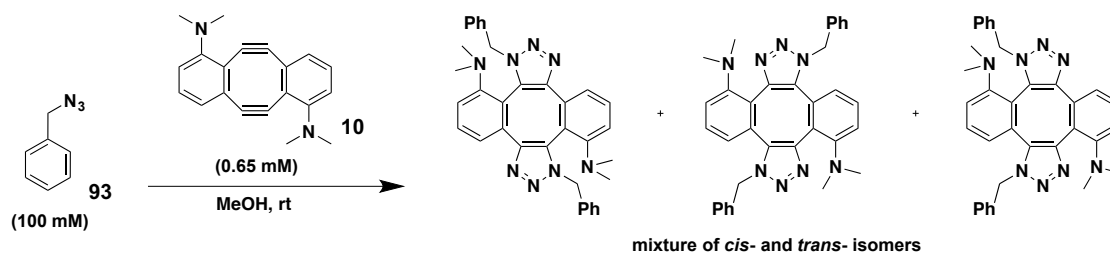


Run	Second order rate constant (M ⁻¹ min ⁻¹)	Second order rate constant (M ⁻¹ s ⁻¹)	Mean second order rate constant k (M ⁻¹ s ⁻¹)	Standard error
1	10.256	0.170933	0.173625	2.69E-4
2	10.579	0.176317		

Table 15: Second order rate constants for SPAAC with diyne **13**.

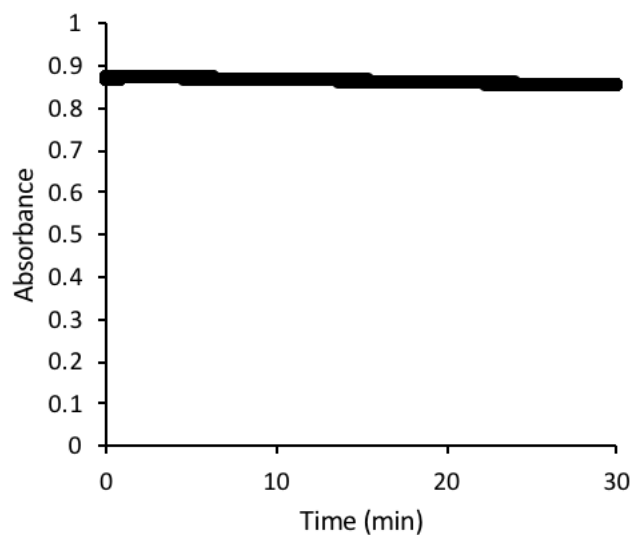
Mean second order rate constant, $k = 0.174 \pm 2.7\text{E-}4 \text{ M}^{-1} \text{ s}^{-1}$

4.1.8 Kinetic analysis of diyne **10**

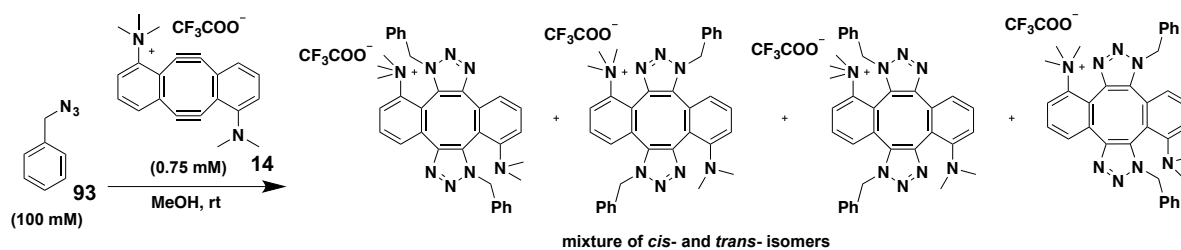


Scheme 63: SPAAC of diyne **10** with benzyl azide.

Time-dependent absorbance of diyne **10** (initial concentration of 1.3 mM) at 372 nm of wavelength was monitored during the reaction with 100 mM benzyl azide. No appreciable change in the absorbance was noted.

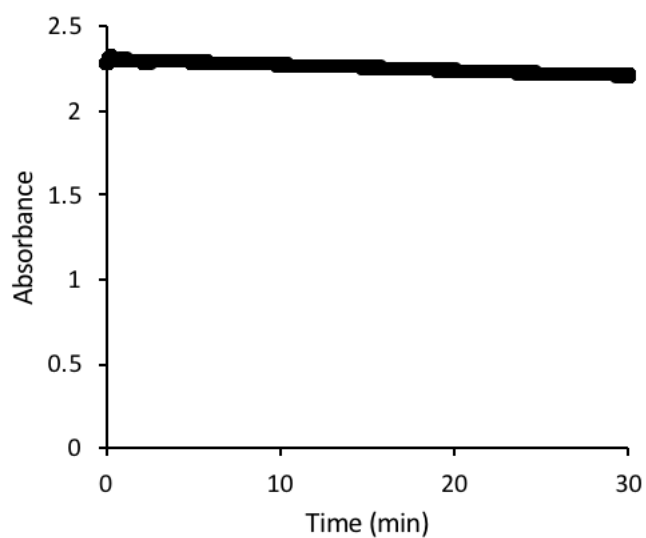


4.1.9 Kinetic analysis of diyne **14**

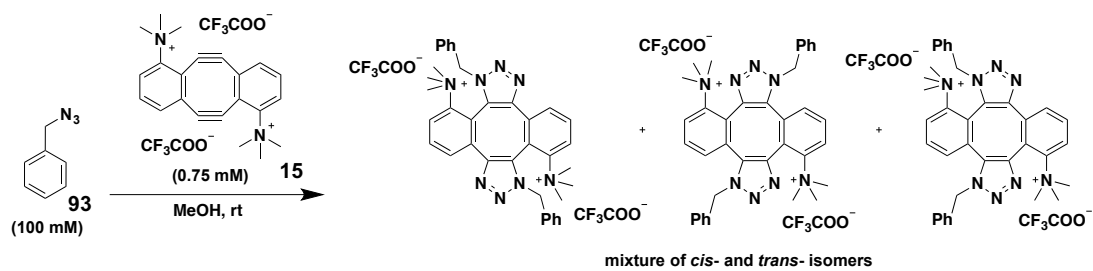


Scheme 64: SPAAC of diyne **14** with benzyl azide.

Time-dependent absorbance of diyne **14** (initial concentration of 1.5 mM) at 372 nm of wavelength was monitored during the reaction with 100 mM benzyl azide. No appreciable change in the absorbance was noted.

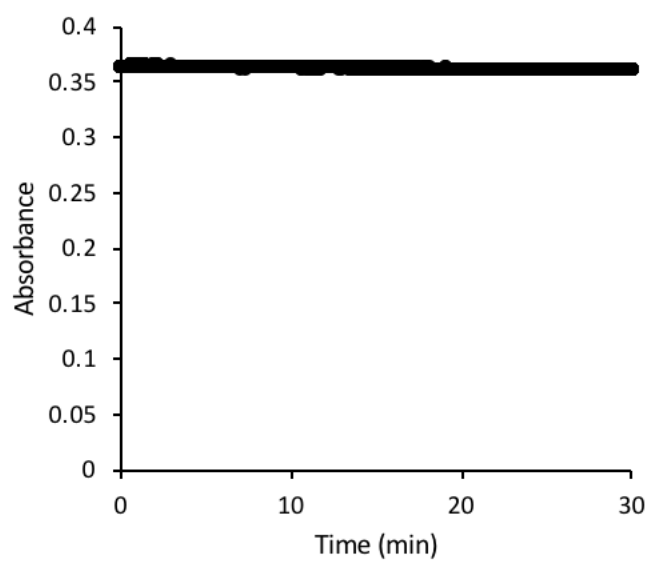


4.1.10 Kinetic analysis of diyne **15**



Scheme 65: SPAAC of diyne **15** with benzyl azide.

Time-dependent absorbance of diyne **15** (initial concentration of 1.5 mM) at 372 nm of wavelength was monitored during the reaction with 100 mM benzyl azide. No appreciable change in the absorbance was noted.



4.1.11 Discussion of kinetic analysis results

The second-order rate constants determined experimentally for substituted Sondheimer dialkynes are depicted in figure 28.

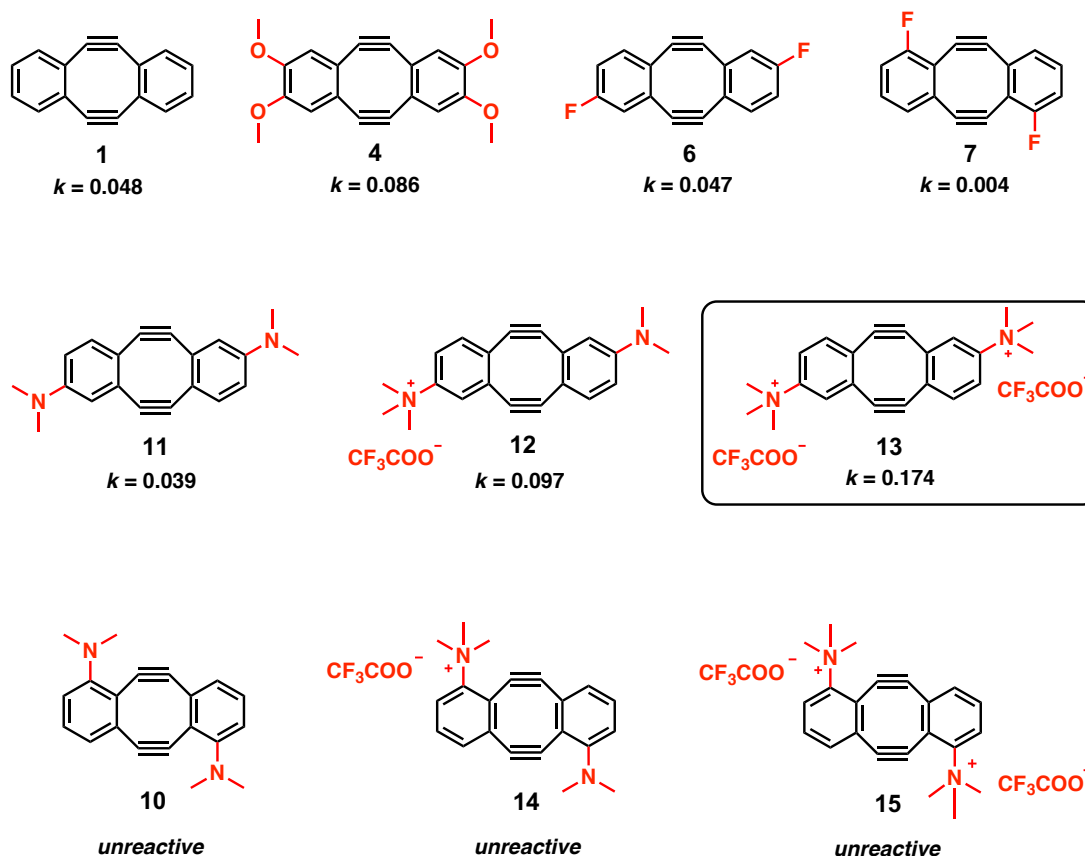


Figure 28: Experimentally determined second-order rate constants (k , in $\text{M}^{-1} \text{s}^{-1}$) of substituted Sondheimer diynes in SPAAC with benzyl azide in MeOH at rt.

We observed that the presence of dimethylamine at the *meta*-position (*m*-NMe₂ **11**, $0.039 \text{ M}^{-1} \text{s}^{-1}$) led to a slight reduction in the rate of SPAAC reaction of Sondheimer dialkyne **1** ($0.048 \text{ M}^{-1} \text{s}^{-1}$)^{76, 116}. However, substitution of a single dimethylamine substituent at the *meta*-position in **11** with a charged trimethylammonium group (*m*-NMe₃⁺ **12**, $0.097 \text{ M}^{-1} \text{s}^{-1}$) led to a 2.5-fold increase in the rate when compared to **11**. Installation of another trimethylammonium substituent at *meta*-position in **12** (di-*m*-NMe₃⁺ **13**, $0.174 \text{ M}^{-1} \text{s}^{-1}$) pleasingly led to a further 1.8-fold increase in the rate over mono-charged diyne **12**. Presence of methoxy-substituent at the *meta*-position (tetra-OMe **4**, $0.086 \text{ M}^{-1} \text{s}^{-1}$) was also found to increase the reactivity of Sondheimer diyne **1** by 1.8-fold, which is consistent with previous studies.^{76, 116}

Presence of a substituent at the *ortho*-position led to a significant decrease in the rate of SPAAC reaction of **1**. A fluoro-substituent at the *meta*-position (*m*-F **6**, $0.047 \text{ M}^{-1} \text{s}^{-1}$) did not

have any considerable effect on the rate of reaction of **1**. On the other hand, a fluoro-substituent at the *ortho*-position (*o*-F **7**, $0.004 \text{ M}^{-1} \text{ s}^{-1}$) resulted in about ten-fold decrease in the rate of reaction compared to **1** and **6**. Moreover, presence of a larger dimethylamine substituent *ortho* to the alkyne (*o*-NMe₂ **10**) led to a further decrease in reactivity making it essentially unreactive towards benzyl azide at rt. Similarly, dialkynes bearing a charged trimethylammonium substituent at the *ortho*-position (*o*-NMe₃⁺ **14**, di-*o*-NMe₃⁺ **15**) were also found to be unreactive. Overall, di-*m*-NMe₃⁺ substituted **13** was found to be the most reactive dialkyne exhibiting 3.6-fold increase in reactivity over Sondheimer dialkyne **1**.

In order to understand this observed contrast in reactivity between the *ortho* and *meta*-amine substituted diynes (**10**, **11**, **12**, **13**) X-ray crystallographic analysis was employed.

4.2 X-ray crystallographic analysis

X-ray crystal structures of *ortho* and *meta*-amine substituted diynes (**10**, **11**, **12**, **13**) were determined successfully with the help of Dr Andrew Bond at the Department of Chemistry, University of Cambridge (Figure 29).

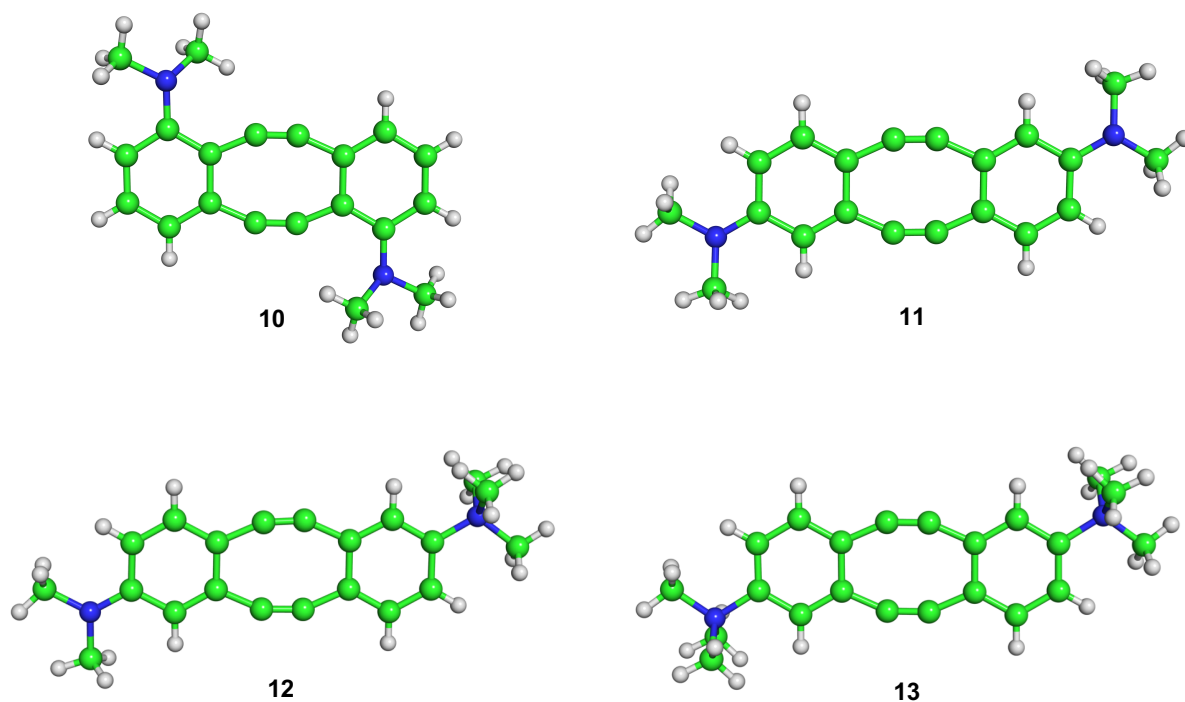


Figure 29: X-ray crystal structures of *ortho* and *meta*-amine substituted dialkynes.

Previously, Bertozzi and co-workers have demonstrated how alkyne bond angles in strained cyclooctyne reagents can be used as a measure to predict their reactivity.¹¹⁷ They observed that a decrease in the alkyne bond angle reflects in an increased azide reactivity of the strained cyclooctyne (Table 16). For instance, installation of methoxy substituents and nitrogen atom within the cyclooctyne ring (DIMAC⁶⁷) leads to only minor deviations in the alkyne bond angles (1° and 2° respectively). However, installation of a fluoro substituent at the propargylic position of cyclooctyne (MOFO⁶⁹) leads to a slight distortion of alkyne bond angle b (by 4°, 159° vs 155°) through a bond polarisation mechanism. This is reflected by a slightly increased reactivity of MOFO over DIMAC ($k_{\text{MOFO}} = 4.3 \times 10^{-3} \text{ M}^{-1} \text{ s}^{-1}$ and $k_{\text{DIMAC}} = 3.0 \times 10^{-3} \text{ M}^{-1} \text{ s}^{-1}$). Installation of another fluorine atom at the propargylic position of MOFO (DIFO2¹¹⁸) leads to a further distortion of alkyne bond angle b (by 4°, 155° vs 151°), which is reflected by a significantly increased azide reactivity of DIFO2 over MOFO ($k_{\text{DIFO2}} = 4.2 \times 10^{-2} \text{ M}^{-1} \text{ s}^{-1}$).

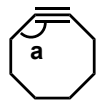
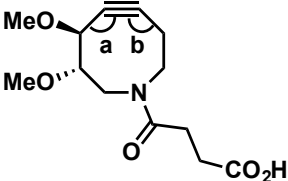
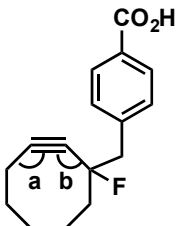
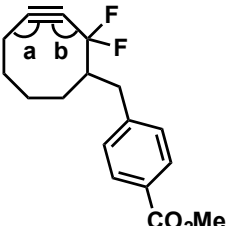
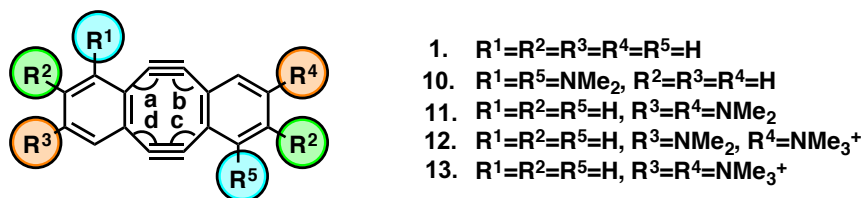
Strained alkyne	angle a (°)	angle b (°)	Rate constant (M ⁻¹ s ⁻¹)
 cyclooctyne	159	N/A	N/A
 DIMAC	158	157	3.0×10^{-3}
 MOFO	160	155	4.3×10^{-3}
 DIFO2	162	151	4.2×10^{-2}

Table 16: Correlation between reactivity and alkyne bond angles of strained cyclooctynes.

Hence, we sought to determine how the presence of different substituents would affect structural changes in our substituted Sondheimer diynes. Alkyne bond angles measured experimentally *via* X-ray crystallography for **10-13** (Figure 29) are depicted in Figure 30. From the resulting structural data obtained we noted that the presence of a dimethylamine substituent at either *ortho* or *meta*-position (**10**, **11**) did not result in any significant structural change on Sondheimer diyne **1** (Figure 30). A charged trimethylammonium substituent (**12**)

at the *meta*-position, however, did result in minor structural changes on the diyne distorting the alkyne bond angles slightly, reflecting an increased reactivity.



Diyne	angle a (°)	angle b (°)	angle c (°)	angle d (°)
1	156.4	155.3	155.3	155.3
10	156.3	156.5	156.3	156.5
11	156.3	155.2	156.3	155.2
12	158.6	153.1	154.5	156.9
13	155.5	156.3	155.5	156.3

Figure 30: X-ray crystal structure data (alkyne bond angles) of **10**, **11**, **12**, and **13**.

These observations suggested that alkyne bond angle distortion is not the sole factor involved in determining the reactivity of substituted Sondheimer dialkynes and that there are other potential factors like steric and electronic effects playing a role. This prompted us to further investigate the observed contrast in reactivity between *ortho*- and *meta*-substituted Sondheimer dialkynes by performing detailed computational studies which will be discussed at length in Chapter 5.

5. Computational Studies: Prediction of SPAAC reactivity

5.1 Prediction of alkyne bond angles and strain energies of substituted Sondheimer dialkynes

Previously, Bertozzi and co-workers have demonstrated how an alkyne bond angle analysis through computational studies can enable prediction of the reactivity of strained alkyne reagents.¹¹⁷ Hence, a computational analysis was performed to calculate the alkyne bond angles for our substituted Sondheimer dialkynes **4**, **6**, **7**, **10-13**. Geometry optimized structures of substituted Sondheimer dialkynes were calculated using Gaussian 09¹¹⁹ with the B3LYP density functional and the 6-31G(d) basis set within the CPCM model for methanol as solvent at standard conditions (Figure 31, see Chapter 8 for further details). The above parameters were selected as previous computational studies with these on similar systems have provided results in accordance with the experiment.^{115, 117, 120-121} Single-point energies were calculated using M06-2X¹²², the polarised, triple- ζ valence quality def2-TZVPP basis set of Weigend and Ahlrichs¹²³ and an ultrafine integration grid within the CPCM model (methanol). The resulting energies were used to correct the energies obtained from the B3LYP optimizations¹²⁴⁻¹²⁵. The computationally obtained geometry optimized structures of the *ortho*- and *meta*-amine substituted diynes **10-13** corroborated with their X-ray crystal structures depicted in figure 29.

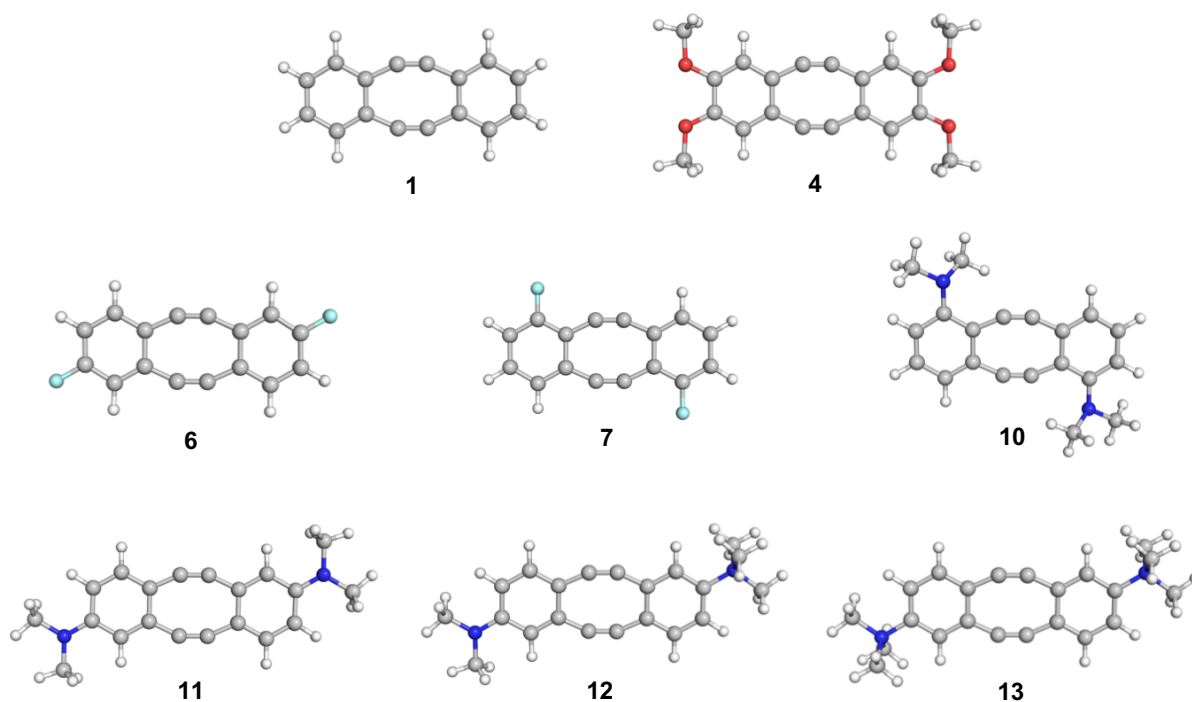
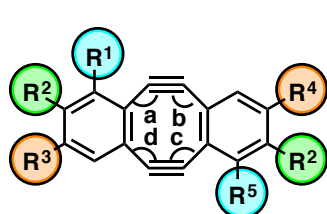


Figure 31: DFT geometry optimized structures of substituted Sondheimer dialkynes.

The alkyne bond angles were measured from the geometry optimized structures (Figure 32). These results indicated that presence of a fluoro or amine substituent at *ortho*- or *meta*-position (6, 7, 10-13) did not result in any significant structural change on Sondheimer dialkyne 1.



1. $R^1=R^2=R^3=R^4=R^5=H$
4. $R^1=R^5=H, R^2=R^3=R^4=OMe$
6. $R^1=R^2=R^5=H, R^3=R^4=F$
7. $R^1=R^5=F, R^2=R^3=R^4=H$
10. $R^1=R^5=NMe_2, R^2=R^3=R^4=H$
11. $R^1=R^2=R^5=H, R^3=R^4=NMe_2$
12. $R^1=R^2=R^5=H, R^3=NMe_2, R^4=NMe_3^+$
13. $R^1=R^2=R^5=H, R^3=R^4=NMe_3^+$

Diyne	angle a (°)	angle b (°)	angle c (°)	angle d (°)
1	155.5 (156.4)	155.5 (155.3)	155.5 (155.3)	155.5 (155.3)
4	155.4	155.2	155.4	155.2
6	155.6	155.3	155.6	155.3
7	154.0	156.3	154.0	156.3
10	156.1 (156.3)	155.9 (156.5)	156.1 (156.3)	155.9 (156.5)
11	155.8 (156.3)	154.8 (155.2)	155.8 (156.3)	154.8 (155.2)
12	156.8 (158.6)	153.8 (153.1)	154.8 (154.5)	155.9 (156.9)
13	155.7 (155.5)	154.9 (156.3)	155.7 (155.5)	154.9 (156.3)

Figure 32. Calculated alkyne bond angles of substituted Sondheimer dialkynes (X-ray crystallography data shown in parenthesis).

Strain energies were also calculated for these substituted Sondheimer dialkynes in accordance with the work previously reported by Orita and co-workers (Table 17).⁷⁶ All of the substituted diynes showed similar values of strain energy.

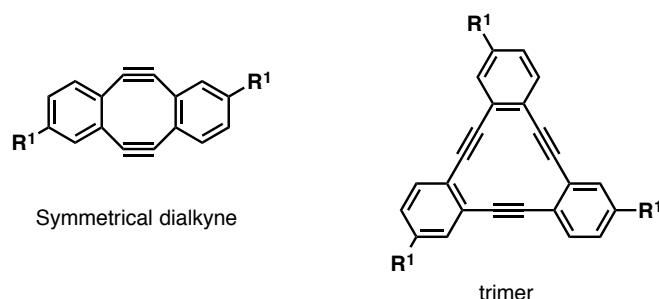
Strain energy of substituted Sondheimer dialkynes were calculated by using the following equations:

Strain energy calculation for symmetrical Sondheimer dialkynes (1, 4, 6, 7, 10, 11, 13)

$$E_{\text{strain}} = E_{\text{diyne}} - (2/3) * E_{\text{trimer}}$$

where E_{diyne} - Single point energy of the dialkyne

E_{trimer} - Single point energy of the corresponding trimer of the dialkyne

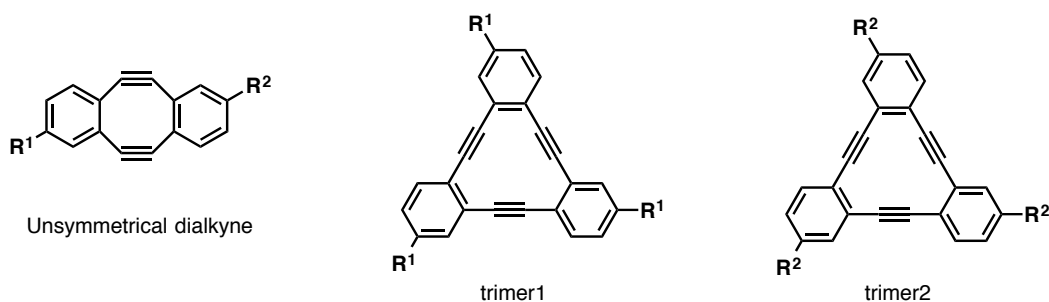


Strain energy calculation for unsymmetrical Sondheimer dialkyne (12)

$$E_{\text{strain}} = E_{\text{diyne}} - (1/3) * (E_{\text{trimer1}} + E_{\text{trimer2}})$$

where E_{diyne} - Single point energy of the dialkyne

E_{trimer1} and E_{trimer2} - Single point energy of the corresponding trimers each bearing the respective substituents of unsymmetrical dialkyne



Compound	E _{diyne}	E _{trimer}	E _{trimer1}	E _{trimer2}	E _{strain}
1	-385512.86	-578313.76	na	na	29.64
4	-672977.48	-1009513.1	na	na	31.27
6	-510076.11	-765158.53	na	na	29.58
7	-510074.69	-765156.93	na	na	29.92
10	-553638.20	-830502.07	na	na	29.85
11	-553632.06	-830491.51	na	na	28.95
12	-603500.57	na	-830502.07	-905293.37	28.34
13	-578570.91	-905293.37	na	na	27.57

Table 17: Strain energies of substituted Sondheimer dialkynes (energies in kcal/mol).

Generally, it was noted that substitution of Sondheimer diyne **1** did not result in any significant structural change and all substituted diynes demonstrated alkyne bond angles around 155°, along with similar strain energy values. This suggested that alkyne bond angle distortion and strain energy are not the sole factors determining the reactivity of these substituted strained alkynes and that there are other potential factors like steric and electronic effects playing a role.

5.2 Transition state barriers

To further investigate the effect of substituent on the reactivity of our amine and fluoro substituted Sondheimer diynes **6-7**, **10-13**, their transition state barriers were calculated in a SPAAC with benzyl azide in MeOH. Previously, Goddard and co-workers have computationally predicted a decrease in reactivity for dibenzocyclooctynes over cyclooctynes due to the resulting steric interference between the incoming azide and hydrogen atom on the benzene ring *ortho* to the alkyne (Figure 33).¹²⁶ A similar decrease in the reactivity in the presence of an *ortho*-substituent has also been observed by Bertozzi and co-workers with biarylazacyclooctynone (BARAC) based alkynes (Figure 33).¹¹⁷ They noted that the presence of a fluoro or methyl substituent *ortho* to the alkyne significantly diminishes the reactivity of BARAC which was reflected by a significant increase in the transition state barrier.

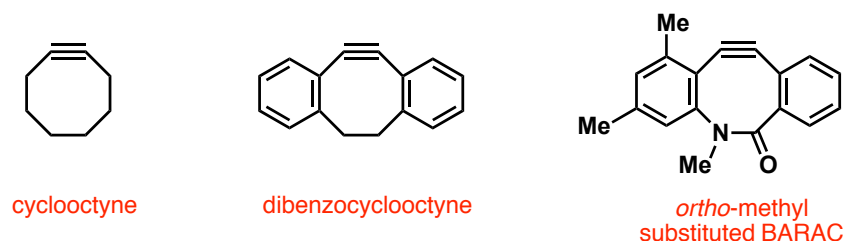


Figure 33. Effect of *ortho*-substituent on the reactivity of strained alkyne.

Investigations began with Sondheimer diyne **1** and the transition states for both first and second cycloaddition with benzyl azide in MeOH at rt were calculated. Due to the conformational flexibility of the benzyl group, multiple transition states were found for first and second cycloaddition (Figure 34, for further analysis details see 9. **Appendix** section). Hence, methyl azide **94** was chosen for further studies as it is less conformationally flexible than benzyl azide, and calculations show that it behaves similarly to benzyl azide in a SPAAC with **1**.¹¹⁷ The first cycloaddition with methyl azide leading to the formation of monoyne intermediate was found to be the rate-determining step, since the second cycloaddition demonstrated a lower activation energy barrier than the first (by 3.6 kcal/mol, Figure 35 and 36). This is in accordance with the results obtained by Hosoya and co-workers for the SPAAC of Sondheimer dialkyne **1** with methyl azide **94**.¹¹⁵

Thereby, the transition states and activation barriers of the first cycloaddition for all of our substituted Sondheimer diynes were calculated (Figure 37-43). Transition states were found for both *anti*- and *syn*-attack of methyl azide on diynes.

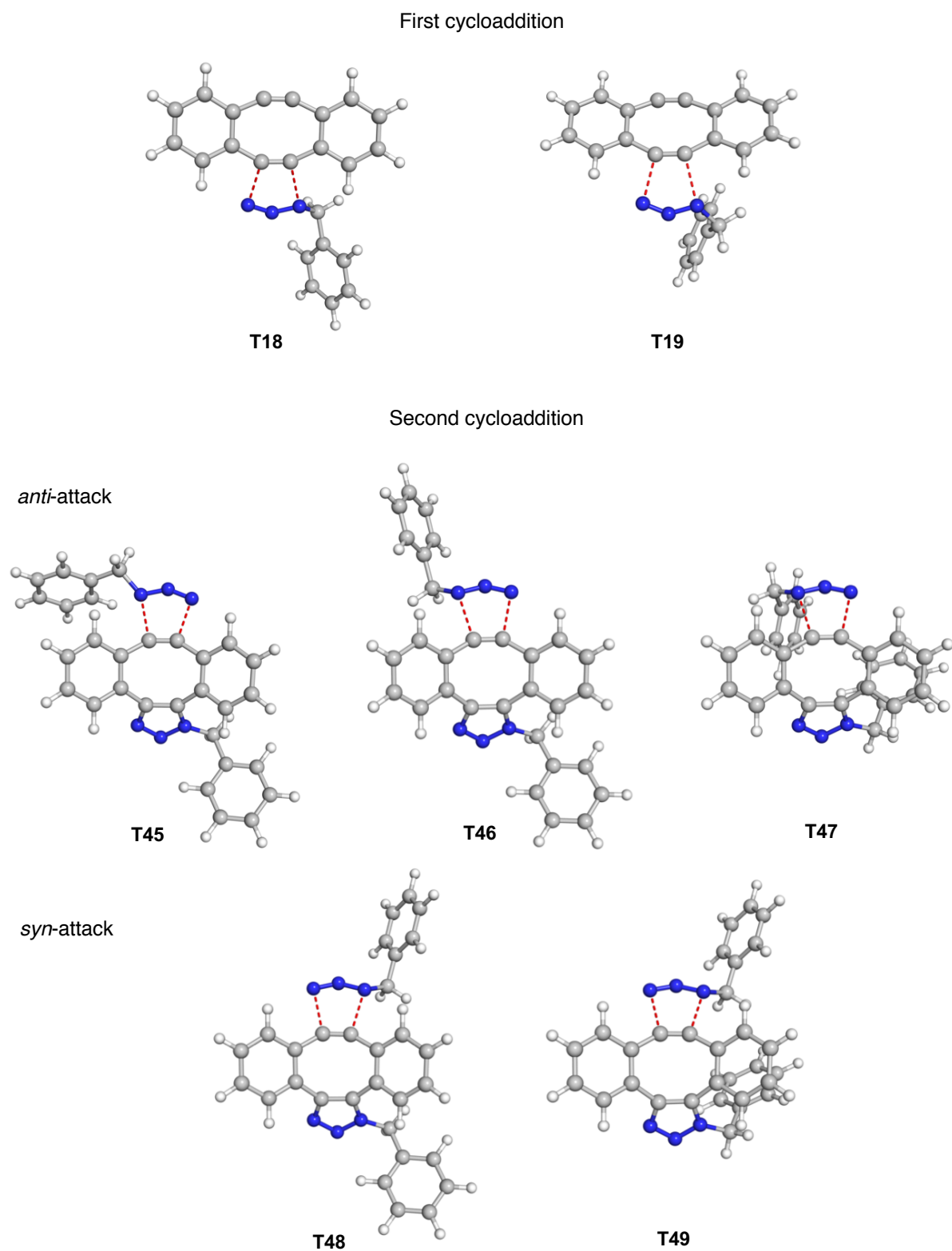


Figure 34. Multiple transition states found for first and second cycloaddition of Sondheimer dialkyne with benzyl azide due to the conformational flexibility of the benzyl group.

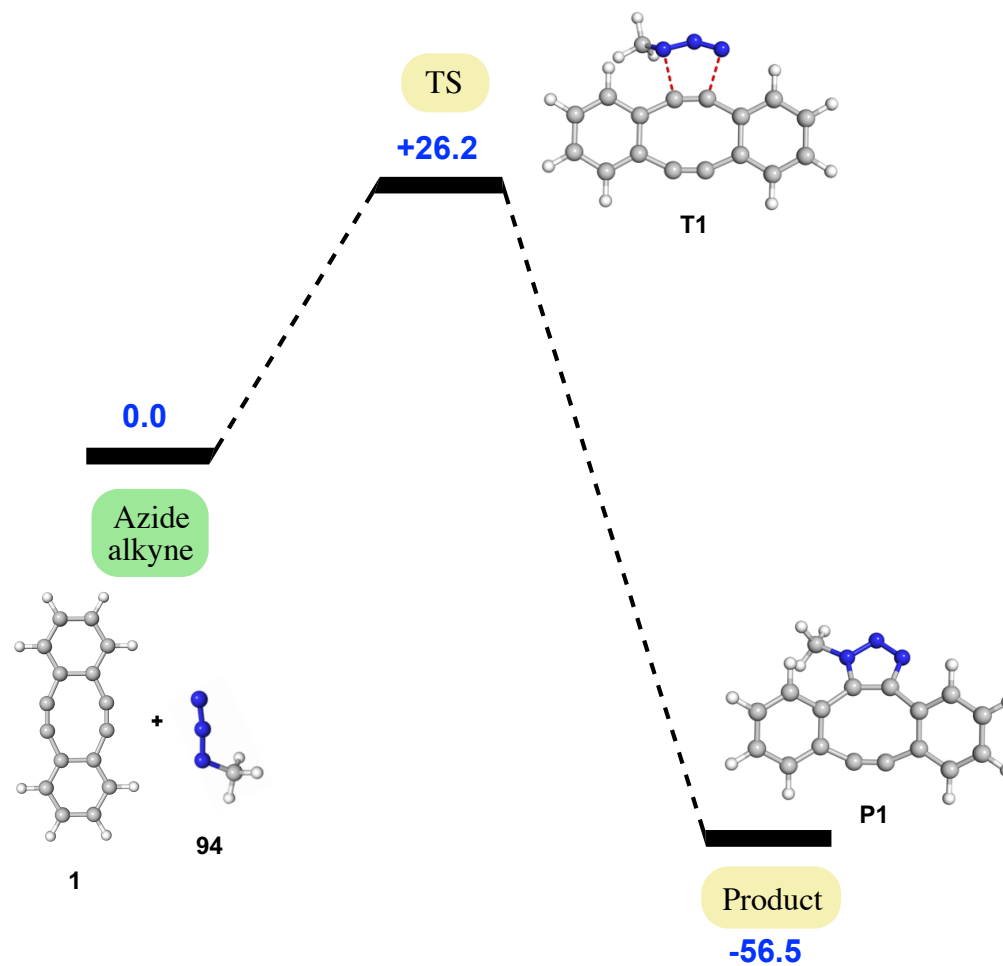


Figure 35: Energy level diagram depicting strain-promoted click reaction between Sondheimer dialkyne and methyl azide (energy values in kcal/mol).

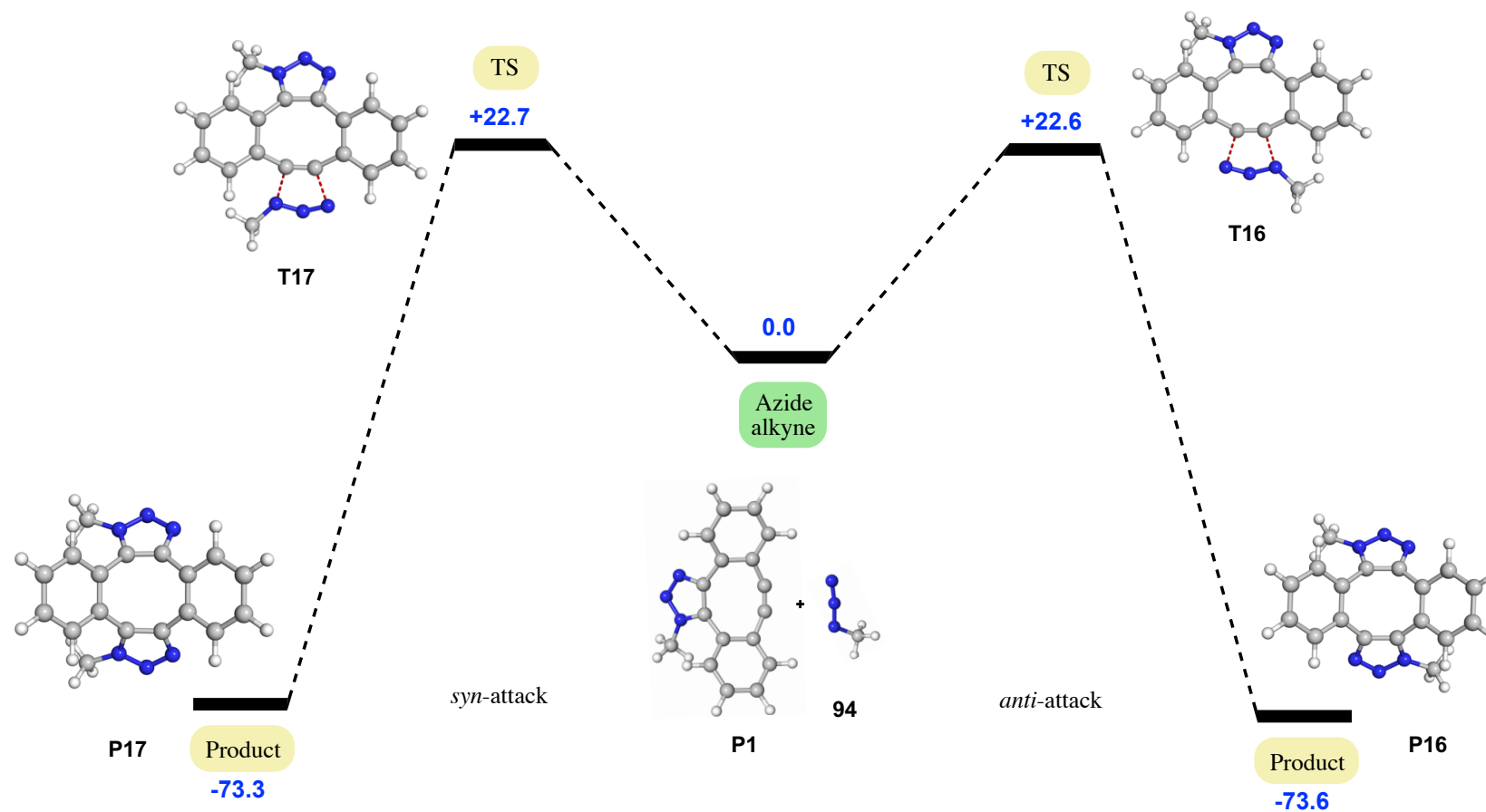


Figure 36: Energy level diagram depicting second strain-promoted azide-alkyne cycloaddition between Sondheimer dialkyne and methyl azide (energy values in kcal/mol).

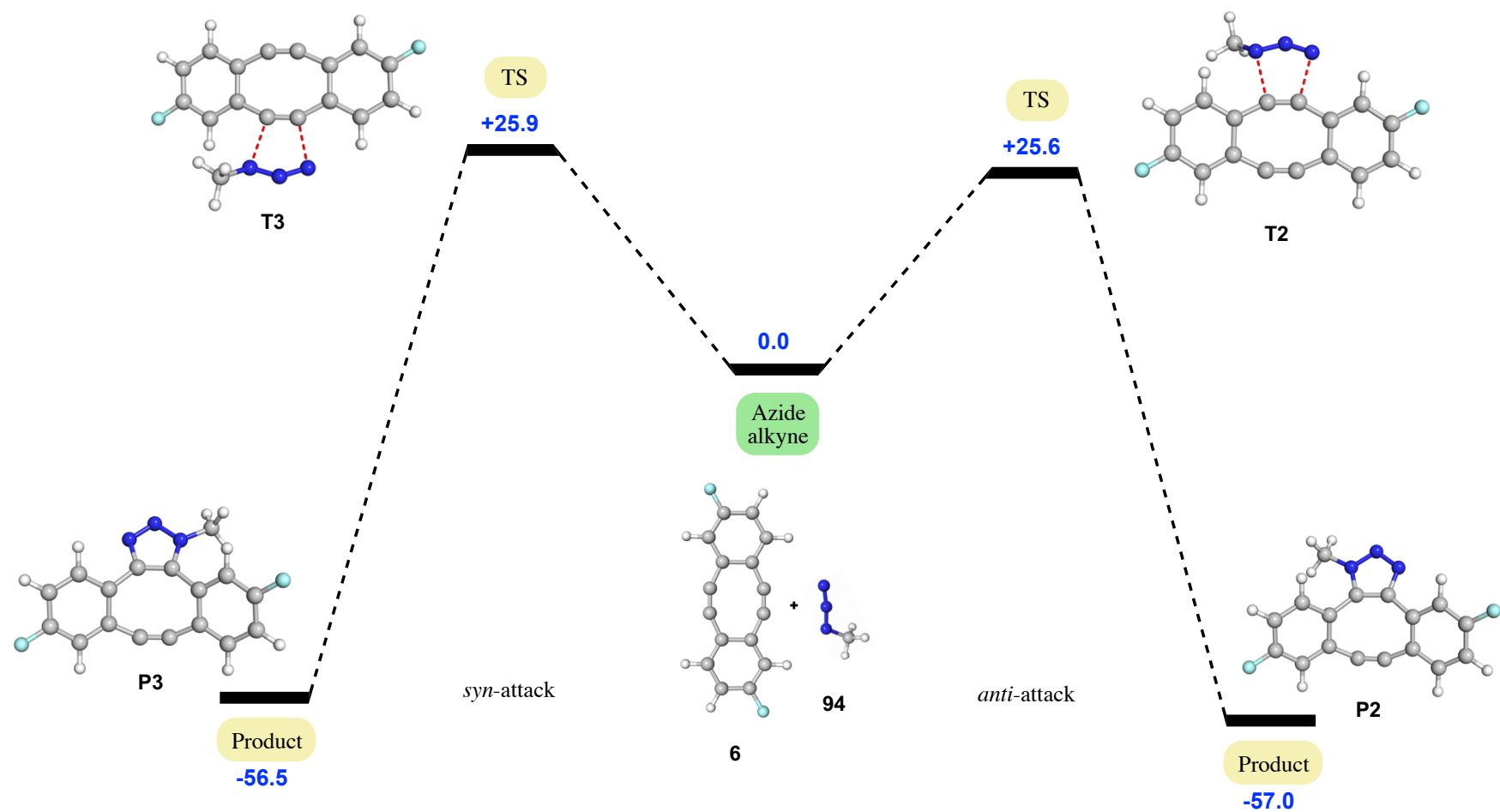


Figure 37: Energy level diagram depicting strain-promoted click reaction between *meta*-fluoro substituted Sondheimer dialkyne and methyl azide (energy values in kcal/mol).

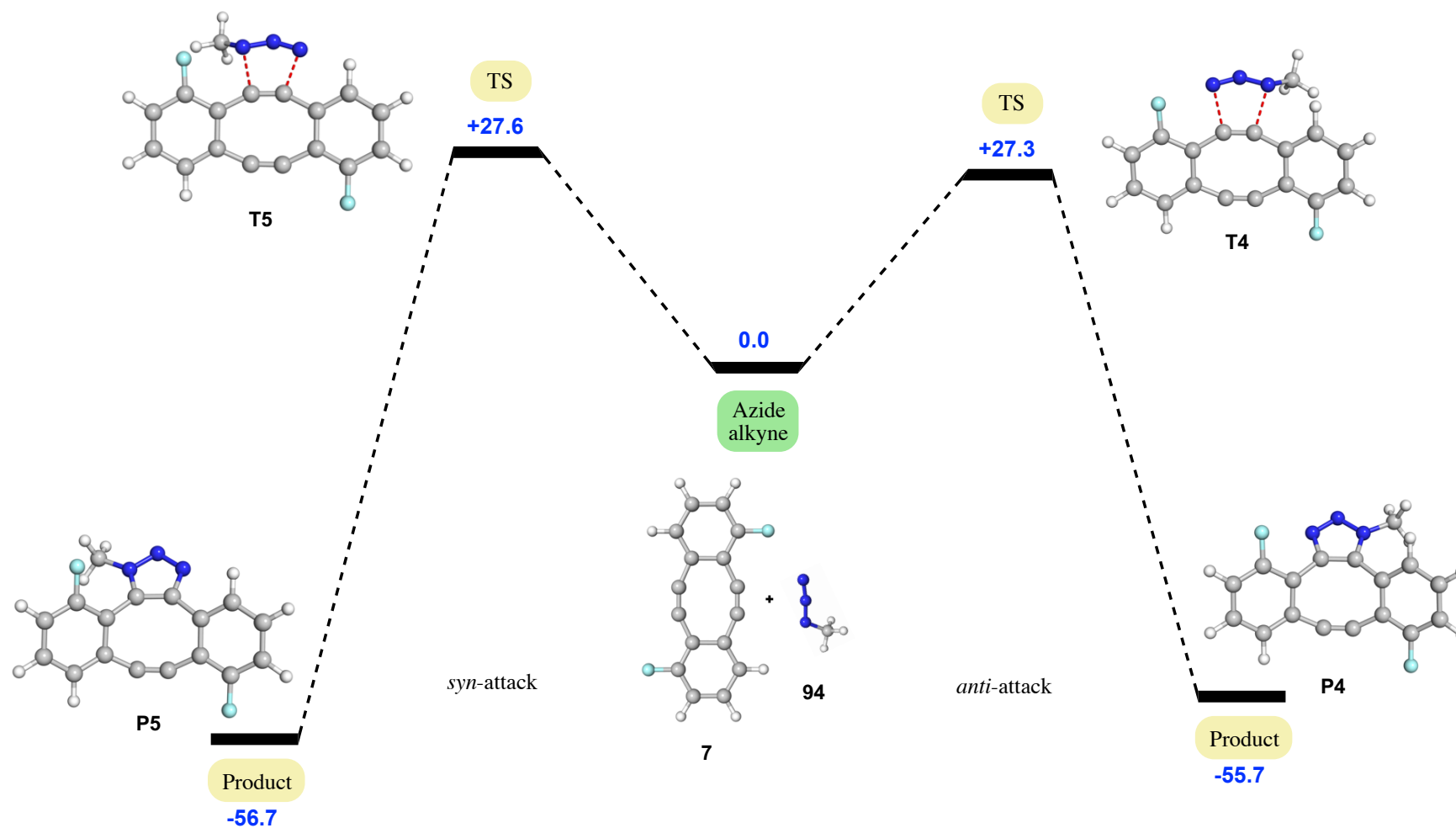


Figure 38: Energy level diagram depicting strain-promoted click reaction between *ortho*-fluoro substituted Sondheimer dialkyne and methyl azide (energy values in kcal/mol).

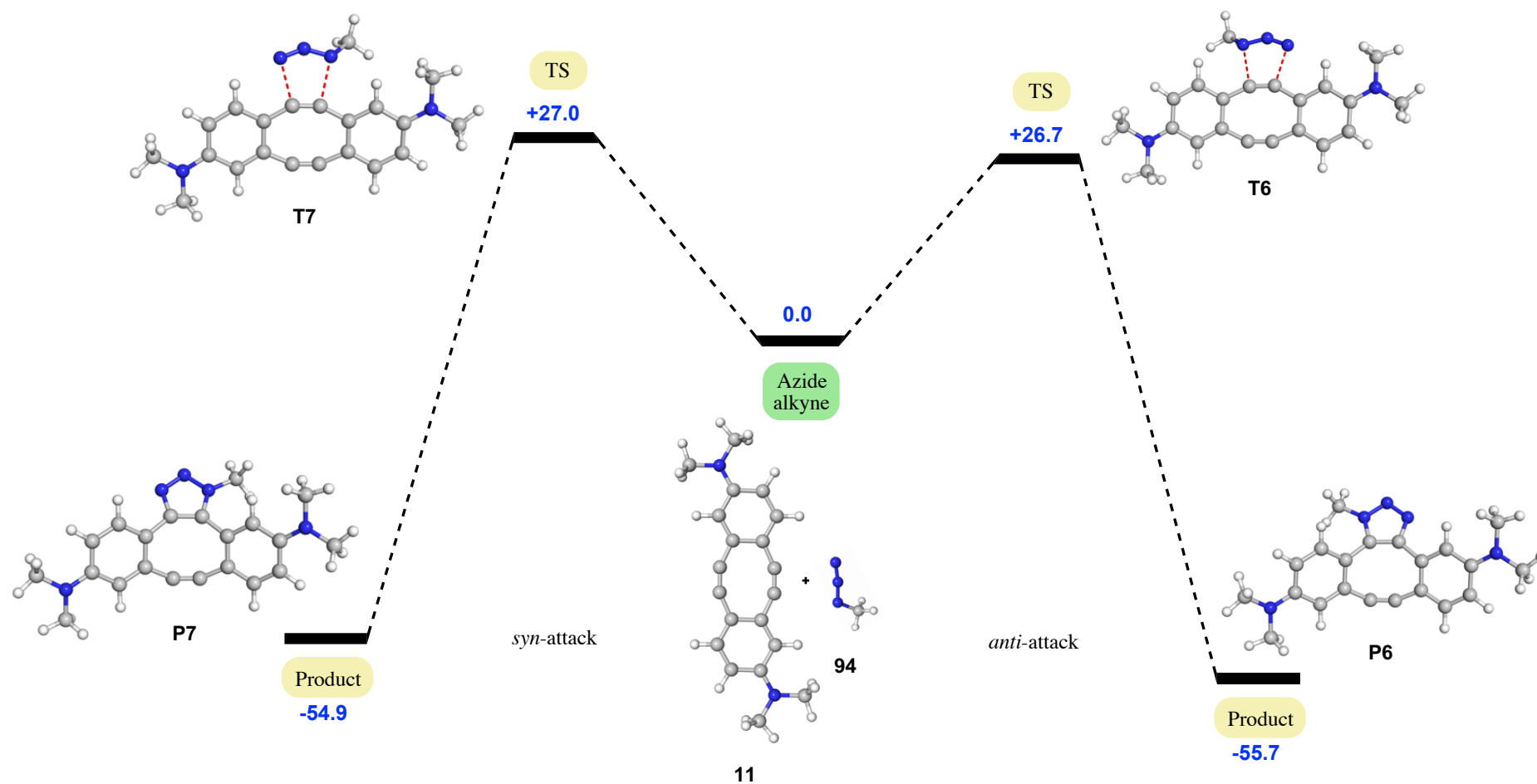


Figure 39: Energy level diagram depicting strain-promoted click reaction between *meta*-dimethylamine substituted Sondheimer dialkyne and methyl azide (energy values in kcal/mol).

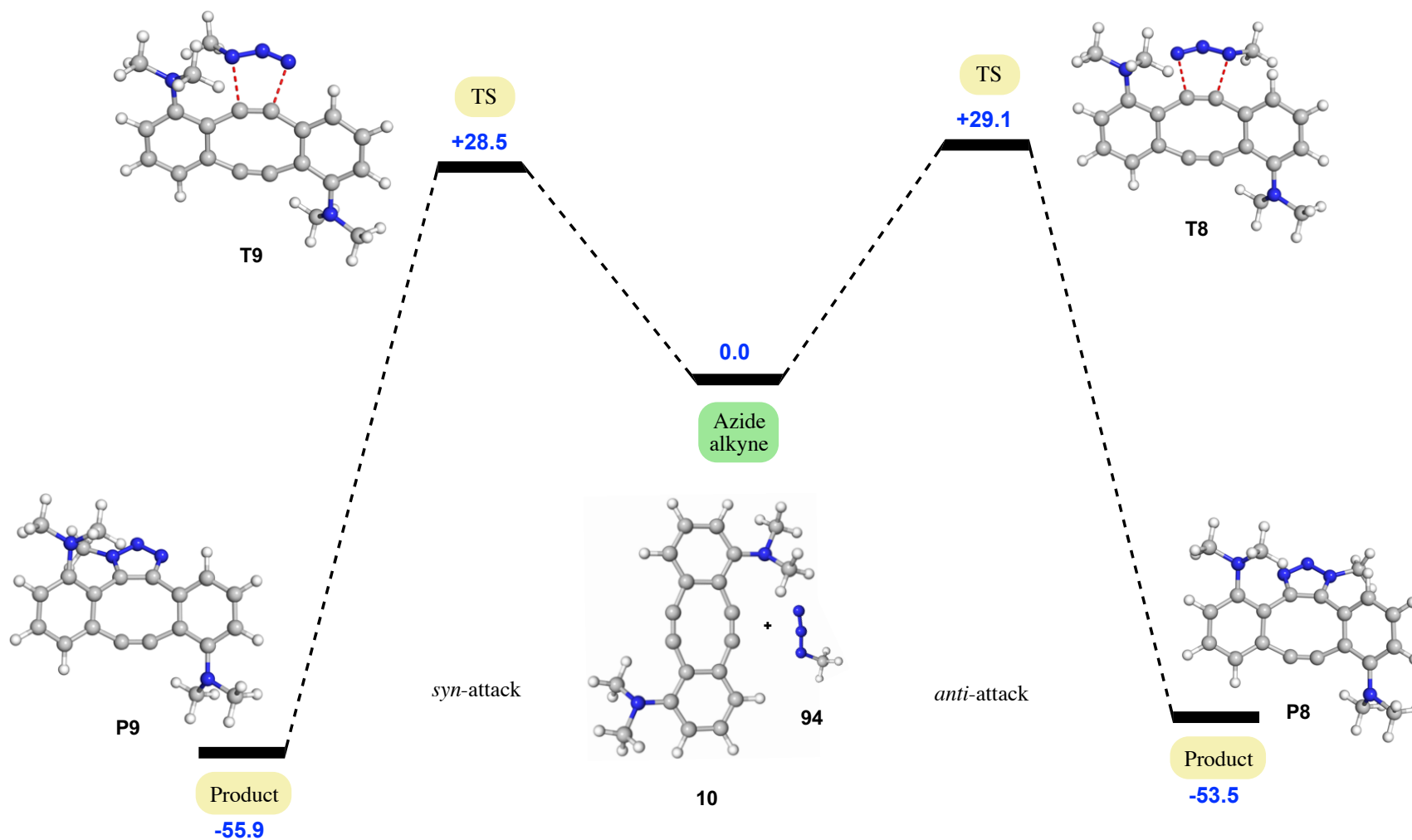


Figure 40: Energy level diagram depicting strain-promoted click reaction between *ortho*-dimethylamine substituted Sondheimer dialkyne and methyl azide (energy values in kcal/mol).

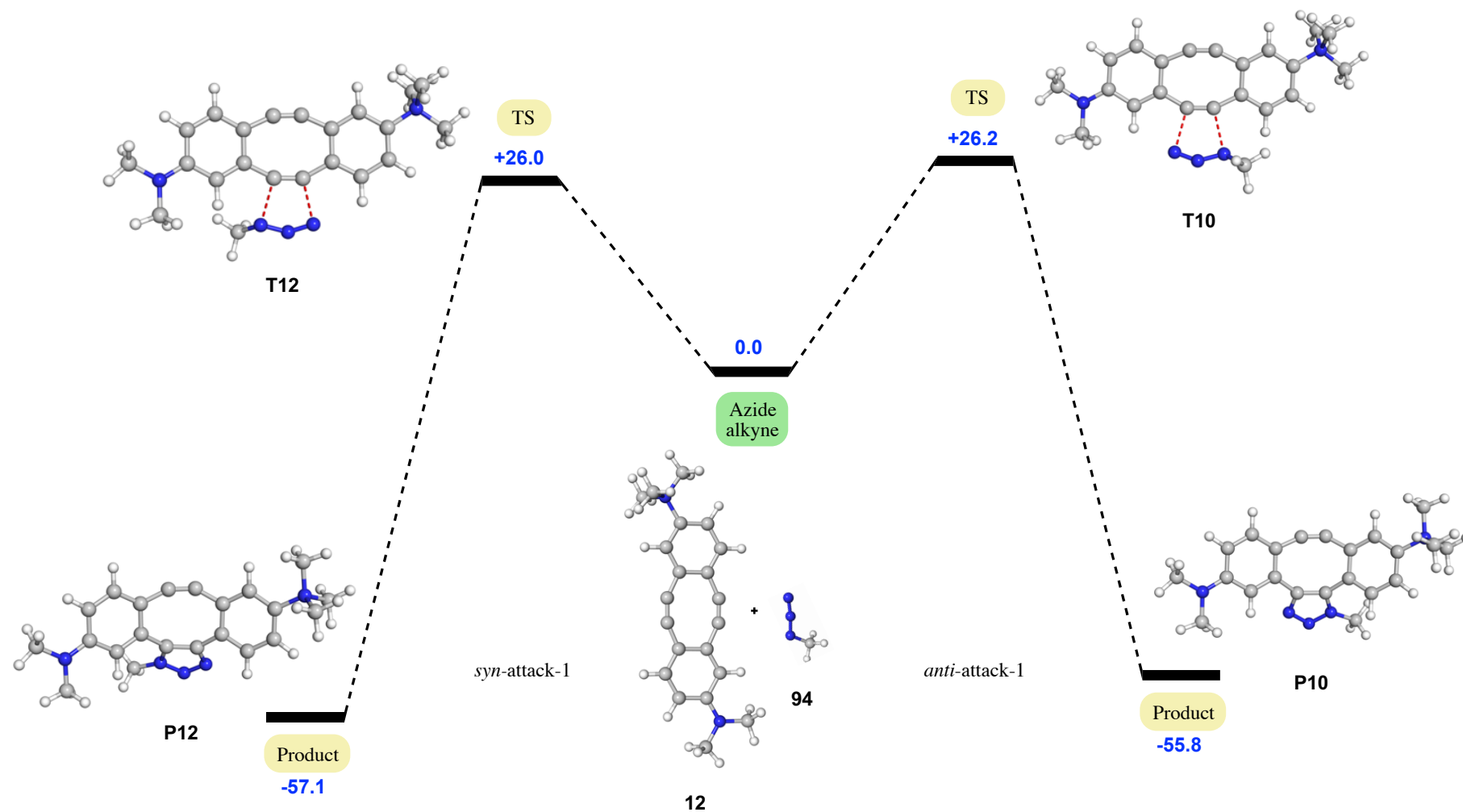


Figure 41: Energy level diagram depicting strain-promoted click reaction between *meta*-trimethylammonium substituted Sondheimer dialkyne and methyl azide (energy values in kcal/mol).

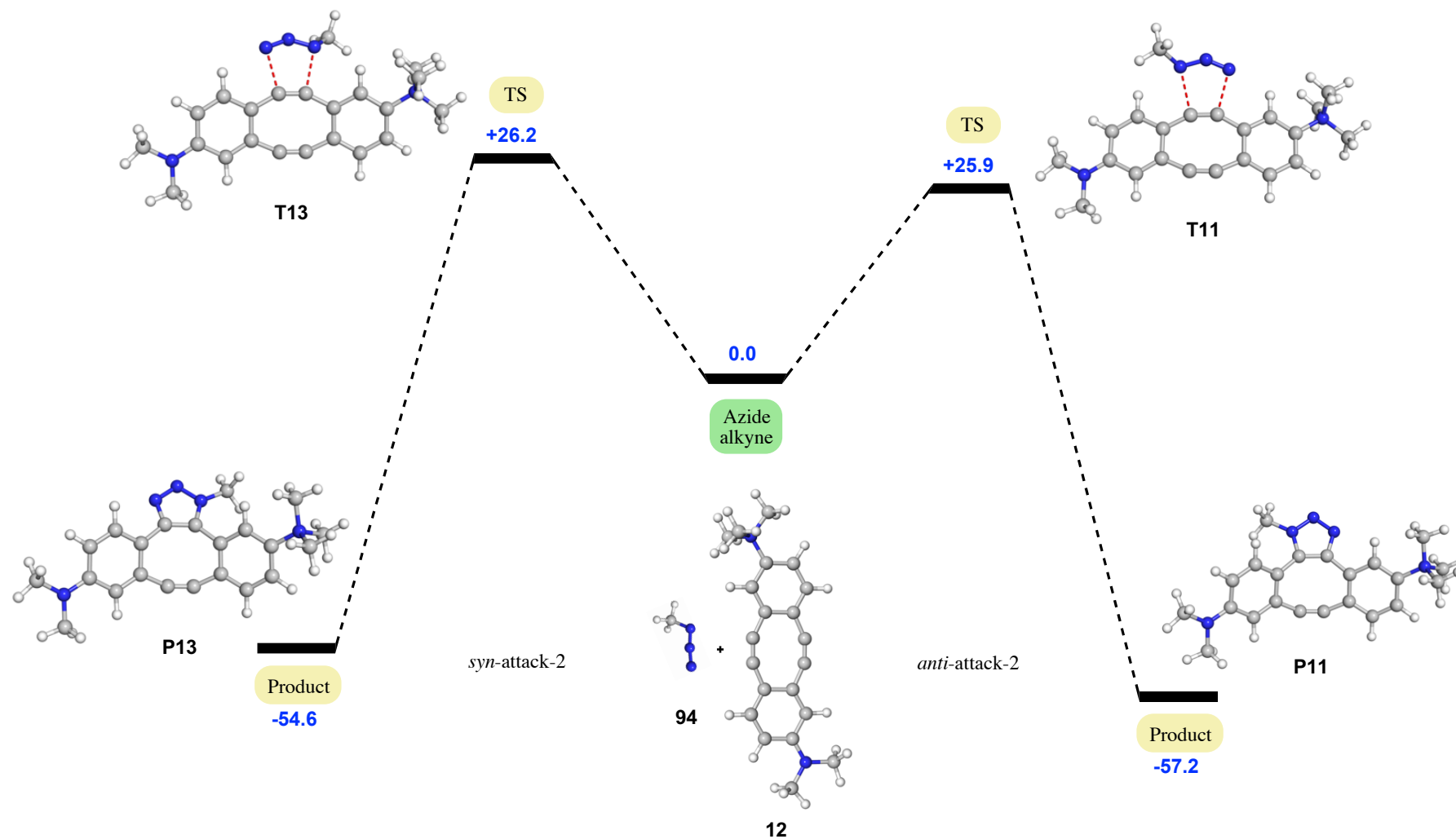


Figure 42: Energy level diagram depicting strain-promoted click reaction between *meta*-trimethylammonium substituted Sondheimer dialkyne and methyl azide approaching from opposite face of the dialkyne (energy values in kcal/mol).

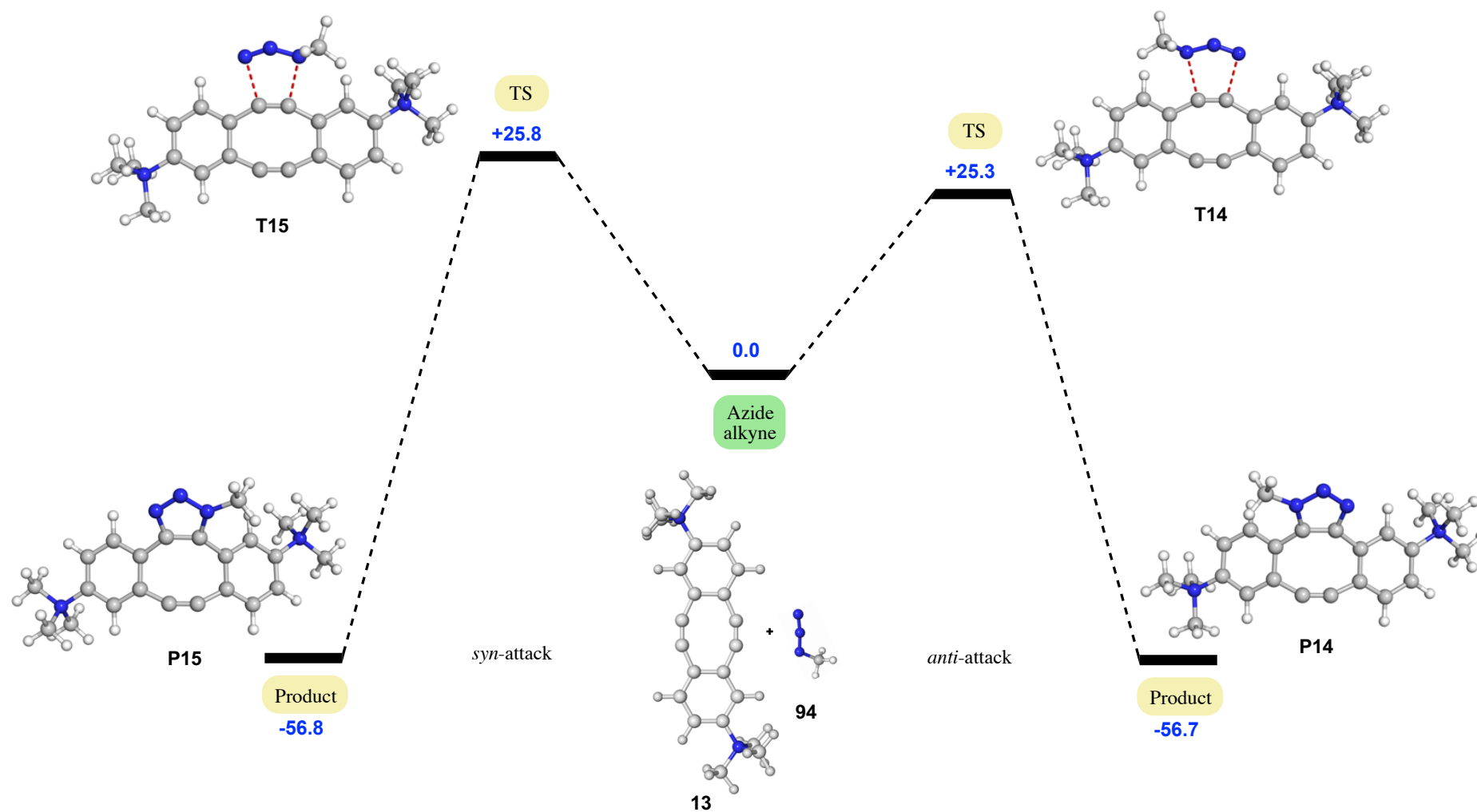


Figure 43: Energy level diagram depicting strain-promoted click reaction between *meta*-di-trimethylammonium substituted Sondheimer dialkyne and methyl azide (energy values in kcal/mol).

In order to investigate the effect of substituent on the rate of SPAAC of Sondheimer dialkyne, the activation barriers obtained above were compared (Figure 44). Here, the transition states with lower activation barrier among *anti*- and *syn*-attack are denoted for rate comparison.

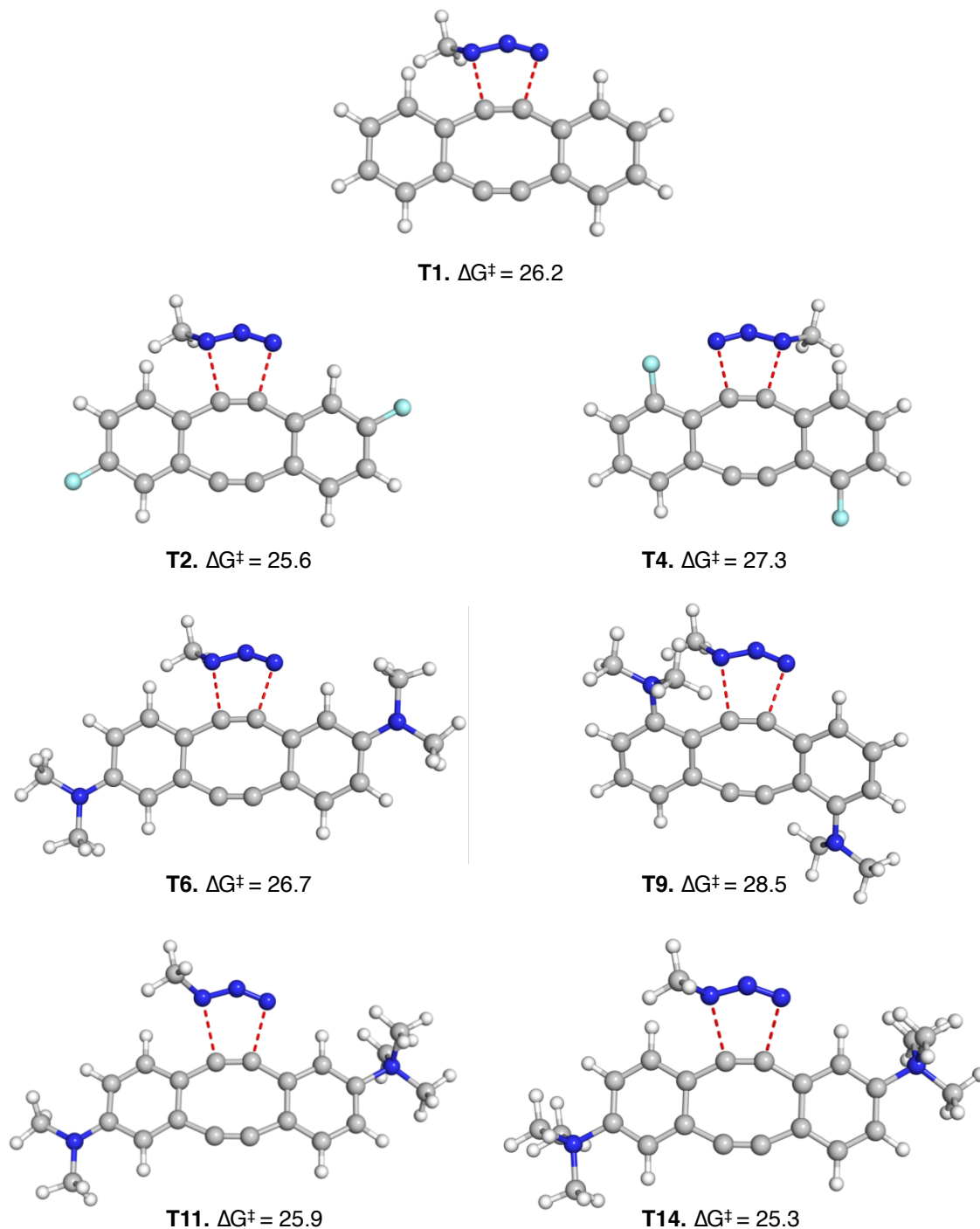


Figure 44: Transition state structures and activation free energies in kcal/mol for cycloaddition of substituted Sondheimer diynes with methyl azide in methanol.

It was observed that substitution of Sondheimer dialkyne with fluoro group at the *meta*-position **6** led to a small decrease in the activation barrier (by 0.6 kcal/mol); whereas, substitution with dimethylamine at *meta*-position **11** led to a small increase in the activation barrier (by 0.5 kcal/mol). However, substitution with either a fluoro **7** or dimethylamine **10** at the *ortho*-position led to large increments in the activation barrier (by 1.1 kcal/mol and 2.3 kcal/mol respectively); thereby suggesting a decreased SPAAC reactivity. This increase in the SPAAC activation barrier of Sondheimer dialkyne in the presence of an *ortho*-substituent was found to be more significant with the bulkier dimethylamine substituent **10** in comparison to fluoro **7**. This was clearly reflected in their relative SPAAC rates observed experimentally (Figure 28). Experimentally determined rate constants have shown that the presence of a fluoro substituent at the *ortho*-position results in about ten-fold decrease in the rate of SPAAC compared to **1** and **6**. Moreover, no reaction was observed in the presence of a bulkier dimethylamine substituent at the *ortho*-position (**10**).

The transition states of *ortho*-substituted diynes **7** and **10** were further analyzed in order to explain their observed inactivity (Figure 45a-b). This demonstrated that the presence of a bulkier dimethylamine substituent in **10** leads to an increased C-N bond distance (by 0.2 Å) on one side in the transition state (Figure 45a). This is consistent with the observation made by Bertozzi and co-workers with *ortho*-substituted BARAC.¹¹⁷ The presence of a relatively smaller fluoro substituent at the *ortho*-position (**7**) similarly resulted in a small increase in the C-N bond distance (by 0.1 Å). The approach of methyl azide towards dialkynes **7** and **10** in a SPAAC was also analysed, and it could be noted from the transition states (side-view) that as the size of the *ortho*-substituent increases, the angle of attack (from the plane of diyne) increases (Figure 45b). These observations confirm that the presence of an *ortho*-substituent on Sondheimer diyne hinders the approach of methyl azide during cycloaddition, and the larger the substituent the more significant is the effect.

5.3 Distortion/Interaction analysis

In order to further explain the relative reactivities observed with substituted Sondheimer diynes, the distortion/interaction (D/I) model developed by Houk and co-workers was applied to selected substrates.¹²⁷⁻¹²⁸ This model deconstructs the activation energy $\Delta E^\ddagger_{\text{act}}$ into distortion energy $\Delta E^\ddagger_{\text{dist}}$ and interaction energy $\Delta E^\ddagger_{\text{int}}$ (Figure 46).

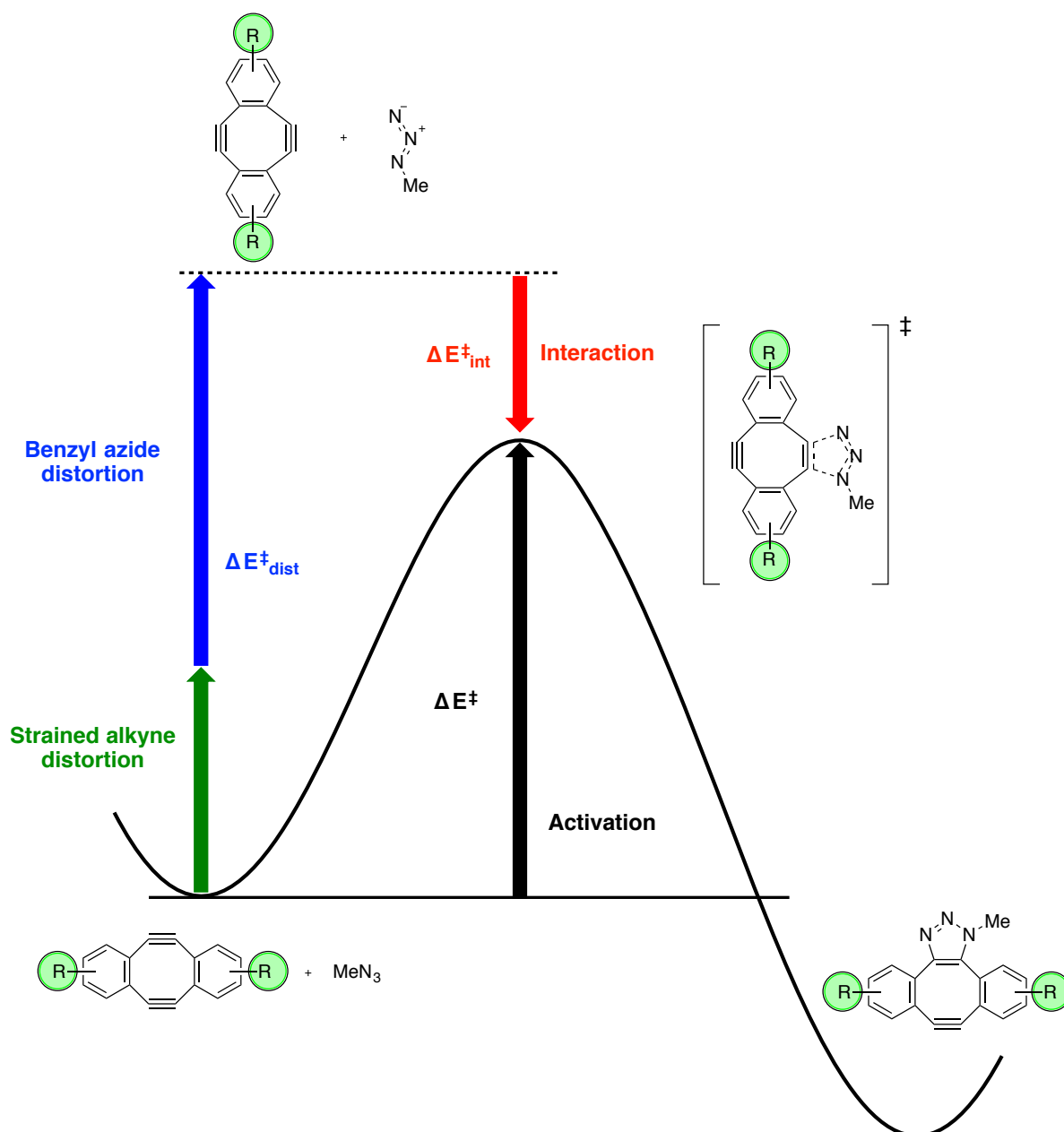


Figure 46: Application of D/I analysis on SPAAC of methyl azide with substituted Sondheimer diynes.

Distortion energy is the energy needed to distort the starting alkyne and azide to transform them into their preferred transition state geometries, whereas the interaction energy is the

energy released upon favorable orbital interactions between these distorted reactants. This model has previously been applied to various SPAAC reaction systems and it has been generally observed that steric effects induced by the presence of a substituent are reflected in an increased distortion energy whereas interaction energy encompasses the electronic effects introduced by the substituent.^{117, 121, 129} Hence, this model was applied to calculate the distortion ($\Delta E_{\text{dist}}^\ddagger$) and interaction energies ($\Delta E_{\text{int}}^\ddagger$) for our reaction in order to investigate the steric and electronic effects of different substituents on Sondheimer diyne SPAAC reactivity. The results from D/I analysis (Table 18) demonstrated that presence of an *ortho*-substituent next to the alkyne has a significant effect on the distortion energy. For instance, installation of an *ortho*-fluoro (**7**) caused an increase in the distortion energy $\Delta E_{\text{dist}}^\ddagger$ (by 1.3 kcal/mol) and a slight increase in the interaction energy $\Delta E_{\text{int}}^\ddagger$ (by 0.4 kcal/mol) leading to an overall increase in the activation energy ΔE^\ddagger (by 0.9 kcal/mol). The most significant effect was observed with the bulkier dimethylamine substituent at *ortho*-position (**10**), which led to a considerable increase in the distortion energy $\Delta E_{\text{dist}}^\ddagger$ (by 1.8 kcal/mol) and no change in the interaction energy, leading to an even higher overall activation barrier ΔE^\ddagger (by 1.8 kcal/mol). This clearly reflects the steric hindrance offered to the SPAAC reaction in the presence of an *ortho*-substituent which becomes more significant in the presence of an even bulkier substituent, overall resulting in an observed sluggish reactivity of these diynes. This is also in accordance with the D/I analysis results shown previously with BARAC in the presence of an *ortho*-fluoro/methyl substituent.¹¹⁷

Diyne	$\Delta E_{\text{dist}}^\ddagger$ (kcal/mol)	$\Delta E_{\text{int}}^\ddagger$ (kcal/mol)	ΔE^\ddagger (kcal/mol)	ΔG^\ddagger (kcal/mol)
1	23.7	-10.3	13.4	26.2
6	23.7	-10.7	13.0	25.6
11	23.8	-9.6	14.2	26.7
7	25.0	-10.7	14.3	27.3
10	25.5	-10.3	15.2	28.5

Table 18: Table depicting calculated distortion energies ($\Delta E_{\text{dist}}^\ddagger$), interaction energies ($\Delta E_{\text{int}}^\ddagger$), overall electronic energies of activation (ΔE^\ddagger), and free energies of activation (ΔG^\ddagger). $\Delta E_{\text{dist}}^\ddagger$, $\Delta E_{\text{int}}^\ddagger$, ΔE^\ddagger denoted here are calculated using the single-point energies obtained with M06-2X¹²², the polarised, triple- ζ valence quality def2-TZVPP basis set of Weigend and Ahlrichs¹²³ and an ultrafine integration grid within the CPCM model (methanol).

On the other hand, installation of a substituent at the *meta*-position of Sondheimer diyne did not have a considerable effect on the D/I energetics. For instance, presence of a *meta*-fluoro substituent on Sondheimer diyne (**6**) did not affect the distortion energy but caused a slight increase in the interaction energy $\Delta E_{\text{int}}^{\ddagger}$ (by 0.4 kcal/mol), thereby leading to a slight decrease in the activation energy ΔE^{\ddagger} (by 0.4 kcal/mol). A similar increase in the interaction energy $\Delta E_{\text{int}}^{\ddagger}$ (by 0.4 kcal/mol) for Sondheimer dialkyne was observed in the presence of an *ortho*-fluoro substituent (**7**). Previously, a *meta*-fluoro substitution on BARAC has been found to enhance the reaction rate by increasing the interaction energy.¹¹⁷ This effect has been attributed to electronic modulation by the fluoro substituent which provides enhanced stabilizing interactions in the transition state. Installation of a *meta*-dimethylamine substituent (**11**) was found to slightly increase the distortion $\Delta E_{\text{dist}}^{\ddagger}$ (by 0.1 kcal/mol) and decrease the interaction energy $\Delta E_{\text{int}}^{\ddagger}$ (by 0.7 kcal/mol) leading to a slight increase in the overall activation energy ΔE^{\ddagger} (by 0.8 kcal/mol).

6. Conclusions and future work

Ten different substituted variants of Sondheimer dialkyne **4-7**, **10-15** were successfully synthesised and evaluated for their water solubility (Figure 47). Out of these, *meta*-trimethylammonium substituted derivatives **12-15** were found to be particularly water soluble and stable, potentially due to the presence of a charged substituent. In an effort to generate stapled peptide-based inhibitors of the oncogenic p53-MDM2 PPI, the strain-promoted double-click stapling of p53-based diazido peptide **2** with dialkynes **4-7**, **10-15** was carried out (Figure 47).

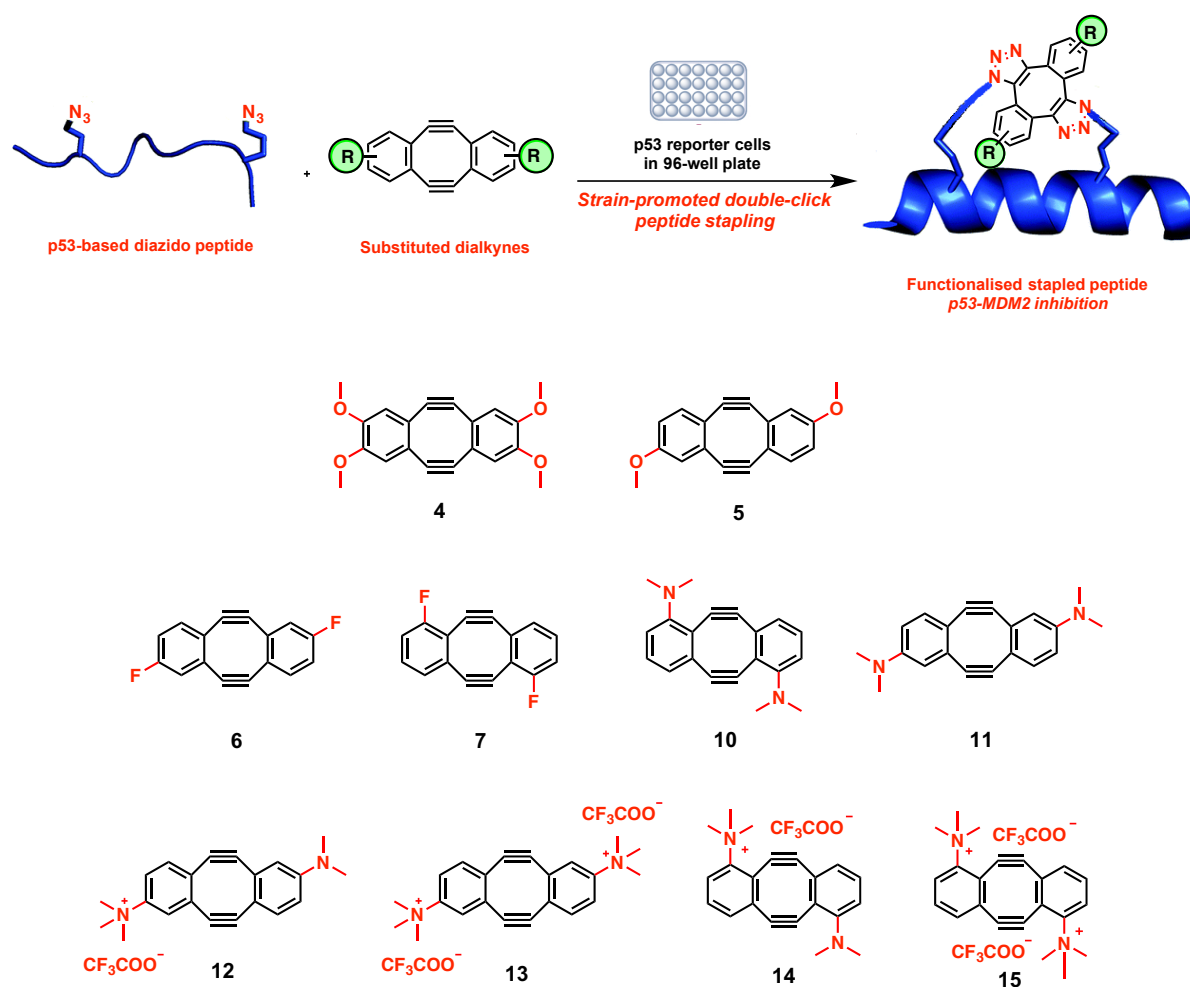


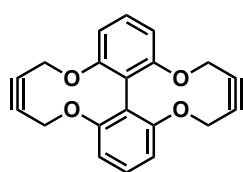
Figure 47: Strain-promoted double-click stapling with substituted Sondheimer dialkynes for inhibition of p53-MDM2 interaction.

The resultant functionalised stapled peptides **81**, **87-92** were tested for their cellular activity in a p53 reporter cell-based assay, and for their *in vitro* binding affinity with MDM2. Three stapled peptides **87-89** were found to have inhibitory activity, thus demonstrating the utility

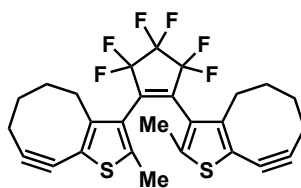
of the novel dialkynes in the preparation of PPI inhibitors. Minor changes in aromatic substitution pattern around the aromatic rings of the stapled peptides was found to have a significant effect upon both binding affinity and cellular activity. *meta*-Fluoro functionalised stapled peptide **88** was found to be the most potent inhibitor (fold activation: 3.9 ± 0.7) in a p53-reporter cell-based assay and twice as active than the unsubstituted counterpart **3** (fold activation: 1.9 ± 0.1). Through X-ray crystallography, the structure of MDM2-bound functionalised stapled peptide **91** was elucidated, which confirmed its α -helical conformation and indicated a shift of the staple moiety away from the MDM2 surface, presumably due to the presence of the charged trimethylammonium group.

Kinetic studies were performed to investigate the effect of substituent on the SPAAC reactivity of substituted Sondheimer dialkynes, with benzyl azide as a model substrate. These studies revealed a *meta*-trimethylammonium substituted dialkyne **13** to be most reactive, with a 3.6-fold increase in the reaction rate observed over Sondheimer dialkyne **1**. These studies also demonstrated all *ortho*-amine substituted Sondheimer dialkynes **10**, **14**, **15** to be unreactive with benzyl azide in contrast to their azide-reactive *meta*-substituted counterparts **11-13**. This observed contrast in azide reactivity was investigated through X-ray crystallographic studies and density functional theory (DFT) calculations. These suggested that the azide reactivity of substituted Sondheimer dialkynes was influenced by both steric and electronic effects associated with presence of the additional substituent.

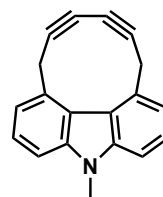
In the future, the substituted Sondheimer dialkynes reported in this thesis could conceivably be used to develop potent stapled peptide inhibitors of other therapeutically relevant PPIs (for instance, cancer specific targets HNF1 β –importin α and Tankyrase/Wnt PPI). The synthetic methodology employed in this thesis was unsuccessful in the preparation of nitro-substituted and heteroaromatic (pyridine and furan) based variants of Sondheimer dialkyne. Thus, the development of new synthetic routes, which provide efficient access to these derivatives (and indeed other substituted Sondheimer dialkynes) is of interest. The Spring group is also interested in the development of novel strained dialkyne reagents aided by DFT calculations, and their application in biocompatible double strain-promoted click chemistry. We are currently investigating the SPAAC reactivity and stability of biphenyl **95**, thiophene-fused cyclooctyne **96** and carbazole **97** based strained dialkynes through DFT studies (Figure 48). This work is being carried out in collaboration with Professor Martin Wells at University of Leeds and Professor Igor Kamarov at University of Kyiv.



Biphenyl based 95



Thiophene-fused
cyclooctyne based 96



Carbazole based 97

Figure 48: DFT investigations into the azide-reactivity and stability of alternative strained dialkyne reagents.

7. Experimental

7.1 General Information

7.1.1 Solvents and reagents

Tetrahydrofuran was dried over sodium wire and distilled from a mixture of calcium hydride and lithium aluminium hydride with triphenylmethane as indicator. Diethyl ether was distilled from a mixture of calcium hydride and lithium aluminium hydride. Dichloromethane, methanol, hexane, acetonitrile and toluene were distilled from calcium hydride. Petroleum ether refers to the fraction of petroleum ether boiling in the range 40-60 °C. All other reagents and solvents were used as supplied, without prior purification.

7.1.2 Chromatography

Flash column chromatography was carried out using Kieselgel 60 silica (230-400 mesh) with distilled solvents under a positive pressure of nitrogen. TLC was carried out on glass Merck Kieselgel 60 F254 plates, visualised by ultraviolet irradiation (254 and 365 nm)

7.1.3 NMR Spectroscopy

NMR spectra were recorded on a Bruker Ultrashield 500 (^1H : 500 MHz and ^{13}C : 126 MHz) spectrometers. Chemical shifts are quoted in ppm and are referenced to the residual non-deuterated solvent peak, and are reported based on appearance rather than interpretation. ^1H spectra are reported as follows: δ_{H} (*spectrometer frequency, solvent*): ppm (*no. of protons, multiplicity, J-coupling constant(s), assignment*). ^{13}C spectra are reported as follows δ_{C} (*spectrometer frequency, solvent*): ppm (*assignment*). Spectral assignment was aided by the results of DEPT, COSY, HMBC and HSQC experiments where appropriate.

7.1.4 IR Spectroscopy

IR spectra were recorded neat on a Perkin Elmer Spectrum One FT-IR spectrophotometer fitted with an attenuated total reflectance (ATR) sampling accessory. Absorption maxima are reported in wavenumbers (cm^{-1}).

7.1.5 High Resolution Mass Spectrometry

Accurate masses were recorded on a Waters LCT Premier Time of Flight mass spectrometer or Micromass Quadrupole-Time of Flight mass spectrometer. Reported mass values are within the error limits of ± 5 ppm.

7.1.6 Liquid Chromatography-Mass Spectrometry

LCMS chromatographs were obtained on an Agilent 1200 series LC using a Supelcosil ABZ+PLUS column (33 mm x 4.6 mm, 3 μ m), together with an ESCi Multi-Mode Ionisation Waters ZQ spectrometer using MassLynx 4.1 software. Chromatographs were monitored by absorbance using diode array detection at a wavelength range of 190-600 nm.

7.1.7 UV Spectroscopy

All UV measurements were recorded using a Varian Cary 300 UV–visible spectrophotometer.

7.1.8 High-performance Liquid Chromatography

Analytical HPLC chromatographs were obtained on an Agilent 1260 Infinity, eluting with a gradient of 5-95% MeCN (with 0.05% TFA) in water (with 0.1% TFA) over 15 minutes. Semi-preparative HPLC was run on an Agilent 1260 Infinity, eluting with a gradient of 40-70% MeCN (with 0.05% TFA) in water (with 0.1% TFA) over 20 minutes. Retention times are reported to the nearest 0.01 min.

7.1.9 Melting points

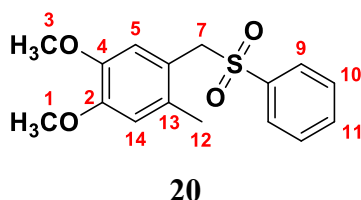
All melting points were measured on a Büchi B545 melting point apparatus and are uncorrected. Solvents are reported in parentheses where solids were purified by recrystallization.

7.1.10 Naming and numbering of compounds

Where given, systematic compound names are those generated by ChemBioDraw Ultra 13.0 following IUPAC conventions. The numbering of atoms for spectral assignment purposes is arbitrary and not necessarily consistent with the IUPAC name.

7.2 Experimental procedures and data

1,2-Dimethoxy-4-methyl-5-((phenylsulfonyl)methyl)benzene



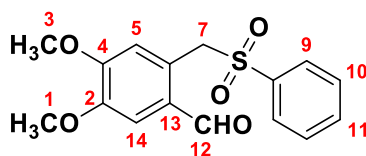
A suspension of 3,4-dimethoxytoluene (1.5 g, 10 mmol), and paraformaldehyde (0.45 g, 15 mmol) in dry CCl_4 (17 mL) was cooled to 0 °C under N_2 . To this suspension a solution of HBr/AcOH (33%, 4.0 mL) was added dropwise over 3–5 min, and the resulting mixture was stirred for 4 h at 0 °C. The reaction mixture was poured into cold water (33 mL), and the organic layer was separated, washed with 5% $\text{NaHCO}_3(\text{aq})$, and dried over anhydrous MgSO_4 . Evaporation of the solvents *in vacuo* afforded a white solid. To this resulting residue, benzenesulfinic acid sodium salt dihydrate (2.4 g, 12 mmol) and DMF (17 mL) were added. After stirring at 80 °C overnight, the reaction mixture was cooled to rt. The reaction mixture was diluted with water (30 mL) and extracted with EtOAc (3×50 mL). The organic layers were combined, dried (MgSO_4), filtered and concentrated *in vacuo*. Purification *via* flash column chromatography on silica gel ($\text{EtOAc}/\text{hexane} = 1:8$) gave **20** (2.6 g, 86%) as a white solid.

mp: 158-160 °C

δ_{H} (500 MHz, CDCl_3): 7.71-7.60 (3H, m, H9, H11), 7.54-7.45 (2H, m, H10), 6.61 (1H, s, H14), 6.44 (1H, s, H5), 4.31 (2H, s, H7), 3.86 (3H, s, H3), 3.68 (3H, s, H1), 2.05 (3H, s, H12).
 δ_{C} (126 MHz, CDCl_3): 149.1 (C4), 146.8 (C2), 138.3 (C8), 133.7 (Ar CH), 131.0 (C6), 128.9 (Ar CH), 128.8 (Ar CH), 118.0 (C13), 114.4 (C5), 113.3 (C14), 59.9 (C7), 55.8 (C1, C3), 18.9 (C12).

Characterisation data is in accordance with that previously reported.⁷⁶

4,5-Dimethoxy-2-((phenylsulfonyl)methyl)benzaldehyde



23

To a suspension of **20** (1.2 g, 4.0 mmol) in CCl₄ (37 mL) at 80 °C under N₂ were added NBS (0.75 g, 4.2 mmol) and BPO (97 mg, 0.40 mmol), and then the resulting mixture was heated at 80 °C. After stirring at this temperature for 6 h, the reaction mixture was cooled to rt. The reaction mixture was diluted with saturated aqueous NH₄Cl (37 mL) and extracted with CH₂Cl₂ (3 × 37 mL). The organic layers were combined, dried (MgSO₄), filtered and concentrated *in vacuo*. To the resulting residue were added CaCO₃ (4.0 g, 40 mmol), dimethoxyethane (13 mL), and H₂O (13 mL). After the resulting mixture had been heated at 120 °C overnight, it was cooled to rt, and the remaining CaCO₃ was neutralised with 1M HCl solution. The reaction mixture was diluted with water (12 mL) and extracted with CH₂Cl₂ (3 × 20 mL). The organic layers were combined, dried (MgSO₄), filtered and concentrated *in vacuo*. To this crude product were added MnO₂ (3.5 g, 40 mmol) and CH₂Cl₂ (13 mL). After the resulting mixture was heated to 50 °C overnight, it was cooled to rt and filtered, and the filtrate was concentrated *in vacuo*. Purification *via* flash column chromatography on silica gel (EtOAc/hexane = 1:1) gave **23** as a pale-yellow solid (0.64 g, 50%).

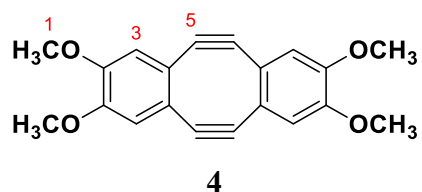
mp: 145-147 °C

δ_H (500 MHz, CDCl₃): 9.76 (1H, s, H12), 7.71 (2H, dd, *J* 8.43, 1.18, Ar H), 7.66-7.61 (1H, m, Ar H), 7.51-7.46 (2H, m, Ar H), 7.26 (1H, s, H14), 6.80 (1H, s, H5), 4.92 (2H, s, H7), 3.96 (3H, s, H1), 3.91 (3H, s, H3).

δ_C (126 MHz, CDCl₃): 189.5 (C12), 153.0 (C2), 149.5 (C4), 137.9 (C8), 133.9 (Ar CH), 129.0 (Ar CH), 128.7 (Ar CH), 128.0 (C6), 123.7 (C13), 115.5 (C5), 114.1 (C14), 57.3 (C7), 56.3 (C3), 56.1 (C1).

Characterisation data is in accordance with that previously reported.⁷⁶

2,3,8,9-Tetramethoxy-5,6,11,12-tetrahydrodibenzo[a,e]cyclooctene



A mixture of **23** (0.19 g, 0.58 mmol) and $\text{ClP}(\text{O})(\text{OEt})_2$ (0.10 mL, 0.69 mmol) in THF (12 mL) was cooled to $-78\text{ }^\circ\text{C}$, and then LiHMDS (1.0 M in THF, 1.2 mL, 1.2 mmol) was added. After stirring at $-78\text{ }^\circ\text{C}$ for 30 min, the reaction mixture was warmed to rt and stirred for a further 1.5 h. LDA (1.0 M in THF/hexane, 2.9 mL, 2.9 mmol) was then added at $-78\text{ }^\circ\text{C}$ and the reaction mixture was stirred at this temperature for 2 h, and saturated aqueous NH_4Cl (3.0 mL) was poured into the mixture. The reaction mixture was diluted with water (6 mL) and extracted with EtOAc ($3 \times 10\text{ mL}$). The organic layers were combined, dried (MgSO_4), filtered and concentrated *in vacuo*. Purification *via* flash column chromatography on silica gel (PE/EtOAc = 1:1) gave **4** as a yellow solid (0.041 g, 22%).

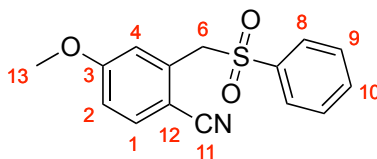
mp: $205\text{ }^\circ\text{C}$ (dec.)

δ_{H} (400 MHz, CDCl_3): 6.26 (4H, s, H3), 3.78 (12 H, s, H1).

δ_{C} (101 MHz, CDCl_3): 149.0 (C2), 126.2 (C4), 111.4 (C3), 108.9 (C5), 56.2 (C1).

Characterisation data is in accordance with that previously reported.⁷⁶

4-methoxy-2-((phenylsulfonyl)methyl)benzonitrile



27

To a suspension of 4-methoxy-2-methylbenzonitrile (4.0 g, 27 mmol) in CCl_4 (80 mL) at 80 °C under N_2 were added NBS (5.8 g, 33 mmol) and BPO (0.33 g, 1.4 mmol) and then the resulting mixture was heated at 80 °C. After stirring at this temperature for 6 h, the reaction mixture was cooled to rt. The reaction mixture was diluted with saturated aqueous NH_4Cl (80 mL) and extracted with CH_2Cl_2 (3×80 mL). The organic layers were combined, dried (MgSO_4), filtered and concentrated *in vacuo*. To the resulting residue were added benzenesulfinic acid sodium salt dihydrate (6.7 g, 41 mmol) and DMF (80 mL). After the resulting mixture had been stirred at 80 °C overnight, it was cooled to rt. The reaction mixture was diluted with water (100 mL) and extracted with EtOAc (3×100 mL). The organic layers were combined, dried (MgSO_4), filtered and concentrated *in vacuo*. Purification *via* flash column chromatography on silica gel (EtOAc/hexane = 1:2) gave **27** (6.2 g, 81%) as a white solid.

mp: 144-145 °C

ν_{max} (neat): 2944, 2221 ($\text{C}\equiv\text{N}$), 1609, 1499, 1291 ($\text{S}=\text{O}$), 1147 ($\text{S}=\text{O}$), 1082, 1025.

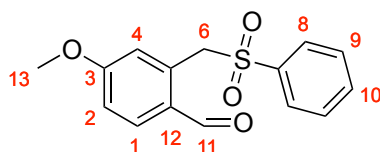
δ_{H} (500 MHz, CDCl_3): 7.73 (2H, dd, J 8.4, 1.2, H8), 7.69-7.62 (1H, m, H10), 7.53-7.47 (2H, m, H9), 7.44 (1H, d, J 8.7, H1), 7.10 (1H, d, J 2.5, H4), 6.93 (1H, dd, J 8.7, 2.5, H2), 4.52 (2H, s, H6), 3.87 (3H, s, H13).

δ_{C} (126 MHz, CDCl_3): 162.8 (C3), 137.7 (C7), 134.4 (Ar CH), 134.4 (Ar CH), 133.8 (C12), 129.4 (C9), 128.8 (C8), 117.4 (C4), 117.1 (C11), 115.7 (C2), 106.0 (C5), 60.7 (C6), 55.9 (C13).

HRMS (ES^+): found 288.0686; $\text{C}_{15}\text{H}_{14}\text{NO}_3^{32}\text{S}$ [$\text{M}+\text{H}$] $^+$ requires 288.0689.

Characterisation data is in accordance with that previously reported.¹³⁰

4-methoxy-2-((phenylsulfonyl)methyl)benzaldehyde



28

To a solution of **27** (1.0 g, 3.5 mmol) in CH₂Cl₂ (10 mL), was added DIBAL-H (1.0 M in hexane, 5.2 mL, 5.2 mmol) at -78 °C. After the mixture had been stirred at this temperature for 2 h, saturated aqueous NH₄Cl (25 mL) was poured into the mixture followed by 1M HCl (25 mL). The product was then extracted with CH₂Cl₂ (3 × 50 mL). The organic layers were combined, dried (MgSO₄), filtered and concentrated *in vacuo*. Purification *via* flash column chromatography on silica gel (EtOAc/hexane = 1:2) gave **28** (0.60 g, 59%) as a white solid.

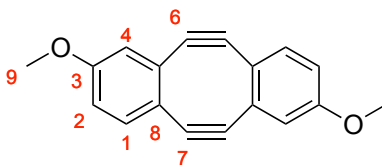
δ_{H} (500 MHz, CDCl₃): 9.65 (1H, s, H11), 7.73-7.70 (2H, m, H8), 7.63 (1H, d, *J* 8.5, H1), 7.62-7.57 (1H, m, H10), 7.48-7.42 (2H, m, H9), 7.01 (1H, dd, *J* 8.5, 2.5, H2), 6.97 (1H, d, *J* 2.5, H4), 5.04 (2H, s, H6), 3.88 (3H, s, H13).

δ_{C} (126 MHz, CDCl₃): 190.8 (C11), 163.4 (C3), 138.5 (C7), 137.4 (C1), 133.9 (C10), 131.4 (C12), 128.9 (C9), 128.8 (C8), 128.1 (C5), 119.5 (C4), 114.6 (C2), 57.7 (C6), 55.9 (C13).

HRMS (ES⁺): found 291.0683; C₁₅H₁₅O₄³²S [M+H]⁺ requires 291.0686.

Characterisation data is in accordance with that previously reported.¹³¹

2,8-Dimethoxy-5,6,11,12-tetrahydrodibenzo[a,e]cyclooctene



5

A mixture of **28** (0.50 g, 1.7 mmol) and ClP(O)(OEt)_2 (0.30 mL, 2.1 mmol) in THF (35 mL) was cooled to -78°C , and then LiHMDS (1.0 M in THF, 3.8 mL, 3.8 mmol) was added. After stirring at -78°C for 30 min, the reaction mixture was warmed to rt and stirred for a further 1.5 h. LDA (1.0 M in THF/hexane, 8.6 mL, 8.6 mmol) was then added at -78°C and the reaction mixture was stirred at this temperature for 2 h, and saturated aqueous NH_4Cl (13 mL) was poured into the mixture. The reaction mixture was brought to rt, diluted with water (26 mL) and extracted with EtOAc (3×40 mL). The organic layers were combined, dried (MgSO_4), filtered and concentrated *in vacuo*. Purification *via* flash column chromatography on silica gel (EtOAc/hexane = 1:3) gave **5** as a yellow solid (0.088 g, 39%).

mp: 171-173 (dec) $^\circ\text{C}$

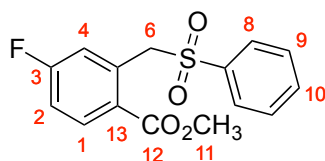
ν_{max} (neat): 2916, 2849, 2145 ($\text{C}\equiv\text{C}$), 1595, 1562, 1421, 1318, 1213, 1065, 1024.

δ_{H} (500 MHz, CDCl_3): 6.67 (2H, d, J 8.4, Ar H), 6.39 (2H, dd, J 8.4, 2.6, Ar H), 6.34 (2H, d, J 2.6, Ar H), 3.72 (6H, s, H9).

δ_{C} (126 MHz, CDCl_3): 160.4 (C3), 135.0 (C5), 128.0 (C1), 124.0 (C8), 114.7 (C4), 112.0 (C2), 110.3 ($\text{C}\equiv\text{C}$), 107.4 ($\text{C}\equiv\text{C}$), 55.5 (C9).

HRMS (ES⁺): found 261.0904; $\text{C}_{18}\text{H}_{13}\text{O}_2$ $[\text{M}+\text{H}]^+$ requires 261.0910.

Methyl 4-fluoro-2-((phenylsulfonyl)methyl)benzoate



32

To a suspension of methyl 4-fluoro-2-methylbenzoate **30** (2.0 g, 12 mmol) in CCl₄ (59 mL) at 80 °C under N₂ were added NBS (2.2 g, 12 mmol) and AIBN (0.19 g, 1.2 mmol), and then the resulting mixture was heated at 100 °C. After stirring at this temperature for 6 h, the reaction mixture was cooled to rt. The reaction mixture was diluted with saturated aqueous NH₄Cl (60 mL) and extracted with CH₂Cl₂ (3 × 60 mL). The organic layers were combined, dried (MgSO₄), filtered and concentrated *in vacuo*. To the resulting crude product (3.2 g, 13 mmol) were added benzenesulfinic acid sodium salt dihydrate (2.6 g, 16 mmol) and DMF (20 mL). After the resulting mixture had been stirred at 80 °C overnight, it was cooled to rt. The reaction mixture was diluted with water (40 mL) and extracted with EtOAc (3 × 40 mL). The organic layers were combined, dried (MgSO₄), filtered and concentrated *in vacuo*. Purification *via* flash column chromatography on silica gel (PE/Et₂O = 2:1) gave **32** (2.6 g, 70%) as a white solid.

mp: 122-124 °C

ν_{max} (neat): 2954 (C-H), 1717 (C=O), 1589, 1306 (S=O), 1273, 1252, 1151 (S=O), 1117.

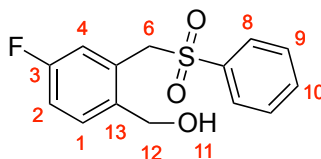
δ_{H} (500 MHz, CDCl₃): 7.93 (1H, dd, *J* 8.52, 5.81, Ar H), 7.71-7.65 (2H, m, Ar H), 7.62 (1H, t, *J* 7.47, Ar H), 7.52-7.43 (2H, m, Ar H), 7.14-7.04 (2H, m, Ar H), 5.04 (2H, s, H₆), 3.74 (3H, s, H₁₁).

δ_{C} (126 MHz, CDCl₃): 166.1 (C₁₂), 164.2 (d, *J* 255.14, C₃), 138.2 (Ar C), 133.7 (Ar CH), 133.5 (d, *J* 9.02, Ar CH), 132.4 (d, *J* 8.76, Ar CH), 128.9 (Ar CH), 128.6 (Ar CH), 126.8 (Ar C), 120.4 (d, *J* 22.68, Ar CH), 115.9 (d, *J* 21.14, Ar CH), 58.9 (C₆), 52.2 (C₁₁).

δ_{F} (376 MHz, CDCl₃): -105.7.

HRMS (ES⁺): found 309.0584; C₁₅H₁₄O₄F³²S [M+H]⁺ requires 309.0597.

(4-Fluoro-2-((phenylsulfonyl)methyl)phenyl)methanol



33

To a solution of **32** (2.5 g, 8.0 mmol) in CH₂Cl₂ (24 mL), was added DIBAL-H (1.0 M in hexane, 19 mL, 19 mmol) at -78 °C. After the mixture had been stirred at this temperature for 2 h, saturated aqueous NH₄Cl (100 mL) was poured into the mixture followed by 1M HCl (100 mL). The reaction mixture was warmed to rt and the product was then extracted with CH₂Cl₂ (3 × 200 mL). The organic layers were combined, dried (MgSO₄), filtered and concentrated *in vacuo* to afford the pure product **33** as a white solid (2.0 g, 90%).

mp: 145-149 °C

ν_{max} (neat): 3479 (O-H), 1592, 1499, 1447, 1305 (S=O), 1146 (S=O), 1081.

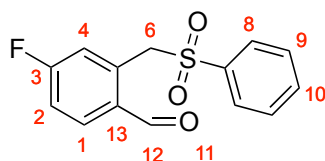
δ_{H} (500 MHz, CDCl₃): 7.80-7.74 (2H, m, Ar H), 7.69 (1H, t, *J* 7.69, Ar H), 7.59-7.51 (2H, m, Ar H), 7.41 (1H, dd, *J* 8.49, 5.77, H1), 7.05 (1H, td, *J* 8.29, 2.67, H2), 6.68 (1H, dd, *J* 9.17, 2.66, H4), 4.61 (2H, s, H12), 4.50 (2H, s, H6), 2.61 (1H, br. s, H11).

δ_{C} (126 MHz, CDCl₃): 161.8 (d, *J* 247.68, C3), 137.8 (Ar C), 136.9 (Ar C), 134.3 (Ar CH), 132.2 (d, *J* 8.24, C1), 129.3 (Ar CH), 128.6 (Ar CH), 128.2 (d, *J* 7.97, Ar C), 119.2 (d, *J* 22.66, C4), 116.4 (d, *J* 20.77, C2), 62.5 (C12), 59.4 (C6).

δ_{F} (376 MHz, CDCl₃): -113.4.

HRMS (ES⁺): found 303.0465; C₁₄H₁₃O₃F³²SNa [M+Na]⁺ requires 303.0462.

4-Fluoro-2-((phenylsulfonyl)methyl)benzaldehyde



34

To a solution of **33** (2.1 g, 7.4 mmol) in CH₂Cl₂ (22 mL) was added DMP (3.5 g, 8.2 mmol) at rt. After the reaction mixture had been stirred for 3 h, the reaction mixture was diluted with CH₂Cl₂ (15 mL) and poured into saturated Na₂S₂O₃ solution (30 mL). Mixture was stirred to dissolve the solid and layers were separated. The CH₂Cl₂ layer was then extracted with saturated aqueous Na₂S₂O₃ (2 × 30 mL) followed by saturated aqueous NaHCO₃ (2 × 30 mL). CH₂Cl₂ was then removed *in vacuo* and purification *via* flash column chromatography on silica gel (EtOAc/hexane = 1:2) gave pure product **34** (1.3 g, 63%) as a white solid.

mp: 138-140 °C

ν_{max} (neat): 2988, 1693 (C=O), 1585, 1447, 1306 (S=O), 1238, 1150 (S=O), 1083.

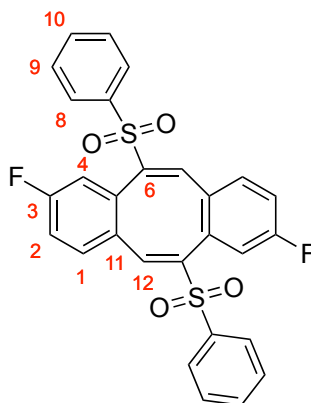
δ_{H} (400 MHz, CDCl₃): 9.81 (1H, s, H11), 7.82-7.72 (3H, m, Ar H), 7.65 (1H, t, *J* 7.48, Ar H), 7.54-7.46 (2H, m, Ar H), 7.32-7.18 (2H, m, Ar H), 5.04 (2H, s, H6).

δ_{C} (126 MHz, CDCl₃): 190.4 (C11), 165.0 (d, *J* 258.44, C3), 138.1 (Ar C), 137.1 (d, *J* 9.92, Ar CH), 134.1 (Ar CH), 132.2 (d, *J* 9.39, Ar C), 131.3 (d, *J* 3.08, Ar C), 129.0 (Ar CH), 128.6 (Ar CH), 121.1 (d, *J* 22.97, C4), 116.6 (d, *J* 21.60, Ar CH), 57.2 (C6).

δ_{F} (376 MHz, CDCl₃): -102.3.

HRMS (ES⁺): found 279.0489; C₁₄H₁₂O₃³²SF [M+H]⁺ requires 279.0491.

(5*E*,11*E*)-2,8-difluoro-6,12-bis(phenylsulfonyl)dibenzo[*a,e*][8]annulene



35

A mixture of **34** (0.80 g, 2.9 mmol) and ClP(O)(OEt)₂ (0.50 mL, 3.5 mmol) in THF (58 mL) was cooled to $-78\text{ }^{\circ}\text{C}$, and then LiHMDS (1.0 M in THF, 5.8 mL, 5.8 mmol) was added. After stirring at $-78\text{ }^{\circ}\text{C}$ for 30 min, the reaction mixture was warmed to rt and stirred for a further 1.5 h. Saturated aqueous NH₄Cl (8.0 mL) was poured into the mixture. The reaction mixture was diluted with water (90 mL) and extracted with EtOAc ($3 \times 100\text{ mL}$). The organic layers were combined, dried (MgSO₄), filtered and concentrated *in vacuo*. Purification *via* flash column chromatography on silica gel (EtOAc/hexane = 3:8) gave **35** as a pale yellow solid (0.28 g, 19%).

mp: $203\text{ }^{\circ}\text{C}$ (dec.)

ν_{max} (neat): 2923, 1579, 1493, 1447, 1319 (S=O), 1222, 1151 (S=O), 1084.

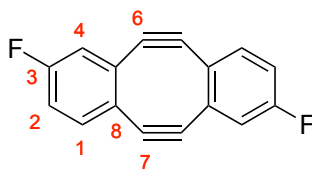
δ_{H} (500 MHz, CDCl₃): 7.66 (2H, t, J 7.19, Ar H), 7.54-7.44 (8H, m, Ar H), 7.33 (2H, s, Ar H), 7.21 (2H, dd, J 9.33, 2.50, Ar H), 7.06-6.94 (4H, m, Ar H).

δ_{C} (126 MHz, CDCl₃): 162.0 (d, J 250.77, C3), 144.4 (Ar C), 138.6 (Ar CH), 136.6 (Ar C), 134.1 (Ar CH), 131.2 (Ar C), 131.1 (d, J 8.80, Ar C), 129.1 (Ar CH), 128.9 (d, J 8.59, Ar CH), 128.1 (Ar CH), 117.9 (d, J 23.49, Ar CH), 117.1 (d, J 21.88, Ar CH).

δ_{F} (376 MHz, CDCl₃): -110.6.

HRMS (ES⁺): found 521.0704; C₂₈H₁₉F₂O₄³²S₂ [M+H]⁺ requires 521.0693.

2,8-Difluoro-5,6,11,12-tetrahydrodibenzo[a,e]cyclooctene



6

A solution of **35** (0.11 g, 0.21 mmol) in THF (5.3 mL) was cooled to $-78\text{ }^{\circ}\text{C}$, and then LDA (1.0 M in THF/hexane, 0.85 mL, 0.85 mmol). The reaction mixture was stirred at this temperature for 2 h, and saturated aqueous NH_4Cl (9 mL) was poured into the mixture. The reaction mixture was cooled to rt, diluted with water (25 mL) and extracted with CH_2Cl_2 ($3 \times 35\text{ mL}$). The organic layers were combined, dried (MgSO_4), filtered and concentrated *in vacuo*. Purification *via* flash column chromatography on silica gel ($\text{EtOAc/hexane} = 1:8$) gave **6** as a yellow solid (15 mg, 30%).

ν_{max} (neat): 2922, 1569, 1461, 1243, 977, 778.

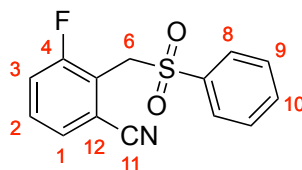
δ_{H} (500 MHz, CDCl_3): 6.98-6.91 (2H, m, Ar H), 6.73 (2H, t, J 8.74, Ar H), 6.59 (2H, d, Ar H).

δ_{C} (126 MHz, CDCl_3): 158.6 (d, J 254.49, C3), 134.3 (Ar C), 131.0 (d, J 8.54, Ar CH), 123.2 (d, J 2.93, Ar CH), 119.8 (d, J 16.54, Ar C), 117.8 (d, J 21.06, Ar CH), 111.4 ($\text{C}\equiv\text{C}$), 104.9 ($\text{C}\equiv\text{C}$).

δ_{F} (376 MHz, CDCl_3): -107.7.

HRMS (ES⁺): found 236.0428; $\text{C}_{16}\text{H}_6\text{F}_2$ $[\text{M}+\text{H}]^+$ requires 236.0438.

3-Fluoro-2-((phenylsulfonyl)methyl)benzonitrile



38

To a suspension of 3-fluoro-2-methylbenzonitrile **36** (5.3 g, 39 mmol) in CCl₄ (196 mL) at 80 °C under N₂ were added NBS (7.3 g, 41 mmol) and AIBN (0.64 g, 3.9 mmol), and then the resulting mixture was heated at 100 °C. After stirring at this temperature for 6 h, the reaction mixture was cooled to rt. The reaction mixture was diluted with saturated aqueous NH₄Cl (150 mL) and extracted with CH₂Cl₂ (3 × 150 mL). The organic layers were combined, dried (MgSO₄), filtered and concentrated *in vacuo*. To the resulting residue (8.6 g, 40 mmol) were added benzenesulfinic acid sodium salt dihydrate (7.9 g, 48 mmol) and DMF (60 mL). After the resulting mixture had been stirred at 80 °C overnight, it was cooled to rt. The reaction mixture was diluted with water (100 mL) and extracted with EtOAc (3 × 100 mL). The organic layers were combined, dried (MgSO₄), filtered and concentrated *in vacuo*. Purification *via* flash column chromatography on silica gel (PE/Et₂O = 2:1) gave **38** (6.6 g, 61%) as a white solid.

mp: 156-158 °C

ν_{\max} (neat): 2236 (C≡N), 1575, 1321 (S=O), 1253, 1137 (S=O), 1084.

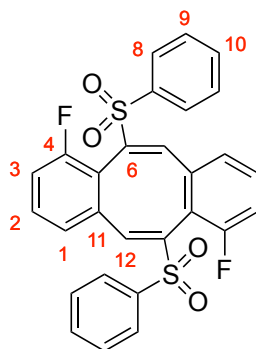
δ_{H} (500 MHz, CDCl₃): 7.84-7.78 (2H, m, Ar H), 7.70 (1H, t, *J* 7.49, Ar H), 7.59-7.52 (2H, m, Ar H), 7.51-7.45 (2H, m, Ar H), 7.39-7.31 (1H, m, Ar H), 4.63 (2H, s, H₆).

δ_{C} (126 MHz, CDCl₃): 161.4 (d, *J* 254.59, C₄), 138.0 (Ar C), 134.5 (Ar CH), 131.5 (d, *J* 8.98, Ar CH), 129.4 (Ar CH), 129.1 (d, *J* 3.85, Ar CH), 128.7 (Ar CH), 120.7 (d, *J* 22.15, Ar CH), 119.7 (d, *J* 17.48, Ar C), 116.3 (CN), 115.6 (Ar C), 55.0 (C₆).

δ_{F} (376 MHz, CDCl₃): -109.8.

HRMS (ES⁺): found 276.0498; C₁₄H₁₁NO₂³²SF [M+H]⁺ requires 276.0495.

(5*E*,11*E*)-1,7-difluoro-6,12-bis(phenylsulfonyl)dibenzo[*a,e*][8]annulene



40

To a solution of **38** (1.1 g, 3.9 mmol) in CH₂Cl₂ (19 mL), was added DIBAL-H (1.0 M in hexane, 7.8 mL, 7.8 mmol) at -78 °C. After the mixture had been stirred at this temperature for 2 h, saturated aqueous NH₄Cl (50 mL) was poured into the mixture followed by 1M HCl (50 mL). The product was then extracted with CH₂Cl₂ (3 × 100 mL). The organic layers were combined, dried (MgSO₄), filtered and concentrated *in vacuo*. Purification *via* flash column chromatography on silica gel (EtOAc/hexane = 1:2) gave **39** (0.70 g, 65%) as a crude white solid consisting of an inseparable mixture of the desired aldehyde product (major) and starting material. A mixture of crude **39** (0.52 g, 1.9 mmol) and ClP(O)(OEt)₂ (0.32 mL, 2.2 mmol) in THF (37 mL) was cooled to -78 °C, and then LiHMDS (1.0 M in THF, 3.7 mL, 3.7 mmol) was added. After stirring at -78 °C for 30 min, the reaction mixture was warmed to rt and stirred for a further 1.5 h. Saturated aqueous NH₄Cl (5.0 mL) was poured into the mixture. The reaction mixture was diluted with water (50 mL) and extracted with EtOAc (3 × 60 mL). The organic layers were combined, dried (MgSO₄), filtered and concentrated *in vacuo*. Purification *via* flash column chromatography on silica gel (EtOAc/hexane = 3:8) gave **40** as a pale yellow solid (0.22 g, 23%).

mp: 190-193 °C

ν_{max} (neat): 1571, 1446, 1319 (S=O), 1260, 1146 (S=O), 1085.

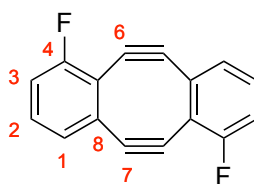
δ_{H} (500 MHz, CDCl₃): 7.67 (2H, t, *J* 7.11), 7.57-7.46 (10H, m, Ar H), 7.33-7.27 (2H, m, Ar H), 6.95-6.86 (4H, m, Ar H).

δ_{C} (126 MHz, CDCl₃): 160.2 (d, *J* 253.97, C4), 142.7 (Ar C), 140.6 (Ar CH), 138.5 (Ar C), 138.0 (Ar C), 134.0 (Ar CH), 131.5 (d, *J* 8.80, Ar CH), 129.2 (Ar CH), 128.6 (Ar CH), 122.6 (Ar CH), 117.4 (d, *J* 17.06, Ar C), 116.3 (d, *J* 21.80, Ar CH).

δ_F (376 MHz, $CDCl_3$): -105.5.

HRMS (ES⁺): found 521.0693; $C_{28}H_{19}O_4^{32}S_2F_2$ $[M+H]^+$ requires 521.0693.

1,7-Difluoro-5,6,11,12-tetrahydrodibenzo[a,e]cyclooctene



7

A solution of **40** (0.13 g, 0.24 mmol) in THF (4.9 mL) was cooled to $-78\text{ }^{\circ}\text{C}$, and then LDA (1.0 M in THF/hexane, 0.98 mL, 0.98 mmol). The reaction mixture was stirred at this temperature for 2 h, and saturated aqueous NH_4Cl (7.0 mL) was poured into the mixture. The reaction mixture was cooled to rt, diluted with water (20 mL) and extracted with CH_2Cl_2 (3×30 mL). The organic layers were combined, dried ($MgSO_4$), filtered and concentrated *in vacuo*. Purification *via* flash column chromatography on silica gel (EtOAc/hexane = 1:8) gave **7** as a yellow solid (15 mg, 26%).

mp: $140\text{ }^{\circ}\text{C}$ (dec.)

ν_{max} (neat): 2156 ($C\equiv C$), 1574, 1448, 1181, 877, 815.

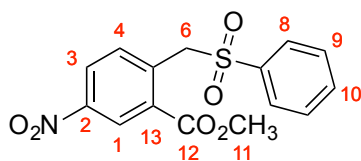
δ_H (500 MHz, $CDCl_3$): 6.74-6.68 (2H, m, Ar H), 6.62 (2H, td, J 8.41, 2.61, Ar H), 6.48 (2H, dd, J 8.70, 2.60, Ar H).

δ_C (126 MHz, $CDCl_3$): 163.0 (d, J 250.97, C4), 135.3 (d, J 10.12), 128.2 (d, J 8.78, Ar CH), 115.22 (Ar CH), 115.23 (d, J 45.55, Ar C), 109.9 ($\underline{C}\equiv C$), 107.4 ($\underline{C}\equiv C$).

δ_F (376 MHz, $CDCl_3$): -109.5.

HRMS (ES⁺): found 236.0427; $C_{16}H_6F_2$ $[M+H]^+$ requires 236.0438.

Methyl 5-nitro-2-((phenylsulfonyl)methyl)benzoate



43

To a suspension of methyl 2-methyl-5-nitrobenzoate (5.0 g, 26 mmol) in CCl₄ (128 mL) at 80 °C under N₂ were added NBS (4.8 g, 27 mmol) and BPO (0.62 mg, 2.6 mmol), and then the resulting mixture was heated at 100 °C. After stirring at this temperature for 6 h, the reaction mixture was cooled to rt. The reaction mixture was diluted with saturated aqueous NH₄Cl (120 mL) and extracted with CH₂Cl₂ (3 × 120 mL). The organic layers were combined, dried (MgSO₄), filtered and concentrated *in vacuo*. To the resulting residue (7.7 g, 28 mmol) were added benzenesulfinic acid sodium salt dihydrate (5.6 g, 34 mmol) and DMF (42 mL). After the resulting mixture had been stirred at 80 °C overnight, it was cooled to rt. The reaction mixture was diluted with water (50 mL) and extracted with EtOAc (3 × 50 mL). The organic layers were combined, dried (MgSO₄), filtered and concentrated *in vacuo*. Purification *via* flash column chromatography on silica gel (EtOAc/hexane = 1:1) gave **43** (6.4 g, 74%) as a yellow solid.

mp: 134-135 °C

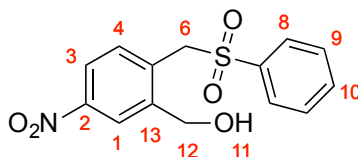
ν_{max} (neat): 2952, 1722 (C=O), 1527 (NO₂), 1346, 1306 (NO₂), 1254 (S=O), 1135 (S=O), 1067, 732.

δ_{H} (400 MHz, CDCl₃): 8.74 (1H, d, *J* 2.5, H1), 8.32 (1H, dd, *J* 8.5, 2.5, H3), 7.71-7.61 (3H, m, Ar H), 7.56 (1H, d, *J* 8.5, H4), 7.53-7.47 (2H, m, Ar H), 5.15 (2H, s, H6), 3.84 (3H, s, H11).

δ_{C} (126 MHz, CDCl₃): 165.2 (C2), 147.8 (Ar C), 138.1 (Ar C), 136.1 (Ar C), 134.7 (Ar CH), 134.1 (Ar CH), 132.1 (Ar C), 129.2 (Ar CH), 128.6 (Ar CH), 126.3 (Ar CH), 125.9 (Ar CH), 58.7 (C6), 52.9 (C11).

HRMS (ES⁺): found 336.0546; C₁₅H₁₄NO₆³²S [M+H]⁺ requires 336.0542.

(5-nitro-2-((phenylsulfonyl)methyl)phenyl)methanol



44

To a solution of **43** (0.28 g, 0.84 mmol) in CH₂Cl₂ (2.6 mL), was added DIBAL-H (1.0 M in hexane, 2.0 mL, 2.0 mmol) at -78 °C. After the mixture had been stirred at this temperature for 2 h, saturated aqueous NH₄Cl (10 mL) was poured into the mixture followed by 1M HCl (10 mL). The reaction mixture was warmed to rt and the product was then extracted with EtOAc (3 × 20 mL). The organic layers were combined, dried (MgSO₄), filtered and concentrated *in vacuo*. Purification *via* flash column chromatography on silica gel (EtOAc/hexane = 1:1) gave **44** as a white solid (0.24 g, 91%).

mp: 146-147 °C

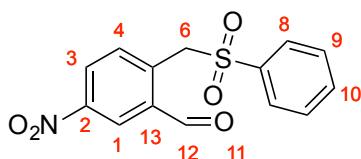
ν_{\max} (neat): 3487 (O-H), 3099, 2870, 1590, 1518, 1446, 1347, 1304 (S=O).

δ_{H} (400 MHz, CD₃OD): 8.34 (1H, d, *J* 2.6, Ar H), 8.03 (1H, dd, *J* 8.5, 2.6, Ar H), 7.79-7.71 (3H, m, Ar H), 7.60 (2H, t, *J* 7.8, Ar H), 7.31 (1H, *J* 8.5, Ar H), 4.76 (2H, s, H6), 4.67 (2H, s, H12).

δ_{C} (101 MHz, CD₃OD): 150.5, 146.5, 140.6, 136.4 (Ar CH), 135.7 (Ar CH), 135.3, 131.4 (Ar CH), 130.5 (Ar CH), 124.2 (Ar CH), 123.5 (Ar CH), 62.8 (C12), 60.0 (C6).

HRMS (ES⁺): found 328.0240; C₁₄H₁₁NO₅³²S [M+Na]⁺ requires 328.0250.

5-nitro-2-((phenylsulfonyl)methyl)benzaldehyde



45

To a solution of **44** (0.16 g, 0.52 mmol) in CH₂Cl₂ (8 mL) was added DMP (0.27 g, 0.63 mmol) at rt. After the reaction mixture had been stirred for 3 h, the reaction mixture was poured into saturated Na₂S₂O₃ solution (8 mL). Mixture was stirred to dissolve the solid and layers were separated. The CH₂Cl₂ layer was then extracted with saturated aqueous Na₂S₂O₃ (2 × 8 mL) followed by saturated aqueous NaHCO₃ (2 × 8 mL). CH₂Cl₂ was then removed *in vacuo* and purification *via* flash column chromatography on silica gel (PE/EtOAc = 1:1) gave pure product **45** (0.14 g, 87%) as a white solid.

mp: 187-188 °C

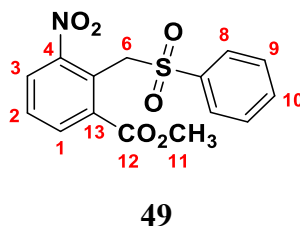
ν_{max} (neat): 1702 (C=O), 1611, 1589, 1522, 1446, 1400, 1350, 1303 (S=O).

δ_{H} (400 MHz, CDCl₃): 9.95 (1H, s, H12), 8.62 (1H, d, *J* 2.42, Ar H), 8.41 (1H, d, *J* 2.43, Ar H), 7.79-7.61 (4H, m, Ar H), 7.57-7.47 (2H, m, Ar H), 5.08 (2H, s, H6)

δ_{C} (101 MHz, CDCl₃): 189.5 (C12), 148.4 (Ar C), 137.9 (Ar C), 135.6 (Ar C), 135.3 (Ar C), 135.2 (Ar CH), 134.4 (Ar CH), 129.3 (Ar CH), 128.5 (Ar CH), 128.2 (Ar CH), 127.5 (Ar CH), 57.4 (C6).

HRMS (ES⁺): found 330.0401; C₁₄H₁₃NO₅³²S [M+Na]⁺ requires 330.0407.

Methyl 3-nitro-2-((phenylsulfonyl)methyl)benzoate



To a suspension of methyl 2-methyl-3-nitrobenzoate (1.0 g, 5.1 mmol) in CCl₄ (51 mL) at 80 °C under N₂ were added NBS (0.96 g, 5.4 mmol) and BPO (0.12 g, 0.51 mmol), and then the resulting mixture was heated at 100 °C. After stirring at this temperature for 6 h, the reaction mixture was cooled to rt. The reaction mixture was diluted with saturated aqueous NH₄Cl (50 mL) and extracted with CH₂Cl₂ (3 × 50 mL). The organic layers were combined, dried (MgSO₄), filtered and concentrated *in vacuo*. To the resulting residue (1.4 g, 5.0 mmol) were added benzenesulfinic acid sodium salt dihydrate (0.98 g, 6.0 mmol) and DMF (8.5 mL). After the resulting mixture had been stirred at 80 °C overnight, it was cooled to rt. The reaction mixture was diluted with water (25 mL) and extracted with EtOAc (3 × 25 mL). The organic layers were combined, dried (MgSO₄), filtered and concentrated *in vacuo*. Purification *via* flash column chromatography on silica gel (EtOAc/hexane = 2:1) gave **49** (0.89 g, 57%) as a yellow solid.

mp: 102-104 °C

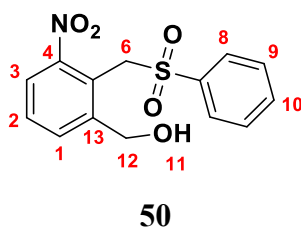
ν_{max} (neat): 1720 (C=O), 1533 (NO₂), 1447, 1302 (S=O), 1268, 1149 (S=O), 1083.

δ_{H} (500 MHz, CDCl₃): 8.11 (1H, d, *J* 7.86, H1), 8.00 (1H, d, *J* 7.93, H3), 7.68-7.56 (4H, m, Ar H), 7.52-7.44 (2H, m), 5.70 (2H, br. s, H6), 3.86 (3H, d, *J* 1.83, H11), 3.05 (0.6 H, s).

δ_{C} (126 MHz, CDCl₃): 166.2 (C12), 151.7 (C4), 138.0 (Ar C), 134.7 (C1), 134.2 (Ar CH), 134.1 (Ar C), 133.7 (Ar CH), 129.6 (C2), 129.3 (Ar CH), 128.3 (C3), 127.3 (Ar CH), 123.1 (Ar C), 53.1 (C11), 52.2 (C6), 44.5.

HRMS (ES⁺): found 358.0363; C₁₅H₁₃NO₆Na³²S [M+Na]⁺ requires 358.0361.

(3-Nitro-2-((phenylsulfonyl)methyl)phenyl)methanol



To a solution of **49** (0.49 g, 1.5 mmol) in CH₂Cl₂ (4.5 mL), was added DIBAL-H (1.0 M in hexane, 3.4 mL, 3.4 mmol) at -78 °C. After the mixture had been stirred at this temperature for 2 h, saturated aqueous NH₄Cl (10 mL) was poured into the mixture followed by 1M HCl (10 mL). The reaction mixture was warmed to rt and the product was then extracted with CH₂Cl₂ (3 × 20 mL). The organic layers were combined, dried (MgSO₄), filtered and concentrated *in vacuo* to afford the pure product **50** as a white solid (0.38 g, 84%).

mp: 88-89 °C

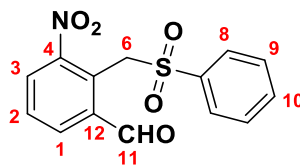
ν_{max} (neat): 3525 (O-H), 1736 (C=O), 1532 (NO₂), 1355, 1308 (S=O), 1148 (S=O), 1085.

δ_{H} (500 MHz, CDCl₃): 7.88 (1H, dd, *J* 8.13, 1.34, Ar H), 7.84-7.78 (3H, m, Ar H), 7.74-7.59 (4H, m, Ar H), 5.22 (2H, br. s, H6), 4.86 (2H, s, H12), 3.07 (0.7 H, s), 2.83 (1H, br. s, H11).

δ_{C} (126 MHz, CDCl₃): 151.1 (C4), 143.9 (C13), 138.0 (Ar C), 134.7 (Ar CH), 134.5 (Ar CH), 130.0 (Ar CH), 129.6 (Ar CH), 128.3 (Ar CH), 125.2 (Ar CH), 120.4 (Ar C), 63.0 (C12), 53.4 (C6), 44.5.

HRMS (ES⁺): found 330.0415; C₁₄H₁₃NO₅Na³²S [M+Na]⁺ requires 330.0412.

3-Nitro-2-((phenylsulfonyl)methyl)benzaldehyde



51

To a solution of **50** (0.78 g, 2.5 mmol) in CH₂Cl₂ (7.6 mL) was added DMP (1.2 g, 2.8 mmol) at rt. After the reaction mixture had been stirred for 3 h, the reaction mixture was diluted with CH₂Cl₂ (25 mL) and poured into saturated Na₂S₂O₃ solution (35 mL). Mixture was stirred to dissolve the solid and layers were separated. The CH₂Cl₂ layer was then extracted with saturated aqueous Na₂S₂O₃ (2 × 35 mL) followed by saturated aqueous NaHCO₃ (2 × 35 mL). CH₂Cl₂ was then removed *in vacuo* to yield pure product **51** (0.67 g, 87%) as a white solid.

mp: 200-202 °C

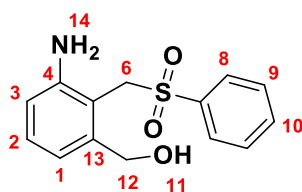
ν_{max} (neat): 1730 (C=O), 1534 (NO₂), 1447, 1354, 1304 (S=O), 1150 (S=O), 1084.

δ_{H} (400 MHz, CDCl₃): 10.17 (1H, s, H11), 8.20-8.11 (2H, m, Ar H), 7.82-7.66 (4H, m, Ar H), 7.59-7.52 (2H, m, Ar H), 5.65 (2H, s, H6).

δ_{C} (126 MHz, CDCl₃): 189.9 (C11), 151.7 (C4), 138.0 (Ar C), 137.0 (Ar CH), 136.8 (Ar C), 134.4 (Ar CH), 130.2 (Ar CH), 129.7 (Ar CH), 129.4 (Ar CH), 128.4 (Ar CH), 127.4 (Ar C), 123.2 (Ar C), 50.9 (C6).

HRMS (ES⁺): found 304.0280; C₁₄H₁₂NO₅³²S [M+H]⁺ requires 304.0280.

(3-Amino-2-((phenylsulfonyl)methyl)phenyl)methanol



52

Zn powder (0.39 g, 0.59 mmol) and NH₄Cl (79 mg, 1.5 mmol) were added to a solution of nitro-compound **51** (18 mg, 0.06 mmol) in a 5:1 mixture of acetone:water (1.2 mL) at rt. After 2 h the reaction mixture was filtered through a pad of Celite[®] and concentrated *in vacuo*. The residue was extracted with diethyl ether (5 mL), washed with brine (5 mL), dried (MgSO₄), filtered and concentrated *in vacuo*. Purification *via* flash column chromatography on silica gel (EtOAc/hexane = 1:1) gave **52** (14 mg, 86%) as a white solid.

mp: 139-141 °C

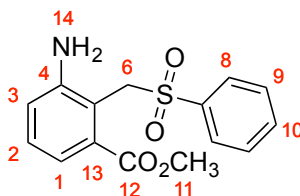
ν_{max} (neat): 3525 (O-H), 3356 (NH₂), 1470, 1307 (S=O), 1143 (S=O), 1083.

δ_{H} (500 MHz, CDCl₃): 7.99 (2H, dd, *J* 8.44, 1.22, Ar H), 7.77-7.56 (3H, m, Ar H), 7.20 (1H, t, *J* 7.76, Ar H), 6.89-6.79 (2H, m, Ar H), 4.66 (2H, s, H₆), 4.48 (2H, s, H₁₂).

δ_{C} (126 MHz, CDCl₃): 147.9 (Ar C), 142.0 (Ar C), 139.1 (Ar C), 134.2 (Ar CH), 130.2 (Ar CH), 129.5 (Ar CH), 128.2 (Ar CH), 121.1 (Ar CH), 118.2 (Ar CH), 112.6 (Ar C), 64.0 (C₁₂), 55.9 (C₆).

HRMS (ES⁺): found 278.0845; C₁₄H₁₆NO₃³²S [M+H]⁺ requires 278.0851.

Methyl 3-amino-2-((phenylsulfonyl)methyl)benzoate



54

Zn powder (0.21 g, 3.3 mmol) and NH₄Cl (0.26 g, 4.9 mmol) were added to a solution of nitro-compound **49** (0.10 g, 0.30 mmol) in a 5:1 mixture of acetone:water (6.6 mL) at rt. After 2 h the reaction mixture was filtered through a pad of Celite® and concentrated *in vacuo*. The residue was extracted with diethyl ether (20 mL), washed with brine (20 mL), dried over MgSO₄. The solvent was evaporated *in vacuo* to give pure product **54** as a liquid (69 mg, 75%).

mp: 103°C

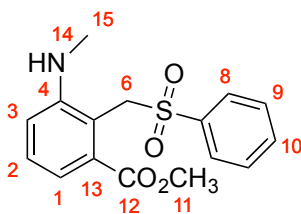
ν_{max} (neat): 3427 (NH₂), 3372 (NH₂), 1711 (C=O), 1466, 1302 (S=O), 1146 (S=O), 1081.

δ_{H} (500 MHz, CDCl₃): 7.82-7.75 (2H, m, Ar H), 7.62 (1H, app tt, *J* 7.47, 1.22, Ar H), 7.54-7.44 (2H, m, Ar H), 7.29 (1H, d, *J* 8.60, Ar H), 7.19 (1H, t, *J* 7.86, Ar H), 6.98 (1H, d, *J* 7.96, Ar H), 5.24 (2H, br. s, H₆), 4.51 (2H, br. s, H₁₄), 3.63 (3H, s, H₁₁), 2.44 (1H, br. s, H₁₁).

δ_{C} (126 MHz, CDCl₃): 167.6 (C₁₂), 148.1 (Ar C), 138.3 (Ar C), 133.6 (Ar CH), 131.5 (Ar C), 129.2 (Ar CH), 128.8 (Ar CH), 128.7 (Ar CH), 122.1 (Ar CH), 121.8 (Ar CH), 114.9 (Ar C), 54.3 (C₆), 52.0 (C₁₁).

HRMS (ES⁺): found 306.0791; C₁₅H₁₆NO₄³²S [M+H]⁺ requires 306.0795.

Methyl 3-(methylamino)-2-((phenylsulfonyl)methyl)benzoate



55

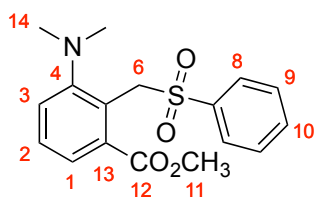
A solution of **54** (30 mg, 0.10 mmol) in methanol (0.50 mL) was heated to 50 °C and then 37% aqueous formaldehyde solution (0.016 mL, 0.60 mmol) was added. The mixture was stirred for 5 minutes at rt and then sodium cyanoborohydride (7.4 mg, 0.12 mmol) was added. 1M HCl was added to adjust the pH (6-8) of the reaction mixture. After the reaction mixture had been stirred for overnight, the reaction mixture was poured into a water-ice mixture (~5.0 mL) and extracted with CH₂Cl₂ (3 × 6.0 mL). The remaining aqueous layer was neutralized with saturated NaHCO₃ solution and extracted with CH₂Cl₂ (3 × 6.0 mL). The organic layers were combined, dried (MgSO₄), filtered and concentrated *in vacuo*. Purification *via* flash column chromatography on silica gel (EtOAc/hexane = 1:3) gave minor product **55** (5.0 mg, 16%) as a colourless liquid.

ν_{max} (neat): 2989 (C-H), 1714 (C=O), 1591, 1447, 1320 (S=O), 1150 (S=O), 1082.

δ_{H} (500 MHz, CDCl₃): 7.77 (2H, dd, *J* 8.39, 1.22, H8), 7.62 (1H, t, *J* 7.47, H10), 7.48 (2H, t, *J* 7.86, H9), 7.30 (1H, t, *J* 7.95, H1), 7.23 (1H, dd, *J* 7.75, 1.21, H2), 6.96 (1H, d, *J* 8.16, H3), 5.22 (2H, br. s, H6), 3.62 (3H, s, H11), 2.90 (3H, s, H15).

δ_{C} (126 MHz, CDCl₃): 167.9 (C12), 150.0 (Ar C), 138.3 (Ar C), 133.6 (Ar CH), 131.4 (Ar C), 129.5 (Ar CH), 128.8 (Ar CH), 128.7 (Ar CH), 120.2 (Ar CH), 115.8 (Ar CH), 114.6 (Ar C), 54.6 (C6), 52.0 (C11), 31.1 (C15).

Methyl 3-(dimethylamino)-2-((phenylsulfonyl)methyl)benzoate



56

To a solution of **54** (0.10 g, 0.34 mmol) in glacial acetic acid (2.0 mL) under Ar (g) were added paraformaldehyde (0.10 g, 3.4 mmol) and sodium cyanoborohydride (0.11 g, 1.7 mmol). After the reaction mixture had been stirred for overnight, the reaction mixture was poured into a water-ice mixture (~5.0 mL) and extracted with CH₂Cl₂ (2 × 5.0 mL). The remaining aqueous layer was neutralized with saturated NaHCO₃ solution and extracted with CH₂Cl₂ (2 × 5.0 mL). The organic layers were combined, dried (MgSO₄), filtered and concentrated *in vacuo*. Purification *via* flash column chromatography on silica gel (EtOAc/hexane = 1:3) gave **56** (0.11 g, 93%) as a colourless liquid.

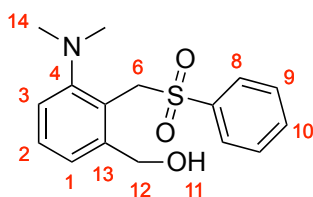
ν_{\max} (neat): 2944, 1714 (C=O), 1446, 1306, 1263 (S=O), 1115, 1033, 1003 (S=O), 689.

δ_{H} (400 MHz, CDCl₃): 7.67 (1H, d, *J* 8.1, H1), 7.57 (2H, d, *J* 7.6, H8), 7.52 (1H, t, *J* 7.5, H10), 7.41-7.32 (3H, m, Ar H), 7.16 (1H, d, *J* 8.1, H3), 5.37 (2H, s, H6), 3.94 (3H, s, H11), 2.32 (6H, s, H14).

δ_{C} (101 MHz, CDCl₃): 168.5 (C12), 155.2 (Ar C), 139.2 (Ar C), 133.9 (Ar C), 133.1 (Ar CH), 129.3 (Ar CH), 128.5 (Ar CH), 128.4 (Ar CH), 126.4 (Ar CH), 124.7, 124.3 (Ar CH), 52.7 (C6), 52.5 (C11), 45.2 (C14).

HRMS (ES⁺): found 334.1106; C₁₇H₂₀NO₄³²S [M+H]⁺ requires 334.1108.

(3-(Dimethylamino)-2-((phenylsulfonyl)methyl)phenyl)methanol



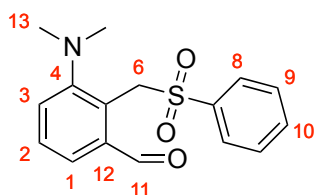
57

To a solution of **56** (1.9 g, 5.7 mmol) in CH₂Cl₂ (18.0 mL), was added DIBAL-H (1.0 M in hexane, 13 mL, 13 mmol) at -78 °C. After the mixture had been stirred at this temperature for 2 h, saturated aqueous NH₄Cl (60 mL) was poured into the mixture followed by 1M HCl (60 mL). The product was then extracted with CH₂Cl₂ (3 × 120 mL). The organic layers were combined, dried (MgSO₄), filtered and concentrated *in vacuo* to afford the pure product **57** as a pale-yellow oil (1.7 g, 96%).

δ_{H} (400 MHz, CDCl₃): 7.67-7.53 (3H, m, Ar H), 7.49-7.40 (2H, m, Ar H), 7.38-7.32 (2H, m, Ar H), 7.00-6.94 (1H, m, Ar H), 4.94 (2H, s, H6), 4.83 (2H, d, *J* 6.68, H12), 3.25 (1H, t, *J* 6.70, H11), 2.18 (6H, s, H14).

δ_{C} (126 MHz, CDCl₃): 150.0 (Ar C), 141.7 (Ar C), 139.2 (Ar C), 134.1 (Ar CH), 130.4 (Ar CH), 129.4 (Ar CH), 128.2 (Ar CH), 119.6 (Ar CH), 112.3 (Ar CH), 112.2 (Ar C), 64.2 (C12), 56.0 (C6), 31.1 (C14).

3-(Dimethylamino)-2-((phenylsulfonyl)methyl)benzaldehyde



58

To a solution of **57** (1.7 g, 5.5 mmol) in CH₂Cl₂ (20 mL) was added DMP (2.54 g, 6.0 mmol) at rt. After the reaction mixture had been stirred for 3 h, the reaction mixture was poured into saturated Na₂S₂O₃ solution (20 mL). Mixture was stirred to dissolve the solid and layers were separated. The CH₂Cl₂ layer was then extracted with saturated aqueous Na₂S₂O₃ (2 × 20 mL) followed by saturated aqueous NaHCO₃ (2 × 20 mL). CH₂Cl₂ was then removed *in vacuo* and purification *via* flash column chromatography on silica gel (EtOAc/hexane = 1:4) gave pure product **58** (1.4 g, 82%) as a white solid.

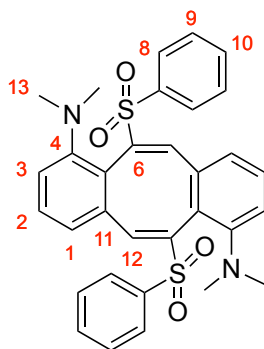
ν_{max} (neat): 2938, 1692 (C=O), 1583, 1447, 1307 (S=O), 1157 (S=O), 1083.

δ_{H} (400 MHz, CDCl₃): 10.17 (1H, s, H11), 7.68 (1H, dd, *J* 7.7, 1.4, H1), 7.63-7.59 (2H, m, Ar H), 7.59-7.52 (1H, m, Ar H), 7.48 (1H, t, *J* 7.8, H2), 7.42 (2H, t, *J* 7.8, H9), 7.31 (1H, dd, *J* 7.9, 1.4, H3), 5.28 (2H, s, H6), 2.36 (6H, s, H13).

δ_{C} (126 MHz, CDCl₃): 193.4 (C11), 150.5 (Ar C), 138.3 (Ar C), 134.9 (Ar C), 133.8 (Ar CH), 130.1 (Ar CH), 128.8 (Ar CH), 128.7 (Ar CH), 125.7 (Ar CH), 117.6 (Ar CH), 112.9 (Ar C), 53.8 (C6), 31.0 (C13).

HRMS (ES⁺): found 304.0997; C₁₆H₁₈NO₃³²S [M+H]⁺ requires 304.1002.

(5*E*,11*E*)-*N*¹,*N*¹,*N*⁷,*N*⁷-tetramethyl-6,12-bis(phenylsulfonyl)dibenzo[*a,e*][8]annulene-1,7-diamine



59

A mixture of **58** (1.3 g, 4.3 mmol) and ClP(O)(OEt)₂ (0.64 mL, 4.7 mmol) in THF (86 mL) was cooled to −78 °C, and then LiHMDS (1.0 M in THF, 9.4 mL, 9.4 mmol) was added. After stirring at −78 °C for 30 min, the reaction mixture was warmed to rt and stirred for a further 1.5 h. Saturated aqueous NH₄Cl (10 mL) was poured into the mixture. The reaction mixture was diluted with water (10 mL) and extracted with EtOAc (3 × 20 mL). The organic layers were combined, dried (MgSO₄), filtered and concentrated *in vacuo*. Purification *via* flash column chromatography on silica gel (EtOAc/hexane = 1:2) gave **59** as a pale yellow solid (0.32 g, 26%).

mp: 197-199°C

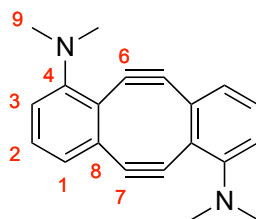
ν_{max} (neat): 1574, 1296 (S=O), 1140 (S=O), 727.

δ_{H} (400 MHz, CDCl₃): 7.55 (2H, tt, *J* 6.0, 2.6, Ar H), 7.46-7.38 (10H, m, Ar H), 7.18 (2H, t, *J* 7.9, H2), 6.76 (2H, d, *J* 7.9, H1), 6.61 (2H, d, *J* 7.9, H3), 2.42 (12H, s, H13).

δ_{C} (101 MHz, CDCl₃): 154.1 (Ar C), 147.3 (Ar C), 140.9 (Ar CH), 140.6 (Ar C), 138.8 (Ar C), 133.0 (Ar CH), 129.9 (Ar CH), 128.7 (Ar CH), 128.2 (Ar CH), 120.9 (Ar C), 119.0 (Ar CH), 118.1 (Ar CH), 42.9 (C13).

HRMS (ES⁺): found 571.1715; C₃₂H₃₁N₂O₄³²S₂ [M+H]⁺ requires 571.1720.

N¹,N¹,N⁷,N⁷-tetramethyl-5,6,11,12-tetrahydrodibenzo[a,e]cyclooctene-1,7-diamine



10

A solution of **59** (0.10 g, 0.20 mmol) in THF (3.5 mL) was cooled to -78°C , and then LDA (1.0 M in THF/hexane, 0.85 mL, 0.85 mmol). The reaction mixture was stirred at this temperature for 2 h, and saturated aqueous NH_4Cl (1.0 mL) was poured into the mixture. The reaction mixture was cooled to rt, diluted with water (4.0 mL) and extracted with CH_2Cl_2 (3×5.0 mL). The organic layers were combined, dried (MgSO_4), filtered and concentrated *in vacuo*. Purification *via* flash column chromatography on silica gel ($\text{CH}_2\text{Cl}_2/\text{hexane} = 1:1$) gave **10** as an orange solid (27 mg, 54%).

mp: $186\text{--}190^{\circ}\text{C}$ (dec.)

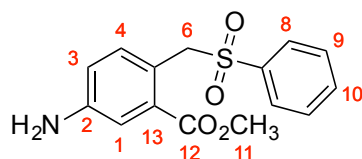
ν_{max} (neat): 3049, 2960, 2804, 2137 ($\text{C}\equiv\text{C}$), 1433, 1346, 1130, 1002, 785.

δ_{H} (400 MHz, CDCl_3): 6.79 (2H, dd, J 8.6, 7.4, H2), 6.47 (2H, d, J 8.6, Ar H), 6.30 (2H, d, J 7.4, Ar H), 2.92 (12H, s, H9).

δ_{C} (101 MHz, CDCl_3): 150.28 (C4), 134.56 (Ar C), 129.63 (C2), 119.3 (Ar C), 118.9 (Ar CH), 117.6 (Ar CH), 110.9 ($\text{C}\equiv\text{C}$), 108.7 ($\text{C}\equiv\text{C}$), 42.6 (C9).

HRMS (ES⁺): found 287.1540; $\text{C}_{20}\text{H}_{19}\text{N}_2$ $[\text{M}+\text{H}]^+$ requires 287.1543.

Methyl 5-amino-2-((phenylsulfonyl)methyl)benzoate



60

Zn powder (2.0 g, 30 mmol) and NH₄Cl (2.4 g, 45 mmol) were added to a solution of nitro-compound **43** (1.0 g, 3.0 mmol) in a 5:1 mixture of acetone:water (60 mL) at rt. After 2 h the reaction mixture was filtered through a pad of Celite® and concentrated *in vacuo*. The residue was extracted with diethyl ether (200 mL), washed with brine (200 mL), dried over MgSO₄. The solvent was evaporated *in vacuo* to give pure product **60** as a liquid (0.64 g, 70%).

mp: 168-169 °C

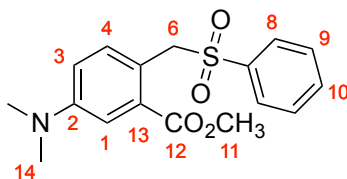
ν_{\max} (neat): 3100-2800 (N-H), 3076, 2957 1720 (C=O), 1286 (S=O), 1137 (S=O), 1066, 691.

δ_{H} (400 MHz, CDCl₃): 7.65-7.61 (2H, m, Ar H), 7.60-7.54 (1H, m, Ar H), 7.46-7.39 (2H, m, Ar H), 7.15 (1H, d, *J* 2.6, H1), 7.07 (1H, d, *J* 8.2, H4), 6.74 (1H, dd, *J* 8.2, 2.6, H3), 4.90 (2H, s, H6), 3.84 (2H, br. s, NH₂), 3.69 (3H, s, H11).

δ_{C} (101 MHz, CDCl₃): 167.3 (C12), 147.1 (C2), 138.6 (Ar C), 134.7 (C4), 133.5 (Ar CH), 131.7 (Ar C), 128.8 (Ar CH), 128.8 (Ar CH), 118.2 (C3), 118.1 (Ar C), 117.1 (C1), 59.1 (C6), 52.2 (C11).

HRMS (ES⁺): found 306.0790; C₁₅H₁₆NO₄³²S [M+H]⁺ requires 306.0800.

Methyl 5-(dimethylamino)-2-((phenylsulfonyl)methyl)benzoate



61

To a solution of **60** (6.1 g, 20 mmol) in glacial acetic acid (119 mL) under Ar (g) were added paraformaldehyde (6.0 g, 199 mmol) and sodium cyanoborohydride (6.3 g, 100 mmol). After the reaction mixture had been stirred for overnight, the reaction mixture was poured into a water-ice mixture (~240 mL) and extracted with CH₂Cl₂ (2 × 240 mL). The remaining aqueous layer was neutralized with saturated NaHCO₃ solution and extracted with CH₂Cl₂ (2 × 240 mL). The organic layers were combined, dried (MgSO₄), filtered and concentrated *in vacuo*. Purification *via* flash column chromatography on silica gel (EtOAc/hexane = 1:1) gave **61** (5.5 g, 82%) as a colourless liquid.

mp: 150-152 °C

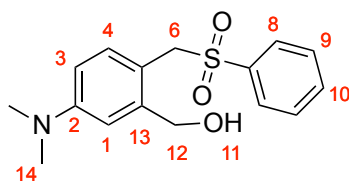
ν_{max} (neat): 2950 (C-H), 1714 (C=O), 1606, 1515, 1446, 1305 (S=O), 1258 (S=O), 1083.

δ_{H} (500 MHz, CDCl₃): 7.66-7.60 (2H, m, Ar H), 7.57 (1H, t, *J* 7.00, Ar H), 7.47-7.40 (2H, m, Ar H), 7.16 (1H, s, H1), 7.12 (1H, d, *J* 8.6, Ar H), 6.76 (1H, dd, *J* 8.55, 2.85, Ar H), 4.90 (2H, s, H6), 3.70 (3H, s, H11), 2.98 (6H, s, H14).

δ_{C} (126 MHz, CDCl₃): 167.8 (C12), 150.2 (Ar C), 138.7 (Ar C), 134.3 (Ar CH), 133.3 (Ar CH), 131.3 (Ar C), 129.6 (Ar C), 128.7 (Ar CH), 128.7 (Ar CH), 115.2 (Ar CH), 114.2 (Ar CH), 59.1 (C6), 52.0 (C11), 40.2 (C14).

HRMS (ES⁺): found 334.1105; C₁₇H₂₀NO₄³²S [M+H]⁺ requires 334.1113.

(5-(Dimethylamino)-2-((phenylsulfonyl)methyl)phenyl)methanol



62

To a solution of **61** (0.34 g, 1.0 mmol) in CH₂Cl₂ (3.1 mL), was added DIBAL-H (1.0 M in hexane, 2.2 mL, 2.2 mmol) at -78 °C. After the mixture had been stirred at this temperature for 2 h, saturated aqueous NH₄Cl (10 mL) was poured into the mixture followed by 1M HCl (10 mL). The reaction mixture was warmed to rt and the product was then extracted with CH₂Cl₂ (3 × 20 mL). The organic layers were combined, dried (MgSO₄), filtered and concentrated *in vacuo* to afford the pure product **62** as an off-white solid (0.29 g, 94%).

mp: 140-141 °C

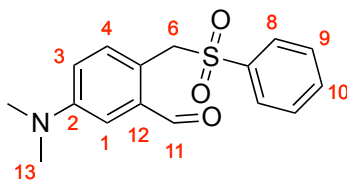
ν_{\max} (neat): 3452 (O-H), 2898 (C-H), 1610, 1515, 1360, 1298 (S=O), 1205 (C-N), 1147.

δ_{H} (500 MHz, CDCl₃): 7.80-7.73 (2H, m, Ar H), 7.64 (1H, t, *J* 7.48, Ar H), 7.56-7.48 (2H, m, Ar H), 6.79-6.73 (2H, m, Ar H), 6.50 (1H, dd, *J* 8.58, 2.72, Ar H), 4.57 (2H, s, H₁₂), 4.42 (2H, s, H₆), 2.97 (6H, s, H₁₄).

δ_{C} (126 MHz, CDCl₃): 151.0 (Ar C), 141.7 (Ar C), 138.4 (Ar C), 133.8 (Ar CH), 133.5 (Ar CH), 129.1 (Ar CH), 128.6 (Ar CH), 113.8 (Ar CH), 112.3 (Ar C), 111.7 (Ar CH), 63.8 (C₁₂), 59.6 (C₆), 40.2 (C₁₄).

HRMS (ES⁺): found 306.1149; C₁₆H₂₀NO₃³²S [M+H]⁺ requires 306.1164.

5-(Dimethylamino)-2-((phenylsulfonyl)methyl)benzaldehyde



63

To a solution of **62** (0.29 g, 0.95 mmol) in CH₂Cl₂ (2.9 mL) was added DMP (0.44 g, 1.1 mmol) at rt. After the reaction mixture had been stirred for 3 h, the reaction mixture was diluted with CH₂Cl₂ (4.0 mL) and poured into saturated Na₂S₂O₃ solution (5 mL). Mixture was stirred to dissolve the solid and layers were separated. The CH₂Cl₂ layer was then extracted with saturated aqueous Na₂S₂O₃ (2 × 7.0 mL) followed by saturated aqueous NaHCO₃ (2 × 7.0 mL). CH₂Cl₂ was then removed *in vacuo* and purification *via* flash column chromatography on silica gel (EtOAc/hexane = 1:2) gave pure product **63** (0.21 g, 73%) as a white solid.

mp: 122-125 °C

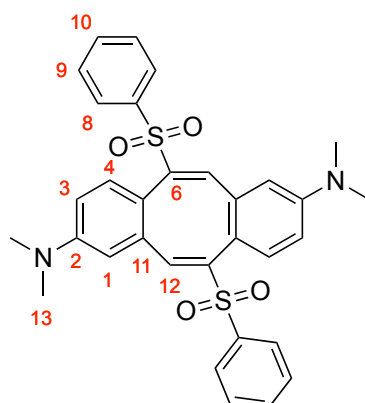
ν_{max} (neat): 2922 (C-H), 1692 (C=O), 1606, 1517, 1305 (S=O), 1206 (C-N), 1148, 1083.

δ_{H} (500 MHz, CDCl₃): 9.76 (1H, s, H11), 7.72-7.64 (2H, m, Ar H), 7.58 (1H, t, *J* 7.47, Ar H), 7.49-7.40 (2H, m, Ar H), 7.23 (1H, d, *J* 8.53, Ar H), 6.98 (1H, d, *J* 2.87, H1), 6.83 (1H, dd, *J* 8.53, 2.87, Ar H), 4.87 (2H, s, H6), 3.03 (6H, s, H13).

δ_{C} (126 MHz, CDCl₃): 192.5 (C11), 150.7 (Ar C), 138.5 (Ar C), 135.2 (Ar C), 134.7 (Ar CH), 133.5 (Ar CH), 128.75 (Ar CH), 128.71 (Ar CH), 117.0 (C1), 116.2 (Ar CH), 114.9 (Ar C), 57.4 (C6), 40.1 (C13)

HRMS (ES⁺): found 304.1014; C₁₆H₁₈NO₃³²S [M+H]⁺ requires 304.1007.

(5*E*,11*E*)-*N*²,*N*²,*N*⁸,*N*⁸-tetramethyl-5,11-bis(phenylsulfonyl)dibenzo[*a,e*][8]annulene-2,8-diamine



64

A mixture of **63** (3.5 g, 12 mmol) and ClP(O)(OEt)₂ (2.0 mL, 14 mmol) in THF (233 mL) was cooled to $-78\text{ }^{\circ}\text{C}$, and then LiHMDS (1.0 M in THF, 23 mL, 23 mmol) was added. After stirring at $-78\text{ }^{\circ}\text{C}$ for 30 min, the reaction mixture was warmed to rt and stirred for a further 1.5 h. Saturated aqueous NH₄Cl (25 mL) was poured into the mixture. The reaction mixture was diluted with water (210 mL) and extracted with EtOAc (3 \times 230 mL). The organic layers were combined, dried (MgSO₄), filtered and concentrated *in vacuo*. Purification *via* flash column chromatography on silica gel (EtOAc/hexane = 2:3) gave **64** as a pale yellow solid (0.86 g, 13%).

mp: 156-158 $^{\circ}\text{C}$

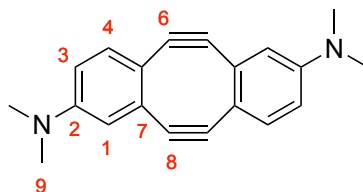
ν_{max} (neat): 2923 (C-H), 1595, 1303 (S=O), 1147 (S=O), 1206 (C-N), 1084.

δ_{H} (500 MHz, CDCl₃): 7.60 (2H, t, *J* 7.39, Ar H), 7.48-7.42 (4H, m, Ar H), 7.42-7.37 (6H, m, Ar H), 6.57 (2H, dd, *J* 8.86, 2.70, Ar H), 6.21 (2H, d, *J* 2.62, H1), 2.90 (12H, s, H13).

δ_{C} (126 MHz, CDCl₃): 150.2 (C2), 144.4 (Ar C), 139.7 (Ar C), 139.1 (Ar CH), 136.9 (Ar C), 133.4 (Ar CH), 131.7 (Ar CH), 128.7 (Ar CH), 127.9 (Ar CH), 115.5 (Ar C), 111.7 (Ar CH), 109.4 (Ar CH), 40.0 (C13).

HRMS (ES⁺): found 571.1711; C₃₂H₃₁N₂O₄³²S₂ [M+H]⁺ requires 571.1720.

***N*²,*N*²,*N*⁸,*N*⁸-tetramethyl-5,6,11,12-tetrahydrodibenzo[*a,e*]cyclooctene-2,8-diamine**



11

A solution of **64** (0.27 g, 0.47 mmol) in THF (9.4 mL) was cooled to $-78\text{ }^{\circ}\text{C}$, and then LDA (1.0 M in THF/hexane, 2.4 mL, 2.4 mmol). The reaction mixture was stirred at this temperature for 2 h, and saturated aqueous NH_4Cl (3.0 mL) was poured into the mixture. The reaction mixture was cooled to rt, diluted with water (10 mL) and extracted with CH_2Cl_2 ($3 \times 12\text{ mL}$). The organic layers were combined, dried (MgSO_4), filtered and concentrated *in vacuo*. Purification *via* flash column chromatography on silica gel ($\text{CH}_2\text{Cl}_2/\text{hexane} = 1:1$) gave **11** as an orange solid (67 mg, 50%).

mp: 160 °C (dec.)

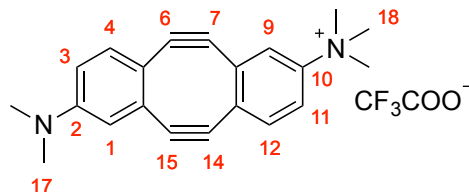
 ν_{\max} (neat): 2917 (C-H), 2132 (C \equiv C), 1588, 1215 (C-N), 1051, 805.

δ_{H} (400 MHz, CDCl_3): 6.64 (2H, d, J 8.52, Ar H), 6.21 (2H, d, J 2.63, H1), 6.14 (2H, dd, J 8.45, 2.59, Ar H), 2.92 (12H, s, H9).

δ_{C} (126 MHz, CDCl_3): 150.4 (C2), 134.9 (Ar C), 127.5 (Ar CH), 117.7 (Ar C), 111.6 (C1), 109.3 (Ar CH), 107.2 ($\text{C}\equiv\text{C}$), 40.1 (C9).

HRMS (ES⁺): found 286.1460; C₂₀H₁₈N₂ [M+H]⁺ requires 286.1470.

8-(dimethylamino)-*N*²,*N*²,*N*²-trimethyl-5,6,11,12-tetradehydrodibenzo[*a,e*]cyclooctene-2-aminium trifluoroacetate



12

A solution of **11** (25 mg, 0.09 mmol) in CH₂Cl₂ (1.3 mL) was taken in a dry round bottom flask. Methyl trifluoromethanesulfonate (0.019 mL, 0.17 mmol) was added to the reaction mixture dropwise at rt and the mixture was stirred for 2 h. CH₂Cl₂ was then removed *in vacuo* and preparative HPLC purification (30-60% MeCN) gave pure product **12** (11 mg, 30%) as an orange solid.

mp: 160 °C (dec.)

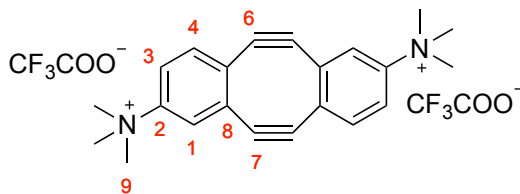
ν_{max} (neat): 2916 (C-H), 2134 (C \equiv C), 1664, 1170 (C-N), 1125 (C-N), 802.

δ_{H} (500 MHz, CD₃CN): 7.28 (1H, dd, *J* 8.40, 3.05, Ar H), 7.12 (1H, d, *J* 2.90, Ar H), 6.93 (1H, d, *J* 8.65, Ar H), 6.38 (1H, d, *J* 2.70, ArH), 6.73 (1H, d, *J* 8.64, Ar H), 6.30 (1H, dd, *J* 8.70, 2.75, Ar H), 3.42 (9H, s, H18), 2.92 (6H, s, H17).

δ_{C} (126 MHz, CD₃CN): 152.1 (Ar C), 147.9 (Ar C), 137.3 (Ar C), 135.1 (Ar C), 133.4 (Ar C), 129.4 (Ar CH), 128.3 (Ar CH), 120.6 (Ar CH), 118.9 (Ar CH), 116.6 (Ar C), 115.1 (C \equiv C), 113.9 (Ar CH), 112.9 (C \equiv C), 111.6 (Ar CH), 107.3 (C \equiv C), 105.8 (C \equiv C), 57.5 (C18), 40.1 (C17).

HRMS (ES⁺): found 301.1705; C₂₁H₂₁N₂ [M]⁺ requires 301.1705.

***N*²,*N*²,*N*²,*N*⁸,*N*⁸,*N*⁸-hexamethyl-5,6,11,12-tetradehydrodibenzo[*a,e*]cyclooctene-2,8-diaminium trifluoroacetate**



13

A solution of **11** (21 mg, 0.070 mmol) in CH₂Cl₂ (1.1 mL) was taken in a dry round bottom flask. Methyl trifluoromethanesulfonate (0.016 mL, 0.15 mmol) was added to the reaction mixture dropwise at rt and the mixture was stirred for 2 h. CH₂Cl₂ was then removed *in vacuo*. The resulting crude product (32 mg, 0.11 mmol) was dissolved in MeCN (1.6 mL) and methyl trifluoromethanesulfonate (0.023 mL, 0.21 mmol) was added dropwise. After having stirred the reaction mixture for 3 h MeCN was removed *in vacuo* and preparative HPLC purification (30-60% MeCN) gave pure product **13** (20 mg, 49%) as a light brown solid.

mp: 120 °C (dec.)

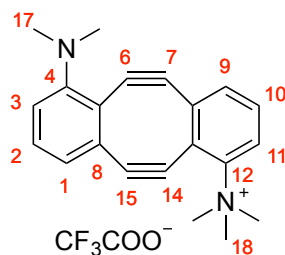
ν_{max} (neat): 2970 (C-H), 1670, 1172 (C-N), 1120 (C-N), 799.

δ_{H} (500 MHz, CD₃CN): 7.49 (2H, dd, *J* 8.75, 2.80, H3), 7.34 (2H, d, *J* 2.76, H1), 7.08 (2H, d, *J* 8.67, H4), 3.46 (18H, s, H9).

δ_{C} (126 MHz, CD₃CN): 148.3 (C2), 135.1 (Ar C), 135.0 (Ar C), 129.3 (Ar CH), 122.9 (Ar CH), 121.0 (Ar CH), 110.1 ($\underline{\text{C}}\equiv\text{C}$), 110.0 ($\underline{\text{C}}\equiv\text{C}$), 57.6 (C9).

HRMS (ES⁺): found 158.0968; C₂₂H₂₄N₂ [M]²⁺ requires 158.0964.

7-(dimethylamino)-*N*¹,*N*¹,*N*¹-trimethyl-5,6,11,12-tetradehydrodibenzo[*a,e*]cyclooctene-1-aminium trifluoroacetate



14

A solution of **10** (18 mg, 0.06 mmol) in CH₂Cl₂ (1.0 mL) was taken in a dry round bottom flask. Methyl trifluoromethanesulfonate (0.012 mL, 0.11 mmol) was added to the reaction mixture dropwise at rt and the mixture was stirred for 1 h. CH₂Cl₂ was then removed *in vacuo* and preparative HPLC purification (30-60% MeCN) gave pure product **14** (10 mg, 37%) as an orange solid.

mp: 115-116 °C (dec.)

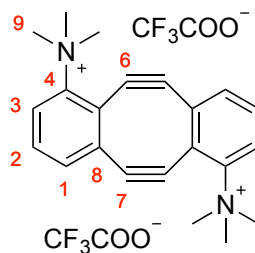
ν_{max} (neat): 3034, 2851, 2801, 2150 (C≡C), 1690, 1681, 1469, 1193, 1109, 782.

δ_{H} (500 MHz, CD₃CN): 7.32 (1H, dd, *J* 8.9, 0.9, H11), 7.18 (1H, dd, *J* 8.9, 7.6, H10), 6.98-6.92 (2H, m, Ar H), 6.67 (1H, dd, *J* 8.9, 1.0, H1), 6.39 (1H, dd, *J* 7.2, 1.0, H3), 3.58 (9H, s, H18), 2.98 (6H, s, H17).

δ_{C} (126 MHz, CD₃CN): 151.1 (C12), 143.7 (C4), 138.0 (Ar C), 132.4 (Ar C), 132.0 (C10), 131.8 (Ar CH), 129.2 (Ar CH), 125.8 (Ar C), 121.1 (C11), 120.4 (C1), 120.0 (C3), 119.8 (Ar C), 114.7 (C≡C), 112.9 (C≡C), 108.1 (C≡C), 101.8 (C≡C), 57.1 (C18), 42.3 (C17).

HRMS (ES⁺): found 301.1698; C₂₁H₂₁N₂ [M]⁺ requires 301.1699.

***N*¹,*N*¹,*N*¹,*N*⁷,*N*⁷,*N*⁷-hexamethyl-5,6,11,12-tetradehydrodibenzo[*a,e*]cyclooctene-1,7-diaminium trifluoroacetate**



15

A solution of **10** (18 mg, 0.06 mmol) in CH₂Cl₂ (1.1 mL) was taken in a dry round bottom flask. Methyl trifluoromethanesulfonate (0.013 mL, 0.12 mmol) was added to the reaction mixture dropwise at rt and the mixture was stirred for 2 h. CH₂Cl₂ was then removed *in vacuo*. The resulting crude product was dissolved in MeCN (1.6 mL) and methyl trifluoromethanesulfonate (0.027 mL, 0.25 mmol) was added dropwise. After having stirred the reaction mixture for 5 h MeCN was removed *in vacuo* and preparative HPLC purification (30-60% MeCN) gave pure product **15** (20 mg, 55%) as a light brown solid.

mp: 168-170 °C (dec.)

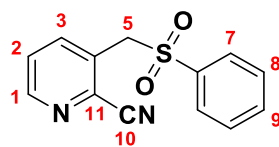
ν_{max} (neat): 3049, 2159 (C≡C), 1771, 1731, 1185, 1135, 787.

δ_{H} (500 MHz, CD₃CN): 7.51 (2H, dd, *J* 8.9, 0.9, H3), 7.32 (2H, dd, *J* 8.9, 7.6, H2), 7.14 (2H, dd, *J* 7.6, 0.9, H1), 3.60 (18H, s, H9).

δ_{C} (126 MHz, CD₃CN): 144.3 (C4), 135.4 (C8), 133.1 (C2), 130.8 (C1), 126.0 (C5), 123.8 (C3), 116.8 (C7), 104.0 (C6), 57.4 (C9).

HRMS (ES⁺): found 158.0960; C₂₂H₂₄N₂ [M]²⁺ requires 158.0964.

3-((Phenylsulfonyl)methyl)picolinonitrile



66

To a suspension of 3-methylpicolinonitrile (1.2 g, 10 mmol) in CCl₄ (100 mL) at 80 °C under N₂ were added NBS (1.9 g, 11 mmol) and BPO (24 mg, 1.0 mmol), and then the resulting mixture was heated at 100 °C. After stirring at this temperature for 6 h, the reaction mixture was cooled to rt. The reaction mixture was diluted with saturated aqueous NH₄Cl (100 mL) and extracted with CH₂Cl₂ (3 × 100 mL). The organic layers were combined, dried (MgSO₄), filtered and concentrated *in vacuo*. To the resulting residue (0.71 g, 3.6 mmol) were added benzenesulfinic acid sodium salt dihydrate (0.71 g, 4.3 mmol) and DMF (5.4 mL). After the resulting mixture had been stirred at 80 °C overnight, it was cooled to rt. The reaction mixture was diluted with water (15 mL) and extracted with EtOAc (3 × 15 mL). The organic layers were combined, dried (MgSO₄), filtered and concentrated *in vacuo*. Purification *via* flash column chromatography on silica gel (EtOAc/hexane = 1:8) gave **66** (0.67 g, 26%) as a white solid.

mp: 163-164 °C

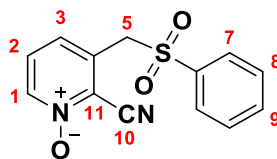
ν_{max} (neat): 2239 (C≡N), 1567 (C=N), 1308 (S=O), 1154 (S=O), 1131, 1080.

δ_{H} (500 MHz, CDCl₃): 8.71 (1H, dd, *J* 4.73, 1.60, H1), 8.08 (1H, dd, *J* 8.09, 1.60, H3), 7.76-7.70 (3H, m, Ar H), 7.64-7.53 (3H, m, Ar H), 4.59 (2H, s, H5).

δ_{C} (126 MHz, CDCl₃): 151.0 (C1), 139.7 (C3), 137.1 (C6), 135.0 (C4), 134.8 (Ar CH), 129.6 (Ar CH), 129.4 (C11), 128.6 (Ar CH), 126.7 (C2), 114.8 (C10), 58.8 (C5).

HRMS (ES⁺): found 259.0532; C₁₃H₁₁N₂O₂³²S [M+H]⁺ requires 259.0536.

2-cyano-3-((phenylsulfonyl)methyl)pyridine 1-oxide



69

To a solution of **67** (40 mg, 0.16 mmol) in CH₂Cl₂ (2 mL) was added *m*-CPBA (80 mg, 0.47 mmol) at rt. After the reaction mixture had been stirred for 16 h, the solvent was evaporated *in vacuo*. Purification *via* flash column chromatography on silica gel (CH₂Cl₂/acetone = 4:1) gave **69** as a solid (40 mg, 94%).

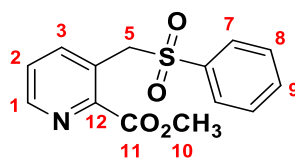
ν_{max} (neat): 2343 (C≡N), 1429 (C=N), 1310 (S=O), 1152 (S=O), 1084.

δ_{H} (500 MHz, CDCl₃): 8.26 (1H, dd, *J* 6.26, 1.30, H1), 7.86-7.48 (7H, m, Ar H), 4.51 (2H, s, H5).

δ_{C} (126 MHz, CDCl₃): 139.8 (Ar CH), 137.1 (Ar C), 135.1 (Ar CH), 133.0 (Ar C), 129.9 (Ar CH), 128.6 (Ar CH), 128.2 (Ar C), 128.0 (Ar CH), 127.1 (Ar CH), 109.9 (C10), 58.8 (C5).

HRMS (ES⁺): found 275.0493; C₁₃H₁₁N₂O₃³²S [M+H]⁺ requires 275.0490.

Methyl 3-((phenylsulfonyl)methyl)picolinate



73

To a suspension of methyl 3-methylpicolinate (1.0 g, 6.6 mmol) in CCl_4 (66 mL) at 80 °C under N_2 were added NBS (1.2 g, 7.0 mmol) and BPO (0.16 g, 0.66 mmol), and then the resulting mixture was heated at 100 °C. After stirring at this temperature for 6 h, the reaction mixture was cooled to rt. The reaction mixture was diluted with saturated aqueous NH_4Cl (66 mL) and extracted with CH_2Cl_2 (3×66 mL). The organic layers were combined, dried (MgSO_4), filtered and concentrated *in vacuo*. To the resulting residue (0.92 g, 4.0 mmol) were added benzenesulfinic acid sodium salt dihydrate (0.79 g, 4.8 mmol) and DMF (7.0 mL). After the resulting mixture had been stirred at 80 °C overnight, it was cooled to rt. The reaction mixture was diluted with water (21 mL) and extracted with EtOAc (3×21 mL). The organic layers were combined, dried (MgSO_4), filtered and concentrated *in vacuo*. Purification *via* flash column chromatography on silica gel (EtOAc/hexane = 4:1) gave **73** (0.60 g, 42%) as a pale-yellow liquid.

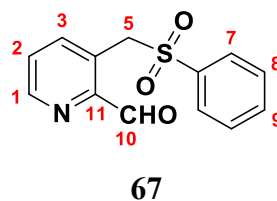
ν_{max} (neat): 1719 (C=O), 1585, 1570 (C=N), 1447, 1304 (S=O), 1152 (S=O), 1122, 1080.

δ_{H} (500 MHz, CDCl_3): 8.70 (1H, dd, J 4.68, 1.56, H1), 7.82 (1H, dd, J 7.89, 1.53, Ar H), 7.69-7.58 (3H, m, Ar H), 7.53-7.41 (3H, m, Ar H), 5.05 (2H, s, H5), 3.80 (3H, s, H10).

δ_{C} (126 MHz, CDCl_3): 165.7 (C11), 149.4 (Ar CH), 147.6 (Ar C), 141.5 (Ar CH), 137.9 (Ar C), 133.9 (Ar CH), 129.1 (Ar CH), 128.6 (Ar CH), 126.2 (Ar CH), 126.0 (Ar C), 58.0 (C5), 52.9 (C10).

HRMS (ES⁺): found 292.0651; $\text{C}_{14}\text{H}_{14}\text{NO}_4^{32}\text{S}$ $[\text{M}+\text{H}]^+$ requires 292.0644.

3-((Phenylsulfonyl)methyl)picolinaldehyde



To a solution of methyl 3-((phenylsulfonyl)methyl)picolinate **73** (0.20 g, 0.67 mmol) in CH₂Cl₂ (2.0 mL) was added DIBAL-H (1.0 M in hexane, 1.5 mL, 1.5 mmol) at -78 °C. After the mixture had been stirred at this temperature for 2 h, saturated aqueous NH₄Cl (5.0 mL) was poured into the mixture followed by 1M HCl (5.0 mL). The reaction mixture was warmed to rt and the product was then extracted with CH₂Cl₂ (3 × 10 mL). The organic layers were combined, dried (MgSO₄), filtered and concentrated *in vacuo* to give pure product **67** as a white solid (0.17 g, 97%).

mp: 144-145 °C

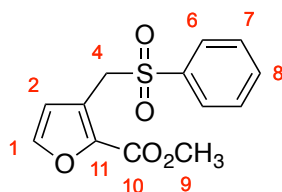
ν_{\max} (neat): 1710 (C=O), 1571, 1570 (C=N), 1447, 1308 (S=O), 1153 (S=O), 1084.

δ_{H} (500 MHz, CDCl₃): 9.79 (1H, d, *J* 0.69, H10), 8.82 (1H, app dd, *J* 4.65, 1.60, H1), 7.97 (1H, d, *J* 6.94, H3), 7.72-7.47 (6H, m, Ar H), 5.10 (2H, s, H5).

δ_{C} (126 MHz, CDCl₃): 194.3 (C10), 150.2 (C1), 150.0 (C11), 141.5 (C3), 138.0 (Ar C), 134.1 (Ar CH), 129.0 (Ar CH), 128.6 (Ar CH), 126.8 (C2), 125.2 (Ar C), 56.0 (C5).

HRMS (ES⁺): found 262.0543; C₁₃H₁₂NO₃³²S [M+H]⁺ requires 262.0538.

Methyl 3-((phenylsulfonyl)methyl)furan-2-carboxylate



77

To a suspension of methyl 3-methylfuran-2-carboxylate (2.0 g, 14 mmol) in CCl_4 (75 mL) at 80 °C under N_2 were added NBS (2.7 g, 15 mmol) and BPO (0.34 g, 1.4 mmol), and then the resulting mixture was heated at 100 °C. After stirring at this temperature for 6 h, the reaction mixture was cooled to rt. The reaction mixture was diluted with saturated aqueous NH_4Cl (70 mL) and extracted with CH_2Cl_2 (3 \times 70 mL). The organic layers were combined, dried (MgSO_4), filtered and concentrated *in vacuo*. To the resulting residue (3.5 g, 16 mmol) were added benzenesulfinic acid sodium salt dihydrate (3.2 g, 20 mmol) and DMF (24 mL). After the resulting mixture had been stirred at 80 °C overnight, it was cooled to rt. The reaction mixture was diluted with water (48 mL) and extracted with EtOAc (3 \times 48 mL). The organic layers were combined, dried (MgSO_4), filtered and concentrated *in vacuo*. Purification *via* flash column chromatography on silica gel (EtOAc/hexane = 1:2) gave **77** (3.2 g, 80%) as a pale yellow solid.

mp: 110-113 °C

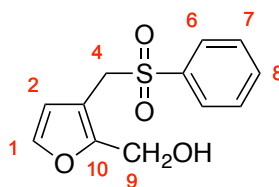
ν_{max} (neat): 2989 (C-H), 1697 (C=O), 1445, 1306 (S=O), 1132, 1175, 1117.

δ_{H} (400 MHz, CDCl_3): 7.78-7.40 (6H, m, Ar H), 6.69 (1H, s, H2), 4.69 (2H, s, H4), 3.66 (3H, s, H9).

δ_{C} (100 MHz, CDCl_3): 158.4 (C10), 145.5 (C1), 142.0 (Ar C), 137.6 (Ar C), 133.9 (Ar CH), 128.8 (Ar CH), 128.5 (Ar CH), 121.8 (Ar C), 114.6 (C2), 53.0 (C9), 51.8 (C4).

HRMS (ES⁺): found 281.0477; $\text{C}_{13}\text{H}_{13}\text{O}_5^{32}\text{S}$ $[\text{M}+\text{H}]^+$ requires 281.0484.

(3-((phenylsulfonyl)methyl)furan-2-yl)methanol



78

To a solution of **77** (3.0 g, 11 mmol) in CH₂Cl₂ (32 mL), was added DIBAL-H (1.0 M in hexane, 25 mL, 25 mmol) at -78 °C. After the mixture had been stirred at this temperature for 2 h, saturated aqueous NH₄Cl (100 mL) was poured into the mixture followed by 1M HCl (100 mL). The reaction mixture was warmed to rt and the product was then extracted with CH₂Cl₂ (3 × 200 mL). The organic layers were combined, dried (MgSO₄), filtered and concentrated *in vacuo* to afford the pure product **78** as a black solid (2.5 g, 94%).

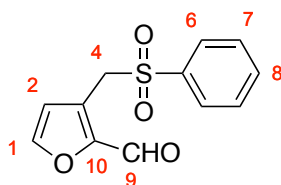
ν_{max} (neat): 3453 (O-H), 2927 (C-H), 1770, 1585, 1447, 1305 (S=O), 1142 (S=O), 1083.

δ_{H} (400 MHz, CDCl₃): 7.82-7.76 (2H, m, Ar H), 7.68 (1H, t, *J* 7.49, Ar H), 7.60-7.52 (2H, m, Ar H), 7.30 (1H, d, *J* 1.87, H1), 5.99 (1H, d, *J* 1.85, H2), 4.53 (2H, s, H4), 4.27 (2H, s, H9).

δ_{C} (100 MHz, CDCl₃): 154.3 (C10), 142.1 (C1), 137.6 (Ar C), 134.1 (Ar CH), 129.2 (Ar CH), 128.6 (Ar CH), 112.5 (C2), 109.3 (Ar C), 55.6 (C4), 53.5 (C9).

HRMS (ES⁺): found 275.0340; C₁₂H₁₂O₄³²SNa [M+Na]⁺ requires 275.0349.

3-((phenylsulfonyl)methyl)furan-2-carbaldehyde



79

To a solution of **78** (2.3 g, 9.3 mmol) in CH₂Cl₂ (28 mL) was added DMP (4.5 g, 10 mmol) at rt. After the reaction mixture had been stirred for 3 h, the reaction mixture was diluted with CH₂Cl₂ (20 mL) and poured into saturated Na₂S₂O₃ solution (40 mL). Mixture was stirred to dissolve the solid and layers were separated. The CH₂Cl₂ layer was then extracted with saturated aqueous Na₂S₂O₃ (2 × 40 mL) followed by saturated aqueous NaHCO₃ (2 × 40 mL). CH₂Cl₂ was then removed *in vacuo* and purification *via* flash column chromatography on silica gel (EtOAc/hexane = 1:1) gave pure product **79** (2.3 g, 98%) as a brown solid.

mp: 71-74 °C

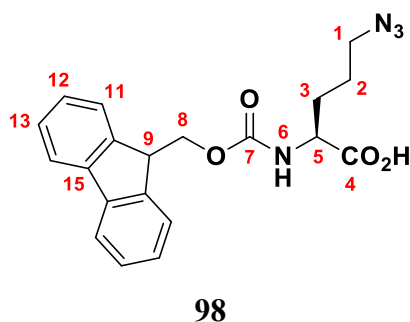
ν_{\max} (neat): 2987, 1672 (C=O), 1588, 1475, 1447, 1425, 1307 (S=O), 1145 (S=O), 1083.

δ_{H} (400 MHz, CDCl₃): 9.48 (1H, s, H₉), 7.82-7.44 (6H, m, Ar H), 6.78 (1H, d, *J* 1.48, H₂), 4.70 (2H, s, H₄).

δ_{C} (100 MHz, CDCl₃): 178.9 (C₉), 149.7 (Ar C), 147.1 (Ar CH), 137.5 (Ar C), 134.1 (Ar CH), 129.0 (Ar CH), 128.5 (Ar CH), 121.9 (Ar C), 115.4 (C₂), 52.2 (C₄).

HRMS (ES⁺): found 251.0374; C₁₂H₁₁O₄³²S [M+H]⁺ requires 251.0378.

Fmoc-Orn(N₃)-OH



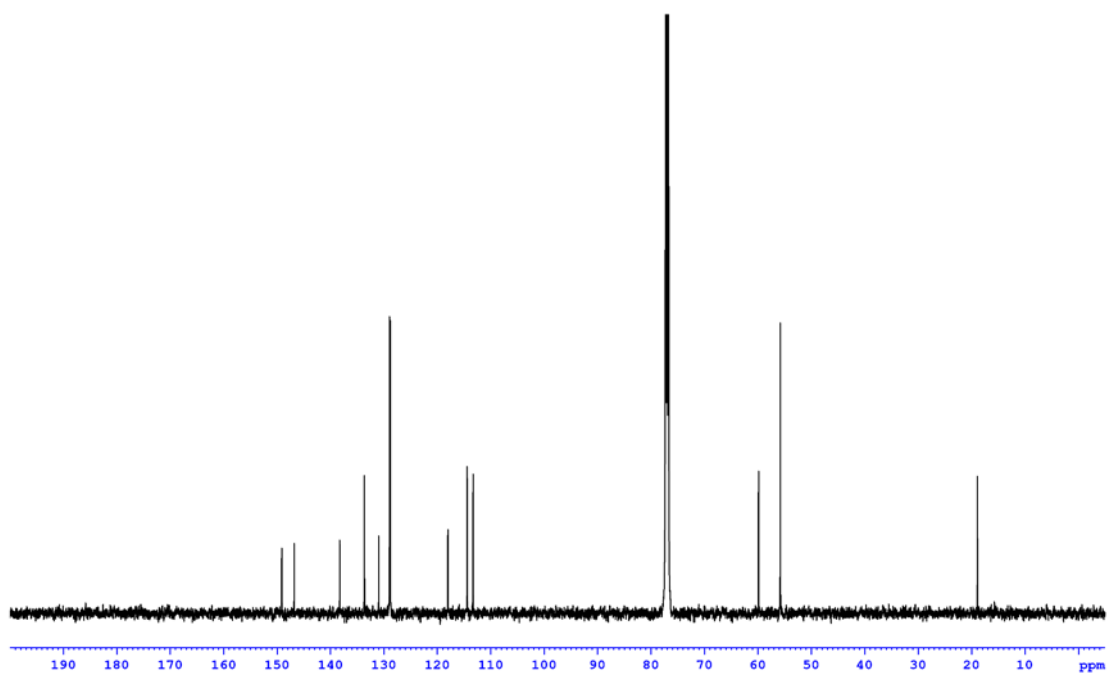
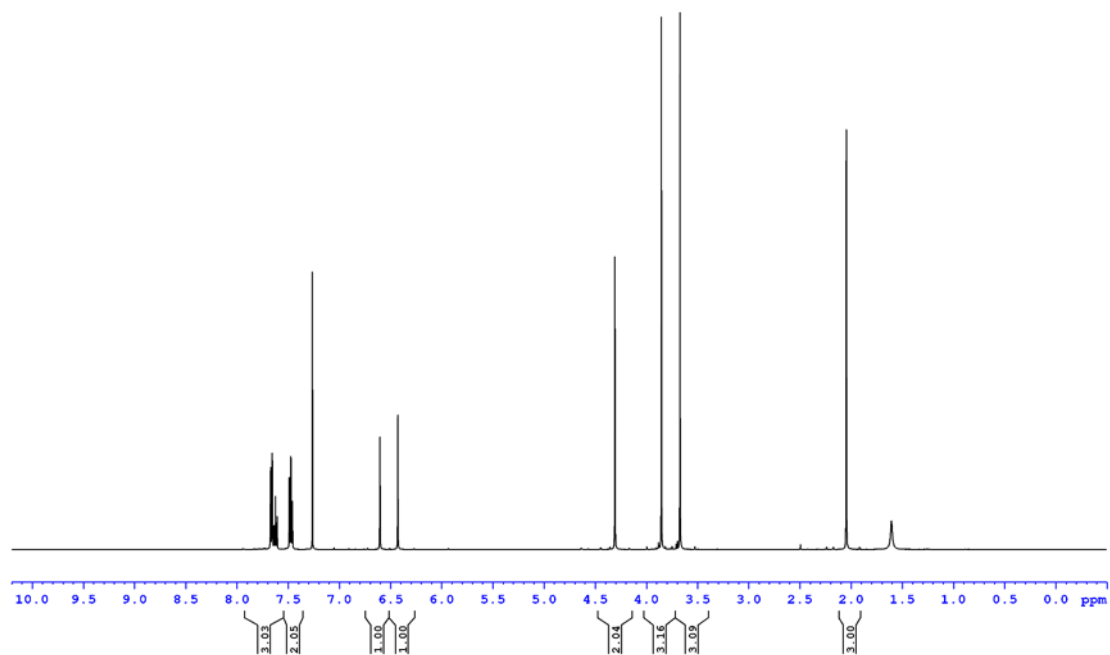
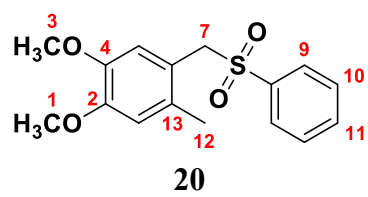
Fmoc-Orn-OH·HCl (4.0 g, 10 mmol) was dissolved in a biphasic mixture of H₂O (50 mL), MeOH (100 mL) and CH₂Cl₂ (85 mL). CuSO₄·5H₂O (16 mg, 0.060 mmol) and imidazole-1-sulfonyl azide hydrochloride (8.6 g, 32 mmol) were added, and the mixture was adjusted to pH 9 with aqueous K₂CO₃ solution. After stirring vigorously for 18 h, the organic solvents were removed *in vacuo*. The remaining aqueous phase was washed with diethyl ether (2 × 20 mL), acidified to pH 2 with concentrated HCl and extracted with diethyl ether (3 × 30 mL). The organic extracts were dried over MgSO₄ and concentrated *in vacuo*. The oily residue was dissolved in CH₂Cl₂, and the solvent was removed under a stream of nitrogen to give **98** (2.1 g, 53%) as a white solid.

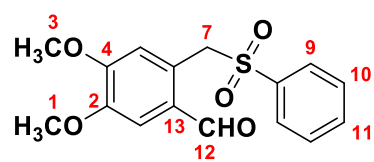
mp: 133-135 °C

δ_H (500 MHz, CDCl₃): 7.79 (2H, d, *J* 7.48, H14), 7.61 (2H, d, *J* 6.5, H11), 7.43 (2H, app t, *J* 7.1, H13), 7.38-7.30 (2H, app tt, *J* 7.44, 1.49, H12), 5.35 (1H, d, *J* 8.09, H6), 4.70-4.34 (3H, m, H8, H5), 4.24 (1H, t, *J* 6.71, H9), 3.44-3.09 (2H, m, H1), 2.16-1.19 (4H, m, H2, H3).

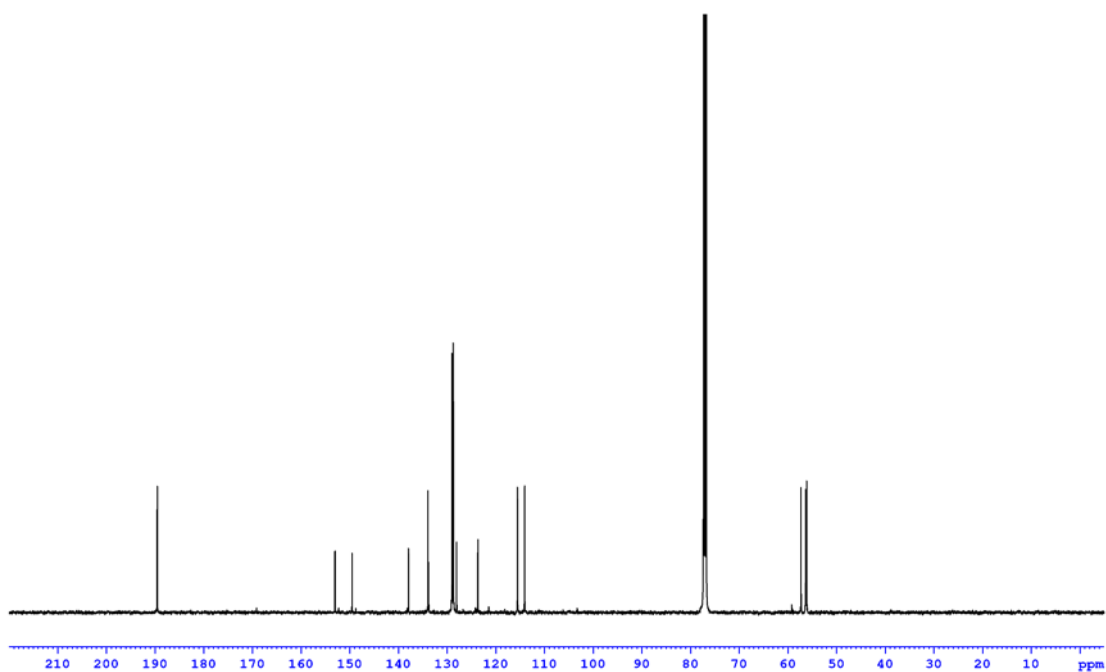
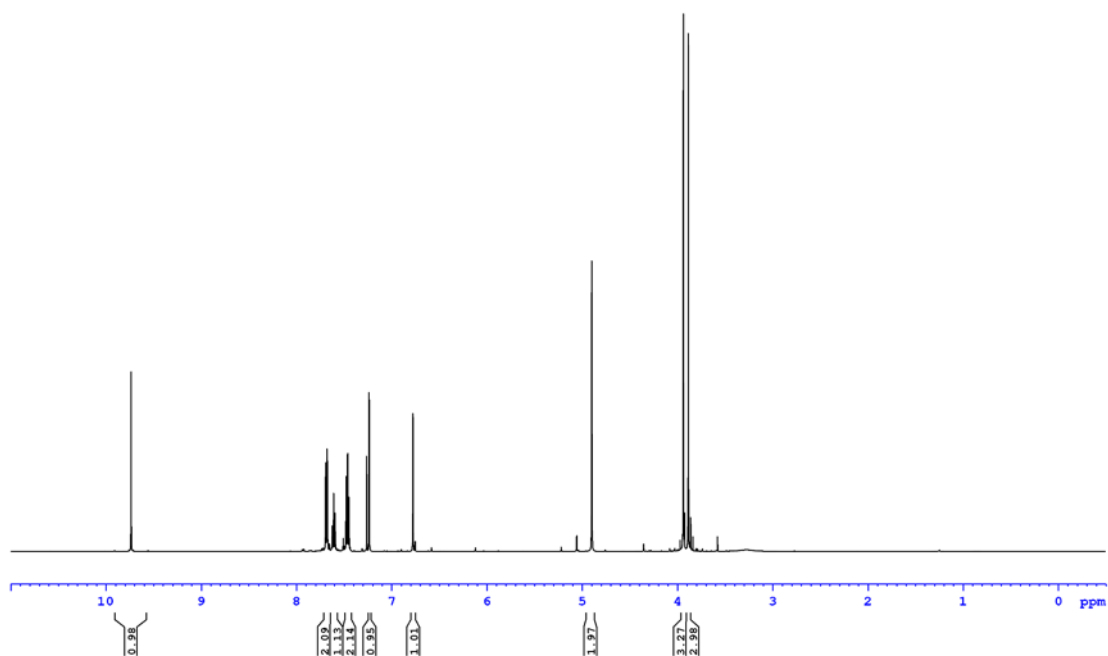
δ_C (126 MHz, CDCl₃): 176.0 (C10), 156.1 (C5), 143.6 (Ar C), 141.3 (Ar C), 127.8 (Ar CH), 127.1 (Ar CH), 125.0 (Ar CH), 120.0 (Ar CH), 67.1 (C8), 53.3 (C9), 50.8 (C1), 47.1 (C5), 29.6 (C3), 24.8 (C2).

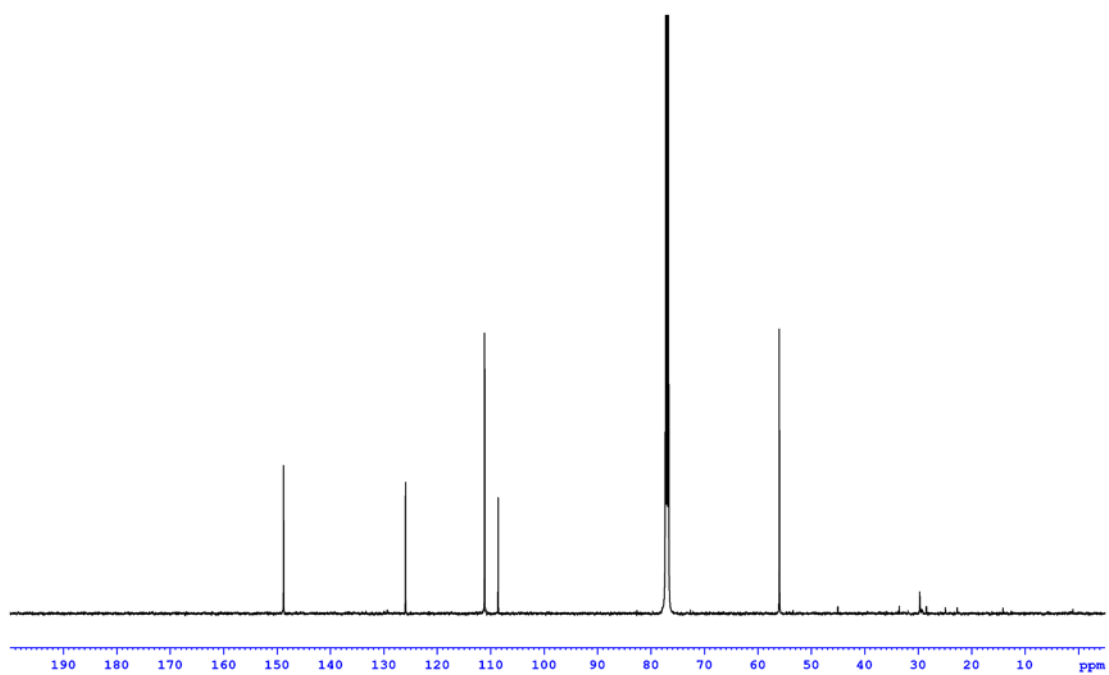
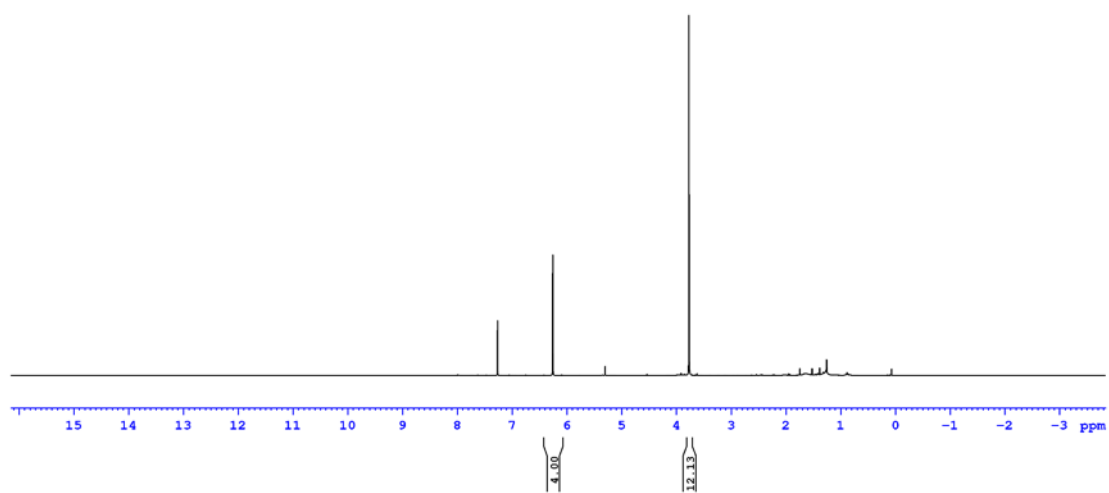
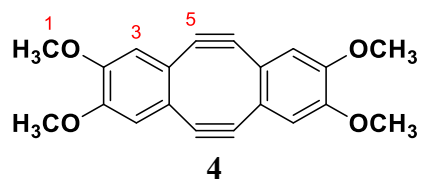
Characterisation data is in accordance with that previously reported.¹³²

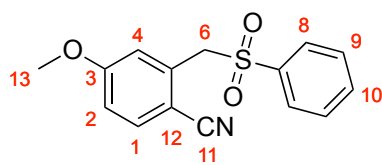




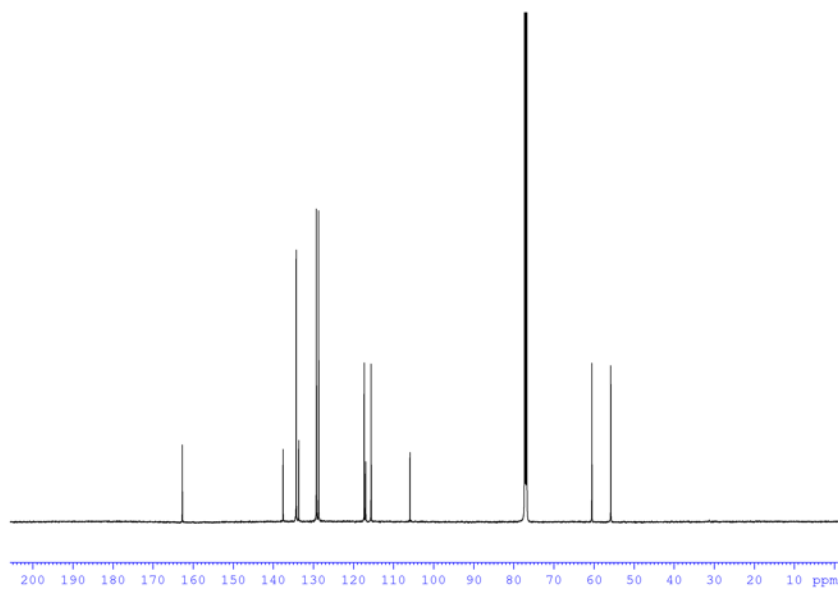
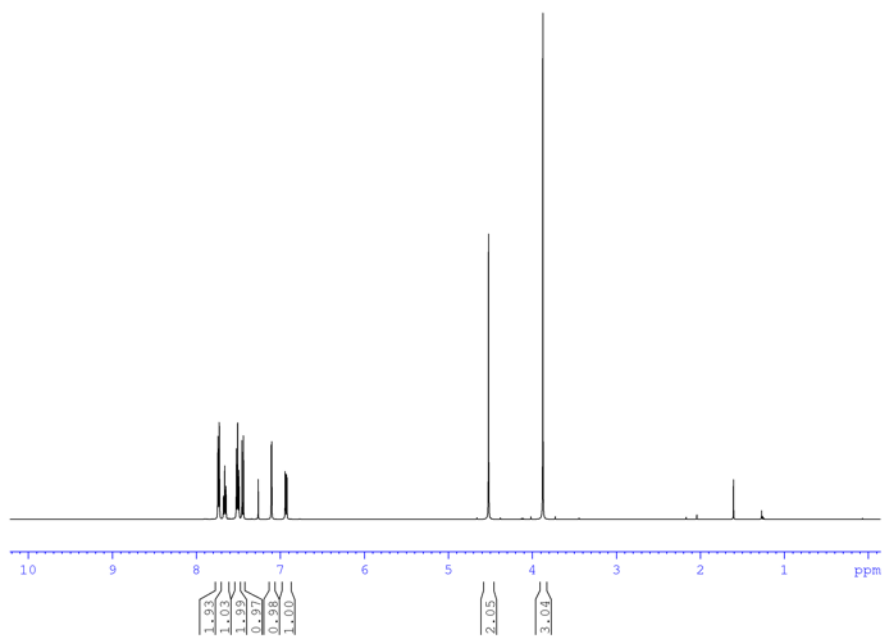
23

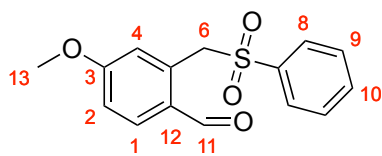




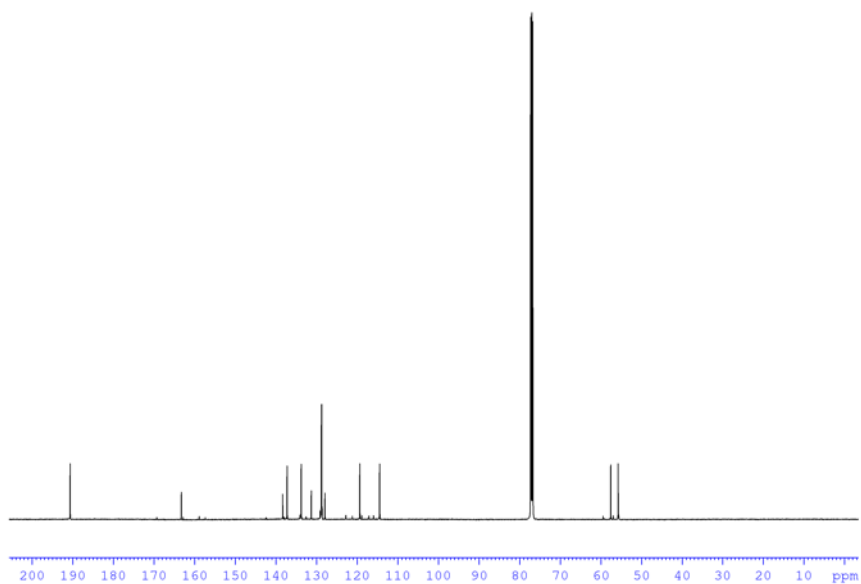
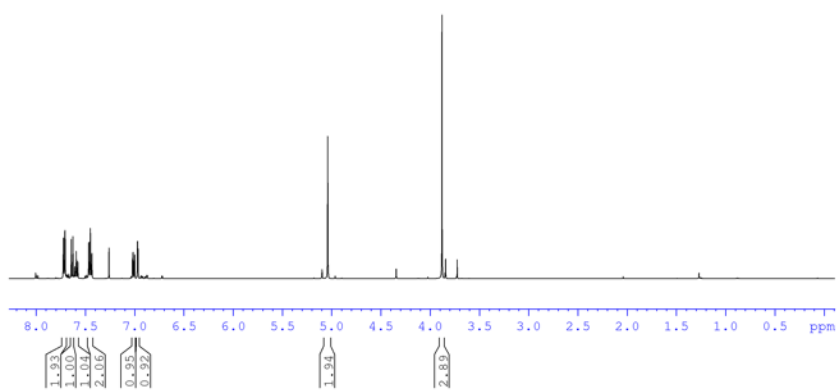


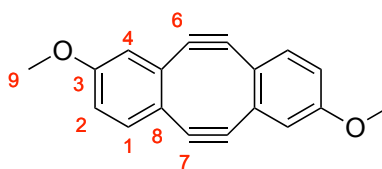
27



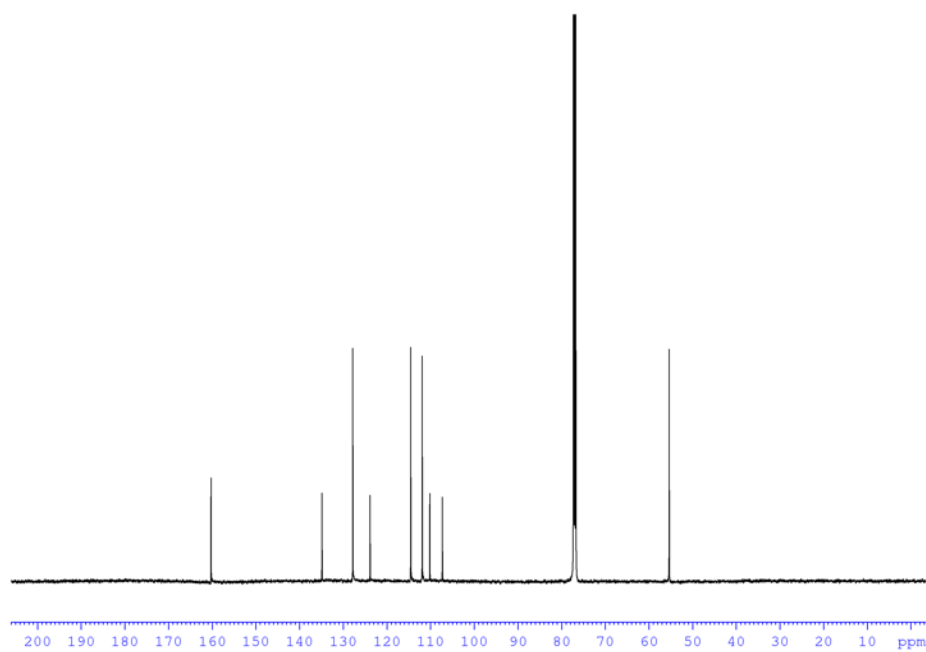
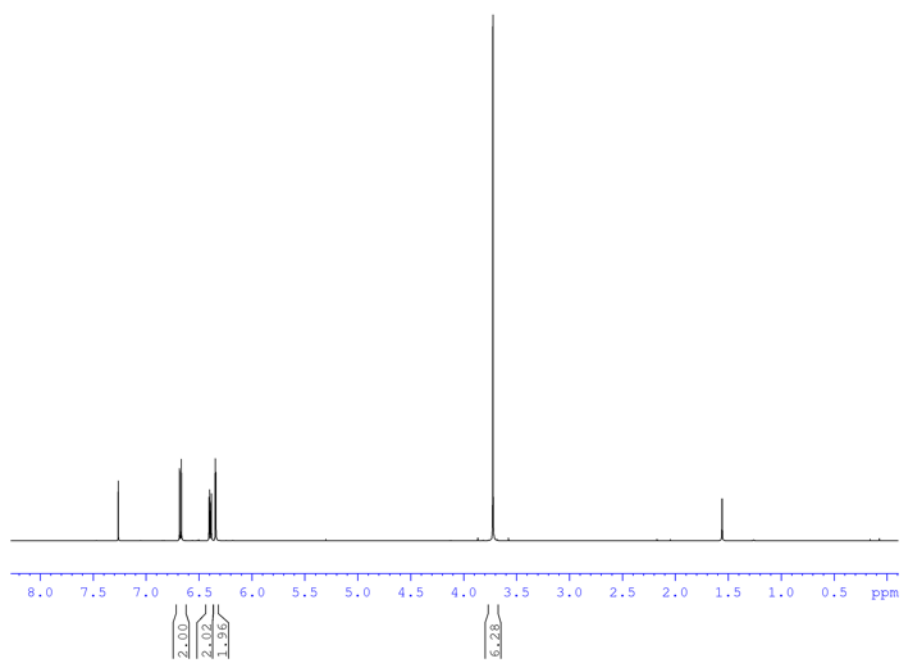


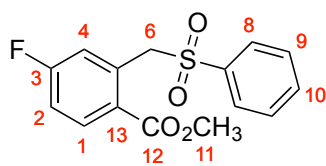
28



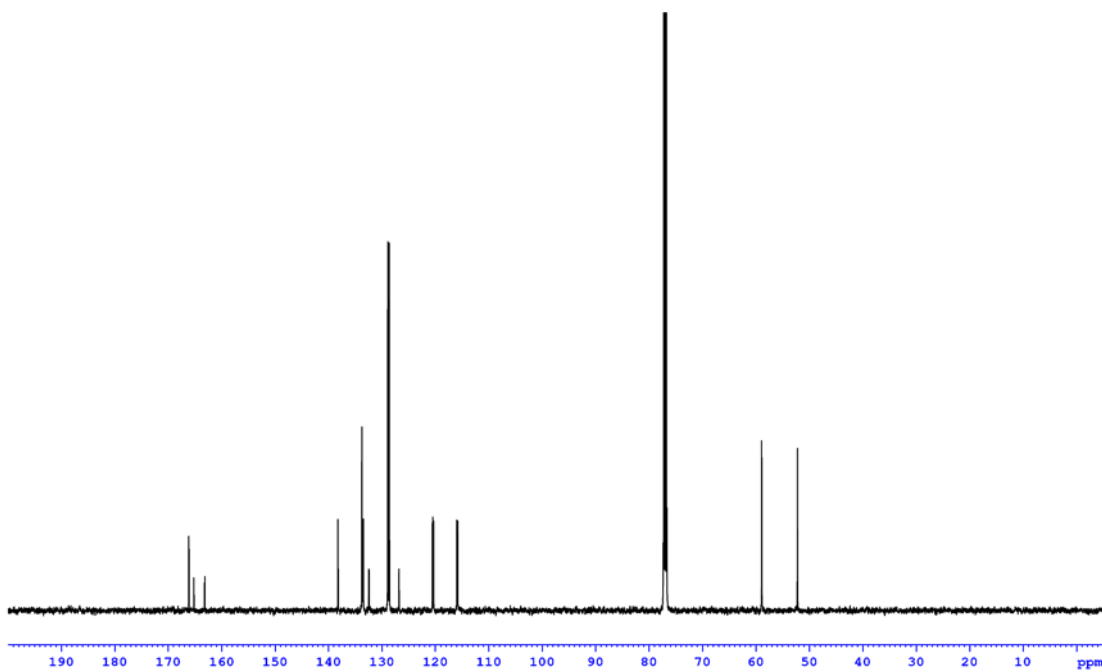
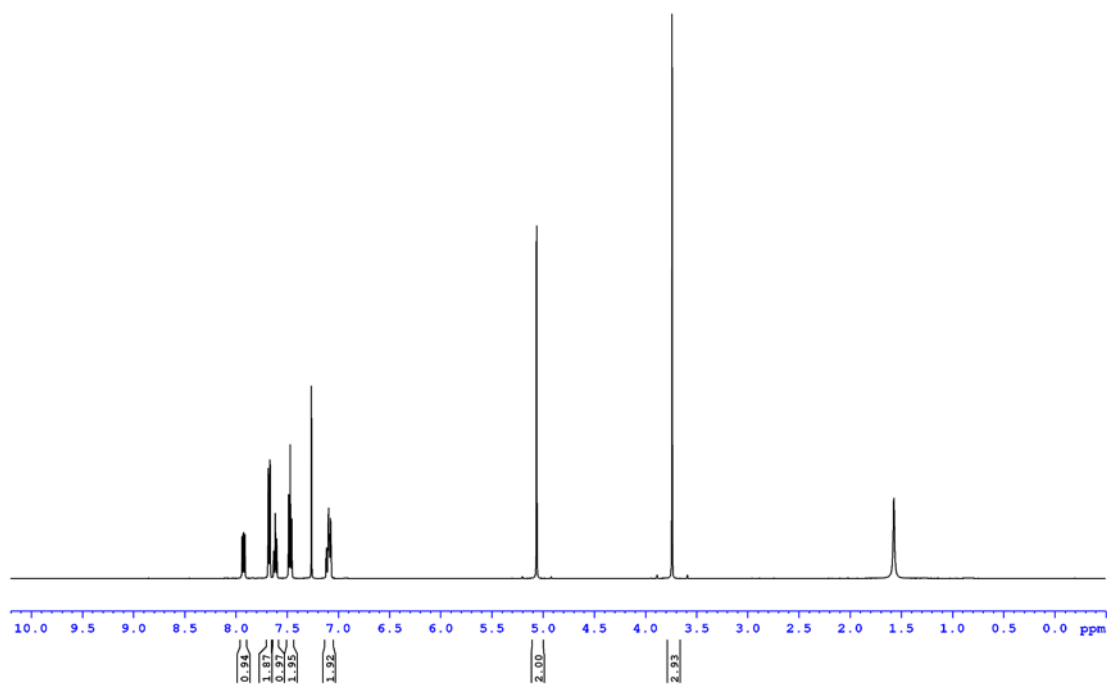


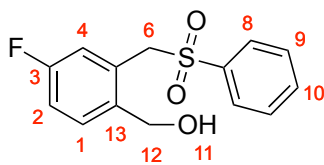
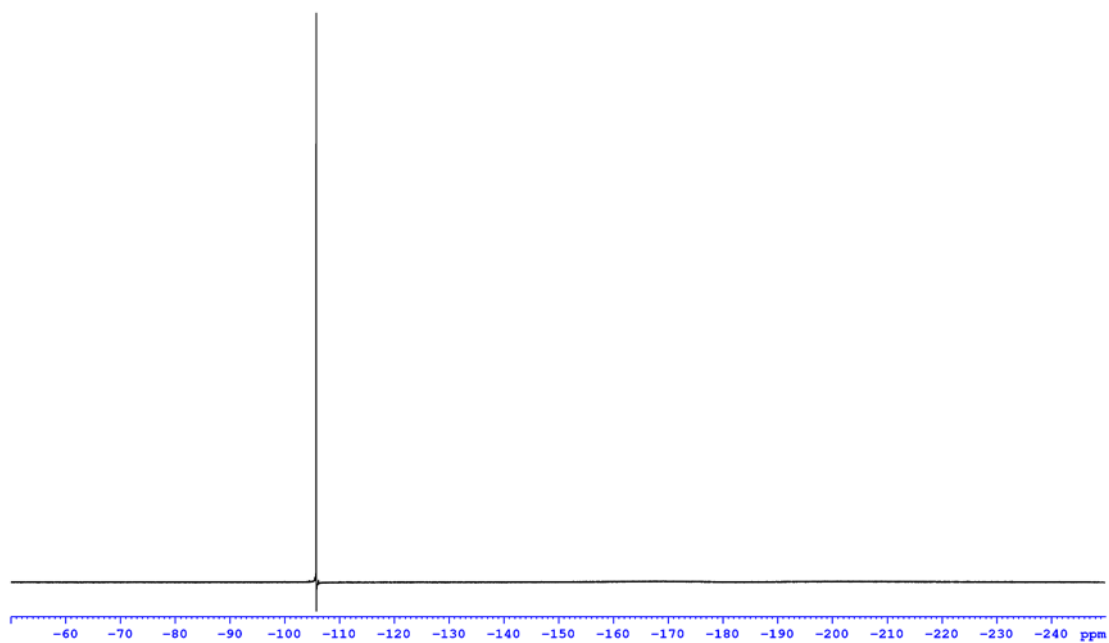
5



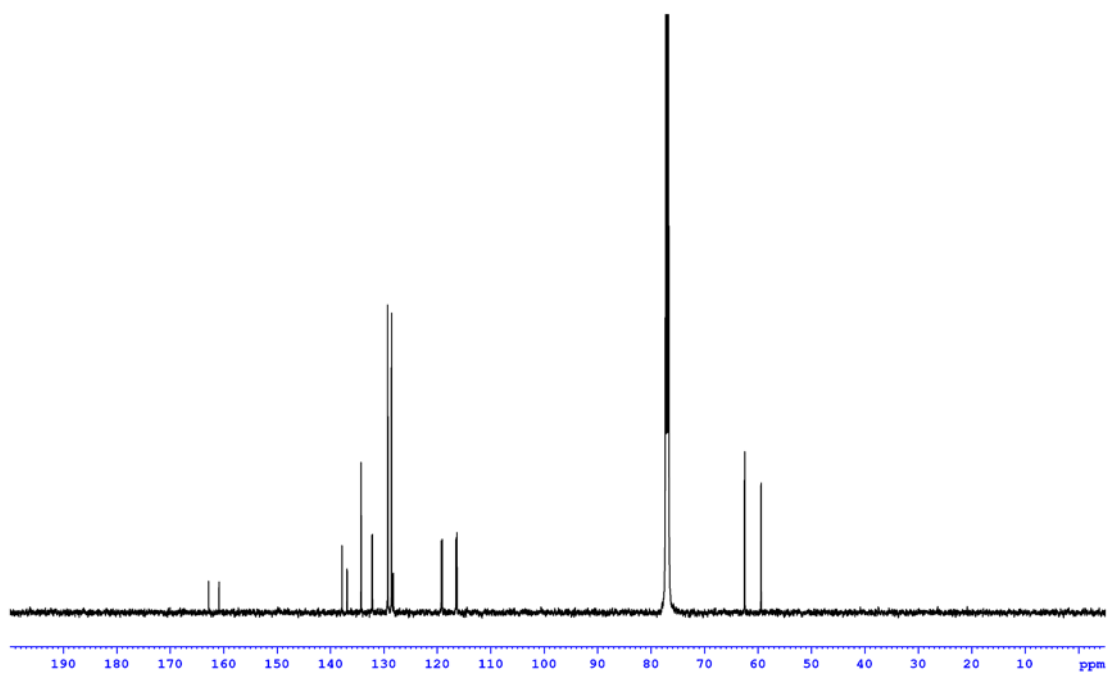
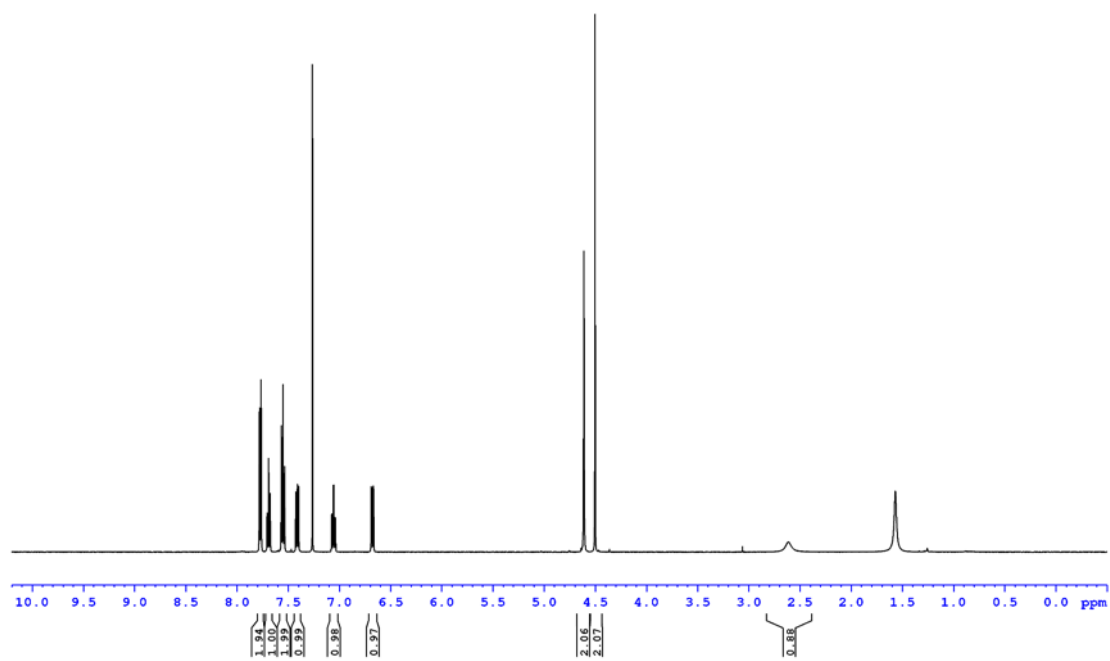


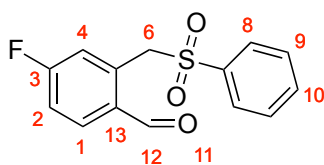
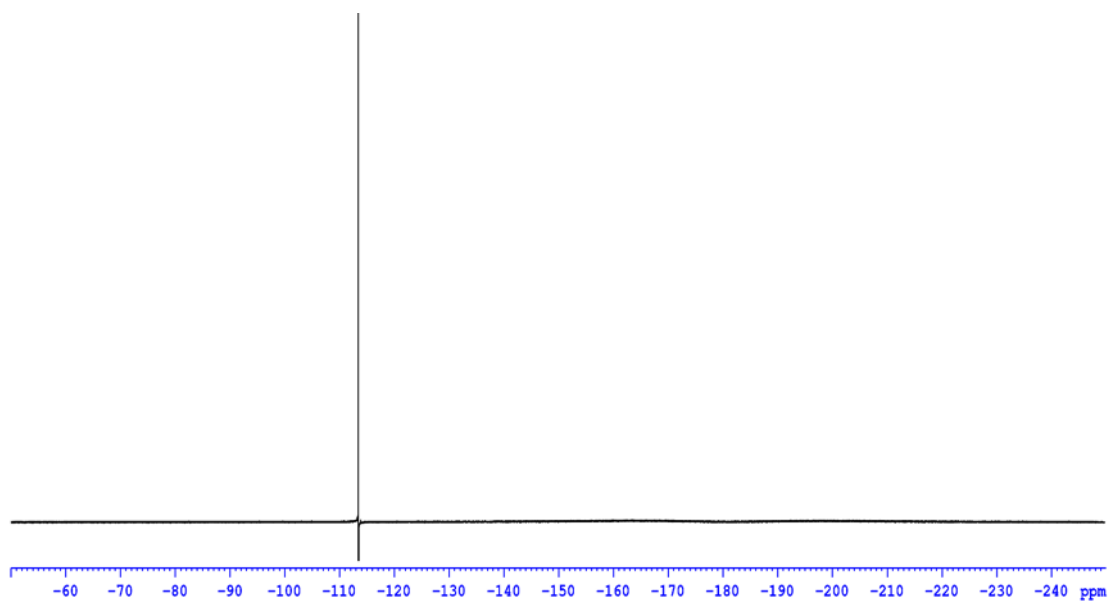
32



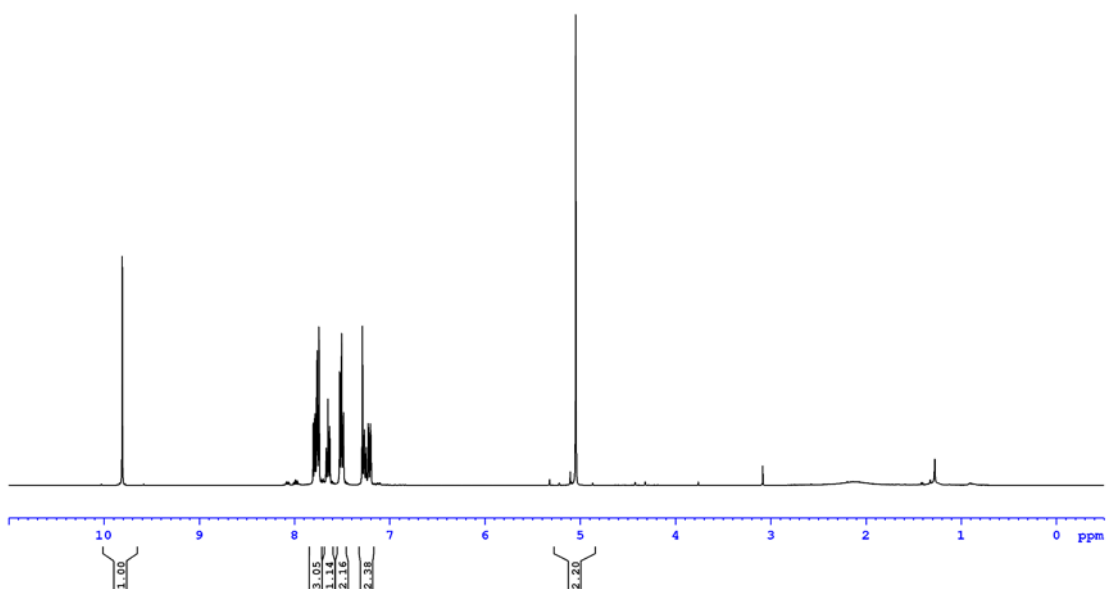


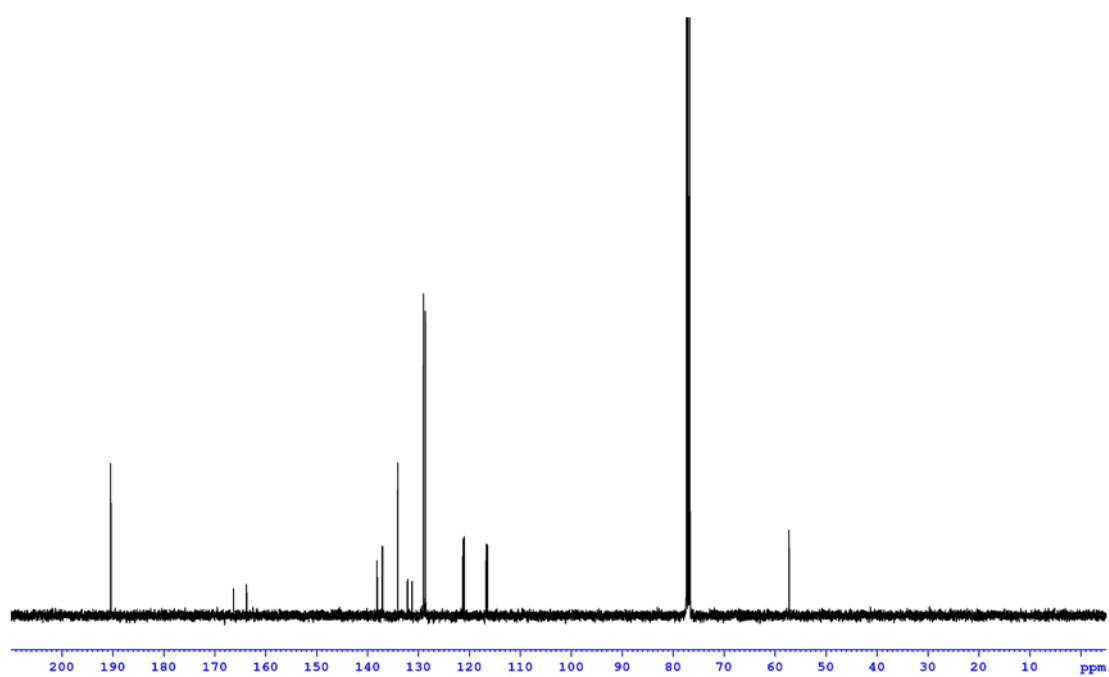
33

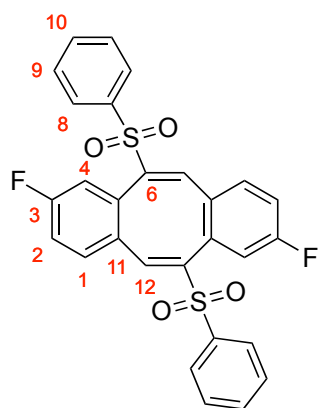




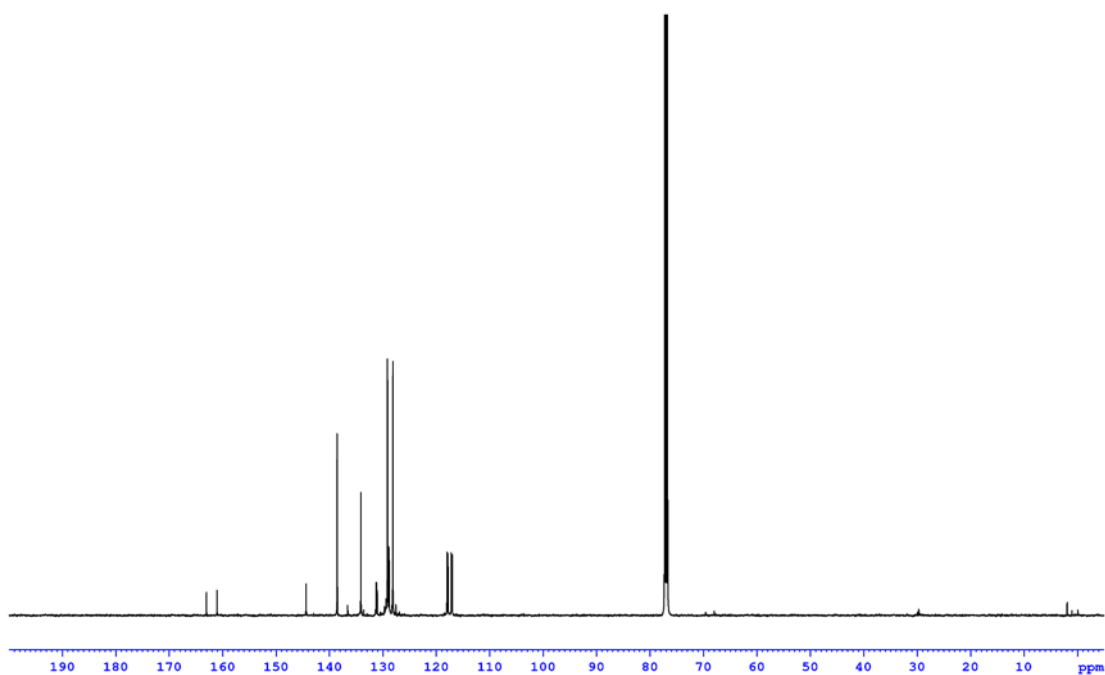
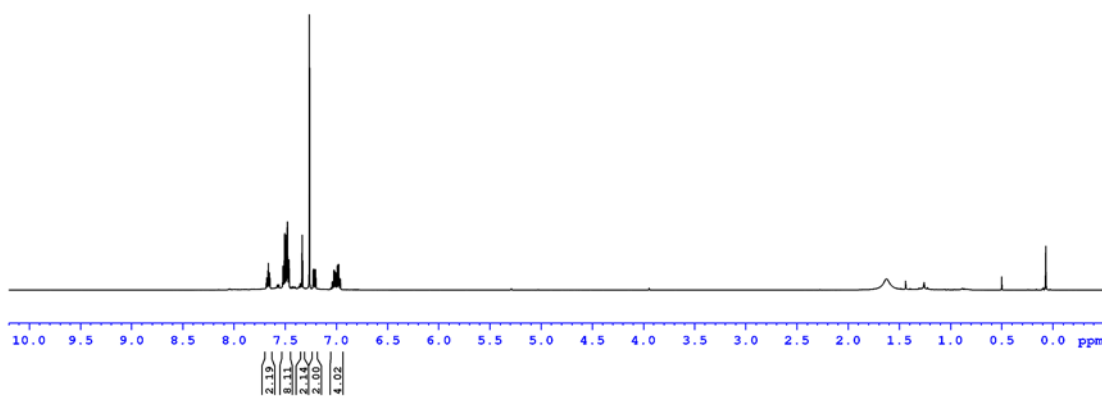
34



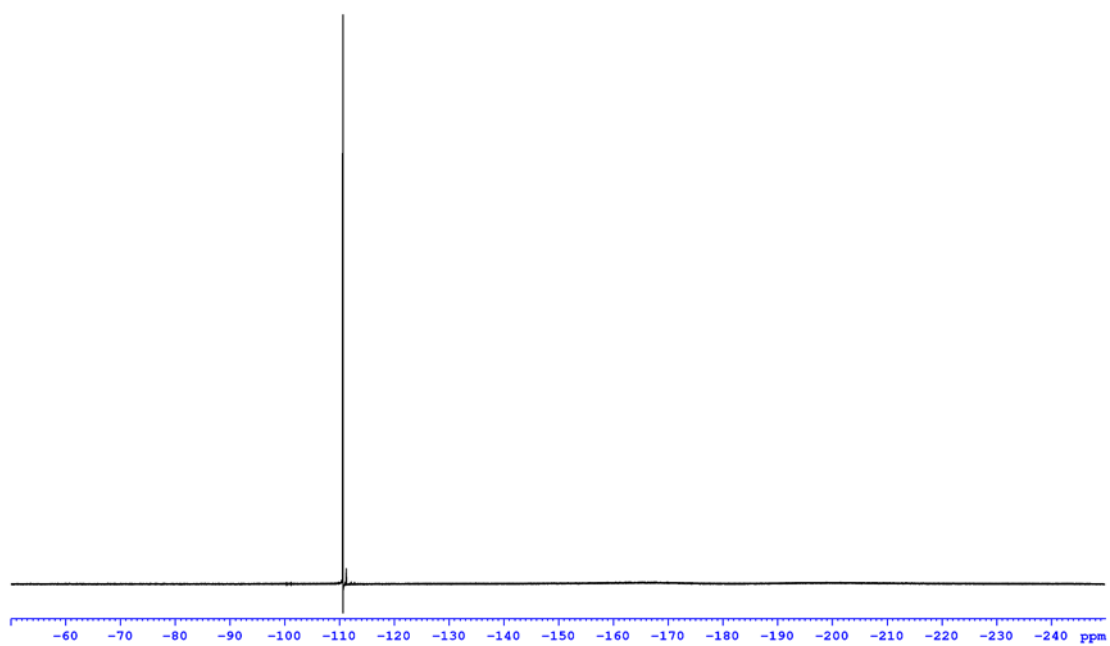


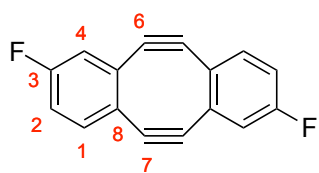


35

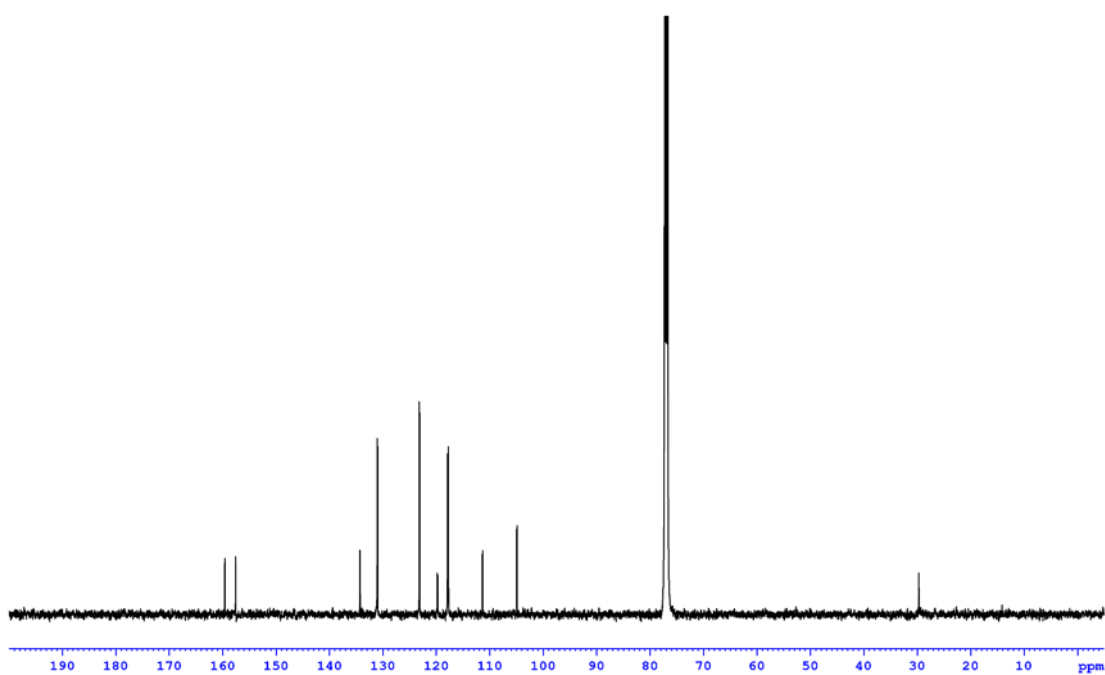
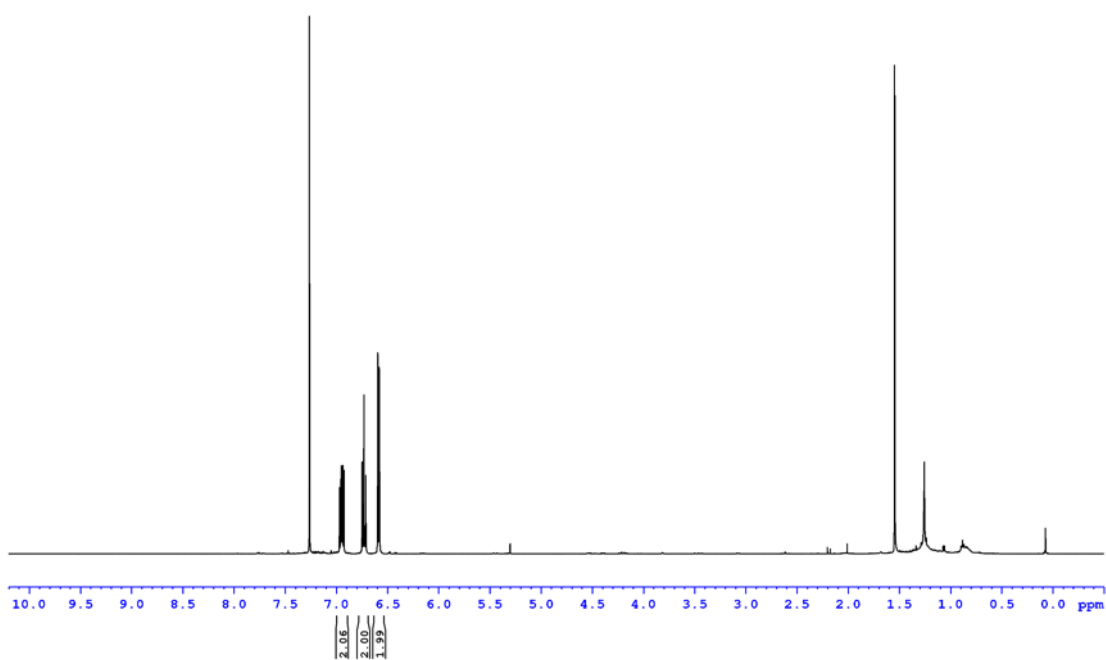


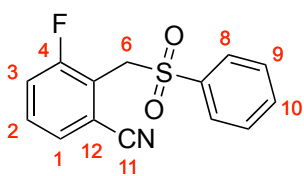
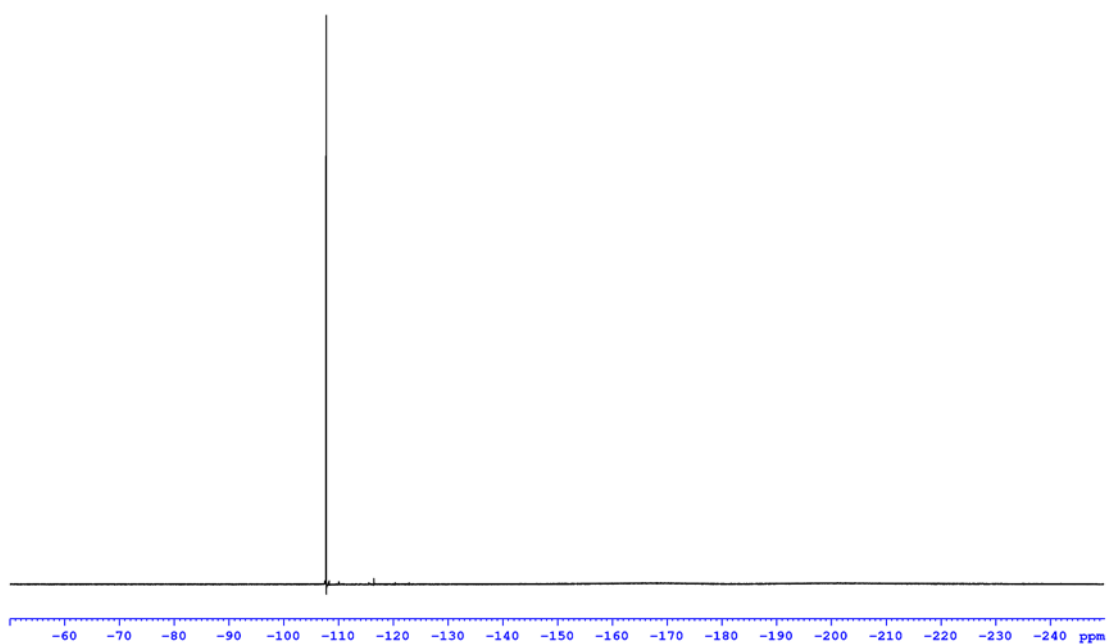
153



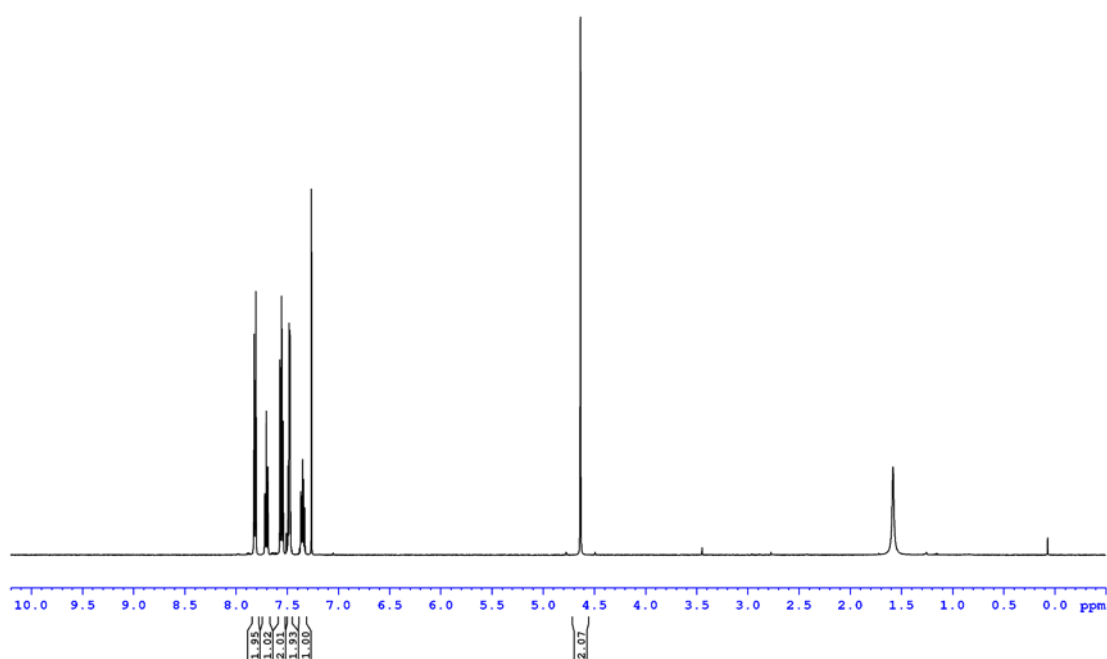


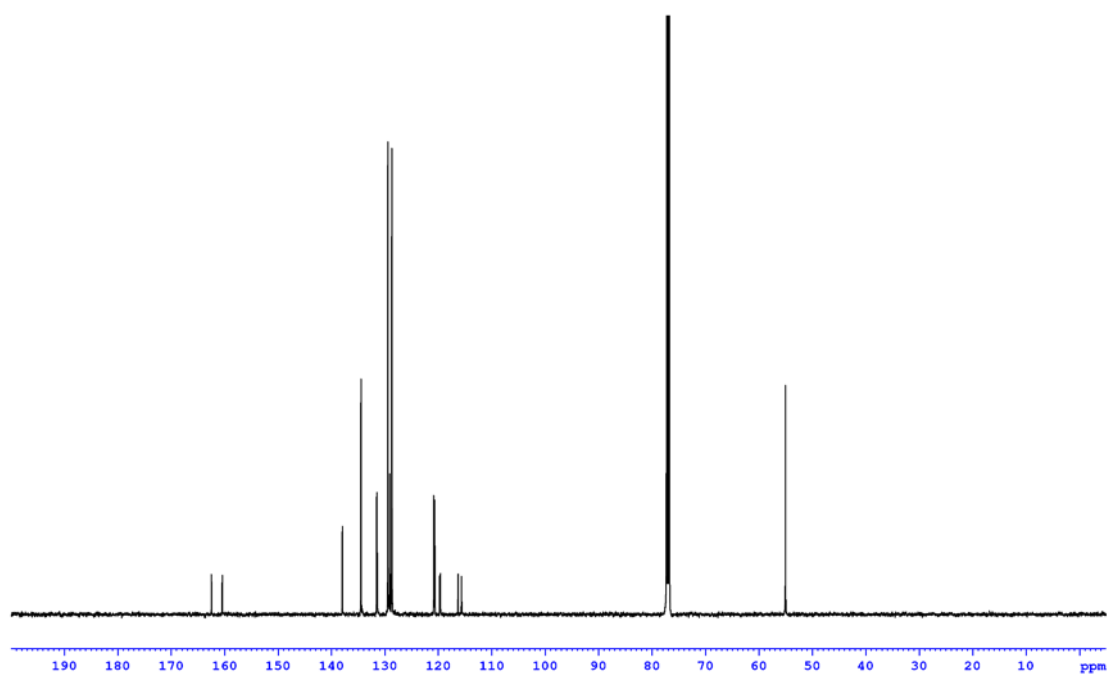
6

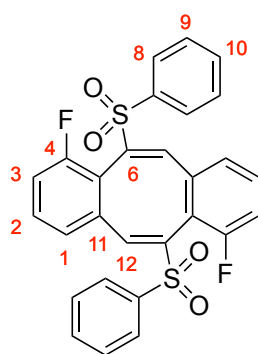




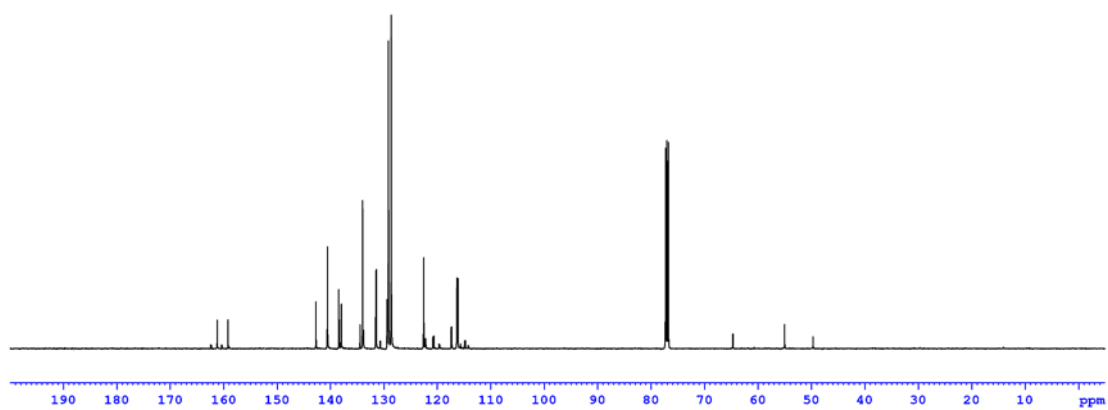
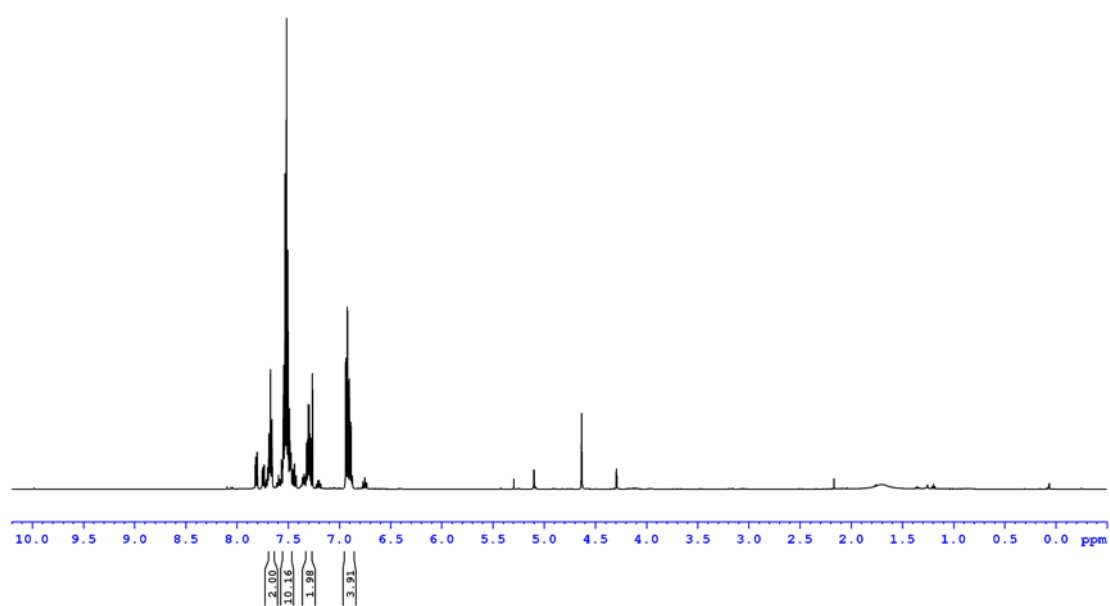
38

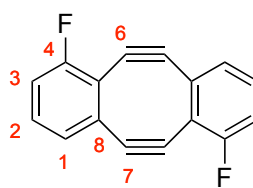
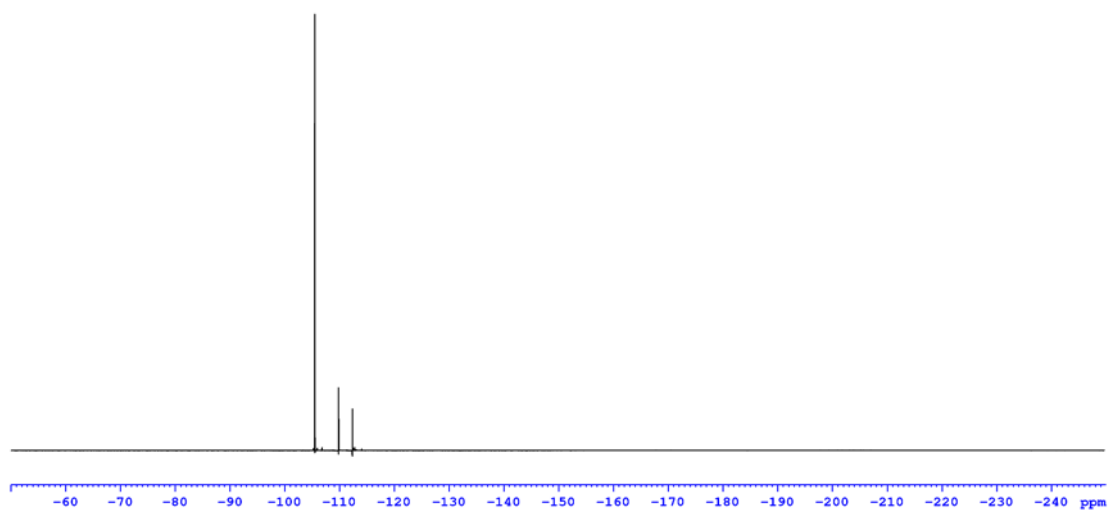




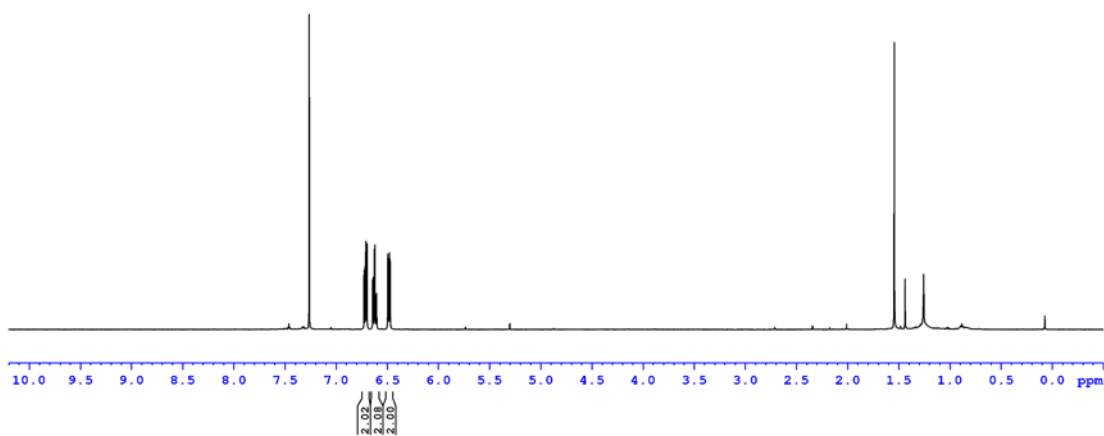


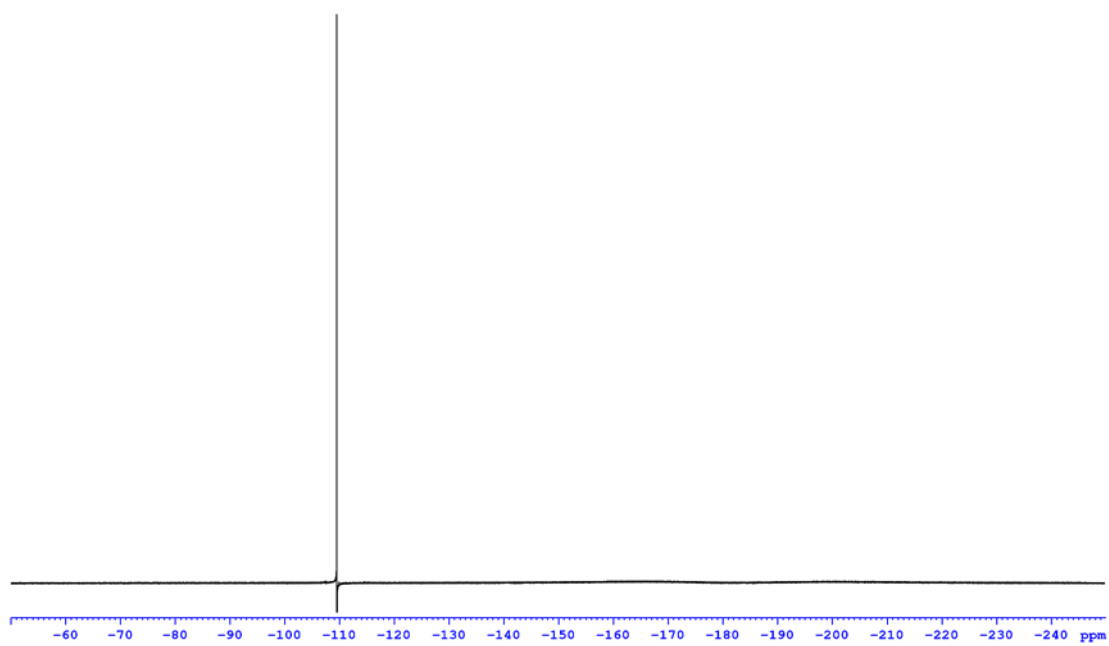
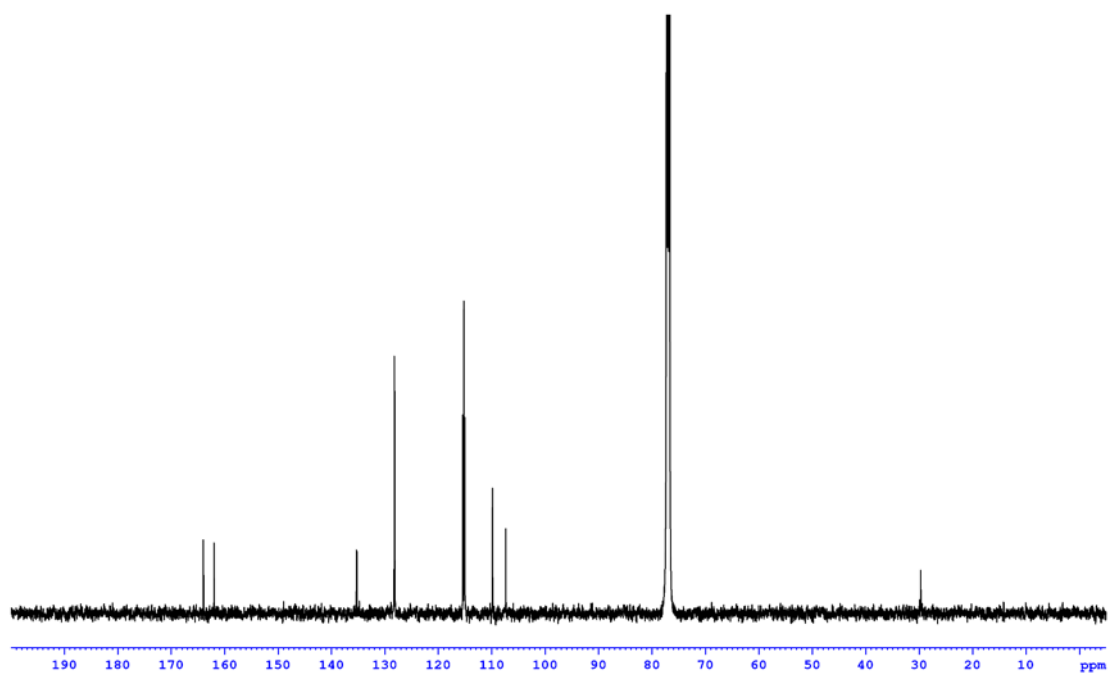
40

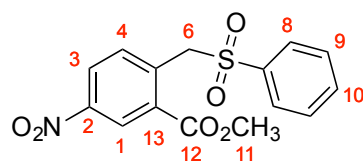




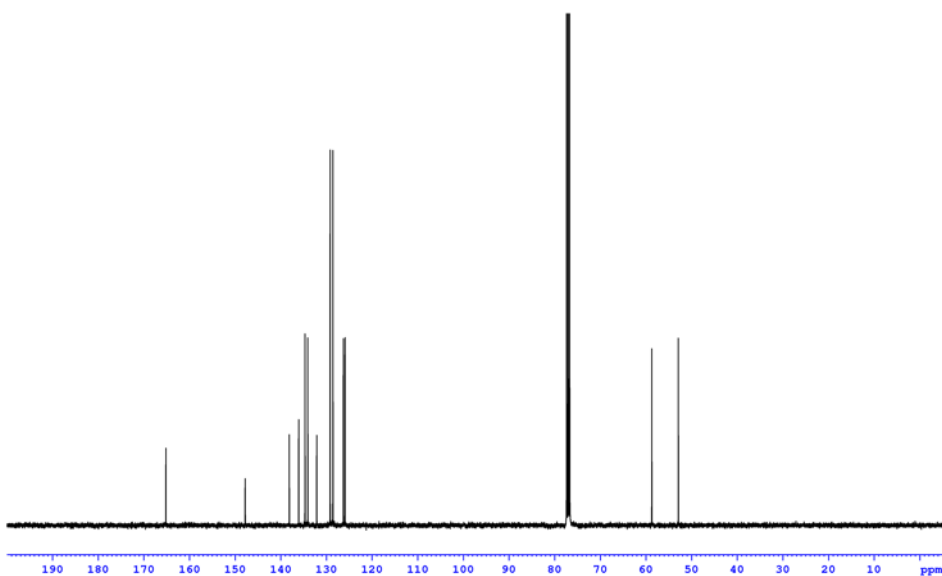
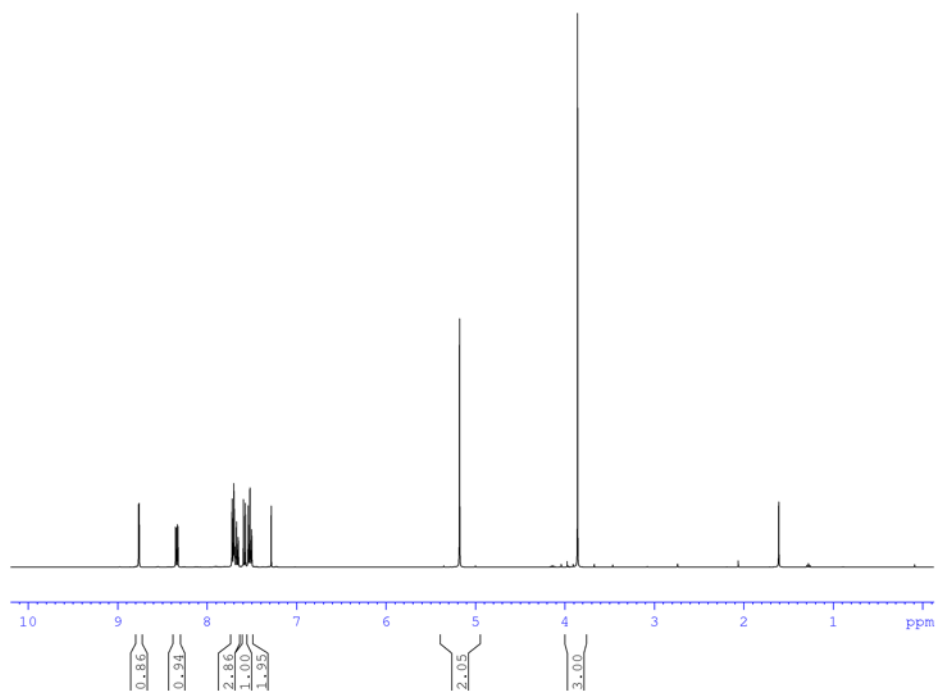
7

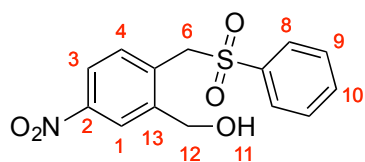




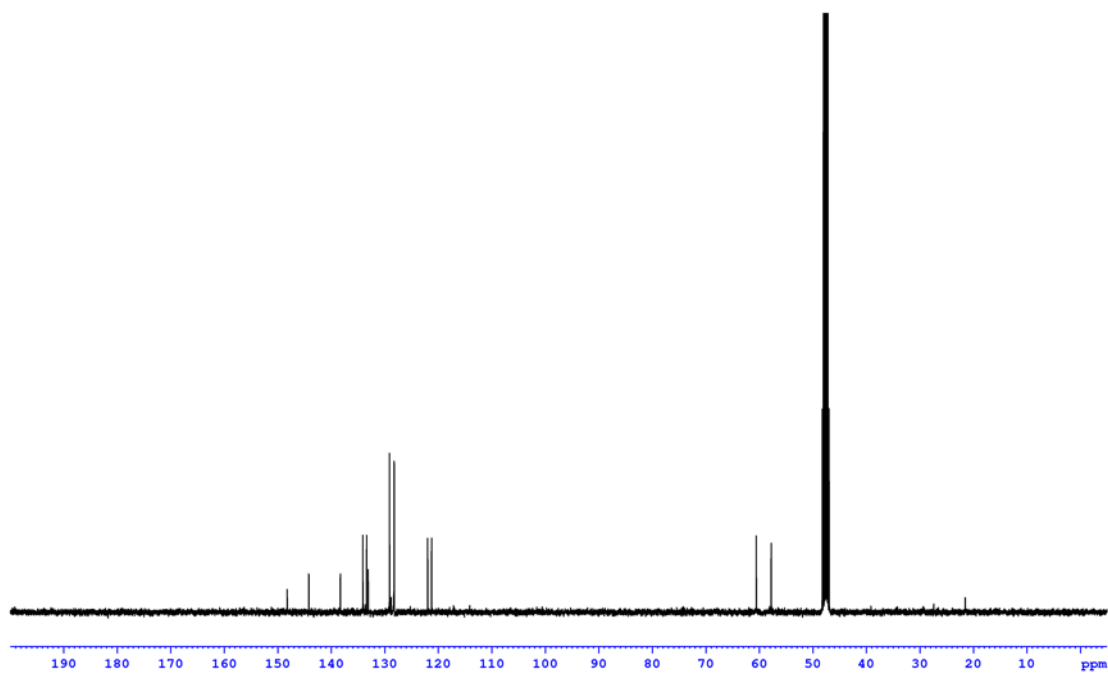
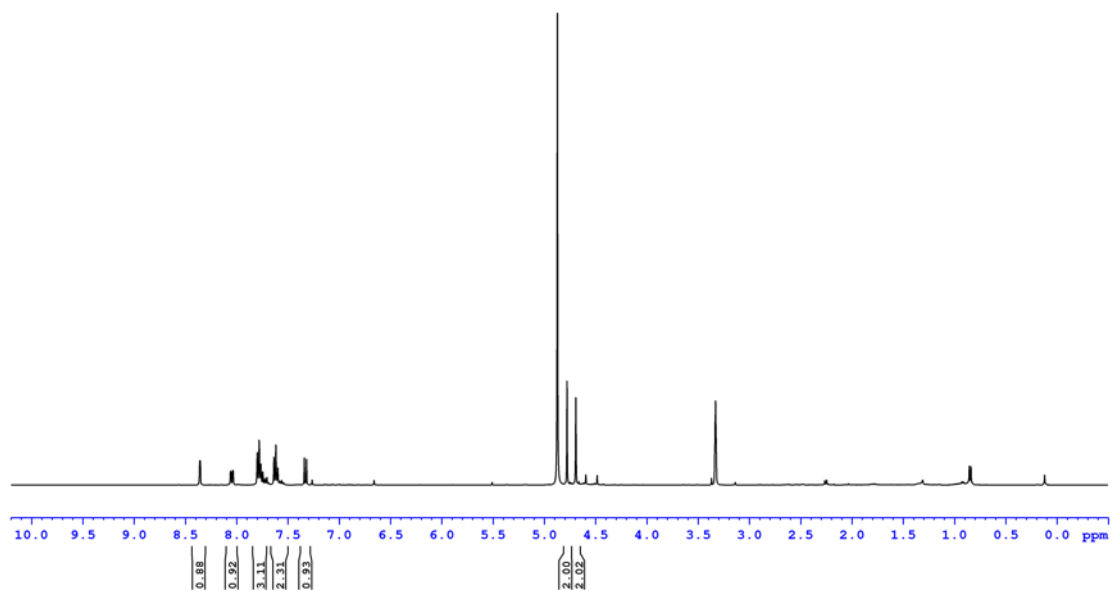


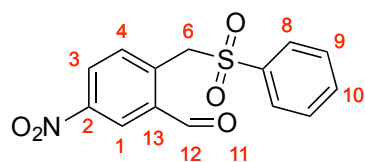
43



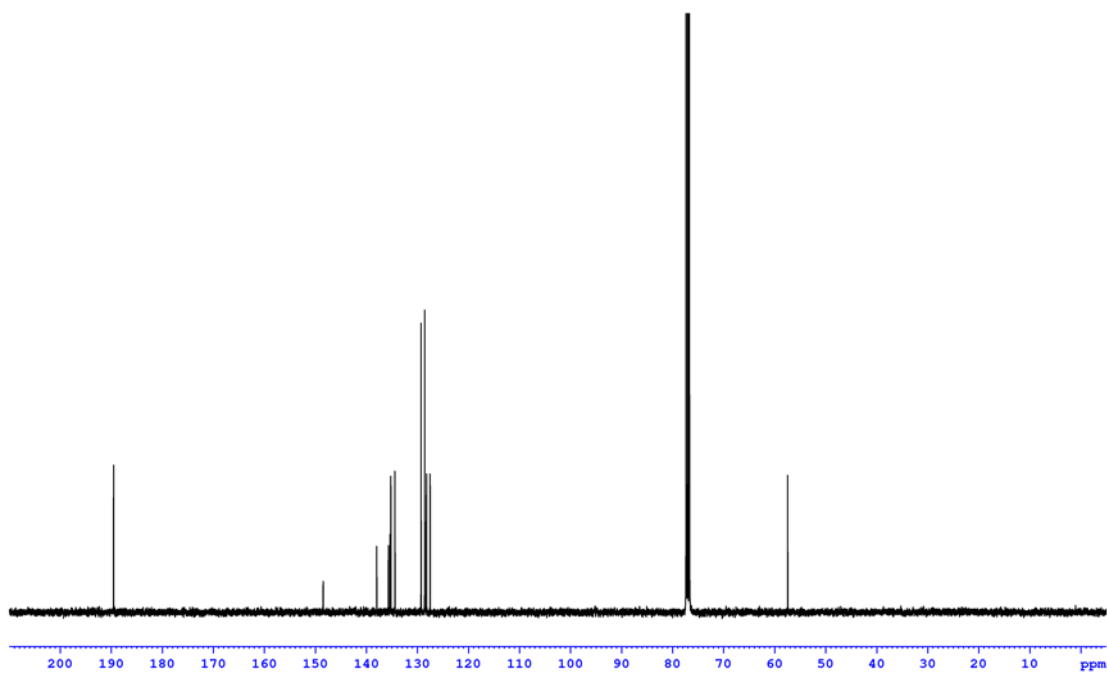
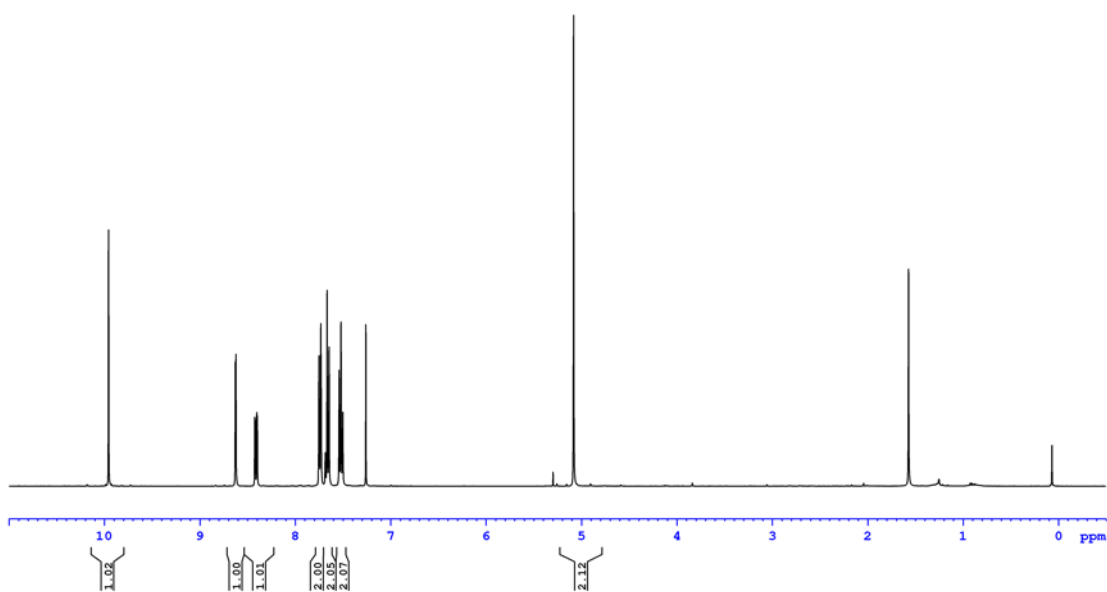


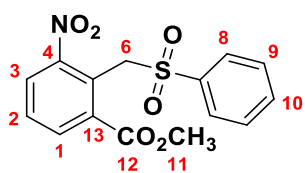
44



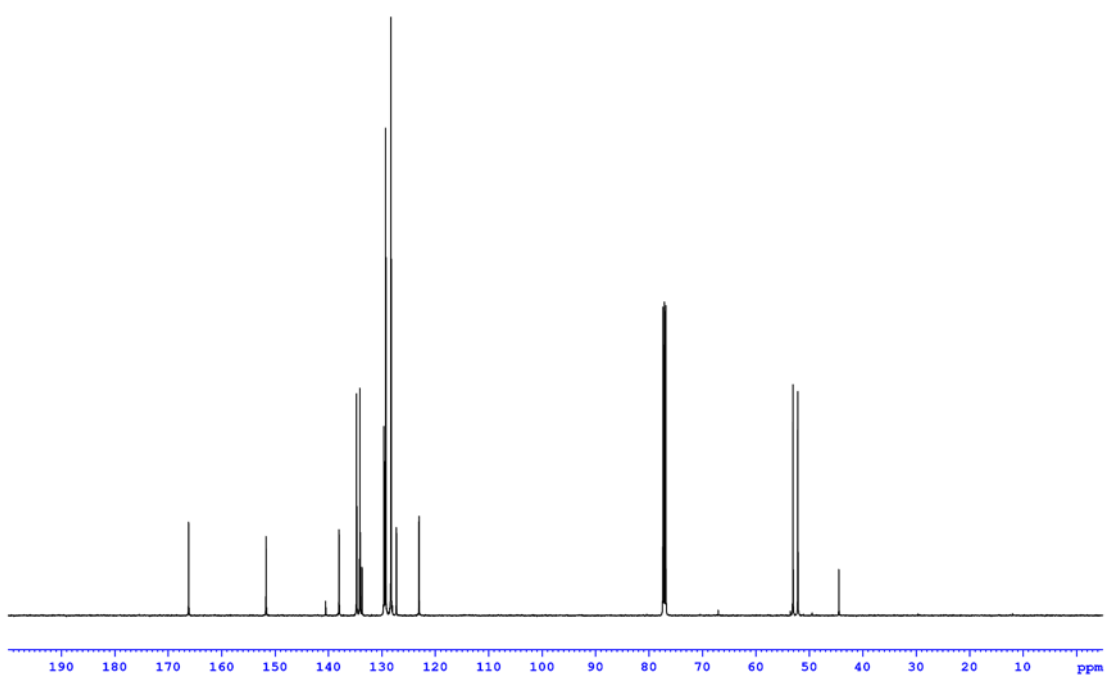
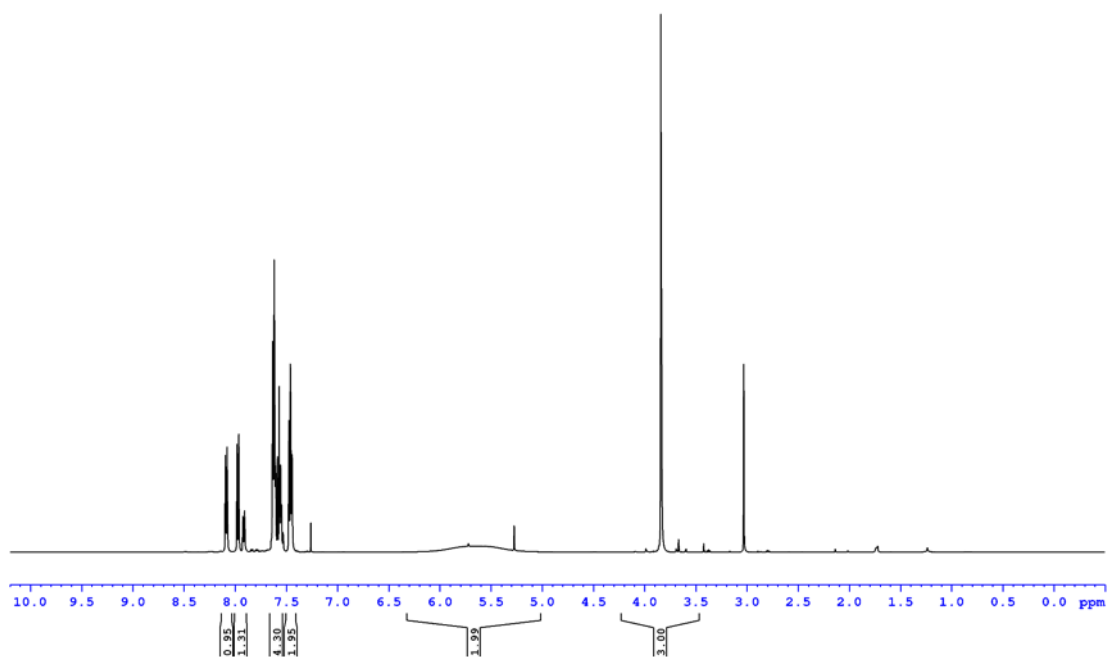


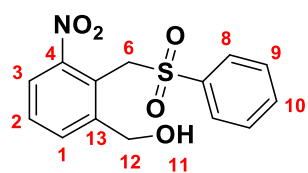
45



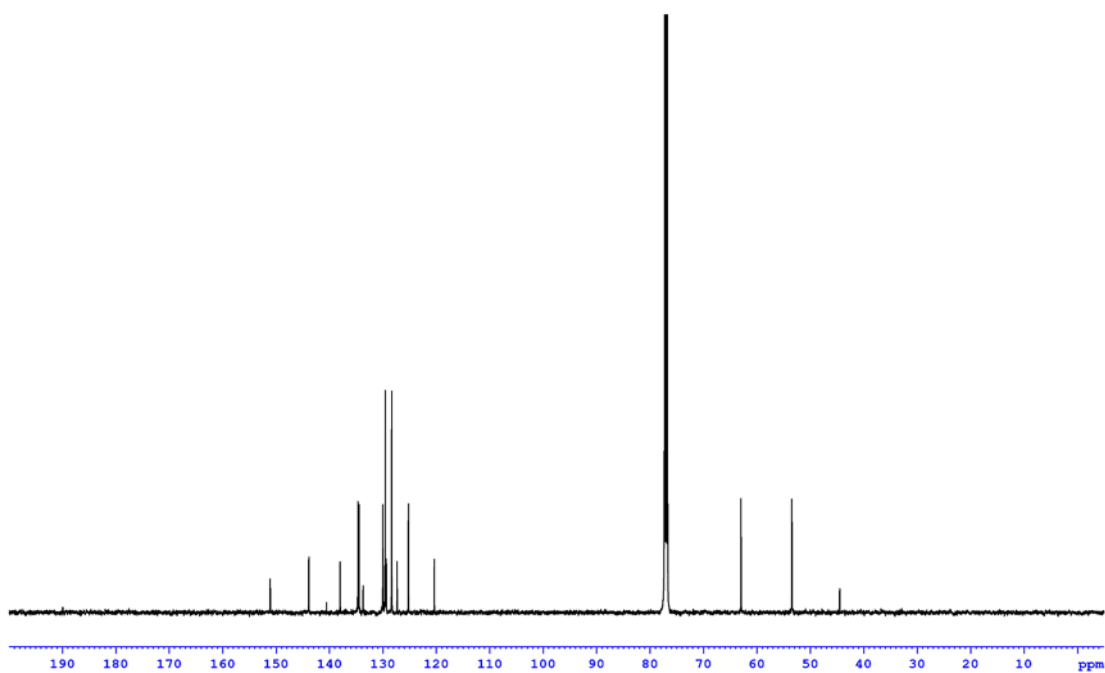
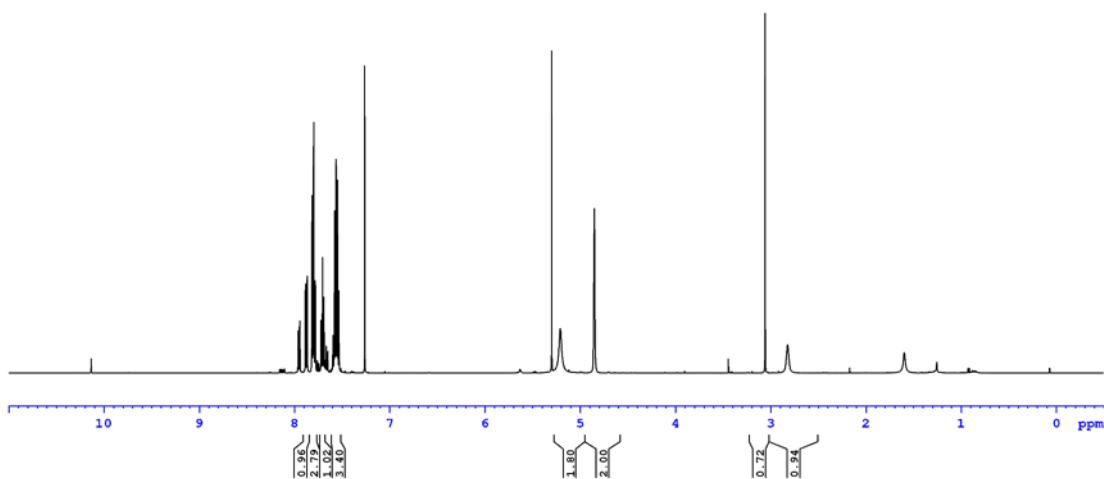


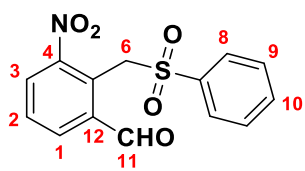
49



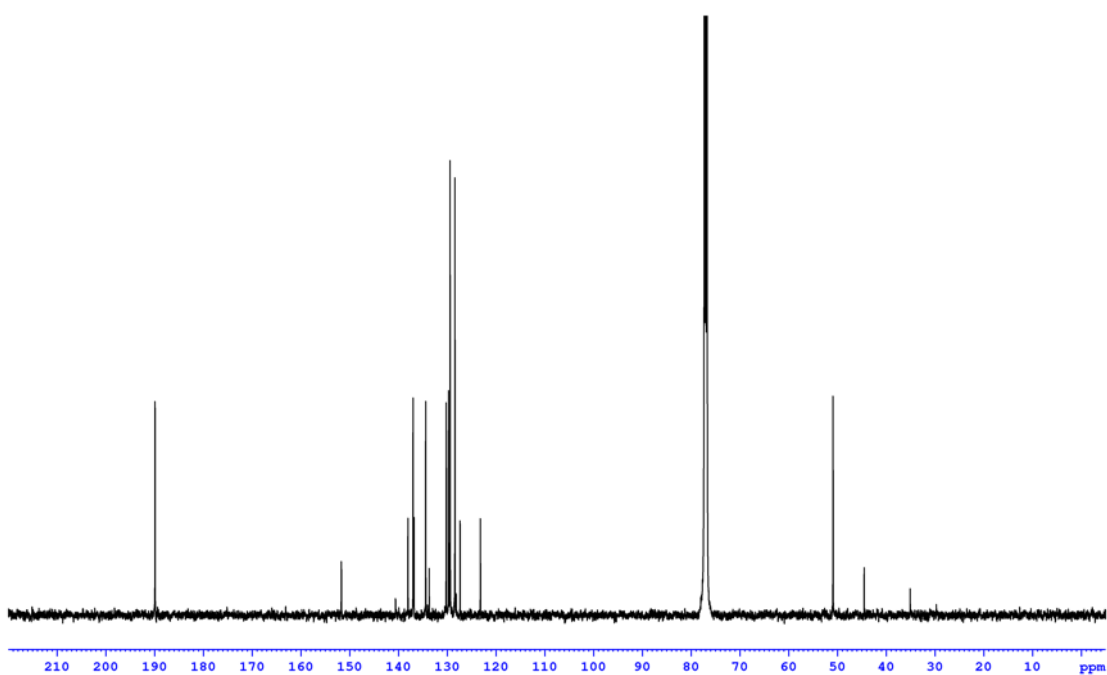
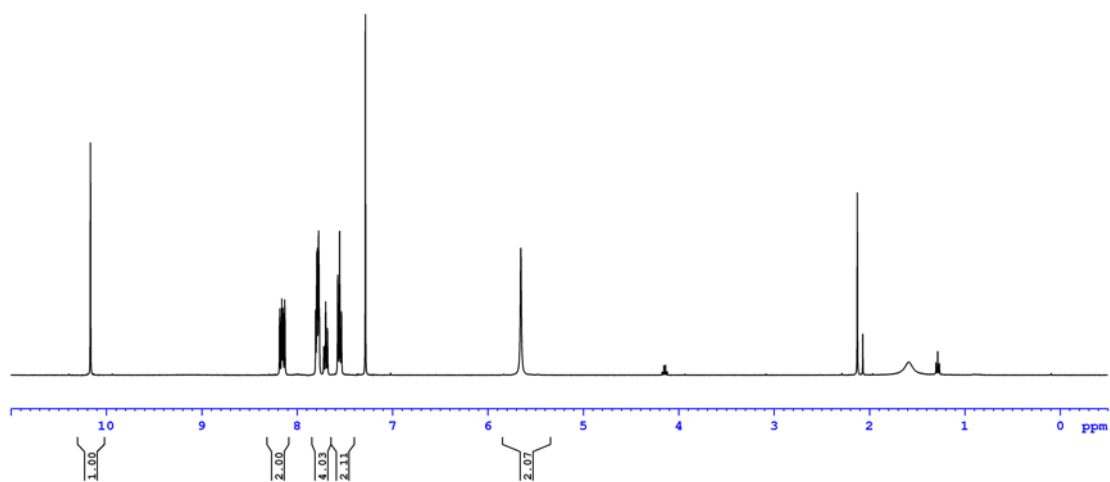


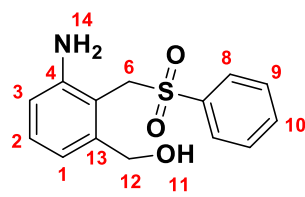
50



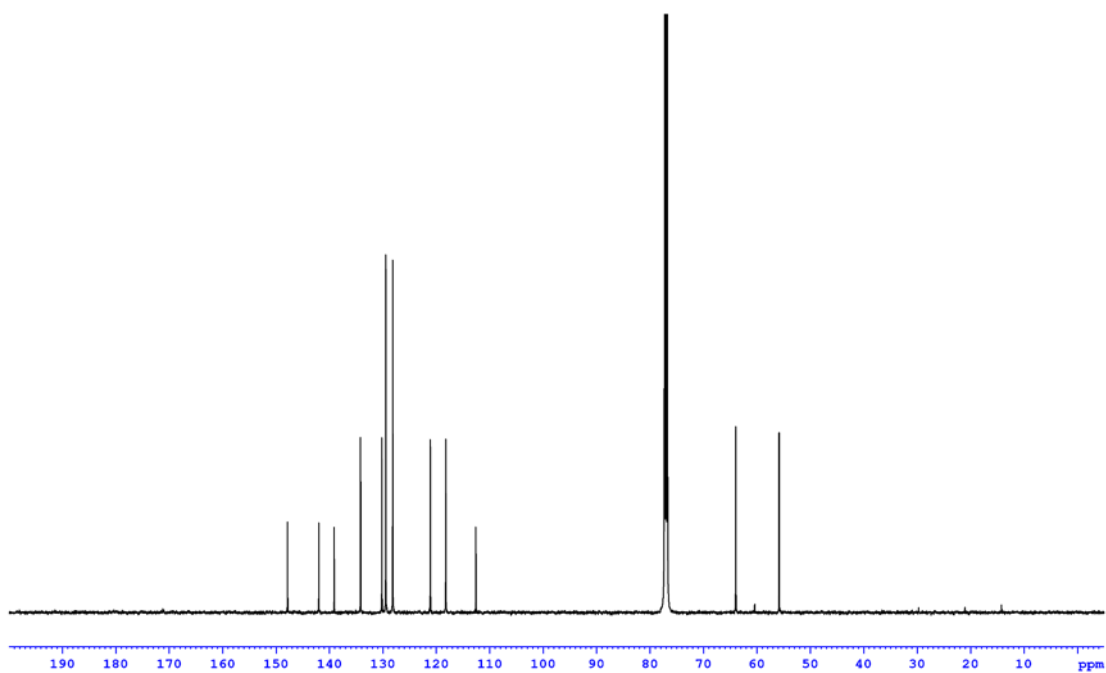
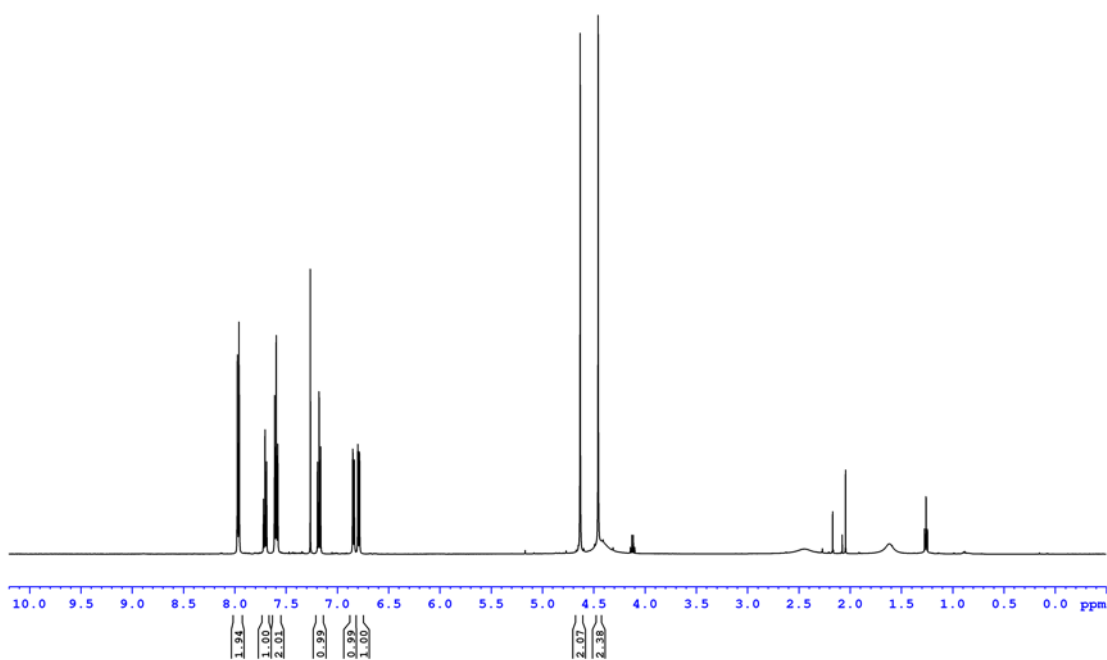


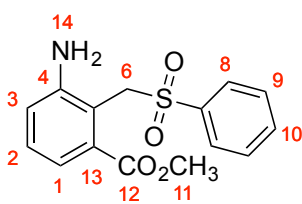
51



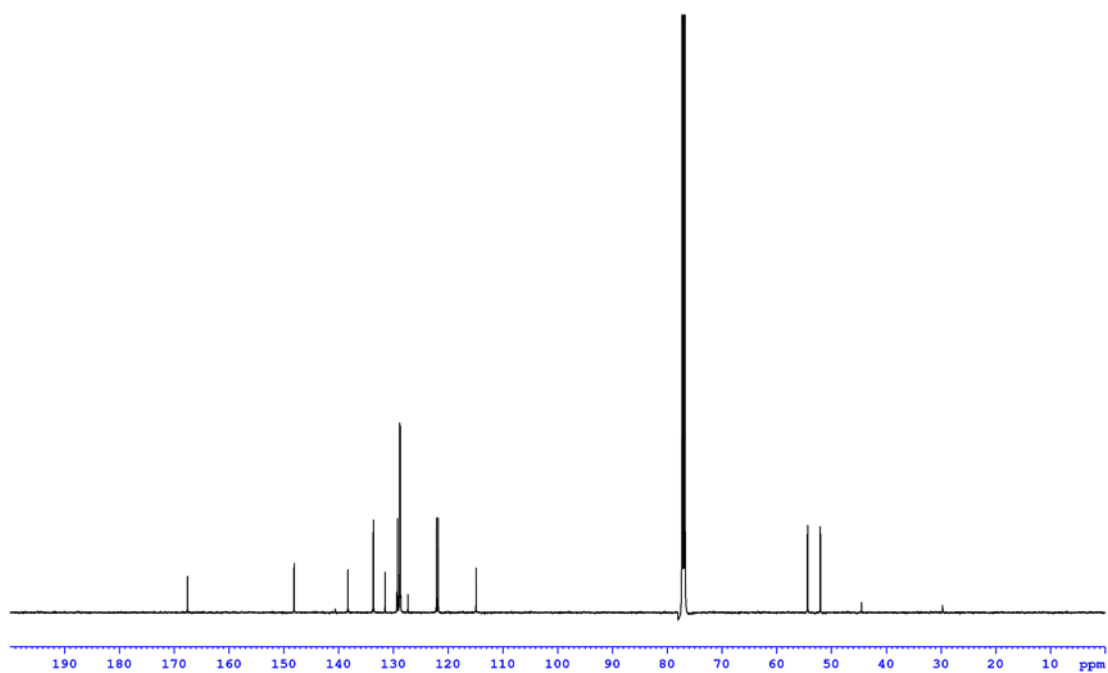
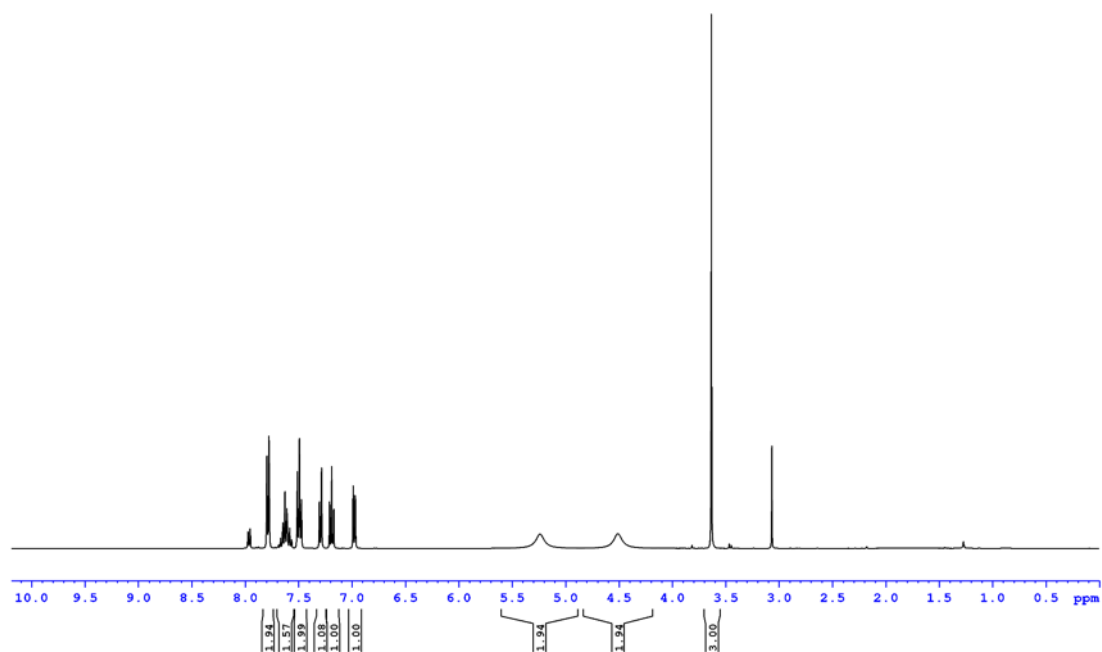


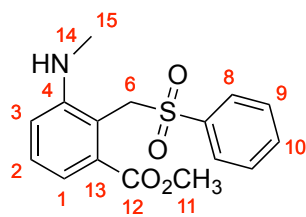
52



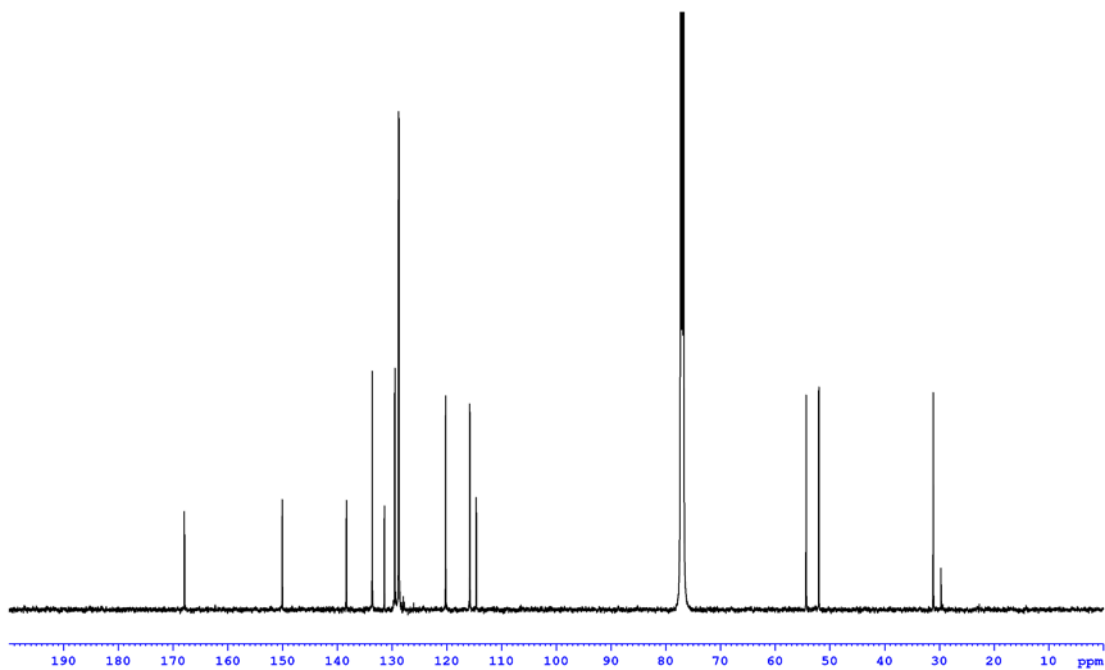
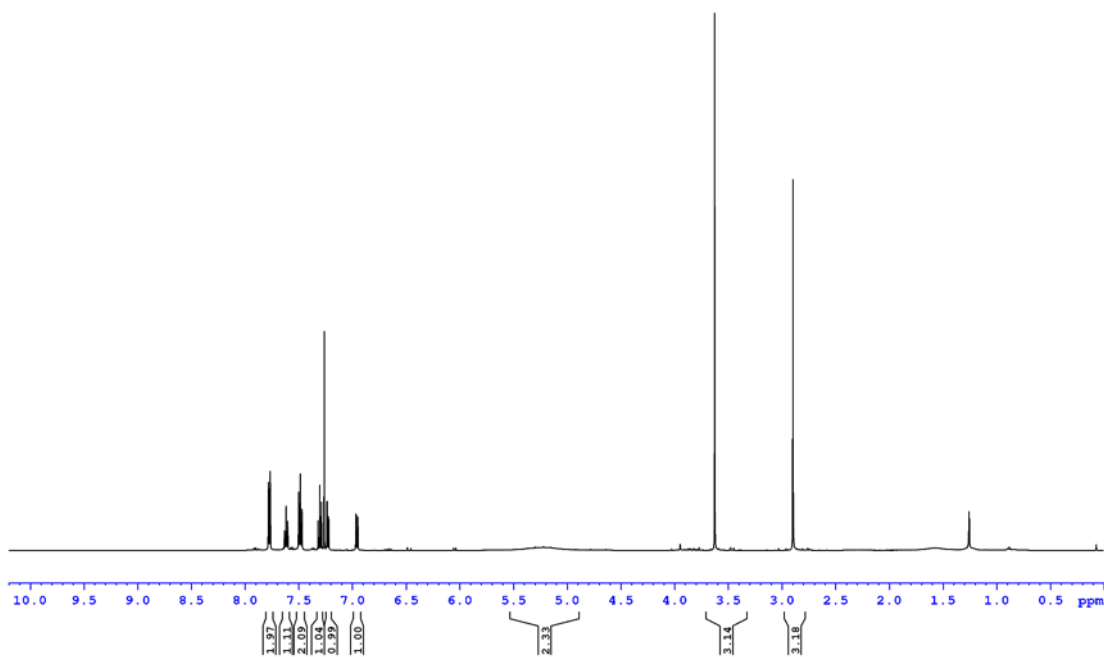


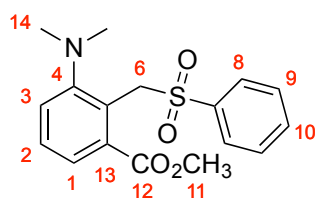
54



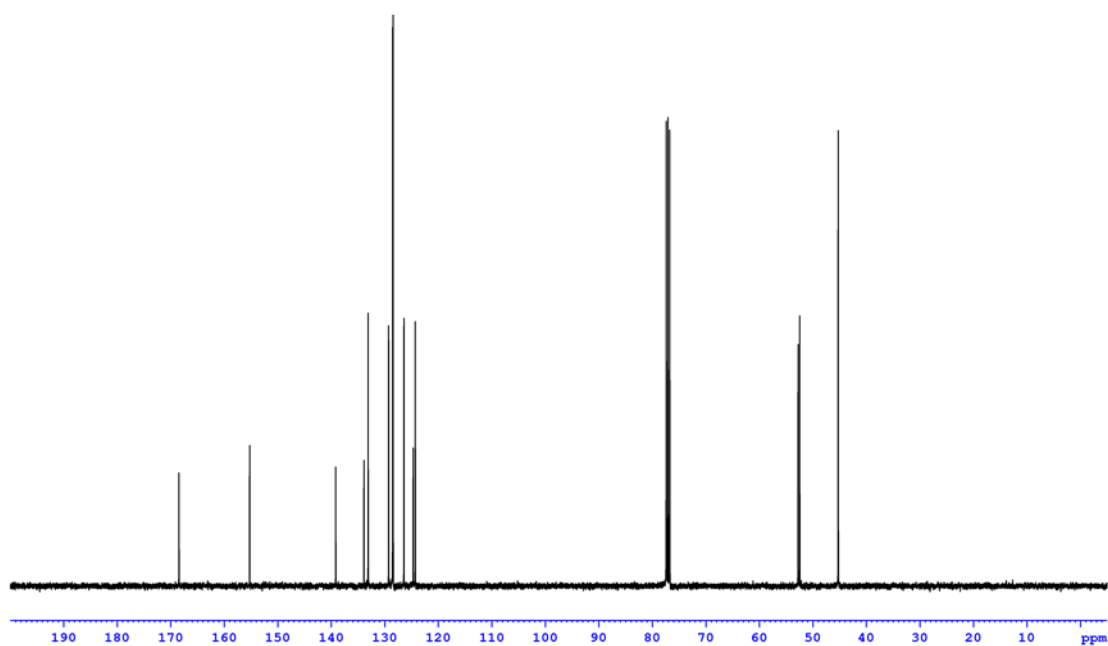
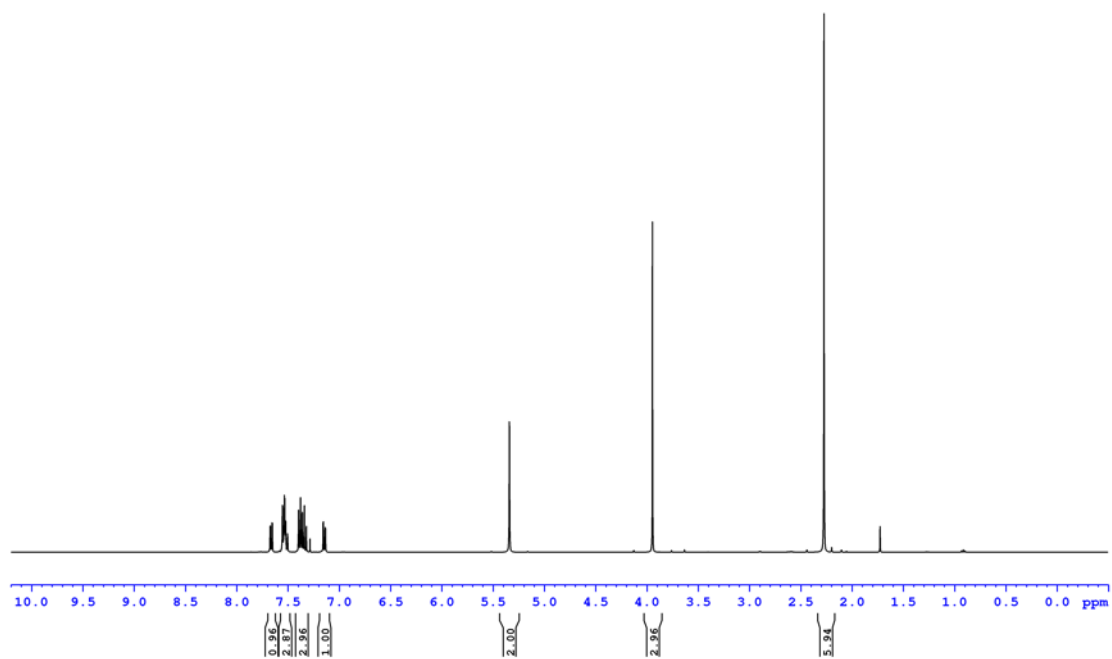


55

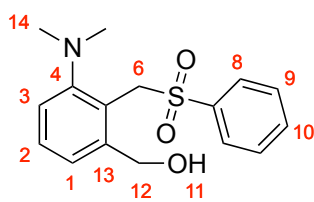




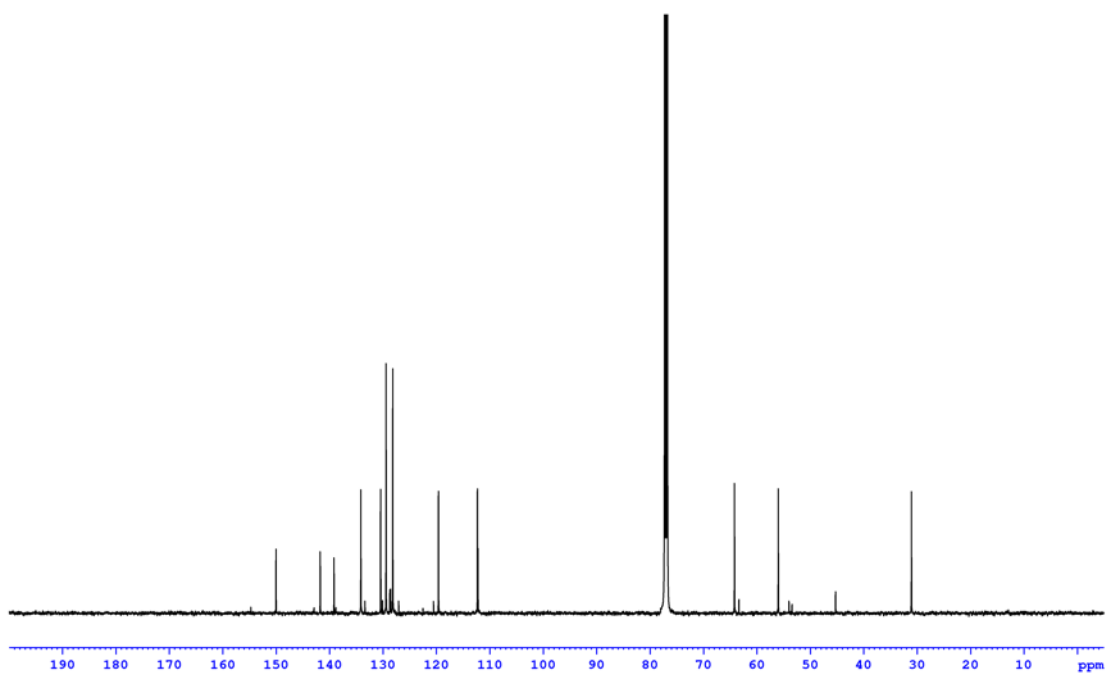
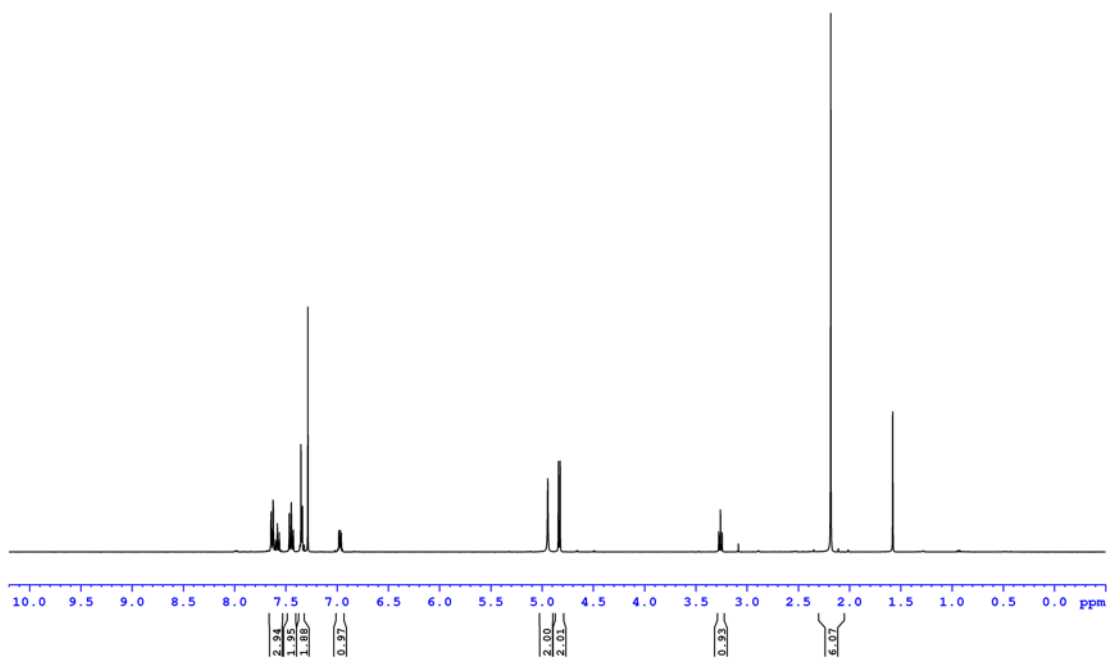
56

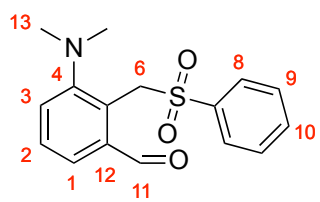


170

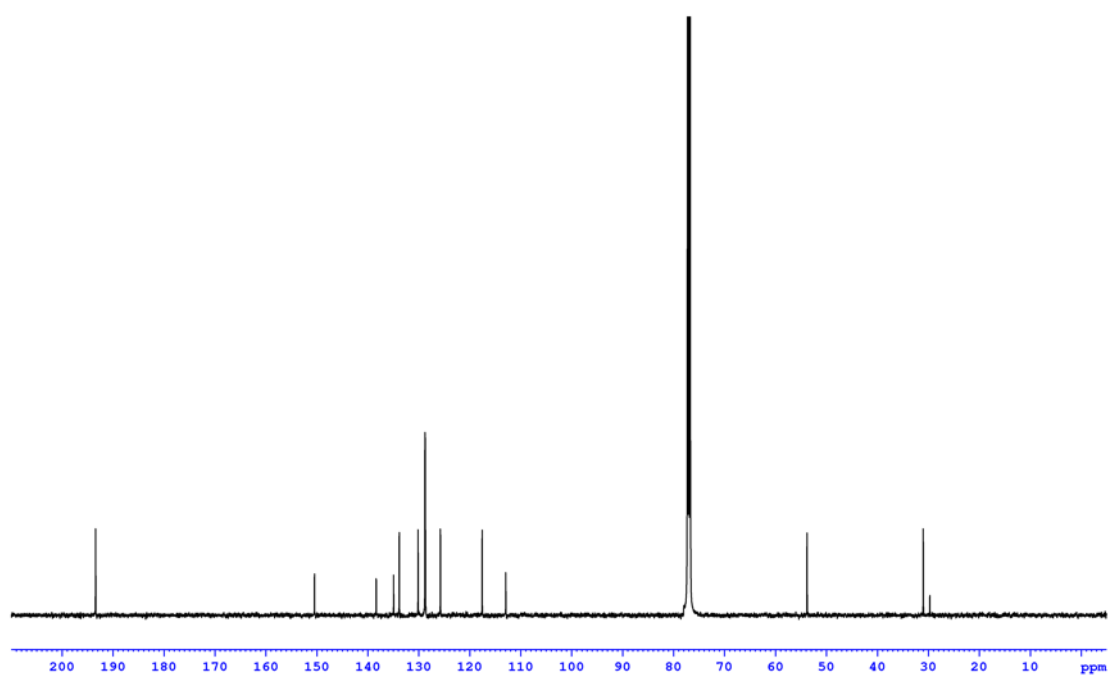
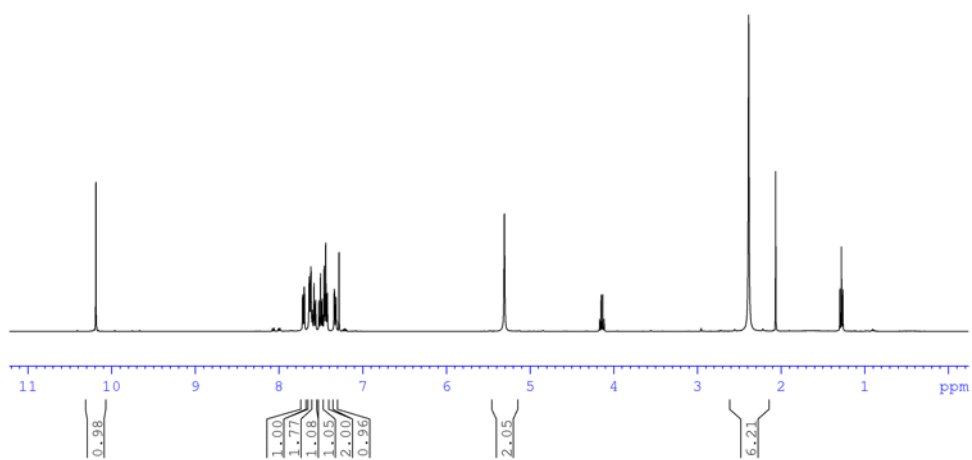


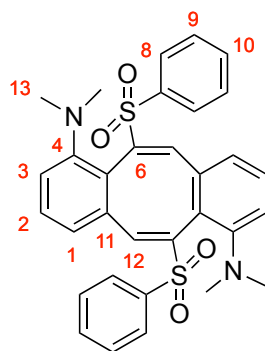
57



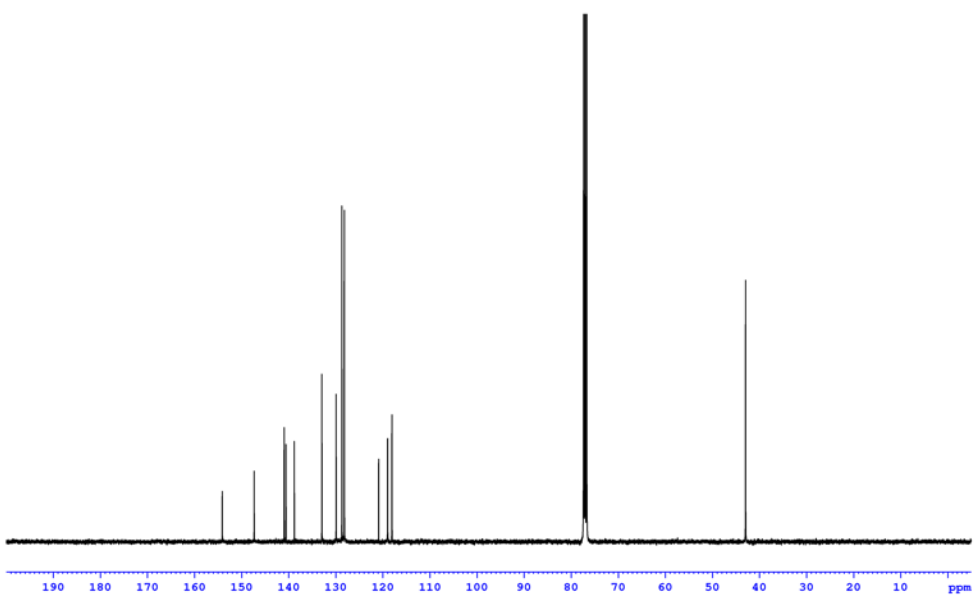
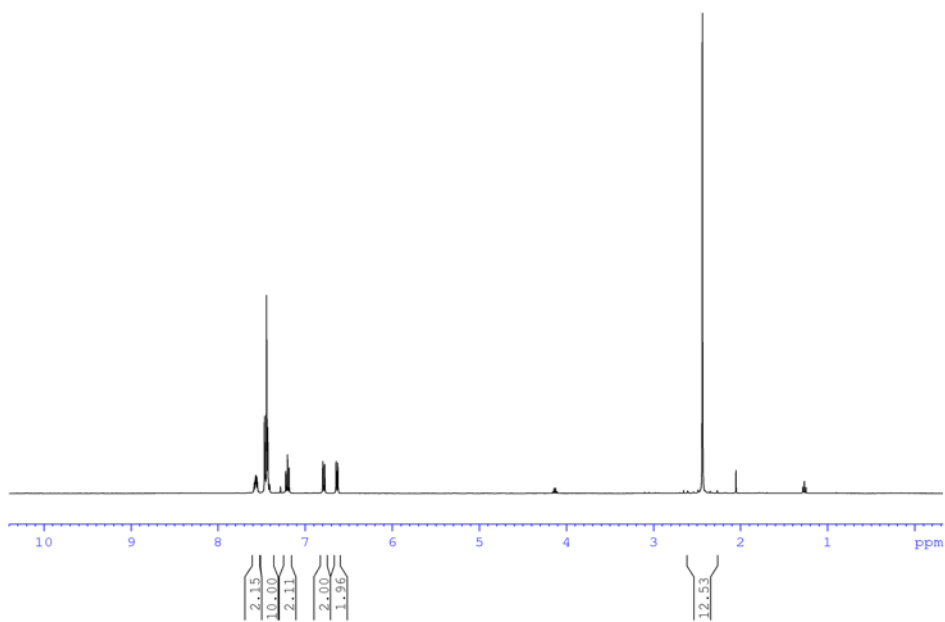


58

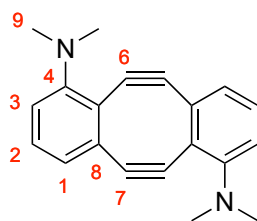




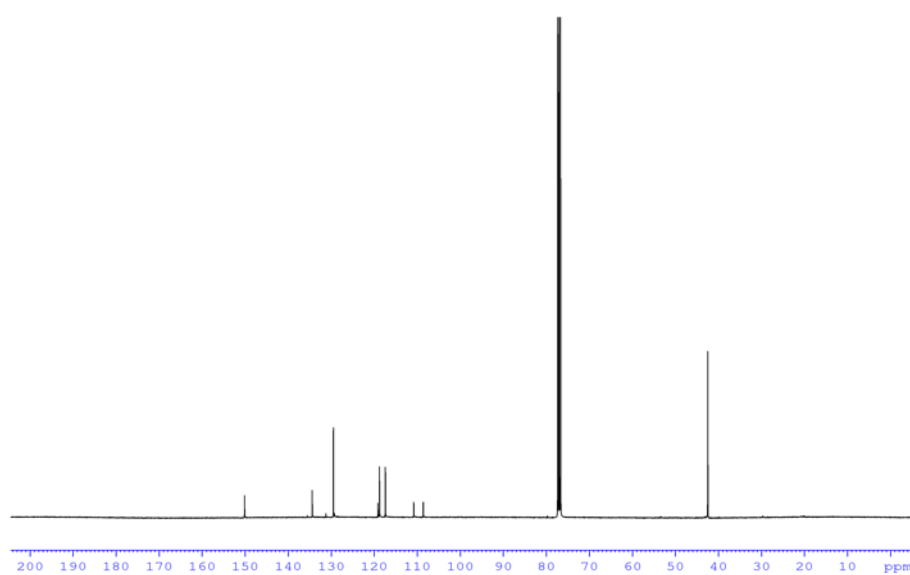
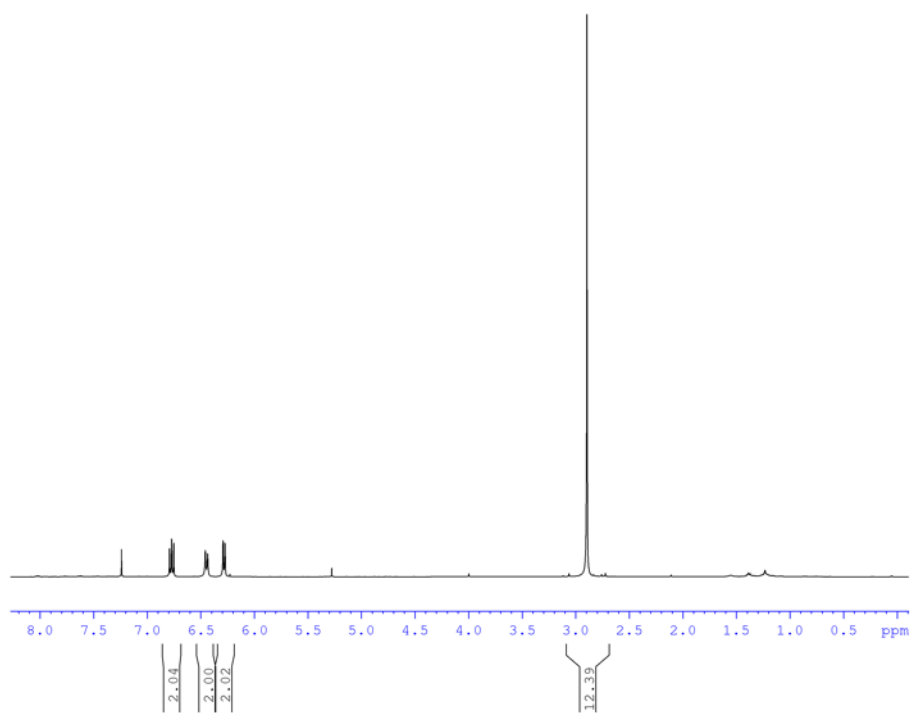
59

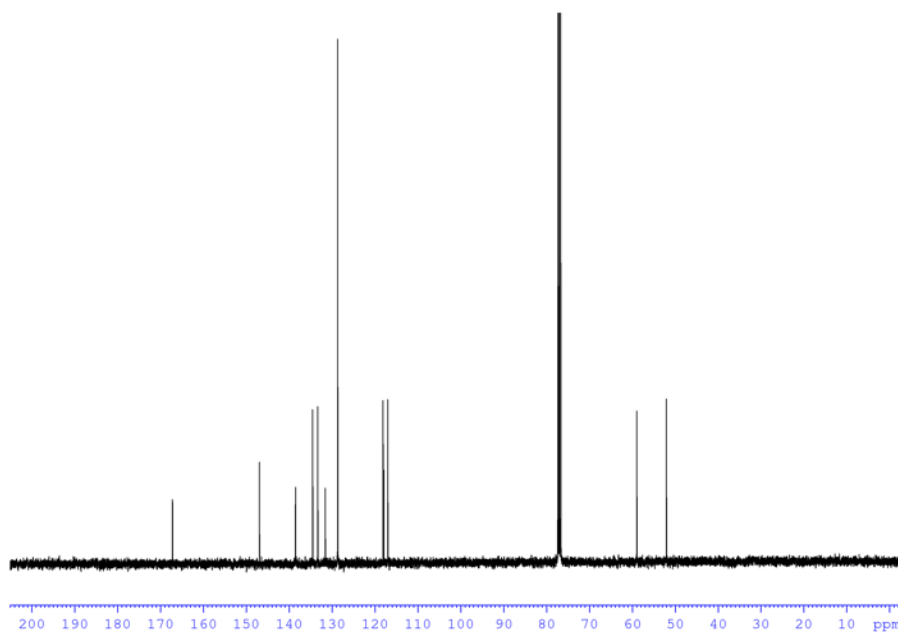


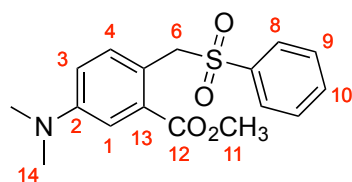
173



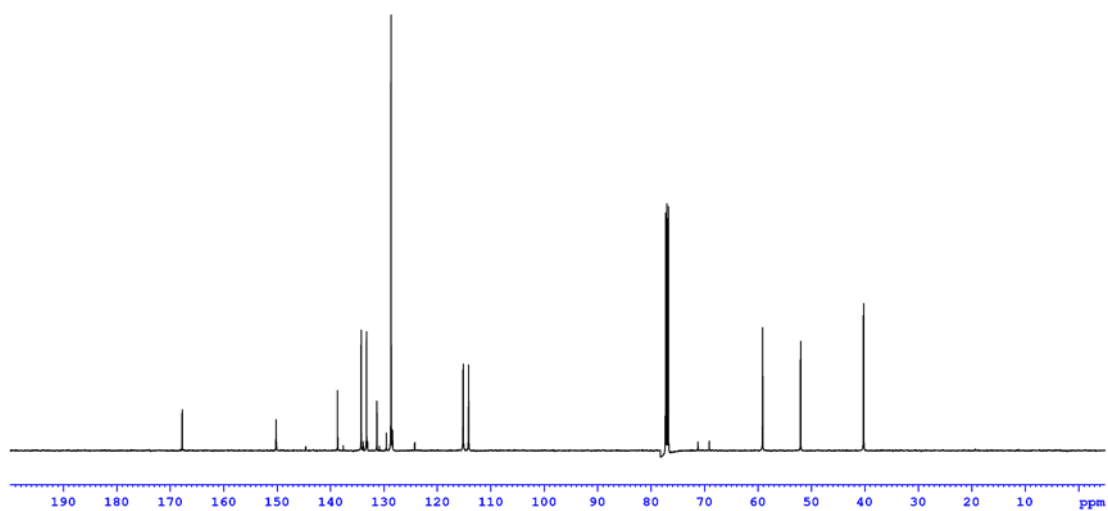
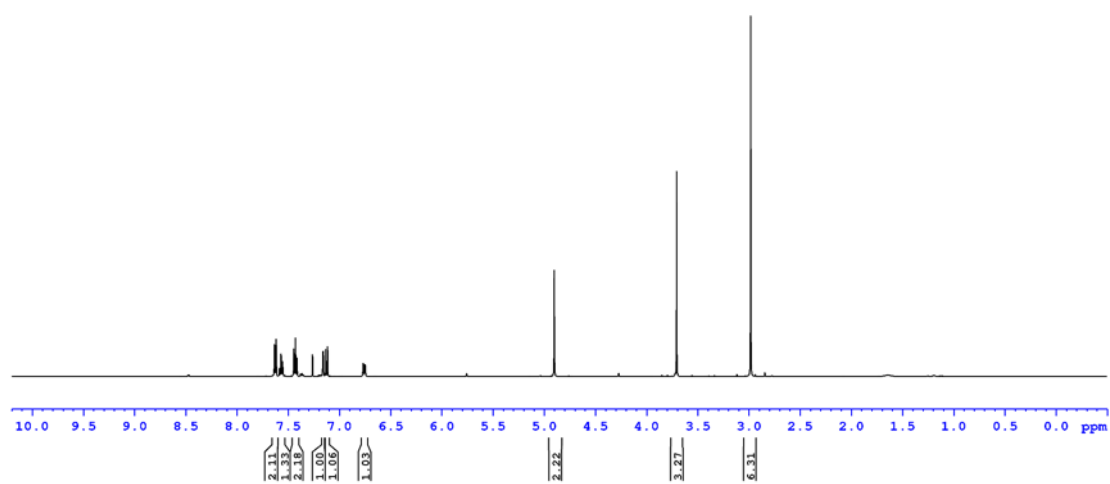
10

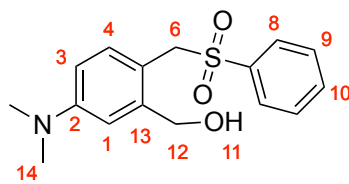




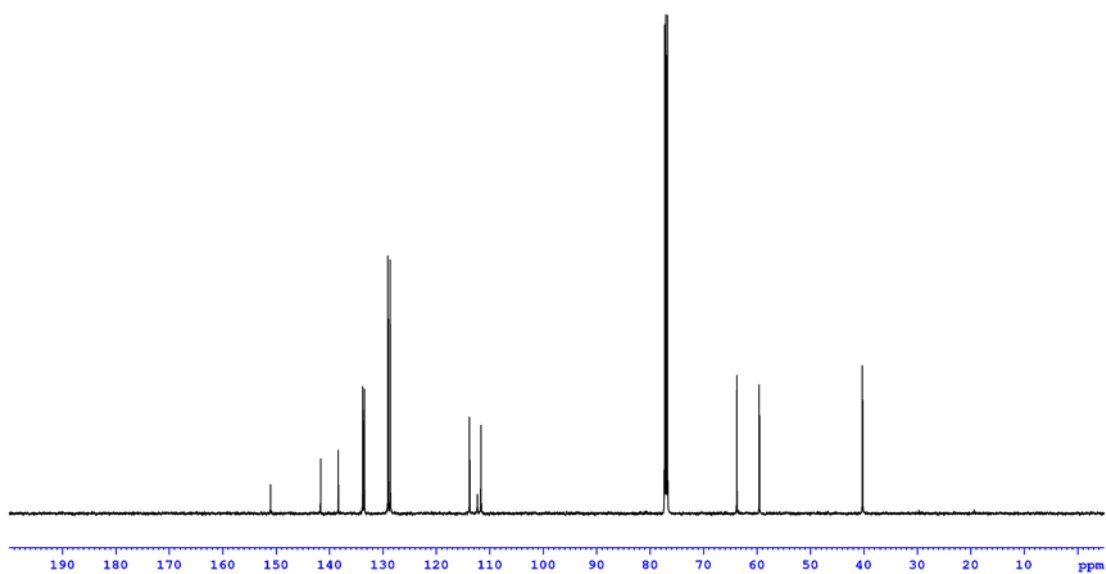
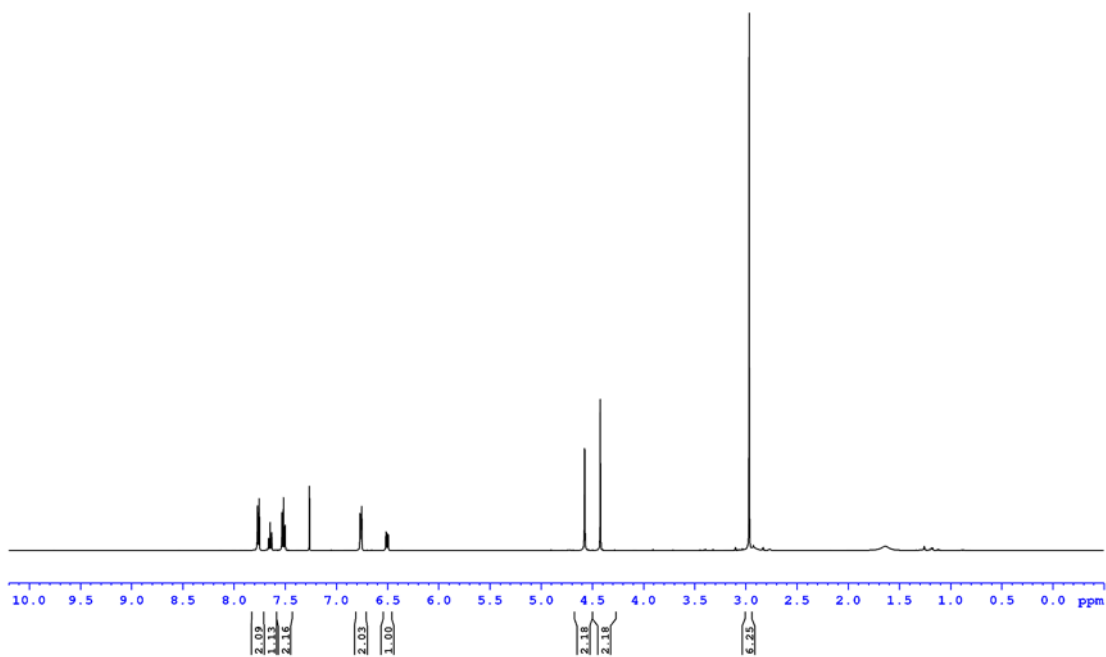


61

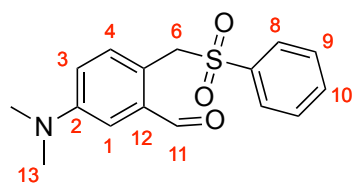




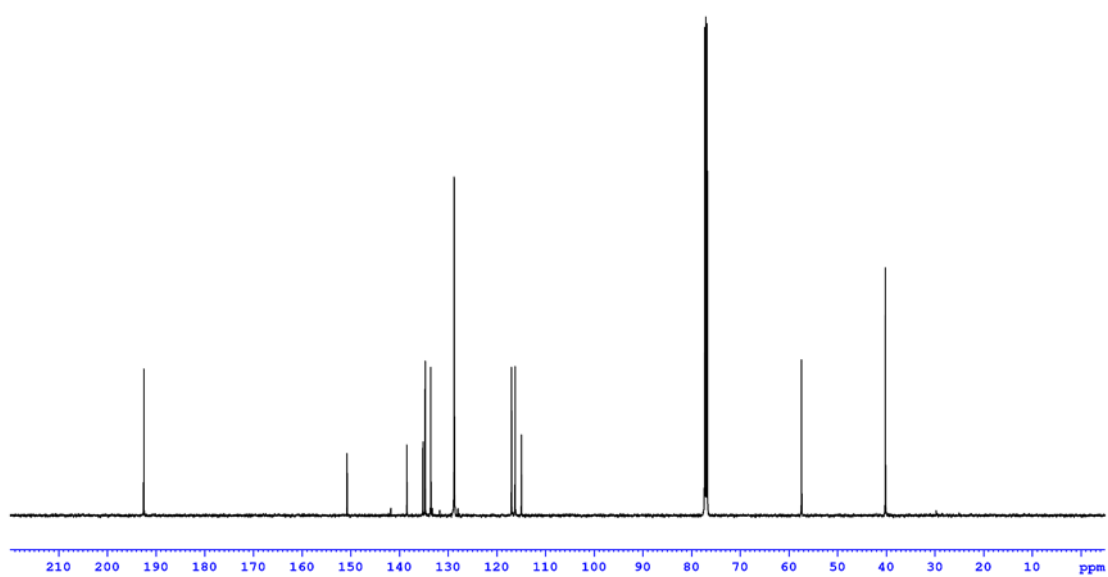
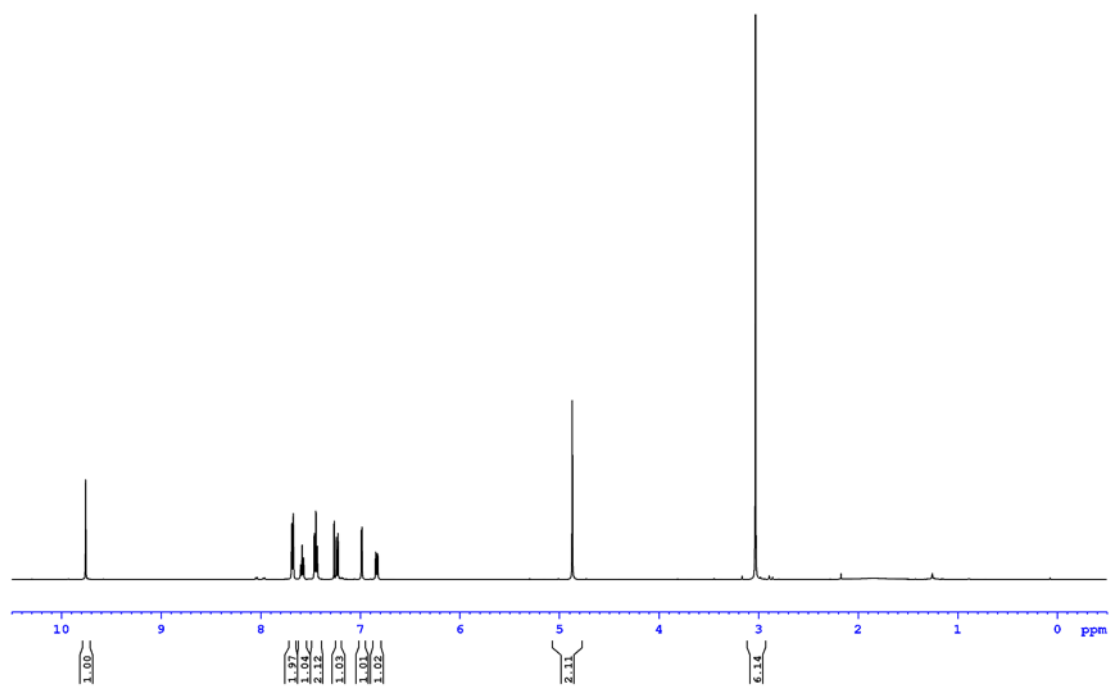
62



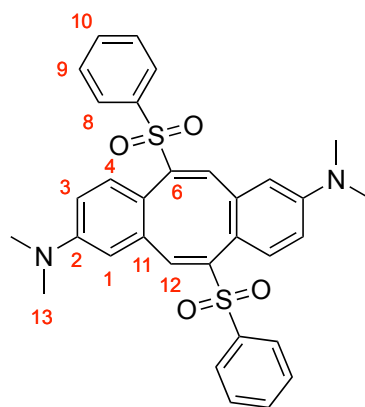
177



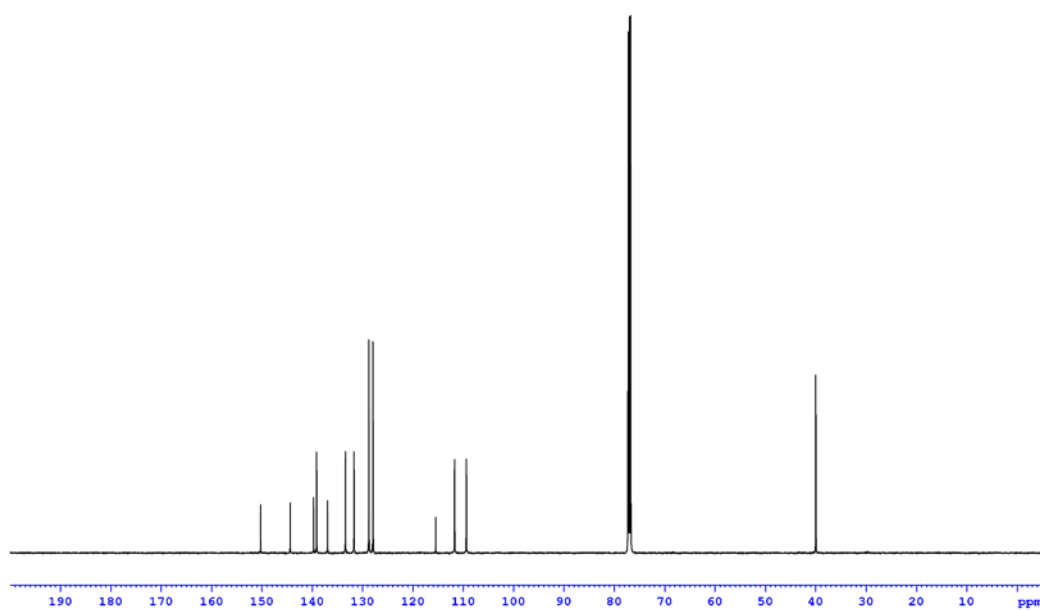
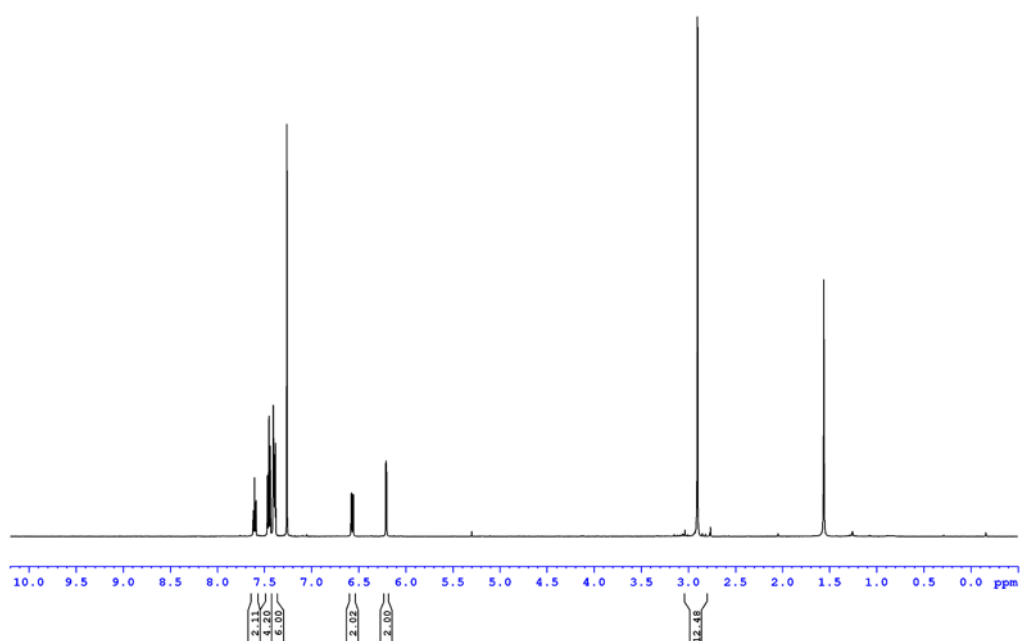
63

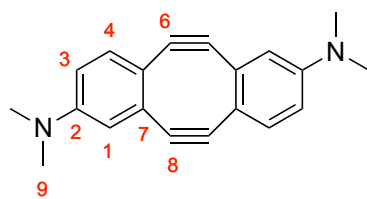


178

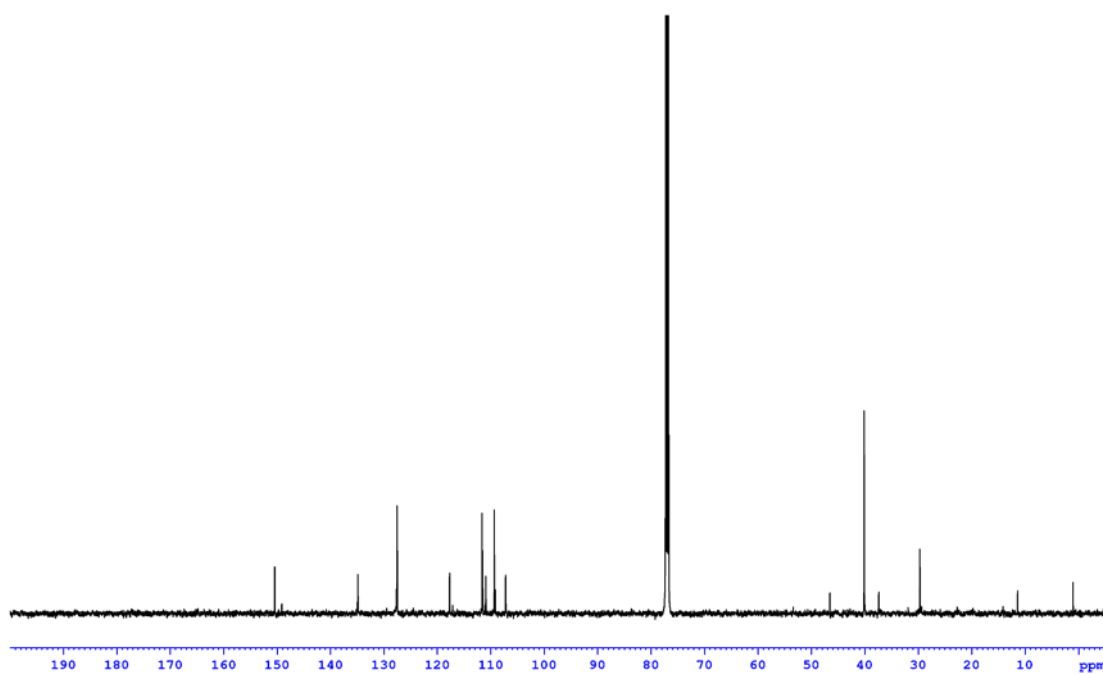
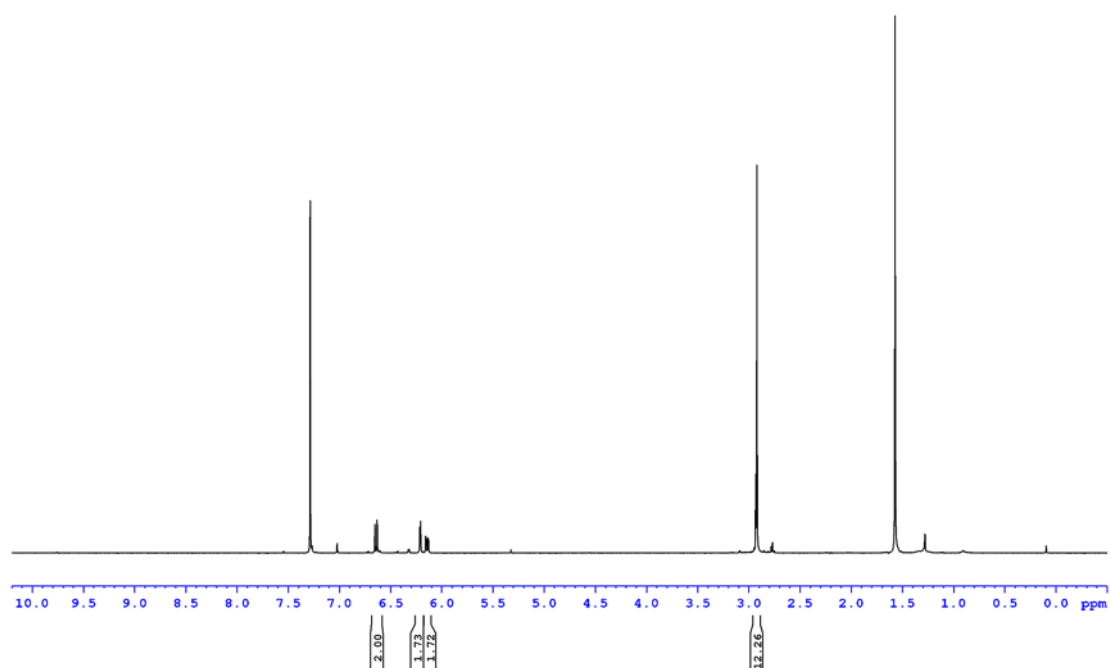


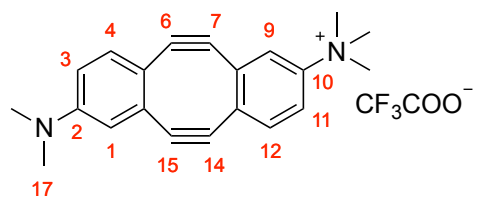
64



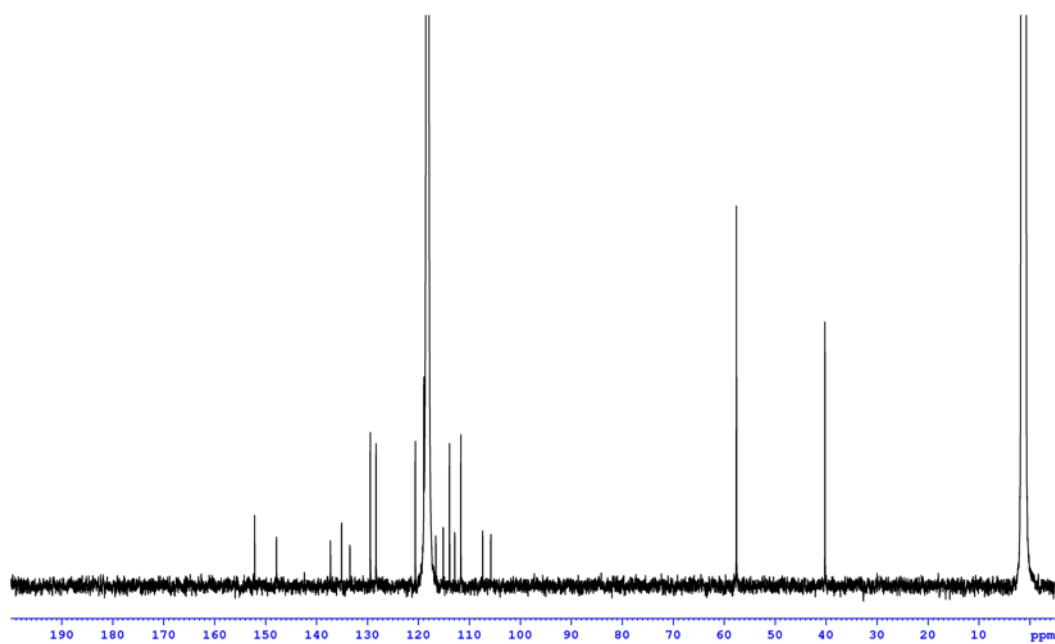
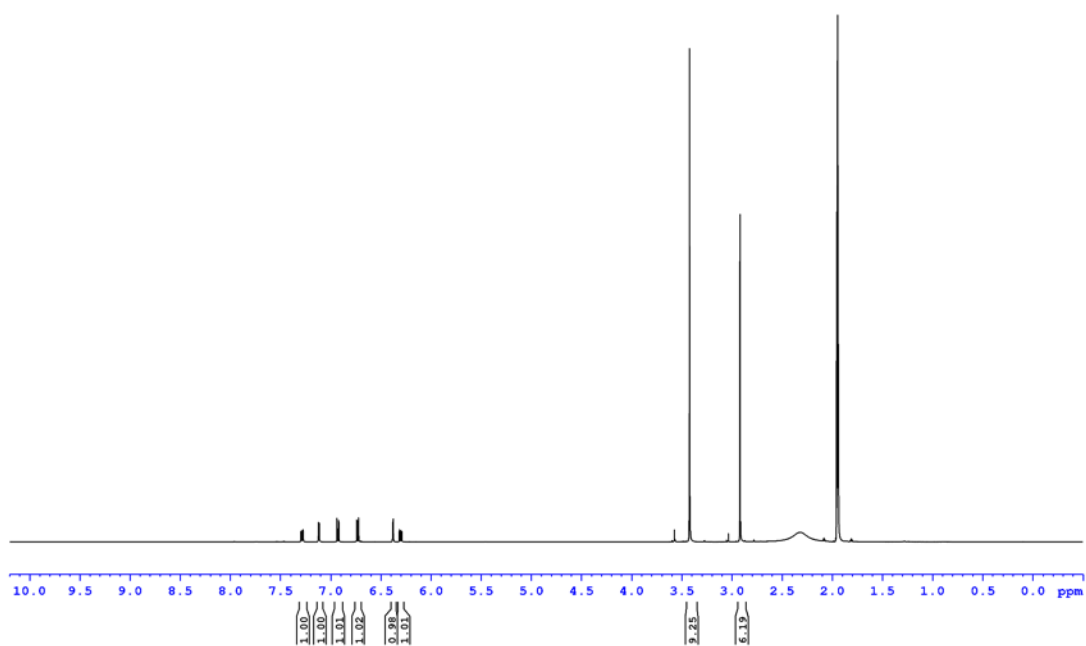


11

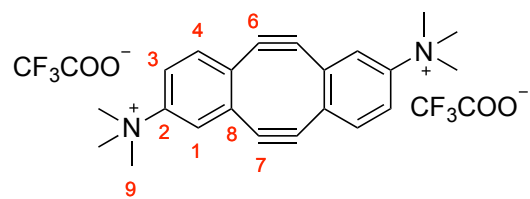




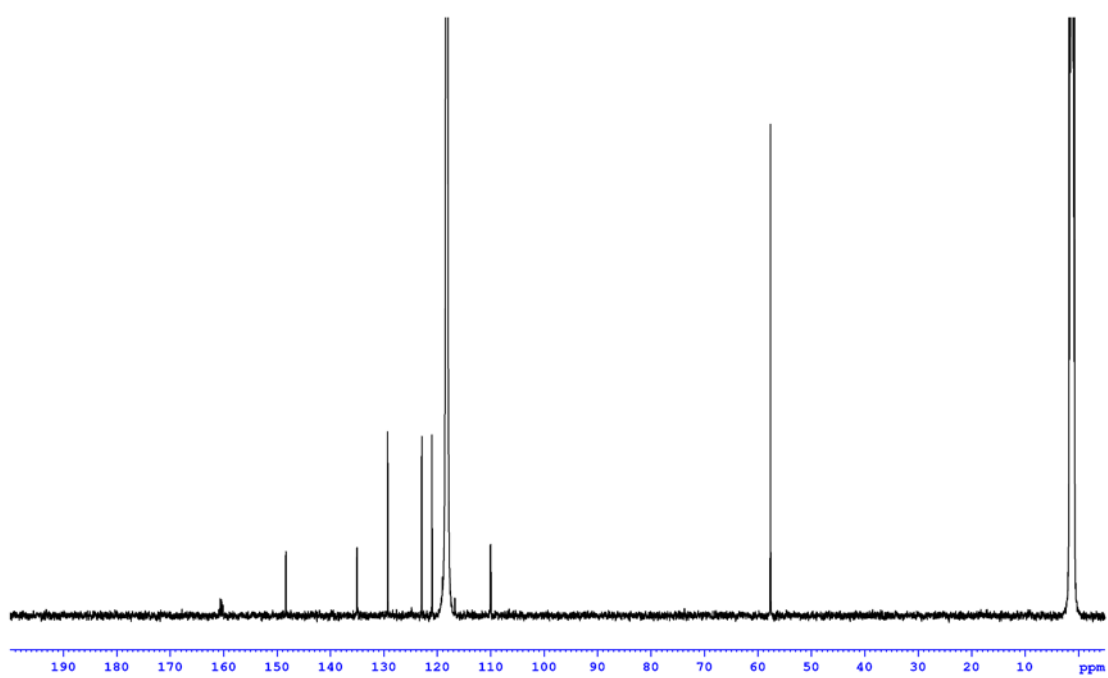
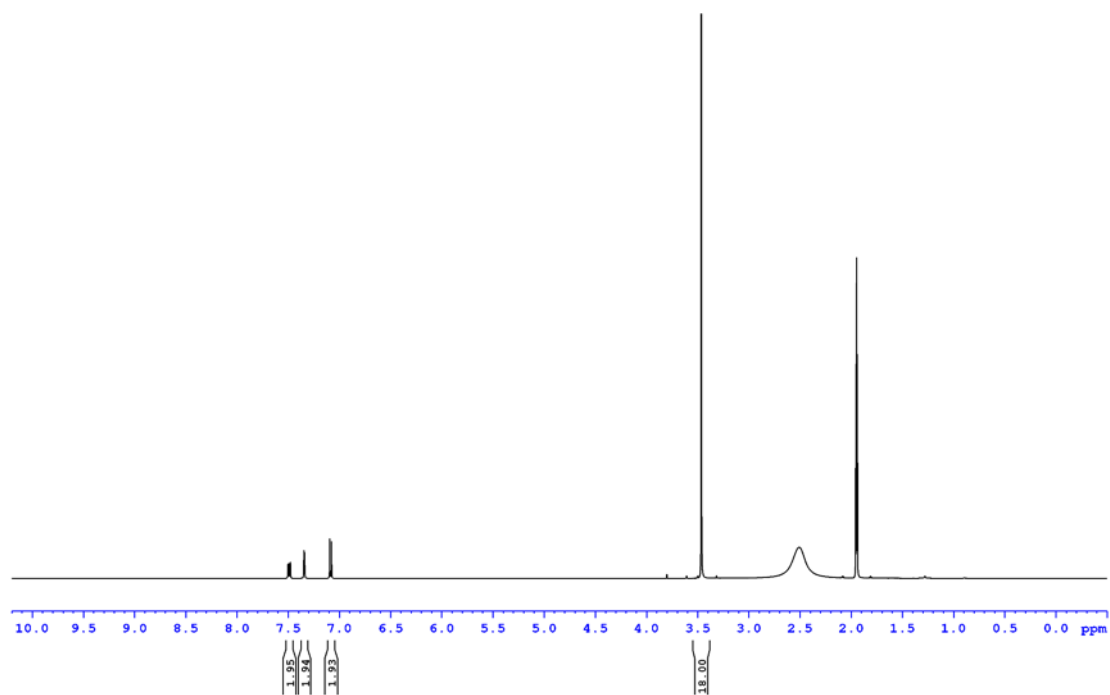
12

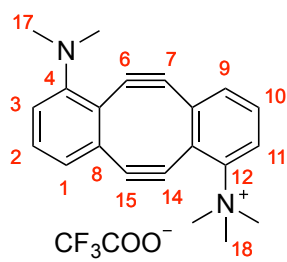


181

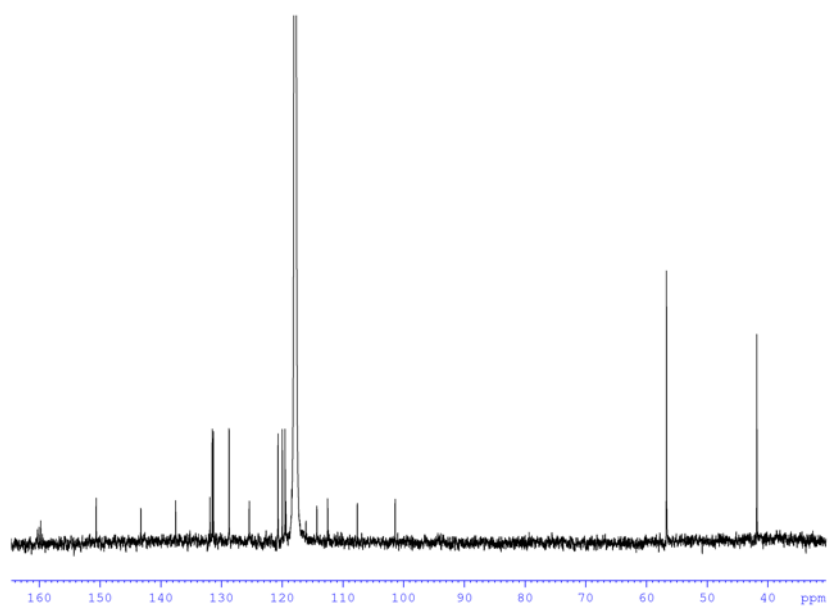
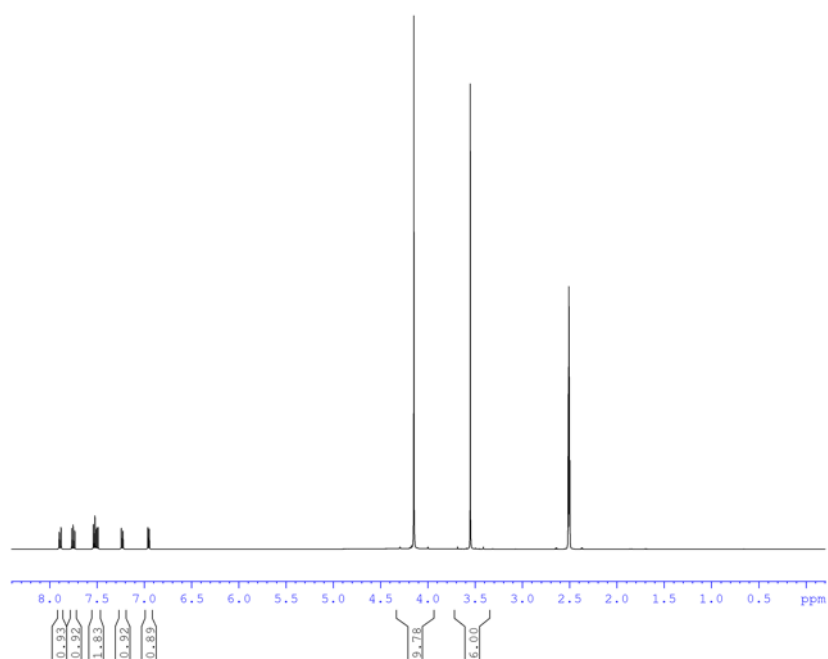


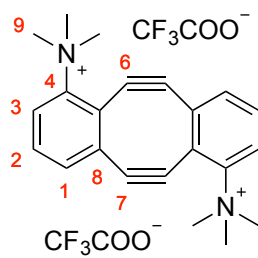
13



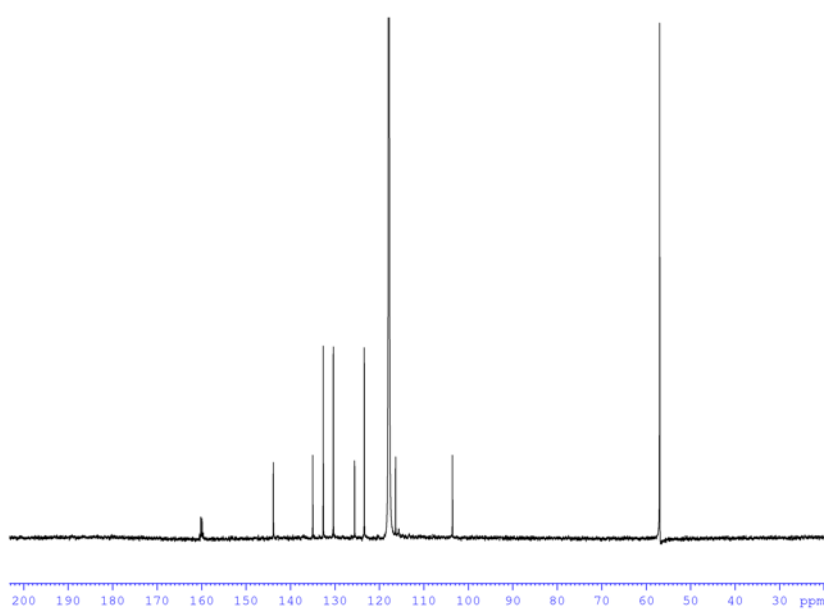
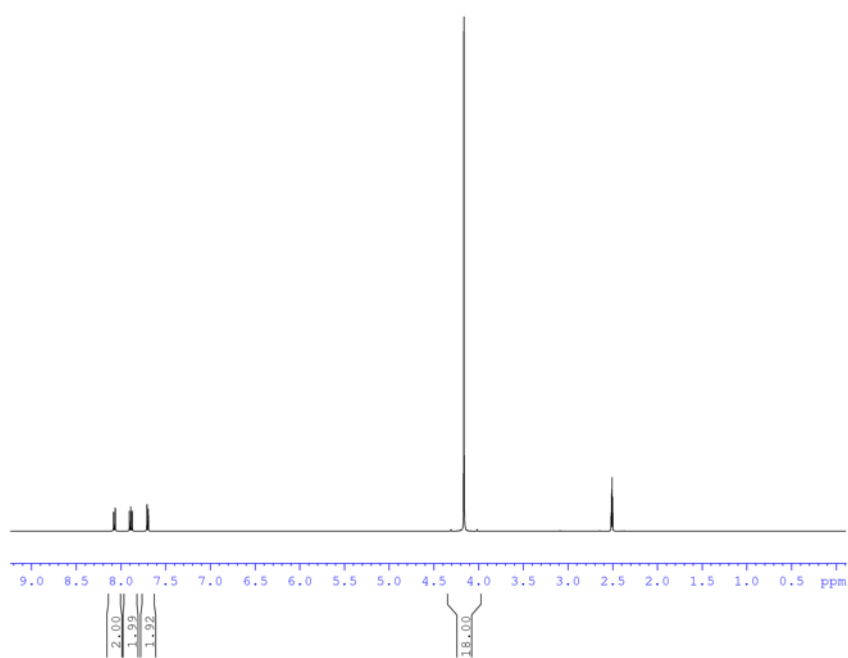


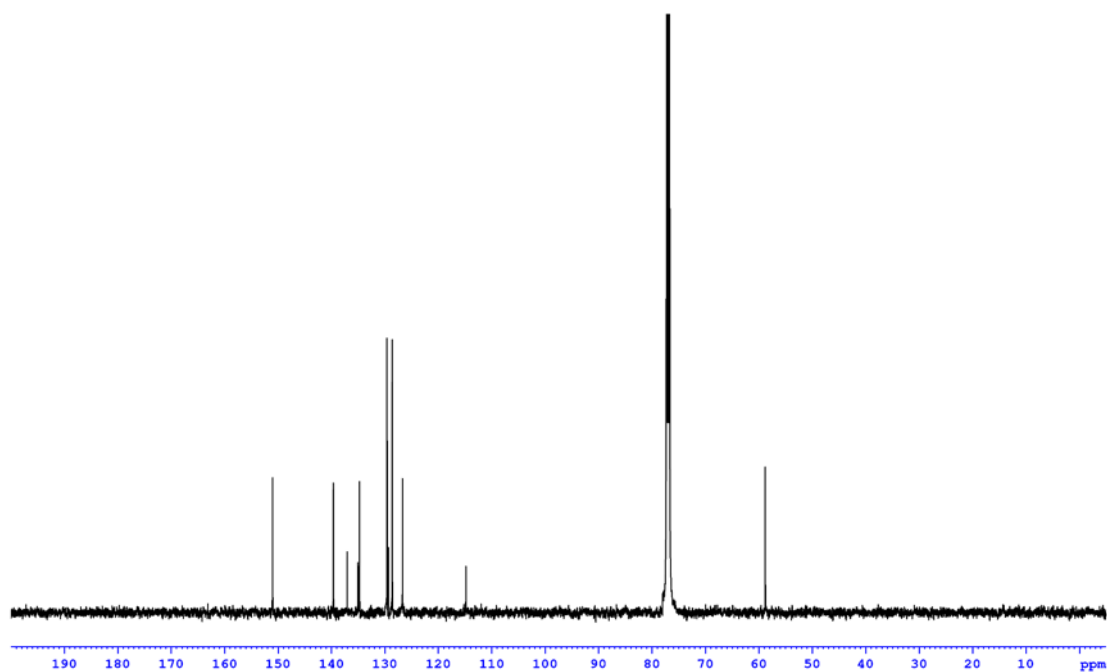
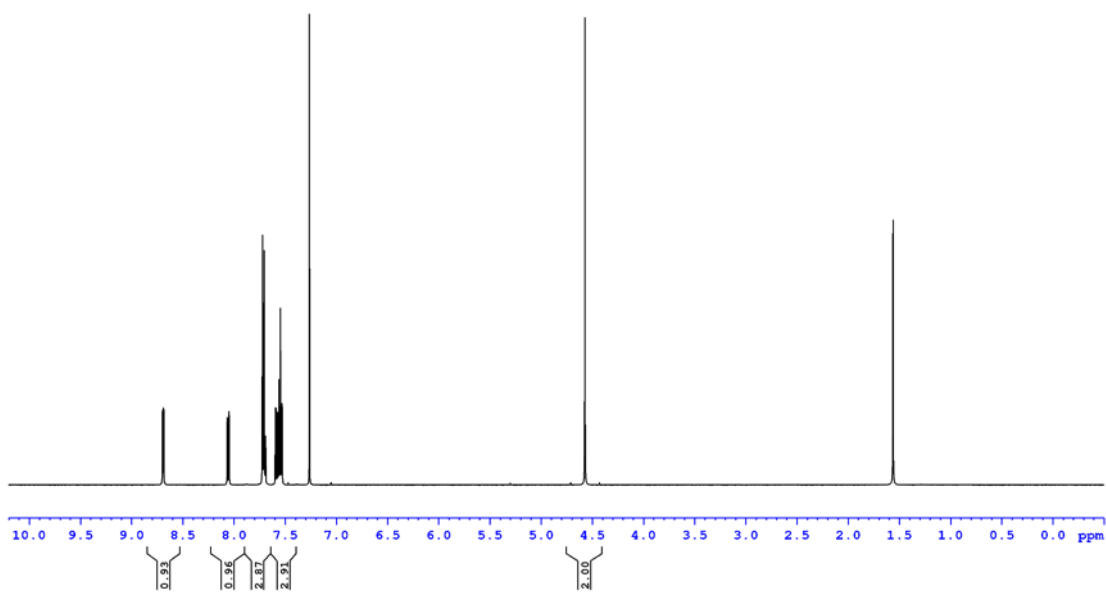
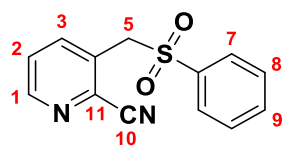
14

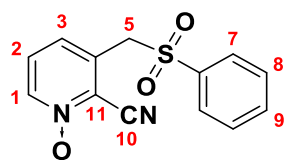




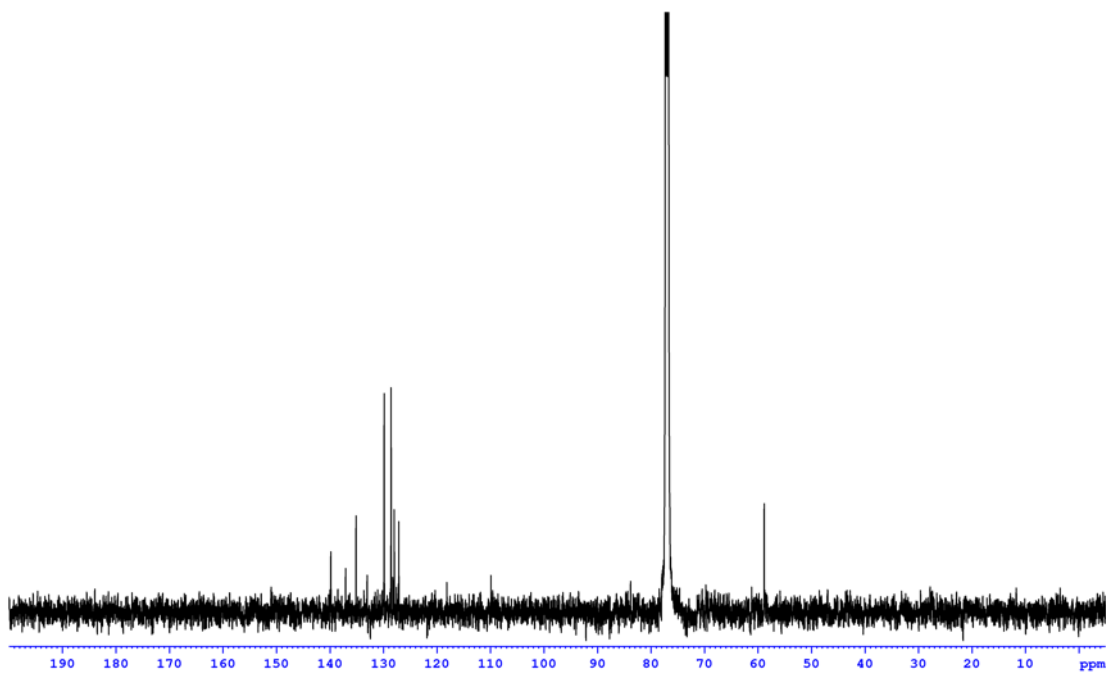
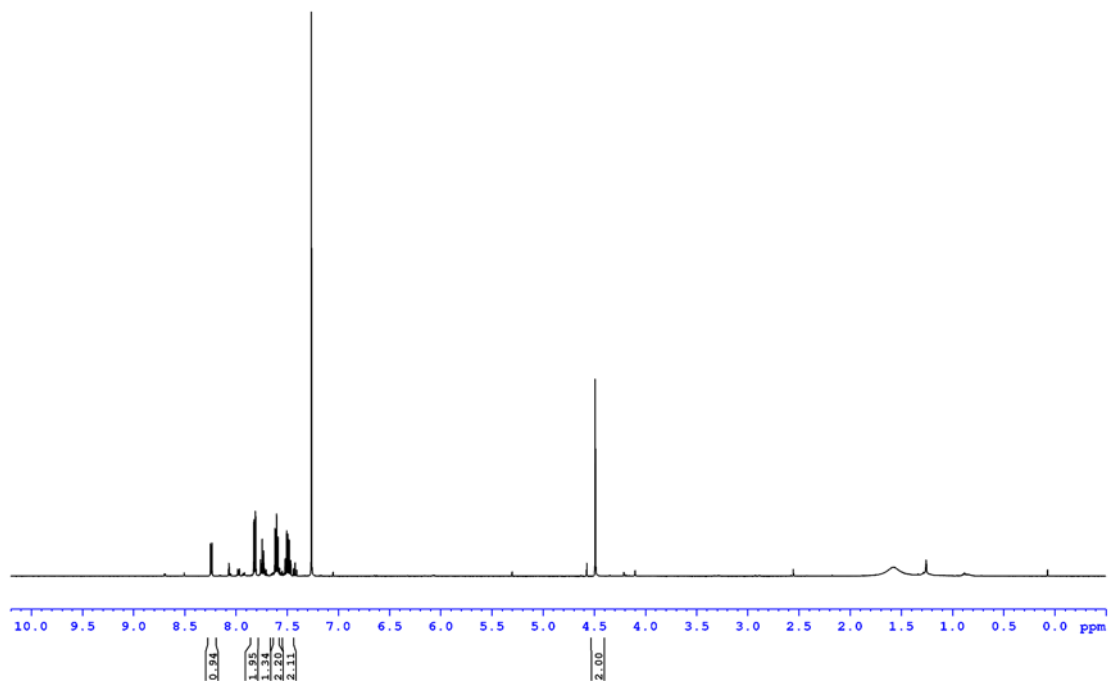
15

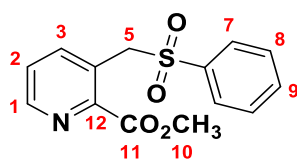




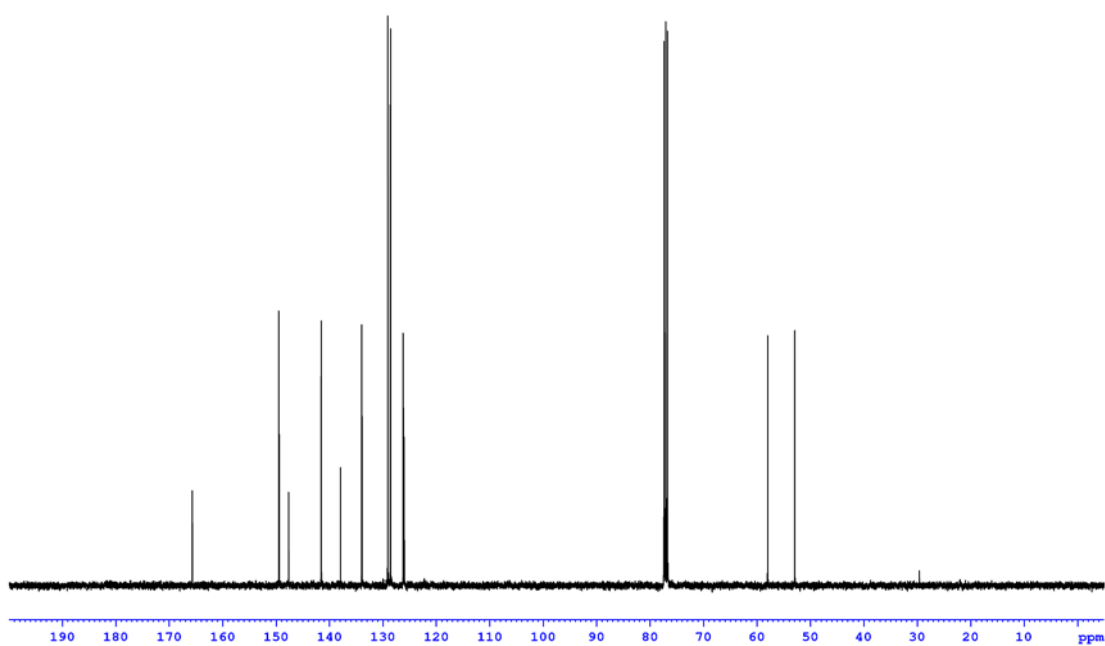
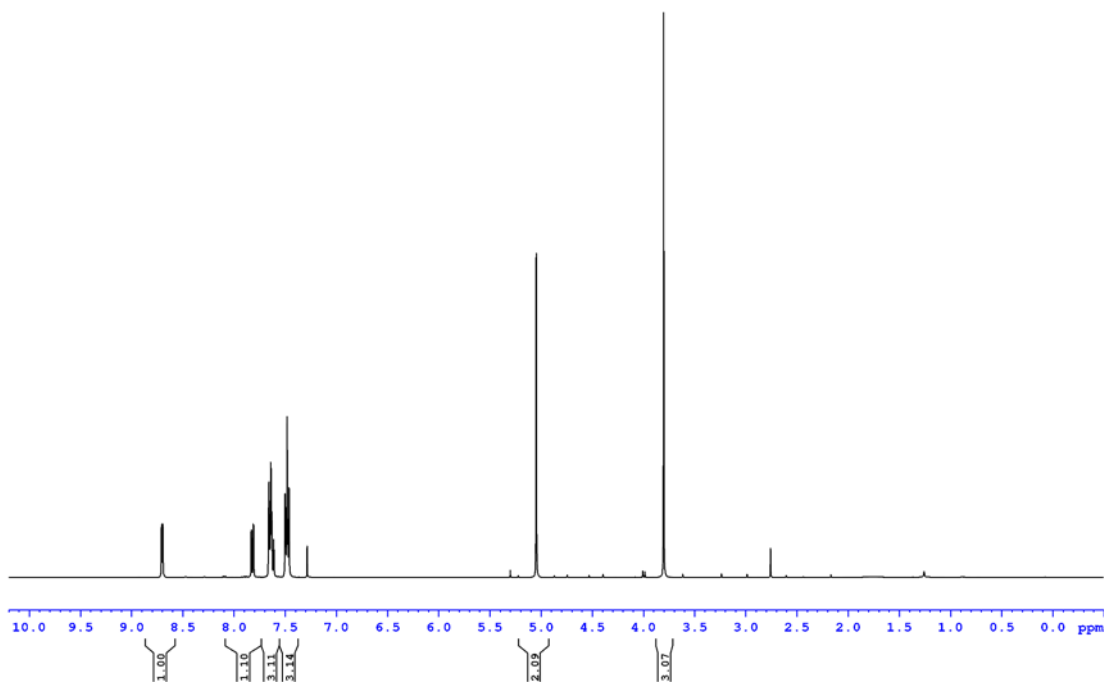


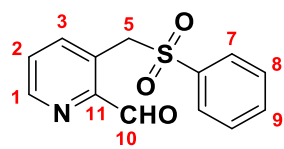
69



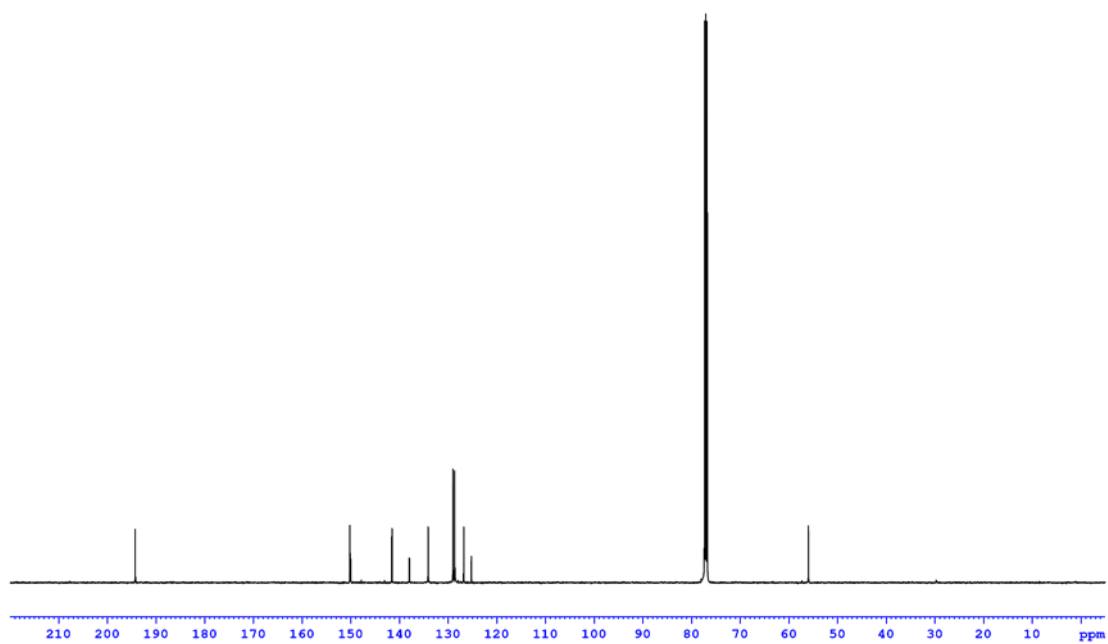
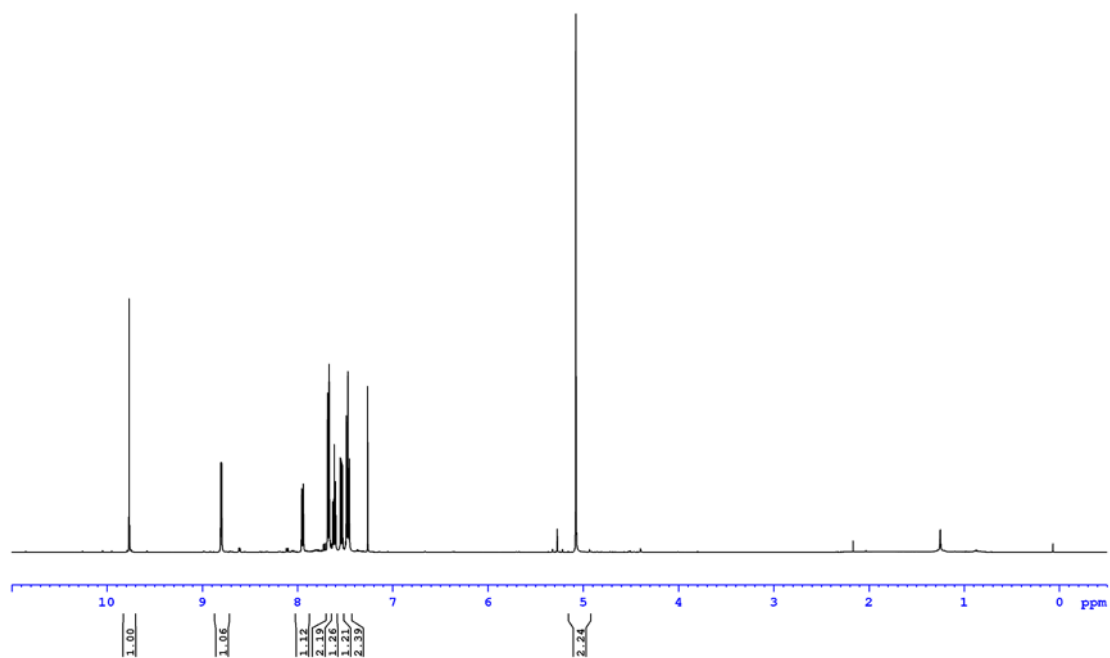


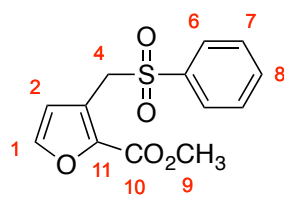
73



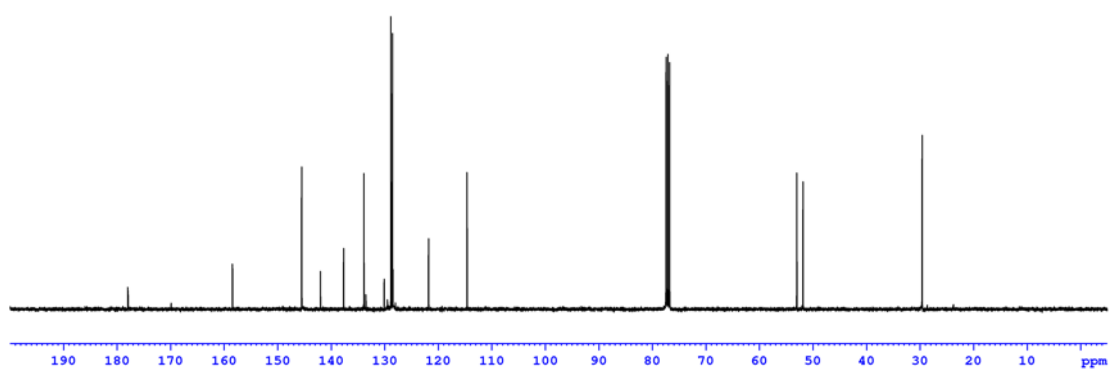
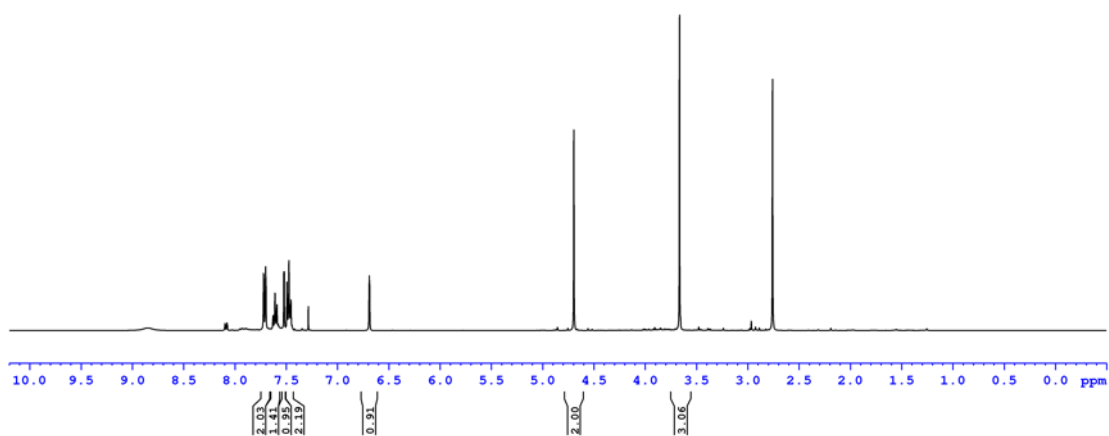


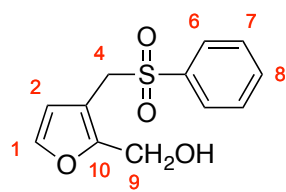
67



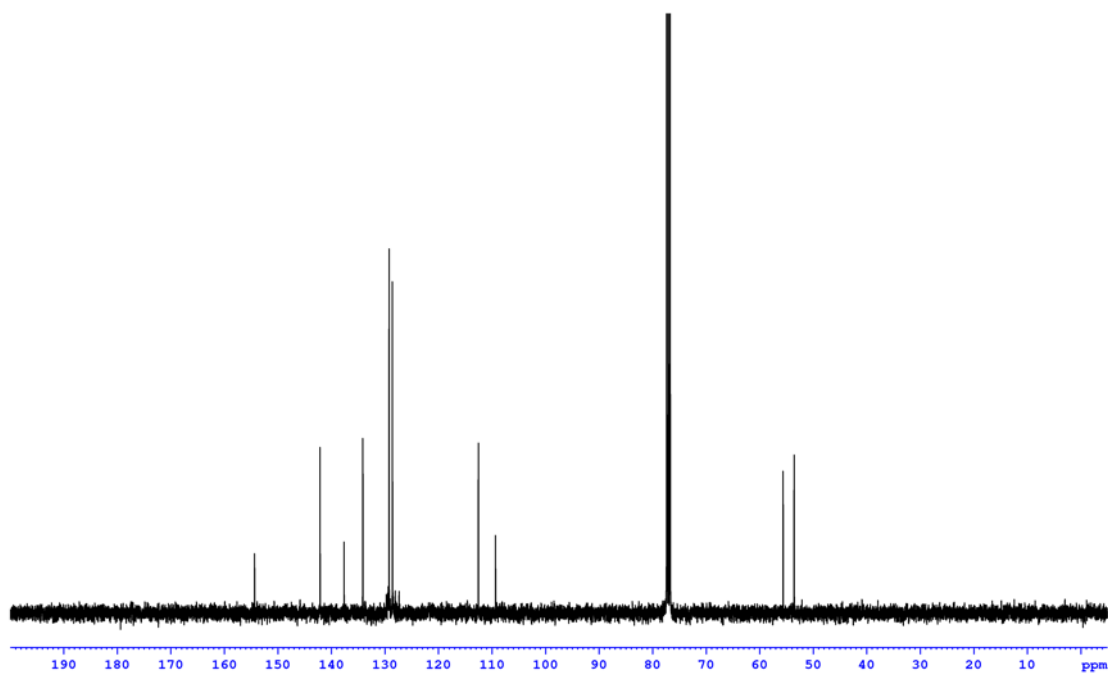
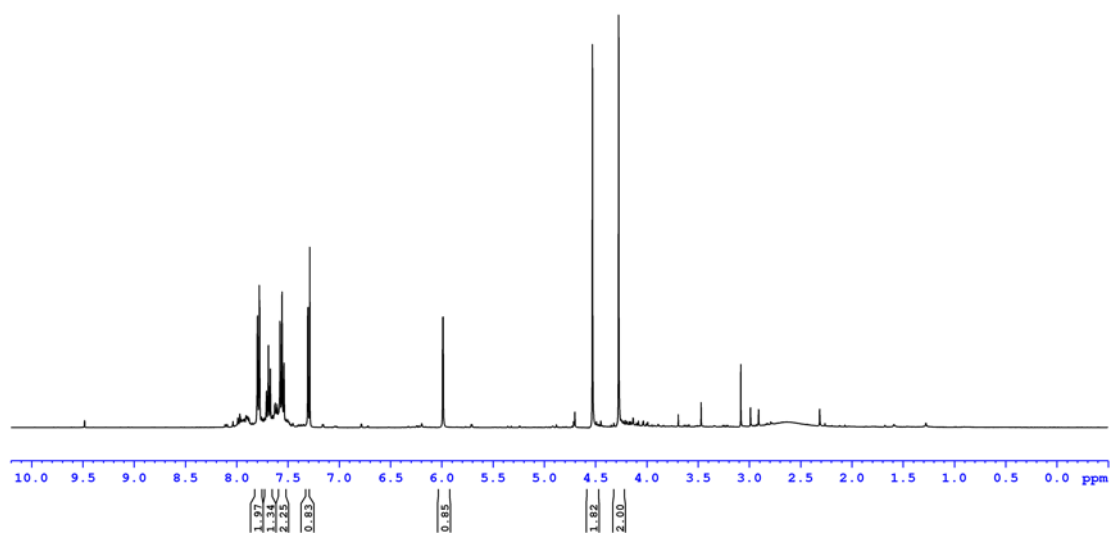


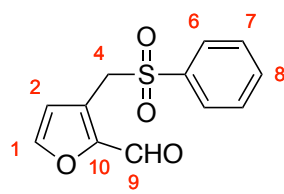
77



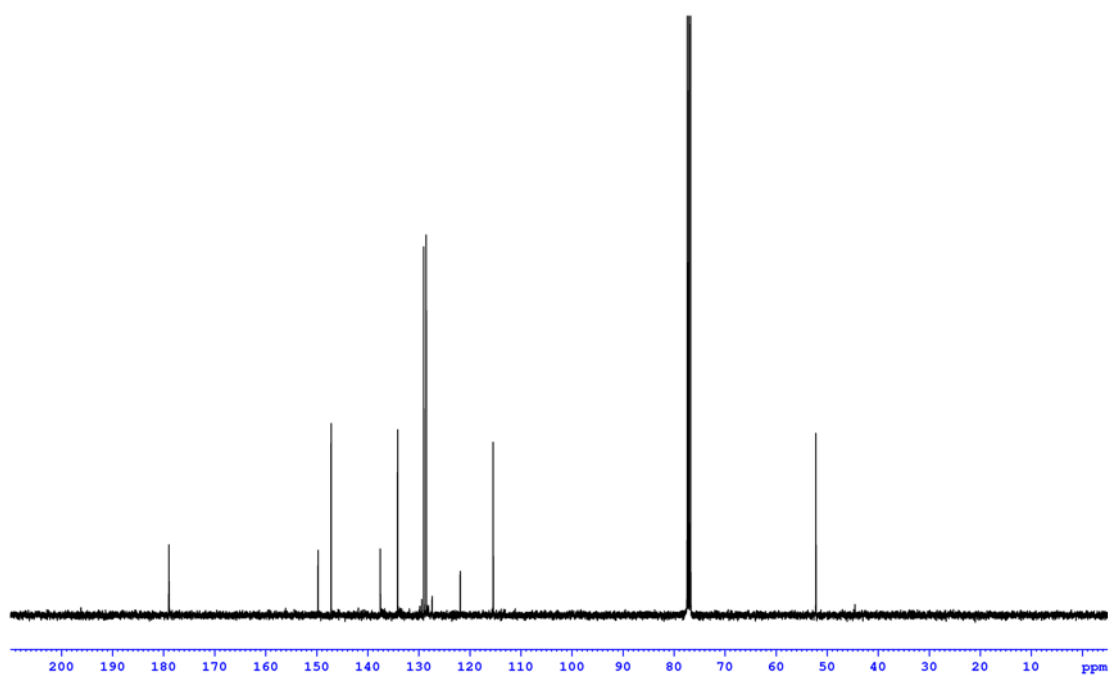
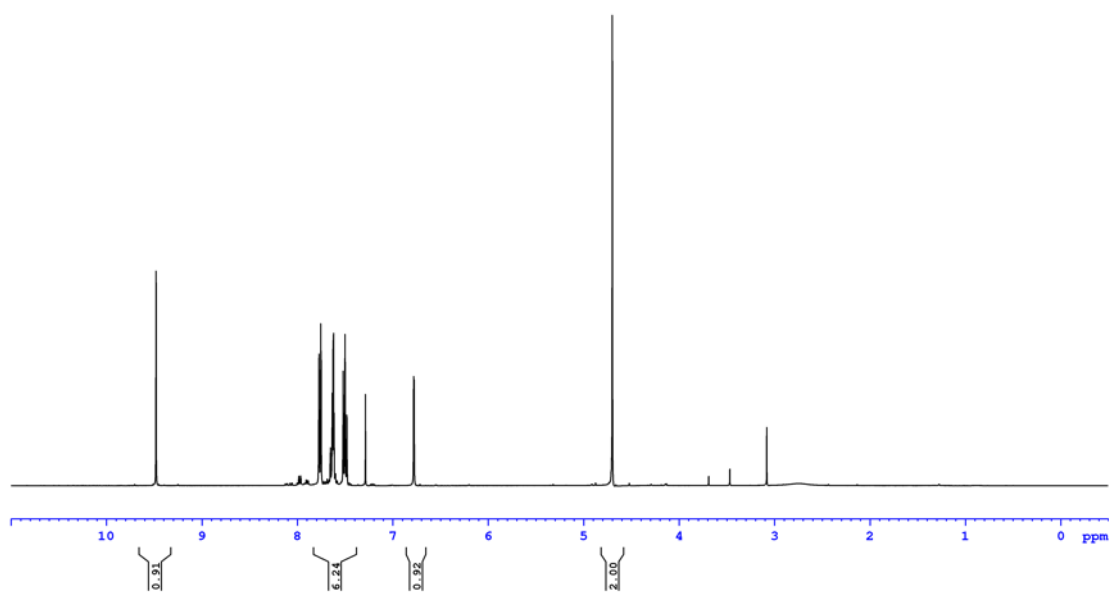


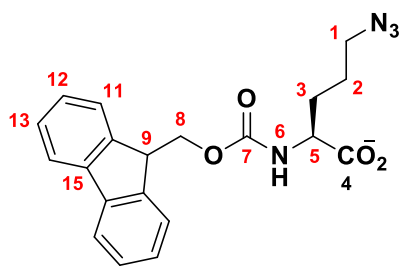
78



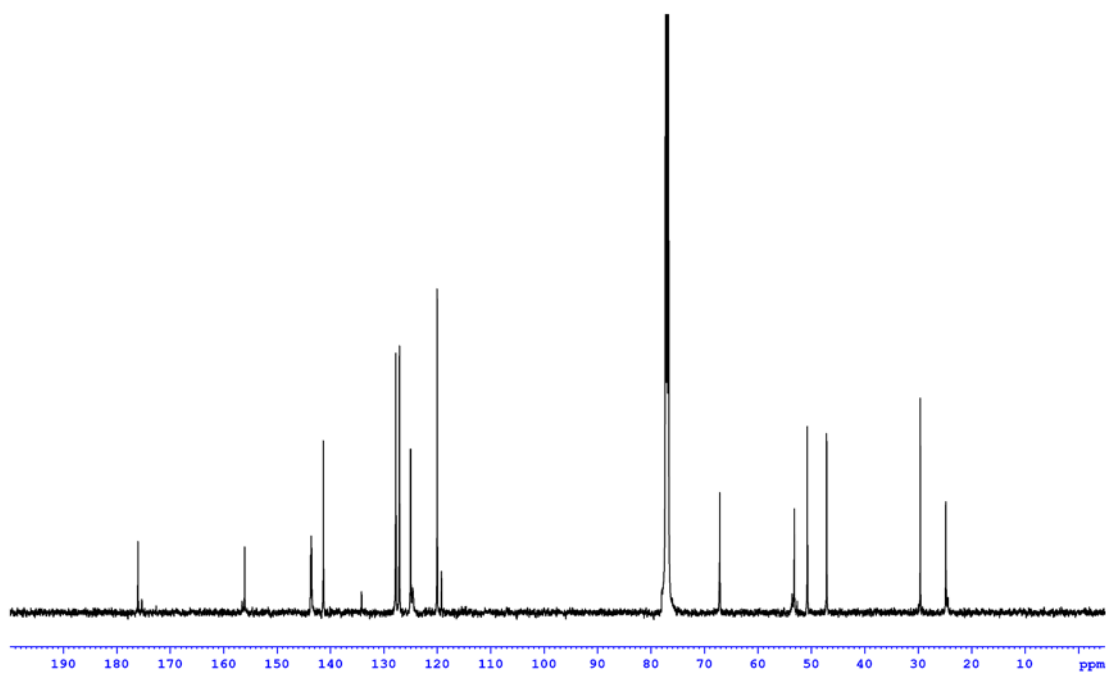
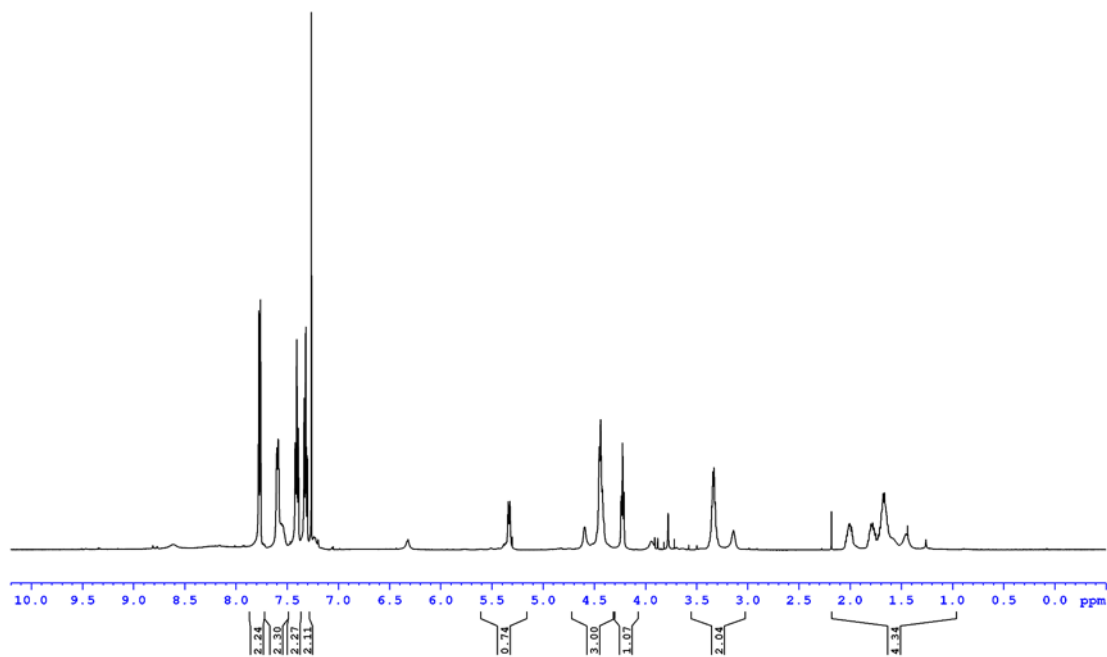


79





98



7.2.1 Peptide synthesis procedure

Peptide synthesis was carried out on solid-phase using an Fmoc-protecting group strategy on a CEM Liberty Automated Microwave Peptide Synthesiser. Merck Rink Amide MBHA resin LL (0.29-0.39 mmol/g) was used. Peptide couplings were conducted with Fmoc-protected amino acids (5 equiv) in DMF, HATU or HBTU (5 equiv) in DMF as the coupling reagent, and *N,N*-diisopropylethylamine (10 equiv) in NMP as the base. Double coupling was used for arginine for 15 min each without microwave irradiation. Single coupling was used for all other amino acids, with 25 W power at 75 °C over 15 min. Fmoc deprotection was carried out using 20% piperidine in DMF, with 45 W power at 75 °C over 3 min.

N-terminal capping was carried out manually by treating the resin-bound peptide with acetic anhydride (10 equiv) and *N,N*-diisopropylethylamine (10 equiv) in dichloromethane for 45 min. Cleavage was carried out with a cocktail of 95% trifluoroacetic acid, 2.5% water and 2.5% triisopropylsilane for 2 h. The cleavage solution was then evaporated under a stream of nitrogen and triturated with diethyl ether prior to purification by preparative HPLC.

Peptide yields were estimated based on absorbance in the HPLC chromatograph at 220 nm. Concentration of peptides in stock solutions were determined by amino acid analysis at the Peptide Nucleic Acid Chemistry Facility at the Department of Biochemistry, University of Cambridge.

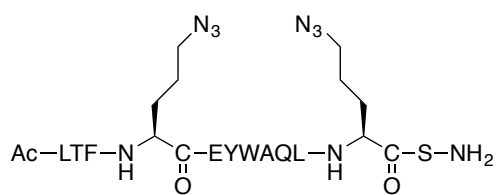
7.2.2 General strain-promoted double-click peptide stapling procedure

A solution of diazido PDI-E peptide (1 eq) and dialkyne (1.1 eq) in 1:1 *t*-BuOH/H₂O (1 mL/mg peptide) was stirred at rt for 16 h (1:1 MeCN/H₂O employed for trimethylammonium substituted diynes). Reaction mixture was lyophilised and purified by HPLC to give the stapled peptide.

7.2.3 Peptide LCMS and HPLC data

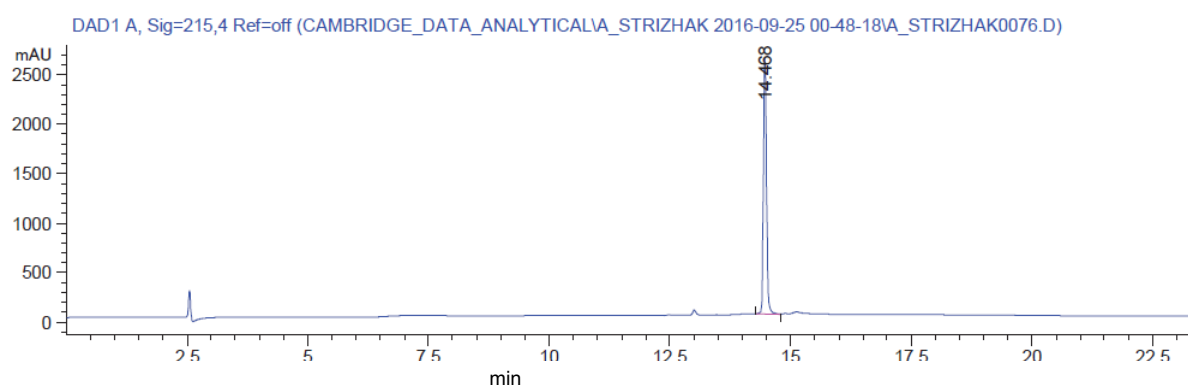
Data on PDI-E was previously reported.⁶¹

Peptide	Mass	<i>m/z</i> found	<i>m/z</i> calcd
2	1577.8	790.3	790.4 [M+2H] ²⁺
87	1838.1	920.7	920.0 [M+2H] ²⁺
81	1898.1	950.2	950.1 [M+2H] ²⁺
88	1814.0	908.7	908.0 [M+2H] ²⁺
89	1814.0	908.7	908.0 [M+2H] ²⁺
90	1864.2	933.5	933.1 [M+2H] ²⁺
91	1879.2	940.6	940.6 [M+2H] ²⁺
92	1894.2	947.8	948.1 [M+2H] ²⁺

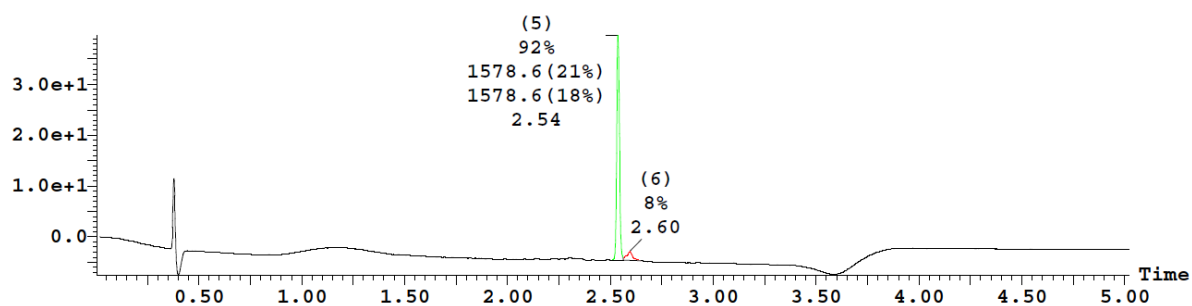


PDI-E 2

Analytical HPLC Spectra (5-95% MeCN over 15 mins)

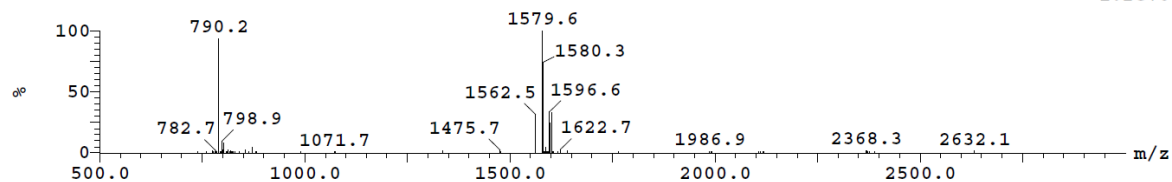


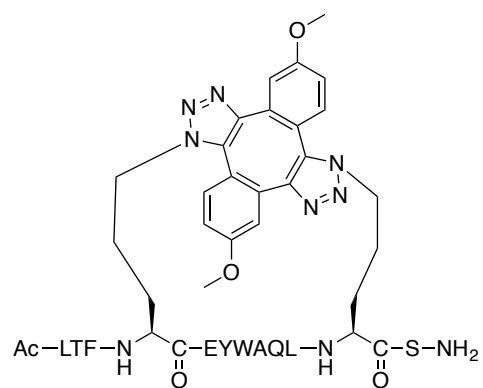
LCMS Spectra



Peak ID	Compound	Time	Mass Found	BPM
5	Found	2.54	1602,1580	1580

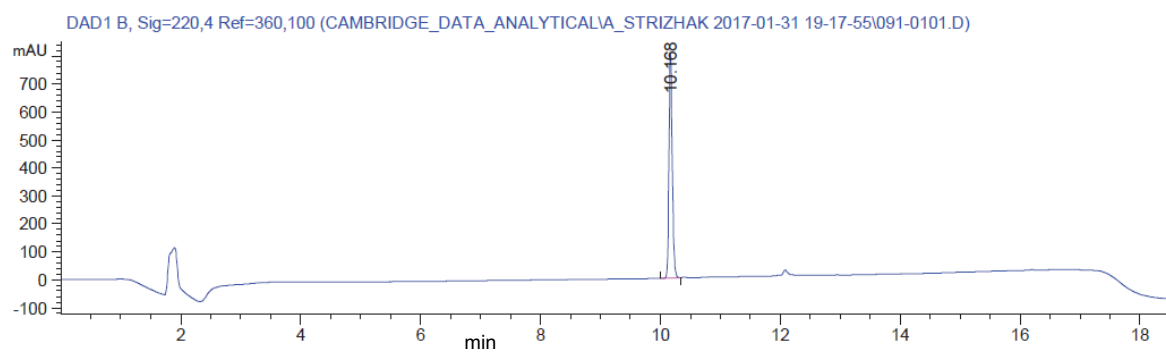
1:MS ES+
1.2e+007





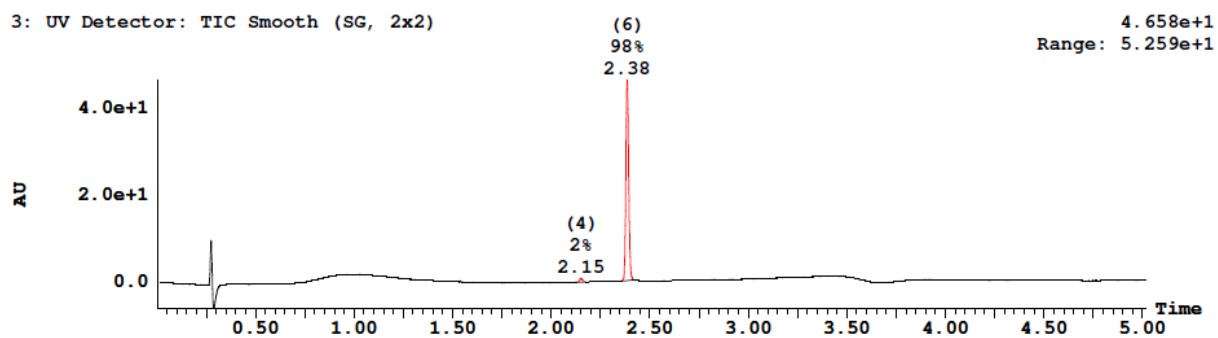
87

Analytical HPLC Spectra (5-95% MeCN over 15 mins)



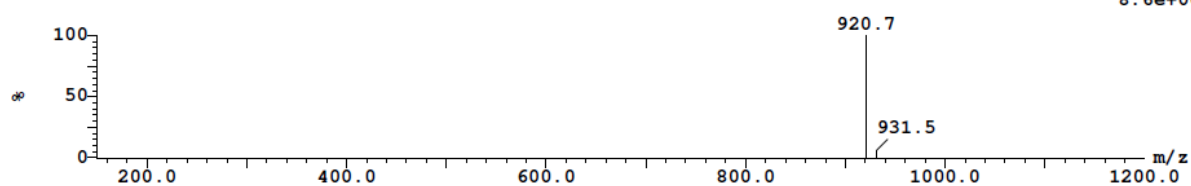
LCMS Spectra

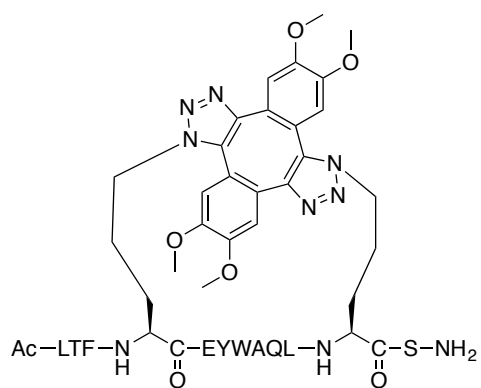
3: UV Detector: TIC Smooth (SG, 2x2)



Peak ID	Compound	Time	Mass Found	BPM
6		2.38	921	

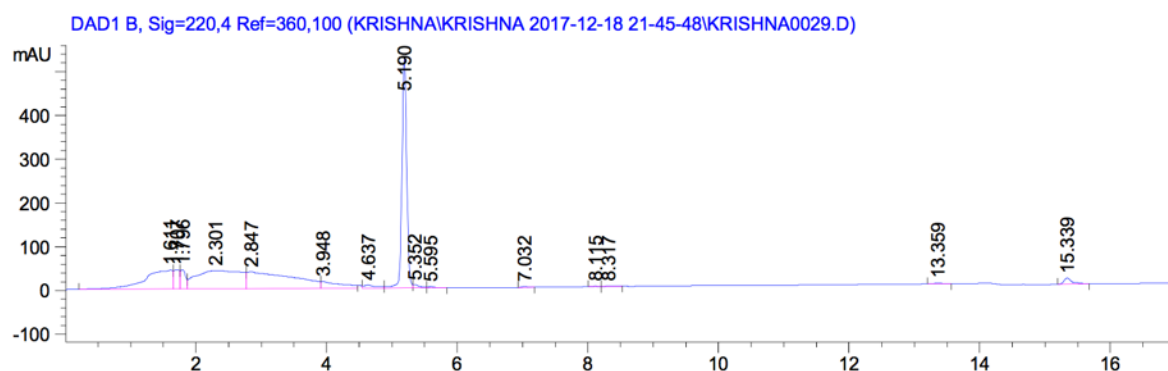
1:MS ES+
8.6e+007





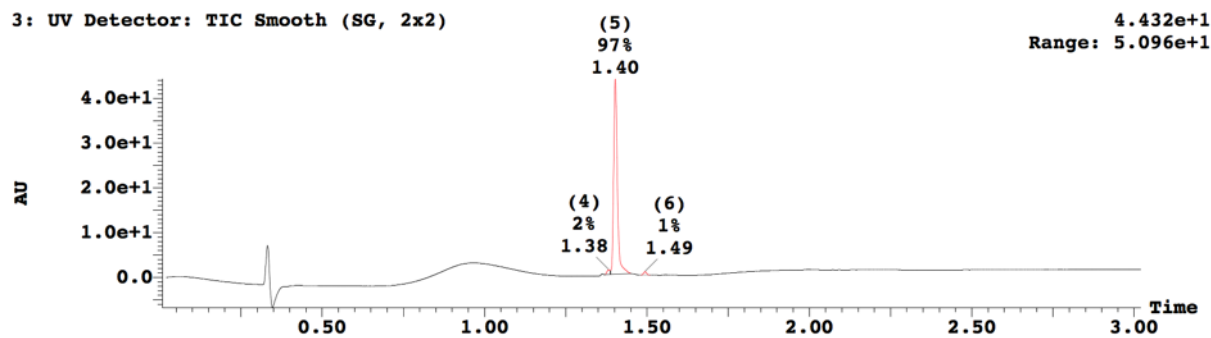
81

Analytical HPLC Spectra (40-70% MeCN over 20 mins)



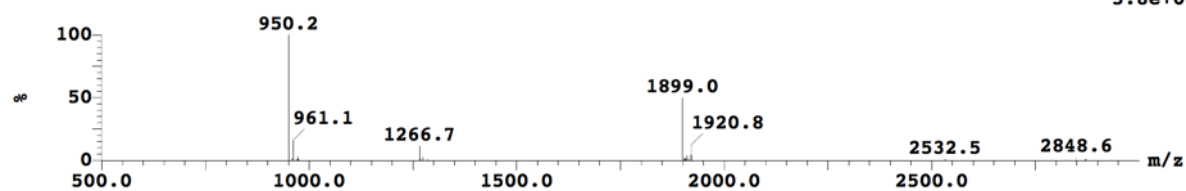
LCMS Spectra

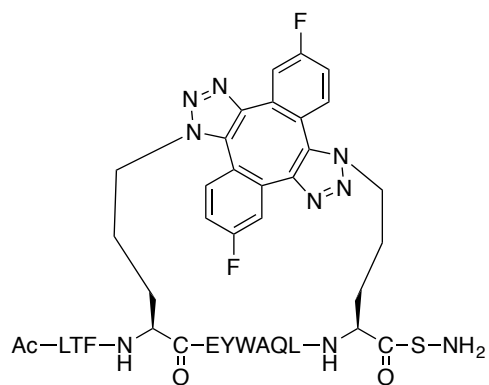
3: UV Detector: TIC Smooth (SG, 2x2)



Peak ID	Compound	Time	Mass Found	BPM
5		1.41		950

1:MS ES+
5.8e+007

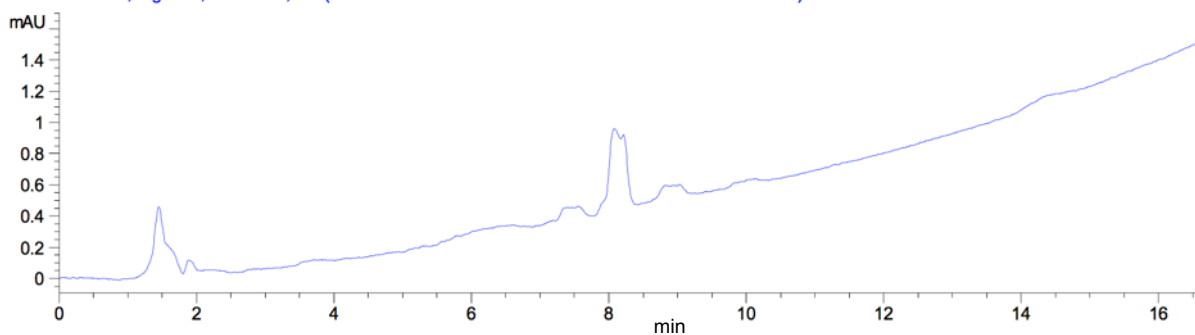




88

Analytical HPLC Spectra (40-70% MeCN over 20 mins)

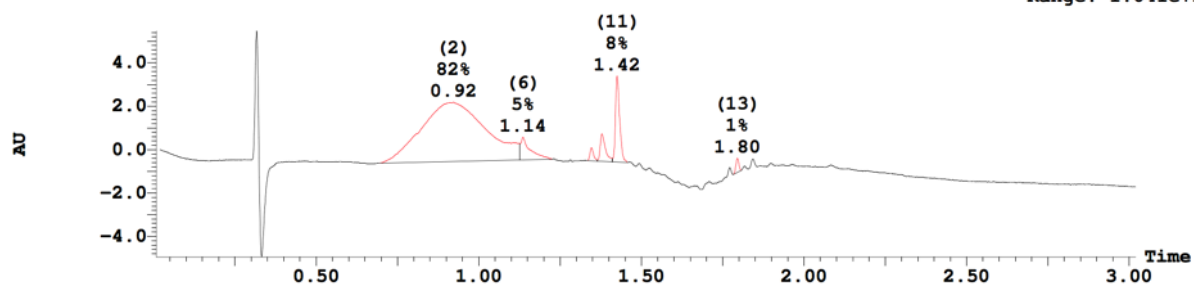
DAD1 A, Sig=254,4 Ref=360,100 (KRISHNA\KRISHNA 2017-08-30 18-15-59\KRISHNA0027.D)



LCMS Spectra

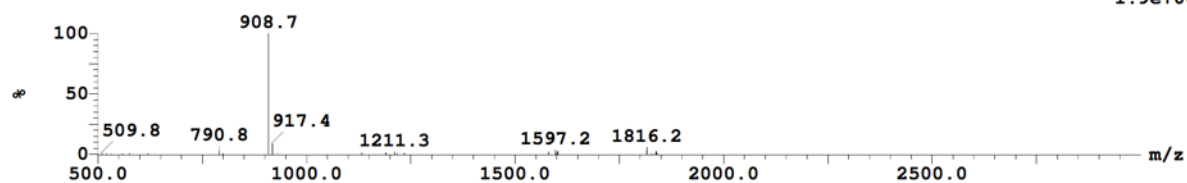
3: UV Detector: TIC Smooth (SG, 2x2)

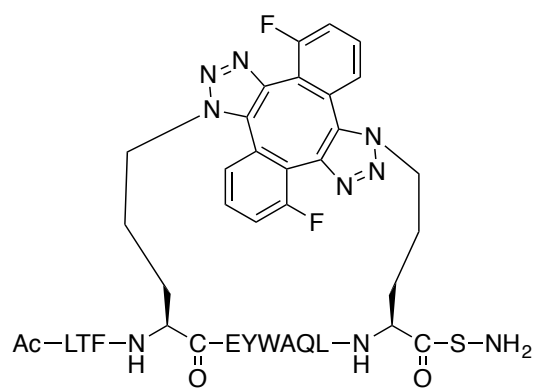
5.475
Range: 1.041e+1



Peak ID	Compound	Time	Mass Found	BPM
11		1.43		909

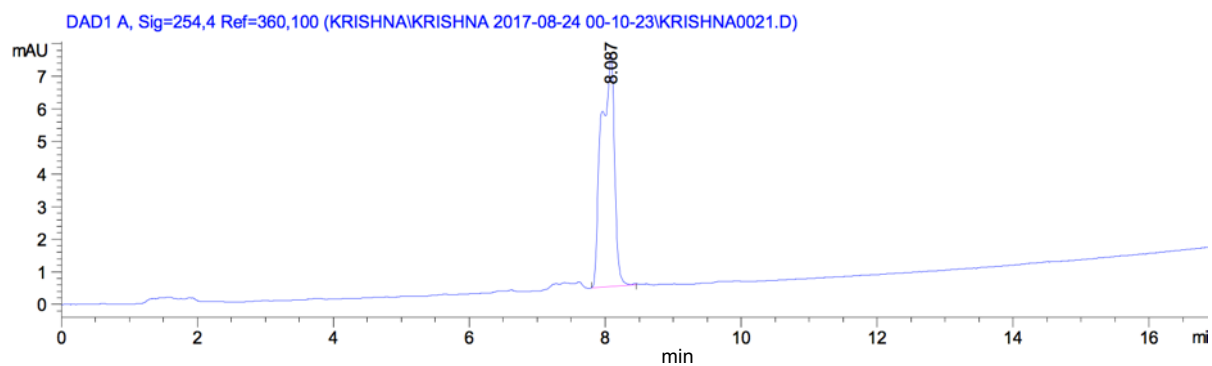
1:MS ES+
1.9e+007





89

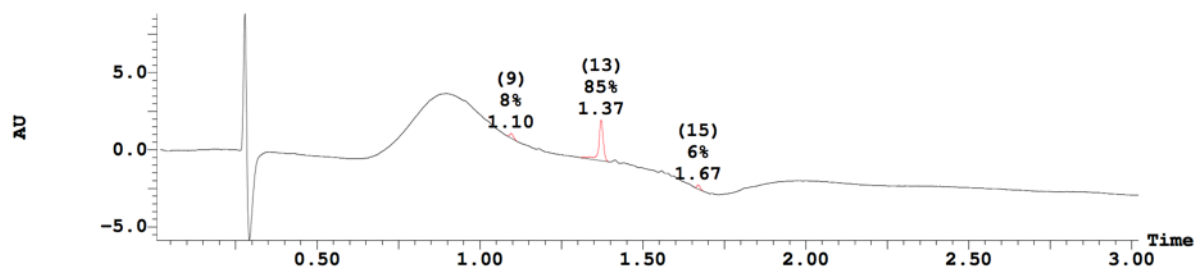
Analytical HPLC Spectra (40-70% MeCN over 20 mins)



LCMS Spectra

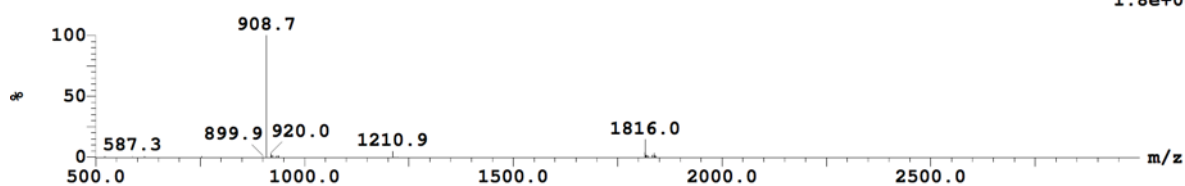
3: UV Detector: TIC Smooth (SG, 2x2)

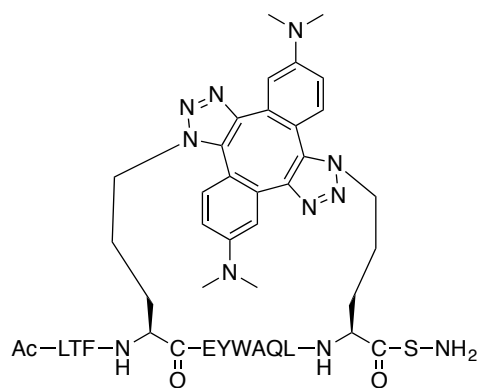
8.837
Range: 1.469e+1



Peak ID	Compound	Time	Mass Found	BPM
13		1.38	909	

1:MS ES+
1.8e+007

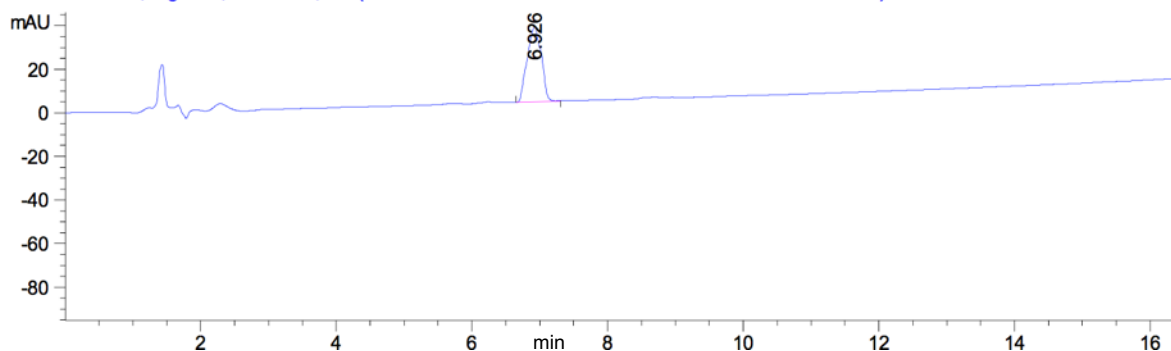




90

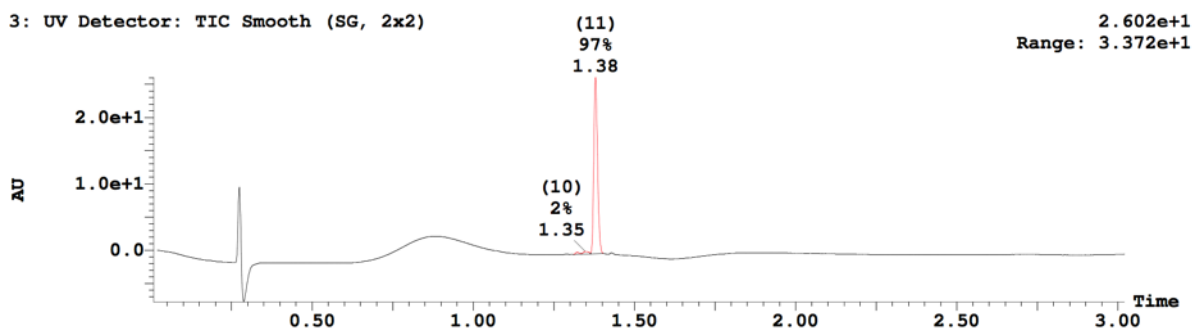
Analytical HPLC Spectra (40-70% MeCN over 20 mins)

DAD1 B, Sig=220,4 Ref=360,100 (KRISHNA\KRISHNA 2017-08-23 23-46-04\KRISHNA0020.D)



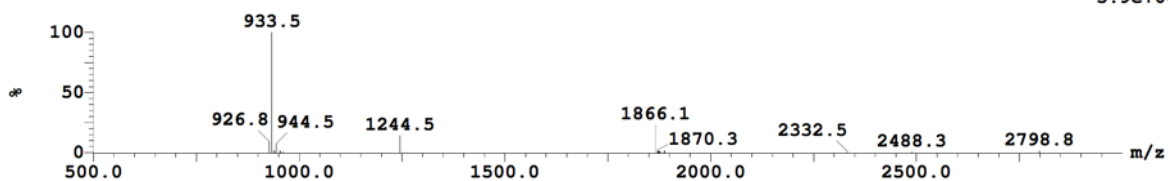
LCMS Spectra

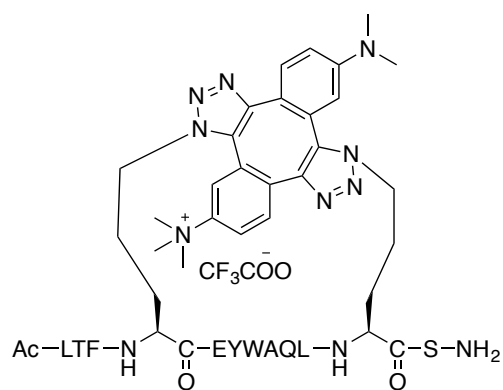
3: UV Detector: TIC Smooth (SG, 2x2)



Peak ID	Compound	Time	Mass Found	BPM
11		1.38		934

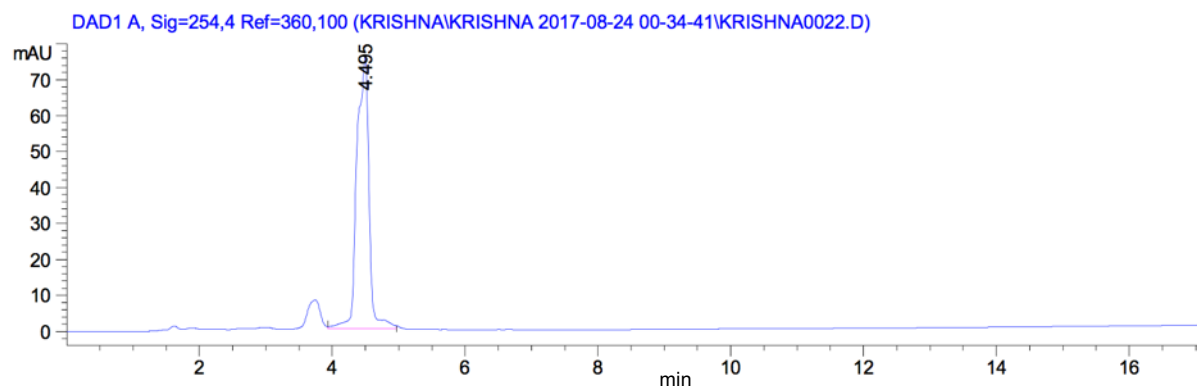
1:MS ES+
5.9e+007



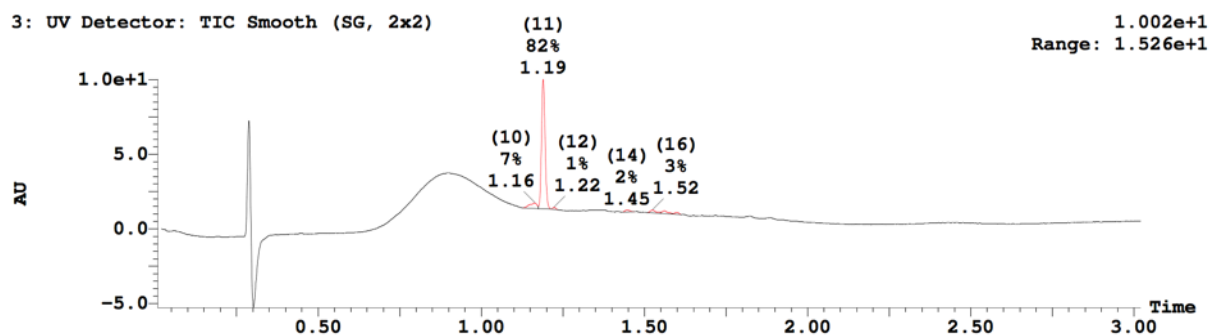


91

Analytical HPLC Spectra (40-70% MeCN over 20 mins)



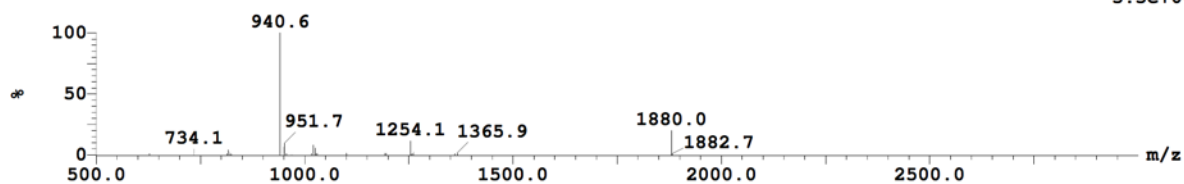
LCMS Spectra

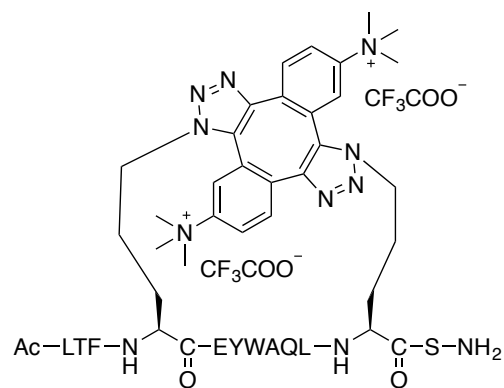


Peak ID Compound Time Mass Found BPM

11 1.19 941

1:MS ES+
3.3e+007

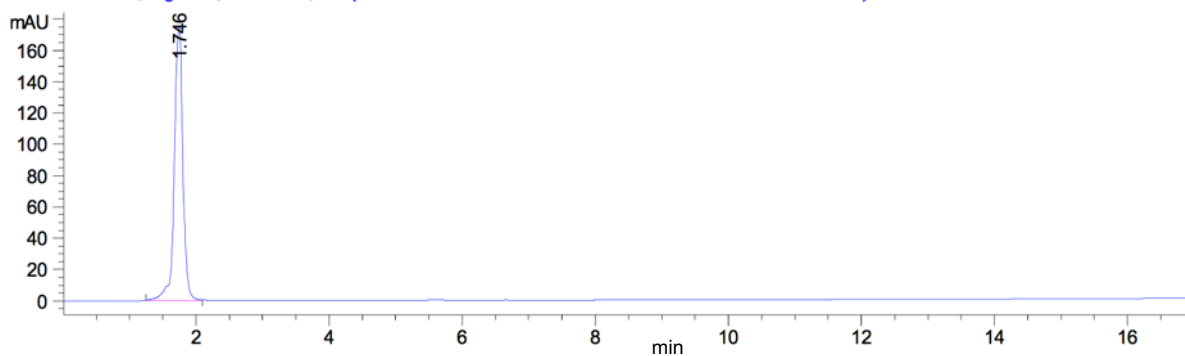




92

Analytical HPLC Spectra (40-70% MeCN over 20 mins)

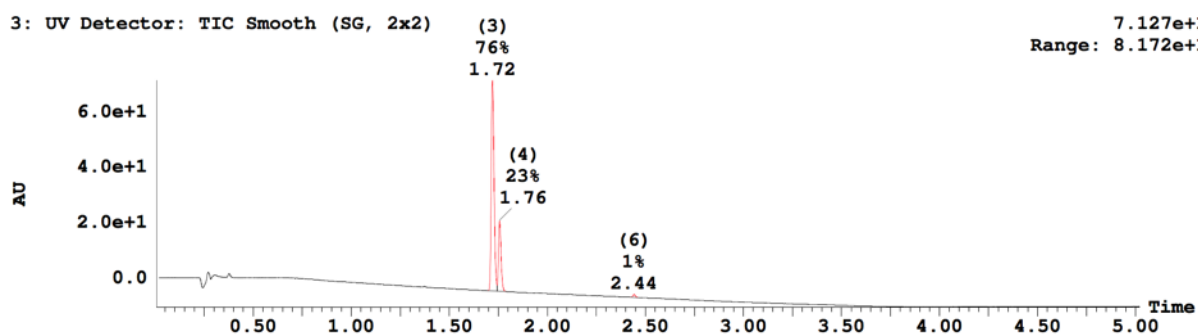
DAD1 A, Sig=254,4 Ref=360,100 (KRISHNA\KRISHNA 2017-08-24 00-58-59\KRISHNA0023.D)



LCMS Spectra

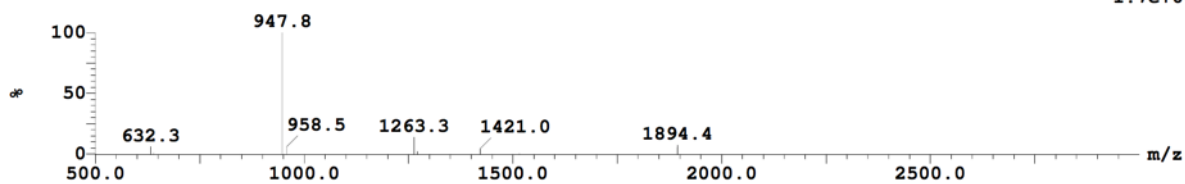
3: UV Detector: TIC Smooth (SG, 2x2)

7.127e+1
Range: 8.172e+1



Peak ID	Compound	Time	Mass Found	BPM
3		1.74		948

1:MS ES+
1.7e+008



7.2.4 X-ray crystallography

7.2.4.1 X-ray crystallography of *meta*-trimethylammonium functionalised peptide **91** in complex with MDM2

7.2.4.1.1 Expression and purification of MDM2₁₇₋₁₀₈-E69AK70A

The protein was expressed and purified following the methods described previously.⁶¹ The plasmid pGEX6P1- MDM2₁₇₋₁₀₈-E69AK70A, kindly provided by Dr J. Reeks (Newcastle University, UK), was transformed into BL21 (DE3) cells for expression. The cells were cultured in two litres of Hyper-Broth medium (Molecular Dimension) with 100 µg/ml ampicillin at 37 °C until the OD₆₀₀ reached 0.4. The cell culture was then incubated at 18 °C for one hour before induction with 0.2 mM IPTG. Protein was expressed at 18 °C for 16 hours before the cells were centrifuged at 4000 g for 10 minutes at 4 °C. The cell pellet was resuspended in 50 mL lysis buffer (20 mM Tris pH 8, 200 mM NaCl, 5 mM DTT, 10% sucrose, cOmplete mini protease inhibitors cocktail (Roche Diagnostics)) and then lysed by EmuSiFlex. The soluble fraction of the lysate was collected after centrifugation at 15000 g for 30 minutes at 4°C and then filtered through Minisart 0.45 µm syringe filter (Sartorius Stedium).

The GST-tagged MDM2₁₇₋₁₀₈-E69AK70A was purified by affinity chromatography using PureCube Glutathione Agarose beads (Cube Biotech). 2 mL beads were equilibrated with 10 mL of the lysis buffer and then mixed with the lysate. After incubation at 18 °C for one hour, the beads were washed with 40 mL of the lysis buffer and then eluted by the lysis buffer with 10 mM reduced glutathione. The eluted fractions were analysed by SDS-PAGE and the ones containing GST-tagged MDM2₁₇₋₁₀₈-E69AK70A were combined and concentrated to 4 mL using Amicon Ultra-4 centrifugal filter with 3 kDa cut off at 18 °C. The GST tag was cleaved by incubation with PreScission 3C protease at the molar ratio of 30:1 at 4 °C overnight. 0.9 mg of the stapled peptide **91** was added to the cleaved GST-tagged MDM2₁₇₋₁₀₈-E69AK70A and incubated for one hour on ice. The mixture was then purified by size exclusion chromatography using Superdex 75 10/300 column (GE Healthcare) in the buffer of 20 mM HEPES pH 7.4, 200 mM NaCl, 5 mM DTT. The peak fractions were analysed by SDS-PAGE and the ones containing MDM2₁₇₋₁₀₈-E69AK70A were combined and concentrated to 12 mg/ml using Amico Ultra-4 centrifugal filter with 3 kDa cut off.

7.2.4.1.2 Crystallisation and structure determination of MDM2-91 peptide complex

Crystallisation of the MDM2₁₇₋₁₀₈-E69AK70A-51 stapled peptide complex was performed in 96-well MRC 2-drop crystallisation plates using JCSG+ Crystal Screen (Molecular Dimensions). Mosquito Crystal (TTPLabtech Ltd) system was used to set up two crystallisation drops for each condition. One drop contains 200 nL of protein plus 200 nL of reservoir and the other drop contains 200 nL of protein plus 100 nL of reservoir. Crystals appeared after eight days in the conditions of 1.1 M sodium malonate dibasic, 0.1 M HEPES pH 7.0, 0.5% v/v Jeffamine ED-2003. Three crystals were harvested and flash-cooled in liquid nitrogen. Diffraction data was collected at Diamond synchrotron I04 beamline and processed by autoPROC¹³³ to the resolution of 2.0 Å.

The structure of MDM2₁₇₋₁₀₈-E69AK70A-**91** stapled peptide was solved by molecular replacement in Phaser.¹³⁴ The coordinates of MDM2 in the structure of MDM2₁₇₋₁₀₈-E69AK70A-E1 stapled peptide (PDB code 5AFG) were used as a search model. The structure solution from *Phaser* was refined without the stapled peptide by several rounds of manual building using *Coot*¹³⁵ and refinement using REFMAC5¹³⁶. The refined data shows clear electron density to build the stapled peptide in both the 2Fo-Fc map and Fo-Fc map (Figure 7.2.4.1.2a and b). The stapled peptide was therefore manually built using Coot and refined using PHENIX¹³⁷ (Figure 7.2.4.1.2c). The geometrical restraint file for the stapled linker was generated using Grade Web Server (Global Phasing Ltd.). The statistics of data processing and refinement are shown in Table 7.2.4.1.2.

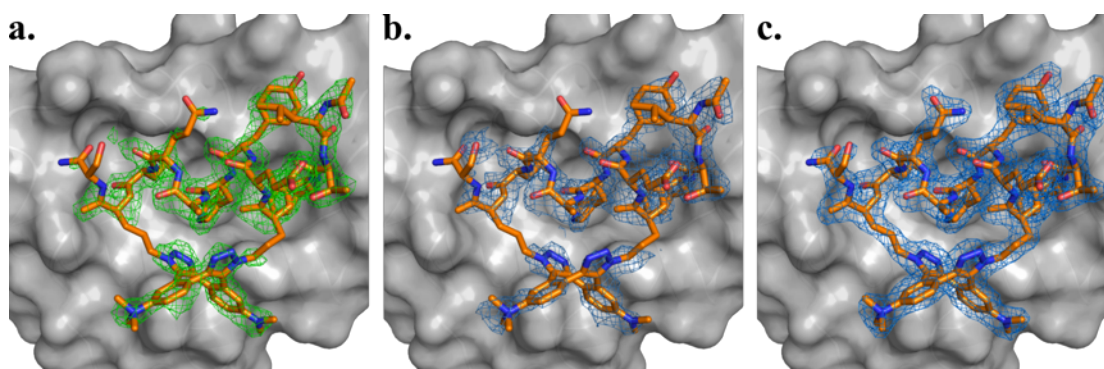


Figure 7.2.4.1.2. Electron density maps of the bound **91** peptide. The structure of MDM2 is shown as surface and coloured in grey. The structure of stapled peptide is shown in sticks. **a.** Difference density map (Fo-Fc) contoured at 2σ before modeling the peptide. **b.** Electron

density map (2Fo-Fc) contoured at 0.5σ before modeling the peptide. **c.** Final electron density map (2Fo-Fc) contoured at 1σ after peptide modeling and structure refinement.

Table 7.2.4.1.2. Crystallographic statistics of peptide-MDM2 complex (PDB code: 6H22)

Data Collection	
Wavelength (Å)	0.9795
Resolution range (Å)	48.06 - 2.006 (2.078 - 2.006)
Space group	P 2 ₁ 2 ₁ 2 ₁
Unit cell (Å)	a=64.416 b=72.186 c=45.124 $\alpha=\beta=\gamma=90^\circ$
Molecules per asymmetric unit	2
Total reflections	77879 (6731)
Unique reflections	14427 (1253)
Multiplicity	5.4 (5.4)
Completeness (%)	98.54 (86.83)
Mean I/sigma(I)	9.46 (2.20)
R-merge	0.1103 (0.7797)
CC _{1/2}	0.998 (0.898)
Refinement	
Resolution range (Å)	48.06 - 2.006 (2.078 - 2.006)
R-work	0.2107 (0.3239)
R-free	0.2384 (0.3977)
Number of non-hydrogen atoms	1965
Macromolecules	1700
Ligands	74
Water	191
Protein residues	213
Root-mean-square deviation	
Bonds	0.005
Angles	0.88
Average B-factor	30.1

Macromolecules	29.6
Ligands	28.6
Solvent	35
Ramachandran favored (%)	100
Ramachandran outliers (%)	0
Clashscore	1.99

7.2.4.1.3 Analysis of the MDM2-91 peptide structure

The analysis of the crystallographic data of MDM2-**91** peptide complex shows that one asymmetric unit contains two macromolecules that have the same structures apart from the small variation at the N-termini (r.m.s.d of 0.108) (Figure 7.2.4.1.3.1a and b). As the complex is eluted from size exclusion chromatography as monomers (data not shown), the possibility that the complex forms a dimer is emitted. The fact that two complexes present in one asymmetric unit is due to the structural heterogeneity.

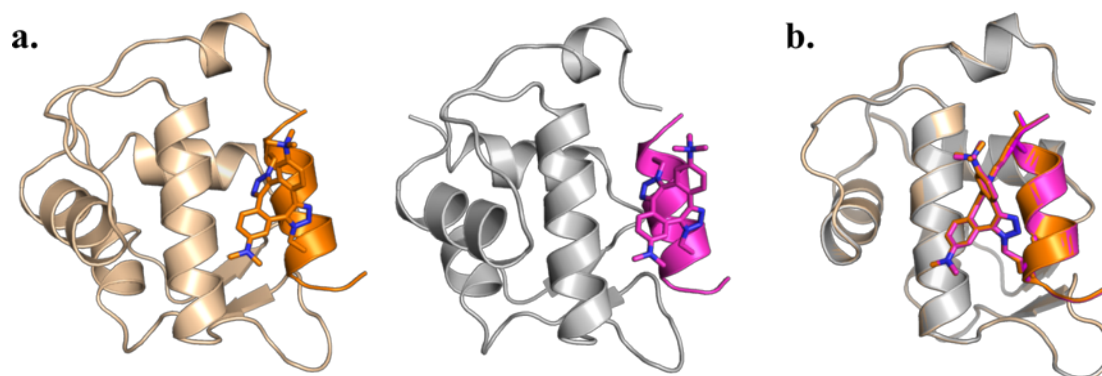


Figure 7.2.4.1.3.1. Crystal structure of MDM2-**91** peptide in one asymmetric unit. Structures of MDM2 are shown as cartoon and coloured in light orange and grey. Structures of peptides are shown as cartoon and coloured in orange and magenta with the staple shown as sticks. a. Asymmetric unit of the crystal structure of MDM2-**91** peptide complex. b. Superimposition of two MDM2-**91** peptide complex structures in one asymmetric unit. The root-mean-square deviation (r.m.s.d) is 0.108.

In comparison with the structure of MDM2-E1 peptide complex (PDB code 5AFG), both peptides form hydrophobic interactions with MDM2 through residue F3, W7, and L10 (Figure 7.2.4.1.3.2a). However, the staple compound of **91** peptide shifts away from the MDM2

protein surface (Figure 7.2.4.1.3.2b). The trimethylammonium group moves even further compared to the dimethylamine group, indicating that the hydrophobic interface on MDM2 seem to expel the staple compound due to its charged groups.

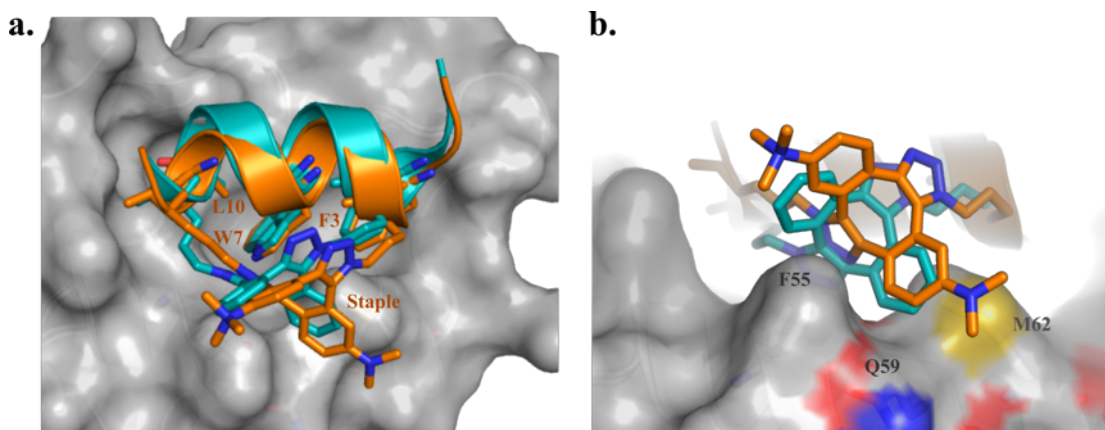
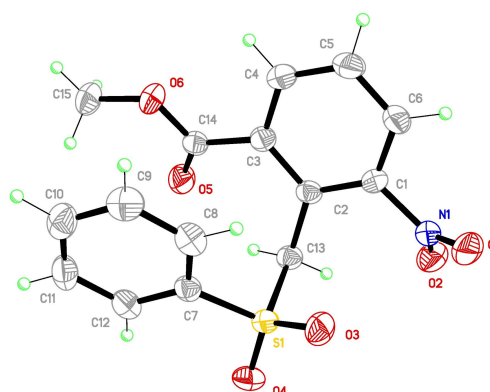
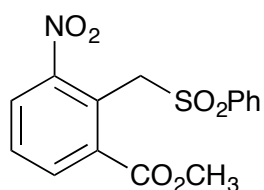


Figure 7.2.4.1.3.2. Comparison of structures of MDM2-**91** peptide complex (PDB code 6H22) and MDM2-E1 peptide complex (PDB code 5AFG). The structure of MDM2 is shown as surface and coloured in grey. The peptides are shown as cartoon and the staple shown as sticks. E1 peptide is coloured in cyan and **91** peptide is in orange. a. **91** peptide associates with MDM2 through hydrophobic interactions mediated by residue F3, W7, and L10, which is conserved in E1 peptide-MDM2 interactions. b. The staple of 51 peptide shifts away from the MDM2 surface formed by F55, Q59, and M62 compared to the staple of E1 peptide.

7.2.4.2 X-ray crystallographic data

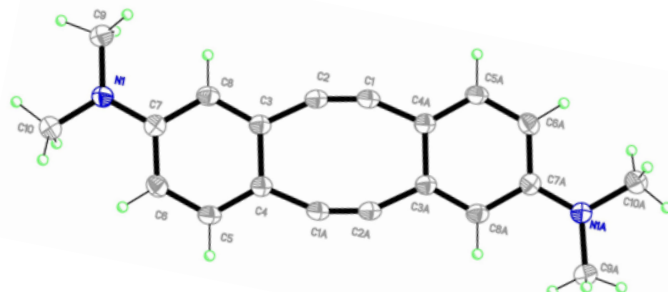
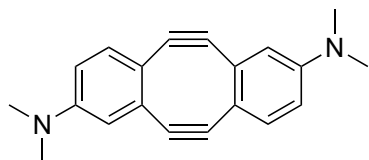
Methyl 3-nitro-2-((phenylsulfonyl)methyl)benzoate (49)



Key data and refinement for compound 49	
Empirical formula	C ₁₅ H ₁₃ NO ₆ S
Formula weight	335.32
Temperature	180 K
Wavelength	0.71073 Å
Crystal system	Monoclinic
Space group	P 2 ₁ /n
Unit cell dimensions	a = 14.9043 Å α = 90.00°
	b = 7.2865 Å β = 111.95°
	c = 14.8024 Å γ = 90.00°
Volume	1491.0 Å ³
Z	4
Density (calculated)	1.494 Mg/m ³
Absorption coefficient	0.249 mm ⁻¹
F (000)	696
Crystal size	0.40 × 0.30 × 0.07 mm ³
Theta range for data collected	3.72 to 27.44°

Reflections collected	8424
Independent reflections	3315
Completeness to theta = 27.44°	100.0 %
Refinement method	Full-matrix least-squares on F ²
Data / restraint / parameters	3315/0/209
Goodness-of-fit on F ²	1.025

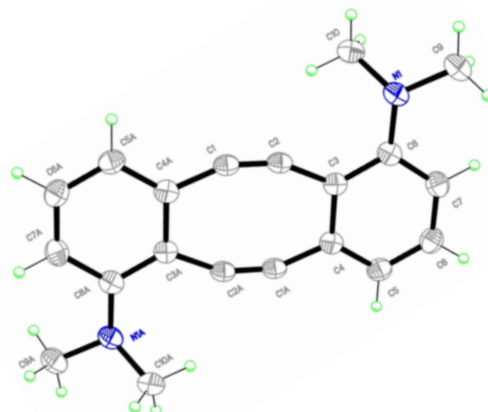
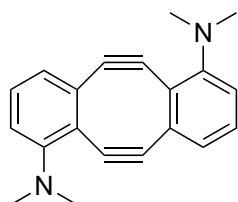
***N*²,*N*²,*N*⁸,*N*⁸-tetramethyl-5,6,11,12-tetrahydridibenzo[*a,e*]cyclooctene-1,7-diamine**
(11)



Key data and refinement for compound <i>11</i>	
Empirical formula	C ₂₀ H ₁₈ N ₂
Formula weight	286.36
Temperature	180 K
Wavelength	1.54178 Å
Crystal system	Monoclinic
Space group	P 2 ₁ /n
Unit cell dimensions	a = 7.4232 Å α = 90.00°
	b = 6.1731 Å β = 100.98°
	c = 16.2142 Å γ = 90.00°
Volume	729.4 Å ³
Z	2
Density (calculated)	1.304 Mg/m ³
Absorption coefficient	0.591 mm ⁻¹
F (000)	304
Crystal size	0.15 × 0.08 × 0.04 mm ³
Theta range for data collected	5.56 to 66.71°
Reflections collected	8217

Independent reflections	1295
Completeness to theta = 66.71°	97.3 %
Refinement method	Full-matrix least-squares on F ²
Data / restraint / parameters	1295/0/103
Goodness-of-fit on F ²	1.055

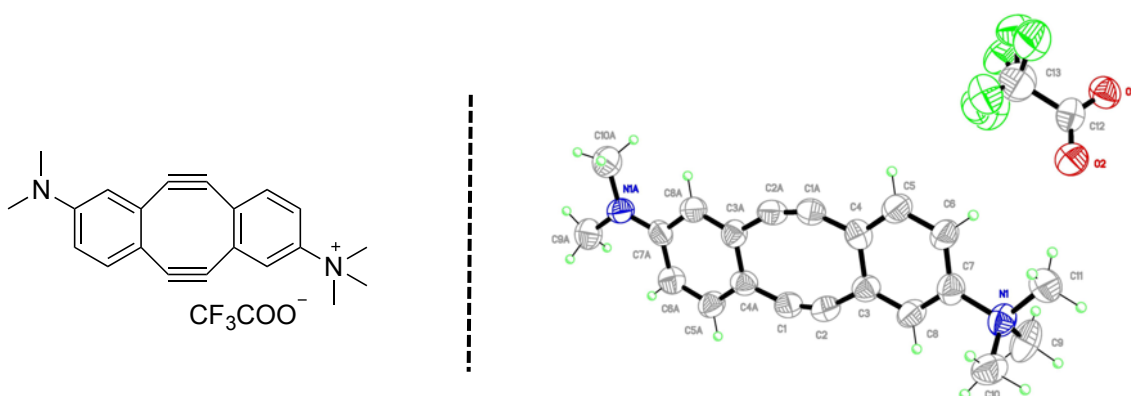
***N*¹,*N*¹,*N*⁷,*N*⁷-tetramethyl-5,6,11,12-tetrahydridibenzo[*a,e*]cyclooctene-1,7-diamine**
(10)



Key data and refinement for compound <i>10</i>	
Empirical formula	C ₂₀ H ₁₈ N ₂
Formula weight	286.36
Temperature	180 K
Wavelength	1.54178 Å
Crystal system	Orthorhombic
Space group	P b c a
Unit cell dimensions	a = 11.0677 Å α = 90°
	b = 11.5283 Å β = 90°
	c = 11.9927 Å γ = 90°
Volume	1530.17 Å ³
Z	4
Density (calculated)	1.243 Mg/m ³
Absorption coefficient	0.564 mm ⁻¹
F (000)	608
Crystal size	0.18 × 0.14 × 0.04 mm ³
Theta range for data collected	6.66 to 66.52°

Reflections collected	16437
Independent reflections	1348
Completeness to theta = 66.52°	99.9 %
Refinement method	Full-matrix least-squares on F ²
Data / restraint / parameters	1348/0/102
Goodness-of-fit on F ²	1.053

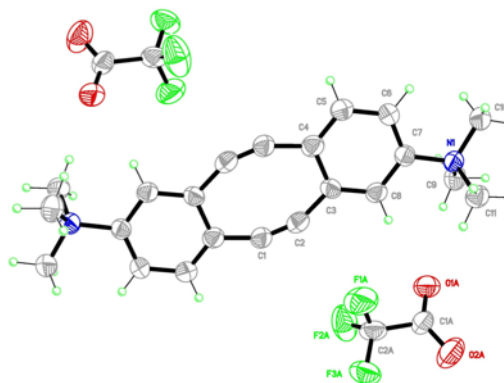
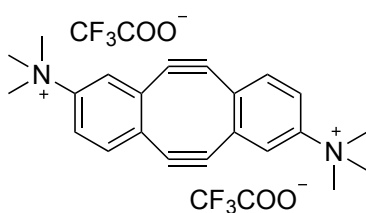
8-(dimethylamino)-*N*²,*N*²,*N*²-trimethyl-5,6,11,12-tetradehydrodibenzo[*a,e*]cyclooctene-2-aminium trifluoroacetate (12)



Key data and refinement for compound 12	
Empirical formula	C ₂₃ H ₂₁ F ₃ N ₂ O ₂
Formula weight	414.42
Temperature	180 K
Wavelength	1.54178 Å
Crystal system	Monoclinic
Space group	P 2 ₁ /n
Unit cell dimensions	a = 22.283 Å α = 90.00°

	$b = 6.3777 \text{ \AA}$ $\beta = 102.72^\circ$
	$c = 14.6736 \text{ \AA}$ $\gamma = 90.00^\circ$
Volume	2034.2 \AA^3
Z	4
Density (calculated)	1.353 Mg/m^3
Absorption coefficient	0.891 mm^{-1}
F (000)	864
Crystal size	$0.10 \times 0.10 \times 0.01 \text{ mm}^3$
Theta range for data collected	4.067 to 50.453°
Reflections collected	2123
Independent reflections	2123
Completeness to $\theta = 50.453^\circ$	99.7 %
Refinement method	Full-matrix least-squares on F^2
Data / restraint / parameters	2123/48/306
Goodness-of-fit on F^2	1.031

***N*²,*N*²,*N*²,*N*⁸,*N*⁸,*N*⁸-hexamethyl-5,6,11,12-tetrahydrodibenzo[a,e]cyclooctene-2,8-diaminium trifluoroacetate (13)**

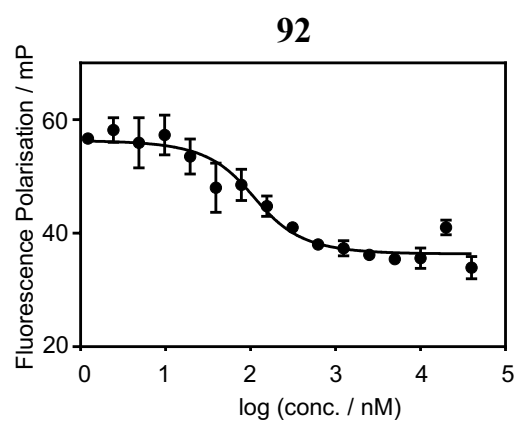
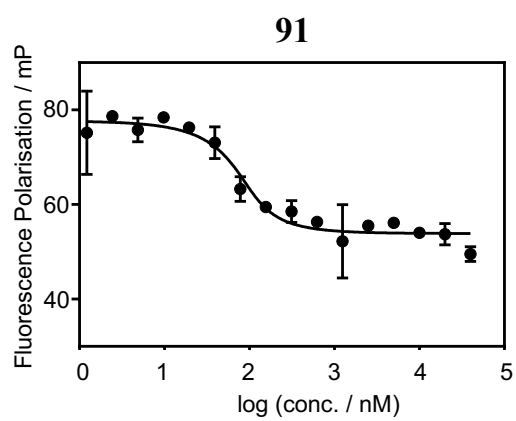
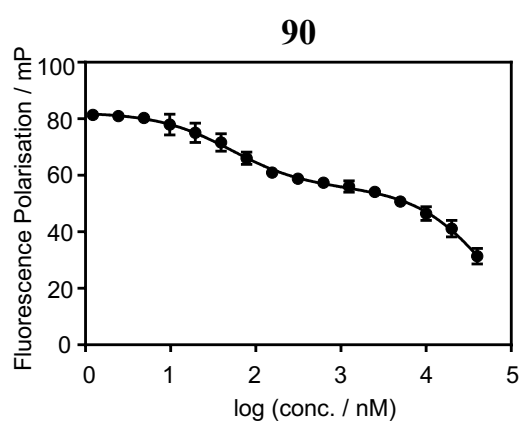
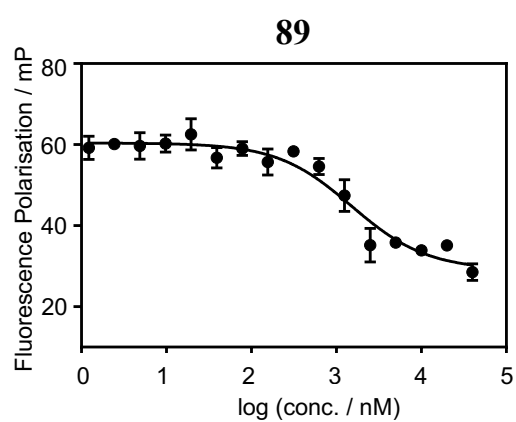
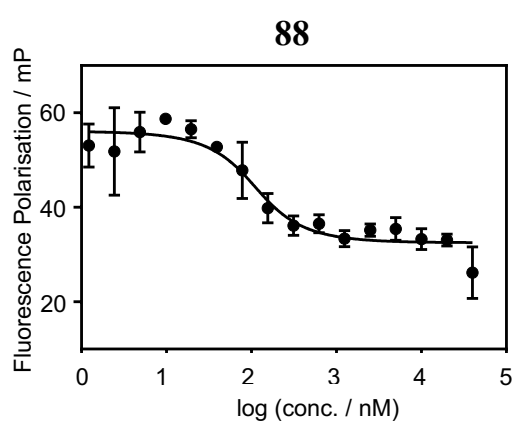
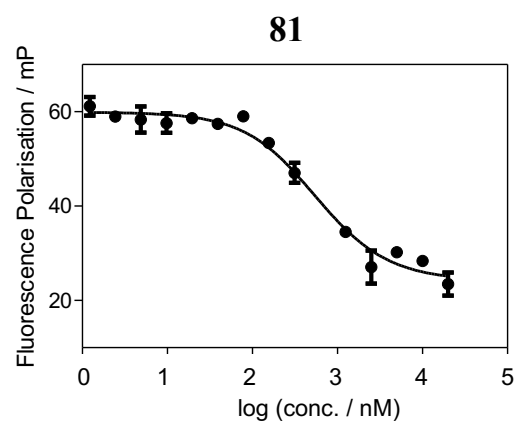
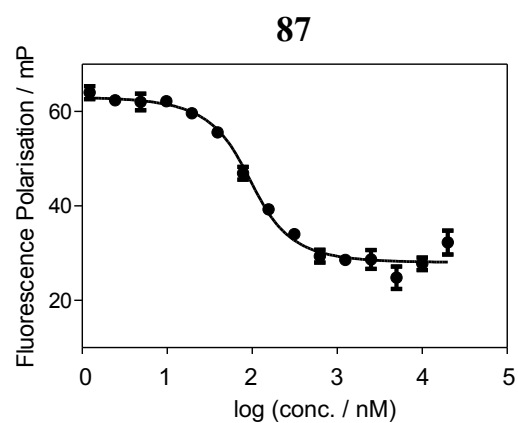


Key data and refinement for compound 13	
Empirical formula	C ₂₆ H ₂₄ F ₆ N ₂ O ₄
Formula weight	542.47
Temperature	180 K
Wavelength	1.54178 Å
Crystal system	Monoclinic
Space group	P 2 ₁ /n
Unit cell dimensions	a = 5.6108 Å α = 90.00°
	b = 8.7794 Å β = 94.73°
	c = 25.5148 Å γ = 90.00°
Volume	1252.6 Å ³
Z	2
Density (calculated)	1.438 Mg/m ³
Absorption coefficient	1.102 mm ⁻¹
F (000)	560
Crystal size	0.16 × 0.05 × 0.01 mm ³
Theta range for data collected	3.476 to 66.715°
Reflections collected	2263
Independent reflections	2263
Completeness to theta = 66.715°	99.6 %
Refinement method	Full-matrix least-squares on F ²
Data / restraint / parameters	2263/0/176
Goodness-of-fit on F ²	1.054

7.2.5 Competitive fluorescence polarisation assay

Competitive fluorescence polarisation (FP) assays were performed as previously described^{61, 89} in 384-well microplates (Corning) on a CLARIOstar microplate reader (BMG labtech) using excitation filter 540–20 nm, dichroic mirror LP 566 nm, and emission filter 590–20 nm. All peptides were dissolved in DMSO as stock solutions. The stock concentration of the TAMRA-labeled tracer (TAMRA-RFMDYWEGL-NH₂) was determined based on the 5-TAMRA absorbance at 556 nm (extinction coefficient $\epsilon = 89,000 \text{ M}^{-1} \text{ cm}^{-1}$) measured on a NanoDrop 2000 (Thermo Scientific) and concentrations of all peptides were determined by amino acid analysis (Department of Biochemistry, University of Cambridge). K_d of the TAMRA-labelled tracer was obtained from previously reported experiments⁶¹. For the competitive fluorescence polarisation assay, TAMRA-labelled tracer (50 nM) was incubated with MDM2 (95 nM) in PBS buffer containing 0.05% (v/v) Tween 20 at 25 °C for 1 hr. The unlabeled peptides or positive controls (nutlin) were diluted 2-fold serially in PBS buffer containing 0.05% (v/v) Tween 20 for a 16-point titration curve (20 μL per well). To each well containing the unlabeled compound was added the TAMRA-labelled tracer/MDM2 solution (20 μL) and the mixture was incubated for 1 hr at 25 °C before the measurement was taken. Titrations were performed in triplicate. Data were fitted in GraphPad Prism 5.0 using the equations as described previously.¹³⁸ Data for **50** (inseparable mixture of two conformational isomers) was fitted using a competitive two-site binding model from GraphPad Prism 7.0, and the K_d from the tighter binding is reported below.

Binding curves for FP assay



7.2.6 Cellular p53 reporter assay

The basic assay was carried out as previously described in the literature^{109, 139} and is briefly described as follows. T22 mouse prostate fibroblast cells stably transfected with a p53-responsive β -galactosidase reporter,¹⁰⁹ kindly provided by Prof. Sir David Lane, were grown in Dulbecco's Modified Eagle Medium (DMEM) with 10% fetal bovine serum and penicillin/streptomycin. Cells were seeded for 24 h at 8000 cells per 100 μ L well in a 96-well black-walled clear flat-bottom polystyrene plate (Greiner #655090), then treated with peptide in triplicate for 18 h at 37 °C in DMEM with 10% serum and a final DMSO concentration of 1%. β -galactosidase activity was quantified using a FluoReporter LacZ/Galactosidase Quantitation kit (Invitrogen). Fluorescence measurements were read on a Tecan Infinite 200 Pro plate reader. Elevated levels of p53 resulting from inhibition of MDM2 leads to the production of β -galactosidase, which is quantified using the profluorescent substrate 3-carboxyumbelliferyl β -D- galactopyranoside (CUG).

The *in situ* stapling version of the assay was identical to the basic assay conditions in all aspects, except that the cells were treated with pure unstapled PDI-E peptide (50 μ M) and substituted Sondheimer dialkynes (0.5 mM). Control cells were treated with only substituted Sondheimer dialkynes (0.5 mM), only unstapled PDI-E peptide (50 μ M), or only 1% DMSO.

7.2.7 Kinetic analysis method

To 1.5 mL solution of substituted dialkyne in MeOH (fixed concentration) taken in a quartz cuvette, we added 1.5 mL of MeOH solution of benzyl azide in 3 different concentrations (20, 100, and 200 mM; final concentration at 10, 50, and 100 mM, respectively; unless specified otherwise). The consumption of the dialkyne was monitored by UV spectroscopy at a wavelength that is characteristic for the absorbance of that dialkyne but almost no significant absorption is observed for benzyl azide and products. The experiments were repeated in duplicate for each concentration of azide. The observed absorbance data were plotted versus time and fitted to a first order exponential decay curve. The pseudo-first order rate constants (k_0) were determined by least-squares fitting of the data to the following exponential equation ($y = A \cdot \exp(-k_0 \cdot x) + y_0$) using Origin where A , y_0 are constants. The pseudo-first order rate constants determined were plotted versus concentration of benzyl azide and fitted to a straight line by linear regression method using Microsoft Office Excel 16. The slope of the straight line indicated the second order rate constant (k) for the first cycloaddition in a double strain-promoted click reaction of diyne with benzyl azide, which is the rate-determining step of the reaction.¹¹⁵

7.2.8 log P determination of *meta*-amine substituted dialkynes **13**, **11**

7.2.8.1 log P determination of quaternary ammonium substituted dialkyne **13**

Analytical grade n-octanol was pre-saturated with distilled water. Similarly, distilled water (adjusted to pH 7.4 with phosphate buffer) was pre-saturated with analytical grade n-octanol. Both phases were left for separation for 24 hours at rt. A stock solution of quaternary amine substituted Sondheimer dialkyne **13** (0.3 mg/mL) was prepared in pre-saturated distilled water. 2.0 mL of this solution was taken and shaken with 2.0 mL of pre-saturated n-octanol and left for separation for 24 hours. Similarly, another 1.8 mL sample of the stock solution of **13** in water was shaken with 1.8 mL of pre-saturated n-octanol and left for separation for 24 hours. The two layers were separated and the resulting amount of diyne **13** in water layer was measured for both the samples using UV spectroscopy.

Absorbance of stock solution of dialkyne **13** in pre-saturated water at 288 nm = 3.73

Run 1

Absorbance of 2.0 mL water sample of dialkyne **13** at 288 nm after shaking with 2.0 mL pre-saturated n-octanol = 3.62

Fraction of dialkyne **13** in water phase after partitioning = $3.62/3.73 = 0.9705$

Fraction of dialkyne **13** in n-octanol phase after partitioning = $1 - 0.9705 = 0.0295$

n-Octanol-water partition coefficient; $P = 0.030$

$\log P = -1.52$

Run 2

Absorbance of 1.8 mL water sample of dialkyne **13** at 288 nm after shaking with 1.8 mL pre-saturated n-octanol = 3.61

Fraction of dialkyne **13** in water phase after partitioning = $3.61/3.73 = 0.9678$

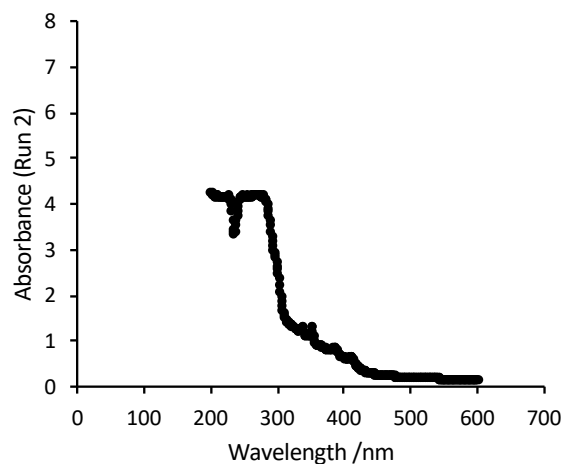
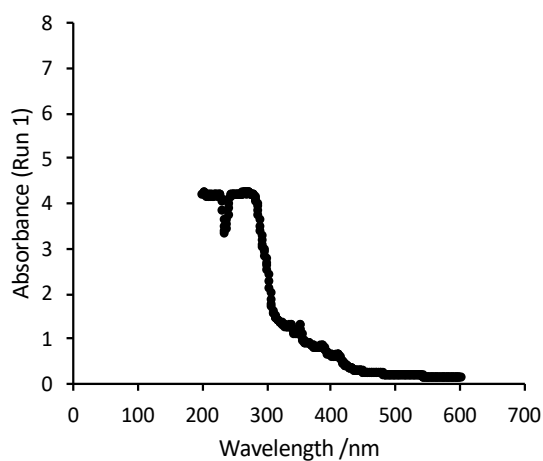
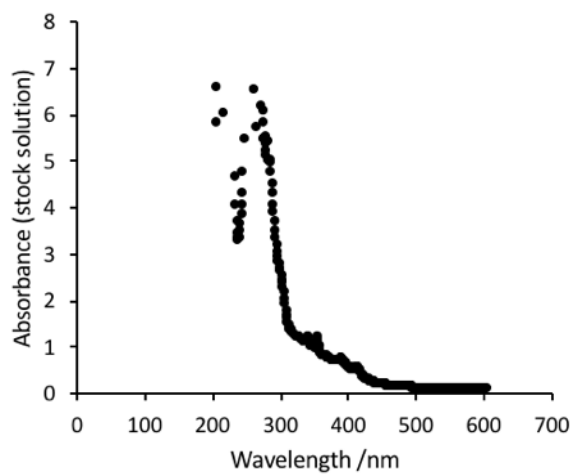
Fraction of dialkyne **13** in n-octanol phase after partitioning = $1 - 0.9678 = 0.0322$

n-Octanol-water partition coefficient; $P = 0.033$

$\log P = -1.48$

Mean $\log P = -1.50$

Error = ± 0.02



7.2.8.2 log P determination of uncharged dimethylamine substituted dialkyne **11**

Absorbance of stock solution of dialkyne **11** in pre-saturated n-octanol at 336 nm = 4.46

Run 1

Absorbance of 2.0 mL n-octanol sample of dialkyne **11** at 336 nm after shaking with 2.0 mL pre-saturated distilled water = 4.20

Fraction of dialkyne **11** in n-octanol phase after partitioning = $4.20/4.46 = 0.9417$

Fraction of dialkyne **11** in water phase after partitioning = $1 - 0.9417 = 0.0583$

n-Octanol-water partition coefficient; $P = 16.15$

$\log P = 1.21$

Run 2

Absorbance of 1.8 mL n-octanol sample of dialkyne **11** at 336 nm after shaking with 1.8 mL pre-saturated distilled water = 4.06

Fraction of dialkyne **11** in n-octanol phase after partitioning = $4.06/4.46 = 0.9103$

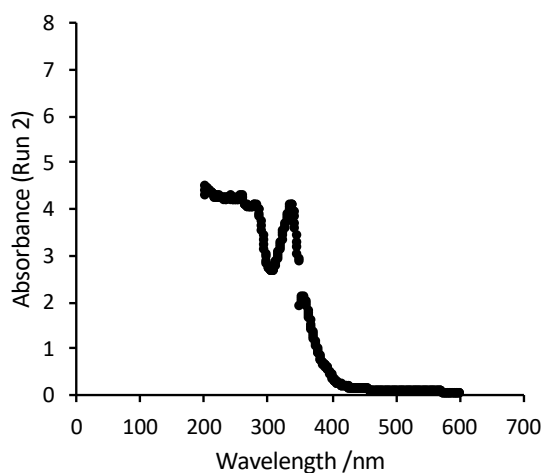
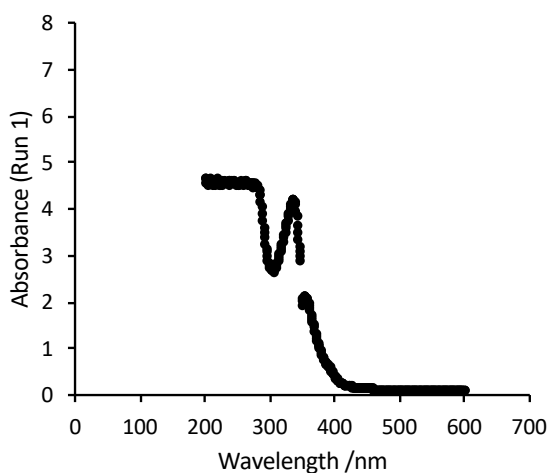
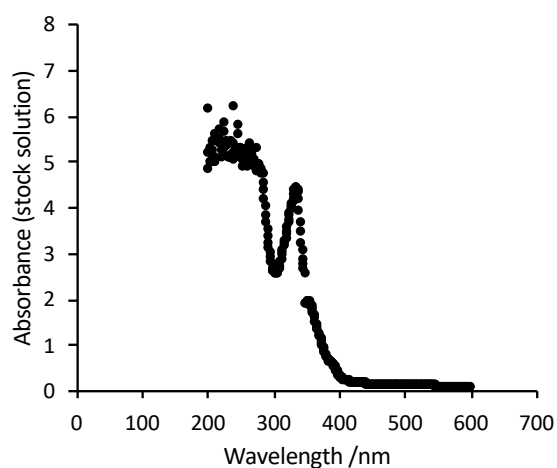
Fraction of dialkyne **11** in water phase after partitioning = $1 - 0.9103 = 0.0897$

n-Octanol-water partition coefficient (P) = 10.15

$\log P = 1.00$

Mean $\log P = 1.10$

Error = ± 0.10



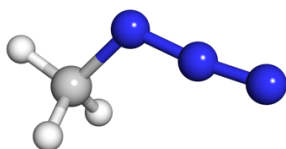
8. Computational data

All quantum mechanical calculations were performed with Gaussian 09 Rev D.01. All geometries were optimized using the B3LYP density functional and the 6-31G(d) basis set within the conductor-like polarisable continuum solvation model (CPCM)¹⁴⁰⁻¹⁴¹ for methanol, using the default integration grid. Vibrational frequencies were computed for all optimized structures to verify that they were either minima (zero imaginary frequencies) or transition states (a single imaginary frequency). Single-point energies E (M06-2X) were calculated using M06-2X¹²², the polarised, triple- ζ valence quality def2-TZVPP basis set of Weigend and Ahlrichs¹²³ and an ultrafine integration grid within the CPCM model (methanol). The resulting energies were used to correct the energies obtained from the B3LYP optimizations¹²⁴⁻¹²⁵. The strain-promoted click reaction of substituted Sondheimer dialkynes with methyl azide was modelled at 298.15 K at 1 atm in methanol. Methyl azide was employed as it is less conformationally flexible than benzyl azide, and calculations showed that it behaves similarly to benzyl azide in a SPAAC with Sondheimer dialkyne.¹¹⁷ Transition states were calculated for both *anti*- and *syn*-attack of methyl azide on diynes. Previous computational studies with similar methods provided results in accordance with the experiment.^{115, 117, 126} Computationally obtained structures were illustrated with PyMOL. The Gibbs free energy G (M06-2X) values were determined by the addition of G_{corr} (thermal correction to Gibbs free energy) to E (M06-2X). $G_{\text{corr}} = G(\text{B3LYP}) - E(\text{B3LYP})$.

8.1 Cartesian coordinates and energies of all stationary points. Absolute energies depicted in hartrees.

8.1.1 Reactants: azide and substituted Sondheimer dialkynes

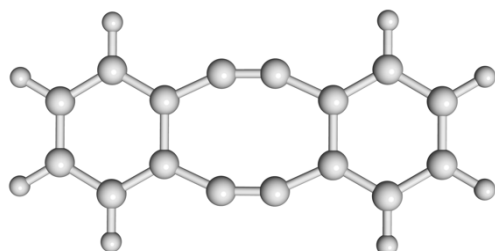
94: Methyl azide



<i>E</i> (B3LYP)	<i>H</i> (B3LYP)	<i>G</i> (B3LYP)	<i>E</i> (M06-2X)
-204.097310	-204.041262	-204.073388	-204.088511

	X	Y	Z
6	-1.554491	0.283662	0.000005
1	-1.564307	0.916618	-0.894171
1	-1.563690	0.917485	0.893568
7	-0.391263	-0.630461	0.000032
7	0.718117	-0.096148	-0.000071
7	1.801311	0.271227	0.000036
1	-2.442214	-0.348399	0.000593

1: Sondheimer dialkyne

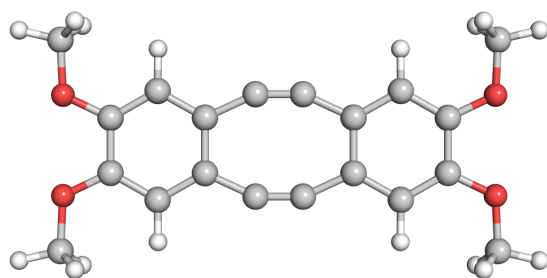


<i>E</i> (B3LYP)	<i>H</i> (B3LYP)	<i>G</i> (B3LYP)	<i>E</i> (M06-2X)
-614.380791	-614.188209	-614.236972	-614.354319

	X	Y	Z
6	-3.131969	-1.404702	0.000001

6	-4.341346	-0.696460	0.000004
6	-4.341346	0.696460	0.000004
6	-3.131969	1.404702	0.000001
6	-1.916748	-0.721724	-0.000001
1	-3.133025	-2.490209	0.000001
1	-5.280381	-1.241481	0.000006
1	-5.280381	1.241481	0.000006
1	-3.133025	2.490209	0.000001
6	-1.916748	0.721724	-0.000002
6	-0.609828	-1.318104	-0.000004
6	0.609828	-1.318104	-0.000005
6	1.916748	-0.721724	-0.000002
6	1.916748	0.721724	-0.000001
6	-0.609828	1.318104	-0.000004
6	0.609828	1.318104	-0.000004
6	3.131969	1.404702	0.000001
1	3.133025	2.490209	0.000001
6	3.131969	-1.404702	0.000001
1	3.133025	-2.490209	0.000001
6	4.341347	-0.696460	0.000004
1	5.280381	-1.241481	0.000006
6	4.341347	0.696460	0.000004
1	5.280381	1.241481	0.000006

4

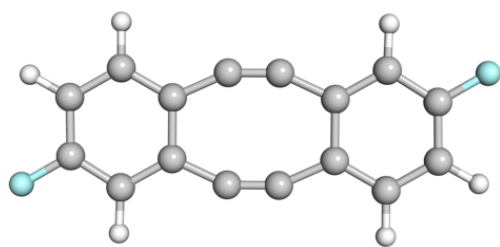


<i>E</i> (B3LYP)	<i>H</i> (B3LYP)	<i>G</i> (B3LYP)	<i>E</i> (M06-2X)
-1072.468622	-1072.134830	-1072.208865	-1072.458685

	X	Y	Z
--	---	---	---

6	3.132971	1.402507	-0.000084
6	4.346654	0.708712	-0.000009
6	4.346693	-0.708709	0.000051
6	3.133088	-1.402613	0.000060
6	1.914219	0.716010	-0.000057
1	3.122929	2.485338	-0.000251
1	3.123135	-2.485449	0.000097
6	1.914273	-0.716233	0.000049
6	0.610147	1.318984	-0.000152
6	-0.610224	1.319330	-0.000042
6	-1.914273	0.716233	-0.000065
6	-1.914220	-0.716010	0.000059
6	0.610223	-1.319330	0.000014
6	-0.610148	-1.318984	0.000162
6	-3.132971	-1.402507	0.000103
1	-3.122929	-2.485338	0.000289
6	-3.133088	1.402613	-0.000086
1	-3.123135	2.485449	-0.000142
6	-4.346693	0.708709	-0.000063
6	-4.346654	-0.708712	0.000021
8	5.573000	1.296160	-0.000094
8	-5.573000	-1.296161	0.000121
6	5.638850	2.721302	0.000149
1	6.701474	2.967113	0.000300
1	5.166573	3.142836	-0.895089
1	5.166392	3.142521	0.895444
6	-5.638850	-2.721302	-0.000100
1	-5.166569	-3.142822	0.895144
1	-6.701473	-2.967114	-0.000244
1	-5.166394	-3.142535	-0.895390
8	5.573098	-1.296019	0.000091
8	-5.573098	1.296019	-0.000112
6	5.639065	-2.721117	-0.000133
1	5.166705	-3.142418	-0.895450
1	6.701697	-2.966898	-0.000184
1	5.166731	-3.142698	0.895066
6	-5.639064	2.721117	0.000103
1	-6.701697	2.966899	0.000160
1	-5.166698	3.142423	0.895415
1	-5.166736	3.142693	-0.895101

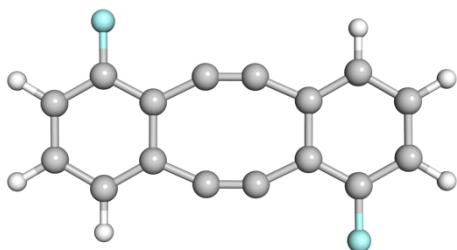
6



<i>E</i> (B3LYP)	<i>H</i> (B3LYP)	<i>G</i> (B3LYP)	<i>E</i> (M06-2X)
-812.845269	-812.667730	-812.720708	-812.858630

	X	Y	Z
6	-1.692594	2.985777	0.000000
6	-1.110798	4.259115	0.000003
6	0.271950	4.358739	0.000003
6	1.110798	3.243451	0.000000
6	-0.899067	1.839244	-0.000003
1	-1.718027	5.157307	0.000006
1	2.186770	3.375969	0.000000
6	0.538742	1.973689	-0.000003
6	-1.369088	0.483122	-0.000006
6	-1.256519	-0.730959	-0.000006
6	-0.538742	-1.973689	-0.000003
6	0.899067	-1.839244	-0.000003
6	1.256519	0.730959	-0.000006
6	1.369088	-0.483122	-0.000006
6	1.692594	-2.985777	0.000000
6	-1.110798	-3.243451	0.000000
1	-2.186770	-3.375969	0.000000
6	-0.271950	-4.358739	0.000003
6	1.110798	-4.259115	0.000003
1	1.718027	-5.157307	0.000006
1	2.773123	-2.887744	0.000000
1	-2.773123	2.887744	0.000000
9	-0.840855	-5.582327	0.000006
9	0.840855	5.582327	0.000006

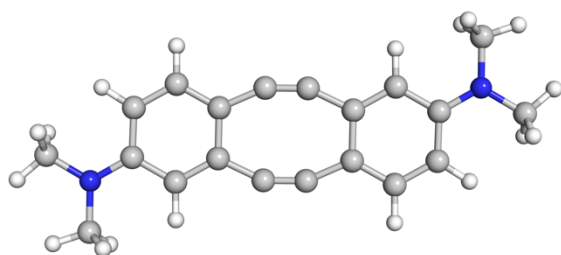
7



<i>E</i> (B3LYP)	<i>H</i> (B3LYP)	<i>G</i> (B3LYP)	<i>E</i> (M06-2X)
-812.844048	-812.666253	-812.719214	-812.856380

	X	Y	Z
6	0.965318	-3.275056	0.000027
6	0.137693	-4.398165	0.000108
6	-1.241769	-4.215602	0.000111
6	-1.796594	-2.927343	0.000033
6	0.466121	-1.978794	-0.000049
1	0.584763	-5.386259	0.000166
1	-1.895929	-5.081520	0.000171
1	-2.873313	-2.795571	0.000033
6	-0.966686	-1.808251	-0.000044
6	1.241769	-0.774894	-0.000143
6	1.385373	0.435783	-0.000139
6	0.966686	1.808251	-0.000044
6	-0.466121	1.978794	-0.000049
6	-1.385373	-0.435783	-0.000139
6	-1.241769	0.774894	-0.000143
6	-0.965318	3.275056	0.000027
6	1.796594	2.927343	0.000033
1	2.873313	2.795571	0.000033
6	1.241769	4.215602	0.000111
1	1.895929	5.081520	0.000171
6	-0.137693	4.398165	0.000108
1	-0.584763	5.386259	0.000166
9	-2.302545	3.449521	0.000022
9	2.302545	-3.449521	0.000022

11

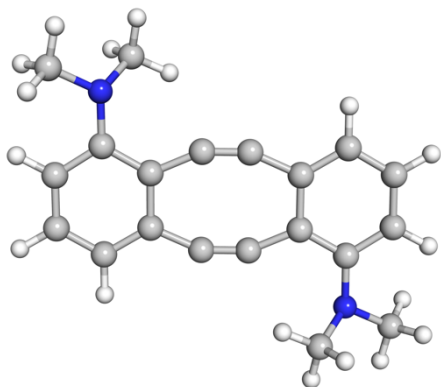


<i>E</i> (B3LYP)	<i>H</i> (B3LYP)	<i>G</i> (B3LYP)	<i>E</i> (M06-2X)
-882.323555	-881.975339	-882.047405	-882.279290

	X	Y	Z
6	-2.816694	1.956418	-0.000078
6	-4.134456	1.502622	-0.000062
6	-4.430246	0.118125	0.000009
6	-3.335893	-0.792052	0.000044
6	-1.736293	1.073436	-0.000020
1	-2.627123	3.026151	-0.000132
1	-4.933615	2.233045	-0.000096
1	-3.512191	-1.860112	0.000079
6	-2.022133	-0.342268	0.000026
6	-0.344262	1.407977	-0.000029
6	0.856482	1.182475	0.000147
6	2.022132	0.342270	0.000046
6	1.736293	-1.073434	-0.000089
6	-0.856483	-1.182474	0.000075
6	0.344262	-1.407976	-0.000117
6	2.816694	-1.956416	-0.000207
1	2.627122	-3.026149	-0.000329
6	3.335893	0.792053	0.000089
1	3.512190	1.860113	0.000192
6	4.430246	-0.118123	0.000000
6	4.134456	-1.502620	-0.000159
1	4.933614	-2.233043	-0.000252
7	5.726444	0.340038	0.000047
7	-5.726444	-0.340040	0.000036
6	6.831899	-0.607260	0.000066
1	7.773447	-0.057904	0.000032

1	6.813544	-1.252463	0.888859
1	6.813513	-1.252529	-0.888680
6	6.004271	1.769695	0.000058
1	7.083690	1.922127	0.000298
1	5.591801	2.265069	-0.889139
1	5.591403	2.265097	0.889052
6	-6.004265	-1.769698	0.000277
1	-5.591505	-2.264938	0.889410
1	-7.083683	-1.922134	0.000417
1	-5.591681	-2.265229	-0.888780
6	-6.831903	0.607254	-0.000197
1	-6.813485	1.252334	-0.889079
1	-7.773448	0.057895	-0.000159
1	-6.813585	1.252647	0.888460

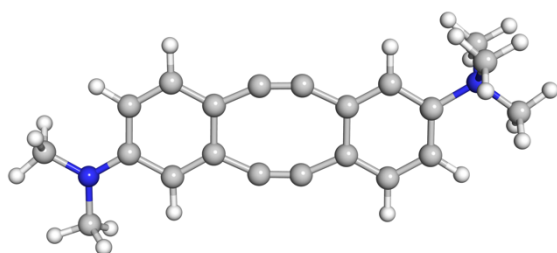
10



<i>E</i> (B3LYP)	<i>H</i> (B3LYP)	<i>G</i> (B3LYP)	<i>E</i> (M06-2X)
-882.313261	-881.965727	-882.034163	-882.269511

	X	Y	Z
6	3.460543	0.145656	-0.040543
6	4.180544	1.364871	0.009569
6	3.534542	2.589936	0.115513
6	2.139306	2.667846	0.186436
6	2.048463	0.216237	0.007699
1	5.263103	1.347217	-0.015199
1	4.126789	3.499513	0.158991
1	1.637914	3.626060	0.273399
6	1.391448	1.494194	0.132769

6	1.135928	-0.884885	-0.106020
6	0.044241	-1.428880	-0.153226
6	-1.391402	-1.494142	-0.132970
6	-2.048467	-0.216159	-0.008107
6	-0.044199	1.429004	0.152877
6	-1.135822	0.884899	0.105304
6	-3.460594	-0.145651	0.040403
6	-2.139090	-2.667890	-0.186215
1	-1.637622	-3.626072	-0.273062
6	-3.534326	-2.590073	-0.115022
1	-4.126503	-3.499715	-0.158132
6	-4.180411	-1.365080	-0.009221
1	-5.262955	-1.347612	0.015812
7	-4.118375	1.085634	0.188807
7	4.117892	-1.085993	-0.189080
6	3.801387	-2.165999	0.750318
1	4.120963	-3.119529	0.318199
1	4.319823	-2.031949	1.714168
1	2.728983	-2.222071	0.934186
6	5.534256	-1.061820	-0.534625
1	6.184197	-0.760337	0.304220
1	5.829986	-2.069358	-0.841741
1	5.709521	-0.384831	-1.374684
6	-5.534931	1.061211	0.533461
1	-5.831054	2.068721	0.840241
1	-6.184253	0.759487	-0.305773
1	-5.710665	0.384317	1.373501
6	-3.800934	2.166935	-0.748713
1	-4.318679	2.034403	-1.713138
1	-4.120647	3.119903	-0.315458
1	-2.728405	2.223100	-0.931743

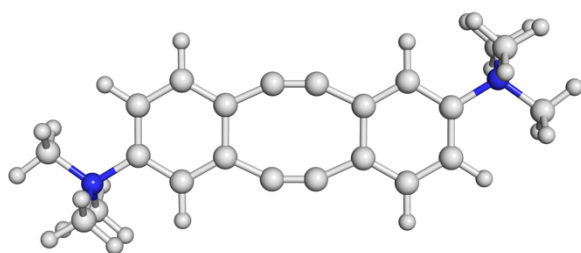


<i>E</i> (B3LYP)	<i>H</i> (B3LYP)	<i>G</i> (B3LYP)	<i>E</i> (M06-2X)
-922.066872	-921.674435	-921.745883	-922.012128

	X	Y	Z
6	-3.134811	-1.960971	-0.000167
6	-4.454067	-1.516626	-0.000171
6	-4.765138	-0.133932	-0.000307
6	-3.678027	0.787451	-0.000193
6	-2.063058	-1.066335	-0.000179
1	-2.936199	-3.028619	-0.000104
1	-5.246870	-2.253697	-0.000124
1	-3.861864	1.853916	0.000032
6	-2.364816	0.344213	-0.000172
6	-0.669313	-1.378253	-0.000140
6	0.531627	-1.153251	0.000334
6	1.677382	-0.297107	0.000164
6	1.385639	1.118867	0.000144
6	-1.203076	1.191533	-0.000067
6	-0.010323	1.445214	0.000165
6	2.439951	2.024145	0.000098
1	2.234015	3.088919	0.000097
6	3.004677	-0.718398	0.000126
1	3.201498	-1.783476	0.000247
6	4.042868	0.224730	-0.000017
6	3.772521	1.586897	0.000048
1	4.555150	2.332223	0.000087
7	5.458919	-0.292366	-0.000043
7	-6.061694	0.310777	-0.000469
6	6.488886	0.812575	-0.000806
1	7.470443	0.341136	-0.001533
1	6.369529	1.416639	-0.898640

1	6.370939	1.416602	0.897269
6	5.694320	-1.136285	-1.239033
1	6.728277	-1.481058	-1.223787
1	5.018587	-1.988542	-1.229450
1	5.507846	-0.516057	-2.115244
6	-6.354268	1.739078	-0.000098
1	-5.946190	2.236822	-0.889392
1	-7.434965	1.879654	-0.000760
1	-5.947234	2.236413	0.889910
6	-7.159784	-0.647140	0.000719
1	-7.134055	-1.290085	0.890388
1	-8.105563	-0.105677	0.000686
1	-7.134802	-1.291289	-0.888102
6	5.694649	-1.135028	1.239714
1	5.507989	-0.514038	2.115341
1	5.019136	-1.987473	1.230904
1	6.728731	-1.479460	1.224779

13



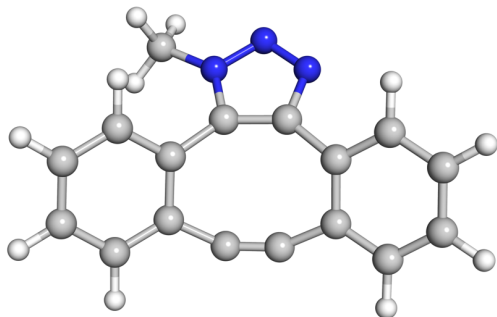
<i>E</i> (B3LYP)	<i>H</i> (B3LYP)	<i>G</i> (B3LYP)	<i>E</i> (M06-2X)
-961.803913	-961.367249	-961.439367	-961.740108

	X	Y	Z
6	2.760049	2.024801	-0.000862
6	4.094289	1.594479	-0.000465
6	4.378870	0.234917	0.000044
6	3.347914	-0.716483	0.000099
6	1.715276	1.108970	-0.000711
1	2.546631	3.087736	-0.001264
1	4.871238	2.345802	-0.000594
1	3.550482	-1.780249	0.000437
6	2.021784	-0.300104	-0.000307

6	0.315151	1.415362	-0.001037
6	-0.876987	1.163600	-0.000173
6	-2.021780	0.300122	-0.000332
6	-1.715272	-1.108952	-0.000727
6	0.876992	-1.163581	-0.000166
6	-0.315146	-1.415344	-0.001045
6	-2.760044	-2.024784	-0.000861
1	-2.546626	-3.087719	-0.001244
6	-3.347911	0.716501	0.000060
1	-3.550477	1.780267	0.000432
6	-4.378865	-0.234902	-0.000001
6	-4.094285	-1.594463	-0.000462
1	-4.871238	-2.345783	-0.000571
7	-5.798087	0.268643	0.000514
7	5.798085	-0.268652	0.000512
6	-6.818546	-0.846251	0.000667
1	-7.803695	-0.382656	0.001325
1	-6.695855	-1.448580	-0.897937
1	-6.694958	-1.449160	0.898746
6	-6.040862	1.110676	-1.239465
1	-7.078896	1.442577	-1.225168
1	-5.376200	1.971622	-1.227517
1	-5.845524	0.493621	-2.115948
6	6.040693	-1.110894	-1.239355
1	5.845280	-0.493978	-2.115919
1	7.078714	-1.442841	-1.225121
1	5.375986	-1.971804	-1.227180
6	6.818585	0.846205	0.000393
1	6.695080	1.449273	0.898377
1	7.803717	0.382574	0.001065
1	6.695863	1.448383	-0.898307
6	-6.040097	1.110321	1.240855
1	-5.845287	0.492686	2.117047
1	-5.374655	1.970667	1.229320
1	-7.077834	1.443151	1.226724
6	6.040205	-1.110145	1.240958
1	5.845506	-0.492367	2.117073
1	5.374750	-1.970482	1.229637
1	7.077934	-1.442998	1.226764

8.1.2 Products: triazole

P1

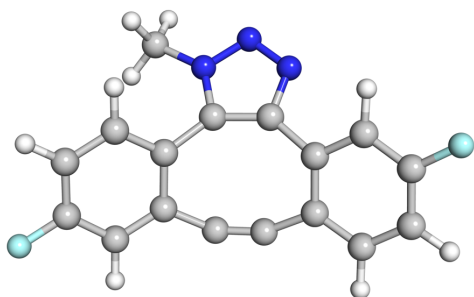


<i>E</i> (B3LYP)	<i>H</i> (B3LYP)	<i>G</i> (B3LYP)	<i>E</i> (M062X)
-818.589639	-818.335584	-818.392334	-818.562492

	X	Y	Z
6	-2.450505	2.639813	-0.607583
1	-2.960837	2.953824	0.305632
1	-3.033145	1.865598	-1.105545
7	-1.105257	2.142945	-0.317763
7	-0.091879	3.016017	-0.433250
7	1.014431	2.361146	-0.234513
6	-0.655577	0.875006	-0.032197
6	0.748499	1.038981	0.000515
6	1.967433	0.191820	0.167478
6	2.119985	-1.101505	-0.410745
6	0.914461	-1.663550	-0.909863
6	-0.295498	-1.777491	-0.969448
6	-1.581343	-1.477549	-0.435215
6	-1.672908	-0.196552	0.185744
6	-2.802530	0.066277	0.970333
1	-2.872123	1.003154	1.512813
6	-2.637501	-2.389910	-0.341246
1	-2.547410	-3.353323	-0.832818
6	3.082087	0.755047	0.802495
1	2.987872	1.739451	1.247740
6	3.352921	-1.765844	-0.365319
1	3.439588	-2.748600	-0.818043
6	4.446383	-1.174516	0.265154

1	5.398474	-1.695550	0.301411
6	4.304973	0.081451	0.857535
1	5.147797	0.544287	1.362734
6	-3.773508	-2.078191	0.407541
1	-4.586173	-2.794637	0.480793
6	-3.843404	-0.861572	1.083641
1	-4.705635	-0.624037	1.699171
1	-2.333279	3.498788	-1.268145

P2: *anti*-attack

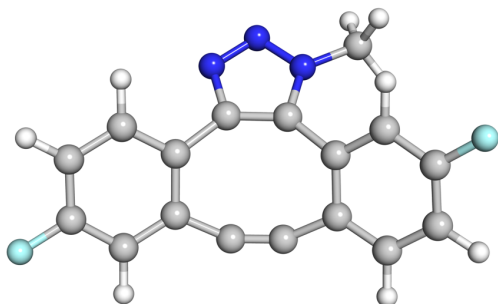


<i>E</i> (B3LYP)	<i>H</i> (B3LYP)	<i>G</i> (B3LYP)	<i>E</i> (M062X)
-1017.054820	-1016.815754	-1016.876636	-1017.067632

	X	Y	Z
6	-2.734256	0.608699	0.973307
6	-3.906549	-0.138748	1.114780
6	-4.025642	-1.323435	0.403328
6	-3.001092	-1.811597	-0.399058
6	-1.688147	0.193203	0.139903
1	-4.711371	0.192696	1.761295
1	-3.107213	-2.767595	-0.898684
6	-1.822322	-1.069691	-0.511341
6	-0.523357	1.096433	-0.095708
6	0.889233	1.039156	-0.108342
6	1.962039	0.006800	-0.003209
6	1.885232	-1.285083	-0.601554
6	-0.622066	-1.554483	-1.104192
6	0.590982	-1.638800	-1.062027
6	2.996988	-2.138794	-0.606645

6	3.171245	0.381918	0.592628
1	3.280613	1.355888	1.053997
6	4.250823	-0.494516	0.579279
6	4.196461	-1.747950	-0.017271
1	5.065824	-2.395965	-0.006986
1	2.912072	-3.115888	-1.070376
1	-2.638184	1.528342	1.539688
9	5.400005	-0.102568	1.170532
9	-5.158754	-2.046091	0.514026
6	-2.036244	3.132172	-0.570361
1	-2.461844	3.493994	0.368142
1	-2.746942	2.471833	-1.066285
7	-0.776124	2.425062	-0.341134
7	0.357999	3.132377	-0.472334
7	1.352954	2.308432	-0.325009
1	-1.807973	3.981824	-1.213571

P3: *syn*-attack

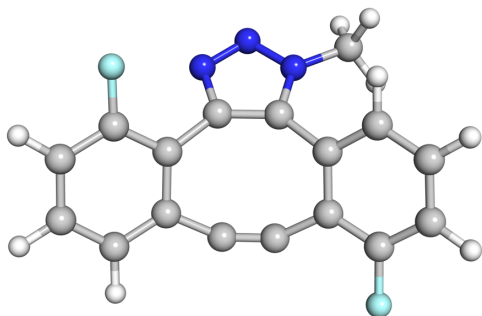


<i>E</i> (B3LYP)	<i>H</i> (B3LYP)	<i>G</i> (B3LYP)	<i>E</i> (M062X)
-1017.053918	-1016.814922	-1016.875938	-1017.066693

	X	Y	Z
6	-2.947566	1.029752	0.866590
6	-4.209127	0.439063	0.959336
6	-4.425920	-0.773255	0.317617
6	-3.425374	-1.422182	-0.392068
6	-1.900133	0.426629	0.157422
1	-5.012896	0.909499	1.515291
1	-3.622236	-2.375966	-0.868086
6	-2.160141	-0.827574	-0.466806

6	-0.641963	1.206903	-0.037309
6	0.746929	0.965080	-0.138709
6	1.704172	-0.173373	-0.010989
6	1.504975	-1.422607	-0.671456
6	-1.018343	-1.440239	-1.049198
6	0.179583	-1.626290	-1.145969
6	2.505574	-2.400875	-0.658980
6	2.882574	-0.001596	0.722750
1	3.065190	0.896867	1.299923
6	3.847342	-1.006141	0.733973
6	3.696550	-2.195358	0.036504
1	4.478323	-2.946357	0.062104
1	2.334987	-3.338552	-1.176893
1	-2.773185	1.986107	1.346354
9	4.970848	-0.801862	1.452354
9	-5.645196	-1.349480	0.393732
6	2.618017	2.646417	-0.729225
1	2.521436	3.546038	-1.336567
1	3.126644	1.868535	-1.297794
7	1.259578	2.215404	-0.396614
7	0.295622	3.147434	-0.434145
7	-0.838379	2.550078	-0.210867
1	3.190213	2.879355	0.171371

P4: *anti*-attack

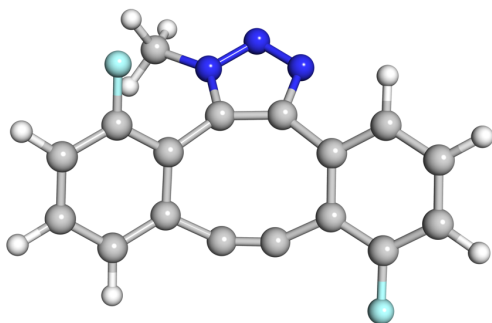


<i>E</i> (B3LYP)	<i>H</i> (B3LYP)	<i>G</i> (B3LYP)	<i>E</i> (M062X)
-1017.050609	-1016.811583	-1016.872742	-1017.062829

	X	Y	Z
--	---	---	---

6	-3.163146	0.172667	0.650531
6	-4.223870	-0.729186	0.705991
6	-4.080427	-1.986543	0.124532
6	-2.872655	-2.343045	-0.475243
6	-1.942772	-0.114866	0.032444
1	-5.140191	-0.428981	1.202875
1	-4.903226	-2.693640	0.155772
1	-2.735524	-3.330659	-0.902210
6	-1.813711	-1.428868	-0.510344
6	-0.937119	0.966151	-0.178368
6	0.464841	1.103901	-0.108964
6	1.652756	0.286805	0.271853
6	1.852322	-1.021158	-0.258451
6	-0.490534	-1.739557	-0.929002
6	0.719031	-1.626821	-0.863973
6	3.055853	-1.677926	-0.000808
6	2.647119	0.827213	1.095042
1	2.496043	1.797783	1.554296
6	3.833630	0.130653	1.349925
1	4.588428	0.574194	1.991043
6	4.056365	-1.124075	0.786665
1	4.969810	-1.681036	0.964368
9	3.228235	-2.910849	-0.519047
9	-3.341946	1.371259	1.245195
6	1.908591	3.123653	-0.801905
1	2.668152	2.447696	-1.194117
1	2.276392	3.602441	0.108104
7	0.670309	2.388591	-0.547529
7	-0.487340	2.997386	-0.854140
7	-1.449776	2.152132	-0.628699
1	1.673522	3.887755	-1.542437

P5: *syn*-attack

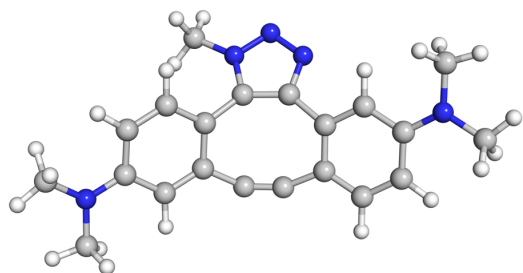


<i>E</i> (B3LYP)	<i>H</i> (B3LYP)	<i>G</i> (B3LYP)	<i>E</i> (M062X)
-1017.053566	-1016.814451	-1016.875344	-1017.064794

	X	Y	Z
6	-2.828176	-0.323301	0.811012
6	-3.711934	-1.392639	0.937752
6	-3.403536	-2.596348	0.311331
6	-2.203810	-2.734330	-0.390625
6	-1.649610	-0.378813	0.064028
1	-4.615363	-1.262348	1.523220
1	-4.084955	-3.437076	0.392725
1	-1.929285	-3.685261	-0.833904
6	-1.322504	-1.654608	-0.490296
6	-0.836321	0.844750	-0.182476
6	0.509499	1.259185	-0.080724
6	1.835071	0.648328	0.224109
6	2.225330	-0.633014	-0.259949
6	0.022894	-1.742249	-0.950335
6	1.191043	-1.434704	-0.803231
6	3.542897	-1.058893	-0.075309
6	2.796367	1.425672	0.881884
1	2.516141	2.406115	1.249351
6	4.103551	0.963568	1.058063
1	4.826673	1.585041	1.576994
6	4.493395	-0.285726	0.573677
1	5.502315	-0.663547	0.697951
9	3.885103	-2.276576	-0.545898
9	-3.140878	0.824900	1.456166
6	-2.860843	2.178603	-1.046369
1	-2.859522	2.992084	-1.770959
1	-3.485634	2.440539	-0.192206

7	-1.474220	1.975166	-0.630385
7	-0.622934	3.002725	-0.768229
7	0.561506	2.580326	-0.432297
1	-3.238737	1.269141	-1.514448

P6: anti-attack

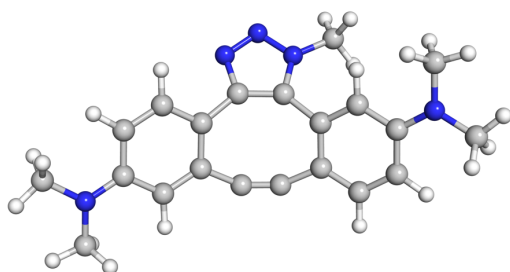


<i>E</i> (B3LYP)	<i>H</i> (B3LYP)	<i>G</i> (B3LYP)	<i>E</i> (M062X)
-1086.532653	-1086.123057	-1086.201861	-1086.487282

	X	Y	Z
6	-2.602195	1.136132	0.878840
6	-3.848678	0.543796	1.059152
6	-4.214591	-0.615475	0.334093
6	-3.227520	-1.185600	-0.508319
6	-1.638132	0.622344	0.000951
1	-2.372395	2.021377	1.464039
1	-4.534534	0.991849	1.766898
1	-3.415671	-2.115934	-1.028419
6	-1.971054	-0.601158	-0.653741
6	-0.381519	1.373789	-0.266113
6	1.013804	1.141664	-0.340080
6	1.947399	-0.024627	-0.281235
6	1.665666	-1.290042	-0.876301
6	-0.870444	-1.226842	-1.312346
6	0.323858	-1.472912	-1.282459
6	2.668841	-2.269601	-0.907670
1	2.451599	-3.229575	-1.366915
6	3.207491	0.186409	0.276214
1	3.407268	1.155028	0.712883

6	4.221644	-0.806072	0.262241
6	3.923613	-2.042742	-0.363558
1	4.666388	-2.828960	-0.413745
7	5.448881	-0.571761	0.838102
7	-5.466032	-1.177809	0.453128
6	6.499054	-1.576386	0.747274
1	7.384954	-1.214836	1.269858
1	6.192538	-2.520320	1.215945
1	6.778355	-1.788359	-0.294545
6	5.754506	0.731336	1.412482
1	6.758449	0.706542	1.836965
1	5.719776	1.533089	0.661362
1	5.054348	0.988569	2.217235
6	-5.755657	-2.453386	-0.187794
1	-5.144737	-3.275324	0.214266
1	-6.806419	-2.699403	-0.030214
1	-5.584308	-2.397789	-1.268939
6	-6.391964	-0.672740	1.457819
1	-6.601973	0.391669	1.300378
1	-7.335101	-1.214121	1.376377
1	-6.009145	-0.798158	2.481481
6	-1.643674	3.587444	-0.649728
1	-1.337677	4.421324	-1.281719
1	-1.996649	3.972911	0.309611
7	-0.472750	2.729857	-0.481098
7	0.735883	3.294890	-0.649953
7	1.623482	2.347779	-0.561312
1	-2.443991	3.027751	-1.133206

P7: *syn*-attack

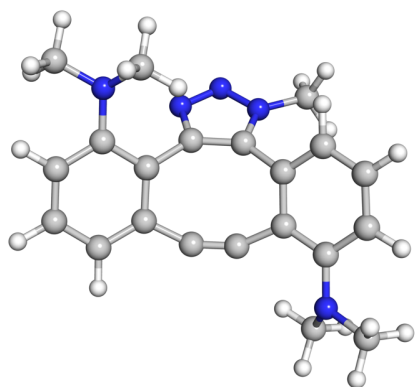


<i>E</i> (B3LYP)	<i>H</i> (B3LYP)	<i>G</i> (B3LYP)	<i>E</i> (M062X)
-1086.530566	-1086.121023	-1086.200124	-1086.485734

	X	Y	Z
6	-2.766373	1.329717	0.874223
6	-4.043621	0.798582	1.028661
6	-4.421219	-0.399799	0.376429
6	-3.442690	-1.027949	-0.429058
6	-1.783391	0.717940	0.085650
1	-2.526092	2.262207	1.375087
1	-4.749798	1.327321	1.656818
1	-3.664403	-1.948892	-0.952863
6	-2.158675	-0.494786	-0.559991
6	-0.510432	1.449001	-0.173744
6	0.856934	1.144674	-0.370922
6	1.761658	-0.044324	-0.327375
6	1.449802	-1.259326	-1.006311
6	-1.093985	-1.140401	-1.251455
6	0.090144	-1.391821	-1.388965
6	2.414581	-2.272333	-1.062531
1	2.181542	-3.191419	-1.591901
6	2.980250	0.056111	0.343383
1	3.186481	0.955241	0.907827
6	3.949098	-0.983265	0.321100
6	3.645724	-2.141439	-0.434797
1	4.357311	-2.954193	-0.506957
7	5.133999	-0.863321	1.008104
7	-5.681861	-0.943416	0.530316
6	6.134003	-1.918341	0.919738
1	6.992840	-1.648073	1.534230
1	5.742195	-2.875899	1.286893
1	6.484165	-2.066064	-0.111316
6	5.437025	0.350668	1.753228
1	6.399589	0.231398	2.250952
1	5.499145	1.231927	1.099392
1	4.681740	0.549102	2.524513
6	-6.087745	-2.069843	-0.298386
1	-5.436589	-2.936650	-0.134033
1	-7.103034	-2.362533	-0.027827
1	-6.072037	-1.830622	-1.372538
6	-6.710778	-0.184962	1.227656
1	-6.942753	0.768757	0.729617
1	-7.623820	-0.780184	1.270560
1	-6.408131	0.035166	2.258187
6	2.760640	2.745637	-1.068390

1	3.407473	2.949403	-0.212123
1	2.664083	3.650098	-1.669160
7	1.412341	2.375745	-0.639928
7	0.496136	3.354620	-0.591611
7	-0.650226	2.805906	-0.306341
1	3.191669	1.944726	-1.667995

P8: *anti*-attack

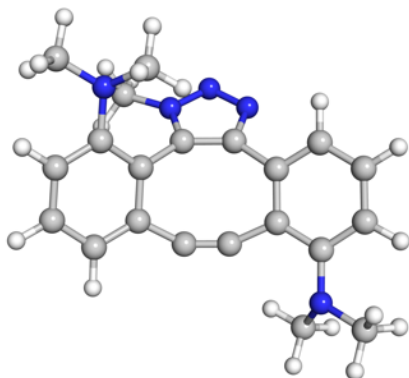


<i>E</i> (B3LYP)	<i>H</i> (B3LYP)	<i>G</i> (B3LYP)	<i>E</i> (M062X)
-1086.515368	-1086.106705	-1086.18269	-1086.472951

	X	Y	Z
6	-3.163639	-0.777736	0.303487
6	-3.798333	-2.040011	0.306424
6	-3.156932	-3.184529	-0.158270
6	-1.835527	-3.123823	-0.591218
6	-1.847248	-0.682321	-0.225794
1	-4.803779	-2.129568	0.699513
1	-3.681404	-4.135875	-0.140995
1	-1.302168	-4.016119	-0.901831
6	-1.183171	-1.885778	-0.604392
6	-1.250583	0.646034	-0.578110
6	-0.007897	1.286474	-0.410257
6	1.306401	1.027152	0.249106
6	2.055916	-0.148737	-0.044557
6	0.210473	-1.725339	-0.863393
6	1.273373	-1.168294	-0.651233
6	3.381056	-0.315714	0.440459
6	1.849341	1.984611	1.109687

1	1.272586	2.862029	1.382725
6	3.131494	1.800075	1.632232
1	3.550940	2.546100	2.301057
6	3.894478	0.689557	1.287213
1	4.899681	0.603182	1.680897
7	4.107160	-1.475079	0.144503
7	-3.831575	0.359574	0.795061
6	-3.177265	1.123862	1.857412
1	-3.598760	2.134284	1.890818
1	-3.324714	0.657012	2.846352
1	-2.106810	1.208743	1.673519
6	-5.271768	0.278951	0.989245
1	-5.567353	-0.320228	1.868535
1	-5.657499	1.293112	1.134998
1	-5.752116	-0.143685	0.102600
6	5.350427	-1.704270	0.870848
1	5.674882	-2.731248	0.681173
1	6.165768	-1.028608	0.562659
1	5.189560	-1.591623	1.946190
6	4.189383	-1.922330	-1.249228
1	4.945429	-1.353569	-1.814621
1	4.468566	-2.980290	-1.268620
1	3.227434	-1.820628	-1.750876
6	0.796095	3.525576	-1.383840
1	0.428262	4.060634	-2.259296
1	0.872866	4.216494	-0.541479
7	-0.161815	2.458588	-1.107496
7	-1.383699	2.544829	-1.661997
7	-2.037948	1.465015	-1.343493
1	1.777330	3.098892	-1.594287

P9: *syn*-attack

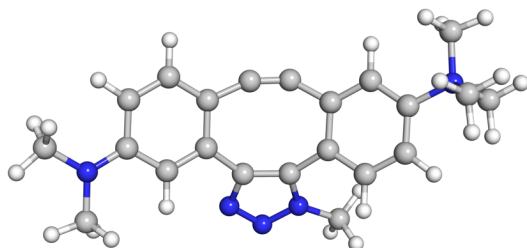


<i>E (B3LYP)</i>	<i>H (B3LYP)</i>	<i>G (B3LYP)</i>	<i>E (M062X)</i>
-1086.519209	-1086.110331	-1086.185783	-1086.477490

	X	Y	Z
6	-2.885048	0.804449	-0.515374
6	-3.457994	2.089666	-0.640232
6	-2.801959	3.226122	-0.179427
6	-1.520810	3.132691	0.361707
6	-1.635140	0.681938	0.148516
1	-4.420191	2.201062	-1.124615
1	-3.275283	4.197743	-0.289174
1	-0.968649	4.019139	0.655319
6	-0.929624	1.873810	0.493114
6	-1.107192	-0.643658	0.592578
6	0.073138	-1.406772	0.470720
6	1.435199	-1.235132	-0.116515
6	2.217748	-0.063390	0.093661
6	0.445258	1.661058	0.815966
6	1.464274	1.031187	0.588331
6	3.575641	0.003660	-0.322100
6	2.010107	-2.320448	-0.783926
1	1.423492	-3.217725	-0.946907
6	3.329273	-2.243831	-1.232435
1	3.768141	-3.087991	-1.757253
6	4.106100	-1.112098	-0.998086
1	5.136117	-1.103171	-1.333025
7	4.323616	1.173201	-0.114266
7	-3.546373	-0.337607	-1.016903
6	-2.822316	-1.136128	-2.013637
1	-3.289972	-2.122726	-2.090727
1	-2.847266	-0.661824	-3.008659
1	-1.781711	-1.274035	-1.721802
6	-4.957655	-0.201907	-1.363736
1	-5.127110	0.380701	-2.284876
1	-5.370679	-1.202847	-1.520622
1	-5.506381	0.269643	-0.544296
6	5.598400	1.291095	-0.811751
1	5.943593	2.325626	-0.726014
1	6.384698	0.636809	-0.398457
1	5.472934	1.060192	-1.872798
6	4.388734	1.726413	1.242295

1	5.114348	1.182349	1.869295
1	4.699939	2.774322	1.186816
1	3.413183	1.691169	1.726526
6	-3.226274	-1.179228	1.937675
1	-3.280468	-0.142235	2.272118
1	-4.001222	-1.362369	1.192384
7	-1.908929	-1.442298	1.368855
7	-1.307823	-2.603424	1.676284
7	-0.123525	-2.588597	1.132348
1	-3.345444	-1.849740	2.788478

P10: *anti*-attack-1

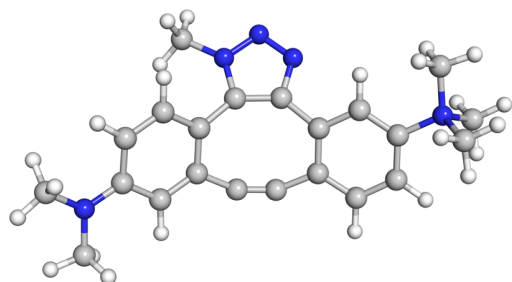


<i>E</i> (B3LYP)	<i>H</i> (B3LYP)	<i>G</i> (B3LYP)	<i>E</i> (M062X)
-1126.275403	-1125.821251	-1125.900342	-1126.219656

	X	Y	Z
6	2.887587	-2.228721	-1.028972
6	4.139698	-2.064378	-0.462564
6	4.470233	-0.863634	0.219133
6	3.484172	0.158295	0.273528
6	1.915731	-1.217390	-0.965164
1	2.645902	-3.159488	-1.533188
1	4.858128	-2.870598	-0.537990
1	3.706517	1.097055	0.761295
6	2.227867	0.008675	-0.304821
6	0.578940	-1.332700	-1.391832
6	-0.610454	-1.060399	-1.459488
6	-1.680624	-0.465384	-0.735974
6	-1.336138	0.704099	0.000984
6	1.321305	1.196453	-0.312230
6	-0.065903	1.451188	-0.230094
6	-2.270669	1.185651	0.922771

1	-2.019121	2.027085	1.558429
6	-2.958349	-1.030964	-0.617937
1	-3.176616	-1.902834	-1.217419
6	-3.876286	-0.487694	0.276023
6	-3.531673	0.605409	1.069330
1	-4.213634	1.029203	1.796514
7	-5.257823	-1.072906	0.422386
7	5.696914	-0.690594	0.805809
6	-5.467942	-1.540791	1.850137
1	-6.469425	-1.964205	1.924517
1	-4.714297	-2.293696	2.077190
1	-5.370919	-0.694033	2.525627
6	-5.494294	-2.256725	-0.486086
1	-6.513441	-2.600812	-0.315981
1	-5.378393	-1.942763	-1.522094
1	-4.790416	-3.048942	-0.236060
6	6.020141	0.556700	1.488079
1	5.327871	0.753775	2.316595
1	7.027128	0.486340	1.899120
1	5.989558	1.414853	0.803742
6	6.702494	-1.742424	0.721484
1	6.975641	-1.960394	-0.319506
1	7.600889	-1.419565	1.247261
1	6.352194	-2.673322	1.185881
6	-6.291019	-0.016687	0.077148
1	-6.185045	0.825975	0.756659
1	-6.121528	0.302902	-0.950477
1	-7.280397	-0.461419	0.183336
6	-1.298075	3.700976	-0.509108
1	-2.096797	3.193208	-1.049495
1	-0.966119	4.572146	-1.073261
7	-0.140054	2.815777	-0.381971
7	1.075589	3.363109	-0.528708
7	1.949984	2.400388	-0.477027
1	-1.660423	4.021783	0.469800

P11: *anti*-attack-2

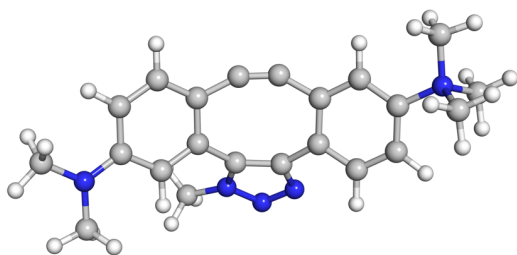


<i>E</i> (B3LYP)	<i>H</i> (B3LYP)	<i>G</i> (B3LYP)	<i>E</i> (M062X)
-1126.277017	-1125.823063	-1125.902076	-1126.221865

	X	Y	Z
6	-2.914467	1.133047	0.878282
6	-4.149959	0.518468	1.053198
6	-4.496570	-0.651575	0.334162
6	-3.493188	-1.211229	-0.497438
6	-1.938380	0.634366	0.004077
1	-2.704594	2.021827	1.464502
1	-4.845730	0.956906	1.757233
1	-3.657580	-2.150568	-1.008928
6	-2.252897	-0.596653	-0.642157
6	-0.689127	1.398390	-0.255208
6	0.706743	1.173385	-0.345185
6	1.655352	0.022381	-0.340666
6	1.403230	-1.229833	-0.963454
6	-1.134157	-1.212125	-1.271447
6	0.057347	-1.434438	-1.367258
6	2.420891	-2.186693	-1.060624
1	2.216379	-3.134422	-1.546141
6	2.933054	0.248056	0.193320
1	3.111629	1.205027	0.659566
6	3.927473	-0.722456	0.101877
6	3.683025	-1.942070	-0.532361
1	4.442824	-2.709539	-0.619171
7	5.297606	-0.484393	0.687247
7	-5.733731	-1.233830	0.452986
6	5.587770	-1.534279	1.743165
1	6.574492	-1.334764	2.160926
1	4.821901	-1.461250	2.514458
1	5.569650	-2.520910	1.285941

6	5.432872	0.869156	1.344318
1	6.448206	0.943353	1.731177
1	5.262864	1.648839	0.603798
1	4.719484	0.945207	2.163348
6	-6.015052	-2.498649	-0.214090
1	-5.394669	-3.320732	0.170898
1	-7.062178	-2.758048	-0.056164
1	-5.848380	-2.419642	-1.294707
6	-6.689762	-0.715376	1.423037
1	-6.919755	0.338663	1.226883
1	-7.618231	-1.281186	1.344360
1	-6.320849	-0.800172	2.455149
6	6.341500	-0.564326	-0.410714
1	6.318289	-1.554163	-0.861162
1	6.110211	0.195317	-1.156520
1	7.319448	-0.380787	0.034424
6	-1.954398	3.622753	-0.570345
1	-2.762477	3.071208	-1.049608
1	-1.654059	4.463017	-1.196255
7	-0.782813	2.759074	-0.428872
7	0.424728	3.332045	-0.584510
7	1.313553	2.386808	-0.528314
1	-2.290085	3.997074	0.399293

P12: *syn*-attack-1



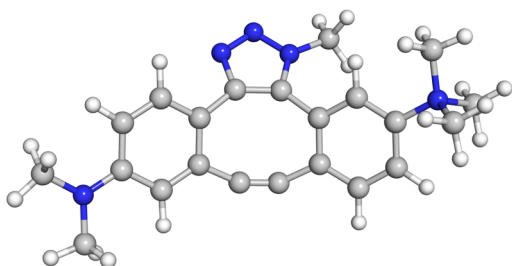
<i>E</i> (B3LYP)	<i>H</i> (B3LYP)	<i>G</i> (B3LYP)	<i>E</i> (M062X)
-1126.276554	-1125.822545	-1125.901852	-1126.221484

	X	Y	Z
6	2.654701	-2.216511	-1.194507
6	3.878564	-2.152982	-0.547248
6	4.206264	-1.042444	0.270890
6	3.265390	0.022981	0.339271

6	1.720572	-1.176314	-1.098866
1	2.401826	-3.099361	-1.773555
1	4.567040	-2.981688	-0.651771
1	3.488494	0.883699	0.954852
6	2.055534	-0.009714	-0.349482
6	0.366307	-1.244986	-1.496258
6	-0.819853	-0.974796	-1.416944
6	-1.865494	-0.358204	-0.678699
6	-1.482301	0.793301	0.063746
6	1.174088	1.197131	-0.330545
6	-0.188473	1.511083	-0.125480
6	-2.441995	1.370322	0.902625
1	-2.177497	2.247728	1.481146
6	-3.170854	-0.865512	-0.593639
1	-3.410738	-1.734276	-1.189463
6	-4.094885	-0.256570	0.248813
6	-3.733550	0.856115	1.009426
1	-4.429479	1.340979	1.683847
7	-5.501897	-0.784962	0.372929
7	5.383874	-0.991250	0.970481
6	-6.489615	0.297514	-0.019313
1	-7.496089	-0.109722	0.076540
1	-6.369751	1.153368	0.641017
1	-6.288364	0.585351	-1.050482
6	-5.759547	-1.210617	1.805919
1	-6.778101	-1.593405	1.869716
1	-5.040126	-1.986052	2.066092
1	-5.641519	-0.351896	2.462932
6	5.704490	0.162935	1.800960
1	4.943644	0.326554	2.574576
1	6.657319	-0.012756	2.299923
1	5.796290	1.081841	1.206479
6	6.346270	-2.080295	0.856537
1	6.697695	-2.205168	-0.176222
1	7.209409	-1.859648	1.484186
1	5.916637	-3.033553	1.190439
6	-5.762251	-1.980181	-0.513352
1	-5.607568	-1.696866	-1.553273
1	-5.097326	-2.793210	-0.226615
1	-6.798280	-2.279799	-0.362038
6	3.108146	2.810861	-0.893971
1	3.031929	3.744662	-1.450827

1	3.545077	2.036070	-1.522442
7	1.746809	2.432167	-0.513550
7	0.842383	3.420867	-0.412116
7	-0.311642	2.873539	-0.169444
1	3.733727	2.965934	-0.012446

P13: *syn*-attack-2

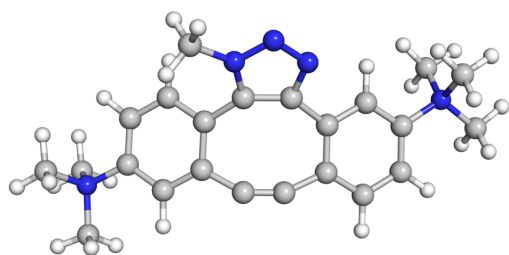


<i>E</i> (B3LYP)	<i>H</i> (B3LYP)	<i>G</i> (B3LYP)	<i>E</i> (M062X)
-1126.272397	-1125.818484	-1125.897842	-1126.217383

	X	Y	Z
6	-3.049711	1.300692	0.920965
6	-4.309860	0.726062	1.045434
6	-4.672168	-0.428299	0.306892
6	-3.677202	-0.991125	-0.527060
6	-2.059703	0.768713	0.084059
1	-2.826607	2.197334	1.489852
1	-5.018428	1.184266	1.724289
1	-3.870668	-1.892680	-1.093608
6	-2.413016	-0.408634	-0.632359
6	-0.800748	1.534309	-0.123711
6	0.565583	1.262917	-0.364000
6	1.480242	0.086259	-0.427890
6	1.189669	-1.068174	-1.208112
6	-1.333182	-0.983179	-1.353860
6	-0.164077	-1.177239	-1.632952
6	2.159703	-2.061782	-1.372651
1	1.939158	-2.924904	-1.990524
6	2.700938	0.130050	0.259301
1	2.886098	0.967474	0.915852

6	3.641136	-0.892343	0.116731
6	3.387492	-1.975816	-0.723508
1	4.107885	-2.771735	-0.870486
7	4.950656	-0.855325	0.862941
7	-5.929100	-0.980916	0.398733
6	6.101452	-0.823216	-0.125860
1	7.033838	-0.802415	0.438527
1	6.064481	-1.712224	-0.751230
1	6.002378	0.073412	-0.736718
6	5.070616	-2.087462	1.741463
1	6.017785	-2.030728	2.277563
1	4.233311	-2.090563	2.438290
1	5.048210	-2.979298	1.119511
6	-6.225118	-2.232656	-0.284109
1	-5.607035	-3.065158	0.082839
1	-7.272663	-2.487791	-0.121347
1	-6.067031	-2.141249	-1.365613
6	-6.882853	-0.456539	1.366535
1	-7.095583	0.603285	1.180608
1	-7.820239	-1.005879	1.275424
1	-6.524345	-0.556825	2.401346
6	5.088363	0.352410	1.759756
1	5.060131	1.257470	1.155333
1	4.287751	0.345619	2.497553
1	6.052266	0.277403	2.260636
6	2.451208	2.931707	-0.938100
1	3.107329	3.054761	-0.073532
1	2.345142	3.891027	-1.444002
7	1.109224	2.517131	-0.529924
7	0.185609	3.476670	-0.384999
7	-0.952234	2.895386	-0.133622
1	2.875161	2.198847	-1.624255

P14: *anti*-attack

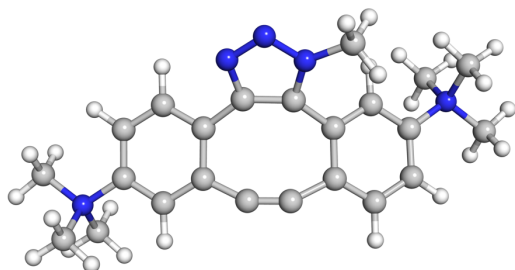


<i>E (B3LYP)</i>	<i>H (B3LYP)</i>	<i>G (B3LYP)</i>	<i>E (M062X)</i>
-1166.014129	-1165.515692	-1165.594682	-1165.949979

	X	Y	Z
6	-2.644069	-2.184701	-1.156190
6	-3.916714	-2.000471	-0.617376
6	-4.193058	-0.818251	0.063570
6	-3.223163	0.179003	0.194841
6	-1.659730	-1.203399	-1.022324
1	-2.413057	-3.105353	-1.679954
1	-4.647731	-2.786956	-0.739882
1	-3.436000	1.111694	0.700908
6	-1.944874	0.015202	-0.345128
6	-0.309175	-1.342027	-1.432327
6	0.878984	-1.092681	-1.377615
6	1.970751	-0.475634	-0.708799
6	1.634259	0.707626	0.004078
6	-1.026275	1.190462	-0.310252
6	0.360060	1.450233	-0.220008
6	2.583725	1.202376	0.904302
1	2.347253	2.054444	1.530382
6	3.241545	-1.051768	-0.598430
1	3.442405	-1.941237	-1.177698
6	4.178018	-0.490947	0.265112
6	3.843636	0.618637	1.039467
1	4.536233	1.053431	1.750002
7	5.557765	-1.076893	0.404518
7	-5.547783	-0.564695	0.674578
6	5.776319	-1.537460	1.834485
1	6.778042	-1.960832	1.903896
1	5.684485	-0.686621	2.505718
1	5.023962	-2.288812	2.070598
6	6.591980	-0.024684	0.045826
1	7.579734	-0.474475	0.143644
1	6.414198	0.292986	-0.980924
1	6.498265	0.820042	0.724612
6	-6.180481	0.650552	0.021545
1	-6.280422	0.451650	-1.044774
1	-7.157961	0.810431	0.476355
1	-5.546100	1.518791	0.184876
6	-6.496883	-1.726253	0.494240

1	-6.083142	-2.607525	0.981950
1	-7.440644	-1.451880	0.963055
1	-6.652542	-1.903974	-0.568472
6	5.784778	-2.266378	-0.500491
1	5.086630	-3.059204	-0.236817
1	5.656384	-1.958698	-1.537068
1	6.806473	-2.607278	-0.340193
6	-5.400955	-0.322251	2.165697
1	-4.929551	-1.198504	2.609265
1	-4.787966	0.560934	2.329951
1	-6.395472	-0.167708	2.583892
6	1.573799	3.718316	-0.460130
1	2.386016	3.219328	-0.987658
1	1.915004	4.047579	0.523359
7	0.424442	2.817441	-0.345237
7	-0.794631	3.359950	-0.480346
7	-1.662149	2.393153	-0.447942
1	1.237138	4.582051	-1.032568

P15: *syn*-attack



<i>E</i> (B3LYP)	<i>H</i> (B3LYP)	<i>G</i> (B3LYP)	<i>E</i> (M062X)
-1166.012662	-1165.514579	-1165.594479	-1165.948927

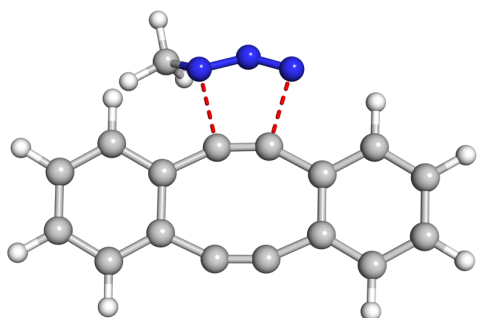
	X	Y	Z
6	-2.399640	-2.057882	-1.434352
6	-3.644033	-2.015671	-0.804388
6	-3.933127	-0.958804	0.051242
6	-3.014499	0.083085	0.234532
6	-1.459797	-1.048344	-1.231537
1	-2.148902	-2.902863	-2.065309
1	-4.338218	-2.824227	-0.984302
1	-3.237707	0.900651	0.907981
6	-1.784003	0.082597	-0.426963

6	-0.096096	-1.116765	-1.624660
6	1.075859	-0.906608	-1.380583
6	2.131931	-0.319974	-0.637043
6	1.755807	0.824640	0.120586
6	-0.887651	1.271908	-0.321541
6	0.471344	1.559100	-0.060304
6	2.719556	1.373804	0.969945
1	2.467917	2.245549	1.561843
6	3.422604	-0.848672	-0.554184
1	3.655665	-1.717070	-1.157543
6	4.359755	-0.258641	0.292918
6	4.008983	0.844212	1.066784
1	4.705266	1.318194	1.744624
7	5.742942	-0.852173	0.345401
7	-5.231176	-0.903827	0.814734
6	6.669518	-0.098081	1.270741
1	7.639575	-0.591460	1.233130
1	6.764222	0.929789	0.924425
1	6.277087	-0.134365	2.285494
6	6.361899	-0.821941	-1.040209
1	7.366168	-1.239646	-0.971723
1	5.757450	-1.417574	-1.720529
1	6.397198	0.214171	-1.375188
6	-5.984797	0.368821	0.474698
1	-6.161954	0.384937	-0.600138
1	-6.928467	0.358800	1.019585
1	-5.396442	1.231729	0.776902
6	-6.144282	-2.065090	0.493499
1	-5.651126	-2.996926	0.763724
1	-7.048207	-1.942281	1.087743
1	-6.393201	-2.043383	-0.566212
6	5.665274	-2.285827	0.837226
1	5.215640	-2.282649	1.829562
1	5.057864	-2.870363	0.149551
1	6.677948	-2.687058	0.874516
6	-4.945873	-0.945047	2.305657
1	-4.418237	-1.872397	2.526158
1	-4.335299	-0.088052	2.581549
1	-5.898686	-0.909583	2.833761
6	-2.790346	2.933217	-0.858670
1	-3.438383	3.056475	0.011856
1	-3.215803	2.199524	-1.542319

7	-1.444700	2.520540	-0.456432
7	-0.534757	3.490255	-0.277763
7	0.605702	2.919979	-0.029430
1	-2.687762	3.892448	-1.365077

8.1.3 Transition states

T1



Imaginary frequency at -353.4 cm^{-1}

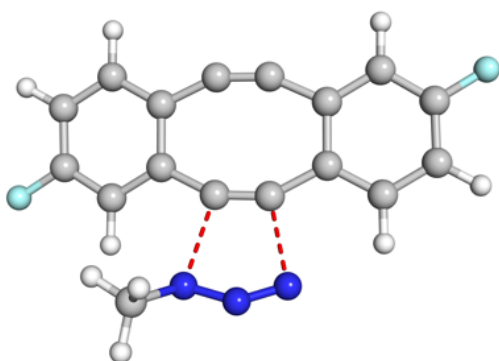
<i>E (B3LYP)</i>	<i>H (B3LYP)</i>	<i>G (B3LYP)</i>	<i>E (M062X)</i>
-818.459875	-818.210551	-818.271791	-818.4213750

<i>Distorted azide E (M06-2X)</i>	<i>Distorted alkyne E (M06-2X)</i>
-204.057463	-614.347525

	X	Y	Z
6	2.346418	3.128101	0.933593
1	1.971761	3.194204	1.960419
1	3.192737	2.441812	0.906091
7	1.335725	2.587206	0.011895
7	0.186289	3.085873	0.043106
7	-0.938043	2.817704	-0.123383
6	0.536421	0.451567	-0.229712
6	-0.699264	0.640370	-0.242487
6	-2.053860	0.114761	-0.168139
6	-2.215966	-1.263144	0.214250
6	-0.991318	-1.969093	0.423406
6	0.215575	-2.129697	0.427952
6	1.570548	-1.747649	0.174447
6	1.728365	-0.375063	-0.223879
6	2.998544	0.060227	-0.608213
1	3.121420	1.078952	-0.957414
6	2.678746	-2.593455	0.225861
1	2.545103	-3.624963	0.536813
6	-3.202420	0.862999	-0.438383

6	1.871517	-1.337608	0.177013
6	0.457253	0.645189	-0.195593
6	-0.792148	0.610553	-0.191356
6	-2.027279	-0.149772	-0.097128
6	-1.936221	-1.538056	0.273601
6	0.612991	-1.959711	0.444525
6	-0.602904	-2.015504	0.453387
6	-3.093490	-2.308057	0.399717
6	-3.291286	0.391464	-0.336023
1	-3.408287	1.430812	-0.613468
6	-4.419701	-0.417332	-0.208296
6	-4.353397	-1.751993	0.159099
1	-5.260620	-2.338761	0.250545
1	-3.009430	-3.352090	0.682860
1	2.881124	1.730029	-0.942805
9	-5.627738	0.136183	-0.451008
9	5.438852	-1.889075	-0.132780
6	1.754607	3.604320	0.950659
1	1.912407	4.636024	0.619085
1	2.711211	3.082603	0.926199
7	0.860120	2.889937	0.026112
7	-0.360272	3.172331	0.055969
7	-1.418360	2.705163	-0.101847
1	1.370663	3.601594	1.976000

T3: *syn*-attack

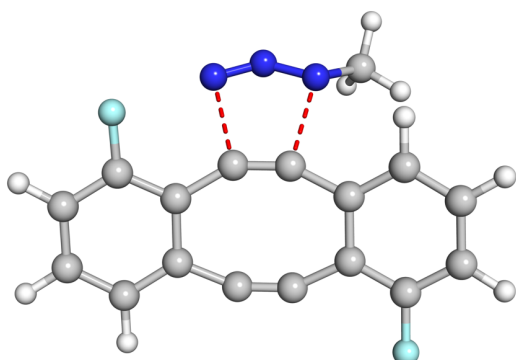


Imaginary frequency at -355.4 cm^{-1}

<i>E</i> (B3LYP)	<i>H</i> (B3LYP)	<i>G</i> (B3LYP)	<i>E</i> (M062X)
-1016.924788	-1016.690512	-1016.755854	-1016.926381

	X	Y	Z
6	-3.094908	1.146423	-0.497547
6	-4.405375	0.659791	-0.437779
6	-4.611337	-0.656136	-0.055130
6	-3.560631	-1.514683	0.260475
6	-2.000503	0.332877	-0.190702
1	-5.252301	1.292683	-0.679423
1	-3.764481	-2.540004	0.547901
6	-2.254415	-1.032287	0.189329
6	-0.617559	0.778523	-0.222440
6	0.605410	0.526316	-0.162723
6	1.742749	-0.371396	-0.118174
6	1.493671	-1.733146	0.273056
6	-1.082900	-1.808650	0.440869
6	0.112319	-2.035227	0.479971
6	2.548613	-2.642574	0.354783
6	3.044465	-0.004790	-0.460673
1	3.266835	0.997133	-0.805485
6	4.067211	-0.949492	-0.377653
6	3.853721	-2.255298	0.034922
1	4.682905	-2.951723	0.090869
1	2.347830	-3.664818	0.658021
1	-2.923612	2.176109	-0.784781
9	5.316547	-0.563515	-0.714140
9	-5.872181	-1.133436	0.013415
6	2.506956	3.088120	1.057712
1	3.316091	2.358134	1.069036
1	2.084515	3.171115	2.064415
7	1.515299	2.606006	0.082671
7	0.396490	3.170238	0.061015
7	-0.734350	2.967735	-0.145493
1	2.915919	4.055853	0.748846

T4: *anti*-attack



Imaginary frequency at -374.8 cm^{-1}

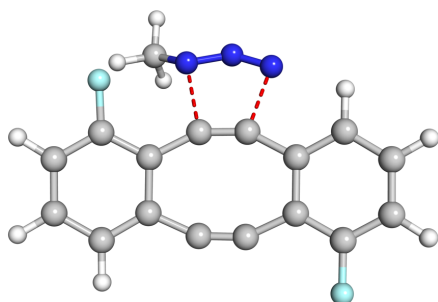
<i>E</i> (B3LYP)	<i>H</i> (B3LYP)	<i>G</i> (B3LYP)	<i>E</i> (M062X)
-1016.921179	-1016.686829	-1016.751638	-1016.922107

<i>Distorted azide</i> <i>E</i> (M06-2X)	<i>Distorted alkyne</i> <i>E</i> (M06-2X)
-204.058010	-812.847000

	X	Y	Z
6	3.315155	0.144191	-0.490142
6	4.421663	-0.689322	-0.323552
6	4.239417	-1.966520	0.195817
6	2.955426	-2.416538	0.523717
6	2.017995	-0.235219	-0.144475
1	5.401360	-0.320926	-0.608288
1	5.094637	-2.620426	0.332928
1	2.804538	-3.421736	0.902664
6	1.854036	-1.579510	0.345501
6	0.849673	0.614858	-0.242800
6	-0.395533	0.723045	-0.282602
6	-1.736782	0.179793	-0.373379
6	-1.911692	-1.174061	0.072394
6	0.490541	-1.955009	0.546768
6	-0.719487	-1.856788	0.457233
6	-3.185906	-1.729901	0.024960
6	-2.841279	0.871520	-0.875492
1	-2.709419	1.883191	-1.242094
6	-4.104597	0.267050	-0.919231
1	-4.950170	0.821702	-1.313378

6	-4.290625	-1.033716	-0.458633
1	-5.261255	-1.517075	-0.476128
9	-3.345979	-3.000051	0.451793
9	3.527996	1.363106	-1.024612
6	-1.745445	3.372258	1.199845
1	-2.687053	2.880854	0.955621
1	-1.874977	4.452588	1.077298
7	-0.746201	2.859124	0.250209
7	0.463089	3.095454	0.488066
7	1.532852	2.646776	0.369323
1	-1.479366	3.148085	2.237996

T5: *syn*-attack



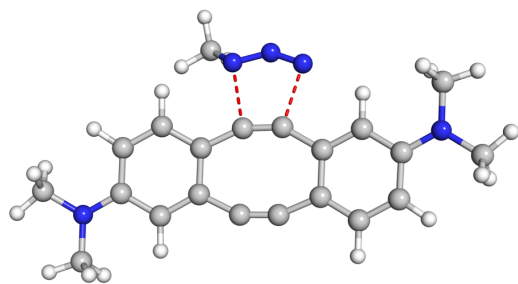
Imaginary frequency at -362.4 cm^{-1}

<i>E</i> (B3LYP)	<i>H</i> (B3LYP)	<i>G</i> (B3LYP)	<i>E</i> (M062X)
-1016.921945	-1016.687620	-1016.752726	-1016.921316

	X	Y	Z
6	3.013127	-0.438494	-0.595811
6	3.941569	-1.475487	-0.499721
6	3.531972	-2.712684	-0.015870
6	2.196047	-2.917174	0.347797
6	1.681063	-0.567650	-0.203611
1	4.963597	-1.291829	-0.812985
1	4.247202	-3.524771	0.065381
1	1.862439	-3.888901	0.695956
6	1.274890	-1.876029	0.242495
6	0.677547	0.475285	-0.241230
6	-0.509575	0.867204	-0.259599
6	-1.935089	0.584888	-0.274840

6	-2.346768	-0.733626	0.121633
6	-0.129777	-1.990208	0.474351
6	-1.297128	-1.650998	0.417240
6	-3.705513	-1.030304	0.144497
6	-2.915752	1.511175	-0.637565
1	-2.616981	2.508986	-0.933875
6	-4.272895	1.164442	-0.614655
1	-5.017442	1.899207	-0.904507
6	-4.681365	-0.105801	-0.216896
1	-5.727214	-0.390926	-0.184502
9	-4.083156	-2.269684	0.523881
9	3.449566	0.737853	-1.095278
6	2.879866	2.699766	1.209158
1	3.186596	3.748461	1.141948
1	3.707694	2.073845	0.881203
7	1.762262	2.425456	0.297930
7	0.697163	3.065875	0.422640
7	-0.451225	2.989613	0.216859
1	2.625702	2.459978	2.247711

T6: *anti*-attack



Imaginary frequency at -343.6 cm⁻¹

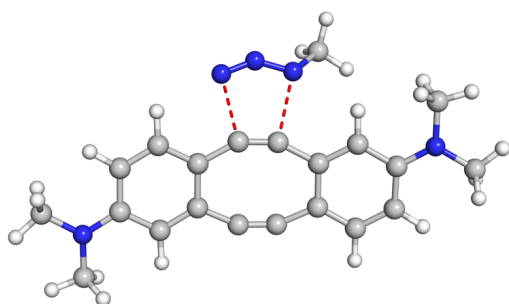
<i>E</i> (B3LYP)	<i>H</i> (B3LYP)	<i>G</i> (B3LYP)	<i>E</i> (M062X)
-1086.402226	-1085.997407	-1086.082296	-1086.345181

<i>Distorted azide</i> <i>E</i> (M06-2X)	<i>Distorted alkyne</i> <i>E</i> (M06-2X)
-204.056918	-882.272960

	X	Y	Z
6	2.829180	1.228001	-0.520621
6	4.137724	0.749623	-0.531159
6	4.434061	-0.579597	-0.147121
6	3.339192	-1.416179	0.199407
6	1.745527	0.429841	-0.143226
1	2.641919	2.248122	-0.837187
1	4.928862	1.419643	-0.843332
1	3.500718	-2.454506	0.459335
6	2.034006	-0.938387	0.194116
6	0.362349	0.844884	-0.108145
6	-0.876096	0.666429	-0.077641
6	-2.003154	-0.251842	0.016308
6	-1.714259	-1.625312	0.338413
6	0.870918	-1.729232	0.456377
6	-0.331096	-1.934296	0.476384
6	-2.775877	-2.525553	0.450415
1	-2.563947	-3.562733	0.694444
6	-3.325011	0.131641	-0.185846
1	-3.522037	1.165674	-0.425767
6	-4.402839	-0.790115	-0.078310
6	-4.095463	-2.131130	0.250253
1	-4.881038	-2.869850	0.346685
7	-5.700157	-0.379833	-0.284023
7	5.726782	-1.052246	-0.114679
6	-6.787013	-1.345277	-0.209628
1	-7.731724	-0.836338	-0.402402
1	-6.672941	-2.147545	-0.952052
1	-6.847918	-1.809143	0.783899
6	-5.988251	0.998532	-0.655115
1	-7.066286	1.119522	-0.763895
1	-5.644721	1.704650	0.112070
1	-5.516000	1.274873	-1.607999
6	5.984523	-2.461094	0.151606
1	5.548142	-3.118410	-0.614606
1	7.062002	-2.627420	0.170450
1	5.582708	-2.760164	1.127004
6	6.815345	-0.215196	-0.599511
1	6.871141	0.724969	-0.037648
1	7.759505	-0.743243	-0.462162
1	6.709541	0.030594	-1.666393
6	1.300512	4.036976	0.975155

1	1.303737	5.061808	0.587486
1	2.318775	3.649635	0.935805
7	0.481224	3.154748	0.132131
7	-0.765483	3.275797	0.191786
7	-1.752051	2.663204	0.055751
1	0.961689	4.041887	2.016818

T7: *syn*-attack



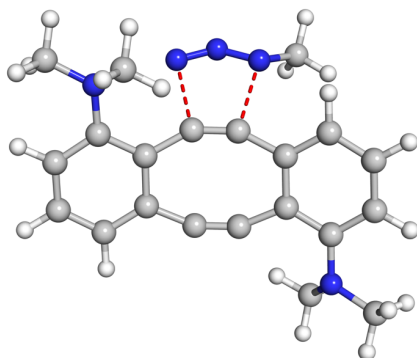
Imaginary frequency at -347.2 cm^{-1}

<i>E</i> (B3LYP)	<i>H</i> (B3LYP)	<i>G</i> (B3LYP)	<i>E</i> (M062X)
-1086.401966	-1085.997188	-1086.081202	-1086.345519

	X	Y	Z
6	2.966225	1.448209	-0.491905
6	4.295739	1.032246	-0.487829
6	4.646779	-0.298287	-0.159400
6	3.588491	-1.188340	0.165066
6	1.911091	0.584598	-0.180001
1	2.743622	2.478896	-0.741857
1	5.062288	1.755395	-0.737217
1	3.796626	-2.218013	0.426547
6	2.261862	-0.772235	0.149094
6	0.509593	0.952964	-0.154513
6	-0.697114	0.636878	-0.048509
6	-1.786817	-0.319205	0.020439
6	-1.437859	-1.672669	0.360671
6	1.145084	-1.620736	0.425400
6	-0.038044	-1.907379	0.495683
6	-2.455853	-2.623195	0.454255
1	-2.201203	-3.645105	0.720829

6	-3.114782	-0.008681	-0.255525
1	-3.345019	1.005229	-0.550470
6	-4.146892	-0.985341	-0.182486
6	-3.785575	-2.298437	0.201620
1	-4.536466	-3.073341	0.289217
7	-5.450166	-0.656835	-0.477474
7	5.956071	-0.722079	-0.157380
6	-6.499646	-1.656331	-0.338601
1	-7.455397	-1.212445	-0.618037
1	-6.322444	-2.519426	-0.993637
1	-6.582002	-2.024265	0.693708
6	-5.806278	0.710275	-0.828895
1	-6.871722	0.753236	-1.055851
1	-5.604551	1.413678	-0.008571
1	-5.258940	1.054282	-1.715686
6	6.290840	-2.067306	0.289599
1	5.804944	-2.829026	-0.332912
1	7.368892	-2.210169	0.210806
1	5.997139	-2.242272	1.334477
6	7.026899	0.231389	-0.410000
1	7.056454	1.031316	0.343945
1	7.983166	-0.292107	-0.389848
1	6.919232	0.698649	-1.396844
6	-2.671298	3.145557	1.267733
1	-3.433206	2.368915	1.335894
1	-3.152815	4.079291	0.956871
7	-1.698917	2.692071	0.262130
7	-0.608201	3.308199	0.190469
7	0.519585	3.150359	-0.071380
1	-2.211868	3.281437	2.252712

T8: *anti*-attack



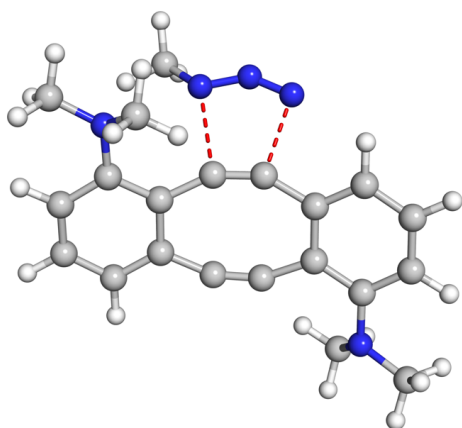
Imaginary frequency at -382.2 cm⁻¹

<i>E (B3LYP)</i>	<i>H (B3LYP)</i>	<i>G (B3LYP)</i>	<i>E (M062X)</i>
-1086.386596	-1085.982671	-1086.062345	-1086.332803

	X	Y	Z
6	-3.288846	-0.831794	0.227783
6	-3.961464	-2.054500	-0.016683
6	-3.286163	-3.189362	-0.446812
6	-1.899067	-3.172259	-0.612380
6	-1.893301	-0.774677	-0.027183
1	-5.028291	-2.118946	0.159492
1	-3.841182	-4.107226	-0.619080
1	-1.358528	-4.067278	-0.902398
6	-1.203622	-1.984997	-0.386830
6	-1.088594	0.431767	0.005614
6	0.028856	0.982205	0.125471
6	1.453899	0.971925	0.404026
6	2.159511	-0.247743	0.132346
6	0.220910	-1.859533	-0.445920
6	1.296677	-1.319141	-0.254318
6	3.554594	-0.343582	0.357733
6	2.141164	2.056787	0.951320
1	1.604106	2.970541	1.180988
6	3.510216	1.945707	1.210777
1	4.045159	2.789608	1.637346
6	4.208663	0.782129	0.908336
1	5.275881	0.749710	1.089937
7	4.239138	-1.542277	0.101628
7	-3.989951	0.291851	0.681283
6	-3.503470	1.000490	1.864992
1	-3.870686	2.032034	1.846476
1	-3.858522	0.524412	2.794690
1	-2.415288	1.030163	1.881295
6	-5.443708	0.278276	0.606762
1	-5.916390	-0.356064	1.376322
1	-5.805577	1.301125	0.750475
1	-5.772606	-0.063490	-0.378121
6	5.594064	-1.673628	0.623697
1	5.894411	-2.722324	0.540890
1	6.334901	-1.066108	0.076662
1	5.623524	-1.393786	1.680033

6	4.099492	-2.155452	-1.222686
1	4.727779	-1.649826	-1.974587
1	4.409682	-3.203470	-1.164629
1	3.062828	-2.130152	-1.557772
6	0.671064	3.657692	-1.698164
1	0.418313	4.717707	-1.808749
1	1.654148	3.583122	-1.232786
7	-0.269452	2.988132	-0.789960
7	-1.422456	2.734701	-1.223608
7	-2.287406	1.955496	-1.132021
1	0.701976	3.183068	-2.685022

T9: *syn*-attack



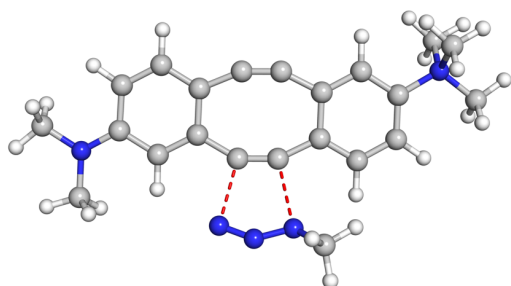
Imaginary frequency at -358.5 cm^{-1}

<i>E</i> (B3LYP)	<i>H</i> (B3LYP)	<i>G</i> (B3LYP)	<i>E</i> (M062X)
-1086.387378	-1085.983427	-1086.063232	-1086.333758

<i>Distorted azide</i> <i>E</i> (M06-2X)	<i>Distorted alkyne</i> <i>E</i> (M06-2X)
-204.056694	-882.260665

	X	Y	Z
6	-3.025150	0.929448	-0.409639
6	-3.624197	2.204579	-0.248737
6	-2.893695	3.315928	0.148734
6	-1.516720	3.222785	0.366280
6	-1.644421	0.800634	-0.097023
1	-4.677236	2.329553	-0.467927

1	-3.395562	4.273684	0.252895
1	-0.929524	4.096965	0.627411
6	-0.892800	1.985169	0.227512
6	-0.887401	-0.432634	-0.057369
6	0.164339	-1.107496	-0.099881
6	1.603603	-1.185254	-0.293716
6	2.367638	0.010792	-0.073048
6	0.518911	1.775416	0.337030
6	1.559185	1.154574	0.202314
6	3.776309	0.009642	-0.218739
6	2.258041	-2.351812	-0.692057
1	1.685837	-3.257319	-0.856145
6	3.643198	-2.338419	-0.876639
1	4.150710	-3.246014	-1.191678
6	4.392050	-1.191907	-0.635324
1	5.467834	-1.233793	-0.754605
7	4.516036	1.187633	-0.014571
7	-3.787755	-0.166300	-0.829633
6	-3.290062	-0.994123	-1.929443
1	-3.753700	-1.983949	-1.874130
1	-3.535813	-0.548754	-2.907705
1	-2.211809	-1.123770	-1.862950
6	-5.238364	-0.031368	-0.862187
1	-5.599545	0.594421	-1.695711
1	-5.672462	-1.028596	-0.980317
1	-5.607380	0.389797	0.076623
6	5.899386	1.204084	-0.473989
1	6.255626	2.238474	-0.456715
1	6.577372	0.603488	0.156119
1	5.962784	0.839455	-1.502561
6	4.355771	1.893484	1.260455
1	4.924195	1.407390	2.070899
1	4.724223	2.918293	1.149693
1	3.306395	1.943145	1.550005
6	-3.294334	-1.752642	2.077171
1	-3.966242	-2.617466	2.119347
1	-3.875182	-0.876953	1.790478
7	-2.276768	-1.924860	1.038128
7	-1.370539	-2.773094	1.199574
7	-0.276299	-3.016945	0.860938
1	-2.850961	-1.588370	3.065699

T10: *anti*-attack-1

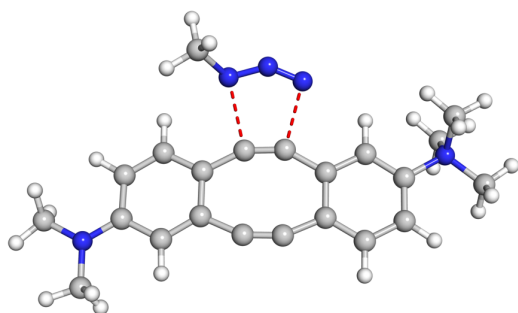
Imaginary frequency at -357.9 cm⁻¹

<i>E</i> (B3LYP)	<i>H</i> (B3LYP)	<i>G</i> (B3LYP)	<i>E</i> (M062X)
-1126.146144	-1125.696971	-1125.780392	-1126.079663

	X	Y	Z
6	2.997356	-2.514413	0.543414
6	4.321876	-2.163121	0.308852
6	4.663001	-0.846527	-0.085476
6	3.608193	0.100949	-0.215861
6	1.959259	-1.589480	0.405169
1	2.762363	-3.533155	0.837258
1	5.088988	-2.917068	0.430706
1	3.827937	1.119554	-0.498855
6	2.283028	-0.241602	0.019670
6	0.571646	-1.845000	0.568801
6	-0.627185	-1.619087	0.558458
6	-1.757205	-0.813245	0.235700
6	-1.439621	0.529827	-0.174421
6	1.179825	0.702022	-0.098918
6	-0.049232	0.928967	-0.127959
6	-2.480300	1.340101	-0.620948
1	-2.258293	2.337033	-0.981790
6	-3.082144	-1.245833	0.241025
1	-3.284956	-2.258772	0.567283
6	-4.102554	-0.387445	-0.187348
6	-3.809301	0.894878	-0.632365
1	-4.571445	1.573224	-0.988889
7	-5.517993	-0.904729	-0.160752
7	5.963253	-0.484143	-0.331631
6	-6.520686	0.111812	-0.652812
1	-7.507689	-0.342890	-0.583721
1	-6.475991	0.996355	-0.019995

1	-6.300108	0.361681	-1.689215
6	-5.899103	-1.271201	1.261551
1	-6.925991	-1.636761	1.255948
1	-5.229422	-2.046911	1.625753
1	-5.812724	-0.377630	1.878883
6	6.289192	0.881905	-0.721858
1	5.997505	1.605807	0.050350
1	7.366058	0.961354	-0.870037
1	5.795073	1.164272	-1.660629
6	7.031469	-1.464675	-0.190234
1	6.888249	-2.317647	-0.866615
1	7.983313	-0.993944	-0.436048
1	7.095665	-1.849711	0.836296
6	-5.633372	-2.127976	-1.051142
1	-5.347369	-1.840617	-2.062357
1	-4.973190	-2.908837	-0.680511
1	-6.667549	-2.471728	-1.027227
6	-0.942376	4.002776	1.026755
1	-0.598198	3.903175	2.061375
1	-1.965009	3.633099	0.952548
7	-0.133381	3.197248	0.098064
7	1.113673	3.301051	0.168927
7	2.099380	2.690604	0.036000
1	-0.932337	5.058102	0.734904

T11: *anti*-attack-2



Imaginary frequency at -349.7 cm^{-1}

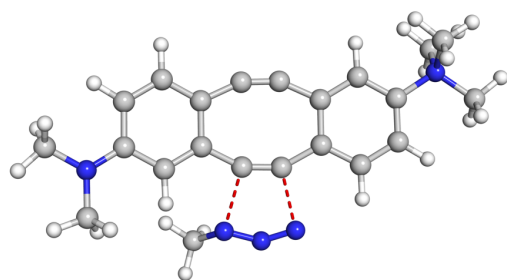
<i>E</i> (B3LYP)	<i>H</i> (B3LYP)	<i>G</i> (B3LYP)	<i>E</i> (M062X)
-1126.147214	-1125.697851	-1125.781360	-1126.080357

	X	Y	Z
--	---	---	---

6	3.116850	1.233699	0.536282
6	4.421493	0.748756	0.547742
6	4.716264	-0.581299	0.160486
6	3.618310	-1.412804	-0.195364
6	2.031157	0.440607	0.151310
1	2.933920	2.252927	0.857621
1	5.214936	1.414193	0.863502
1	3.775497	-2.450152	-0.460856
6	2.319514	-0.924834	-0.191217
6	0.651155	0.857926	0.112317
6	-0.586198	0.670055	0.076160
6	-1.702771	-0.246189	-0.033212
6	-1.427349	-1.619933	-0.367049
6	1.152350	-1.709771	-0.456206
6	-0.042713	-1.935273	-0.505295
6	-2.477002	-2.523209	-0.502318
1	-2.264513	-3.555742	-0.757106
6	-3.032917	0.129782	0.159069
1	-3.232690	1.163247	0.405194
6	-4.067913	-0.804868	0.028802
6	-3.805251	-2.126710	-0.306344
1	-4.585748	-2.865828	-0.418846
7	-5.478757	-0.319763	0.253618
7	6.001675	-1.059262	0.137799
6	-6.504224	-1.419915	0.117015
1	-7.482493	-0.981034	0.306991
1	-6.471294	-1.821834	-0.894051
1	-6.297774	-2.195829	0.852446
6	-5.814510	0.752414	-0.765487
1	-6.841089	1.076849	-0.594746
1	-5.132805	1.590992	-0.642487
1	-5.706869	0.322033	-1.760497
6	6.263921	-2.452701	-0.200490
1	5.884300	-2.698961	-1.199686
1	7.340786	-2.621216	-0.200202
1	5.808343	-3.145144	0.520866
6	7.101084	-0.211287	0.579819
1	6.996174	0.079982	1.634124
1	8.038643	-0.756029	0.468293
1	7.166186	0.703143	-0.022957
6	-5.609224	0.251010	1.653132
1	-5.362318	-0.534901	2.366048

1	-4.927850	1.091017	1.765654
1	-6.637806	0.585058	1.789904
6	1.566200	4.012579	-0.967878
1	1.213383	3.997975	-2.004288
1	2.582864	3.621711	-0.931804
7	0.751513	3.150785	-0.097431
7	-0.493954	3.268824	-0.151010
7	-1.482904	2.661747	-0.019229
1	1.575844	5.043021	-0.596983

T12: *syn*-attack-1



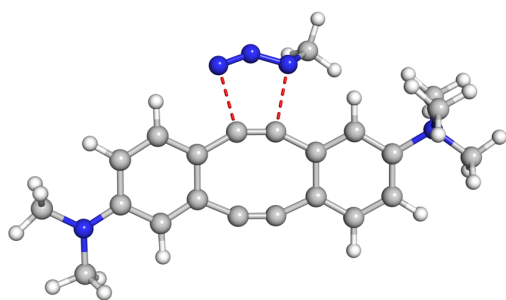
Imaginary frequency at -357.3 cm^{-1}

<i>E</i> (B3LYP)	<i>H</i> (B3LYP)	<i>G</i> (B3LYP)	<i>E</i> (M062X)
-1126.146491	-1125.697299	-1125.780349	-1126.080436

	X	Y	Z
6	-2.715264	-2.590090	0.558344
6	-4.044572	-2.298735	0.273731
6	-4.426560	-1.009450	-0.171896
6	-3.409531	-0.017730	-0.276582
6	-1.713244	-1.624618	0.435509
1	-2.447313	-3.594441	0.872796
1	-4.782795	-3.082688	0.383393
1	-3.652540	0.978997	-0.617312
6	-2.083530	-0.296865	0.029384
6	-0.313324	-1.820755	0.591979
6	0.870055	-1.532228	0.530255
6	1.962883	-0.679772	0.202865
6	1.596399	0.651379	-0.209464
6	-1.009575	0.676375	-0.072437
6	0.190336	1.006679	-0.187591
6	2.616930	1.518421	-0.593662

1	2.369040	2.523530	-0.909827
6	3.304556	-1.057492	0.233798
1	3.540933	-2.064625	0.555280
6	4.298594	-0.150492	-0.152686
6	3.963025	1.129413	-0.574299
1	4.706441	1.849690	-0.885681
7	5.733817	-0.607600	-0.096317
7	-5.728293	-0.717670	-0.491258
6	6.706135	0.467692	-0.519230
1	7.709186	0.051906	-0.436953
1	6.506052	0.749713	-1.551408
1	6.605278	1.324019	0.145482
6	5.930132	-1.794574	-1.020862
1	6.976427	-2.096750	-0.971013
1	5.290487	-2.612934	-0.697829
1	5.666995	-1.485920	-2.032050
6	-6.096680	0.612176	-0.959899
1	-5.549910	0.886074	-1.871335
1	-7.161952	0.624886	-1.189905
1	-5.904730	1.381416	-0.199905
6	-6.757471	-1.740395	-0.356660
1	-6.837891	-2.099320	0.677863
1	-7.720077	-1.317881	-0.644304
1	-6.556506	-2.604441	-1.003856
6	6.087653	-1.005049	1.324402
1	5.941154	-0.137696	1.967188
1	5.444885	-1.822528	1.642146
1	7.129948	-1.323293	1.338736
6	-2.977421	3.075897	1.309464
1	-2.487171	3.219695	2.277612
1	-3.695165	2.259521	1.389798
7	-2.021515	2.689688	0.259551
7	-0.945346	3.327055	0.184343
7	0.182361	3.206622	-0.089817
1	-3.515105	3.987690	1.028788

T13: *syn-attack-2*



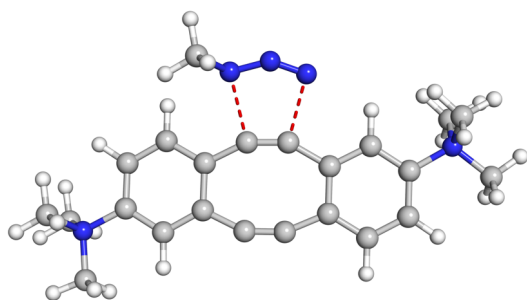
Imaginary frequency at -359.0 cm^{-1}

<i>E (B3LYP)</i>	<i>H (B3LYP)</i>	<i>G (B3LYP)</i>	<i>E (M062X)</i>
-1126.145487	-1125.696280	-1125.779957	-1126.079524

	X	Y	Z
6	-3.240024	1.435476	0.527816
6	-4.562002	1.000785	0.527061
6	-4.904337	-0.320927	0.150909
6	-3.838316	-1.189060	-0.212611
6	-2.178968	0.595722	0.170234
1	-3.027138	2.458783	0.813414
1	-5.334124	1.702297	0.817251
1	-4.035248	-2.213940	-0.499372
6	-2.521250	-0.751278	-0.199508
6	-0.785053	0.976787	0.135735
6	0.425022	0.687461	-0.011380
6	1.509976	-0.262139	-0.106947
6	1.181493	-1.612657	-0.482037
6	-1.394503	-1.574287	-0.512243
6	-0.217073	-1.859740	-0.630548
6	2.191074	-2.561077	-0.602706
1	1.941467	-3.574737	-0.896613
6	2.841618	0.036758	0.186089
1	3.069133	1.041668	0.517329
6	3.834979	-0.947532	0.082844
6	3.525155	-2.238131	-0.325697
1	4.272505	-3.012168	-0.426019
7	5.248708	-0.562159	0.441895
7	-6.205168	-0.754480	0.137407
6	6.221834	-1.707448	0.290068
1	7.206664	-1.339075	0.573248

1	5.926933	-2.519962	0.951805
1	6.233473	-2.033390	-0.748667
6	5.300153	-0.106126	1.888122
1	6.331930	0.151337	2.127772
1	4.660356	0.764543	2.013571
1	4.952102	-0.925048	2.516517
6	-6.524472	-2.117958	-0.266776
1	-6.070692	-2.859531	0.404225
1	-7.605662	-2.252944	-0.238321
1	-6.183524	-2.326367	-1.289102
6	-7.277227	0.145996	0.540236
1	-7.335972	1.025035	-0.115348
1	-8.228262	-0.383538	0.483836
1	-7.142814	0.497319	1.571755
6	5.722983	0.560557	-0.460204
1	5.654397	0.220598	-1.492961
1	5.096064	1.435577	-0.305902
1	6.755161	0.795289	-0.200508
6	2.278542	3.160666	-1.372806
1	2.984949	2.349508	-1.550988
1	2.840644	4.057815	-1.092860
7	1.404680	2.724704	-0.270388
7	0.318944	3.337738	-0.126738
7	-0.798136	3.180046	0.169990
1	1.716861	3.348896	-2.293133

T14: *anti*-attack



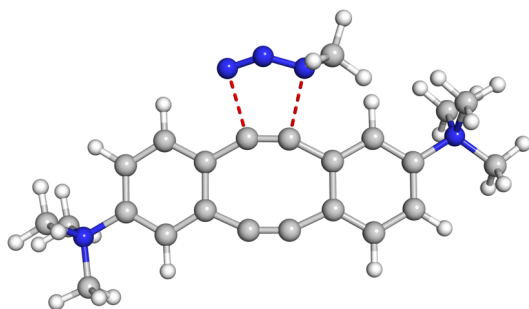
Imaginary frequency at -358.6 cm^{-1}

<i>E</i> (B3LYP)	<i>H</i> (B3LYP)	<i>G</i> (B3LYP)	<i>E</i> (M062X)
-1165.885010	-1165.391416	-1165.475032	-1165.809834

	X	Y	Z
6	-2.726947	-2.501589	-0.597618
6	-4.058826	-2.135118	-0.371116
6	-4.345164	-0.834200	0.021560
6	-3.325344	0.113213	0.180980
6	-1.694831	-1.583780	-0.434007
1	-2.499920	-3.518111	-0.898720
1	-4.826872	-2.883138	-0.507565
1	-3.539419	1.132885	0.469242
6	-1.994255	-0.234928	-0.038209
6	-0.304550	-1.858547	-0.597594
6	0.888061	-1.623239	-0.555492
6	2.031526	-0.828127	-0.239588
6	1.725396	0.507620	0.178376
6	-0.890511	0.697717	0.098842
6	0.338394	0.920798	0.135067
6	2.776919	1.307048	0.628612
1	2.568357	2.302634	1.000386
6	3.349761	-1.286097	-0.257928
1	3.529555	-2.297818	-0.592025
6	4.377724	-0.442233	0.166150
6	4.093803	0.842416	0.624893
1	4.872351	1.506448	0.980898
7	5.813613	-0.897015	0.148463
7	-5.762071	-0.385129	0.271614

6	6.380409	-0.857223	1.556317
1	7.412001	-1.207058	1.517753
1	6.347370	0.163150	1.931738
1	5.776993	-1.511444	2.184462
6	6.621184	0.018021	-0.754578
1	7.652781	-0.333171	-0.760246
1	6.193867	-0.027213	-1.755661
1	6.575992	1.034862	-0.371422
6	-6.126630	0.706903	-0.717232
1	-6.017030	0.305322	-1.724025
1	-7.158538	1.004358	-0.530993
1	-5.461948	1.556242	-0.575646
6	-6.767377	-1.502078	0.113438
1	-6.539919	-2.293307	0.826093
1	-7.751580	-1.086397	0.323651
1	-6.737171	-1.874782	-0.908822
6	5.977786	-2.307595	-0.367834
1	5.437963	-2.994219	0.282191
1	5.608126	-2.362889	-1.390426
1	7.041382	-2.539982	-0.347572
6	-5.892716	0.146010	1.687396
1	-5.618658	-0.651222	2.377384
1	-5.233819	1.001632	1.815590
1	-6.928385	0.448698	1.841236
6	1.236850	3.986980	-0.986005
1	2.257754	3.612783	-0.915444
1	1.229667	5.038786	-0.683204
7	0.423790	3.178661	-0.061236
7	-0.821149	3.286077	-0.128093
7	-1.811894	2.683878	-0.004421
1	0.889116	3.895809	-2.019720

T15: *syn*-attack



Imaginary frequency at -363.7 cm⁻¹

<i>E (B3LYP)</i>	<i>H (B3LYP)</i>	<i>G (B3LYP)</i>	<i>E (M062X)</i>
-1165.883856	-1165.390319	-1165.473499	-1165.809354

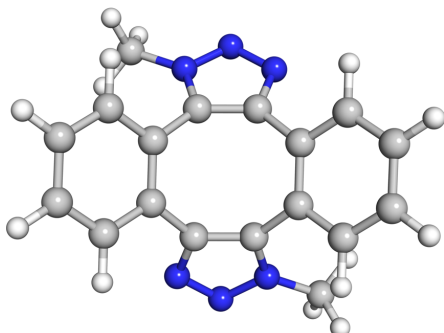
	X	Y	Z
6	-2.470809	-2.527236	-0.695111
6	-3.804582	-2.228261	-0.392119
6	-4.128329	-0.960028	0.071683
6	-3.144297	0.030295	0.208082
6	-1.472902	-1.571773	-0.542204
1	-2.214103	-3.524327	-1.034874
1	-4.544151	-3.005885	-0.518460
1	-3.379154	1.020208	0.577784
6	-1.815140	-0.247189	-0.104755
6	-0.072053	-1.789130	-0.711495
6	1.106145	-1.508210	-0.600250
6	2.216182	-0.686621	-0.240997
6	1.867159	0.628173	0.212204
6	-0.736173	0.711222	0.029344
6	0.467767	1.008507	0.184276
6	2.900844	1.465513	0.636633
1	2.670540	2.463296	0.986738
6	3.549158	-1.099879	-0.279678
1	3.759390	-2.098211	-0.635593
6	4.552859	-0.228188	0.144300
6	4.231899	1.045000	0.610830
1	4.993566	1.735446	0.953224
7	6.002555	-0.636431	0.109148
7	-5.543294	-0.605445	0.450391
6	6.581344	-0.589564	1.511835
1	7.625299	-0.898765	1.459269
1	6.512680	0.424944	1.898112
1	6.010246	-1.273201	2.138988
6	6.773002	0.310644	-0.793181
1	7.814700	-0.008888	-0.811521
1	6.338002	0.261327	-1.790726
1	6.701011	1.322237	-0.400410
6	-6.035003	0.540880	-0.413288
1	-5.964099	0.236871	-1.457088
1	-7.069805	0.751114	-0.143619
1	-5.420742	1.419433	-0.229994

6	-6.504310	-1.757178	0.265139
1	-6.194740	-2.589803	0.894347
1	-7.490434	-1.410735	0.570521
1	-6.522926	-2.044110	-0.784946
6	6.206438	-2.037182	-0.419593
1	5.691717	-2.744778	0.228240
1	5.832207	-2.095987	-1.440318
1	7.276619	-2.237590	-0.407797
6	-5.591930	-0.198057	1.911946
1	-5.233859	-1.034274	2.511161
1	-4.960269	0.674229	2.064256
1	-6.624896	0.041839	2.163425
7	0.486034	3.204405	0.199110
7	-0.629507	3.345705	-0.106640
7	-1.710081	2.728200	-0.252197
6	-2.579036	3.137327	-1.369976
1	-2.009710	3.316191	-2.286883
1	-3.276616	2.317095	-1.539366
1	-3.149826	4.032900	-1.104916

8.1.4 Second click

Products: triazole

P16: *anti*-attack

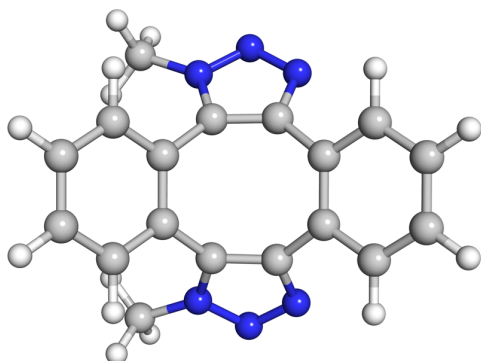


<i>E</i> (B3LYP)	<i>H</i> (B3LYP)	<i>G</i> (B3LYP)	<i>E</i> (M06-2X)
-1022.825245	-1022.509607	-1022.575068	-1022.797320

	X	Y	Z
6	-3.375157	1.594410	-1.668624
1	-4.072137	2.058238	-0.966299
1	-3.595254	0.529592	-1.752625
7	-1.995386	1.774103	-1.229267
7	-1.268428	2.786107	-1.743123
7	-0.073163	2.725084	-1.216718
6	-1.254635	1.033651	-0.353254
6	-0.011215	1.658442	-0.366782
6	1.205203	1.367825	0.414113
6	1.801729	0.087140	0.435023
6	1.254636	-1.033652	-0.353253
6	0.011216	-1.658442	-0.366782
6	-1.205203	-1.367826	0.414113
6	-1.801730	-0.087141	0.435022
6	-2.962130	0.115389	1.200778
1	-3.406258	1.105305	1.241134
6	-1.811478	-2.412898	1.127198
1	-1.356160	-3.397760	1.094620
6	1.811478	2.412897	1.127198
1	1.356161	3.397759	1.094618
6	2.962128	-0.115390	1.200782
1	3.406255	-1.105306	1.241138
6	3.544616	0.929805	1.914349
1	4.440111	0.749457	2.501527

6	2.971800	2.202190	1.869260
1	3.420819	3.025638	2.416905
6	-2.971800	-2.202191	1.869259
1	-3.420819	-3.025638	2.416905
6	-3.544617	-0.929806	1.914345
1	-4.440113	-0.749459	2.501523
6	3.375156	-1.594406	-1.668629
1	3.470843	-2.071611	-2.643830
1	4.072143	-2.058199	-0.966287
7	1.995387	-1.774104	-1.229266
7	1.268428	-2.786107	-1.743123
7	0.073164	-2.725084	-1.216719
1	3.595239	-0.529587	-1.752666
1	-3.470838	2.071582	-2.643842

P17: *syn*-attack



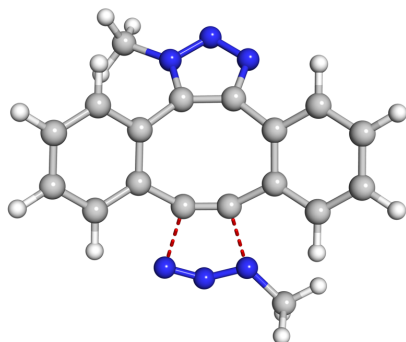
<i>E</i> (B3LYP)	<i>H</i> (B3LYP)	<i>G</i> (B3LYP)	<i>E</i> (M06-2X)
-1022.824745	-1022.509152	-1022.574628	-1022.796745

	X	Y	Z
6	-2.306827	2.899089	-1.406433
1	-2.301772	3.377333	-2.385769
1	-2.650278	3.613620	-0.654230
7	-0.942526	2.464013	-1.126867
7	0.084057	3.062918	-1.761414
7	1.188973	2.490514	-1.359781
6	-0.494432	1.475208	-0.299699
6	0.886465	1.499782	-0.468904
6	1.950551	0.706500	0.177105

6	1.950544	-0.706510	0.177101
6	0.886450	-1.499782	-0.468910
6	-0.494447	-1.475199	-0.299703
6	-1.363399	-0.706510	0.609178
6	-1.363390	0.706523	0.609182
6	-2.204027	1.389848	1.502195
1	-2.188959	2.475148	1.521610
6	-2.204048	-1.389830	1.502183
1	-2.188997	-2.475130	1.521588
6	3.041351	1.388912	0.738810
1	3.040096	2.474496	0.724395
6	3.041338	-1.388935	0.738802
1	3.040073	-2.474519	0.724382
6	4.113769	-0.698327	1.299110
1	4.944634	-1.247823	1.732330
6	4.113776	0.698291	1.299114
1	4.944646	1.247776	1.732337
6	-3.040835	-0.697692	2.375199
1	-3.681478	-1.247463	3.057980
6	-3.040824	0.697716	2.375205
1	-3.681457	1.247492	3.057992
6	-2.306849	-2.899091	-1.406408
1	-2.971036	-2.034000	-1.419081
1	-2.650224	-3.613739	-0.654281
7	-0.942546	-2.464003	-1.126869
7	0.084031	-3.062916	-1.761416
7	1.188952	-2.490516	-1.359787
1	-2.301846	-3.377199	-2.385811
1	-2.970984	2.033977	-1.419273

Transition states

T16: *anti*-attack



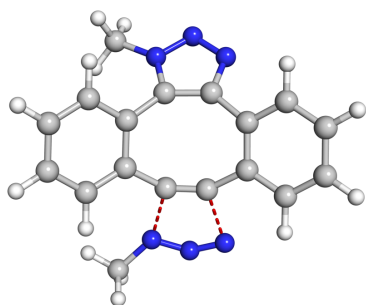
Imaginary frequency at -299.5 cm^{-1}

<i>E</i> (B3LYP)	<i>H</i> (B3LYP)	<i>G</i> (B3LYP)	<i>E</i> (M06-2X)
-1022.674256	-1022.363647	-1022.433574	-1022.634474

	X	Y	Z
6	-3.606833	-1.280026	1.686361
1	-4.392938	-1.665681	1.033130
1	-3.695167	-0.196531	1.764255
7	-2.281946	-1.633613	1.181244
7	-1.689478	-2.731015	1.683111
7	-0.503636	-2.816167	1.149118
6	-1.464269	-0.980253	0.294053
6	-0.297914	-1.764228	0.298985
6	1.029704	-1.709611	-0.367131
6	1.811578	-0.524953	-0.460086
6	1.169228	0.699078	-0.093755
6	0.142282	1.391246	-0.038407
6	-1.230479	1.441872	-0.455628
6	-1.967597	0.225554	-0.415457
6	-3.236579	0.197786	-1.009916
1	-3.793502	-0.733339	-1.035461
6	-1.812556	2.591247	-1.006010
1	-1.242278	3.514212	-1.007214
6	1.593209	-2.912507	-0.814642
1	1.007182	-3.822366	-0.737898
6	3.109950	-0.582788	-0.989652
1	3.687904	0.332592	-1.060088
6	3.645325	-1.790570	-1.431239
1	4.650016	-1.819129	-1.842727

6	2.883315	-2.957501	-1.345279
1	3.290401	-3.903769	-1.689689
6	-3.089258	2.544480	-1.565905
1	-3.523023	3.441983	-1.997150
6	-3.794867	1.341772	-1.585598
1	-4.779084	1.287928	-2.040936
6	4.099241	2.359204	1.152704
1	4.383610	2.808504	2.109946
1	4.409904	3.015965	0.332569
7	2.661851	2.070653	1.110144
7	1.831994	2.996058	1.192688
7	0.722624	3.304579	1.015485
1	4.609022	1.400033	1.055147
1	-3.702793	-1.732674	2.673192

T17: *syn*-attack



Imaginary frequency at -302.6 cm⁻¹

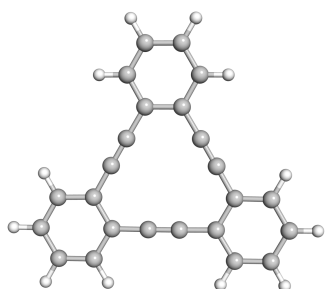
<i>E</i> (B3LYP)	<i>H</i> (B3LYP)	<i>G</i> (B3LYP)	<i>E</i> (M06-2X)
-1022.673918	-1022.363311	-1022.433102	-1022.634384

	X	Y	Z
6	1.718185	-3.316875	-1.570560
1	2.501796	-2.560521	-1.614459
1	1.542528	-3.727534	-2.564732
7	0.464801	-2.705871	-1.133436
7	-0.677050	-3.140265	-1.693413
7	-1.649682	-2.415825	-1.215320
6	0.236339	-1.668675	-0.264810
6	-1.154428	-1.484683	-0.343511
6	-2.149028	-0.556276	0.257304

6	-1.964311	0.852409	0.322051
6	-0.658429	1.360925	0.011859
6	0.561760	1.157541	0.090575
6	1.609478	0.307364	0.567239
6	1.368278	-1.094003	0.508026
6	2.264566	-1.950548	1.161951
1	2.071730	-3.018459	1.172147
6	2.756193	0.790008	1.213099
1	2.925104	1.860901	1.250322
6	-3.389259	-1.081072	0.645369
1	-3.541572	-2.154022	0.590017
6	-3.015931	1.677054	0.747809
1	-2.858295	2.750254	0.774405
6	-4.237577	1.129477	1.135821
1	-5.039832	1.780034	1.472083
6	-4.422208	-0.253308	1.089618
1	-5.369311	-0.690448	1.392607
6	3.649756	-0.085628	1.828321
1	4.530847	0.304859	2.328812
6	3.395048	-1.456894	1.817052
1	4.070620	-2.146055	2.314520
6	2.627251	3.816070	-1.039375
1	2.593144	4.531251	-0.210071
1	2.771361	4.354201	-1.982021
7	1.426003	2.975659	-1.090154
7	0.301185	3.494542	-1.225914
7	-0.845854	3.340217	-1.098950
1	2.021779	-4.120335	-0.895560
1	3.470174	3.139345	-0.894784

8.1.5 Trimers

M1

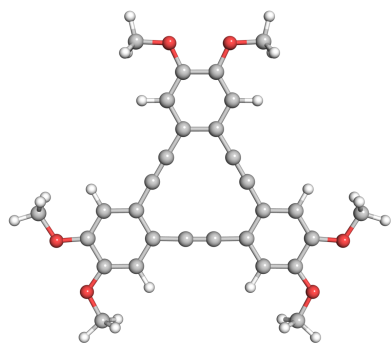


<i>E</i> (B3LYP)	<i>H</i> (B3LYP)	<i>G</i> (B3LYP)	<i>E</i> (M06-2X)
-921.643178	-921.352636	-921.418064	-921.602338

	X	Y	Z
6	-2.414803	-1.511674	0.000175
6	-1.377664	-2.494739	-0.000087
6	-1.723573	-3.857149	-0.000345
1	-0.930566	-4.597855	-0.000586
6	-3.753725	-1.941670	0.000227
6	-4.076067	-3.297816	0.000000
1	-5.118583	-3.598530	0.000051
6	-3.057726	-4.256948	-0.000303
1	-3.300885	-5.315848	-0.000515
6	-0.008734	-2.099160	-0.000225
6	1.157860	-1.752311	-0.000322
6	2.516357	-1.332810	-0.000073
6	2.852119	0.055413	-0.000061
6	3.555531	-2.280225	-0.000019
6	4.205616	0.434471	-0.000051
6	4.892084	-1.884340	0.000037
6	5.216699	-0.523507	0.000008
1	4.452944	1.491028	-0.000070
1	5.672082	-2.638574	0.000067
1	6.256062	-0.207090	0.000016
6	1.824929	1.042589	-0.000090
6	0.938288	1.876211	-0.000052
6	-2.106365	-0.123356	0.000439
6	-1.822396	1.060257	0.000559
6	-1.475695	2.442323	0.000219

6	-2.478554	3.427171	0.000332
6	-0.104310	2.843104	-0.000047
6	-2.151993	4.781140	0.000141
1	-3.517834	3.115131	0.000581
6	0.198795	4.216334	-0.000223
6	-0.810490	5.177812	-0.000151
1	-2.944326	5.524500	0.000238
1	-0.545275	6.229925	-0.000294
1	1.242078	4.521344	-0.000426
1	3.299930	-3.336680	-0.000038
1	-4.542724	-1.194065	0.000462

M2



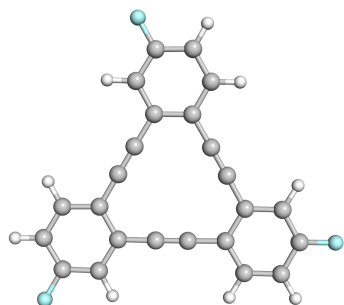
<i>E</i> (B3LYP)	<i>H</i> (B3LYP)	<i>G</i> (B3LYP)	<i>E</i> (M06-2X)
-1608.778708	-1608.276179	-1608.377691	-1608.762781

	X	Y	Z
6	1.030377	2.651818	0.000017
6	-0.377910	2.820328	-0.000176
6	-0.912995	4.125940	-0.000333
1	-1.989714	4.239655	-0.000434
6	1.858283	3.794433	0.000103
6	1.322513	5.077182	-0.000018
6	-0.089883	5.246199	-0.000254
6	-1.248776	1.694772	-0.000222
6	-1.978114	0.719543	-0.000217
6	-2.812297	-0.433420	-0.000013
6	-2.253621	-1.737055	0.000067
6	-4.215787	-0.288183	-0.000008
6	-3.116564	-2.853452	0.000197

6	-5.058624	-1.393638	0.000116
6	-4.498406	-2.701174	0.000242
1	-2.676083	-3.842500	0.000177
6	-0.843364	-1.928222	-0.000031
6	0.365839	-2.072381	-0.000122
6	1.611269	1.352666	0.000274
6	2.090529	0.233228	0.000447
6	2.630778	-1.083274	0.000124
6	4.029113	-1.272007	0.000124
6	1.781353	-2.218930	-0.000118
6	4.588383	-2.544687	-0.000071
1	4.665254	-0.395871	0.000367
6	2.357525	-3.506927	-0.000247
6	3.736361	-3.683803	-0.000223
1	-4.628254	0.712874	-0.000122
1	1.696988	-4.364797	-0.000366
1	2.931452	3.650847	0.000310
8	5.920377	-2.810650	-0.000011
8	-0.525102	6.532876	-0.000291
8	-5.394821	-3.721677	0.000333
6	6.826942	-1.708614	0.000577
1	6.699270	-1.089062	0.896010
1	7.825081	-2.148063	0.000806
1	6.699890	-1.088607	-0.894629
6	-4.893630	-5.057840	0.000042
1	-4.293248	-5.257687	0.895340
1	-5.773237	-5.702572	-0.000258
1	-4.292972	-5.257177	-0.895182
6	-1.932840	6.766956	-0.000098
1	-2.051381	7.851080	0.000285
1	-2.405937	6.346986	-0.895514
1	-2.405783	6.346351	0.895103
8	4.367671	-4.886468	-0.000329
8	-6.415768	-1.338382	0.000112
8	2.048840	6.224873	0.000093
6	3.566104	-6.067128	-0.000455
1	2.935505	-6.119676	0.894817
1	2.935513	-6.119491	-0.895744
1	4.269120	-6.900887	-0.000536
6	-7.037014	-0.053603	0.000011
1	-6.767086	0.518856	0.895234
1	-6.767153	0.518675	-0.895349

1	-8.110629	-0.245282	0.000071
6	3.472029	6.120416	0.000204
1	3.842956	7.145993	0.000169
1	3.832647	5.600512	0.895529
1	3.832788	5.600398	-0.894996

M3

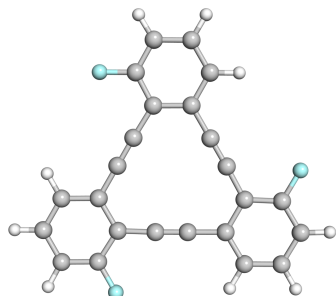


<i>E</i> (B3LYP)	<i>H</i> (B3LYP)	<i>G</i> (B3LYP)	<i>E</i> (M06-2X)
-1219.339831	-1219.071994	-1219.143764	-1219.358660

	X	Y	Z
6	2.648612	-1.046202	-0.000124
6	1.809026	-2.200874	0.000057
6	2.394475	-3.477572	0.000143
1	1.777786	-4.369036	0.000273
6	4.044952	-1.216134	-0.000205
6	4.619112	-2.483760	-0.000110
1	5.694975	-2.619492	-0.000177
6	3.777063	-3.591399	0.000063
6	0.392346	-2.066520	0.000174
6	-0.816953	-1.935197	0.000260
6	-2.230474	-1.771110	0.000102
6	-2.810179	-0.466408	-0.000005
6	-3.076238	-2.895106	0.000105
6	-4.208510	-0.334656	-0.000102
6	-4.461043	-2.758069	0.000001
6	-4.998813	-1.474833	-0.000100
1	-4.671770	0.645336	-0.000179
1	-5.116848	-3.621677	0.000006
6	-1.985486	0.693359	0.000000

6	-1.267159	1.675032	0.000013
6	2.083082	0.259571	-0.000284
6	1.592361	1.372585	-0.000383
6	1.000881	2.666853	-0.000132
6	1.814421	3.811795	-0.000123
6	-0.418741	2.817399	0.000052
6	1.222350	5.066379	0.000071
1	2.894738	3.722752	-0.000276
6	-0.969122	4.111901	0.000232
6	-0.157810	5.242527	0.000248
1	-0.577603	6.242364	0.000390
1	-2.633237	-3.885369	0.000197
1	-2.048202	4.223516	0.000362
1	4.680742	-0.337135	-0.000358
9	4.322223	-4.825021	0.000157
9	-6.339699	-1.329756	-0.000205
9	2.018643	6.154931	0.000053

M4

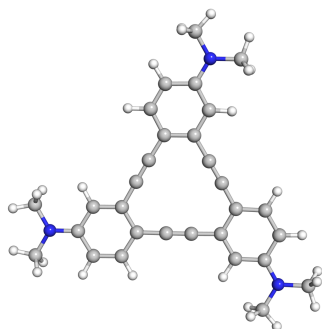


<i>E</i> (B3LYP)	<i>H</i> (B3LYP)	<i>G</i> (B3LYP)	<i>E</i> (M06-2X)
-1219.338186	-1219.070218	-1219.141952	-1219.356104

	X	Y	Z
6	-0.242083	2.827831	0.000081
6	1.167534	2.603692	0.000048
6	2.044547	3.701685	0.000019
1	3.113719	3.519402	-0.000051
6	-0.686076	4.157970	0.000137
6	0.176305	5.244244	0.000158

1	-0.232089	6.248924	0.000212
6	1.552154	5.005787	0.000104
1	2.242069	5.843523	0.000164
6	1.674485	1.274322	-0.000178
6	2.109044	0.138534	-0.000240
6	2.571571	-1.203695	-0.000018
6	1.670996	-2.311082	0.000452
6	3.945097	-1.486106	-0.000311
6	2.181527	-3.620329	0.000560
6	4.452812	-2.776838	-0.000154
6	3.556766	-3.847809	0.000279
1	1.487957	-4.454168	0.000789
1	5.526861	-2.927064	-0.000352
1	3.935815	-4.864725	0.000433
6	0.266443	-2.083847	0.000457
6	-0.934490	-1.892492	0.000299
6	-1.172061	1.755112	0.000169
6	-1.940063	0.812229	0.000161
6	-2.838586	-0.290913	-0.000146
6	-4.227887	-0.079862	-0.000345
6	-2.328464	-1.623949	0.000080
6	-5.111386	-1.158068	-0.000434
1	-4.604262	0.937332	-0.000387
6	-3.258613	-2.673240	-0.000053
6	-4.630452	-2.469061	-0.000309
1	-6.181789	-0.979085	-0.000663
1	-5.296647	-3.324832	-0.000409
9	-2.014904	4.382779	0.000174
9	-2.789189	-3.936577	0.000110
9	4.805607	-0.448869	-0.000798

M5

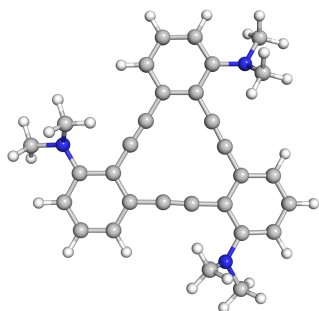


<i>E (B3LYP)</i>	<i>H (B3LYP)</i>	<i>G (B3LYP)</i>	<i>E (M06-2X)</i>
-1323.557878	-1323.033912	-1323.132563	-1323.490290

	X	Y	Z
6	2.824818	0.309107	0.004934
6	2.633165	-1.105851	0.006863
6	3.740326	-1.963543	0.012295
1	3.550573	-3.029099	0.008724
6	4.148837	0.786759	0.007335
6	5.242640	-0.064534	0.013570
1	6.236518	0.365460	0.012928
6	5.067911	-1.473415	0.020931
6	1.317893	-1.654698	0.000991
6	0.187396	-2.110619	-0.002861
6	-1.141960	-2.610824	-0.008606
6	-2.266877	-1.729977	-0.009705
6	-1.398407	-3.994592	-0.009487
6	-3.566208	-2.252539	-0.013639
6	-2.685466	-4.508434	-0.013484
6	-3.813156	-3.646125	-0.021180
1	-4.390134	-1.550698	-0.009836
1	-2.815715	-5.583464	-0.009457
6	-2.075450	-0.318230	-0.003827
6	-1.911676	0.889573	0.001202
6	1.721292	1.203267	-0.000655
6	0.766234	1.960491	-0.006590
6	-0.363744	2.828692	-0.013166
6	-0.170222	4.215548	-0.020755
6	-1.687383	2.291867	-0.008032
6	-1.255579	5.123617	-0.027495
1	0.848692	4.580662	-0.019234
6	-2.760137	3.202816	-0.007736
6	-2.564998	4.574999	-0.014910
1	-3.432047	5.223573	-0.010598
1	-0.556128	-4.680401	-0.004726
1	-3.773980	2.813183	0.000626
1	4.314849	1.860173	0.003152
7	-1.047254	6.483255	-0.050588
7	-5.095125	-4.143278	-0.036909
7	6.143682	-2.329738	0.037179

6	-5.320801	-5.580599	0.029538
1	-4.931558	-6.017828	0.959922
1	-6.392630	-5.774895	-0.015363
1	-4.848528	-6.099242	-0.814263
6	-6.232679	-3.237134	0.036097
1	-6.240021	-2.535085	-0.807385
1	-7.154075	-3.818516	-0.003509
1	-6.235531	-2.652243	0.966809
6	-2.178611	7.395637	0.044843
1	-2.733134	7.270504	0.985788
1	-1.812939	8.421721	-0.001541
1	-2.880179	7.250580	-0.786073
6	0.306134	7.015946	0.022593
1	0.920174	6.659678	-0.813893
1	0.263833	8.103958	-0.033062
1	0.811293	6.738980	0.959115
6	5.934082	-3.769953	-0.009817
1	5.429434	-4.083086	-0.934683
1	6.900421	-4.272545	0.036845
1	5.331966	-4.115397	0.840330
6	7.499472	-1.800950	-0.019602
1	8.206608	-2.630245	0.011133
1	7.680718	-1.230851	-0.941518
1	7.711329	-1.144354	0.834135

M6

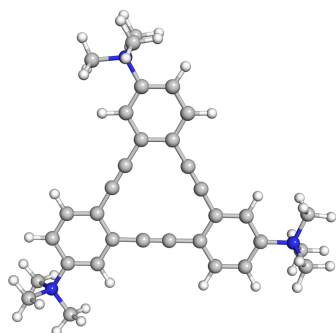


<i>E</i> (B3LYP)	<i>H</i> (B3LYP)	<i>G</i> (B3LYP)	<i>E</i> (M06-2X)
-1323.536391	-1323.013516	-1323.106089	-1323.473471

	X	Y	Z
6	1.539390	2.428080	-0.041268
6	0.178257	2.790587	-0.293844
6	-0.179548	4.149281	-0.348119
1	-1.215412	4.423038	-0.525517
6	2.509186	3.445641	0.188328
6	2.104232	4.800723	0.086966
1	2.818225	5.609794	0.234661
6	0.783346	5.134225	-0.193771
1	0.491459	6.177218	-0.257736
6	-0.887305	1.834793	-0.384860
6	-1.852045	1.101401	-0.216196
6	-2.867441	0.108464	-0.112092
6	-2.462691	-1.260370	0.083959
6	-4.256277	0.422822	-0.129161
6	-3.401519	-2.288179	0.271098
6	-5.163702	-0.649663	0.071266
6	-4.753956	-1.964619	0.254963
1	-3.074721	-3.315165	0.408940
1	-6.216699	-0.416645	0.185142
1	-5.497946	-2.733857	0.443098
6	-1.091970	-1.627031	0.054525
6	0.019027	-2.128905	0.053249
6	1.888036	1.058528	-0.155069
6	2.035237	-0.136368	-0.296719
6	2.379325	-1.512501	-0.409256
6	3.676592	-1.939675	-0.763351
6	1.383177	-2.494684	-0.152235
6	4.015344	-3.281086	-0.733211
1	4.440937	-1.213292	-1.020405
6	1.742638	-3.892150	-0.155748
6	3.071489	-4.262892	-0.420531
1	5.029420	-3.571583	-0.996152
1	3.363922	-5.302227	-0.413114
7	0.731757	-4.844751	0.075828
7	-4.741647	1.718644	-0.264624
7	3.852177	3.095775	0.265806
6	0.008786	-4.660725	1.337152
1	-0.896762	-5.262048	1.239491
1	0.547887	-4.993479	2.237258
1	-0.265867	-3.611256	1.444517
6	1.051716	-6.246691	-0.189615

1	1.780504	-6.676564	0.515385
1	0.117900	-6.809732	-0.132577
1	1.442858	-6.353952	-1.202519
6	-6.158681	1.908243	-0.560657
1	-6.842670	1.689671	0.272582
1	-6.288123	2.953044	-0.856268
1	-6.446061	1.258872	-1.392368
6	-4.189796	2.766052	0.595966
1	-4.347042	3.717900	0.084935
1	-4.673986	2.818457	1.588161
1	-3.119892	2.608613	0.719628
6	4.311891	2.229063	1.350068
1	5.328250	1.993974	1.047977
1	4.320794	2.723878	2.336597
1	3.761471	1.297482	1.414606
6	4.797583	4.156245	-0.043120
1	4.819981	4.962712	0.706150
1	5.790557	3.703959	-0.103122
1	4.553079	4.601844	-1.010732

M7



<i>E</i> (B3LYP)	<i>H</i> (B3LYP)	<i>G</i> (B3LYP)	<i>E</i> (M06-2X)
-1442.774635	-1442.118217	-1442.219637	-1442.677913

	X	Y	Z
6	-0.594246	-2.781643	-0.033138

6	-1.865251	-2.142869	-0.023825
6	-3.036984	-2.922126	-0.008096
1	-3.984811	-2.403011	0.002520
6	-0.545374	-4.184406	-0.029857
6	-1.707638	-4.946033	-0.014559
1	-1.618141	-6.025052	-0.012876
6	-2.953045	-4.310588	-0.003690
6	-1.967989	-0.725746	-0.024297
6	-2.036308	0.487057	-0.023920
6	-2.110596	1.906417	-0.030809
6	-0.923100	2.688882	-0.013830
6	-3.352185	2.562768	-0.041530
6	-1.013940	4.092825	-0.004734
6	-3.432996	3.949535	-0.032852
6	-2.259742	4.710409	-0.012106
1	-0.089022	4.653516	0.006767
1	-4.416510	4.407600	-0.036712
6	0.356028	2.068219	-0.005152
6	1.441875	1.522821	-0.001303
6	0.601715	-2.010133	-0.038794
6	1.615837	-1.342138	-0.037778
6	2.792201	-0.544789	-0.022783
6	4.055566	-1.165760	-0.029990
6	2.706671	0.873387	0.001671
6	5.213339	-0.396221	0.000752
1	4.087794	-2.244503	-0.056874
6	3.896554	1.620832	0.018238
6	5.138537	0.999218	0.020266
1	6.023392	1.625560	0.035235
1	-4.265153	1.977447	-0.052567
1	3.846954	2.703860	0.030938
1	0.417364	-4.683223	-0.039352
7	6.574986	-1.040357	0.010117
7	-2.386512	6.207764	0.013417
7	-4.191639	-5.168002	0.024201
6	-3.145097	6.681804	-1.213849
1	-4.153263	6.272069	-1.191499
1	-3.188995	7.771833	-1.184625
1	-2.617446	6.338477	-2.104077
6	-3.141042	6.627254	1.263891
1	-2.588337	6.272188	2.132840
1	-3.212484	7.716070	1.270099

1	-4.137385	6.189651	1.247283
6	7.361110	-0.583771	-1.204873
1	7.485723	0.497752	-1.169088
1	8.333949	-1.072355	-1.177586
1	6.813549	-0.875342	-2.101080
6	7.318187	-0.639278	1.270437
1	6.748214	-0.992401	2.129752
1	8.303180	-1.102924	1.249872
1	7.417235	0.443227	1.302214
6	-4.197237	-6.085266	-1.186105
1	-3.315347	-6.721878	-1.162398
1	-5.100862	-6.693258	-1.144854
1	-4.194115	-5.464970	-2.083533
6	-4.198409	-5.994597	1.297798
1	-5.101150	-6.604467	1.298645
1	-3.315378	-6.629272	1.321581
1	-4.197449	-5.309256	2.145487
6	-1.045362	6.906102	0.029393
1	-0.494628	6.604363	0.918246
1	-0.498108	6.648732	-0.874474
1	-1.232818	7.977191	0.055809
6	-5.475020	-4.368827	-0.005166
1	-5.526255	-3.735483	0.879169
1	-5.509987	-3.770441	-0.914603
1	-6.298004	-5.083422	0.001847
6	6.513185	-2.551748	-0.020998
1	5.989153	-2.907426	0.866509
1	6.015099	-2.865402	-0.937839
1	7.540730	-2.920844	-0.015388

References

1. Toogood, P. L., Inhibition of Protein–Protein Association by Small Molecules: Approaches and Progress. *J. Med. Chem.* **2002**, *45* (8), 1543-1558.
2. Zinzalla, G.; Thurston, D. E., Targeting protein-protein interactions for therapeutic intervention: a challenge for the future. *Future Med. Chem.* **2009**, *1* (1), 65-93.
3. Ryan, D. P.; Matthews, J. M., Protein-protein interactions in human disease. *Curr. Opin. Struct. Biol.* **2005**, *15* (4), 441-6.
4. Fletcher, S.; Hamilton, A. D., Targeting protein-protein interactions by rational design: mimicry of protein surfaces. *Journal of the Royal Society, Interface / the Royal Society* **2006**, *3* (7), 215-33.
5. Keskin, O.; Gursoy, A.; Ma, B.; Nussinov, R., Principles of Protein–Protein Interactions: What are the Preferred Ways For Proteins To Interact? *Chem. Rev.* **2008**, *108* (4), 1225-1244.
6. Wilson, A. J., Inhibition of protein-protein interactions using designed molecules. *Chem. Soc. Rev.* **2009**, *38* (12), 3289-300.
7. Verdine, G. L.; Walensky, L. D., The challenge of drugging undruggable targets in cancer: lessons learned from targeting BCL-2 family members. *Clin. Cancer Res.* **2007**, *13* (24), 7264-70.
8. Yin, H.; Hamilton, A. D., Strategies for targeting protein-protein interactions with synthetic agents. *Angew. Chem. Int. Ed. Engl.* **2005**, *44* (27), 4130-63.
9. Munos, B., Lessons from 60 years of pharmaceutical innovation. *Nat Rev Drug Discov* **2009**, *8* (12), 959-968.
10. Berg, T., Modulation of protein-protein interactions with small organic molecules. *Angew. Chem. Int. Ed. Engl.* **2003**, *42* (22), 2462-81.
11. Stites, W. E., Protein–Protein Interactions: Interface Structure, Binding Thermodynamics, and Mutational Analysis. *Chem. Rev.* **1997**, *97* (5), 1233-1250.
12. Ivanov, A. A.; Khuri, F. R.; Fu, H., Targeting protein-protein interactions as an anticancer strategy. *Trends Pharmacol. Sci.* **2013**, *34* (7), 393-400.
13. Arkin, M. R.; Wells, J. A., Small-molecule inhibitors of protein-protein interactions: progressing towards the dream. *Nat Rev Drug Discov* **2004**, *3* (4), 301-17.
14. Clackson, T.; Wells, J., A hot spot of binding energy in a hormone-receptor interface. *Science* **1995**, *267* (5196), 383-386.
15. Wells, J. A.; McClendon, C. L., Reaching for high-hanging fruit in drug discovery at protein-protein interfaces. *Nature* **2007**, *450* (7172), 1001-1009.
16. Vassilev, L. T.; Vu, B. T.; Graves, B.; Carvajal, D.; Podlaski, F.; Filipovic, Z.; Kong, N.; Kammlott, U.; Lukacs, C.; Klein, C.; Fotouhi, N.; Liu, E. A., In Vivo Activation of the p53 Pathway by Small-Molecule Antagonists of MDM2. *Science* **2004**, *303* (5659), 844-848.
17. Dorr, P.; Westby, M.; Dobbs, S.; Griffin, P.; Irvine, B.; Macartney, M.; Mori, J.; Rickett, G.; Smith-Burchnell, C.; Napier, C.; Webster, R.; Armour, D.; Price, D.; Stammen, B.; Wood, A.; Perros, M., Maraviroc (UK-427,857), a Potent, Orally Bioavailable, and Selective Small-Molecule Inhibitor of Chemokine Receptor CCR5 with Broad-Spectrum Anti-Human Immunodeficiency Virus Type 1 Activity. *Antimicrob. Agents Chemother.* **2005**, *49* (11), 4721-4732.
18. Hajduk, P. J.; Galloway, W. R. J. D.; Spring, D. R., Drug discovery: A question of library design. *Nature* **2011**, *470* (7332), 42-43.
19. Galloway, W. R.; Isidro-Llobet, A.; Spring, D. R., Diversity-oriented synthesis as a tool for the discovery of novel biologically active small molecules. *Nature communications* **2010**, *1*, 80.
20. Spring, D. R., Diversity-oriented synthesis; a challenge for synthetic chemists. *Org. Biomol. Chem.* **2003**, *1* (22), 3867-3870.

21. Stockwin, L.; Holmes, S., Antibodies as therapeutic agents: vive la renaissance! *Expert Opin. Biol. Ther.* **2003**, *3* (7), 1133-1152.
22. Hudis, C. A., Trastuzumab — Mechanism of Action and Use in Clinical Practice. *N. Engl. J. Med.* **2007**, *357* (1), 39-51.
23. Cho, H.-S.; Mason, K.; Ramyar, K. X.; Stanley, A. M.; Gabelli, S. B.; Denney, D. W.; Leahy, D. J., Structure of the extracellular region of HER2 alone and in complex with the Herceptin Fab. *Nature* **2003**, *421* (6924), 756-760.
24. Vagner, J.; Qu, H.; Hruby, V. J., Peptidomimetics, a synthetic tool of drug discovery. *Curr. Opin. Chem. Biol.* **2008**, *12* (3), 292-6.
25. Grauer, A.; König, B., Peptidomimetics - A Versatile Route to Biologically Active Compounds. *European J. Org. Chem.* **2009**, *2009* (30), 5099-5111.
26. Avan, I.; Hall, C. D.; Katritzky, A. R., Peptidomimetics via modifications of amino acids and peptide bonds. *Chem. Soc. Rev.* **2014**, *43* (10), 3575-94.
27. Cummings, C. G.; Hamilton, A. D., Disrupting protein-protein interactions with non-peptidic, small molecule alpha-helix mimetics. *Curr. Opin. Chem. Biol.* **2010**, *14* (3), 341-6.
28. Yin, H.; Lee, G.-i.; Sedey, K. A.; Kutzki, O.; Park, H. S.; Orner, B. P.; Ernst, J. T.; Wang, H.-G.; Sebt, S. M.; Hamilton, A. D., Terphenyl-Based Bak BH3 α -Helical Proteomimetics as Low-Molecular-Weight Antagonists of Bcl-xL. *J. Am. Chem. Soc.* **2005**, *127* (29), 10191-10196.
29. Orner, B. P.; Ernst, J. T.; Hamilton, A. D., Toward Proteomimetics: Terphenyl Derivatives as Structural and Functional Mimics of Extended Regions of an α -Helix. *J. Am. Chem. Soc.* **2001**, *123* (22), 5382-5383.
30. Bautista, A. D.; Appelbaum, J. S.; Craig, C. J.; Michel, J.; Schepartz, A., Bridged β 3-Peptide Inhibitors of p53-hDM2 Complexation: Correlation between Affinity and Cell Permeability. *J. Am. Chem. Soc.* **2010**, *132* (9), 2904-2906.
31. Kritzer, J. A.; Lear, J. D.; Hodsdon, M. E.; Schepartz, A., Helical β -Peptide Inhibitors of the p53-hDM2 Interaction. *J. Am. Chem. Soc.* **2004**, *126* (31), 9468-9469.
32. Davis, J. M.; Tsou, L. K.; Hamilton, A. D., Synthetic non-peptide mimetics of [small alpha]-helices. *Chem. Soc. Rev.* **2007**, *36* (2), 326-334.
33. Pauling, L.; Corey, R. B.; Branson, H. R., The Structure of Proteins: Two Hydrogen-Bonded Helical Configurations of the Polypeptide Chain. *Proc. Natl. Acad. Sci. U. S. A.* **1951**, *37* (4), 205-211.
34. Perutz, M. F.; Kendrew, J. C.; Watson, H. C., Structure and function of haemoglobin: II. Some relations between polypeptide chain configuration and amino acid sequence. *J. Mol. Biol.* **1965**, *13* (3), 669-678.
35. Kendrew, J. C.; Dickerson, R. E.; Strandberg, B. E.; Hart, R. G.; Davies, D. R.; Phillips, D. C.; Shore, V. C., Structure of Myoglobin: A Three-Dimensional Fourier Synthesis at 2 [angst]. Resolution. *Nature* **1960**, *185* (4711), 422-427.
36. Cochran, A. G., Antagonists of protein-protein interactions. *Chem. Biol.* **2000**, *7* (4), R85-R94.
37. Cochran, A. G., Protein-protein interfaces: mimics and inhibitors. *Curr. Opin. Chem. Biol.* **2001**, *5* (6), 654-659.
38. Lau, Y. H.; de Andrade, P.; Wu, Y.; Spring, D. R., Peptide stapling techniques based on different macrocyclisation chemistries. *Chem. Soc. Rev.* **2015**, *44* (1), 91-102.
39. Blackwell, H. E.; Grubbs, R. H., Highly Efficient Synthesis of Covalently Cross-Linked Peptide Helices by Ring-Closing Metathesis. *Angewandte Chemie International Edition* **1998**, *37* (23), 3281-3284.
40. Schafmeister, C. E.; Po, J.; Verdine, G. L., An All-Hydrocarbon Cross-Linking System for Enhancing the Helicity and Metabolic Stability of Peptides. *J. Am. Chem. Soc.* **2000**, *122* (24), 5891-5892.

41. Walensky, L. D.; Bird, G. H., Hydrocarbon-stapled peptides: principles, practice, and progress. *J. Med. Chem.* **2014**, *57* (15), 6275-88.
42. Yip, K. W.; Reed, J. C., Bcl-2 family proteins and cancer. *Oncogene* **2008**, *27* (50), 6398-6406.
43. Felix, A. M.; Heimer, E. P.; Wang, C.-T.; Lambros, T. J.; Fournier, A.; Mowles, T. F.; Maines, S.; Campbell, R. M.; Wegrzynski, B. B.; Toome, V.; Fry, D.; Madison, V. S., Synthesis, biological activity and conformational analysis of cyclic GRF analogs. *Int. J. Pept. Protein Res.* **1988**, *32* (6), 441-454.
44. Taylor, J. W., The synthesis and study of side-chain lactam-bridged peptides. *Peptide Science* **2002**, *66* (1), 49-75.
45. Shepherd, N. E.; Hoang, H. N.; Abbenante, G.; Fairlie, D. P., Single Turn Peptide Alpha Helices with Exceptional Stability in Water. *J. Am. Chem. Soc.* **2005**, *127* (9), 2974-2983.
46. Harrison, R. S.; Ruiz-Gómez, G.; Hill, T. A.; Chow, S. Y.; Shepherd, N. E.; Lohman, R.-J.; Abbenante, G.; Hoang, H. N.; Fairlie, D. P., Novel Helix-Constrained Nociceptin Derivatives Are Potent Agonists and Antagonists of ERK Phosphorylation and Thermal Analgesia in Mice. *J. Med. Chem.* **2010**, *53* (23), 8400-8408.
47. Harrison, R. S.; Shepherd, N. E.; Hoang, H. N.; Ruiz-Gómez, G.; Hill, T. A.; Driver, R. W.; Desai, V. S.; Young, P. R.; Abbenante, G.; Fairlie, D. P., Downsizing human, bacterial, and viral proteins to short water-stable alpha helices that maintain biological potency. *Proceedings of the National Academy of Sciences* **2010**, *107* (26), 11686-11691.
48. Rostovtsev, V. V.; Green, L. G.; Fokin, V. V.; Sharpless, K. B., A Stepwise Huisgen Cycloaddition Process: Copper(I)-Catalyzed Regioselective "Ligation" of Azides and Terminal Alkynes. *Angewandte Chemie International Edition* **2002**, *41* (14), 2596-2599.
49. Tornøe, C. W.; Christensen, C.; Meldal, M., Peptidotriazoles on Solid Phase: [1,2,3]-Triazoles by Regiospecific Copper(I)-Catalyzed 1,3-Dipolar Cycloadditions of Terminal Alkynes to Azides. *The Journal of Organic Chemistry* **2002**, *67* (9), 3057-3064.
50. Scrima, M.; Le Chevalier-Isaad, A.; Rovero, P.; Papini, A. M.; Chorev, M.; D'Ursi, A. M., CuI-Catalyzed Azide-Alkyne Intramolecular i-to-(i+4) Side-Chain-to-Side-Chain Cyclization Promotes the Formation of Helix-Like Secondary Structures. *European J. Org. Chem.* **2010**, *2010* (3), 446-457.
51. Kawamoto, S. A.; Coleska, A.; Ran, X.; Yi, H.; Yang, C.-Y.; Wang, S., Design of Triazole-Stapled BCL9 α -Helical Peptides to Target the β -Catenin/B-Cell CLL/lymphoma 9 (BCL9) Protein-Protein Interaction. *J. Med. Chem.* **2012**, *55* (3), 1137-1146.
52. Jackson, D. Y.; King, D. S.; Chmielewski, J.; Singh, S.; Schultz, P. G., General approach to the synthesis of short .alpha.-helical peptides. *J. Am. Chem. Soc.* **1991**, *113* (24), 9391-9392.
53. Galande, A. K.; Bramlett, K. S.; Burris, T. P.; Wittliff, J. L.; Spatola, A. F., Thioether side chain cyclization for helical peptide formation: inhibitors of estrogen receptor-coactivator interactions. *The Journal of Peptide Research* **2004**, *63* (3), 297-302.
54. Pellegrini, M.; Royo, M.; Chorev, M.; Mierke, D. F., Conformational consequences of i, i + 3 cystine linkages: nucleation for α -helicity? *The Journal of Peptide Research* **1997**, *49* (5), 404-414.
55. Kumita, J. R.; Smart, O. S.; Woolley, G. A., Photo-control of helix content in a short peptide. *Proceedings of the National Academy of Sciences* **2000**, *97* (8), 3803-3808.
56. Kneissl, S.; Loveridge, E. J.; Williams, C.; Crump, M. P.; Allemann, R. K., Photocontrollable Peptide-Based Switches Target the Anti-Apoptotic Protein Bcl-xL. *Chembiochem* **2008**, *9* (18), 3046-3054.
57. Spokoyny, A. M.; Zou, Y.; Ling, J. J.; Yu, H.; Lin, Y. S.; Pentelute, B. L., A perfluoroaryl-cysteine S(N)Ar chemistry approach to unprotected peptide stapling. *J. Am. Chem. Soc.* **2013**, *135* (16), 5946-9.

58. Jo, H.; Meinhardt, N.; Wu, Y.; Kulkarni, S.; Hu, X.; Low, K. E.; Davies, P. L.; DeGrado, W. F.; Greenbaum, D. C., Development of α -Helical Calpain Probes by Mimicking a Natural Protein–Protein Interaction. *J. Am. Chem. Soc.* **2012**, *134* (42), 17704-17713.
59. Sletten, E. M.; Bertozzi, C. R., Bioorthogonal Chemistry: Fishing for Selectivity in a Sea of Functionality. *Angewandte Chemie International Edition* **2009**, *48* (38), 6974-6998.
60. Hang, H. C.; Yu, C.; Kato, D. L.; Bertozzi, C. R., A metabolic labeling approach toward proteomic analysis of mucin-type O-linked glycosylation. *Proceedings of the National Academy of Sciences* **2003**, *100* (25), 14846.
61. Lau, Y. H.; de Andrade, P.; Quah, S.-T.; Rossmann, M.; Laraia, L.; Skold, N.; Sum, T. J.; Rowling, P. J. E.; Joseph, T. L.; Verma, C.; Hyvonen, M.; Itzhaki, L. S.; Venkitaraman, A. R.; Brown, C. J.; Lane, D. P.; Spring, D. R., Functionalised staple linkages for modulating the cellular activity of stapled peptides. *Chemical Science* **2014**, *5* (5), 1804-1809.
62. Agard, N. J.; Prescher, J. A.; Bertozzi, C. R., A Strain-Promoted [3 + 2] Azide–Alkyne Cycloaddition for Covalent Modification of Biomolecules in Living Systems. *Journal of the American Chemical Society* **2004**, *126* (46), 15046-15047.
63. Wong, H. N. C.; Garratt, P. J.; Sondheimer, F., Unsaturated eight-membered ring compounds. XI. Synthesis of sym-dibenzo-1,5-cyclooctadiene-3,7-diyne and sym-dibenzo-1,3,5-cyclooctatrien-7-yne, presumably planar conjugated eight-membered ring compounds. *Journal of the American Chemical Society* **1974**, *96* (17), 5604-5605.
64. Orita, A.; Hasegawa, D.; Nakano, T.; Otera, J., Double Elimination Protocol for Synthesis of 5,6,11,12-Tetrahydrodibenzo[a,e]cyclooctene. *Chemistry – A European Journal* **2002**, *8* (9), 2000-2004.
65. This work was carried out by Yuteng Wu in the Spring group.
66. Sutton, D. A.; Yu, S.-H.; Steet, R.; Popik, V. V., Cyclopropenone-caged Sondheimer diyne (dibenzo[a,e]cyclooctadiyne): a photoactivatable linchpin for efficient SPAAC crosslinking. *Chemical Communications* **2016**, *52* (3), 553-556.
67. Sletten, E. M.; Bertozzi, C. R., A Hydrophilic Azacyclooctyne for Cu-Free Click Chemistry. *Organic Letters* **2008**, *10* (14), 3097-3099.
68. Ning, X.; Guo, J.; Wolfert, M. A.; Boons, G.-J., Visualizing Metabolically Labeled Glycoconjugates of Living Cells by Copper-Free and Fast Huisgen Cycloadditions. *Angewandte Chemie International Edition* **2008**, *47* (12), 2253-2255.
69. Agard, N. J.; Baskin, J. M.; Prescher, J. A.; Lo, A.; Bertozzi, C. R., A Comparative Study of Bioorthogonal Reactions with Azides. *ACS Chemical Biology* **2006**, *1* (10), 644-648.
70. Stockmann, H.; Neves, A. A.; Stairs, S.; Ireland-Zecchini, H.; Brindle, K. M.; Leeper, F. J., Development and evaluation of new cyclooctynes for cell surface glycan imaging in cancer cells. *Chemical Science* **2011**, *2* (5), 932-936.
71. Debets, M. F.; van Berkel, S. S.; Schoffelen, S.; Rutjes, F. P. J. T.; van Hest, J. C. M.; van Delft, F. L., Aza-dibenzocyclooctynes for fast and efficient enzyme PEGylation via copper-free (3+2) cycloaddition. *Chemical Communications* **2010**, *46* (1), 97-99.
72. Baskin, J. M.; Prescher, J. A.; Laughlin, S. T.; Agard, N. J.; Chang, P. V.; Miller, I. A.; Lo, A.; Codelli, J. A.; Bertozzi, C. R., Copper-free click chemistry for dynamic *in vivo* imaging. *Proceedings of the National Academy of Sciences* **2007**, *104* (43), 16793-16797.
73. Jewett, J. C.; Sletten, E. M.; Bertozzi, C. R., Rapid Cu-Free Click Chemistry with Readily Synthesized Biarylazacyclooctynones. *Journal of the American Chemical Society* **2010**, *132* (11), 3688-3690.
74. Mbua, N. E.; Guo, J.; Wolfert, M. A.; Steet, R.; Boons, G.-J., Strain-Promoted Alkyne–Azide Cycloadditions (SPAAC) Reveal New Features of Glycoconjugate Biosynthesis. *ChemBioChem* **2011**, *12* (12), 1912-1921.
75. Sletten, E. M.; Bertozzi, C. R., From Mechanism to Mouse: A Tale of Two Bioorthogonal Reactions. *Accounts of Chemical Research* **2011**, *44* (9), 666-676.

76. Xu, F.; Peng, L.; Shinohara, K.; Morita, T.; Yoshida, S.; Hosoya, T.; Orita, A.; Otera, J., Substituted 5,6,11,12-Tetrahydrodibenzo[a,e]cyclooctenes: Syntheses, Properties, and DFT Studies of Substituted Sondheimer–Wong Diynes. *The Journal of Organic Chemistry* **2014**, *79* (23), 11592-11608.
77. Thanks to Alexander Strizhak for assistance with the synthesis of this molecule.
78. Dess, D. B.; Martin, J. C., Readily accessible 12-I-5 oxidant for the conversion of primary and secondary alcohols to aldehydes and ketones. *The Journal of Organic Chemistry* **1983**, *48* (22), 4155-4156.
79. MacMillan, K. S.; Nguyen, T.; Hwang, I.; Boger, D. L., Total Synthesis and Evaluation of iso-Duocarmycin SA and iso-Yatakemycin. *Journal of the American Chemical Society* **2009**, *131* (3), 1187-1194.
80. Chandrappa, S.; Vinaya, K.; Ramakrishnappa, T.; Rangappa, K. S., An Efficient Method for Aryl Nitro Reduction and Cleavage of Azo Compounds Using Iron Powder/Calcium Chloride. *Synlett* **2010**, *2010* (20), 3019-3022.
81. Borch, R. F.; Bernstein, M. D.; Durst, H. D., Cyanohydridoborate anion as a selective reducing agent. *Journal of the American Chemical Society* **1971**, *93* (12), 2897-2904.
82. Chandrasekharam, M.; Chiranjeevi, B.; Gupta, K. S. V.; Sridhar, B., Iron-Catalyzed Regioselective Direct Oxidative Aryl–Aryl Cross-Coupling. *The Journal of Organic Chemistry* **2011**, *76* (24), 10229-10235.
83. Reeves, J. T.; Fandrick, D. R.; Tan, Z.; Song, J. J.; Lee, H.; Yee, N. K.; Senanayake, C. H., Room Temperature Palladium-Catalyzed Cross Coupling of Aryltrimethylammonium Triflates with Aryl Grignard Reagents. *Organic Letters* **2010**, *12* (19), 4388-4391.
84. OECD, Paris, 1981, Test Guideline 107, Decision of the Council C(81) 30 final. *OECD, Paris, 1981, Test Guideline 107, Decision of the Council C(81) 30 final*.
85. Ley, S. V.; Baxendale, I. R.; Bream, R. N.; Jackson, P. S.; Leach, A. G.; Longbottom, D. A.; Nesi, M.; Scott, J. S.; Storer, R. I.; Taylor, S. J., Multi-step organic synthesis using solid-supported reagents and scavengers: a new paradigm in chemical library generation. *Journal of the Chemical Society, Perkin Transactions 1* **2000**, (23), 3815-4195.
86. Booth, R. J.; Hodges, J. C., Solid-Supported Reagent Strategies for Rapid Purification of Combinatorial Synthesis Products. *Acc. Chem. Res.* **1999**, *32* (1), 18-26.
87. Hu, B.; Gilkes, D. M.; Chen, J., Efficient p53 Activation and Apoptosis by Simultaneous Disruption of Binding to MDM2 and MDMX. *Cancer Research* **2007**, *67* (18), 8810.
88. Phan, J.; Li, Z.; Kasprzak, A.; Li, B.; Sebti, S.; Guida, W.; Schönbrunn, E.; Chen, J., Structure-based Design of High Affinity Peptides Inhibiting the Interaction of p53 with MDM2 and MDMX. *Journal of Biological Chemistry* **2010**, *285* (3), 2174-2183.
89. Lau, Y. H.; Wu, Y.; Rossmann, M.; Tan, B. X.; de Andrade, P.; Tan, Y. S.; Verma, C.; McKenzie, G. J.; Venkitaraman, A. R.; Hyvönen, M.; Spring, D. R., Double Strain-Promoted Macrocyclization for the Rapid Selection of Cell-Active Stapled Peptides. *Angewandte Chemie International Edition* **2015**, *54* (51), 15410-15413.
90. Levine, A. J., p53, the Cellular Gatekeeper for Growth and Division. *Cell* **1997**, *88* (3), 323-331.
91. Fridman, J. S.; Lowe, S. W., Control of apoptosis by p53. *Oncogene* **2003**, *22* (56), 9030-9040.
92. Vousden, K. H.; Lu, X., Live or let die: the cell's response to p53. *Nat. Rev. Cancer* **2002**, *2* (8), 594-604.
93. Hollstein, M.; Sidransky, D.; Vogelstein, B.; Harris, C., p53 mutations in human cancers. *Science* **1991**, *253* (5015), 49-53.
94. Chene, P., Inhibiting the p53-MDM2 interaction: an important target for cancer therapy. *Nat. Rev. Cancer* **2003**, *3* (2), 102-9.

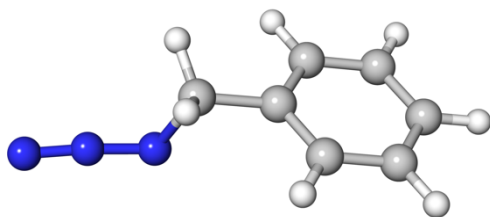
95. Kubbutat, M. H. G.; Jones, S. N.; Vousden, K. H., Regulation of p53 stability by Mdm2. *Nature* **1997**, 387 (6630), 299-303.
96. Honda, R.; Tanaka, H.; Yasuda, H., Oncoprotein MDM2 is a ubiquitin ligase E3 for tumor suppressor p53. *FEBS Lett.* **1997**, 420 (1), 25-27.
97. Haupt, Y.; Maya, R.; Kazaz, A.; Oren, M., Mdm2 promotes the rapid degradation of p53. *Nature* **1997**, 387 (6630), 296-299.
98. Alarcon-Vargas, D.; Ronai, Z. e., p53–Mdm2—the affair that never ends. *Carcinogenesis* **2002**, 23 (4), 541-547.
99. Vogelstein, B.; Lane, D.; Levine, A. J., Surfing the p53 network. *Nature* **2000**, 408 (6810), 307-310.
100. Moll, U. M.; Petrenko, O., The MDM2-p53 Interaction. *Mol. Cancer Res.* **2003**, 1 (14), 1001-1008.
101. Shieh, S.-Y.; Ahn, J.; Tamai, K.; Taya, Y.; Prives, C., The human homologs of checkpoint kinases Chk1 and Cds1 (Chk2) phosphorylate p53 at multiple DNA damage-inducible sites. *Genes Dev.* **2000**, 14 (3), 289-300.
102. Sakaguchi, K.; Saito, S. i.; Higashimoto, Y.; Roy, S.; Anderson, C. W.; Appella, E., Damage-mediated Phosphorylation of Human p53 Threonine 18 through a Cascade Mediated by a Casein 1-like Kinase: EFFECT ON Mdm2 BINDING. *J. Biol. Chem.* **2000**, 275 (13), 9278-9283.
103. Wu, X.; Bayle, J. H.; Olson, D.; Levine, A. J., The p53-mdm-2 autoregulatory feedback loop. *Genes Dev.* **1993**, 7 (7a), 1126-1132.
104. Momand, J.; Jung, D.; Wilczynski, S.; Niland, J., The MDM2 gene amplification database. *Nucleic Acids Res.* **1998**, 26 (15), 3453-3459.
105. Eymin, B.; Gazzeri, S.; Brambilla, C.; Brambilla, E., Mdm2 overexpression and p14(ARF) inactivation are two mutually exclusive events in primary human lung tumors. *Oncogene* **2002**, 21 (17), 2750-61.
106. Leite, K. R. M.; Franco, M. F.; Srougi, M.; Nesrallah, L. J.; Nesrallah, A.; Bevilacqua, R. G.; Darini, E.; Carvalho, C. M.; Meirelles, M. I.; Santana, I.; Camara-Lopes, L. H., Abnormal Expression of MDM2 in Prostate Carcinoma. *Mod. Pathol.* **2001**, 14 (5), 428-436.
107. Kussie, P. H.; Gorina, S.; Marechal, V.; Elenbaas, B.; Moreau, J.; Levine, A. J.; Pavletich, N. P., Structure of the MDM2 Oncoprotein Bound to the p53 Tumor Suppressor Transactivation Domain. *Science* **1996**, 274 (5289), 948-953.
108. Joerger, Andreas C.; Wilcken, R.; Andreeva, A., Tracing the Evolution of the p53 Tetramerization Domain. *Structure(London, England:1993)* **2014**, 22 (9), 1301-1310.
109. Brown, C. J.; Quah, S. T.; Jong, J.; Goh, A. M.; Chiam, P. C.; Khoo, K. H.; Choong, M. L.; Lee, M. A.; Yurlova, L.; Zolghadr, K.; Joseph, T. L.; Verma, C. S.; Lane, D. P., Stapled Peptides with Improved Potency and Specificity That Activate p53. *ACS Chemical Biology* **2013**, 8 (3), 506-512.
110. Chang, Y. S.; Graves, B.; Guerlavais, V.; Tovar, C.; Packman, K.; To, K.-H.; Olson, K. A.; Kesavan, K.; Gangurde, P.; Mukherjee, A.; Baker, T.; Darlak, K.; Elkin, C.; Filipovic, Z.; Qureshi, F. Z.; Cai, H.; Berry, P.; Feyfant, E.; Shi, X. E.; Horstick, J.; Annis, D. A.; Manning, A. M.; Fotouhi, N.; Nash, H.; Vassilev, L. T.; Sawyer, T. K., Stapled α -helical peptide drug development: A potent dual inhibitor of MDM2 and MDMX for p53-dependent cancer therapy. *Proceedings of the National Academy of Sciences* **2013**, 110 (36), E3445-E3454.
111. Stewart, M. L.; Fire, E.; Keating, A. E.; Walensky, L. D., The MCL-1 BH3 helix is an exclusive MCL-1 inhibitor and apoptosis sensitizer. *Nature Chemical Biology* **2010**, 6, 595.
112. Phillips, C.; Roberts, L. R.; Schade, M.; Bazin, R.; Bent, A.; Davies, N. L.; Moore, R.; Pannifer, A. D.; Pickford, A. R.; Prior, S. H.; Read, C. M.; Scott, A.; Brown, D. G.; Xu, B.; Irving, S. L., Design and Structure of Stapled Peptides Binding to Estrogen Receptors. *Journal of the American Chemical Society* **2011**, 133 (25), 9696-9699.

113. Adrian, G.; David, B.; Gernot, H.; Christoph, R.; Christian, O.; N., G. T., Constrained Peptides with Target-Adapted Cross-Links as Inhibitors of a Pathogenic Protein–Protein Interaction. *Angewandte Chemie International Edition* **2014**, *53* (9), 2489-2493.
114. Anil, B.; Riedinger, C.; Endicott, J. A.; Noble, M. E. M., The structure of an MDM2–Nutlin-3a complex solved by the use of a validated MDM2 surface-entropy reduction mutant. *Acta Crystallographica Section D* **2013**, *69* (8), 1358-1366.
115. Kii, I.; Shiraishi, A.; Hiramatsu, T.; Matsushita, T.; Uekusa, H.; Yoshida, S.; Yamamoto, M.; Kudo, A.; Hagiwara, M.; Hosoya, T., Strain-promoted double-click reaction for chemical modification of azido-biomolecules. *Organic & Biomolecular Chemistry* **2010**, *8* (18), 4051-4055.
116. Sutton, D. A.; Popik, V. V., Sequential Photochemistry of Dibenzo[a,e]dicyclopropa[c,g][8]annulene-1,6-dione: Selective Formation of Didehydrodibenzo[a,e][8]annulenes with Ultrafast SPAAC Reactivity. *The Journal of Organic Chemistry* **2016**, *81* (19), 8850-8857.
117. Gordon, C. G.; Mackey, J. L.; Jewett, J. C.; Sletten, E. M.; Houk, K. N.; Bertozzi, C. R., Reactivity of Biarylazacyclooctynones in Copper-Free Click Chemistry. *Journal of the American Chemical Society* **2012**, *134* (22), 9199-9208.
118. Codelli, J. A.; Baskin, J. M.; Agard, N. J.; Bertozzi, C. R., Second-Generation Difluorinated Cyclooctynes for Copper-Free Click Chemistry. *Journal of the American Chemical Society* **2008**, *130* (34), 11486-11493.
119. Frisch, M. J.; Trucks, G. W.; Schlegel, H. B.; Scuseria, G. E.; Robb, M. A.; Cheeseman, J. R.; Scalmani, G.; Barone, V.; Petersson, G. A.; Nakatsuji, H.; Li, X.; Caricato, M.; Marenich, A. V.; Bloino, J.; Janesko, B. G.; Gomperts, R.; Mennucci, B.; Hratchian, H. P.; Ortiz, J. V.; Izmaylov, A. F.; Sonnenberg, J. L.; Williams; Ding, F.; Lipparini, F.; Egidi, F.; Goings, J.; Peng, B.; Petrone, A.; Henderson, T.; Ranasinghe, D.; Zakrzewski, V. G.; Gao, J.; Rega, N.; Zheng, G.; Liang, W.; Hada, M.; Ehara, M.; Toyota, K.; Fukuda, R.; Hasegawa, J.; Ishida, M.; Nakajima, T.; Honda, Y.; Kitao, O.; Nakai, H.; Vreven, T.; Throssell, K.; Montgomery Jr., J. A.; Peralta, J. E.; Ogliaro, F.; Bearpark, M. J.; Heyd, J. J.; Brothers, E. N.; Kudin, K. N.; Staroverov, V. N.; Keith, T. A.; Kobayashi, R.; Normand, J.; Raghavachari, K.; Rendell, A. P.; Burant, J. C.; Iyengar, S. S.; Tomasi, J.; Cossi, M.; Millam, J. M.; Klene, M.; Adamo, C.; Cammi, R.; Ochterski, J. W.; Martin, R. L.; Morokuma, K.; Farkas, O.; Foresman, J. B.; Fox, D. J. *Gaussian 09 Rev. D.01*, Wallingford, CT, 2013.
120. Ess, D. H.; Houk, K. N., Activation Energies of Pericyclic Reactions: Performance of DFT, MP2, and CBS-QB3 Methods for the Prediction of Activation Barriers and Reaction Energetics of 1,3-Dipolar Cycloadditions, and Revised Activation Enthalpies for a Standard Set of Hydrocarbon Pericyclic Reactions. *The Journal of Physical Chemistry A* **2005**, *109* (42), 9542-9553.
121. Ess, D. H.; Jones, G. O.; Houk, K. N., Transition States of Strain-Promoted Metal-Free Click Chemistry: 1,3-Dipolar Cycloadditions of Phenyl Azide and Cyclooctynes. *Organic Letters* **2008**, *10* (8), 1633-1636.
122. Zhao, Y.; Truhlar, D. G., The M06 suite of density functionals for main group thermochemistry, thermochemical kinetics, noncovalent interactions, excited states, and transition elements: two new functionals and systematic testing of four M06-class functionals and 12 other functionals. *Theoretical Chemistry Accounts* **2008**, *120* (1), 215-241.
123. Weigend, F.; Ahlrichs, R., Balanced basis sets of split valence, triple zeta valence and quadruple zeta valence quality for H to Rn: Design and assessment of accuracy. *Physical Chemistry Chemical Physics* **2005**, *7* (18), 3297-3305.
124. Lam, Y.-h.; Grayson, M. N.; Holland, M. C.; Simon, A.; Houk, K. N., Theory and Modeling of Asymmetric Catalytic Reactions. *Accounts of Chemical Research* **2016**, *49* (4), 750-762.

125. Grayson, M. N.; Yang, Z.; Houk, K. N., Chronology of CH \cdots O Hydrogen Bonding from Molecular Dynamics Studies of the Phosphoric Acid-Catalyzed Allylboration of Benzaldehyde. *Journal of the American Chemical Society* **2017**, *139* (23), 7717-7720.
126. Chenoweth, K.; Chenoweth, D.; Goddard Iii, W. A., Cyclooctyne-based reagents for uncatalyzed click chemistry: A computational survey. *Organic & Biomolecular Chemistry* **2009**, *7* (24), 5255-5258.
127. Ess, D. H.; Houk, K. N., Theory of 1,3-Dipolar Cycloadditions: Distortion/Interaction and Frontier Molecular Orbital Models. *Journal of the American Chemical Society* **2008**, *130* (31), 10187-10198.
128. Ess, D. H.; Houk, K. N., Distortion/Interaction Energy Control of 1,3-Dipolar Cycloaddition Reactivity. *Journal of the American Chemical Society* **2007**, *129* (35), 10646-10647.
129. Schoenebeck, F.; Ess, D. H.; Jones, G. O.; Houk, K. N., Reactivity and Regioselectivity in 1,3-Dipolar Cycloadditions of Azides to Strained Alkynes and Alkenes: A Computational Study. *Journal of the American Chemical Society* **2009**, *131* (23), 8121-8133.
130. Taber, D. F.; Jiang, Q.; Chen, B.; Zhang, W.; Campbell, C. L., Synthesis of (-)-Calicoferol B. *The Journal of Organic Chemistry* **2002**, *67* (14), 4821-4827.
131. Ghera, E.; Maurya, R.; Ben-David, Y., New syntheses of phenanthrenes and of related systems by intramolecular annulation processes. *The Journal of Organic Chemistry* **1988**, *53* (9), 1912-1918.
132. Le Chevalier Isaad, A.; Barbetti, F.; Rovero, P.; D'Ursi, A. M.; Chelli, M.; Chorev, M.; Papini, A. M., N α -Fmoc-Protected ω -Azido- and ω -Alkynyl-L-amino Acids as Building Blocks for the Synthesis of "Clickable" Peptides. *European J. Org. Chem.* **2008**, *2008* (31), 5308-5314.
133. Vonnrhein, C.; Flensburg, C.; Keller, P.; Sharff, A.; Smart, O.; Paciorek, W.; Womack, T.; Bricogne, G., Data processing and analysis with the autoPROC toolbox. *Acta Crystallographica Section D* **2011**, *67* (4), 293-302.
134. McCoy, A. J.; Grosse-Kunstleve, R. W.; Adams, P. D.; Winn, M. D.; Storoni, L. C.; Read, R. J., Phaser crystallographic software. *Journal of Applied Crystallography* **2007**, *40* (4), 658-674.
135. Emsley, P.; Lohkamp, B.; Scott, W. G.; Cowtan, K., Features and development of Coot. *Acta Crystallographica Section D* **2010**, *66* (4), 486-501.
136. Vagin, A. A.; Steiner, R. A.; Lebedev, A. A.; Potterton, L.; McNicholas, S.; Long, F.; Murshudov, G. N., REFMAC5 dictionary: organization of prior chemical knowledge and guidelines for its use. *Acta Crystallographica Section D* **2004**, *60* (12 Part 1), 2184-2195.
137. Adams, P. D.; Afonine, P. V.; Bunkoczi, G.; Chen, V. B.; Davis, I. W.; Echols, N.; Headd, J. J.; Hung, L.-W.; Kapral, G. J.; Grosse-Kunstleve, R. W.; McCoy, A. J.; Moriarty, N. W.; Oeffner, R.; Read, R. J.; Richardson, D. C.; Richardson, J. S.; Terwilliger, T. C.; Zwart, P. H., PHENIX: a comprehensive Python-based system for macromolecular structure solution. *Acta Crystallographica Section D* **2010**, *66* (2), 213-221.
138. Zhi-Xin, W., An exact mathematical expression for describing competitive binding of two different ligands to a protein molecule. *FEBS Letters* **1995**, *360* (2), 111-114.
139. Heng, L. Y.; Peterson, d. A.; J., M. G.; R., V. A.; R., S. D., Linear Aliphatic Dialkynes as Alternative Linkers for Double-Click Stapling of p53-Derived Peptides. *ChemBioChem* **2014**, *15* (18), 2680-2683.
140. Barone, V.; Cossi, M., Quantum Calculation of Molecular Energies and Energy Gradients in Solution by a Conductor Solvent Model. *The Journal of Physical Chemistry A* **1998**, *102* (11), 1995-2001.
141. Maurizio, C.; Nadia, R.; Giovanni, S.; Vincenzo, B., Energies, structures, and electronic properties of molecules in solution with the C-PCM solvation model. *Journal of Computational Chemistry* **2003**, *24* (6), 669-681.

Appendix: DFT studies with benzyl azide

93 Benzyl azide

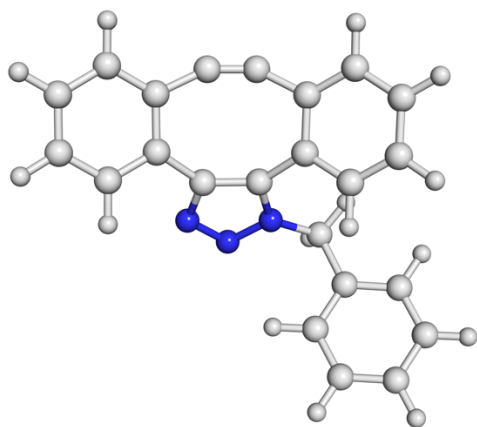


<i>E</i> (B3LYP)	<i>H</i> (B3LYP)	<i>G</i> (B3LYP)	<i>E</i> (M06-2X)
-435.149488	-435.007608	-435.053196	-435.128821

	X	Y	Z
6	-2.422311	1.209037	-0.169603
6	-3.098306	0.000298	-0.354834
6	-2.422682	-1.208666	-0.169842
6	-1.075895	-1.207089	0.197837
6	-0.390522	-0.000179	0.385451
6	-1.075541	1.206994	0.198076
1	-2.943571	2.152312	-0.307881
1	-4.147345	0.000499	-0.637987
1	-2.944199	-2.151771	-0.308299
1	-0.552890	-2.149264	0.343698
1	-0.552235	2.148975	0.344107
6	1.069277	-0.000461	0.765620
1	1.314949	0.887090	1.360027
1	1.314679	-0.888324	1.359688
7	1.902040	-0.000391	-0.481416
7	3.120794	0.000057	-0.299679
7	4.263809	0.000459	-0.257416

A.1 Products: triazole

P18

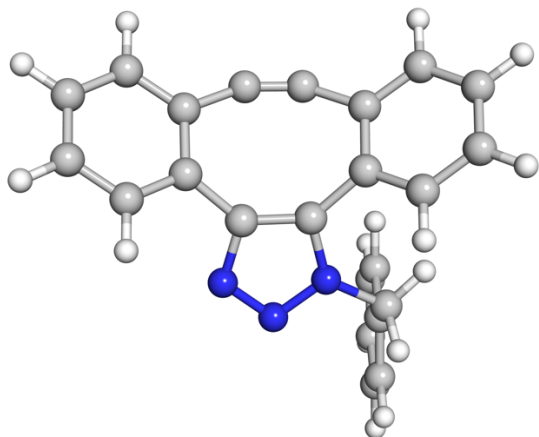


<i>E</i> (B3LYP)	<i>H</i> (B3LYP)	<i>G</i> (B3LYP)
-1049.640089	-1049.300223	-1049.368890

	X	Y	Z
6	-4.335439	-2.308814	-0.943689
6	-5.432894	-1.447235	-1.012201
6	-5.409576	-0.242669	-0.306121
6	-4.292322	0.098233	0.458711
6	-3.189530	-0.762883	0.534175
6	-3.221659	-1.972459	-0.171490
1	-4.345494	-3.248226	-1.489678
1	-6.298716	-1.711941	-1.612751
1	-6.256045	0.436704	-0.355366
1	-4.276970	1.041594	0.999344
1	-2.376642	-2.651758	-0.115020
6	-2.023411	-0.387090	1.434796
1	-2.016433	0.685843	1.627390
1	-2.114364	-0.895037	2.399597
7	-0.694042	-0.765129	0.931194
7	-0.280319	-2.017284	1.193706
7	0.950666	-2.118957	0.790031
6	0.302043	-0.015791	0.343532
6	1.381232	-0.925737	0.274627
6	2.814455	-0.927850	-0.147798
6	3.724621	0.131363	0.134275
6	3.104629	1.330533	0.577322

6	2.165191	2.097289	0.677778
6	0.852213	2.482724	0.283321
6	-0.005827	1.391922	-0.048390
6	-1.206301	1.685604	-0.705813
1	-1.852100	0.875610	-1.026094
6	0.448160	3.801077	0.048136
1	1.114709	4.613154	0.320360
6	3.333705	-2.096605	-0.719379
1	2.657912	-2.915421	-0.940947
6	5.093514	-0.011773	-0.128349
1	5.763597	0.810952	0.100494
6	5.581388	-1.191286	-0.688391
1	6.642584	-1.295298	-0.894036
6	4.697731	-2.227935	-0.992854
1	5.066998	-3.145518	-1.441643
6	-0.778282	4.064040	-0.564323
1	-1.081177	5.090261	-0.749338
6	-1.592014	3.005670	-0.963562
1	-2.531757	3.196700	-1.472700

P19

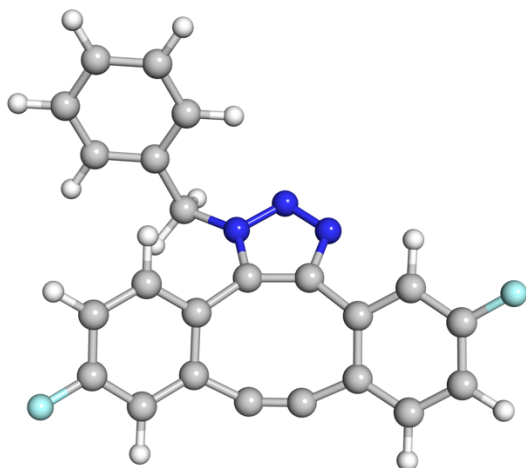


<i>E</i> (B3LYP)	<i>H</i> (B3LYP)	<i>G</i> (B3LYP)
-1049.638946	-1049.298980	-1049.369211

	X	Y	Z
6	-3.878617	-0.985986	2.069505

6	-4.879784	-1.854623	1.624172
6	-5.040328	-2.083930	0.256646
6	-4.199894	-1.450586	-0.662523
6	-3.196739	-0.579645	-0.224344
6	-3.044788	-0.349464	1.150227
1	-3.751295	-0.800092	3.132407
1	-5.531512	-2.347412	2.340339
1	-5.816977	-2.756412	-0.097008
1	-4.325380	-1.633958	-1.726665
1	-2.271742	0.329188	1.502778
6	-2.301468	0.124676	-1.224519
1	-2.658841	-0.030769	-2.245066
1	-2.281129	1.195998	-1.034041
7	-0.906847	-0.361134	-1.168201
7	-0.710236	-1.662740	-1.432988
7	0.530985	-1.936855	-1.159177
6	0.244432	0.242966	-0.712350
6	1.172248	-0.820128	-0.692657
6	2.581544	-1.052267	-0.261547
6	3.146225	-0.494686	0.922960
6	2.377837	0.547800	1.508206
6	1.561076	1.433966	1.491480
6	0.729818	2.301733	0.723439
6	0.232244	1.717000	-0.478122
6	-0.334890	2.569034	-1.434259
1	-0.655086	2.163274	-2.389315
6	0.546998	3.665521	0.976483
1	0.923268	4.085712	1.903667
6	3.347377	-1.987596	-0.969666
1	2.934424	-2.425188	-1.872020
6	4.412806	-0.896780	1.368863
1	4.816267	-0.457733	2.275882
6	5.146015	-1.837113	0.647456
1	6.128639	-2.141320	0.995512
6	4.615353	-2.372840	-0.527457
1	5.185382	-3.096217	-1.103228
6	-0.073904	4.480298	0.028021
1	-0.205843	5.539130	0.229227
6	-0.488788	3.937650	-1.187149
1	-0.936134	4.570912	-1.947095

P20: *anti*-attack

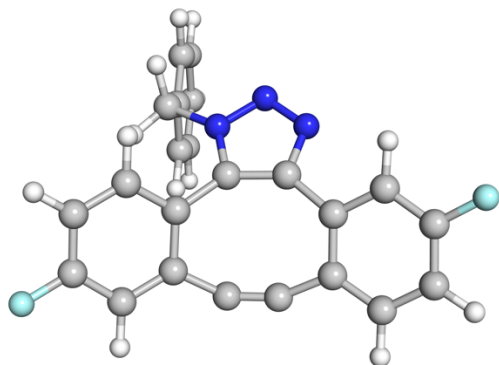


<i>E</i> (B3LYP)	<i>H</i> (B3LYP)	<i>G</i> (B3LYP)
-1248.105223	-1247.780392	-1247.853373

	X	Y	Z
6	-1.626332	1.320503	-0.647140
6	-2.246365	2.541463	-0.926807
6	-1.628437	3.709321	-0.505579
6	-0.395569	3.704386	0.136376
6	-0.408739	1.249876	0.041013
1	-3.191115	2.584201	-1.457123
1	0.083998	4.638682	0.404570
6	0.228716	2.479607	0.386752
6	0.138394	-0.077448	0.449260
6	1.364506	-0.779539	0.410864
6	2.785051	-0.522712	0.029291
6	3.479059	0.689327	0.314920
6	1.577806	2.342505	0.819721
6	2.640516	1.757915	0.723747
6	4.857644	0.795921	0.085027
6	3.518403	-1.588058	-0.504378
1	3.036805	-2.531595	-0.730930
6	4.882948	-1.443847	-0.730964
6	5.575889	-0.275843	-0.438687
1	6.641642	-0.211309	-0.627864
1	5.361918	1.728948	0.313240
1	-2.107753	0.408488	-0.980531

9	5.558467	-2.489700	-1.253834
9	-2.223300	4.894284	-0.751021
6	-5.434704	-1.326608	-0.315301
6	-5.207438	-2.478895	-1.071084
6	-3.959551	-3.104105	-1.018541
6	-2.944196	-2.585257	-0.212248
6	-3.164420	-1.427073	0.543896
6	-4.417128	-0.802027	0.483623
1	-6.400312	-0.829941	-0.352404
1	-5.996137	-2.885346	-1.698057
1	-3.774173	-4.000729	-1.603642
1	-1.980182	-3.082619	-0.169150
1	-4.597335	0.100118	1.063430
6	-2.108450	-0.863128	1.481362
1	-2.295866	0.191640	1.683819
1	-2.134256	-1.391932	2.438812
7	-0.720164	-0.994413	1.014568
7	-0.095469	-2.153547	1.289206
7	1.142871	-2.031689	0.917481

P21: *anti*-attack

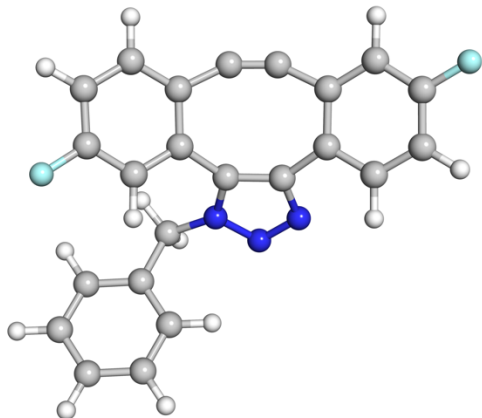


<i>E</i> (B3LYP)	<i>H</i> (B3LYP)	<i>G</i> (B3LYP)
-1248.104307	-1247.779450	-1247.853127

	X	Y	Z
6	-0.964580	2.272525	-1.491240
6	-1.368113	3.602777	-1.345020

6	-1.052553	4.263614	-0.166724
6	-0.306695	3.665738	0.842595
6	-0.257700	1.601389	-0.484785
1	-1.917836	4.114419	-2.127037
1	-0.030246	4.231301	1.724947
6	0.115668	2.344490	0.674030
6	0.024303	0.142719	-0.624499
6	1.129472	-0.733201	-0.541931
6	2.550945	-0.685515	-0.092375
6	2.999320	0.044180	1.048259
6	1.077187	1.693264	1.499499
6	2.055419	0.971665	1.559219
6	4.313435	-0.096588	1.516072
6	3.468056	-1.524135	-0.735732
1	3.172316	-2.103804	-1.601727
6	4.766953	-1.630597	-0.251229
6	5.211759	-0.941895	0.870481
1	6.233166	-1.060454	1.214688
1	4.628294	0.468332	2.387091
1	-1.202484	1.755868	-2.415680
9	5.627388	-2.443409	-0.901246
9	-1.451908	5.541039	-0.002693
6	-4.751519	-3.219032	0.125940
6	-4.739668	-2.982820	1.501815
6	-3.981786	-1.927703	2.018772
6	-3.240951	-1.113217	1.162310
6	-3.243134	-1.348966	-0.219499
6	-4.004417	-2.405892	-0.729788
1	-5.340207	-4.035496	-0.283061
1	-5.319723	-3.614618	2.168790
1	-3.972752	-1.735625	3.088129
1	-2.658005	-0.290614	1.569576
1	-4.012968	-2.593321	-1.800535
6	-2.449434	-0.455844	-1.151361
1	-2.735013	-0.626926	-2.192168
1	-2.627028	0.592773	-0.920332
7	-0.992137	-0.686274	-1.043987
7	-0.559112	-1.942561	-1.236910
7	0.707156	-1.971486	-0.945685

P22: *syn*-attack

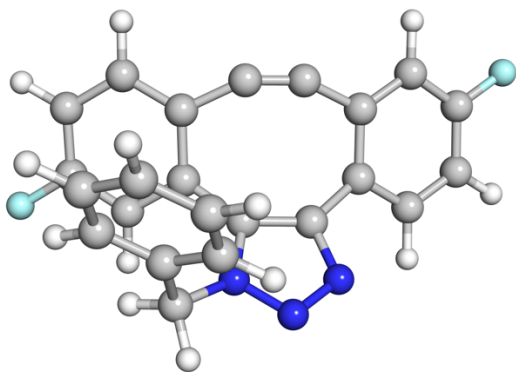


<i>E</i> (B3LYP)	<i>H</i> (B3LYP)	<i>G</i> (B3LYP)
-1248.104388	-1247.779562	-1247.852716

	X	Y	Z
6	-3.357192	-1.822028	-0.678230
6	-4.725962	-1.817006	-0.953410
6	-5.474520	-0.705246	-0.589914
6	-4.902399	0.404426	0.016172
6	-2.724823	-0.734523	-0.061186
1	-5.207386	-2.660093	-1.436989
1	-5.511620	1.263615	0.272377
6	-3.526505	0.394593	0.274065
6	-1.299697	-0.893770	0.356197
6	-0.132369	-0.104122	0.453474
6	0.312661	1.281466	0.121120
6	-0.433216	2.438184	0.499703
6	-2.793200	1.506819	0.767674
6	-1.779419	2.170437	0.872587
6	0.101615	3.718605	0.318364
6	1.539730	1.474604	-0.520871
1	2.126593	0.638630	-0.881305
6	2.031234	2.764671	-0.706869
6	1.349946	3.893748	-0.277982
1	1.774584	4.879585	-0.431721

1	-0.479324	4.582255	0.623654
1	-2.767226	-2.693592	-0.938312
9	3.221520	2.908608	-1.325535
9	-6.801042	-0.693790	-0.843583
6	4.212738	-2.763402	-1.030762
6	5.401072	-2.029525	-1.055390
6	5.520122	-0.881689	-0.268972
6	4.453942	-0.469359	0.532517
6	3.260891	-1.203578	0.564988
6	3.149470	-2.356952	-0.221955
1	4.111900	-3.657546	-1.639816
1	6.227225	-2.348686	-1.684623
1	6.438272	-0.301036	-0.284076
1	4.549362	0.430548	1.135468
1	2.232824	-2.938173	-0.199822
6	2.150720	-0.760689	1.505331
1	2.198665	-1.328532	2.439130
1	2.255542	0.294855	1.757214
7	0.784260	-0.974304	1.003567
7	0.244492	-2.185656	1.217891
7	-0.992003	-2.144208	0.820110

P23: *syn*-attack

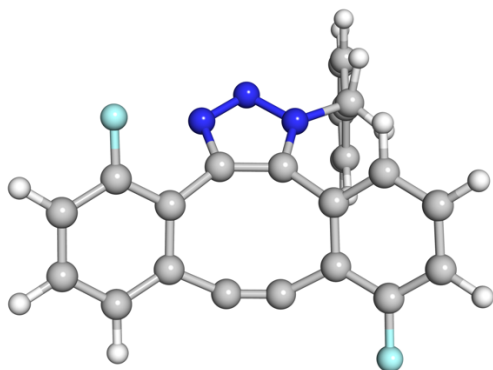


<i>E</i> (B3LYP)	<i>H</i> (B3LYP)	<i>G</i> (B3LYP)
-1248.104177	-1247.779254	-1247.852290

	X	Y	Z
--	---	---	---

6	3.773851	-0.570060	-1.238765
6	5.078966	-0.483526	-0.750937
6	5.272293	-0.093017	0.567766
6	4.214518	0.233021	1.404914
6	2.665766	-0.260460	-0.439328
1	5.932551	-0.718455	-1.377503
1	4.401160	0.549664	2.424705
6	2.910223	0.157622	0.901487
6	1.303792	-0.552637	-0.973414
6	0.006709	-0.006998	-0.885356
6	-0.657048	1.213492	-0.339370
6	-0.493495	1.628621	1.015032
6	1.752918	0.584765	1.606867
6	0.625287	1.037558	1.668473
6	-1.260879	2.678276	1.532430
6	-1.515737	1.954655	-1.157014
1	-1.617434	1.738159	-2.214555
6	-2.244596	3.011658	-0.616093
6	-2.158263	3.371915	0.720985
1	-2.753727	4.193432	1.103555
1	-1.128935	2.970731	2.568592
1	3.609366	-0.894595	-2.260028
9	-3.065092	3.704244	-1.432590
9	6.530337	-0.015141	1.052670
6	-2.917839	-3.210469	1.445385
6	-3.961512	-2.499452	2.046143
6	-4.432709	-1.327379	1.452940
6	-3.859945	-0.864804	0.264913
6	-2.817595	-1.573259	-0.342459
6	-2.351068	-2.751623	0.256723
1	-2.548078	-4.124719	1.901434
1	-4.403570	-2.858606	2.971391
1	-5.242002	-0.768340	1.914413
1	-4.226634	0.051132	-0.191622
1	-1.541832	-3.307754	-0.209438
6	-2.224118	-1.086188	-1.651600
1	-2.367302	-1.820737	-2.447667
1	-2.695793	-0.157927	-1.967405
7	-0.760866	-0.908864	-1.586477
7	-0.011545	-1.911429	-2.078391
7	1.220685	-1.694589	-1.725836

P24: *anti*-attack

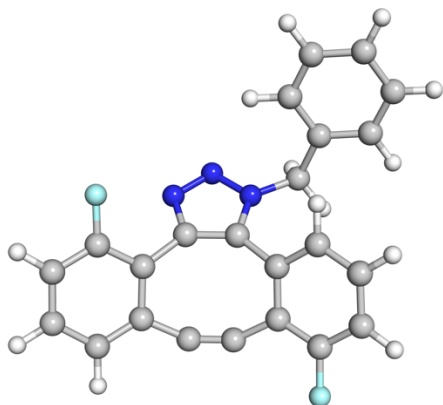


<i>E</i> (B3LYP)	<i>H</i> (B3LYP)	<i>G</i> (B3LYP)
-1248.100029	-1247.775160	-1247.849370

	X	Y	Z
6	-3.276786	-2.079371	-0.572709
6	-4.534695	-2.389051	-0.060073
6	-4.995423	-1.715133	1.068356
6	-4.213779	-0.718323	1.652075
6	-2.434058	-1.116479	-0.009930
1	-5.127691	-3.151241	-0.554133
1	-5.970696	-1.954262	1.480169
1	-4.574621	-0.162159	2.510521
6	-2.958055	-0.411012	1.115782
6	-1.021892	-0.993988	-0.471767
6	-0.100963	0.045926	-0.709807
6	-0.101986	1.536045	-0.756610
6	-0.589892	2.308884	0.336359
6	-2.161761	0.699559	1.510286
6	-1.385045	1.608366	1.283605
6	-0.426027	3.694149	0.309316
6	0.450719	2.208580	-1.853112
1	0.778180	1.643474	-2.719708
6	0.579868	3.602187	-1.855190
1	1.014476	4.099214	-2.716308

6	0.158616	4.356621	-0.762008
1	0.252679	5.436773	-0.738132
9	-0.886893	4.407123	1.356569
9	-2.881070	-2.744346	-1.678619
6	4.270986	-0.788822	2.092646
6	5.226901	-1.731974	1.703103
6	5.275641	-2.162226	0.375983
6	4.368849	-1.654367	-0.557599
6	3.409676	-0.710689	-0.175024
6	3.370170	-0.278420	1.157882
1	4.231351	-0.446323	3.123001
1	5.931063	-2.126099	2.430644
1	6.017098	-2.893162	0.065469
1	4.406939	-1.993050	-1.589864
1	2.632929	0.459244	1.465645
6	2.443997	-0.143815	-1.195637
1	2.412762	0.942590	-1.132964
1	2.747119	-0.414888	-2.210080
7	1.061942	-0.630507	-0.997233
7	0.878565	-1.960399	-0.960760
7	-0.364834	-2.181233	-0.652202

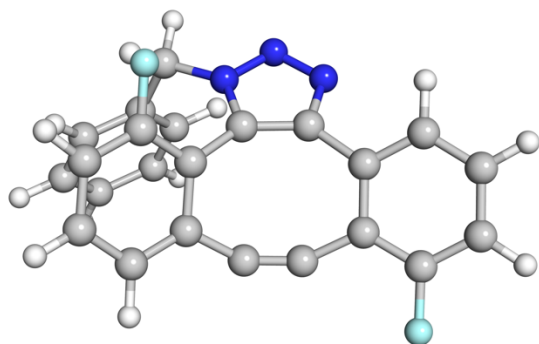
P25: *anti*-attack



<i>E</i> (B3LYP)	<i>H</i> (B3LYP)	<i>G</i> (B3LYP)
-1248.101152	-1247.776254	-1247.849125

	X	Y	Z
6	-3.178778	-2.116106	-0.640297
6	-4.541815	-2.267061	-0.886847
6	-5.416001	-1.243603	-0.528975
6	-4.920398	-0.070250	0.039602
6	-2.628649	-0.978665	-0.042772
1	-4.891178	-3.182055	-1.353083
1	-6.480411	-1.354147	-0.709941
1	-5.586291	0.747543	0.293073
6	-3.546830	0.068826	0.268178
6	-1.200167	-0.977948	0.387283
6	-0.114933	-0.077764	0.377728
6	0.183240	1.299765	-0.109352
6	-0.678834	2.394166	0.194621
6	-2.910153	1.275321	0.670477
6	-1.977493	2.056339	0.659725
6	-0.276090	3.685831	-0.145498
6	1.367073	1.563011	-0.807008
1	2.016206	0.742660	-1.089884
6	1.729155	2.870380	-1.151211
1	2.654720	3.045135	-1.690089
6	0.916650	3.948099	-0.806142
1	1.178081	4.970260	-1.057262
9	-1.102635	4.706883	0.158514
9	-2.367223	-3.125569	-1.020420
6	4.433609	-2.486864	-0.802895
6	5.537324	-1.645946	-0.965059
6	5.547205	-0.392889	-0.348765
6	4.456152	0.017063	0.420071
6	3.347493	-0.822696	0.588745
6	3.346220	-2.080985	-0.026757
1	4.418281	-3.463613	-1.278655
1	6.382651	-1.964422	-1.568682
1	6.399003	0.270290	-0.471491
1	4.465872	0.997129	0.890932
1	2.495764	-2.743410	0.102624
6	2.209688	-0.369300	1.489713
1	2.319237	-0.806744	2.486415
1	2.215836	0.715168	1.603497
7	0.867217	-0.771932	1.045836
7	0.433612	-1.984793	1.434150
7	-0.795267	-2.114414	1.033201

P26: *syn*-attack

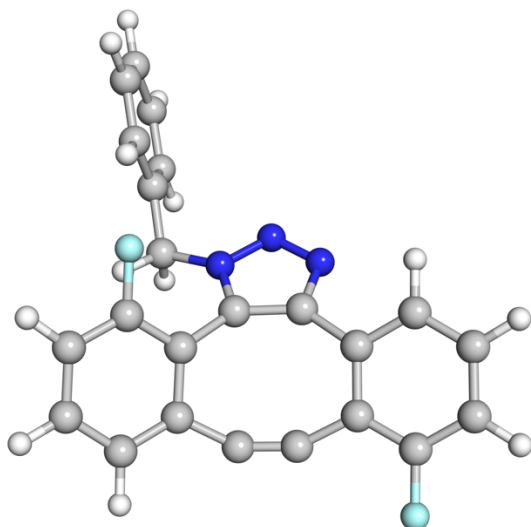


<i>E</i> (B3LYP)	<i>H</i> (B3LYP)	<i>G</i> (B3LYP)
-1248.104286	-1247.779238	-1247.852361

	X	Y	Z
6	-1.309851	1.866271	-1.504066
6	-1.973283	3.054725	-1.208215
6	-1.820730	3.610508	0.058816
6	-0.977442	3.005284	0.993400
6	-0.514503	1.176505	-0.587941
1	-2.587700	3.519363	-1.971462
1	-2.337031	4.531568	0.309440
1	-0.806304	3.463331	1.961400
6	-0.306314	1.823452	0.668459
6	0.033248	-0.173315	-0.903474
6	1.282313	-0.827642	-0.898904
6	2.674957	-0.545080	-0.448313
6	2.967366	0.116289	0.779016
6	0.769408	1.264810	1.417847
6	1.878216	0.763015	1.413994
6	4.292475	0.185127	1.215871
6	3.740262	-1.090191	-1.175262
1	3.531766	-1.603699	-2.106792
6	5.055686	-0.992668	-0.713270
1	5.863438	-1.418576	-1.300187
6	5.345298	-0.357515	0.495048
1	6.357993	-0.272263	0.873586
9	4.541256	0.815447	2.382815
9	-1.463614	1.359327	-2.751662
6	-3.217289	-2.448697	2.051226

6	-4.152897	-1.493040	2.460129
6	-4.476835	-0.433041	1.612017
6	-3.864602	-0.326042	0.360269
6	-2.930115	-1.280239	-0.055843
6	-2.611862	-2.344531	0.799344
1	-2.962757	-3.277249	2.706400
1	-4.625777	-1.575993	3.434802
1	-5.201581	0.314169	1.923222
1	-4.114622	0.504411	-0.295117
1	-1.886822	-3.090063	0.482648
6	-2.294183	-1.180814	-1.429301
1	-2.512020	-2.069235	-2.027027
1	-2.662450	-0.316196	-1.977062
7	-0.821422	-1.137367	-1.381114
7	-0.167088	-2.275549	-1.668860
7	1.089816	-2.090166	-1.392786

P27: *syn*-attack

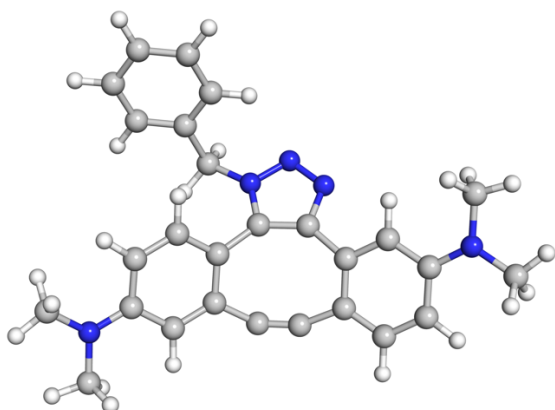


<i>E</i> (B3LYP)	<i>H</i> (B3LYP)	<i>G</i> (B3LYP)
-1248.102229	-1247.777300	-1247.850476

	X	Y	Z
6	0.681674	2.305443	0.864519
6	0.723125	3.695506	0.930929
6	-0.196677	4.428434	0.185936

6	-1.168969	3.771668	-0.571479
6	-0.218603	1.594198	0.070446
1	1.466733	4.172340	1.559811
1	-0.174055	5.512947	0.217684
1	-1.925696	4.334766	-1.106657
6	-1.204372	2.374686	-0.606756
6	-0.107516	0.116011	-0.084584
6	-0.940578	-1.011261	0.059438
6	-2.382713	-1.292983	0.309379
6	-3.429697	-0.551526	-0.309905
6	-2.292270	1.599948	-1.105050
6	-3.048702	0.661382	-0.935962
6	-4.748961	-0.988643	-0.167792
6	-2.727158	-2.429828	1.050549
1	-1.940146	-3.008058	1.520864
6	-4.059334	-2.831713	1.181004
1	-4.298820	-3.713411	1.767213
6	-5.086918	-2.116211	0.564961
1	-6.127033	-2.410878	0.651278
9	-5.721047	-0.268598	-0.765742
9	1.575970	1.614099	1.613629
6	5.275681	-0.924281	1.171758
6	6.005977	-1.689884	0.257992
6	5.537555	-1.841465	-1.048239
6	4.341208	-1.233717	-1.436008
6	3.603676	-0.467448	-0.526400
6	4.083789	-0.313482	0.781707
1	5.638057	-0.797322	2.188243
1	6.936100	-2.161745	0.562587
1	6.100078	-2.432203	-1.765903
1	3.978089	-1.355410	-2.453448
1	3.525590	0.287473	1.492175
6	2.323859	0.206692	-0.973268
1	2.306910	1.253429	-0.678404
1	2.237247	0.169717	-2.063123
7	1.106905	-0.435482	-0.423978
7	1.040033	-1.774404	-0.475449
7	-0.175766	-2.123015	-0.172339

P28: *anti*-attack

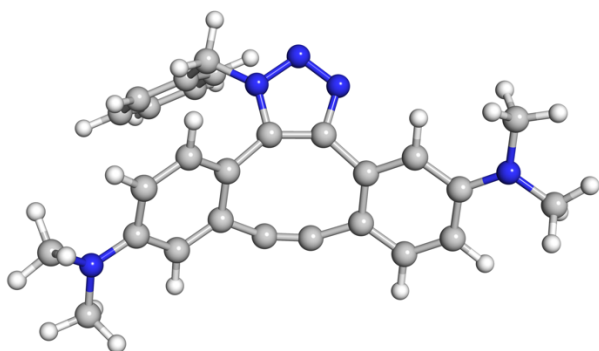


<i>E</i> (B3LYP)	<i>H</i> (B3LYP)	<i>G</i> (B3LYP)
-1317.583246	-1317.087790	-1317.178647

	X	Y	Z
6	-2.150208	-0.364696	0.510444
6	-3.178915	-1.255070	0.804512
6	-3.132594	-2.595181	0.351752
6	-1.959866	-3.002290	-0.332325
6	-1.014152	-0.733205	-0.222860
1	-2.236779	0.651761	0.880092
1	-4.018350	-0.898112	1.387761
1	-1.827566	-4.032759	-0.635599
6	-0.922929	-2.109087	-0.592551
6	-0.018863	0.290301	-0.643219
6	1.385709	0.471508	-0.659486
6	2.611026	-0.317966	-0.323763
6	2.759107	-1.705486	-0.617979
6	0.357371	-2.498817	-1.087062
6	1.565874	-2.365583	-0.990270
6	4.002404	-2.320004	-0.409583
1	4.111564	-3.376051	-0.638622
6	3.705607	0.378527	0.185669
1	3.578384	1.432025	0.392812
6	4.963008	-0.239906	0.410779
6	5.088191	-1.614032	0.084894
1	6.028255	-2.132090	0.227845

7	6.019320	0.473492	0.927081
7	-4.168790	-3.472554	0.578213
6	7.314987	-0.167516	1.102146
1	8.012960	0.550499	1.533186
1	7.249647	-1.026210	1.782814
1	7.732047	-0.520065	0.148310
6	5.883189	1.898143	1.197186
1	6.821788	2.274143	1.604905
1	5.652458	2.469301	0.287191
1	5.092147	2.095284	1.932243
6	-4.018480	-4.881475	0.240000
1	-3.221416	-5.369663	0.820029
1	-4.956430	-5.398179	0.446154
1	-3.792980	-5.009654	-0.825153
6	-5.292468	-3.066231	1.411226
1	-5.780329	-2.172623	1.004650
1	-6.029825	-3.869467	1.429830
1	-4.990988	-2.850091	2.446902
6	-4.647652	3.586821	0.364916
6	-3.959456	4.528502	1.133431
6	-2.567971	4.608083	1.043444
6	-1.866359	3.755337	0.188240
6	-2.549916	2.805165	-0.580570
6	-3.945727	2.728168	-0.482939
1	-5.729729	3.513139	0.430535
1	-4.503116	5.193499	1.798768
1	-2.024504	5.337595	1.637835
1	-0.785641	3.828718	0.116257
1	-4.486370	1.990124	-1.070864
6	-1.831495	1.895226	-1.565165
1	-2.416643	0.994178	-1.751120
1	-1.700942	2.409386	-2.522525
7	-0.481654	1.479640	-1.166254
7	0.527400	2.319731	-1.466993
7	1.638843	1.722535	-1.156251

P29: *anti*-attack

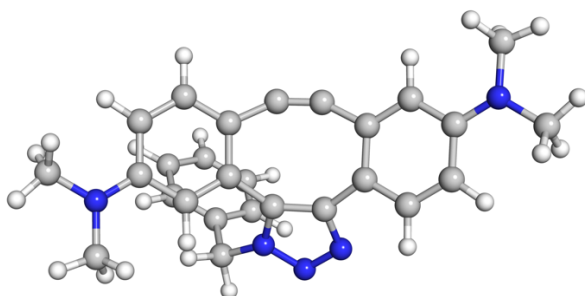


<i>E</i> (B3LYP)	<i>H</i> (B3LYP)	<i>G</i> (B3LYP)
-1317.583128	-1317.087679	-1317.178376

	X	Y	Z
6	1.843610	-0.814109	-1.711492
6	2.934097	-1.672835	-1.603629
6	3.256333	-2.286631	-0.368708
6	2.368886	-2.062281	0.713737
6	1.003049	-0.521212	-0.629978
1	1.631179	-0.378678	-2.684057
1	3.530144	-1.864126	-2.486890
1	2.508436	-2.574423	1.656921
6	1.262005	-1.226555	0.582094
6	-0.053107	0.520549	-0.750407
6	-1.437187	0.666216	-0.505058
6	-2.530194	-0.129808	0.129849
6	-2.347928	-0.898139	1.318292
6	0.207504	-1.132447	1.541634
6	-1.001955	-1.100518	1.701543
6	-3.467204	-1.478937	1.932781
1	-3.326706	-2.058604	2.840436
6	-3.813983	-0.002516	-0.397074
1	-3.933245	0.593047	-1.291680
6	-4.947620	-0.602253	0.210560
6	-4.741756	-1.334741	1.407058
1	-5.574474	-1.800684	1.918882
7	-6.198784	-0.475389	-0.345923
7	4.368187	-3.086194	-0.227916
6	-7.356922	-1.046241	0.327386

1	-8.247060	-0.858538	-0.273455
1	-7.254368	-2.132118	0.449491
1	-7.515480	-0.605054	1.321590
6	-6.394118	0.338077	-1.538248
1	-7.443698	0.295012	-1.829997
1	-6.128899	1.390840	-1.367616
1	-5.794286	-0.032135	-2.379321
6	4.588869	-3.816278	1.013018
1	3.803100	-4.560967	1.208977
1	5.545604	-4.336274	0.953537
1	4.632350	-3.132784	1.868921
6	5.161844	-3.433918	-1.398686
1	5.552947	-2.535477	-1.890824
1	6.012523	-4.039718	-1.084762
1	4.585446	-4.006512	-2.140232
6	2.447493	3.955512	1.779619
6	3.742040	3.477438	2.006344
6	4.335147	2.619075	1.079293
6	3.635790	2.237848	-0.069051
6	2.342077	2.715701	-0.304000
6	1.752858	3.578938	0.630275
1	1.980683	4.624895	2.497084
1	4.283101	3.772696	2.901154
1	5.339388	2.240658	1.249424
1	4.098002	1.562450	-0.784520
1	0.747619	3.953457	0.454678
6	1.604139	2.331323	-1.573715
1	1.382691	3.213894	-2.179109
1	2.206073	1.655688	-2.178035
7	0.285327	1.729705	-1.315248
7	-0.783341	2.543453	-1.428232
7	-1.811914	1.906412	-0.952856

P30: *syn*-attack

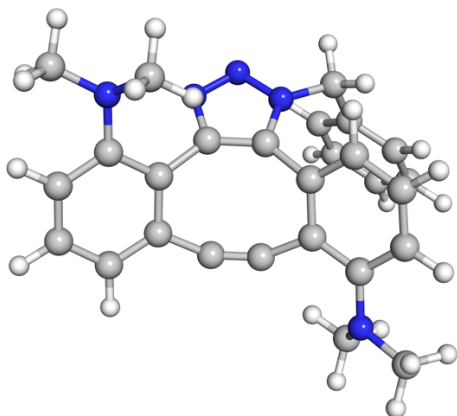


<i>E (B3LYP)</i>	<i>H (B3LYP)</i>	<i>G (B3LYP)</i>
-1317.581073	-1317.085704	-1317.177075

	X	Y	Z
6	-3.421504	0.073184	1.631566
6	-4.745221	-0.138844	1.258419
6	-5.098973	-0.345637	-0.097004
6	-4.048721	-0.330662	-1.044730
6	-2.368461	0.082232	0.707795
1	-3.197505	0.248812	2.679081
1	-5.505573	-0.136688	2.029720
1	-4.250525	-0.484194	-2.097033
6	-2.721772	-0.136787	-0.655096
6	-1.013014	0.502296	1.159258
6	0.330428	0.193888	0.854809
6	1.090966	-0.800351	0.037803
6	0.818127	-1.003633	-1.346274
6	-1.610180	-0.234144	-1.540793
6	-0.448160	-0.520633	-1.770736
6	1.674534	-1.822533	-2.092250
1	1.476435	-1.966829	-3.150166
6	2.131293	-1.513108	0.632854
1	2.279351	-1.413694	1.700436
6	2.981502	-2.375783	-0.111219
6	2.747262	-2.479154	-1.504527
1	3.379283	-3.103396	-2.123513
7	3.990467	-3.079674	0.501922
7	-6.407060	-0.568091	-0.478449
6	4.875535	-3.921211	-0.291577
1	5.605349	-4.391751	0.367368
1	4.321436	-4.716316	-0.807641
1	5.422440	-3.340853	-1.047267
6	4.223981	-2.941904	1.932548
1	5.043307	-3.599225	2.223917
1	4.499463	-1.914204	2.208116
1	3.339069	-3.227130	2.516134
6	-6.750191	-0.608714	-1.892942
1	-6.210269	-1.412304	-2.407846
1	-7.817541	-0.808848	-1.994592
1	-6.525997	0.337291	-2.408577

6	-7.476985	-0.413179	0.497024
1	-7.532998	0.608545	0.901939
1	-8.429911	-0.645003	0.019723
1	-7.348003	-1.104992	1.337844
6	4.171280	2.629192	-1.632780
6	3.473715	3.801502	-1.927524
6	2.435380	4.220254	-1.089473
6	2.099911	3.471361	0.038218
6	2.795331	2.291872	0.339221
6	3.830217	1.876477	-0.505666
1	4.977346	2.295333	-2.280384
1	3.735459	4.386613	-2.804865
1	1.889381	5.132775	-1.312897
1	1.293432	3.799538	0.688928
1	4.370681	0.959901	-0.283412
6	2.455662	1.489420	1.582113
1	3.094387	0.612095	1.657562
1	2.596000	2.087302	2.486000
7	1.040613	1.081268	1.634156
7	0.221174	1.853248	2.370465
7	-1.001789	1.502509	2.098649

P31: *anti*-attack

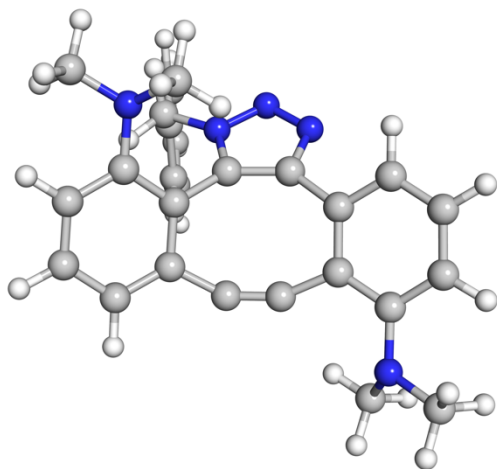


<i>E</i> (B3LYP)	<i>H</i> (B3LYP)	<i>G</i> (B3LYP)
-1317.566386	-1317.071709	-1317.159593

	X	Y	Z
6	3.956377	0.252859	-0.245531
6	4.833418	1.030014	-1.034976
6	4.363233	1.894042	-2.019678
6	2.995506	2.058656	-2.217821
6	2.560058	0.340283	-0.499621
1	5.900863	0.972002	-0.860164
1	5.071934	2.472191	-2.606118
1	2.611918	2.769619	-2.942014
6	2.103803	1.301637	-1.449388
6	1.609058	-0.684453	0.037038
6	0.341584	-0.676327	0.646055
6	-0.641713	0.323912	1.157802
6	-1.170258	1.331688	0.301773
6	0.691522	1.503937	-1.445286
6	-0.377294	1.538895	-0.860454
6	-2.240683	2.165654	0.723319
6	-1.104895	0.231400	2.472643
1	-0.668102	-0.491485	3.154313
6	-2.119256	1.086619	2.910648
1	-2.479060	1.013594	3.932894
6	-2.697980	2.013781	2.049802
1	-3.510284	2.629630	2.415382
7	-2.757017	3.147098	-0.129949
7	4.460800	-0.603066	0.751117
6	3.952160	-0.436564	2.113030
1	4.134649	-1.353573	2.683386
1	4.450194	0.398200	2.635210
1	2.879329	-0.247754	2.108522
6	5.883532	-0.910695	0.735110
1	6.520366	-0.074449	1.073419
1	6.061200	-1.755954	1.407672
1	6.198373	-1.203722	-0.270081
6	-3.676409	4.126678	0.436659
1	-3.819907	4.927293	-0.294268
1	-4.666704	3.705753	0.678172
1	-3.252334	4.566341	1.343260
6	-3.120836	2.769862	-1.499289
1	-4.095878	2.257313	-1.534865
1	-3.183398	3.673610	-2.112898
1	-2.366688	2.117948	-1.939445
6	-1.236160	-2.673891	1.100622

1	-0.956988	-3.714669	1.280876
1	-1.609765	-2.258088	2.035094
6	-2.284771	-2.571813	0.008048
6	-2.057142	-3.148230	-1.249513
6	-3.499356	-1.920564	0.249663
6	-3.028628	-3.072699	-2.247329
1	-1.114791	-3.653778	-1.444572
6	-4.475338	-1.847566	-0.748111
1	-3.682780	-1.466815	1.220264
6	-4.241538	-2.422518	-1.998295
1	-2.841670	-3.523954	-3.217963
1	-5.414803	-1.339931	-0.547241
1	-4.998904	-2.365937	-2.775334
7	0.029862	-2.010442	0.746617
7	1.011657	-2.781096	0.240321
7	1.958308	-1.992633	-0.177394

P32: *syn*-attack



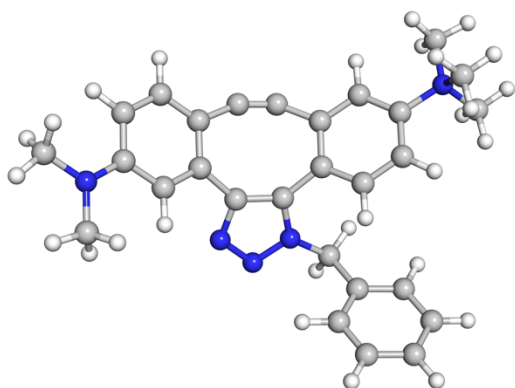
<i>E</i> (B3LYP)	<i>H</i> (B3LYP)	<i>G</i> (B3LYP)
-1317.569255	-1317.074559	-1317.162301

	X	Y	Z
6	-1.370242	2.560688	0.237072
6	-1.631208	3.451508	1.301125
6	-1.036375	3.288378	2.548303
6	-0.110435	2.269176	2.763049
6	-0.518696	1.448924	0.478512

1	-2.294083	4.293526	1.142977
1	-1.263948	3.991396	3.344555
1	0.412517	2.175289	3.708839
6	0.169577	1.376191	1.725410
6	-0.419655	0.317769	-0.492978
6	0.584625	-0.372767	-1.201479
6	2.076755	-0.403870	-1.239532
6	2.873283	-0.438299	-0.058446
6	1.247552	0.438751	1.737923
6	2.159612	-0.072927	1.110607
6	4.277023	-0.656218	-0.118459
6	2.704872	-0.540647	-2.480848
1	2.108402	-0.516421	-3.386043
6	4.088490	-0.709381	-2.547531
1	4.571323	-0.808002	-3.515924
6	4.863422	-0.780335	-1.392655
1	5.929894	-0.946024	-1.484823
7	5.040438	-0.678187	1.059011
7	-1.970162	2.738189	-1.028927
6	-1.063482	2.918132	-2.168774
1	-1.614068	2.736796	-3.097295
1	-0.652320	3.940620	-2.203703
1	-0.233097	2.214003	-2.120890
6	-3.119036	3.633656	-1.110592
1	-2.849875	4.700448	-1.028687
1	-3.602582	3.485288	-2.081005
1	-3.843067	3.393882	-0.327483
6	6.490529	-0.609735	0.924640
1	6.918989	-0.414488	1.912134
1	6.938154	-1.541855	0.540138
1	6.771876	0.213022	0.262205
6	4.633168	-1.585830	2.136614
1	4.958442	-2.620988	1.941188
1	5.088005	-1.253848	3.075189
1	3.551352	-1.578605	2.267218
6	-2.962506	-0.136993	-0.459884
1	-2.950118	0.626868	0.315721
1	-3.554637	0.242665	-1.295052
6	-3.541202	-1.431156	0.076080
6	-4.607558	-2.054932	-0.579750
6	-3.037753	-2.001849	1.253695
6	-5.164083	-3.231608	-0.070735

1	-5.005525	-1.618352	-1.492547
6	-3.587035	-3.179630	1.759692
1	-2.212413	-1.523188	1.775592
6	-4.653510	-3.797240	1.098615
1	-5.993108	-3.704780	-0.589836
1	-3.187776	-3.612760	2.672775
1	-5.083686	-4.712763	1.495295
7	-1.573215	-0.293948	-0.923258
7	-1.321162	-1.242936	-1.838436
7	-0.030960	-1.288871	-2.012473

P33: *anti*-attack



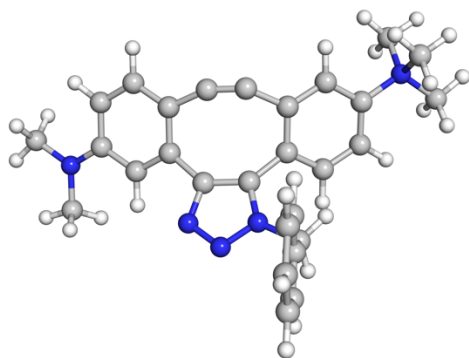
<i>E</i> (B3LYP)	<i>H</i> (B3LYP)	<i>G</i> (B3LYP)
-1357.325836	-1356.786076	-1356.876925

	X	Y	Z
6	3.979591	-2.487219	-0.484859
6	5.110354	-1.892068	0.046645
6	5.100906	-0.518298	0.405787
6	3.905927	0.216310	0.177223
6	2.799723	-1.757063	-0.700753
1	3.999354	-3.542403	-0.740034
1	5.998359	-2.493435	0.194183
1	3.866900	1.270427	0.414261
6	2.768221	-0.369870	-0.367550
6	1.563483	-2.292182	-1.109875
6	0.351793	-2.338044	-1.264280

6	-0.872874	-1.867396	-0.714312
6	-0.862972	-0.509473	-0.282519
6	1.615380	0.523608	-0.692389
6	0.205300	0.449980	-0.686030
6	-1.938508	-0.069909	0.494320
1	-1.935889	0.936092	0.896985
6	-1.985324	-2.684207	-0.466374
1	-1.953857	-3.698681	-0.836580
6	-3.058653	-2.188855	0.268611
6	-3.030816	-0.891869	0.777548
1	-3.834638	-0.491093	1.382906
7	-4.261787	-3.049470	0.560937
7	6.203539	0.083218	0.954008
6	-4.374807	-3.268838	2.058170
1	-5.239800	-3.905262	2.244759
1	-3.461109	-3.751984	2.402528
1	-4.502730	-2.308583	2.552930
6	-4.189038	-4.406248	-0.099877
1	-5.110475	-4.935981	0.137956
1	-4.103464	-4.275382	-1.177508
1	-3.337086	-4.956505	0.295743
6	6.178773	1.500036	1.296972
1	5.403165	1.721839	2.041253
1	7.143245	1.780086	1.720308
1	5.998241	2.128384	0.414995
6	7.422183	-0.686089	1.173141
1	7.829564	-1.078640	0.232053
1	8.174886	-0.040612	1.625458
1	7.247471	-1.532047	1.850326
6	-5.515928	-2.362838	0.052780
1	-5.638496	-1.409015	0.560575
1	-5.410817	-2.208285	-1.020399
1	-6.366343	-3.009741	0.266943
6	-4.187680	3.969742	0.451814
6	-3.443511	4.873417	1.213368
6	-2.052476	4.900648	1.088674
6	-1.406581	4.033242	0.205297
6	-2.147120	3.120865	-0.556874
6	-3.541754	3.095649	-0.424443
1	-5.269746	3.937828	0.544069
1	-3.943533	5.550395	1.900358
1	-1.466320	5.601005	1.677295

1	-0.325934	4.066539	0.106424
1	-4.125495	2.388238	-1.008722
6	-1.490031	2.201307	-1.573979
1	-2.136028	1.352385	-1.799777
1	-1.313794	2.738297	-2.510688
7	-0.171909	1.677448	-1.184809
7	0.896207	2.441269	-1.467401
7	1.961523	1.761837	-1.160737

P34: *anti*-attack



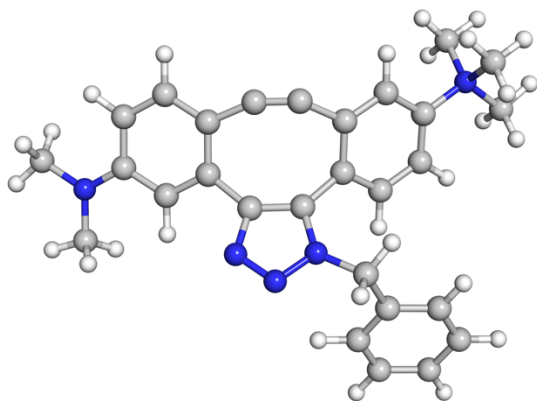
<i>E</i> (B3LYP)	<i>H</i> (B3LYP)	<i>G</i> (B3LYP)
-1357.324992	-1356.785191	-1356.876863

	X	Y	Z
6	3.482172	-1.968774	1.789862
6	4.737266	-1.834423	1.223139
6	4.933579	-0.991512	0.097165
6	3.807953	-0.282226	-0.401454
6	2.371921	-1.269791	1.288015
1	3.346579	-2.630185	2.640188
1	5.564122	-2.392202	1.643851
1	3.921595	0.388089	-1.242006
6	2.544779	-0.399106	0.169774
6	1.038556	-1.439321	1.705896
6	-0.181709	-1.393569	1.640297
6	-1.246650	-1.387777	0.695291
6	-1.018072	-0.585462	-0.463048
6	1.465372	0.495998	-0.341647
6	0.067198	0.435327	-0.525721

6	-1.888357	-0.742139	-1.542348
1	-1.703109	-0.204111	-2.466174
6	-2.380667	-2.200949	0.773871
1	-2.530821	-2.774728	1.680069
6	-3.255894	-2.288687	-0.310896
6	-3.005004	-1.585670	-1.482906
1	-3.640975	-1.656201	-2.353659
7	-4.458700	-3.187443	-0.176921
7	6.164269	-0.863751	-0.492086
6	-5.330285	-3.184576	-1.410292
1	-6.173303	-3.846163	-1.216166
1	-5.687619	-2.172890	-1.595548
1	-4.755975	-3.557917	-2.256424
6	-5.311832	-2.723537	0.988741
1	-6.173995	-3.386064	1.063151
1	-4.726397	-2.768738	1.904236
1	-5.629858	-1.700036	0.793162
6	6.344997	0.014056	-1.642108
1	6.117344	1.059539	-1.395845
1	7.383072	-0.038999	-1.969815
1	5.707159	-0.287138	-2.482894
6	7.311646	-1.583549	0.046863
1	7.153483	-2.669514	0.023394
1	8.190234	-1.356347	-0.556729
1	7.524085	-1.290307	1.083466
6	-4.005644	-4.615828	0.059920
1	-3.389015	-4.921454	-0.784462
1	-3.432625	-4.664690	0.982979
1	-4.891956	-5.245452	0.136609
6	-2.224738	4.413209	1.966298
6	-2.178864	5.718440	1.467198
6	-1.925872	5.933719	0.111281
6	-1.715090	4.847766	-0.741805
6	-1.759043	3.538975	-0.249353
6	-2.019770	3.329675	1.111976
1	-2.426237	4.239127	3.019657
1	-2.342561	6.561841	2.132263
1	-1.891219	6.945048	-0.284175
1	-1.515634	5.018228	-1.796714
1	-2.062625	2.317074	1.505793
6	-1.549265	2.363371	-1.182165
1	-2.320931	1.610593	-1.030913

1	-1.588950	2.683233	-2.226239
7	-0.243307	1.701546	-0.970480
7	0.852602	2.466642	-1.077281
7	1.874284	1.748508	-0.712107

P35: *anti*-attack

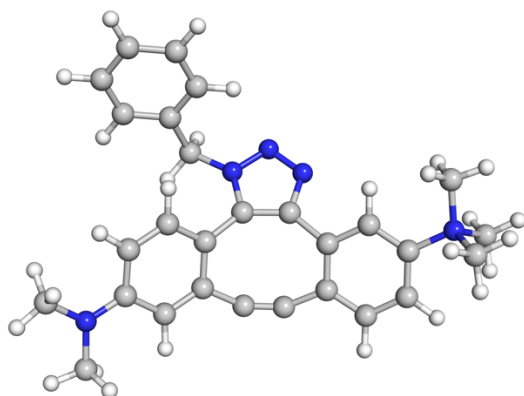


<i>E</i> (B3LYP)	<i>H</i> (B3LYP)	<i>G</i> (B3LYP)
-1357.325998	-1356.786242	-1356.877055

	X	Y	Z
6	-3.959879	-2.491956	-0.480022
6	-5.093662	-1.899494	0.047714
6	-5.089962	-0.524543	0.402829
6	-3.898023	0.214254	0.172688
6	-2.782612	-1.757708	-0.696733
1	-3.974922	-3.548111	-0.731451
1	-5.979517	-2.503814	0.196057
1	-3.863675	1.269360	0.405978
6	-2.757181	-0.369186	-0.368895
6	-1.543550	-2.289634	-1.100700
6	-0.331686	-2.332396	-1.254490
6	0.890311	-1.856696	-0.702965
6	0.875004	-0.493038	-0.277855
6	-1.607527	0.527589	-0.694963
6	-0.196904	0.460018	-0.687042
6	1.946197	-0.045894	0.494921
1	1.940442	0.963014	0.890055
6	2.002689	-2.662124	-0.443074
1	1.981662	-3.683566	-0.802289
6	3.075967	-2.158443	0.294773
6	3.046901	-0.860481	0.788851
1	3.844435	-0.445612	1.388441

7	4.245212	-3.073006	0.558054
7	-6.195334	0.073782	0.949053
6	5.337698	-2.405380	1.359701
1	6.139480	-3.130806	1.489085
1	5.706754	-1.539396	0.812820
1	4.942090	-2.114548	2.331445
6	4.847964	-3.519848	-0.760589
1	5.698333	-4.166973	-0.544721
1	4.100461	-4.065430	-1.332234
1	5.168067	-2.633688	-1.307508
6	-6.176218	1.491355	1.289192
1	-6.000824	2.119080	0.405691
1	-7.140773	1.767735	1.714759
1	-5.399661	1.717834	2.031020
6	-7.411809	-0.699286	1.167080
1	-7.235584	-1.543612	1.845910
1	-8.167483	-0.055638	1.617042
1	-7.816183	-1.094637	0.225862
6	3.778127	-4.286493	1.340373
1	3.339736	-3.941217	2.275802
1	3.039881	-4.830205	0.755559
1	4.642439	-4.921607	1.532820
6	2.034544	4.913025	1.100890
6	3.425711	4.895477	1.225162
6	4.176322	4.000803	0.459201
6	3.536628	3.125988	-0.420804
6	2.141724	3.141397	-0.552722
6	1.394766	4.044879	0.213674
1	1.443323	5.606187	1.692956
1	3.920926	5.572777	1.915311
1	5.258610	3.976401	0.551138
1	4.125380	2.425355	-1.008236
1	0.313852	4.070671	0.115522
6	1.491442	2.220134	-1.572834
1	1.313919	2.757834	-2.508890
1	2.142561	1.375163	-1.798716
7	0.175423	1.688712	-1.186932
7	-0.895724	2.447297	-1.471761
7	-1.958381	1.763721	-1.165474

P36: *anti*-attack

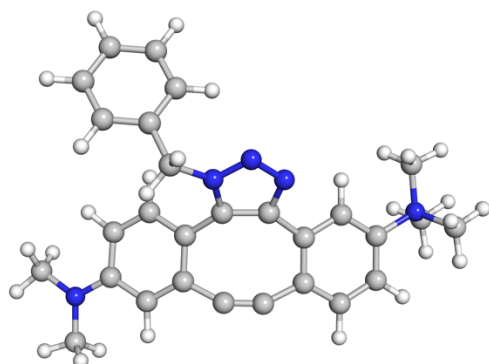


<i>E</i> (B3LYP)	<i>H</i> (B3LYP)	<i>G</i> (B3LYP)
-1357.327440	-1356.787575	-1356.878113

	X	Y	Z
6	-2.439869	-0.339971	0.481045
6	-3.478179	-1.215867	0.780932
6	-3.443135	-2.567875	0.361040
6	-2.263706	-3.001816	-0.296387
6	-1.300618	-0.733686	-0.234741
1	-2.521723	0.682905	0.832169
1	-4.319388	-0.838691	1.348647
1	-2.132116	-4.040583	-0.569370
6	-1.224442	-2.117683	-0.569506
6	-0.284917	0.266445	-0.658149
6	1.123866	0.413041	-0.681043
6	2.339955	-0.398838	-0.381712
6	2.480023	-1.779122	-0.687920
6	0.061285	-2.528063	-1.020270
6	1.273102	-2.434397	-1.048307
6	3.720629	-2.411385	-0.540767
1	3.815286	-3.462898	-0.787893
6	3.465189	0.288256	0.097916
1	3.344555	1.337611	0.320856
6	4.686805	-0.361993	0.254886
6	4.826748	-1.712067	-0.072453
1	5.768826	-2.236950	0.032604
7	5.895181	0.375998	0.775593
7	-4.485976	-3.427607	0.597970

6	6.394485	-0.291944	2.042954
1	7.259280	0.265122	2.403354
1	5.590508	-0.272178	2.777749
1	6.679762	-1.317941	1.822111
6	5.606115	1.821137	1.107093
1	6.531069	2.262462	1.475189
1	5.284832	2.339792	0.205512
1	4.840766	1.867451	1.880156
6	-4.359849	-4.841189	0.265826
1	-3.570312	-5.336737	0.848664
1	-5.305144	-5.341154	0.477866
1	-4.138274	-4.978855	-0.799096
6	-5.632112	-2.982291	1.380159
1	-6.104520	-2.104677	0.923143
1	-6.372160	-3.782151	1.412554
1	-5.356499	-2.725251	2.412981
6	6.991442	0.357613	-0.272526
1	7.266783	-0.672643	-0.487004
1	6.611209	0.842970	-1.170672
1	7.850540	0.899477	0.123328
6	-4.832025	3.671933	0.376289
6	-4.123132	4.600608	1.141659
6	-2.730661	4.653563	1.047144
6	-2.048281	3.787175	0.190270
6	-2.752972	2.849917	-0.575354
6	-4.149682	2.799303	-0.473230
1	-5.915036	3.619254	0.445359
1	-4.651625	5.276460	1.808194
1	-2.171413	5.372999	1.639052
1	-0.966642	3.840695	0.115103
1	-4.706342	2.071710	-1.059165
6	-2.057307	1.927286	-1.564016
1	-2.664732	1.043003	-1.758215
1	-1.908325	2.442694	-2.517776
7	-0.717959	1.472580	-1.164869
7	0.311487	2.291406	-1.458023
7	1.407022	1.664416	-1.159298

P37: *anti*-attack

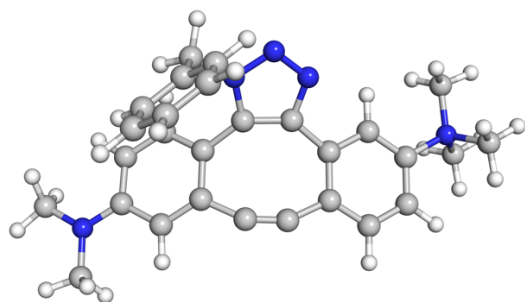


<i>E</i> (B3LYP)	<i>H</i> (B3LYP)	<i>G</i> (B3LYP)
-1357.327440	-1356.787575	-1356.878118

	X	Y	Z
6	-2.439945	-0.339986	-0.480949
6	-3.478320	-1.215827	-0.780718
6	-3.443268	-2.567868	-0.360897
6	-2.263742	-3.001895	0.296282
6	-1.300584	-0.733797	0.234639
1	-2.521816	0.682924	-0.831978
1	-4.319622	-0.838593	-1.348257
1	-2.132121	-4.040687	0.569156
6	-1.224401	-2.117809	0.569298
6	-0.284835	0.266320	0.657950
6	1.123947	0.413027	0.680683
6	2.340052	-0.398851	0.381487
6	2.480113	-1.779125	0.687726
6	0.061376	-2.528260	1.019873
6	1.273165	-2.434340	1.048125
6	3.720737	-2.411385	0.540686
1	3.815367	-3.462902	0.787802
6	3.465326	0.288242	-0.098050
1	3.344698	1.337583	-0.321058
6	4.686980	-0.361966	-0.254809
6	4.826911	-1.712050	0.072510
1	5.769001	-2.236932	-0.032495
7	5.895386	0.376079	-0.775370
7	-4.486222	-3.427514	-0.597671
6	6.394673	-0.291563	-2.042845

1	7.259675	0.265371	-2.402957
1	6.679608	-1.317716	-1.822290
1	5.590815	-0.271355	-2.777765
6	6.991653	0.357343	0.272784
1	7.850743	0.899385	-0.122864
1	6.611378	0.842338	1.171108
1	7.267031	-0.672980	0.486873
6	-4.360106	-4.841127	-0.265660
1	-4.137933	-4.978827	0.799125
1	-5.305614	-5.340938	-0.477124
1	-3.570989	-5.336809	-0.848963
6	-5.632186	-2.982263	-1.380161
1	-5.356345	-2.725336	-2.412949
1	-6.372235	-3.782119	-1.412625
1	-6.104688	-2.104603	-0.923338
6	5.606410	1.821314	-1.106397
1	4.841157	1.867967	-1.879537
1	5.284956	2.339671	-0.204696
1	6.531414	2.262761	-1.474217
6	-4.832291	3.672049	-0.375682
6	-4.123528	4.600605	-1.141327
6	-2.731027	4.653395	-1.047254
6	-2.048477	3.786976	-0.190537
6	-2.753030	2.849862	0.575378
6	-4.149786	2.799395	0.473673
1	-5.915329	3.619485	-0.444420
1	-4.652152	5.276482	-1.807731
1	-2.171870	5.372716	-1.639387
1	-0.966809	3.840390	-0.115717
1	-4.706339	2.071873	1.059802
6	-2.057205	1.927191	1.563894
1	-1.908086	2.442532	2.517666
1	-2.664582	1.042882	1.758102
7	-0.717898	1.472541	1.164502
7	0.311521	2.291488	1.457385
7	1.407072	1.664519	1.158661

P38: *anti*-attack

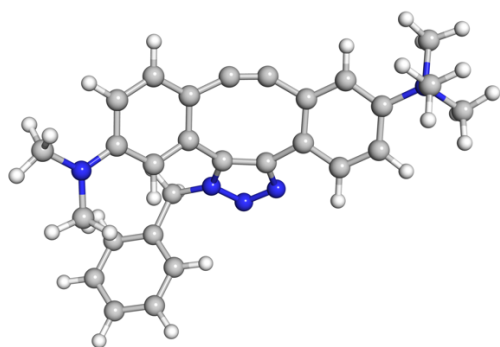


<i>E</i> (B3LYP)	<i>H</i> (B3LYP)	<i>G</i> (B3LYP)
-1357.258178	-1356.718482	-1356.809128

	X	Y	Z
6	-2.272888	-0.839709	-1.681107
6	-3.394273	-1.650605	-1.537252
6	-3.689268	-2.284846	-0.305378
6	-2.732949	-2.139811	0.731284
6	-1.372650	-0.603978	-0.633662
1	-2.085615	-0.397233	-2.655235
1	-4.037004	-1.797212	-2.396133
1	-2.838551	-2.679762	1.663036
6	-1.606768	-1.341256	0.561619
6	-0.273073	0.386305	-0.784382
6	1.122564	0.472452	-0.568280
6	2.202985	-0.294800	0.105729
6	2.039695	-1.070903	1.287462
6	-0.491197	-1.344638	1.442748
6	0.697978	-1.284198	1.687478
6	3.160910	-1.606604	1.937648
1	3.017770	-2.189489	2.840989
6	3.506606	-0.102377	-0.379868
1	3.604073	0.515701	-1.260124
6	4.603207	-0.645152	0.281401
6	4.444572	-1.401716	1.445511
1	5.285081	-1.834118	1.977974
7	6.006810	-0.413467	-0.239752
7	-4.825265	-3.033746	-0.129994
6	6.658001	-1.742137	-0.561924
1	7.663424	-1.556488	-0.944542

1	6.708746	-2.347620	0.340964
1	6.049275	-2.247190	-1.312176
6	6.822868	0.312852	0.809836
1	7.828669	0.478168	0.419043
1	6.333054	1.262826	1.024704
1	6.867848	-0.291772	1.713546
6	-5.053296	-3.735978	1.125635
1	-5.043627	-3.041786	1.974893
1	-6.034006	-4.211626	1.095165
1	-4.300827	-4.516494	1.308230
6	-5.738266	-3.245123	-1.244830
1	-5.267434	-3.803820	-2.066181
1	-6.600234	-3.815464	-0.897444
1	-6.105547	-2.291054	-1.643098
6	6.034586	0.424368	-1.495216
1	5.476724	-0.084803	-2.279985
1	5.596344	1.399845	-1.288024
1	7.076829	0.539060	-1.794036
6	-2.294354	4.518339	1.442381
6	-3.467054	3.998327	1.996880
6	-4.105847	2.920130	1.384428
6	-3.573175	2.361683	0.220741
6	-2.401505	2.879830	-0.340629
6	-1.764467	3.963325	0.278783
1	-1.796977	5.361763	1.913163
1	-3.882178	4.435798	2.900548
1	-5.019494	2.513904	1.809462
1	-4.072232	1.520435	-0.254106
1	-0.853231	4.368730	-0.153705
6	-1.837071	2.287779	-1.616918
1	-2.551359	1.607411	-2.074289
1	-1.593246	3.067418	-2.342016
7	-0.552554	1.584225	-1.401783
7	0.559878	2.327774	-1.581539
7	1.556629	1.661716	-1.098552

P39: *syn*-attack

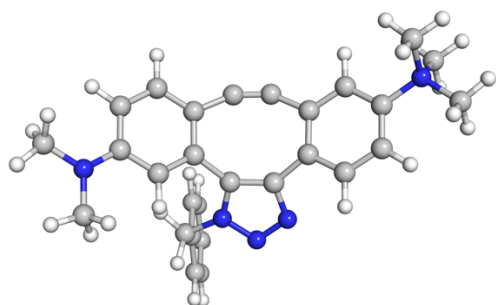


<i>E</i> (B3LYP)	<i>H</i> (B3LYP)	<i>G</i> (B3LYP)
-1357.325773	-1356.785981	-1356.876941

	X	Y	Z
6	-1.000782	3.432511	-0.900468
6	-2.239622	3.557580	-0.292733
6	-2.868327	2.435395	0.303379
6	-2.209267	1.178062	0.195581
6	-0.344016	2.197023	-0.978940
1	-0.512335	4.314001	-1.304214
1	-2.702550	4.534992	-0.249096
1	-2.666553	0.303076	0.637467
6	-0.986393	1.035210	-0.455791
6	1.011000	2.009685	-1.331285
6	2.100436	1.465061	-1.278061
6	2.928290	0.505352	-0.636341
6	2.242323	-0.629149	-0.116420
6	-0.408145	-0.331603	-0.635618
6	0.834906	-0.980790	-0.465676
6	2.986077	-1.545570	0.631209
1	2.489826	-2.416357	1.043564
6	4.305751	0.661210	-0.435188
1	4.778512	1.535710	-0.859903
6	5.013951	-0.288660	0.298615
6	4.355163	-1.383704	0.854386
1	4.868356	-2.125803	1.450401
7	6.487050	-0.084143	0.556253
7	-4.067358	2.550375	0.957564
6	7.214013	-1.401467	0.731466

1	8.278188	-1.184359	0.810903
1	6.879206	-1.887115	1.644388
1	7.015700	-2.028860	-0.136556
6	6.650150	0.735514	1.822132
1	7.715412	0.881788	2.005107
1	6.151526	1.693158	1.678640
1	6.190284	0.191277	2.645936
6	-4.636347	1.408796	1.665850
1	-3.961769	1.037504	2.449296
1	-5.568722	1.715797	2.139515
1	-4.860476	0.581840	0.981910
6	-4.701802	3.856453	1.088283
1	-4.896126	4.303753	0.106008
1	-5.658094	3.737870	1.597552
1	-4.085992	4.556974	1.669435
6	7.162829	0.645120	-0.586655
1	6.962954	0.107086	-1.512520
1	6.791040	1.664946	-0.643303
1	8.231544	0.665618	-0.378924
6	-4.362009	-3.034285	1.404624
6	-5.700793	-2.833092	1.068486
6	-6.021074	-2.147302	-0.107200
6	-5.006786	-1.663344	-0.933318
6	-3.658727	-1.863737	-0.600825
6	-3.344424	-2.556657	0.572675
1	-4.102240	-3.567174	2.315154
1	-6.489714	-3.206855	1.715039
1	-7.060365	-1.984506	-0.378898
1	-5.262797	-1.127112	-1.844327
1	-2.307243	-2.730850	0.839992
6	-2.604828	-1.340992	-1.564743
1	-2.586374	-1.958712	-2.467777
1	-2.836562	-0.320062	-1.870851
7	-1.229966	-1.353338	-1.054696
7	-0.569995	-2.524161	-1.125387
7	0.656852	-2.306352	-0.760658

P40: *syn*-attack

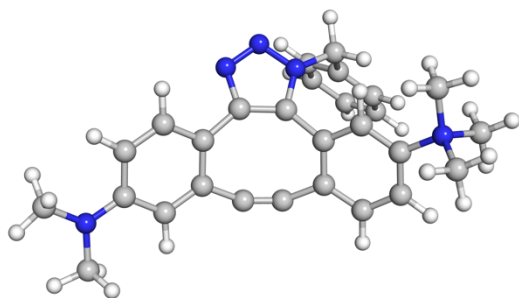


<i>E</i> (B3LYP)	<i>H</i> (B3LYP)	<i>G</i> (B3LYP)
-1357.326241	-1356.786501	-1356.878344

	X	Y	Z
6	1.439733	2.767134	1.946408
6	2.502884	3.395457	1.317581
6	2.933003	2.977944	0.032103
6	2.277871	1.854960	-0.546552
6	0.783151	1.676450	1.359710
1	1.091177	3.138366	2.905203
1	2.978224	4.233772	1.810572
1	2.577631	1.513728	-1.528976
6	1.246833	1.182168	0.105613
6	-0.460192	1.141414	1.768130
6	-1.544809	0.618530	1.576244
6	-2.523941	0.187215	0.641348
6	-2.009804	-0.273495	-0.607250
6	0.692386	-0.063188	-0.505666
6	-0.572511	-0.591988	-0.843396
6	-2.931756	-0.595270	-1.605041
1	-2.568824	-0.947770	-2.563465
6	-3.904177	0.270705	0.852677
1	-4.247700	0.615412	1.820405
6	-4.790155	-0.069175	-0.170261
6	-4.312180	-0.492093	-1.406401
1	-4.969047	-0.751719	-2.224541
7	-6.268375	0.046108	0.104478
7	3.941706	3.625553	-0.631397
6	-7.114834	-0.363201	-1.077232
1	-8.158329	-0.251952	-0.786164

1	-6.894798	0.289986	-1.919944
1	-6.908403	-1.403094	-1.324920
6	-6.615494	1.484231	0.439097
1	-7.687776	1.541845	0.626623
1	-6.064608	1.791362	1.325136
1	-6.339915	2.107556	-0.410708
6	4.367285	3.176926	-1.951561
1	3.546819	3.224497	-2.679213
1	5.169250	3.824597	-2.305136
1	4.747635	2.147141	-1.927852
6	4.606549	4.765903	-0.012565
1	5.094879	4.487004	0.930321
1	5.370825	5.143614	-0.691388
1	3.900655	5.580771	0.194283
6	-6.643414	-0.851957	1.268200
1	-6.381984	-1.876629	1.006317
1	-6.099334	-0.539788	2.156683
1	-7.716271	-0.759841	1.436905
6	3.448802	-3.676488	2.037199
6	4.006784	-4.772208	1.371841
6	4.241179	-4.702877	-0.002765
6	3.914608	-3.543514	-0.710339
6	3.355469	-2.443277	-0.051335
6	3.128644	-2.517379	1.330038
1	3.269132	-3.722451	3.107763
1	4.259972	-5.673277	1.923618
1	4.677150	-5.549455	-0.525921
1	4.095927	-3.492827	-1.780959
1	2.700676	-1.666293	1.854448
6	3.019766	-1.179478	-0.816812
1	3.381513	-0.300140	-0.287541
1	3.477645	-1.191156	-1.808873
7	1.561570	-1.007074	-1.003167
7	0.907854	-2.006785	-1.617953
7	-0.364501	-1.756938	-1.532923

P41: *syn*-attack

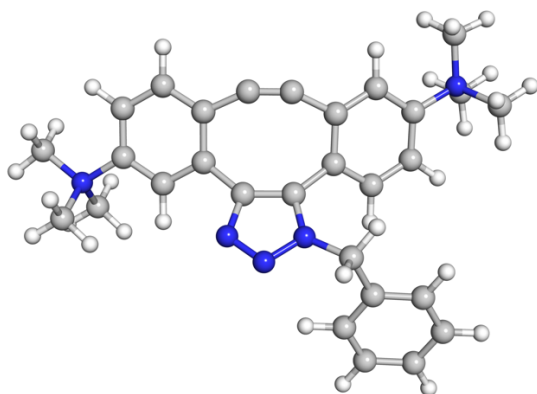


<i>E</i> (B3LYP)	<i>H</i> (B3LYP)	<i>G</i> (B3LYP)
-1357.322623	-1356.782777	-1356.873825

	X	Y	Z
6	3.559524	0.058367	-1.636035
6	4.871967	-0.205902	-1.261227
6	5.224396	-0.420288	0.095257
6	4.172237	-0.393585	1.040957
6	2.508289	0.106829	-0.710431
1	3.342041	0.237791	-2.683862
1	5.629867	-0.244271	-2.033936
1	4.362941	-0.580359	2.089651
6	2.857508	-0.137510	0.647964
6	1.166844	0.565031	-1.157278
6	-0.181582	0.320726	-0.822161
6	-0.965081	-0.632427	0.015863
6	-0.698364	-0.828992	1.399019
6	1.743284	-0.209573	1.525616
6	0.572062	-0.349297	1.829682
6	-1.573587	-1.594949	2.175102
1	-1.380913	-1.717046	3.234973
6	-2.029104	-1.336503	-0.563665
1	-2.166480	-1.260438	-1.632969
6	-2.866183	-2.134660	0.218999
6	-2.663431	-2.237670	1.595102
1	-3.313378	-2.829462	2.228710
7	-4.009390	-2.902293	-0.395425
7	6.525751	-0.648960	0.477081
6	-5.320947	-2.407321	0.185515
1	-6.132176	-2.977228	-0.267372

1	-5.315439	-2.556456	1.262920
1	-5.418278	-1.347995	-0.049403
6	-3.849109	-4.382991	-0.100014
1	-4.674154	-4.915809	-0.572745
1	-2.894954	-4.711964	-0.509747
1	-3.873609	-4.541019	0.975579
6	6.830357	-0.978634	1.862600
1	6.341387	-1.909094	2.185585
1	7.907971	-1.104942	1.969935
1	6.517294	-0.175159	2.540767
6	7.566776	-0.780663	-0.532955
1	7.638682	0.124006	-1.148924
1	8.527222	-0.924421	-0.037219
1	7.392521	-1.636462	-1.201171
6	-4.087414	-2.747039	-1.895821
1	-4.259211	-1.701077	-2.142676
1	-3.164079	-3.109844	-2.344582
1	-4.927740	-3.346207	-2.242784
6	-3.619761	3.131112	1.744040
6	-2.938605	4.346545	1.823602
6	-2.032665	4.701826	0.819158
6	-1.811061	3.845531	-0.258945
6	-2.489779	2.621735	-0.343579
6	-3.393951	2.271804	0.665310
1	-4.325521	2.848207	2.520107
1	-3.112258	5.015324	2.662050
1	-1.502062	5.648359	0.873980
1	-1.107351	4.123604	-1.039097
1	-3.927141	1.326052	0.608390
6	-2.264311	1.697154	-1.525821
1	-2.944623	0.849229	-1.483528
1	-2.432213	2.214879	-2.472715
7	-0.872762	1.212508	-1.614201
7	-0.036726	1.927301	-2.384899
7	1.176242	1.535709	-2.126134

P42: *anti*-attack

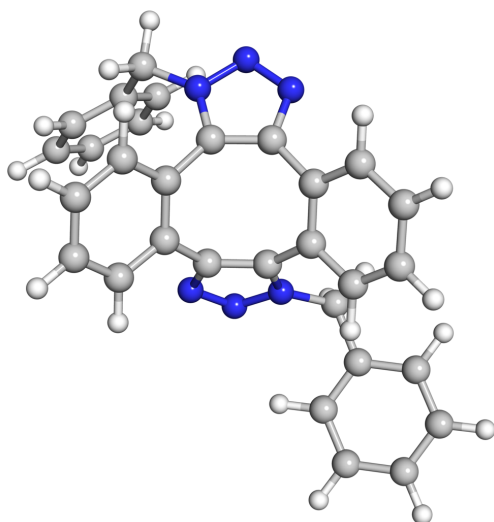


<i>E</i> (B3LYP)	<i>H</i> (B3LYP)	<i>G</i> (B3LYP)
-1397.064481	-1396.480260	-1396.571463

	X	Y	Z
6	-3.722489	-2.582736	-0.598434
6	-4.884230	-1.986089	-0.110618
6	-4.850774	-0.640445	0.244252
6	-3.682656	0.112654	0.097805
6	-2.543192	-1.848081	-0.735956
1	-3.732500	-3.633060	-0.866645
1	-5.774688	-2.591059	-0.014531
1	-3.654434	1.165434	0.346850
6	-2.511658	-0.466225	-0.398243
6	-1.285048	-2.387096	-1.107643
6	-0.070028	-2.400720	-1.123706
6	1.168708	-1.893092	-0.647607
6	1.144404	-0.520499	-0.276127
6	-1.364062	0.442592	-0.690757
6	0.048493	0.406714	-0.681987
6	2.236979	-0.036465	0.450131
1	2.235224	0.982876	0.816168
6	2.288783	-2.692995	-0.393034
1	2.253441	-3.724492	-0.712281
6	3.381350	-2.152669	0.279093
6	3.348592	-0.833286	0.726290
1	4.167476	-0.393913	1.283187
7	4.611068	-2.976843	0.554090
7	-6.070667	0.053715	0.794276
6	4.851017	-3.057849	2.051319
1	5.733648	-3.674642	2.219706

1	5.015096	-2.058074	2.446696
1	3.973678	-3.508867	2.513405
6	5.807977	-2.331405	-0.121432
1	6.684983	-2.944899	0.083153
1	5.612143	-2.286476	-1.192287
1	5.951090	-1.330150	0.278514
6	-6.466928	1.196310	-0.122861
1	-6.681863	0.784066	-1.107966
1	-7.352043	1.675141	0.295595
1	-5.649819	1.911600	-0.182288
6	-7.261563	-0.867858	0.916338
1	-7.019313	-1.680522	1.599510
1	-8.087297	-0.282453	1.317642
1	-7.524873	-1.249605	-0.068752
6	4.501234	-4.391252	0.033434
1	3.671049	-4.893822	0.526824
1	4.359561	-4.368799	-1.045725
1	5.434491	-4.898682	0.272967
6	-5.769664	0.596327	2.179056
1	-5.488657	-0.238658	2.819937
1	-4.956005	1.315188	2.115231
1	-6.669253	1.083936	2.554468
6	2.177830	4.928981	1.089525
6	3.570251	4.954800	1.196930
6	4.339160	4.081809	0.424294
6	3.716674	3.185177	-0.445960
6	2.320360	3.157485	-0.560981
6	1.554541	4.039247	0.212147
1	1.572618	5.605146	1.686947
1	4.052408	5.649051	1.879347
1	5.422644	4.091313	0.503038
1	4.320121	2.502430	-1.039413
1	0.472276	4.032697	0.127390
6	1.689318	2.215322	-1.573795
1	1.485612	2.744696	-2.508994
1	2.361864	1.389304	-1.806209
7	0.389827	1.646540	-1.175739
7	-0.699230	2.381831	-1.453075
7	-1.743706	1.673810	-1.149599

P43: *anti*-attack

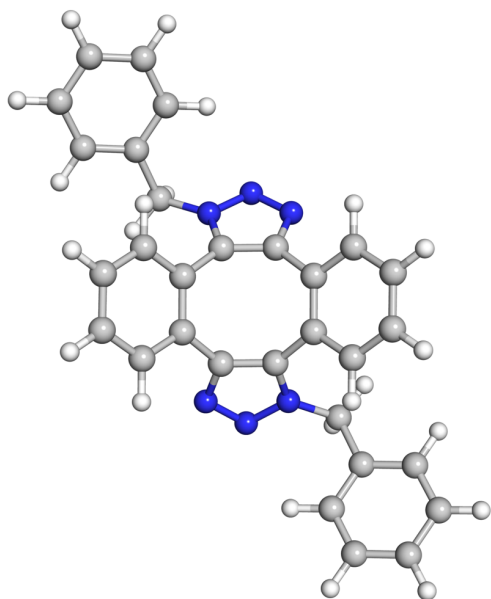


<i>E</i> (B3LYP)	<i>H</i> (B3LYP)	<i>G</i> (B3LYP)	<i>E</i> (M06-2X)
-1484.927446	-1484.440049	-1484.529983	-1484.878639

	X	Y	Z
6	5.681269	-2.351654	0.948877
6	6.760713	-1.624518	0.440254
6	6.558303	-0.736284	-0.617810
6	5.281541	-0.573373	-1.160015
6	4.196365	-1.302090	-0.657306
6	4.406846	-2.195593	0.401190
1	5.830900	-3.044838	1.772159
1	7.752086	-1.748626	0.867127
1	7.390441	-0.163497	-1.017733
1	5.128049	0.125710	-1.978525
1	3.572504	-2.767891	0.795925
6	2.832180	-1.150737	-1.311039
1	2.794370	-0.242826	-1.915475
1	2.626829	-1.998636	-1.971212
7	1.704838	-1.104506	-0.373506
7	1.151830	-2.265520	0.036725
7	0.152512	-1.975665	0.826661
6	1.037158	-0.033404	0.152727
6	0.032580	-0.619130	0.917023
6	-0.986844	0.010203	1.776924
6	-1.879362	0.988369	1.286675

6	-1.858303	1.404820	-0.129130
6	-0.865987	1.981887	-0.913604
6	0.525957	2.326724	-0.570966
6	1.432789	1.373930	-0.052479
6	2.744882	1.773271	0.251467
1	3.436109	1.049892	0.671096
6	0.972517	3.635171	-0.806998
1	0.274495	4.356801	-1.219730
6	-1.092285	-0.400371	3.114040
1	-0.412987	-1.163906	3.480164
6	-2.814887	1.563933	2.162495
1	-3.473494	2.346988	1.798324
6	-2.899072	1.154589	3.491782
1	-3.628578	1.613359	4.152475
6	-2.042061	0.159295	3.966157
1	-2.103898	-0.170848	4.998944
6	2.281730	4.013693	-0.516394
1	2.604157	5.033935	-0.702785
6	3.168723	3.081159	0.023859
1	4.187347	3.367623	0.268043
6	-3.819306	-2.709339	-2.272281
6	-4.233848	-3.530336	-1.218676
6	-4.650739	-2.957385	-0.016343
6	-4.650631	-1.567882	0.133636
6	-4.240385	-0.741192	-0.917604
6	-3.824516	-1.322775	-2.123413
1	-3.495191	-3.149919	-3.211121
1	-4.231059	-4.610434	-1.336312
1	-4.972394	-3.588537	0.807439
1	-4.972335	-1.125246	1.072994
1	-3.502455	-0.686063	-2.943477
6	-4.268796	0.767856	-0.759944
1	-4.909412	1.234377	-1.512310
1	-4.647519	1.046555	0.223737
7	-2.950488	1.389834	-0.950132
7	-2.653265	1.919467	-2.155830
7	-1.400737	2.289678	-2.132256

P44: *anti*-attack

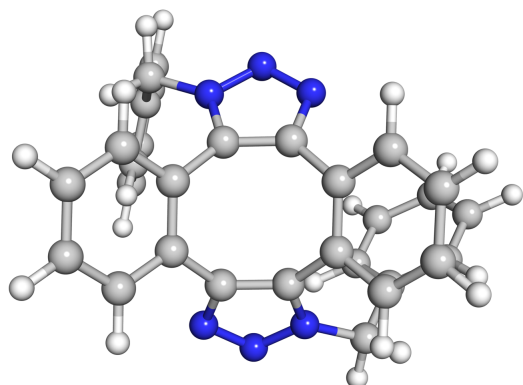


<i>E</i> (B3LYP)	<i>H</i> (B3LYP)	<i>G</i> (B3LYP)	<i>E</i> (M06-2X)
-1484.927135	-1484.439820	-1484.528875	-1484.878087

	X	Y	Z
6	-6.714799	1.539584	-0.013057
6	-7.517327	0.449837	0.335478
6	-7.075434	-0.847132	0.067638
6	-5.834937	-1.051972	-0.540804
6	-5.027301	0.035834	-0.895143
6	-5.479030	1.335257	-0.628852
1	-7.052219	2.551993	0.191572
1	-8.479454	0.611281	0.813673
1	-7.690311	-1.701217	0.337724
1	-5.492271	-2.064581	-0.739367
1	-4.861658	2.185711	-0.902970
6	-3.709968	-0.214692	-1.611300
1	-3.414568	-1.261166	-1.518233
1	-3.803010	0.011537	-2.677592
7	-2.588814	0.603769	-1.135307
7	-2.406517	1.830981	-1.666765
7	-1.333977	2.345655	-1.126780
6	-1.599698	0.309246	-0.238335
6	-0.794918	1.443842	-0.255102

6	0.404893	1.765957	0.540343
6	1.544360	0.930056	0.560433
6	1.599693	-0.309101	-0.238379
6	0.794868	-1.443664	-0.255269
6	-0.404913	-1.765875	0.540182
6	-1.544366	-0.929968	0.560394
6	-2.651937	-1.300275	1.340727
1	-3.518245	-0.648137	1.374800
6	-0.426744	-2.964900	1.267479
1	0.445981	-3.609672	1.234928
6	0.426742	2.964931	1.267722
1	-0.446003	3.609679	1.235253
6	2.651966	1.300357	1.340715
1	3.518309	0.648256	1.374700
6	2.652329	2.488396	2.068920
1	3.519169	2.754035	2.666636
6	1.538724	3.328862	2.024781
1	1.531260	4.259812	2.584101
6	-1.538691	-3.328849	2.024574
1	-1.531216	-4.259841	2.583825
6	-2.652278	-2.488360	2.068849
1	-3.519074	-2.754031	2.666615
6	6.714441	-1.539903	-0.012761
6	7.517341	-0.450316	0.335402
6	7.075814	0.846720	0.067259
6	5.835297	1.051776	-0.541065
6	5.027290	-0.035879	-0.895033
6	5.478661	-1.335366	-0.628468
1	7.051568	-2.552366	0.192083
1	8.479472	-0.611927	0.813529
1	7.690972	1.700694	0.337051
1	5.492937	2.064444	-0.739856
1	4.861007	-2.185703	-0.902318
6	3.710002	0.214909	-1.611169
1	3.414646	1.261373	-1.517811
1	3.803043	-0.010996	-2.677537
7	2.588804	-0.603575	-1.135380
7	2.406470	-1.830728	-1.666980
7	1.333917	-2.345394	-1.127040

P45: *anti*-attack

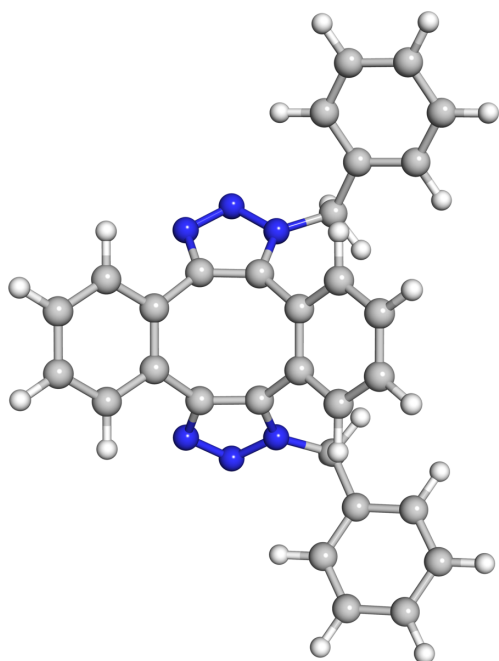


<i>E</i> (B3LYP)	<i>H</i> (B3LYP)	<i>G</i> (B3LYP)	<i>E</i> (M06-2X)
-1484.927353	-1484.439860	-1484.529261	-1484.878643

	X	Y	Z
6	3.677088	2.256017	1.514825
6	4.189211	3.411991	0.918442
6	4.416247	3.439442	-0.458874
6	4.129233	2.315619	-1.237309
6	3.616989	1.154641	-0.647292
6	3.395419	1.132588	0.736778
1	3.502028	2.227263	2.586738
1	4.412090	4.285085	1.525516
1	4.816516	4.333498	-0.928883
1	4.305388	2.340057	-2.309745
1	2.999974	0.236582	1.209141
6	3.308150	-0.061977	-1.498104
1	3.779379	0.018552	-2.479730
1	3.666451	-0.975805	-1.023111
7	1.864060	-0.237347	-1.732082
7	1.235752	0.616094	-2.564669
7	-0.043686	0.352549	-2.516178
6	0.969763	-1.069599	-1.118221
6	-0.258506	-0.663698	-1.629795
6	-1.605212	-1.210866	-1.385110
6	-2.125675	-1.356835	-0.079658
6	-1.358391	-0.930083	1.107586
6	-0.126777	-1.329153	1.614323
6	0.836974	-2.304843	1.073838

6	1.349371	-2.192327	-0.237528
6	2.253477	-3.160764	-0.705806
1	2.621948	-3.094982	-1.725434
6	1.280451	-3.353633	1.892975
1	0.893356	-3.424844	2.904695
6	-2.405637	-1.565034	-2.481297
1	-2.005036	-1.436165	-3.481971
6	-3.409356	-1.901433	0.089607
1	-3.794847	-2.053043	1.093589
6	-4.187368	-2.260589	-1.009246
1	-5.176611	-2.681257	-0.855675
6	-3.687668	-2.080035	-2.300610
1	-4.288410	-2.351153	-3.163808
6	2.194265	-4.295159	1.423831
1	2.521206	-5.102063	2.073031
6	2.674435	-4.204733	0.115771
1	3.372701	-4.943522	-0.265996
6	-1.739547	3.979203	0.323344
6	-2.679763	4.146004	-0.698496
6	-3.720869	3.227296	-0.838851
6	-3.820080	2.143113	0.037320
6	-2.884750	1.972392	1.063366
6	-1.842743	2.900102	1.200673
1	-0.927710	4.692112	0.438288
1	-2.599288	4.987955	-1.380474
1	-4.454014	3.348770	-1.631417
1	-4.628987	1.426357	-0.078986
1	-1.111045	2.773242	1.994637
6	-3.012996	0.809366	2.029411
1	-3.118503	1.157666	3.059816
1	-3.886606	0.201901	1.789785
7	-1.825239	-0.056383	2.048738
7	-0.943643	0.075849	3.062616
7	0.076415	-0.700518	2.809381

P46: *syn*-attack

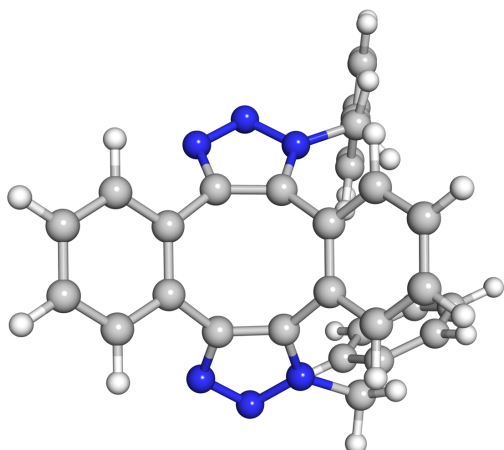


<i>E</i> (B3LYP)	<i>H</i> (B3LYP)	<i>G</i> (B3LYP)	<i>E</i> (M06-2X)
-1484.926792	-1484.439387	-1484.527915	-1484.877476

	X	Y	Z
6	-6.323739	-1.420315	0.102330
6	-6.316942	-2.735525	0.574988
6	-5.185854	-3.531848	0.386477
6	-4.065865	-3.012658	-0.267074
6	-4.067829	-1.696899	-0.746352
6	-5.208030	-0.904305	-0.558624
1	-7.200776	-0.794887	0.244808
1	-7.187231	-3.135619	1.087768
1	-5.169537	-4.554405	0.753299
1	-3.184765	-3.634822	-0.404358
1	-5.220307	0.116124	-0.930276
6	-2.860120	-1.179735	-1.511059
1	-2.000114	-1.834627	-1.360243
1	-3.069598	-1.147920	-2.584310
7	-2.445035	0.181626	-1.154038
7	-3.025185	1.227693	-1.778106
7	-2.465138	2.320642	-1.332153
6	-1.473046	0.608800	-0.293542
6	-1.494782	1.993036	-0.427982
6	-0.706557	3.036843	0.256546

6	0.706308	3.037099	0.256623
6	1.494871	1.993404	-0.427655
6	1.473013	0.609149	-0.293376
6	0.706908	-0.272357	0.606316
6	-0.706895	-0.272570	0.606241
6	-1.390403	-1.116154	1.495773
1	-2.475038	-1.104407	1.509598
6	1.390571	-1.115707	1.495962
1	2.475206	-1.103603	1.509941
6	-1.389838	4.107400	0.854114
1	-2.475460	4.106687	0.839773
6	1.389136	4.107916	0.854220
1	2.474761	4.107619	0.839995
6	0.697747	5.160486	1.450417
1	1.246786	5.976631	1.911261
6	-0.698895	5.160223	1.450385
1	-1.248261	5.976141	1.911240
6	0.697640	-1.955828	2.365726
1	1.247674	-2.599237	3.045759
6	-0.697313	-1.956057	2.365630
1	-1.247219	-2.599635	3.045606
6	6.324280	-1.420686	0.101407
6	6.316995	-2.735605	0.574918
6	5.185465	-3.531486	0.387325
6	4.065488	-3.012148	-0.266166
6	4.067927	-1.696712	-0.746278
6	5.208607	-0.904549	-0.559470
1	7.201694	-0.795624	0.243168
1	7.187274	-3.135793	1.087643
1	5.168766	-4.553803	0.754797
1	3.184042	-3.633974	-0.402763
1	5.221221	0.115635	-0.931777
6	2.860245	-1.179362	-1.510867
1	3.069672	-1.147403	-2.584124
1	2.000195	-1.834199	-1.360095
7	2.445235	0.182008	-1.153640
7	3.025569	1.228124	-1.777454
7	2.465476	2.321056	-1.331528

P47: *syn*-attack



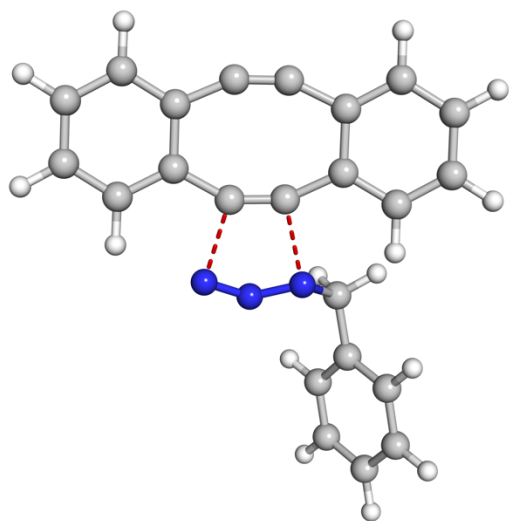
<i>E</i> (B3LYP)	<i>H</i> (B3LYP)	<i>G</i> (B3LYP)	<i>E</i> (M06-2X)
-1484.926240	-1484.438925	-1484.528467	-1484.876592

	X	Y	Z
6	-5.962550	-1.023938	-0.849859
6	-6.349243	-1.948355	0.124172
6	-5.381503	-2.731446	0.756239
6	-4.034124	-2.586534	0.418195
6	-3.640698	-1.664976	-0.560172
6	-4.616930	-0.885035	-1.193974
1	-6.709846	-0.410940	-1.346268
1	-7.397336	-2.055731	0.389404
1	-5.671390	-3.450157	1.517738
1	-3.284078	-3.193893	0.918997
1	-4.322440	-0.169550	-1.956153
6	-2.174440	-1.577093	-0.952195
1	-1.545690	-2.045709	-0.192787
1	-1.997559	-2.098281	-1.897714
7	-1.675569	-0.213027	-1.158955
7	-1.818392	0.358153	-2.372941
7	-1.270454	1.543152	-2.324819
6	-1.003129	0.618890	-0.308081
6	-0.742684	1.745813	-1.081016
6	-0.086820	3.022023	-0.731982
6	1.213253	3.082474	-0.181387
6	2.016339	1.873760	0.085280
6	1.717655	0.730859	0.820025
6	0.551876	0.388541	1.655418

6	-0.753254	0.334810	1.116582
6	-1.830107	0.025663	1.962144
1	-2.834393	0.001480	1.552922
6	0.737323	0.133834	3.024045
1	1.735973	0.201108	3.445152
6	-0.755330	4.218239	-1.036768
1	-1.749322	4.164154	-1.470174
6	1.800805	4.337274	0.045258
1	2.804673	4.375668	0.456837
6	1.122348	5.516328	-0.255216
1	1.594879	6.476029	-0.066464
6	-0.162600	5.456578	-0.799233
1	-0.701030	6.369123	-1.038573
6	-0.340260	-0.183756	3.848843
1	-0.173054	-0.376298	4.904201
6	-1.628454	-0.238118	3.315674
1	-2.476711	-0.474991	3.950659
6	2.727657	-3.635766	-1.791451
6	3.996056	-4.217460	-1.883833
6	4.986345	-3.869384	-0.964139
6	4.710725	-2.940164	0.042588
6	3.443787	-2.355903	0.142076
6	2.452459	-2.713426	-0.782265
1	1.951670	-3.904604	-2.502821
1	4.208826	-4.938257	-2.668441
1	5.974405	-4.316510	-1.029361
1	5.485325	-2.668316	0.755360
1	1.463437	-2.266703	-0.714872
6	3.145832	-1.366748	1.251102
1	2.268834	-1.672332	1.824338
1	3.989908	-1.294632	1.941372
7	2.862788	-0.013045	0.745446
7	3.803814	0.625099	0.023264
7	3.301087	1.766444	-0.367675

A.2 Transition states

T18



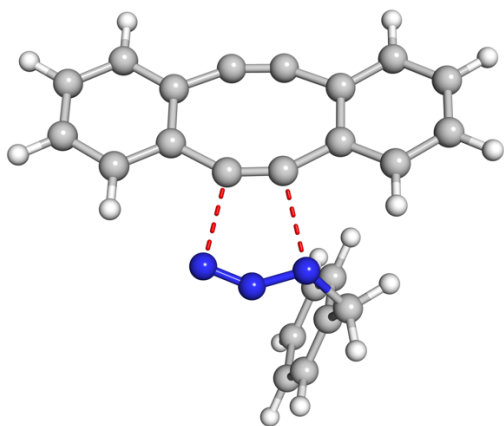
Imaginary frequency at -338 cm^{-1}

<i>E</i> (B3LYP)	<i>H</i> (B3LYP)	<i>G</i> (B3LYP)	<i>E</i> (M06-2X)
-1049.512393	-1049.177136	-1049.250489	-1049.462265

	X	Y	Z
6	-5.630831	-1.937847	0.709562
6	-6.297752	-1.315408	-0.347393
6	-5.705920	-0.227708	-0.996603
6	-4.453627	0.233113	-0.589683
6	-3.776012	-0.387479	0.468859
6	-4.375644	-1.475814	1.113676
1	-6.086092	-2.781140	1.221707
1	-7.274422	-1.672537	-0.662285
1	-6.222018	0.264147	-1.816656
1	-3.999949	1.081448	-1.096664
1	-3.859868	-1.962172	1.938445
6	-2.406028	0.095727	0.900831
1	-2.362496	1.186639	0.902656
1	-2.175609	-0.251178	1.914207
7	-1.324531	-0.314794	-0.032061
7	-0.986266	-1.523515	-0.030474
7	-0.063803	-2.216453	-0.212052
6	0.848187	0.410902	-0.242354
6	1.471306	-0.672340	-0.285934
6	2.729004	-1.402542	-0.228572

6	3.902128	-0.681577	0.189105
6	3.685406	0.707237	0.445828
6	3.057393	1.749678	0.481788
6	1.914685	2.577156	0.246004
6	0.748507	1.856787	-0.188105
6	-0.381567	2.589081	-0.557854
1	-1.249663	2.060414	-0.934121
6	1.881340	3.968270	0.344810
1	2.767128	4.497524	0.682117
6	2.865497	-2.755983	-0.547117
1	1.993054	-3.314155	-0.863875
6	5.131103	-1.335903	0.284065
1	6.005421	-0.777751	0.604310
6	5.235819	-2.693377	-0.038446
1	6.197304	-3.192524	0.036224
6	4.108527	-3.395392	-0.457606
1	4.185740	-4.447845	-0.714452
6	0.724326	4.674015	-0.004879
1	0.709370	5.756878	0.073739
6	-0.395383	3.986804	-0.467305
1	-1.288494	4.531187	-0.759294

T19

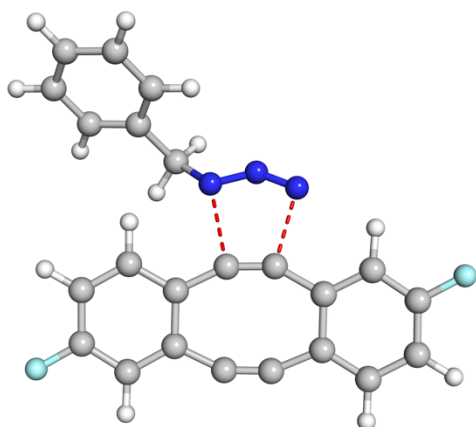


Imaginary frequency at -345.9 cm⁻¹

<i>E</i> (B3LYP)	<i>H</i> (B3LYP)	<i>G</i> (B3LYP)	<i>E</i> (M06-2X)
-1049.512577	-1049.177364	-1049.251092	-1049.463417

	X	Y	Z
6	-3.229350	-1.029019	2.271259
6	-3.962911	-2.209304	2.117404
6	-4.335145	-2.632515	0.840003
6	-3.972803	-1.878974	-0.279364
6	-3.237854	-0.695895	-0.134521
6	-2.870005	-0.277476	1.152063
1	-2.941122	-0.692155	3.263349
1	-4.245148	-2.792991	2.989341
1	-4.908982	-3.546446	0.713050
1	-4.267355	-2.210259	-1.272547
1	-2.301829	0.641195	1.276072
6	-2.826889	0.105257	-1.351849
1	-3.460638	-0.138738	-2.212027
1	-2.929411	1.176085	-1.165912
7	-1.404800	-0.065803	-1.744408
7	-0.973754	-1.233781	-1.900236
7	0.002691	-1.868854	-1.816488
6	0.553579	0.657682	-0.783737
6	1.243137	-0.385031	-0.801021
6	2.418700	-1.122311	-0.362588
6	3.217111	-0.544388	0.685987
6	2.772427	0.737811	1.133082
6	2.088985	1.745400	1.127585
6	1.081091	2.618910	0.610541
6	0.292868	2.044024	-0.445836
6	-0.636645	2.858654	-1.096531
1	-1.201506	2.451592	-1.927251
6	0.869697	3.941356	1.001120
1	1.467097	4.359005	1.805594
6	2.814763	-2.354243	-0.889474
1	2.226189	-2.803609	-1.679785
6	4.342627	-1.217488	1.163093
1	4.931274	-0.768971	1.957358
6	4.712113	-2.451896	0.617781
1	5.591245	-2.966138	0.994384
6	3.953709	-3.011688	-0.407254
1	4.239390	-3.967004	-0.837787
6	-0.089394	4.725596	0.349698
1	-0.244747	5.754520	0.659870
6	-0.827388	4.189330	-0.702660
1	-1.557963	4.800238	-1.224475

T20: *anti*-attack



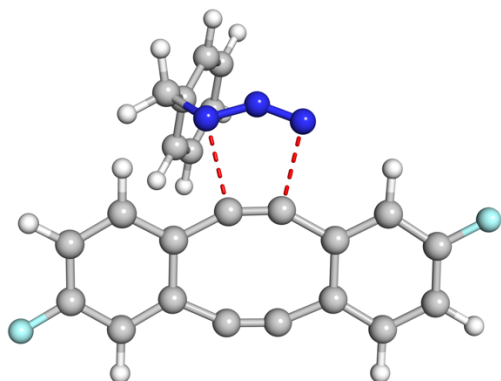
Imaginary frequency at -329.7 cm^{-1}

<i>E</i> (B3LYP)	<i>H</i> (B3LYP)	<i>G</i> (B3LYP)	<i>E</i> (M06-2X)
-1247.977270	-1247.657152	-1247.735106	-1247.967500

	X	Y	Z
6	-1.559765	1.585486	-0.329577
6	-2.196110	2.830946	-0.375425
6	-1.436376	3.975037	-0.190460
6	-0.058882	3.931100	0.016345
6	-0.185673	1.478710	-0.102210
1	-3.263436	2.910427	-0.549956
1	0.502539	4.850862	0.135434
6	0.575225	2.690701	0.049971
6	0.550905	0.232464	-0.034330
6	1.582081	-0.472866	-0.040838
6	3.032799	-0.573481	-0.072211
6	3.794124	0.641088	0.061660
6	1.983605	2.487906	0.179627
6	3.004561	1.825579	0.166410
6	5.189149	0.599425	0.054818
6	3.724389	-1.776576	-0.218687
1	3.194828	-2.714572	-0.319777
6	5.118577	-1.770397	-0.228492
6	5.868813	-0.613508	-0.090507
1	6.952057	-0.660567	-0.099709
1	5.749141	1.522810	0.159337
1	-2.143316	0.686959	-0.488209

9	5.756786	-2.951729	-0.375255
9	-2.041773	5.180496	-0.222090
6	-5.919927	-1.140086	0.233820
6	-5.974883	-2.052975	-0.821561
6	-4.818320	-2.737973	-1.203700
6	-3.615161	-2.514074	-0.532423
6	-3.552328	-1.601989	0.528806
6	-4.714134	-0.913740	0.901254
1	-6.812271	-0.597405	0.533758
1	-6.910666	-2.226563	-1.345676
1	-4.851865	-3.447075	-2.026457
1	-2.718760	-3.045762	-0.838848
1	-4.676044	-0.197444	1.718878
6	-2.266135	-1.380414	1.305051
1	-2.304804	-0.413252	1.816143
1	-2.141676	-2.144939	2.079746
7	-1.063853	-1.347306	0.447711
7	-0.229697	-2.277452	0.521317
7	0.897832	-2.513035	0.324884

T21: *anti*-attack



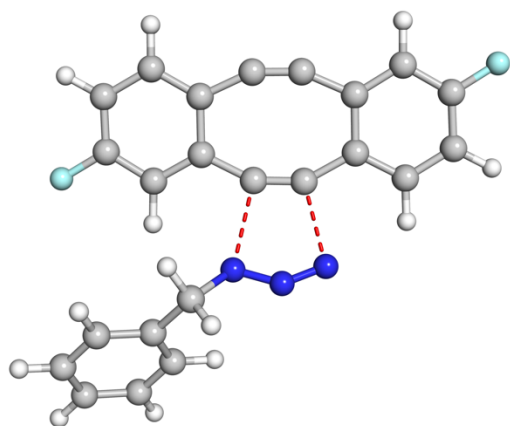
Imaginary frequency at -348.7 cm^{-1}

<i>E</i> (B3LYP)	<i>H</i> (B3LYP)	<i>G</i> (B3LYP)	<i>E</i> (M06-2X)
-1247.977615	-1247.657397	-1247.734683	-1247.968456

	X	Y	Z
6	-2.199757	1.765494	-1.268884
6	-3.142993	2.754505	-0.968328
6	-2.872638	3.640775	0.062433
6	-1.684695	3.600855	0.790075

6	-1.004409	1.658620	-0.553620
1	-4.070990	2.834767	-1.523574
1	-1.501015	4.330097	1.571019
6	-0.740123	2.624083	0.479773
6	0.017911	0.661927	-0.802688
6	1.178706	0.202083	-0.741804
6	2.537912	0.291736	-0.233685
6	2.810651	1.266748	0.789902
6	0.556656	2.510955	1.069613
6	1.692694	2.080432	1.144641
6	4.093605	1.379013	1.328017
6	3.585493	-0.517873	-0.674942
1	3.426317	-1.266670	-1.439643
6	4.853730	-0.364006	-0.116753
6	5.133115	0.559877	0.877760
1	6.135270	0.637880	1.284338
1	4.283442	2.116332	2.101031
1	-2.389086	1.078063	-2.084546
9	5.846846	-1.160004	-0.569058
9	-3.780746	4.590520	0.369390
6	-2.120940	-4.745862	0.944851
6	-2.175153	-4.124968	2.194394
6	-2.309698	-2.735669	2.274033
6	-2.388564	-1.972540	1.108694
6	-2.333667	-2.587397	-0.149986
6	-2.199165	-3.979526	-0.220650
1	-2.020934	-5.825605	0.875552
1	-2.116570	-4.719616	3.101890
1	-2.357353	-2.247579	3.243696
1	-2.494531	-0.892464	1.174608
1	-2.160463	-4.466945	-1.192138
6	-2.394329	-1.757428	-1.414877
1	-2.717214	-2.365255	-2.267501
1	-3.109316	-0.939396	-1.309211
7	-1.115580	-1.087833	-1.768476
7	-0.083119	-1.795283	-1.847933
7	1.074626	-1.748206	-1.704493

T22: *syn*-attack



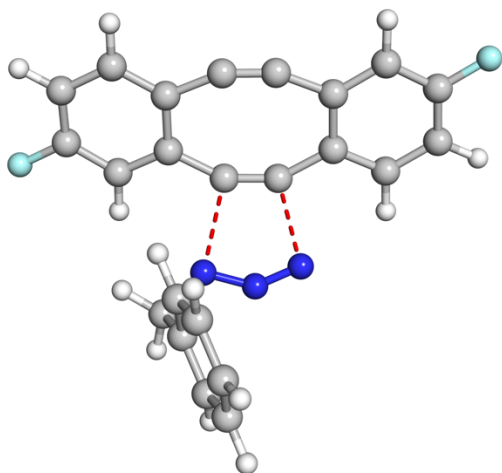
Imaginary frequency at -331.7 cm⁻¹

<i>E</i> (B3LYP)	<i>H</i> (B3LYP)	<i>G</i> (B3LYP)	<i>E</i> (M06-2X)
-1247.977129	-1247.657003	-1247.734669	-1247.967577

	X	Y	Z
6	-3.637206	-1.971277	0.311690
6	-5.032279	-2.075565	0.336446
6	-5.790368	-0.929758	0.155717
6	-5.213585	0.323367	-0.038648
6	-3.001652	-0.741674	0.118015
1	-5.522365	-3.030906	0.489212
1	-5.842439	1.196783	-0.169130
6	-3.823427	0.427994	-0.052806
6	-1.558978	-0.564817	0.073684
6	-0.560556	0.185598	0.037829
6	0.106953	1.471749	0.074295
6	-0.714087	2.639456	-0.108311
6	-3.098929	1.649076	-0.201305
6	-2.109636	2.357379	-0.228094
6	-0.137725	3.909897	-0.101257
6	1.472246	1.647802	0.298954
1	2.124302	0.802842	0.479640
6	2.004857	2.936894	0.308773
6	1.236157	4.071372	0.103165
1	1.697934	5.052331	0.113503
1	-0.768242	4.780914	-0.246040
1	-3.036613	-2.862207	0.442814
9	3.330255	3.072847	0.527003

9	-7.136918	-1.020708	0.170685
6	5.961828	-0.785973	-0.305929
6	6.093473	-1.668014	0.768754
6	4.989652	-2.414603	1.189520
6	3.762839	-2.283300	0.536873
6	3.623540	-1.403225	-0.543948
6	4.732273	-0.652013	-0.954609
1	6.812422	-0.195515	-0.635403
1	7.047745	-1.769862	1.278183
1	5.082942	-3.099813	2.027757
1	2.907401	-2.862499	0.872870
1	4.633575	0.041060	-1.787006
6	2.312695	-1.283549	-1.300754
1	2.279620	-0.328660	-1.834860
1	2.224909	-2.073298	-2.054770
7	1.125941	-1.308676	-0.421174
7	0.343292	-2.284079	-0.474160
7	-0.767767	-2.578859	-0.265278

T23: *syn*-attack



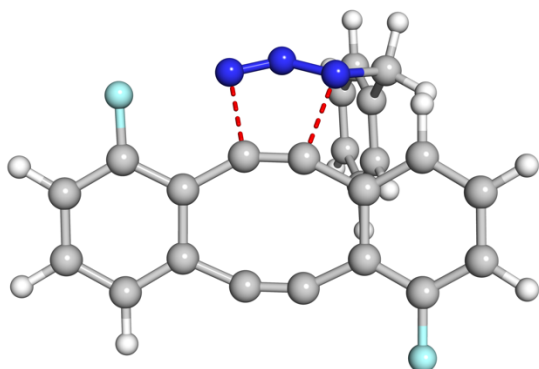
Imaginary frequency at -348.8 cm^{-1}

<i>E</i> (B3LYP)	<i>H</i> (B3LYP)	<i>G</i> (B3LYP)	<i>E</i> (M06-2X)
-1247.977439	-1247.657235	-1247.735846	-1247.968378

	X	Y	Z
6	3.285963	-1.155429	-1.178536

6	4.620876	-1.355675	-0.810491
6	5.150568	-0.593686	0.218697
6	4.405746	0.372287	0.891634
6	2.488727	-0.202167	-0.538612
1	5.237901	-2.094094	-1.310693
1	4.860240	0.952602	1.686640
6	3.078996	0.579447	0.516400
6	1.093724	0.046306	-0.863489
6	0.056000	0.731022	-0.730542
6	-0.684747	1.888927	-0.270415
6	-0.101994	2.665867	0.790910
6	2.213910	1.561683	1.086639
6	1.197815	2.224027	1.187926
6	-0.773079	3.782134	1.291197
6	-1.898725	2.309505	-0.814401
1	-2.347181	1.781097	-1.646213
6	-2.528904	3.439190	-0.292898
6	-2.002867	4.177536	0.755454
1	-2.534210	5.044536	1.131810
1	-0.325997	4.355092	2.096826
1	2.859494	-1.753383	-1.973820
9	-3.703131	3.819747	-0.839627
9	6.435006	-0.784640	0.587085
6	-3.031952	-4.321465	0.786401
6	-2.713200	-3.891606	2.075919
6	-2.452795	-2.538307	2.312224
6	-2.511201	-1.620970	1.262834
6	-2.829246	-2.044152	-0.035416
6	-3.088240	-3.401190	-0.263337
1	-3.238938	-5.371020	0.596036
1	-2.670373	-4.605544	2.893875
1	-2.208411	-2.197512	3.314650
1	-2.309897	-0.569193	1.450928
1	-3.339440	-3.739071	-1.266093
6	-2.868843	-1.054023	-1.179992
1	-3.435909	-1.456951	-2.026664
1	-3.355660	-0.125402	-0.875570
7	-1.531290	-0.626869	-1.666205
7	-0.695545	-1.519989	-1.944796
7	0.452880	-1.729241	-1.958637

T24: *anti*-attack



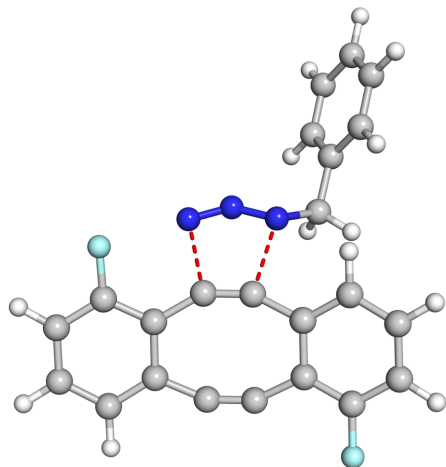
Imaginary frequency at -367.5 cm^{-1}

<i>E</i> (B3LYP)	<i>H</i> (B3LYP)	<i>G</i> (B3LYP)	<i>E</i> (M06-2X)
-1247.973809	-1247.653510	-1247.730366	-1247.964377

	X	Y	Z
6	-3.436507	-1.593984	-0.587617
6	-4.615883	-1.883545	0.099586
6	-4.937882	-1.151645	1.237403
6	-4.097947	-0.119984	1.671695
6	-2.541670	-0.604496	-0.179599
1	-5.258375	-2.673347	-0.274551
1	-5.851061	-1.372416	1.780684
1	-4.358610	0.472599	2.542139
6	-2.925310	0.168129	0.973670
6	-1.278138	-0.309012	-0.823357
6	-0.329452	0.486480	-1.000395
6	0.321411	1.774558	-0.861478
6	-0.076832	2.575877	0.261887
6	-2.042346	1.254347	1.258004
6	-1.144329	2.048958	1.048328
6	0.537621	3.809816	0.448902
6	1.276539	2.281297	-1.745765
1	1.557626	1.695156	-2.613350
6	1.858019	3.537354	-1.527519
1	2.597896	3.913457	-2.226865
6	1.503196	4.306851	-0.422651
1	1.947088	5.277599	-0.231234
9	0.165259	4.555173	1.510149
9	-3.175071	-2.304616	-1.702547
6	3.048813	-1.362221	2.347941

6	3.530667	-2.673052	2.410088
6	3.761139	-3.383445	1.230290
6	3.508189	-2.785253	-0.006559
6	3.024601	-1.472836	-0.078209
6	2.798377	-0.766274	1.111427
1	2.872655	-0.802577	3.262543
1	3.728445	-3.135815	3.373064
1	4.139761	-4.401109	1.270608
1	3.692708	-3.340630	-0.923312
1	2.427852	0.254962	1.068682
6	2.731648	-0.838615	-1.421081
1	3.024893	0.213056	-1.431033
1	3.289997	-1.339582	-2.219945
7	1.294494	-0.819248	-1.795177
7	0.635028	-1.880266	-1.667336
7	-0.438966	-2.273656	-1.439745

T25: *anti*-attack

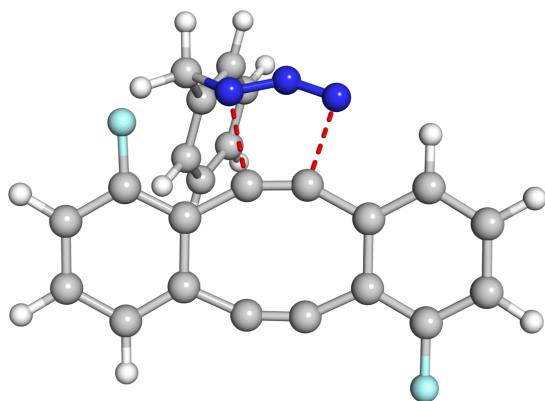


Imaginary frequency at -362.0 cm^{-1}

<i>E</i> (B3LYP)	<i>H</i> (B3LYP)	<i>G</i> (B3LYP)	<i>E</i> (M06-2X)
-1247.973651	-1247.653358	-1247.730579	-1247.962976

	X	Y	Z
6	-2.809328	-2.781952	-0.587091
6	-4.023982	-3.416359	-0.324439
6	-5.022355	-2.721932	0.350248

6	-4.816550	-1.393228	0.738502
6	-2.533200	-1.473631	-0.189666
1	-4.162603	-4.439130	-0.658021
1	-5.968893	-3.208456	0.562664
1	-5.602147	-0.838282	1.240181
6	-3.602158	-0.764351	0.464160
6	-1.267535	-0.796550	-0.385130
6	-0.623333	0.274601	-0.435575
6	-0.521839	1.720779	-0.452320
6	-1.598092	2.446377	0.161803
6	-3.308075	0.610157	0.718426
6	-2.691994	1.655756	0.623972
6	-1.531440	3.835475	0.191174
6	0.527321	2.436112	-1.033613
1	1.325372	1.894373	-1.528246
6	0.546495	3.836553	-0.994436
1	1.370943	4.373779	-1.452276
6	-0.475576	4.547890	-0.371364
1	-0.475659	5.631256	-0.322804
9	-2.541821	4.511773	0.776341
9	-1.877786	-3.476647	-1.269951
6	5.762282	-1.728921	1.117751
6	6.487435	-1.287042	0.009532
6	5.923264	-0.347960	-0.859252
6	4.640413	0.145102	-0.619454
6	3.904699	-0.295058	0.489536
6	4.476816	-1.235464	1.354558
1	6.195509	-2.455505	1.799683
1	7.487695	-1.668809	-0.175641
1	6.484525	0.003469	-1.720771
1	4.207655	0.877559	-1.296607
1	3.916158	-1.581077	2.219930
6	2.502856	0.221061	0.742846
1	2.213570	0.063678	1.787916
1	2.439272	1.290343	0.532905
7	1.491664	-0.391011	-0.158577
7	1.179105	-1.589454	0.055031
7	0.281849	-2.331510	-0.011802

T26: *syn*-attack

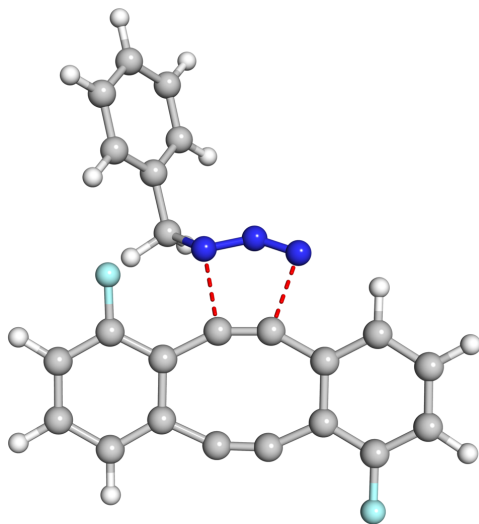
Imaginary frequency at -351.5 cm^{-1}

<i>E</i> (B3LYP)	<i>H</i> (B3LYP)	<i>G</i> (B3LYP)	<i>E</i> (M06-2X)
-1247.974862	-1247.654606	-1247.732116	-1247.963207

	X	Y	Z
6	-1.186721	2.664130	-0.989805
6	-1.616243	3.883397	-0.464882
6	-0.995035	4.391967	0.670004
6	0.064903	3.695860	1.262545
6	-0.170125	1.901507	-0.414829
1	-2.423133	4.410722	-0.962092
1	-1.323817	5.338149	1.087470
1	0.575675	4.102937	2.128645
6	0.490310	2.481003	0.727175
6	0.299568	0.615872	-0.885699
6	1.156786	-0.290856	-0.962950
6	2.469958	-0.818424	-0.630408
6	3.157841	-0.212910	0.476626
6	1.626478	1.736163	1.167709
6	2.503622	0.896538	1.086088
6	4.405550	-0.709278	0.839428
6	3.089040	-1.871243	-1.308034
1	2.577957	-2.337333	-2.141161
6	4.353915	-2.329766	-0.917356
1	4.817895	-3.146669	-1.461069
6	5.020864	-1.758765	0.163200
1	5.996848	-2.104417	0.485882
9	5.041878	-0.138050	1.883968
9	-1.800589	2.221337	-2.108200

6	-4.041747	-3.193864	1.202295
6	-3.807728	-2.550518	2.419364
6	-3.318490	-1.241000	2.429276
6	-3.064758	-0.579894	1.227015
6	-3.293753	-1.218934	0.000464
6	-3.784702	-2.530412	0.000011
1	-4.426297	-4.210029	1.186946
1	-4.008619	-3.064374	3.355433
1	-3.139441	-0.733389	3.373233
1	-2.687733	0.439902	1.239572
1	-3.971636	-3.033548	-0.945930
6	-2.993421	-0.512774	-1.305179
1	-3.556522	-0.963587	-2.130175
1	-3.270605	0.540664	-1.260137
7	-1.556524	-0.495835	-1.667455
7	-0.942277	-1.576287	-1.801859
7	0.137540	-2.024368	-1.772240

T27: *syn*-attack



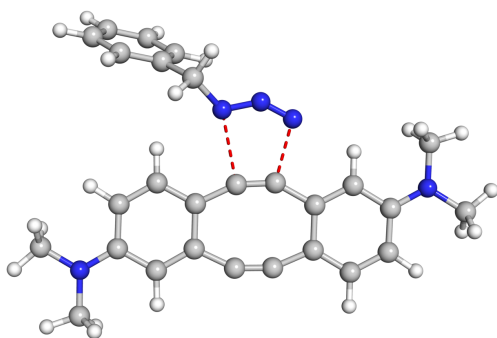
Imaginary frequency at -339.3 cm^{-1}

<i>E</i> (B3LYP)	<i>H</i> (B3LYP)	<i>G</i> (B3LYP)	<i>E</i> (M06-2X)
-1247.975469	-1247.655109	-1247.732083	-1247.962816

	X	Y	Z
6	-1.186721	2.664130	-0.989805

6	-1.616243	3.883397	-0.464882
6	-0.995035	4.391967	0.670004
6	0.064903	3.695860	1.262545
6	-0.170125	1.901507	-0.414829
1	-2.423133	4.410722	-0.962092
1	-1.323817	5.338149	1.087470
1	0.575675	4.102937	2.128645
6	0.490310	2.481003	0.727175
6	0.299568	0.615872	-0.885699
6	1.156786	-0.290856	-0.962950
6	2.469958	-0.818424	-0.630408
6	3.157841	-0.212910	0.476626
6	1.626478	1.736163	1.167709
6	2.503622	0.896538	1.086088
6	4.405550	-0.709278	0.839428
6	3.089040	-1.871243	-1.308034
1	2.577957	-2.337333	-2.141161
6	4.353915	-2.329766	-0.917356
1	4.817895	-3.146669	-1.461069
6	5.020864	-1.758765	0.163200
1	5.996848	-2.104417	0.485882
9	5.041878	-0.138050	1.883968
9	-1.800589	2.221337	-2.108200
6	-4.041747	-3.193864	1.202295
6	-3.807728	-2.550518	2.419364
6	-3.318490	-1.241000	2.429276
6	-3.064758	-0.579894	1.227015
6	-3.293753	-1.218934	0.000464
6	-3.784702	-2.530412	0.000011
1	-4.426297	-4.210029	1.186946
1	-4.008619	-3.064374	3.355433
1	-3.139441	-0.733389	3.373233
1	-2.687733	0.439902	1.239572
1	-3.971636	-3.033548	-0.945930
6	-2.993421	-0.512774	-1.305179
1	-3.556522	-0.963587	-2.130175
1	-3.270605	0.540664	-1.260137
7	-1.556524	-0.495835	-1.667455
7	-0.942277	-1.576287	-1.801859
7	0.137540	-2.024368	-1.772240

T28: *anti*-attack



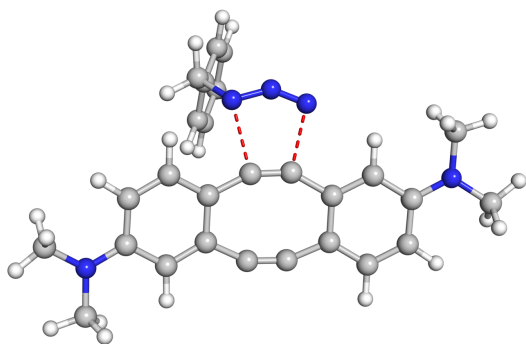
Imaginary frequency at -299.6 cm^{-1}

<i>E</i> (B3LYP)	<i>H</i> (B3LYP)	<i>G</i> (B3LYP)	<i>E</i> (M06-2X)
-1317.454411	-1316.963776	-1317.061237	-1317.385138

	X	Y	Z
6	-2.266260	0.609313	-0.126370
6	-3.338331	1.495927	-0.067837
6	-3.131197	2.894304	0.000156
6	-1.786332	3.352306	0.032023
6	-0.938028	1.043251	-0.116252
1	-2.471383	-0.453492	-0.165581
1	-4.342250	1.090488	-0.074955
1	-1.566690	4.409813	0.104903
6	-0.720147	2.463410	-0.019227
6	0.237018	0.210057	-0.173081
6	1.455295	-0.069693	-0.136694
6	2.834575	0.394756	-0.002072
6	3.040507	1.815574	0.110003
6	0.659762	2.835344	0.038395
6	1.855875	2.604033	0.089140
6	4.344892	2.298210	0.234170
1	4.503658	3.369716	0.316286
6	3.940226	-0.451029	0.020158
1	3.775085	-1.514814	-0.070059
6	5.266961	0.045831	0.151370
6	5.443870	1.445049	0.254808
1	6.434176	1.871870	0.350984
7	6.338297	-0.817421	0.175365
7	-4.182320	3.778781	0.037563
6	7.691815	-0.291057	0.274068

1	8.398593	-1.121021	0.285489
1	7.941340	0.359179	-0.576089
1	7.833087	0.287663	1.196488
6	6.135742	-2.251609	0.024233
1	7.102244	-2.753882	0.071983
1	5.503583	-2.658112	0.824468
1	5.669257	-2.501625	-0.938620
6	-3.936813	5.208564	0.168603
1	-3.332542	5.590279	-0.664185
1	-4.891049	5.735813	0.159535
1	-3.419706	5.454200	1.106727
6	-5.550307	3.280669	0.063118
1	-5.747283	2.665726	0.952493
1	-6.238125	4.126363	0.074958
1	-5.772510	2.675091	-0.824933
6	-3.511587	-4.212052	1.645608
6	-4.844479	-4.178753	1.226566
6	-5.159713	-3.661970	-0.031958
6	-4.146673	-3.181113	-0.864732
6	-2.807566	-3.218389	-0.455359
6	-2.500279	-3.735693	0.809821
1	-3.258525	-4.608547	2.625314
1	-5.631377	-4.548271	1.878396
1	-6.193821	-3.624754	-0.363794
1	-4.398490	-2.774231	-1.841600
1	-1.466562	-3.758083	1.143266
6	-1.716418	-2.742146	-1.398452
1	-1.288892	-3.589067	-1.947003
1	-2.145691	-2.064836	-2.145042
7	-0.638223	-2.006827	-0.711595
7	0.523952	-2.474885	-0.716153
7	1.628211	-2.148793	-0.496705

T29: *anti*-attack



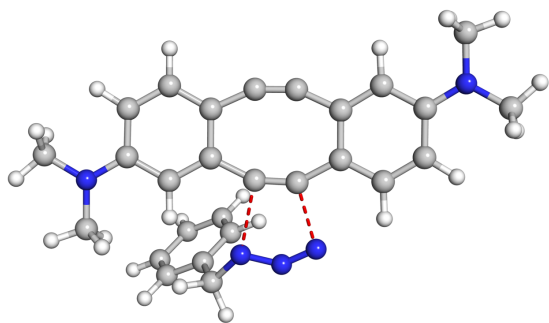
Imaginary frequency at -338.7 cm⁻¹

<i>E</i> (B3LYP)	<i>H</i> (B3LYP)	<i>G</i> (B3LYP)	<i>E</i> (M06-2X)
-1317.455124	-1316.964307	-1317.059232	-1317.387375

	X	Y	Z
6	2.645669	-0.327425	-1.355522
6	3.921134	-0.851390	-1.156679
6	4.155969	-1.859977	-0.192130
6	3.031436	-2.346645	0.527057
6	1.535474	-0.768034	-0.628953
1	2.504192	0.432437	-2.115914
1	4.734469	-0.469632	-1.760730
1	3.142970	-3.146209	1.248161
6	1.758652	-1.830231	0.315116
6	0.182788	-0.283337	-0.775133
6	-1.061539	-0.322257	-0.640242
6	-2.234997	-0.992650	-0.092499
6	-2.010869	-2.063931	0.842982
6	0.565648	-2.308080	0.943248
6	-0.643654	-2.379740	1.082807
6	-3.116069	-2.713672	1.396486
1	-2.952366	-3.521828	2.103752
6	-3.541158	-0.649681	-0.426595
1	-3.690278	0.154035	-1.131617
6	-4.664206	-1.318116	0.134640
6	-4.419118	-2.358864	1.060571
1	-5.240203	-2.897147	1.516933
7	-5.944264	-0.952771	-0.214233
7	5.417905	-2.357586	0.041262
6	-7.080638	-1.678821	0.333862

1	-8.002923	-1.242444	-0.050235
1	-7.062027	-2.741690	0.054381
1	-7.107300	-1.616823	1.429732
6	-6.170179	0.086440	-1.209129
1	-7.243529	0.226911	-1.338881
1	-5.739543	1.046404	-0.896049
1	-5.739982	-0.177511	-2.185318
6	5.604435	-3.488032	0.941093
1	5.088672	-4.392884	0.588071
1	6.669362	-3.710057	1.016284
1	5.238526	-3.257718	1.948830
6	6.530054	-1.932041	-0.797151
1	6.668506	-0.845241	-0.748345
1	7.446415	-2.402173	-0.439099
1	6.388225	-2.211201	-1.851504
6	0.185086	5.307760	1.321404
6	0.881433	4.785546	2.413930
6	1.734614	3.693153	2.235318
6	1.888529	3.125579	0.969594
6	1.193674	3.641520	-0.132747
6	0.340751	4.738766	0.055375
1	-0.475295	6.160696	1.452668
1	0.763218	5.229713	3.398533
1	2.282474	3.285556	3.080635
1	2.552396	2.275357	0.832843
1	-0.199216	5.154851	-0.794531
6	1.341533	3.003417	-1.498718
1	1.179547	3.740717	-2.293189
1	2.347089	2.599429	-1.625951
7	0.438250	1.848057	-1.725085
7	-0.797936	2.063951	-1.693768
7	-1.811114	1.522766	-1.472085

T30: *syn*-attack



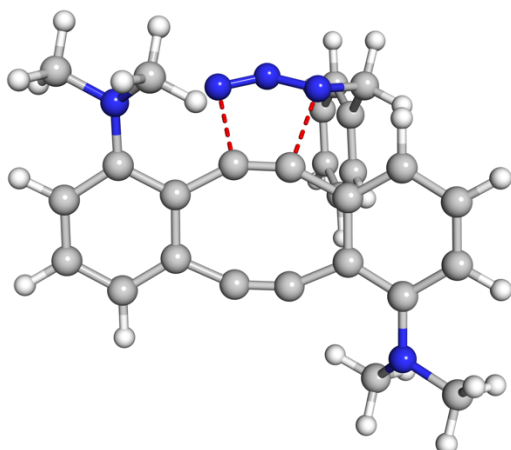
Imaginary frequency at -319.4 cm^{-1}

<i>E</i> (B3LYP)	<i>H</i> (B3LYP)	<i>G</i> (B3LYP)	<i>E</i> (M06-2X)
-1317.453337	-1316.962745	-1317.058319	-1317.385873

	X	Y	Z
6	-3.552175	-1.199672	-1.013578
6	-4.914902	-1.113160	-0.738850
6	-5.433146	-0.089354	0.088527
6	-4.507763	0.854094	0.608937
6	-2.625004	-0.284906	-0.502783
1	-3.201522	-2.004804	-1.647178
1	-5.575439	-1.853152	-1.173546
1	-4.846380	1.668271	1.236802
6	-3.149633	0.769225	0.324752
6	-1.192240	-0.318612	-0.747507
6	-0.067989	0.223050	-0.634439
6	0.857707	1.275959	-0.261030
6	0.326507	2.321235	0.573110
6	-2.171958	1.700785	0.789360
6	-1.061446	2.196707	0.868942
6	1.173033	3.355472	0.973998
1	0.779771	4.141346	1.612551
6	2.185210	1.344507	-0.669191
1	2.555412	0.563049	-1.314915
6	3.040590	2.411270	-0.276459
6	2.504136	3.407791	0.572308
1	3.119218	4.229427	0.916379
7	4.344847	2.468377	-0.714120
7	-6.773593	-0.003258	0.380427
6	5.226176	3.519383	-0.225004
1	6.201914	3.417226	-0.700607

1	4.833587	4.513470	-0.472242
1	5.367287	3.469763	0.864436
6	4.912144	1.372448	-1.487124
1	5.941484	1.618093	-1.749688
1	4.919416	0.428209	-0.923767
1	4.359127	1.212823	-2.421114
6	-7.281578	1.094396	1.191796
1	-7.101262	2.071824	0.722868
1	-8.357460	0.973626	1.320374
1	-6.821801	1.104701	2.188425
6	-7.707870	-0.949280	-0.212785
1	-7.468284	-1.982042	0.071843
1	-8.714773	-0.727392	0.141415
1	-7.709840	-0.890748	-1.310241
6	5.072199	-2.817371	1.455735
6	4.216410	-2.947171	2.553042
6	2.839195	-2.808215	2.371836
6	2.317461	-2.544628	1.102324
6	3.167577	-2.415400	-0.001102
6	4.550373	-2.550003	0.189388
1	6.146362	-2.918250	1.585992
1	4.620906	-3.150562	3.540756
1	2.165972	-2.902686	3.219747
1	1.245854	-2.428408	0.974065
1	5.222471	-2.449078	-0.660291
6	2.639598	-2.170889	-1.407152
1	3.322567	-1.504793	-1.943383
1	2.619074	-3.110624	-1.971092
7	1.304281	-1.553106	-1.454506
7	0.305074	-2.287983	-1.636315
7	-0.866227	-2.240496	-1.579758

T31: *anti*-attack



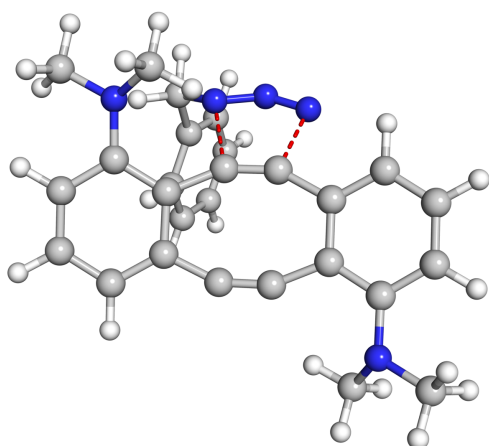
Imaginary frequency at -373.1 cm⁻¹

<i>E</i> (B3LYP)	<i>H</i> (B3LYP)	<i>G</i> (B3LYP)	<i>E</i> (M06-2X)
-1317.439352	-1316.949479	-1317.041191	-1317.375642

	X	Y	Z
6	3.692598	0.987720	-0.211454
6	4.459482	1.621216	-1.220111
6	3.864805	2.329267	-2.256463
6	2.476685	2.476762	-2.313207
6	2.277842	1.049915	-0.309858
1	5.540807	1.577482	-1.172078
1	4.491014	2.803032	-3.007188
1	2.007803	3.067942	-3.092946
6	1.688612	1.861428	-1.341306
6	1.351263	0.318802	0.533829
6	0.209088	0.201934	1.031335
6	-1.142610	0.659592	1.297524
6	-1.735294	1.529361	0.321333
6	0.267386	2.000768	-1.246013
6	-0.822811	1.920855	-0.706489
6	-3.058060	2.009188	0.486691
6	-1.856081	0.333027	2.452167
1	-1.398949	-0.301492	3.203512
6	-3.145016	0.843235	2.632767
1	-3.700451	0.590432	3.531566
6	-3.742973	1.647904	1.669527
1	-4.757453	1.991220	1.830524
7	-3.631905	2.866471	-0.464610

7	4.316349	0.298644	0.835055
6	3.942847	0.613737	2.213767
1	4.166682	-0.244489	2.856175
1	4.503327	1.484554	2.593863
1	2.877298	0.823815	2.290440
6	5.729550	-0.025741	0.707493
1	6.394633	0.841143	0.863116
1	5.980289	-0.777057	1.462963
1	5.935728	-0.452512	-0.277471
6	-4.867616	3.550549	-0.102952
1	-5.056896	4.332959	-0.843666
1	-5.746595	2.884222	-0.082650
1	-4.766223	4.026057	0.876105
6	-3.622587	2.453781	-1.871257
1	-4.413633	1.715927	-2.084721
1	-3.792516	3.331945	-2.502003
1	-2.659480	2.024412	-2.145873
6	-1.026169	-2.880136	1.480754
1	-0.869618	-3.726686	2.159462
1	-1.881039	-2.315364	1.859540
6	-1.278825	-3.364947	0.068282
6	-0.864470	-4.643278	-0.326419
6	-1.912423	-2.537192	-0.869614
6	-1.077712	-5.088795	-1.633314
1	-0.376438	-5.295705	0.394092
6	-2.125288	-2.979405	-2.175712
1	-2.240880	-1.543818	-0.574180
6	-1.708025	-4.257017	-2.560860
1	-0.753992	-6.084492	-1.924142
1	-2.620412	-2.329256	-2.891981
1	-1.876667	-4.602241	-3.577275
7	0.113861	-1.943951	1.620248
7	1.208535	-2.252741	1.082050
7	2.160084	-1.770879	0.606138

T32: *syn*-attack



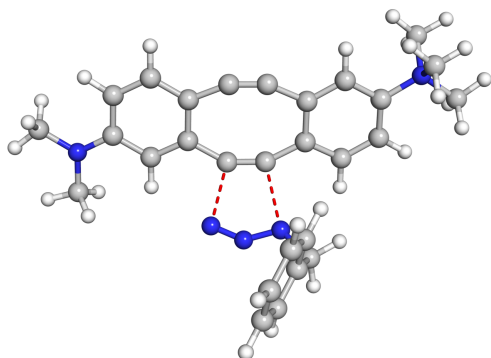
Imaginary frequency at -353.7 cm^{-1}

<i>E</i> (B3LYP)	<i>H</i> (B3LYP)	<i>G</i> (B3LYP)	<i>E</i> (M06-2X)
-1317.440466	-1316.950557	-1317.042257	-1317.376273

	X	Y	Z
6	-1.279640	2.797846	-0.329177
6	-1.511842	3.780767	0.666106
6	-0.797856	3.806320	1.856171
6	0.216812	2.876843	2.098493
6	-0.315808	1.789616	-0.053900
1	-2.247409	4.555120	0.488199
1	-1.007966	4.582386	2.586593
1	0.813996	2.921185	3.003219
6	0.471033	1.890610	1.148260
6	-0.033043	0.628974	-0.871096
6	0.680273	-0.313106	-1.280233
6	1.955677	-1.013308	-1.284428
6	2.804265	-0.850766	-0.137399
6	1.537149	0.939839	1.236157
6	2.302636	0.093239	0.808420
6	4.048473	-1.521788	-0.054175
6	2.384046	-1.812513	-2.345172
1	1.745523	-1.940394	-3.211330
6	3.632528	-2.437083	-2.279334
1	3.967072	-3.054701	-3.108275
6	4.444956	-2.308973	-1.158100
1	5.388910	-2.839510	-1.130484
7	4.876545	-1.350493	1.069262

7	-2.009400	2.809732	-1.523608
6	-1.287572	2.709791	-2.793751
1	-1.969086	2.342801	-3.567431
1	-0.898091	3.691540	-3.109831
1	-0.457633	2.010477	-2.716810
6	-3.163080	3.695499	-1.622285
1	-2.888774	4.758693	-1.727213
1	-3.739430	3.409871	-2.507153
1	-3.808631	3.585593	-0.747154
6	6.257783	-1.805180	0.964459
1	6.818747	-1.400484	1.812221
1	6.360479	-2.903563	0.985898
1	6.712685	-1.429119	0.044369
6	4.309152	-1.629674	2.392300
1	4.259202	-2.712502	2.595094
1	4.941065	-1.166070	3.156436
1	3.307685	-1.209777	2.484082
6	-4.387734	-3.109851	1.372025
1	-3.858586	-2.709404	2.600550
1	-3.211537	-1.474521	2.707501
6	-3.095427	-0.646251	1.590725
6	-3.621941	-1.040735	0.352562
6	-4.268851	-2.278905	0.255009
6	-4.895476	-4.066416	1.282086
1	-3.951891	-3.353312	3.470843
6	-2.801584	-1.155366	3.662009
1	-2.592089	0.313714	1.677299
6	-4.685668	-2.593434	-0.699178
1	-3.472854	-0.150686	-0.864912
1	-4.217157	-0.409317	-1.627332
1	-3.619298	0.898584	-0.605474
7	-2.126521	-0.181571	-1.473368
7	-1.668915	-1.267404	-1.900083
7	-0.650096	-1.786654	-2.154323

T33: *anti*-attack



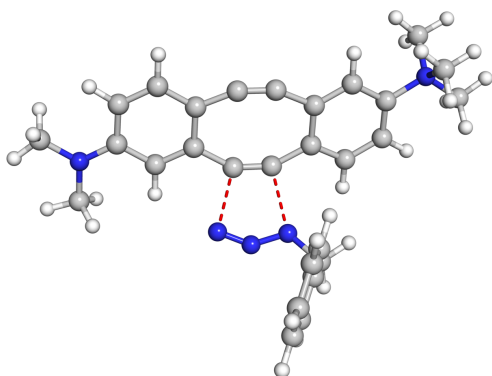
Imaginary frequency at -349.5 cm^{-1}

<i>E</i> (B3LYP)	<i>H</i> (B3LYP)	<i>G</i> (B3LYP)	<i>E</i> (M06-2X)
-1357.198762	-1356.663593	-1356.759753	-1357.121548

	X	Y	Z
6	3.013484	-2.857315	1.473316
6	4.339939	-2.664170	1.105097
6	4.685930	-1.705155	0.122355
6	3.634232	-0.941121	-0.458624
6	1.978491	-2.116566	0.896694
1	2.774119	-3.604766	2.223905
1	5.104852	-3.264357	1.580969
1	3.858756	-0.189783	-1.200644
6	2.307030	-1.126062	-0.093788
6	0.590107	-2.261787	1.156918
6	-0.608591	-2.071630	1.034087
6	-1.736351	-1.522945	0.358342
6	-1.415590	-0.545850	-0.649600
6	1.205743	-0.359866	-0.663493
6	-0.023819	-0.177708	-0.800176
6	-2.454405	-0.051374	-1.434237
1	-2.229639	0.644595	-2.232971
6	-3.061840	-1.899298	0.567677
1	-3.267745	-2.629611	1.340844
6	-4.079886	-1.354134	-0.224572
6	-3.784343	-0.444899	-1.231811
1	-4.544862	-0.021769	-1.872605
7	-5.494990	-1.799168	0.042317
7	5.988292	-1.508278	-0.261618
6	-6.496325	-1.143690	-0.878576

1	-7.482497	-1.518209	-0.608598
1	-6.459441	-0.064389	-0.740406
1	-6.268116	-1.413635	-1.908243
6	-5.883216	-1.447482	1.466425
1	-6.910498	-1.773775	1.628346
1	-5.216878	-1.957019	2.158622
1	-5.799424	-0.368214	1.588180
6	6.319418	-0.514423	-1.275190
1	6.019454	0.495361	-0.966349
1	7.398096	-0.512901	-1.431607
1	5.836579	-0.736981	-2.235889
6	7.051243	-2.303541	0.338569
1	6.907350	-3.376215	0.152768
1	8.006515	-2.009225	-0.095821
1	7.107895	-2.149710	1.424348
6	-5.604783	-3.299263	-0.156251
1	-5.315444	-3.528806	-1.181045
1	-4.944901	-3.805603	0.544613
1	-6.638606	-3.591983	0.027479
6	-0.605020	3.859542	2.304974
6	0.221320	4.987159	2.303253
6	0.676420	5.511706	1.091774
6	0.307347	4.909436	-0.113413
6	-0.519518	3.779120	-0.120841
6	-0.972461	3.259870	1.099948
1	-0.966061	3.450093	3.244515
1	0.505313	5.455903	3.241440
1	1.315150	6.390655	1.082894
1	0.659748	5.323883	-1.055141
1	-1.616977	2.384192	1.105109
6	-0.897257	3.114193	-1.427462
1	-1.928066	2.756329	-1.398347
1	-0.819956	3.818810	-2.263069
7	-0.093884	1.906448	-1.753422
7	1.155655	2.014988	-1.750222
7	2.129426	1.403246	-1.548722

T34: *anti*-attack



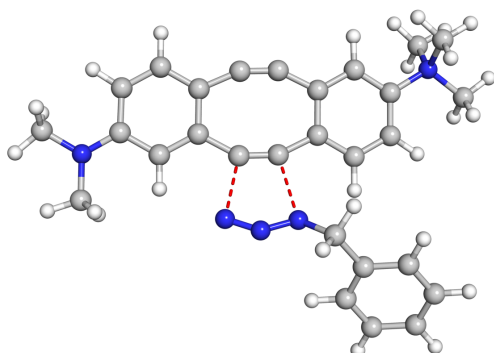
Imaginary frequency at -347.4 cm^{-1}

<i>E</i> (B3LYP)	<i>H</i> (B3LYP)	<i>G</i> (B3LYP)	<i>E</i> (M06-2X)
-1357.198769	-1356.663635	-1356.759186	-1357.121523

	X	Y	Z
6	3.010739	-2.887744	1.458646
6	4.336529	-2.693412	1.088665
6	4.681564	-1.726916	0.112888
6	3.629555	-0.956667	-0.459255
6	1.975321	-2.141069	0.890456
1	2.772234	-3.640956	2.203730
1	5.101773	-3.298526	1.557694
1	3.853091	-0.199416	-1.195617
6	2.303040	-1.143183	-0.092891
6	0.587231	-2.286943	1.152214
6	-0.611621	-2.095099	1.033139
6	-1.740036	-1.542473	0.361484
6	-1.419886	-0.560512	-0.641925
6	1.201325	-0.372089	-0.654593
6	-0.028334	-0.190913	-0.790101
6	-2.458795	-0.062524	-1.424206
1	-2.234314	0.636951	-2.219988
6	-3.065558	-1.919162	0.570060
1	-3.271359	-2.652823	1.340096
6	-4.083894	-1.369818	-0.218984
6	-3.788688	-0.456543	-1.222663
1	-4.549520	-0.030464	-1.861125
7	-5.499188	-1.814341	0.047696
7	5.983266	-1.528962	-0.272692
6	-6.500712	-1.155467	-0.870588

1	-7.486927	-1.530146	-0.601000
1	-6.463111	-0.076602	-0.729264
1	-6.273364	-1.422500	-1.901214
6	-5.885687	-1.465949	1.473062
1	-6.913164	-1.791561	1.635137
1	-5.219122	-1.977996	2.163184
1	-5.800562	-0.387100	1.597521
6	6.313423	-0.527350	-1.278923
1	6.015929	0.480327	-0.960960
1	7.391694	-0.526304	-1.438095
1	5.827749	-0.741159	-2.240182
6	7.046405	-2.331262	0.317743
1	6.900053	-3.402048	0.123157
1	8.001009	-2.034938	-0.116763
1	7.106341	-2.186834	1.404631
6	-5.610804	-3.313782	-0.154638
1	-5.322461	-3.541057	-1.180213
1	-4.951068	-3.822704	0.544482
1	-6.644836	-3.605742	0.029118
6	-0.428921	3.889895	2.311155
6	0.261690	5.104436	2.253178
6	0.564884	5.670912	1.013755
6	0.180495	5.023945	-0.163556
6	-0.512385	3.808321	-0.114493
6	-0.813942	3.247130	1.134568
1	-0.671356	3.446576	3.273151
1	0.558690	5.606543	3.169817
1	1.098589	6.615880	0.960919
1	0.416212	5.469376	-1.127295
1	-1.353909	2.304767	1.184170
6	-0.915006	3.103828	-1.392827
1	-1.937523	2.726706	-1.323894
1	-0.879204	3.791506	-2.245210
7	-0.102102	1.903807	-1.717047
7	1.146984	2.017399	-1.712065
7	2.122589	1.406768	-1.516494

T35: *anti*-attack



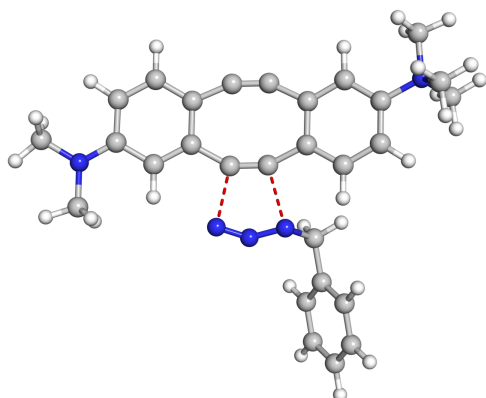
Imaginary frequency at -335.3 cm^{-1}

<i>E</i> (B3LYP)	<i>H</i> (B3LYP)	<i>G</i> (B3LYP)	<i>E</i> (M06-2X)
-1357.198480	-1356.663360	-1356.758323	-1357.120751

	X	Y	Z
6	4.372416	-2.443694	0.234423
6	5.524089	-1.683140	0.067573
6	5.444829	-0.283902	-0.134733
6	4.151753	0.312339	-0.145958
6	3.102059	-1.862470	0.214043
1	4.460848	-3.516230	0.379961
1	6.484371	-2.182333	0.091235
1	4.048787	1.378326	-0.283127
6	2.997104	-0.440184	0.024473
6	1.860153	-2.542025	0.326320
6	0.648916	-2.685588	0.337871
6	-0.683099	-2.218789	0.145316
6	-0.798523	-0.799081	-0.067814
6	1.658059	0.135623	0.023043
6	0.418154	-0.019379	0.011979
6	-2.058158	-0.283583	-0.360827
1	-2.167274	0.774170	-0.565870
6	-1.819416	-3.024703	0.108783
1	-1.695101	-4.086096	0.285360
6	-3.071528	-2.461403	-0.166928
6	-3.196037	-1.100416	-0.412932
1	-4.144819	-0.636225	-0.642489
7	-4.267994	-3.377504	-0.189859
7	6.569973	0.481229	-0.310077
6	-5.548341	-2.656756	-0.538838

1	-6.350173	-3.393699	-0.535753
1	-5.746237	-1.891919	0.210025
1	-5.453954	-2.217313	-1.530502
6	-4.450473	-4.004509	1.179896
1	-5.324099	-4.655472	1.144818
1	-3.563983	-4.582425	1.431597
1	-4.597005	-3.203669	1.903808
6	6.462678	1.920221	-0.515847
1	5.985310	2.418589	0.338018
1	7.462789	2.337120	-0.633926
1	5.885837	2.159551	-1.418823
6	7.885273	-0.144920	-0.291990
1	7.985881	-0.896589	-1.086168
1	8.646859	0.618748	-0.449321
1	8.086590	-0.635304	0.669753
6	-4.062622	-4.466927	-1.225631
1	-3.923792	-3.992059	-2.196135
1	-3.186399	-5.055443	-0.964153
1	-4.948199	-5.102176	-1.231553
6	-3.088904	5.035598	-1.141664
6	-4.433842	4.893413	-0.789244
6	-4.791080	4.009391	0.230963
6	-3.807396	3.271639	0.893570
6	-2.456745	3.414621	0.551330
6	-2.106831	4.301149	-0.475284
1	-2.803555	5.718823	-1.937029
1	-5.197712	5.464729	-1.309449
1	-5.834795	3.887166	0.507438
1	-4.091051	2.580714	1.684309
1	-1.063698	4.412927	-0.757504
6	-1.399631	2.646002	1.323572
1	-0.959324	3.270216	2.108579
1	-1.857525	1.784968	1.820765
7	-0.325907	2.106120	0.463598
7	0.834386	2.563965	0.569818
7	1.953011	2.273295	0.399858

T36: *anti*-attack



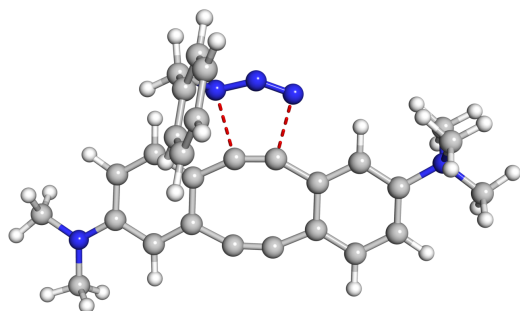
Imaginary frequency at -344.5 cm^{-1}

<i>E (B3LYP)</i>	<i>H (B3LYP)</i>	<i>G (B3LYP)</i>	<i>E (M06-2X)</i>
-1357.198254	-1356.663186	-1356.759121	-1357.120123

	X	Y	Z
6	-3.826967	-2.984163	0.671670
6	-5.054842	-2.393993	0.393399
6	-5.126434	-1.068296	-0.098584
6	-3.903393	-0.361499	-0.279624
6	-2.625207	-2.297128	0.483226
1	-3.800202	-4.005745	1.039168
1	-5.956876	-2.970283	0.554845
1	-3.914976	0.657831	-0.636090
6	-2.673908	-0.943098	-0.000090
6	-1.316012	-2.812476	0.679773
6	-0.096256	-2.832190	0.664217
6	1.169649	-2.294262	0.291207
6	1.125177	-0.951563	-0.215716
6	-1.404307	-0.247584	-0.167467
6	-0.154765	-0.275902	-0.204373
6	2.305307	-0.400824	-0.716748
1	2.284149	0.590753	-1.151996
6	2.381464	-2.990147	0.338442
1	2.370763	-3.993166	0.740421
6	3.545236	-2.389798	-0.144758
6	3.510167	-1.107285	-0.687908
1	4.396071	-0.631116	-1.090957
7	4.864739	-3.119948	-0.116079
7	-6.328281	-0.473848	-0.389042

6	5.354689	-3.333324	-1.535931
1	6.304675	-3.866280	-1.494274
1	4.608379	-3.921241	-2.069054
1	5.488613	-2.367553	-2.018197
6	4.774204	-4.474570	0.546199
1	5.771659	-4.911548	0.535163
1	4.435905	-4.350829	1.573799
1	4.090256	-5.107022	-0.016791
6	-6.375345	0.887134	-0.908938
1	-5.834945	0.977287	-1.860340
1	-7.414975	1.163986	-1.083656
1	-5.945949	1.607804	-0.200804
6	-7.569647	-1.211748	-0.196894
1	-7.701771	-1.513677	0.850488
1	-8.409916	-0.575478	-0.474509
1	-7.604161	-2.115626	-0.819806
6	5.882755	-2.302957	0.657296
1	6.031629	-1.346918	0.161045
1	5.500103	-2.149670	1.665614
1	6.819882	-2.859149	0.681682
6	2.544329	5.756217	-0.987089
6	2.013021	6.765087	-0.177557
6	1.270370	6.425871	0.954739
6	1.057902	5.082420	1.275219
6	1.588019	4.066790	0.471065
6	2.333714	4.415861	-0.663580
1	3.126530	6.014248	-1.867516
1	2.179949	7.809107	-0.427950
1	0.856576	7.204139	1.590087
1	0.479385	4.821704	2.158298
1	2.750958	3.635391	-1.295234
6	1.345647	2.612526	0.821451
1	2.264771	2.031607	0.721555
1	0.998636	2.517410	1.856378
7	0.384518	1.942720	-0.094762
7	-0.819191	2.291527	-0.020564
7	-1.905002	1.876612	-0.122014

T37: *anti*-attack



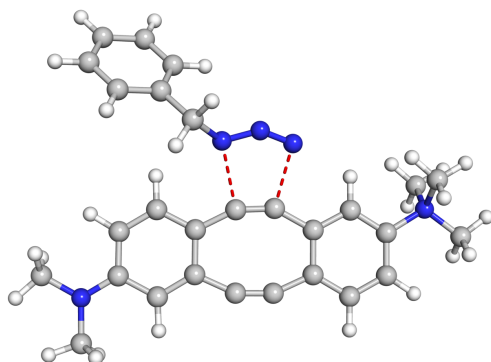
Imaginary frequency at -343.4 cm⁻¹

<i>E</i> (B3LYP)	<i>H</i> (B3LYP)	<i>G</i> (B3LYP)	<i>E</i> (M06-2X)
-1357.199911	-1356.664890	-1356.760410	-1357.122249

	X	Y	Z
6	-2.935476	-0.342703	-1.340893
6	-4.205369	-0.875820	-1.140669
6	-4.439827	-1.873567	-0.163029
6	-3.314092	-2.341826	0.569882
6	-1.826062	-0.763018	-0.599972
1	-2.797113	0.405068	-2.113612
1	-5.018658	-0.510646	-1.754786
1	-3.421289	-3.133382	1.300043
6	-2.049237	-1.814219	0.354378
6	-0.477338	-0.273510	-0.745065
6	0.766024	-0.320290	-0.603728
6	1.928734	-0.986438	-0.051785
6	1.719096	-2.050485	0.895834
6	-0.851999	-2.282300	0.983562
6	0.350809	-2.363343	1.150833
6	2.812314	-2.701392	1.459051
1	2.648724	-3.499300	2.175095
6	3.242035	-0.652312	-0.385007
1	3.393255	0.151194	-1.092062
6	4.322538	-1.337016	0.185373
6	4.122596	-2.353704	1.109880
1	4.938925	-2.892348	1.569862
7	5.711102	-0.923005	-0.235068
7	-5.693612	-2.380211	0.065873
6	6.790838	-1.762486	0.405475
1	7.748742	-1.400677	0.035047

1	6.746492	-1.644192	1.486578
1	6.653145	-2.804519	0.120366
6	5.952412	0.520676	0.163886
1	6.963595	0.794896	-0.138008
1	5.226534	1.157407	-0.337028
1	5.839669	0.598708	1.244757
6	-5.887192	-3.464973	1.020301
1	-5.546137	-3.179428	2.022856
1	-6.950290	-3.697792	1.081987
1	-5.353169	-4.377790	0.721916
6	-6.815691	-1.942984	-0.754637
1	-6.676407	-2.201725	-1.813566
1	-7.725546	-2.428243	-0.401412
1	-6.960805	-0.858018	-0.683497
6	5.856659	-1.066360	-1.738606
1	5.668461	-2.106518	-2.002091
1	5.140809	-0.416230	-2.236002
1	6.871876	-0.778688	-2.011571
6	-0.459169	5.634618	1.033047
6	-0.786285	5.050699	2.258200
6	-1.394009	3.791575	2.287137
6	-1.672128	3.121632	1.095659
6	-1.345664	3.700237	-0.139158
6	-0.736677	4.960696	-0.159204
1	0.009768	6.614350	1.002883
1	-0.572497	5.573941	3.186163
1	-1.654958	3.334398	3.237747
1	-2.145951	2.143333	1.120776
1	-0.483021	5.419939	-1.111863
6	-1.631098	2.964372	-1.431456
1	-2.626775	2.517354	-1.411390
1	-1.598025	3.648862	-2.286447
7	-0.718816	1.823424	-1.698045
7	0.515811	2.040058	-1.687677
7	1.536970	1.513378	-1.477722

T38: *anti*-attack



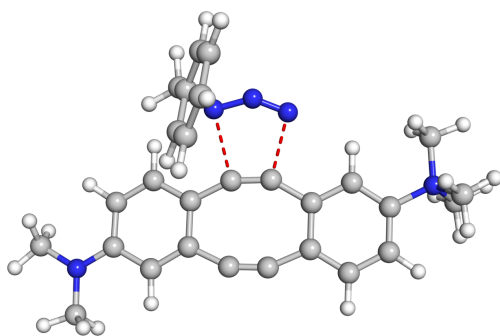
Imaginary frequency at -328.5 cm^{-1}

<i>E</i> (B3LYP)	<i>H</i> (B3LYP)	<i>G</i> (B3LYP)	<i>E</i> (M06-2X)
-1357.199626	-1356.664503	-1356.760313	-1357.121696

	X	Y	Z
6	2.513339	-0.615399	0.287290
6	3.591917	-1.492915	0.344419
6	3.419411	-2.886553	0.160151
6	2.092597	-3.354669	-0.050688
6	1.207233	-1.056410	0.051370
1	2.692522	0.441530	0.449006
1	4.576376	-1.084613	0.534906
1	1.892690	-4.411905	-0.167940
6	1.021565	-2.474214	-0.096300
6	0.030310	-0.227547	-0.023490
6	-1.200018	-0.000257	-0.038947
6	-2.557258	-0.506856	-0.032526
6	-2.754433	-1.925896	-0.180039
6	-0.348353	-2.863073	-0.240898
6	-1.552988	-2.690827	-0.264952
6	-4.044675	-2.446038	-0.205174
1	-4.188117	-3.514746	-0.321174
6	-3.685010	0.303682	0.102464
1	-3.528627	1.367437	0.215581
6	-4.971660	-0.249662	0.083984
6	-5.164374	-1.615915	-0.074570
1	-6.145842	-2.067899	-0.097424
7	-6.138834	0.692678	0.242829
7	4.479259	-3.755578	0.190769
6	-7.472054	-0.014166	0.191572

1	-8.247455	0.741432	0.308710
1	-7.579663	-0.507880	-0.772813
1	-7.529784	-0.732010	1.008042
6	-6.124960	1.719929	-0.873611
1	-6.983085	2.378806	-0.740913
1	-5.203219	2.295110	-0.825848
1	-6.190432	1.190390	-1.823401
6	4.262478	-5.189239	0.041542
1	3.786029	-5.425840	-0.918243
1	5.225281	-5.699063	0.073542
1	3.634561	-5.594566	0.846462
6	5.822895	-3.255644	0.451413
1	5.897305	-2.781883	1.439709
1	6.525793	-4.088017	0.418905
1	6.130155	-2.521115	-0.303871
6	-6.046420	1.395548	1.583889
1	-6.058258	0.637433	2.366228
1	-5.123014	1.968512	1.628027
1	-6.904591	2.060756	1.680366
6	5.368762	3.681626	-0.204840
6	5.024663	4.571168	0.815039
6	3.680597	4.745254	1.156425
6	2.686636	4.036972	0.479462
6	3.023316	3.145265	-0.547002
6	4.372931	2.970259	-0.878138
1	6.411497	3.534341	-0.472683
1	5.797866	5.121907	1.343596
1	3.405307	5.432851	1.951597
1	1.644260	4.173563	0.753566
1	4.646293	2.274820	-1.668516
6	1.954568	2.405433	-1.331508
1	1.537757	3.043216	-2.118660
1	2.395753	1.534651	-1.826360
7	0.860086	1.886981	-0.485890
7	-0.280360	2.393662	-0.576697
7	-1.409215	2.149921	-0.399355

T39: *anti*-attack



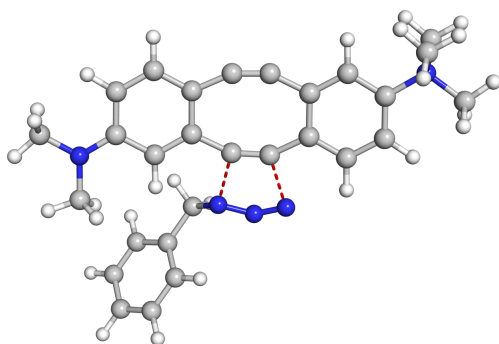
Imaginary frequency at -345.3 cm^{-1}

<i>E</i> (B3LYP)	<i>H</i> (B3LYP)	<i>G</i> (B3LYP)	<i>E</i> (M06-2X)
-1357.199654	-1356.664352	-1356.758993	-1357.122047

	X	Y	Z
6	-2.952830	-0.342284	-1.355558
6	-4.221191	-0.874923	-1.142488
6	-4.447599	-1.865928	-0.156525
6	-3.315899	-2.328174	0.571637
6	-1.837957	-0.756594	-0.619910
1	-2.820747	0.400909	-2.133886
1	-5.039231	-0.514095	-1.752873
1	-3.417406	-3.114017	1.308781
6	-2.053380	-1.800980	0.343525
6	-0.490609	-0.265512	-0.777091
6	0.753940	-0.311056	-0.645371
6	1.920919	-0.967540	-0.090367
6	1.718639	-2.018024	0.868138
6	-0.851165	-2.261529	0.969754
6	0.352800	-2.336080	1.131045
6	2.818416	-2.655661	1.441011
1	2.660554	-3.445579	2.167088
6	3.234234	-0.624443	-0.434267
1	3.370518	0.167286	-1.153356
6	4.315420	-1.288203	0.147942
6	4.119810	-2.297971	1.087598
1	4.946193	-2.820457	1.554107
7	5.733217	-0.923683	-0.221633
7	-5.699114	-2.371910	0.085701
6	6.435716	-2.136364	-0.801643

1	7.450665	-1.844331	-1.071382
1	6.461324	-2.929058	-0.057475
1	5.882315	-2.461628	-1.681948
6	6.474087	-0.450245	1.014499
1	7.491081	-0.187309	0.723198
1	5.951010	0.418594	1.412443
1	6.493005	-1.249501	1.751869
6	-5.885006	-3.448620	1.050702
1	-5.538871	-3.153962	2.048941
1	-6.947210	-3.683258	1.120258
1	-5.350757	-4.362747	0.756966
6	-6.828890	-1.936984	-0.725279
1	-6.700191	-2.200021	-1.784468
1	-7.735595	-2.420148	-0.361255
1	-6.972419	-0.851563	-0.657113
6	5.812740	0.181194	-1.248958
1	5.317055	-0.139660	-2.163798
1	5.350089	1.081081	-0.846913
1	6.867664	0.365891	-1.447031
6	-0.451143	5.593583	1.064232
6	-0.762876	4.991447	2.284587
6	-1.372230	3.732930	2.302317
6	-1.667036	3.081582	1.104534
6	-1.355935	3.678420	-0.125580
6	-0.745381	4.938287	-0.134374
1	0.018835	6.573046	1.042830
1	-0.535941	5.500107	3.217529
1	-1.621359	3.261655	3.249214
1	-2.142165	2.103756	1.121134
1	-0.503689	5.411799	-1.083157
6	-1.658722	2.962296	-1.425049
1	-2.652590	2.511700	-1.397437
1	-1.640162	3.660214	-2.269547
7	-0.747172	1.828391	-1.723256
7	0.486904	2.049672	-1.726204
7	1.512563	1.526892	-1.529906

T40: *syn*-attack



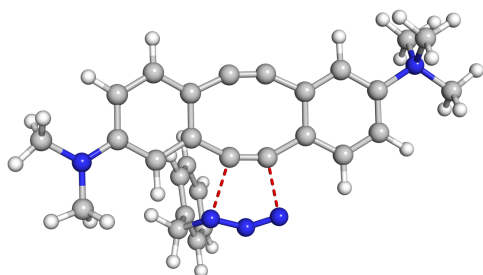
Imaginary frequency at -333.3 cm⁻¹

<i>E</i> (B3LYP)	<i>H</i> (B3LYP)	<i>G</i> (B3LYP)	<i>E</i> (M06-2X)
-1357.198834	-1356.663749	-1356.758882	-1357.122242

	X	Y	Z
6	-0.806991	3.788234	-0.476637
6	-2.165755	3.858378	-0.192092
6	-2.882250	2.708487	0.222004
6	-2.171042	1.475968	0.295281
6	-0.102323	2.585967	-0.382447
1	-0.277681	4.690770	-0.767464
1	-2.664943	4.815076	-0.276079
1	-2.677512	0.573930	0.609349
6	-0.817193	1.396969	-0.006323
6	1.298453	2.402645	-0.545086
6	2.362005	1.807169	-0.503562
6	3.186569	0.684448	-0.208025
6	2.477193	-0.511393	0.169921
6	-0.038057	0.173505	0.069002
6	1.026922	-0.473751	0.153866
6	3.227404	-1.630493	0.523360
1	2.719122	-2.541245	0.812777
6	4.580435	0.690442	-0.234163
1	5.079569	1.605336	-0.529117
6	5.294970	-0.458125	0.126370
6	4.628571	-1.614298	0.510739
1	5.150684	-2.515181	0.800569
7	6.800280	-0.394290	0.087311
7	-4.214200	2.772271	0.542170
6	7.449161	-1.690674	0.510889

1	8.527481	-1.555317	0.443745
1	7.167818	-1.913454	1.538840
1	7.134853	-2.486990	-0.161623
6	7.290922	0.691927	1.026279
1	8.380411	0.703911	0.993457
1	6.899346	1.653521	0.702003
1	6.937622	0.459366	2.030221
6	-4.926167	1.585092	0.999090
1	-4.463125	1.156818	1.897492
1	-5.950937	1.860682	1.248066
1	-4.962109	0.805972	0.226602
6	-4.925032	4.040777	0.447151
1	-4.901651	4.440570	-0.574987
1	-5.967241	3.887305	0.726524
1	-4.498071	4.796434	1.120117
6	7.262545	-0.088362	-1.324740
1	6.903354	-0.879911	-1.981266
1	6.857259	0.871761	-1.636200
1	8.351971	-0.052152	-1.325543
6	-5.221401	-3.278396	1.131592
6	-6.410122	-3.085714	0.426659
6	-6.384531	-2.407610	-0.795814
6	-5.177729	-1.926963	-1.304444
6	-3.978362	-2.122483	-0.603478
6	-4.011698	-2.800282	0.619050
1	-5.230904	-3.801772	2.083942
1	-7.349807	-3.457431	0.825737
1	-7.304862	-2.248491	-1.351235
1	-5.165224	-1.398872	-2.255495
1	-3.092456	-2.950872	1.176272
6	-2.683309	-1.615897	-1.219999
1	-2.390923	-2.242503	-2.070532
1	-2.834220	-0.604589	-1.610678
7	-1.563457	-1.499698	-0.271578
7	-0.694938	-2.403356	-0.247009
7	0.432751	-2.587224	-0.011200

T41: *syn*-attack



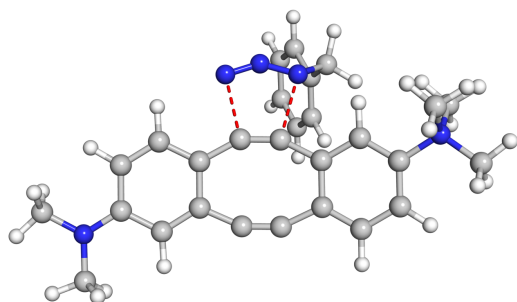
Imaginary frequency at -349.2 cm^{-1}

<i>E</i> (B3LYP)	<i>H</i> (B3LYP)	<i>G</i> (B3LYP)	<i>E</i> (M06-2X)
-1357.199172	-1356.664048	-1356.759522	-1357.122435

	X	Y	Z
6	-1.965418	-3.090449	1.577925
6	-3.279367	-3.212517	1.140718
6	-3.756268	-2.446444	0.048686
6	-2.856364	-1.520459	-0.552657
6	-1.075056	-2.198717	0.975220
1	-1.618993	-3.710500	2.399423
1	-3.929171	-3.919727	1.639808
1	-3.172958	-0.918854	-1.393012
6	-1.549824	-1.375567	-0.103034
6	0.312825	-2.058469	1.251892
6	1.454260	-1.668980	1.071278
6	2.469688	-0.967069	0.361659
6	1.998223	-0.134017	-0.715195
6	-0.591309	-0.453834	-0.688557
6	0.565601	-0.046495	-0.930181
6	2.947110	0.541474	-1.479492
1	2.620426	1.172891	-2.295599
6	3.835458	-1.063374	0.624239
1	4.152126	-1.699091	1.442105
6	4.753862	-0.361536	-0.165413
6	4.319712	0.432265	-1.218831
1	5.003692	0.981209	-1.850744
7	6.219145	-0.511520	0.154828
7	-5.039160	-2.584887	-0.416778
6	7.101544	0.333563	-0.733000
1	8.131889	0.171640	-0.419441
1	6.977724	0.018845	-1.767516

1	6.836982	1.382657	-0.609077
6	6.630410	-1.959902	-0.031955
1	7.693172	-2.045652	0.194787
1	6.052292	-2.587665	0.642738
1	6.434655	-2.237719	-1.067095
6	-5.507820	-1.793864	-1.547247
1	-4.893459	-1.962803	-2.440634
1	-6.531310	-2.084508	-1.783756
1	-5.503390	-0.718090	-1.324782
6	-5.955872	-3.507543	0.240584
1	-6.102931	-3.247474	1.297170
1	-6.924406	-3.463236	-0.257261
1	-5.592828	-4.542588	0.190445
6	6.479794	-0.089016	1.588234
1	6.172211	0.950152	1.698395
1	5.911233	-0.724317	2.263109
1	7.546145	-0.197647	1.785989
6	-1.998542	3.425262	2.380974
6	-1.928357	4.792236	2.095720
6	-2.219241	5.247964	0.808390
6	-2.577173	4.339164	-0.190548
6	-2.649422	2.968490	0.086459
6	-2.357464	2.519681	1.382260
1	-1.778158	3.065803	3.382456
1	-1.651710	5.497703	2.874412
1	-2.170882	6.309323	0.580802
1	-2.806463	4.697666	-1.191401
1	-2.413139	1.457537	1.607844
6	-3.015704	1.984610	-1.004228
1	-3.680400	1.207990	-0.621071
1	-3.538405	2.487080	-1.825826
7	-1.863054	1.234063	-1.565409
7	-0.862027	1.887192	-1.944407
7	0.297145	1.809525	-2.056188

T42: *syn*-attack



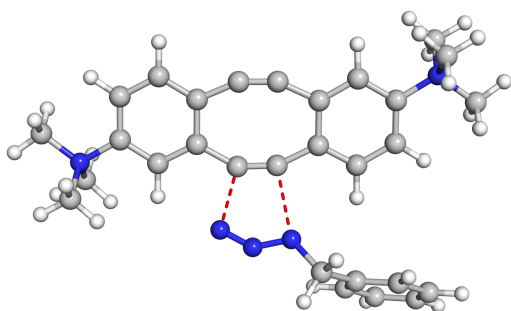
Imaginary frequency at -352.5 cm^{-1}

<i>E</i> (B3LYP)	<i>H</i> (B3LYP)	<i>G</i> (B3LYP)	<i>E</i> (M06-2X)
-1357.198093	-1356.662939	-1356.758095	-1357.121509

	X	Y	Z
6	-3.401031	-0.269952	-1.438946
6	-4.744934	-0.010859	-1.187497
6	-5.146726	0.855618	-0.141821
6	-4.117859	1.462007	0.630177
6	-2.375730	0.315092	-0.686985
1	-3.142059	-0.948061	-2.243332
1	-5.487141	-0.493279	-1.810995
1	-4.361432	2.141442	1.436680
6	-2.779198	1.207397	0.366255
6	-0.961258	0.085762	-0.879390
6	0.234468	0.343208	-0.606845
6	1.263668	1.168643	-0.017341
6	0.873640	2.060791	1.043172
6	-1.689947	1.808870	1.070593
6	-0.527714	2.074131	1.316883
6	1.828918	2.864000	1.655866
1	1.534744	3.525454	2.463381
6	2.593185	1.187911	-0.442600
1	2.862620	0.550646	-1.274935
6	3.528845	2.030946	0.174259
6	3.163181	2.854325	1.231274
1	3.866176	3.502743	1.734514
7	4.941631	2.024923	-0.355465
7	-6.468848	1.107459	0.120323
6	5.850830	2.966516	0.398614
1	6.839267	2.899117	-0.053139

1	5.472069	3.983002	0.307462
1	5.899616	2.659537	1.441901
6	4.939984	2.457892	-1.809896
1	5.969957	2.457542	-2.167085
1	4.342699	1.760867	-2.393397
1	4.513734	3.458779	-1.866164
6	-6.848143	2.006175	1.203262
1	-6.466725	3.023244	1.041708
1	-7.935495	2.057813	1.257760
1	-6.476207	1.650105	2.172677
6	-7.503987	0.490456	-0.698506
1	-7.465921	-0.605340	-0.640033
1	-8.481555	0.815090	-0.342121
1	-7.411376	0.779920	-1.753721
6	5.532835	0.633254	-0.239666
1	5.501983	0.335369	0.807884
1	4.953154	-0.057502	-0.847547
1	6.560976	0.667616	-0.599584
6	0.804276	-3.734046	2.348463
6	0.571350	-5.067504	1.998598
6	0.913976	-5.519758	0.722815
6	1.486333	-4.641075	-0.200201
6	1.722980	-3.303905	0.141974
6	1.376582	-2.858447	1.425339
1	0.543907	-3.377795	3.341428
1	0.128213	-5.750161	2.718412
1	0.739437	-6.555742	0.445600
1	1.755681	-4.998024	-1.191549
1	1.557702	-1.822630	1.701734
6	2.323533	-2.349565	-0.867896
1	3.041314	-1.682541	-0.386393
1	2.859366	-2.895333	-1.652626
7	1.344725	-1.433276	-1.510940
7	0.288983	-1.943850	-1.961035
7	-0.847499	-1.725137	-2.108347

T43: *anti*-attack



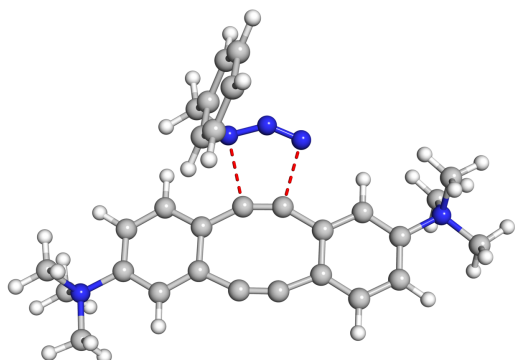
Imaginary frequency at -330.1 cm⁻¹

<i>E</i> (B3LYP)	<i>H</i> (B3LYP)	<i>G</i> (B3LYP)	<i>E</i> (M06-2X)
-1396.936547	-1396.357321	-1396.454293	-1396.848948

	X	Y	Z
6	-4.017210	-2.621617	0.049293
6	-5.208092	-1.890654	0.115396
6	-5.149255	-0.503362	0.110857
6	-3.923185	0.170642	0.035117
6	-2.785771	-1.978246	-0.017612
1	-4.057371	-3.704972	0.053616
1	-6.141119	-2.433446	0.168731
1	-3.878874	1.251691	0.019951
6	-2.726274	-0.542603	-0.026918
6	-1.518840	-2.628778	-0.068824
6	-0.306498	-2.714725	-0.099442
6	1.020130	-2.189059	-0.075002
6	1.086769	-0.753264	-0.065768
6	-1.411350	0.080848	-0.106760
6	-0.168739	-0.039821	-0.132517
6	2.343014	-0.163233	0.027254
1	2.428466	0.914215	0.068647
6	2.181574	-2.952425	-0.026519
1	2.084220	-4.031024	-0.040173
6	3.428174	-2.318740	0.050708
6	3.512026	-0.933225	0.085032
1	4.456978	-0.412797	0.153934
7	4.658705	-3.183477	0.106659
7	-6.401269	0.332613	0.184821
6	5.935461	-2.379509	0.190967
1	6.763555	-3.085870	0.220321

1	6.020710	-1.747028	-0.690907
1	5.927045	-1.782864	1.101498
6	4.738966	-4.039270	-1.144681
1	5.642039	-4.646322	-1.082287
1	3.862778	-4.681230	-1.200492
1	4.778372	-3.377227	-2.009010
6	-6.519016	1.188856	-1.063024
1	-6.554092	0.528209	-1.928613
1	-7.435246	1.774499	-0.987454
1	-5.658610	1.850941	-1.128499
6	-7.656186	-0.502716	0.285267
1	-7.614456	-1.108828	1.188813
1	-8.500956	0.182144	0.338427
1	-7.743963	-1.127721	-0.601595
6	4.597238	-4.077750	1.332031
1	4.528358	-3.442955	2.214823
1	3.726076	-4.725585	1.263885
1	5.506107	-4.678421	1.358697
6	-6.347630	1.226479	1.410468
1	-6.245600	0.593206	2.291069
1	-5.498523	1.901413	1.329817
1	-7.274059	1.798806	1.452699
6	3.361428	4.669770	1.472920
6	4.681898	4.513515	1.040393
6	4.942773	3.850985	-0.160192
6	3.887137	3.346157	-0.924208
6	2.561745	3.504409	-0.500934
6	2.308534	4.169050	0.707125
1	3.151886	5.182781	2.407596
1	5.501089	4.903487	1.638116
1	5.966023	3.720610	-0.501474
1	4.095101	2.827925	-1.857436
1	1.284403	4.289558	1.049997
6	1.423549	2.994265	-1.363454
1	0.915630	3.822633	-1.868077
1	1.813056	2.331698	-2.143923
7	0.428843	2.221384	-0.587408
7	-0.775308	2.551063	-0.609977
7	-1.837148	2.106502	-0.394457

T44: *anti*-attack



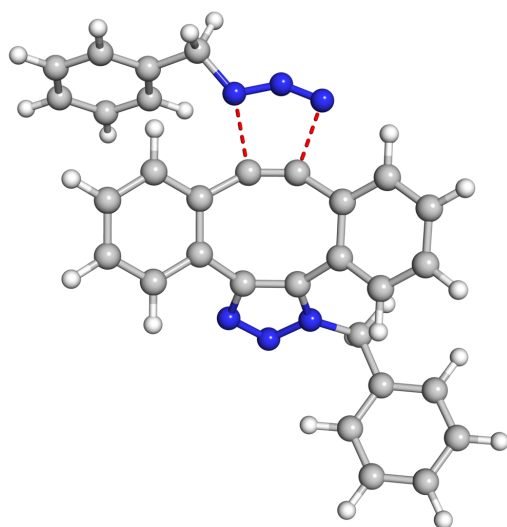
Imaginary frequency at -349.1 cm⁻¹

<i>E</i> (B3LYP)	<i>H</i> (B3LYP)	<i>G</i> (B3LYP)	<i>E</i> (M06-2X)
-1396.937490	-1396.357985	-1396.453340	-1396.851397

	X	Y	Z
6	2.855364	-2.730589	1.549039
6	4.183805	-2.486713	1.182040
6	4.452238	-1.531828	0.210155
6	3.418418	-0.804228	-0.394220
6	1.809584	-2.033713	0.953052
1	2.641397	-3.479785	2.302962
1	4.963705	-3.056097	1.667410
1	3.620163	-0.047275	-1.139525
6	2.090281	-1.036327	-0.042991
6	0.422512	-2.235197	1.216771
6	-0.774013	-2.087547	1.056473
6	-1.927288	-1.575710	0.388035
6	-1.640796	-0.596146	-0.617786
6	0.970240	-0.316517	-0.623695
6	-0.263095	-0.177108	-0.769827
6	-2.700532	-0.138020	-1.401721
1	-2.505586	0.561376	-2.204978
6	-3.235506	-2.006008	0.614026
1	-3.400408	-2.738654	1.390880
6	-4.272858	-1.495925	-0.168696
6	-4.007816	-0.577079	-1.182135
1	-4.793722	-0.180497	-1.813892
7	-5.700158	-1.920906	0.059988
7	5.863879	-1.235435	-0.226872
6	-6.270609	-2.522737	-1.211668

1	-7.295167	-2.834596	-1.008976
1	-6.261740	-1.776007	-2.002256
1	-5.656341	-3.378009	-1.490930
6	-6.523443	-0.710969	0.462862
1	-7.552234	-1.035131	0.618928
1	-6.104853	-0.304236	1.382709
1	-6.480707	0.030903	-0.331479
6	6.205110	0.207929	0.095443
1	6.107556	0.350564	1.170977
1	7.230069	0.393402	-0.225657
1	5.521615	0.866606	-0.435533
6	6.886055	-2.111475	0.458988
1	6.680163	-3.154757	0.224933
1	7.864936	-1.831526	0.073046
1	6.850758	-1.936729	1.532961
6	-5.837965	-2.954159	1.154297
1	-5.274674	-3.845396	0.882117
1	-5.479504	-2.534344	2.092486
1	-6.895514	-3.198047	1.241554
6	5.996395	-1.466485	-1.720933
1	5.737614	-2.503779	-1.929714
1	5.325847	-0.795286	-2.252465
1	7.028547	-1.261925	-2.004850
6	-0.816088	3.972524	2.254747
6	-0.118281	5.181129	2.168954
6	0.210093	5.705299	0.917261
6	-0.156766	5.022077	-0.244809
6	-0.856451	3.811651	-0.167592
6	-1.183392	3.292891	1.093185
1	-1.078512	3.562733	3.226244
1	0.164296	5.712210	3.073694
1	0.748647	6.645999	0.843140
1	0.096881	5.435162	-1.218300
1	-1.730104	2.355739	1.164411
6	-1.239843	3.068930	-1.429121
1	-2.250325	2.663237	-1.352217
1	-1.222017	3.735097	-2.298493
7	-0.389005	1.886239	-1.730707
7	0.854210	2.033364	-1.725668
7	1.849231	1.461217	-1.516738

T45: *anti*-attack



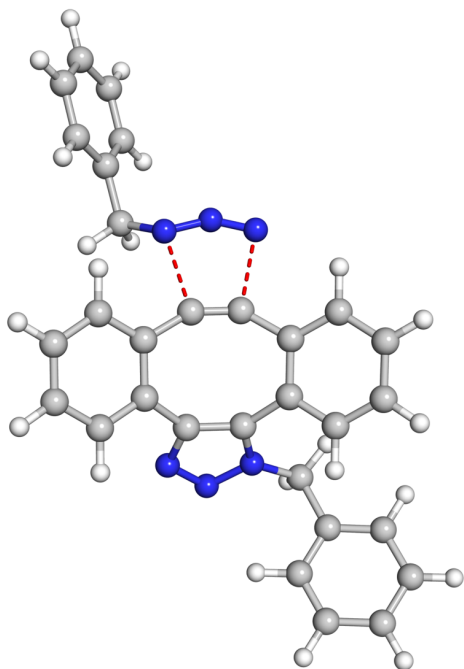
Imaginary frequency at -305.7 cm⁻¹

<i>E</i> (B3LYP)	<i>H</i> (B3LYP)	<i>G</i> (B3LYP)	<i>E</i> (M06-2X)
-1484.776199	-1484.293934	-1484.387072	-1484.715182

	X	Y	Z
6	6.470193	-2.265422	-0.099126
6	7.490492	-1.312551	-0.153267
6	7.220248	-0.039935	-0.660537
6	5.935376	0.277321	-1.105916
6	4.908694	-0.674629	-1.057533
6	5.187647	-1.951350	-0.552788
1	6.672187	-3.258120	0.293909
1	8.488081	-1.559686	0.199119
1	8.005466	0.709809	-0.703428
1	5.729219	1.272498	-1.492606
1	4.401266	-2.699128	-0.516626
6	3.541251	-0.315351	-1.617279
1	3.420877	0.767068	-1.672290
1	3.431325	-0.712791	-2.630768
7	2.399291	-0.855513	-0.867124
7	2.002090	-2.109037	-1.155531
7	0.929684	-2.353773	-0.459198
6	1.553966	-0.258057	0.037401
6	0.593029	-1.253168	0.280568
6	-0.637505	-1.373898	1.105939
6	-1.658301	-0.383565	1.139882

6	-1.348769	0.876452	0.539498
6	-0.510564	1.746702	0.259195
6	0.849758	2.143666	0.496925
6	1.835743	1.118189	0.522639
6	3.126412	1.447931	0.957855
1	3.879983	0.670673	1.024576
6	1.204215	3.458872	0.823851
1	0.442819	4.230168	0.777391
6	-0.862608	-2.582197	1.779663
1	-0.093435	-3.346853	1.749875
6	-2.853415	-0.634253	1.830919
1	-3.623185	0.129375	1.839770
6	-3.050886	-1.841862	2.495928
1	-3.980048	-2.020184	3.029167
6	-2.050810	-2.816095	2.473457
1	-2.194094	-3.759922	2.991524
6	2.503416	3.767131	1.227169
1	2.759855	4.790190	1.486454
6	3.461143	2.757337	1.312214
1	4.469571	2.981155	1.646839
6	-5.597892	-1.469118	-2.130324
6	-6.613299	-1.939161	-1.291960
6	-6.996544	-1.185034	-0.181502
6	-6.365332	0.031685	0.089785
6	-5.351777	0.511116	-0.747810
6	-4.973338	-0.250880	-1.861392
1	-5.292978	-2.051703	-2.995528
1	-7.099095	-2.888075	-1.502145
1	-7.781247	-1.544316	0.478687
1	-6.663810	0.612511	0.959471
1	-4.182389	0.110241	-2.513002
6	-4.715353	1.857119	-0.473002
1	-5.094463	2.606342	-1.178135
1	-4.974636	2.200160	0.535949
7	-3.243905	1.783533	-0.604510
7	-2.605793	2.809337	-0.913003
7	-1.551714	3.308110	-0.922194

T46: *anti*-attack



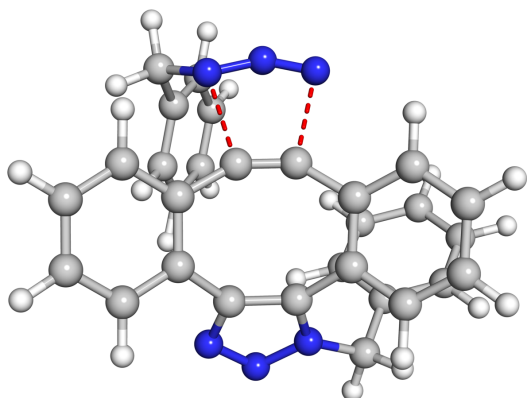
Imaginary frequency at -296.4 cm^{-1}

<i>E</i> (B3LYP)	<i>H</i> (B3LYP)	<i>G</i> (B3LYP)	<i>E</i> (M06-2X)
-1484.778568	-1484.296034	-1484.388817	-1484.717843

	X	Y	Z
6	-7.057888	0.980133	-0.745546
6	-7.819113	-0.160399	-0.478070
6	-7.226331	-1.421781	-0.563646
6	-5.878550	-1.539331	-0.909696
6	-5.110540	-0.399852	-1.182441
6	-5.712651	0.862372	-1.100348
1	-7.511757	1.965337	-0.681510
1	-8.866065	-0.066336	-0.203355
1	-7.808361	-2.314931	-0.353789
1	-5.420492	-2.523871	-0.966831
1	-5.128677	1.751991	-1.315789
6	-3.665883	-0.570959	-1.624985
1	-3.290287	-1.554135	-1.339655
1	-3.592449	-0.491663	-2.713781
7	-2.729604	0.434026	-1.103337
7	-2.620141	1.592514	-1.780035
7	-1.674933	2.290121	-1.218661

6	-1.820176	0.367159	-0.074006
6	-1.132526	1.587913	-0.177248
6	-0.008361	2.248352	0.537782
6	1.210722	1.587840	0.852992
6	1.235883	0.166877	0.679414
6	0.636290	-0.916824	0.744458
6	-0.605762	-1.532653	1.109722
6	-1.803138	-0.816275	0.825636
6	-3.006010	-1.291939	1.364367
1	-3.921165	-0.734590	1.196453
6	-0.668270	-2.728042	1.839167
1	0.251587	-3.272286	2.026045
6	-0.102165	3.623865	0.788606
1	-1.025324	4.137195	0.540191
6	2.281014	2.315230	1.395755
1	3.200806	1.790401	1.632788
6	2.160471	3.681906	1.640054
1	2.995404	4.230861	2.065730
6	0.964685	4.336489	1.339220
1	0.859896	5.400818	1.528742
6	-1.882872	-3.196579	2.339516
1	-1.911718	-4.119625	2.911159
6	-3.050678	-2.467592	2.118430
1	-3.998692	-2.809351	2.522764
6	7.828697	-0.202052	0.150671
6	8.329224	-1.122925	-0.774975
6	7.493726	-1.624667	-1.774653
6	6.161738	-1.208765	-1.847144
6	5.653596	-0.286476	-0.924904
6	6.499404	0.213835	0.074654
1	8.475441	0.195200	0.928253
1	9.365544	-1.444382	-0.717904
1	7.876614	-2.337860	-2.499499
1	5.514228	-1.600890	-2.627956
1	6.114129	0.931940	0.794651
6	4.204568	0.149442	-0.997649
1	4.112297	1.222147	-0.812409
1	3.782951	-0.062140	-1.986337
7	3.360588	-0.467221	0.056698
7	3.039236	-1.669333	-0.058772
7	2.235064	-2.480056	0.149997

T47: *anti*-attack



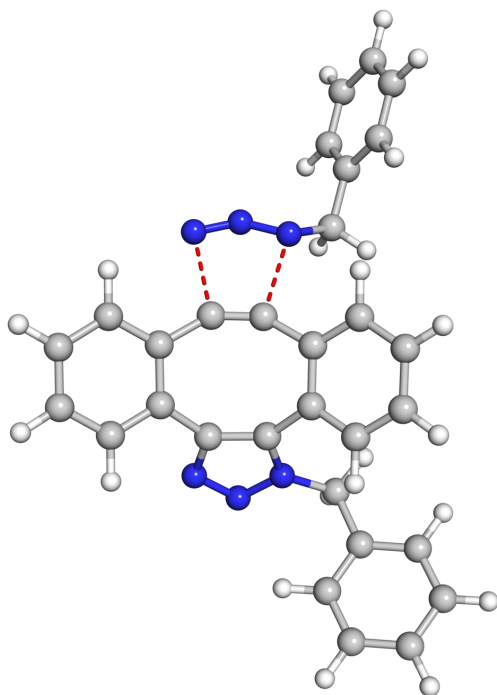
Imaginary frequency at -308.6 cm^{-1}

<i>E</i> (B3LYP)	<i>H</i> (B3LYP)	<i>G</i> (B3LYP)	<i>E</i> (M06-2X)
-1484.779159	-1484.296704	-1484.389517	-1484.721990

	X	Y	Z
6	4.203090	2.523000	0.305445
6	3.149987	3.428567	0.165352
6	2.064466	3.107095	-0.654803
6	2.035535	1.889427	-1.335023
6	3.088134	0.974843	-1.195989
6	4.168436	1.299516	-0.368231
1	5.048042	2.761831	0.945418
1	3.171749	4.377322	0.694403
1	1.236761	3.802477	-0.764104
1	1.188517	1.646720	-1.971435
1	4.985741	0.592838	-0.247233
6	3.091169	-0.335818	-1.961780
1	3.276452	-0.169735	-3.026476
1	3.873974	-0.996837	-1.590410
7	1.796725	-1.031339	-1.925132
7	1.035945	-0.988296	-3.036506
7	-0.126238	-1.495104	-2.738806
6	1.108088	-1.575414	-0.869435
6	-0.150871	-1.858165	-1.418673
6	-1.435819	-2.397404	-0.903281
6	-2.036765	-1.933719	0.300094
6	-1.232550	-1.102634	1.145235

6	-0.117810	-0.843064	1.623022
6	1.248444	-1.278270	1.651390
6	1.792951	-1.776260	0.435074
6	3.036403	-2.420157	0.473353
1	3.437350	-2.862066	-0.433998
6	2.000015	-1.356788	2.832017
1	1.579609	-0.952110	3.746953
6	-2.156592	-3.291566	-1.705571
1	-1.708493	-3.639978	-2.630512
6	-3.324207	-2.368205	0.651043
1	-3.765585	-2.001507	1.572263
6	-4.017625	-3.263491	-0.161257
1	-5.010671	-3.596467	0.126306
6	-3.430647	-3.729630	-1.339221
1	-3.962990	-4.429730	-1.976507
6	3.252548	-1.970416	2.838279
1	3.819067	-2.031751	3.762881
6	3.762559	-2.522173	1.662813
1	4.723171	-3.028263	1.664136
6	-2.198527	4.505351	-0.218232
6	-1.860086	4.050007	-1.494717
6	-2.088292	2.713664	-1.838242
6	-2.651494	1.838791	-0.908320
6	-2.994596	2.287528	0.374835
6	-2.762915	3.627565	0.710468
1	-2.030263	5.543885	0.053163
1	-1.428842	4.733462	-2.221020
1	-1.834667	2.355020	-2.832104
1	-2.829108	0.801485	-1.180576
1	-3.032086	3.988494	1.700474
6	-3.585047	1.333738	1.391674
1	-4.180595	1.872424	2.136952
1	-4.241761	0.604921	0.911907
7	-2.582110	0.498545	2.100504
7	-1.624372	1.058941	2.674172
7	-0.508989	0.998976	2.987995

T48: *syn*-attack

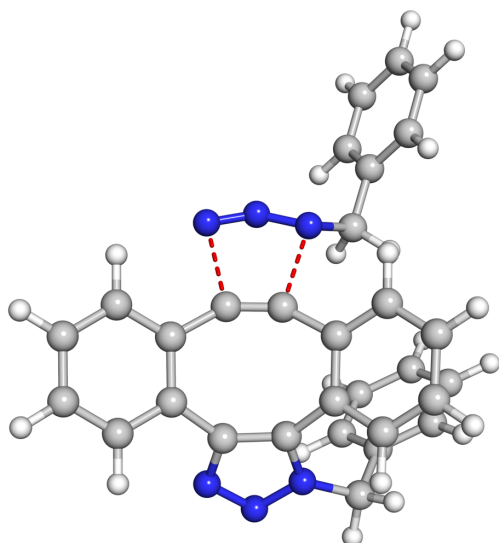


Imaginary frequency at -296.6 cm⁻¹

<i>E</i> (B3LYP)	<i>H</i> (B3LYP)	<i>G</i> (B3LYP)	<i>E</i> (M06-2X)
-1484.778411	-1484.295935	-1484.389760	-1484.717782

	X	Y	Z
6	-6.623117	-1.539960	-0.350657
6	-6.729291	-2.870444	0.061591
6	-5.610072	-3.703405	0.000488
6	-4.391816	-3.205124	-0.465440
6	-4.279497	-1.872592	-0.883295
6	-5.407148	-1.043764	-0.825068
1	-7.489159	-0.885189	-0.306527
1	-7.676724	-3.254483	0.429438
1	-5.680640	-4.738689	0.322531
1	-3.521622	-3.856134	-0.502516
1	-5.333678	-0.011109	-1.152258
6	-2.953324	-1.385994	-1.446405
1	-2.135650	-2.023193	-1.107526
1	-2.970433	-1.422834	-2.539863
7	-2.607487	0.002354	-1.114531
7	-3.099198	0.972152	-1.907868
7	-2.599662	2.104371	-1.503520

6	-1.751040	0.515497	-0.169033
6	-1.751986	1.892012	-0.450219
6	-1.076269	3.101341	0.092061
6	0.319990	3.165362	0.357079
6	1.054322	1.934633	0.332542
6	1.020524	0.713339	0.546086
6	0.272611	-0.382235	1.085814
6	-1.128821	-0.385090	0.836673
6	-1.923927	-1.310182	1.526150
1	-2.998905	-1.298050	1.382955
6	0.828872	-1.338309	1.946872
1	1.899857	-1.322050	2.120239
6	-1.829020	4.277734	0.206942
1	-2.892864	4.238689	-0.003256
6	0.908973	4.391016	0.703786
1	1.978046	4.421988	0.886945
6	0.137095	5.545623	0.818473
1	0.606315	6.485082	1.096185
6	-1.236183	5.487072	0.575272
1	-1.847436	6.380496	0.664806
6	0.019081	-2.270170	2.595444
1	0.465294	-3.000242	3.264293
6	-1.361117	-2.245263	2.398520
1	-2.004310	-2.950305	2.916294
6	7.208906	-1.617127	-1.586122
6	7.702195	-2.183469	-0.409354
6	6.834311	-2.431984	0.658657
6	5.480514	-2.115171	0.547808
6	4.977809	-1.543858	-0.629496
6	5.852798	-1.297604	-1.693778
1	7.876727	-1.424464	-2.421289
1	8.756214	-2.433169	-0.324197
1	7.211851	-2.876792	1.575358
1	4.807840	-2.311971	1.379215
1	5.471815	-0.857435	-2.612302
6	3.511341	-1.180973	-0.744272
1	3.226784	-1.031582	-1.791550
1	2.882061	-1.973423	-0.332173
7	3.146943	0.014404	0.056751
7	3.490818	1.142052	-0.358490
7	3.226917	2.270298	-0.424844

T49: *syn*-attack

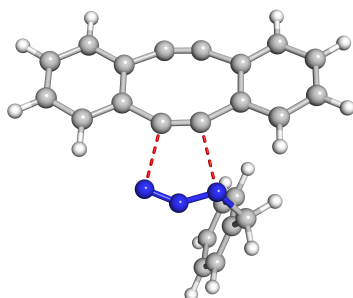
Imaginary frequency at -298.5 cm⁻¹

<i>E</i> (B3LYP)	<i>H</i> (B3LYP)	<i>G</i> (B3LYP)	<i>E</i> (M06-2X)
-1484.778839	-1484.296254	-1484.389578	-1484.719220

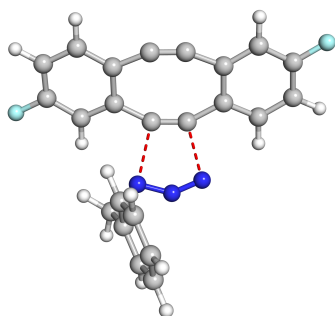
	X	Y	Z
6	-1.455061	3.936379	-0.634286
6	-1.726367	3.474429	-1.923315
6	-0.695125	2.932258	-2.697275
6	0.599541	2.854826	-2.184171
6	0.877749	3.313141	-0.888994
6	-0.158601	3.852081	-0.118904
1	-2.250507	4.358126	-0.026118
1	-2.733931	3.537157	-2.324943
1	-0.899005	2.574028	-3.702603
1	1.398973	2.434218	-2.788743
1	0.046939	4.204603	0.888704
6	2.289052	3.248816	-0.333483
1	2.977075	3.855809	-0.927176
1	2.317421	3.617053	0.691128
7	2.859949	1.893015	-0.385361
7	3.709417	1.614847	-1.393274
7	3.929026	0.331281	-1.381218
6	2.510159	0.755865	0.299579
6	3.207511	-0.256288	-0.375879

6	3.305634	-1.735567	-0.269897
6	2.167952	-2.581232	-0.137112
6	0.907956	-1.960969	0.150838
6	0.325167	-1.028660	0.725333
6	0.462181	0.069869	1.635154
6	1.638665	0.856085	1.499682
6	1.943148	1.781234	2.506696
1	2.870405	2.343787	2.451632
6	-0.406253	0.294920	2.712105
1	-1.304097	-0.309035	2.794277
6	4.559304	-2.331117	-0.461576
1	5.428752	-1.691569	-0.574060
6	2.323166	-3.973858	-0.216795
1	1.442566	-4.601950	-0.129052
6	3.582629	-4.542060	-0.398423
1	3.686755	-5.622111	-0.448681
6	4.703899	-3.718754	-0.515619
1	5.690058	-4.152144	-0.655173
6	-0.102874	1.251988	3.680247
1	-0.781516	1.411163	4.513042
6	1.083448	1.980763	3.590042
1	1.343837	2.704543	4.356321
6	-6.256628	-1.403805	-1.322428
6	-6.940449	-1.456217	-0.106227
6	-6.279099	-1.115391	1.077618
6	-4.940461	-0.724455	1.042818
6	-4.246223	-0.671457	-0.173675
6	-4.915258	-1.014179	-1.354594
1	-6.765634	-1.663445	-2.246621
1	-7.983984	-1.757743	-0.079963
1	-6.807560	-1.149667	2.026429
1	-4.429607	-0.457098	1.964856
1	-4.386166	-0.972502	-2.303811
6	-2.787081	-0.267663	-0.209837
1	-2.495674	0.064193	-1.212184
1	-2.593036	0.551680	0.486082
7	-1.877660	-1.348119	0.251642
7	-1.643076	-2.301458	-0.522170
7	-0.868818	-3.075991	-0.903771

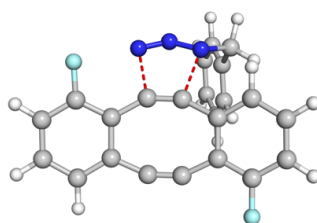
A.3 Summary of transition state barriers (in kcal/mol) with benzyl azide



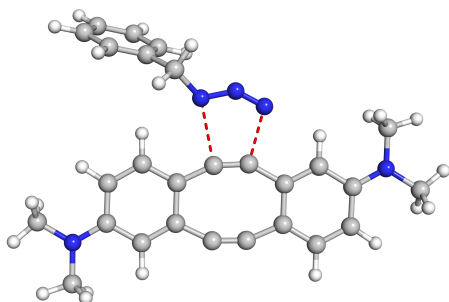
T19 $\Delta G^\ddagger = 25.8$



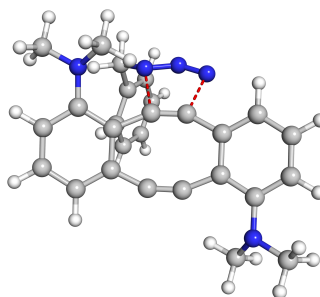
T23 $\Delta G^\ddagger = 25.0$



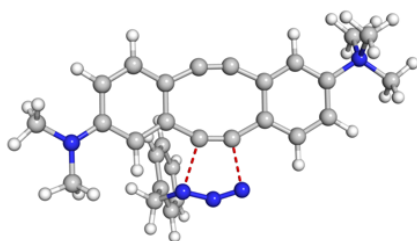
T24 $\Delta G^\ddagger = 27.1$



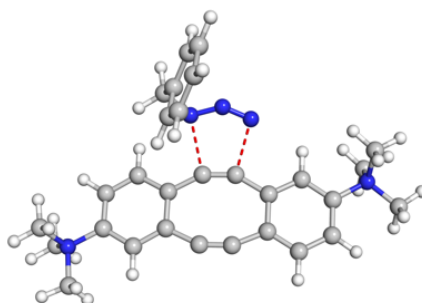
T28 $\Delta G^\ddagger = 27.4$



T32 $\Delta G^\ddagger = 28.2$



T41 $\Delta G^\ddagger = 25.7$



T44 $\Delta G^\ddagger = 25.6$

